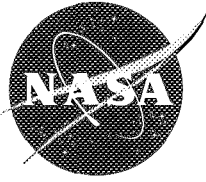


NASA/CP—1998-208536



The 1997 NASA Aerospace Battery Workshop

J.C. Brewer, Compiler

Marshall Space Flight Center, Marshall Space Flight Center, Alabama

July 1998

The NASA STI Program Office...in Profile

Since its founding, NASA has been dedicated to the advancement of aeronautics and space science. The NASA Scientific and Technical Information (STI) Program Office plays a key part in helping NASA maintain this important role.

The NASA STI Program Office is operated by Langley Research Center, the lead center for NASA's scientific and technical information. The NASA STI Program Office provides access to the NASA STI Database, the largest collection of aeronautical and space science STI in the world. The Program Office is also NASA's institutional mechanism for disseminating the results of its research and development activities. These results are published by NASA in the NASA STI Report Series, which includes the following report types:

- **TECHNICAL PUBLICATION.** Reports of completed research or a major significant phase of research that present the results of NASA programs and include extensive data or theoretical analysis. Includes compilations of significant scientific and technical data and information deemed to be of continuing reference value. NASA's counterpart of peer-reviewed formal professional papers but has less stringent limitations on manuscript length and extent of graphic presentations.
- **TECHNICAL MEMORANDUM.** Scientific and technical findings that are preliminary or of specialized interest, e.g., quick release reports, working papers, and bibliographies that contain minimal annotation. Does not contain extensive analysis.
- **CONTRACTOR REPORT.** Scientific and technical findings by NASA-sponsored contractors and grantees.

- **CONFERENCE PUBLICATION.** Collected papers from scientific and technical conferences, symposia, seminars, or other meetings sponsored or cosponsored by NASA.
- **SPECIAL PUBLICATION.** Scientific, technical, or historical information from NASA programs, projects, and mission, often concerned with subjects having substantial public interest.
- **TECHNICAL TRANSLATION.** English-language translations of foreign scientific and technical material pertinent to NASA's mission.

Specialized services that complement the STI Program Office's diverse offerings include creating custom thesauri, building customized databases, organizing and publishing research results...even providing videos.

For more information about the NASA STI Program Office, see the following:

- Access the NASA STI Program Home Page at <http://www.sti.nasa.gov>
- E-mail your question via the Internet to help@sti.nasa.gov
- Fax your question to the NASA Access Help Desk at (301) 621-0134
- Telephone the NASA Access Help Desk at (301) 621-0390
- Write to:
NASA Access Help Desk
NASA Center for AeroSpace Information
800 Elkridge Landing Road
Linthicum Heights, MD 21090-2934

NASA/CP—1998—208536



The 1997 NASA Aerospace Battery Workshop

J.C. Brewer, Compiler

Marshall Space Flight Center, Marshall Space Flight Center, Alabama

*Proceedings of a workshop sponsored by the
NASA Aerospace Flight Battery Systems Program
and held in Huntsville, Alabama
November 18–20, 1997*

National Aeronautics and
Space Administration

Marshall Space Flight Center

July 1998

Available from:

NASA Center for AeroSpace Information
800 Elkridge Landing Road
Linthicum Heights, MD 21090-2934
(301) 621-0390

National Technical Information Service
5285 Port Royal Road
Springfield, VA 22161
(703) 487-4650

Preface

This document contains the proceedings of the 30th annual NASA Aerospace Battery Workshop, hosted by the Marshall Space Flight Center on November 18-20, 1997. The workshop was attended by scientists and engineers from various agencies of the U.S. Government, aerospace contractors, and battery manufacturers, as well as international participation in like kind from a number of countries around the world.

The subjects covered included nickel-cadmium, nickel-hydrogen, silver-zinc, nickel-metal hydride, and lithium- based technologies.

Page intentionally left blank

Introduction

The NASA Aerospace Battery Workshop is an annual event hosted by the Marshall Space Flight Center. The workshop is sponsored by the NASA Aerospace Flight Battery Systems Program which is managed out of NASA Lewis Research Center and receives support in the form of overall objectives, guidelines, and funding from Code S, NASA Headquarters.

The 1997 Workshop was held on three consecutive days and was divided into five sessions. The first day consisted of a General / Secondary Battery Session and a Lithium / Lithium-Ion Battery Focused Session. The second day consisted of a Nickel-Hydrogen Session and a Nickel Electrode Design Focused Session. The third and final day was devoted to an Advanced Nickel-Hydrogen Technology / Nickel Electrode Characteristics Session.

On a personal note, I would like to take this opportunity to thank all of the many people that contributed to the organization and production of this workshop:

The NASA Aerospace Flight Battery Systems Program, for their financial support as well as their input during the initial planning stages of the workshop;

Rao Surampudi, Jet Propulsion Laboratory, and **Joe Stockel**, Office of Research & Development, for serving as Focused Session Organizers, which involved soliciting presentations, organizing the session agenda, and orchestrating the session during the workshop;

Huntsville Hilton, for doing an outstanding job in providing an ideal setting for this workshop and for the hospitality that was shown to all who attended;

Marshall Space Flight Center employees, for their help in mailing the various correspondence, registering attendees, handling the audience microphones, and flipping transparencies during the workshop.

Finally, I want to thank all of you that attended and/or prepared and delivered presentations for this workshop. You were the key to the success of this workshop.

Jeff Brewer
NASA Marshall Space Flight Center

Page intentionally left blank

Table of Contents

Preface	iii
Introduction	v
General / Ni-Cd / Ni-MH Battery Session	1
An Historical Summary and Prospects for the Future of Spacecraft Batteries G. Halpert and S. Surampudi, Jet Propulsion Laboratory	3
Battery System Management -- Optimized Electrokinetic Control in Galvanic, Electrolytic, and Storage Operating Modes Floyd Williamson, ZAE Research, Inc.	29
Advanced Lithium-Ion Energy Technology Ricky J. Roberson and Greg Tyler, Huntsville Integrated Voltaic Equipment	55
Performance of Nickel-Cadmium Batteries on the GOES I-K Series of Weather Satellites Sat P. Singhal, Computer Sciences Corporation; Walter G. Alsbach, Jackson & Tull; and Gopalakrishna M. Rao, NASA Goddard Space Flight Center	83
Near Earth Asteroid Rendezvous Flight Battery Performance Jason E. Jenkins, JHU Applied Physics Laboratory; Jeff W. Hayden and David F. Pickett, Eagle Picher Industries, Inc.	113
Crane Cell Testing Support of Goddard Space Flight Center Steve Hall and Harry Brown, Naval Surface Warfare Center, Crane; and Gopalakrishna Rao, NASA Goddard Space Flight Center	149
Status of Nickel Metal Hydride Cell Development Y. Sone, H. Kusawake, K. Koga, and S. Kuwajima, National Space Development Agency of Japan	161
Battery Systems for X-38 Crew Return Vehicle (CRV) and Deorbit Propulsion Stage (DPS) Eric Darcy, NASA Johnson Space Center	179
Lithium-Ion Focused Session	213
Improved Li-BCX Primary Cells for Space Applications D.M. Spillman, N.M. Waite, M.F. Pyszczek, and E.S. Takeuchi, Wilson Greatbatch Ltd. ...	215
Development of Ultra Low Temperature, Impact Resistant Lithium Battery for the Mars Microprobe H. Frank, F. Deligiannis, E. Davies, B.V. Ratnakumar, and S. Surampudi, Jet Propulsion Laboratory; P.G. Russel and T.B. Reddy, Yardney Technical Products, Inc.	225

Development of 20 to 50-Ah Li-Ion Cells for Aerospace Applications Lynn Marcoux and Gregg Bruce, BlueStar Advanced Technology Corporation	265
Rechargeable Lithium-Ion Battery Development at Eagle-Picher Industries Chad Kelly, Eagle-Picher Industries, Inc.	299
Evaluation of 20 Ah Li Ion Cells Marshall Smart, B.V. Ratnakumar, C.K. Huang, and S. Surampudi, Jet Propulsion Laboratory; Carole Hill and Dan Radzykewycz, Air Force Research Lab, Albuquerque; and R.A. Marsh, Air Force Research Lab, Dayton	311
The Li-Ion Battery Qualification Programme for STRV-1d Vijay V. Thakur, Defence Evaluation and Research Agency	341
Rate Capability Analysis of Li-ion Cells Esther Sans Takeuchi and Randolph A. Leising, Wilson Greatbatch Ltd.	365
Nickel-Hydrogen Session	387
Mars Pathfinder Battery Performance B. Otzinger, D. Perrone, S. Dawson, T. Valdez, S. Surampudi, R. Ewell, and M. Shirbacheh, Jet Propulsion Laboratory	389
Cycle Life Expectations for IPV Nickel-Hydrogen Cells Lawrence H. Thaller, The Aerospace Corporation	411
Life Cycle Testing of Spaceflight Qualified Nickel-Hydrogen Battery Cells Chris Fox, Jennifer Francisco, Kevin Ames, and Ron Repplinger, Eagle-Picher Industries, Inc.	429
EOS-AM1 Nickel Hydrogen Cell Interim Life Test Report C.W. Bennett, Lockheed Martin Missiles and Space; D.J. Keys and G.M. Rao, NASA Goddard Space Flight Center; H.E. Wannemacher, Jackson and Tull; and H. Vaidyanathan, COMSAT Laboratories	457
Characterization and Initial Life-Test Data for Computer Designed Nickel Hydrogen Cells A. Zimmerman, J. Matsumoto, A. Prater, D. Smith, and N. Weber, The Aerospace Corporation	471
Development of a Large Diameter (5.5 Inch) Nickel-Hydrogen (NiH₂) Individual Pressure Vessel (IPV) Battery Cell Dwight Caldwell, Jim Morgan, and Jack Brill, Eagle-Picher Industries, Inc.	485

Charge Temperature Characterization of Nickel-Hydrogen Batteries D. Coates, R. Smith, D. Judd, and J. Brill, Eagle-Picher Industries, Inc.; J. McDermott and G. Gates, Lockheed-Martin	503
Meeting the Demands of the Commercial Aerospace Market: Verification Testing and Product Qualification at a New Battery Manufacturing Facility Jeff Dermott and Dwight Caldwell, Eagle-Picher Industries, Inc.	523
Nickel Electrode Design Focused Session	545
Cause for Second Plateau Discharge in Nickel Electrodes A. Zimmerman and N. Weber, The Aerospace Corporation	547
Fabrication of Nickel Electrodes Using Ethanol Solutions David F. Pickett, Jr., Eagle-Picher Industries, Inc.	559
Effects of Cycling Conditions of Active Material from Discharged Ni Positive Plates Studied by Inelastic Neutron Scattering Spectroscopy Juergen Eckert, Los Alamos National Laboratory; Ravi Varma, Lisa Diebolt, and Margaret Reid	567
Study of Parameters Causing Second Plateau Effect on Nickel Hydrogen Cells Y. Borthomieu, SAFT Defense and Space Division; N. Sac-Epee, CNRS; and T. Jamin, CNES	587
Performance Comparison Between NiH₂ Dry Sinter and Slurry Electrode Cells J.D. Armantrout, Lockheed-Martin	627
Advanced Ni-H₂ / Nickel Electrode Session	663
Lander and Orbiter Battery William Cook, Eagle Picher Inc.	665
IRIDIUM Satellite Batteries: Flight Observations "By the Dozen" Mark R. Toft, Motorola Space Systems Technology Group	689
Behavior of 2-Cell CPV Ni-H₂ Battery During Pulse Discharge Hari Vaidyanathan, COMSAT Laboratories; and Gopalakrishna Rao, NASA Goddard Space Flight Center	713
Nickel-Hydrogen (NiH₂) Single Pressure Vessel (SPV) Battery Development Update Steve Sterz, Beth Parmley, Dwight Caldwell, and John Bennett, Eagle-Picher Industries, Inc.	729
Mechanical Behavior of Nickel Oxide Electrode Under Shallow Cycles and Overcharge G. Davolio, E. Soragni, P. Zannini, and P. Baraldi, University of Modena	733

Characterization of Electrochemically Impregnated Fiber Nickel Electrodes
D. Coates, J. Francisco, D. Chiappetti, and J. Brill, Eagle-Picher Industries, Inc. 755

Nickel Electrode Corrosion During Nominal On-Orbit Operation
Chuck Lurie and Bob Tobias, TRW Space and Electronics Group 777

1997 NASA Aerospace Battery Workshop Attendance List 791

General / Ni-Cd / Ni-MH Battery Session

Page intentionally left blank

**AN HISTORICAL SUMMARY AND
PROSPECTS FOR THE FUTURE OF
SPACECRAFT BATTERIES**



G. HALPERT

ADVANCED TECHNOLOGY PROGRAMS OFFICE

AND

S. SURAMPUDI

DEVICE RESEARCH AND APPLICATIONS SECTION

NASA BATTERY WORKSHOP

HUNTSVILLE, ALABAMA

NOVEMBER 18, 1997

OUTLINE

HISTORICAL EVOLUTION OF BATTERIES IN SPACE

EVOLUTION AND STATUS OF NI-CD AND NI-H₂

PRESENT APPLICATIONS

FUTURE APPLICATIONS

ADVANCED BATTERIES FOR FUTURE MISSIONS



HISTORY OF BATTERIES IN SPACE

APPLICATIONS - FIRST SPACE MISSIONS

1955

10/4/57 SPUTNIK Ag/Zn
1 W FOR 3 WEEKS

12/6/57 VANGUARD Zn/HgO

2/1/58 EXPLORER 1 Zn/HgO
VAN ALLEN RAD BELT

8/7/59 EXPLORER 6 Cyl Ni/Cd
FIRST EARTH PHOTOS

1960

'61-64 RANGERS Pris Ni/Cd
MOON PHOTOS

4/26/62 ARIEL I Pris Ni/Cd
First LEO MISSION

6/23/63 SYNCOM-2 Cyl Ni/Cd
First GEO

1965

5/20/65 APOLLO CM Ag/Zn
LTD CYCLE LIFE



APPLICATIONS - FIRST SPACE MISSIONS

1970

3/13/71 IMP 1 Ag/Cd
NON-MAGNETIC

6/23/77 NTS-2 Ni/H₂
12 HOUR POLAR

9/23/77 AF Ni/H₂
LEO

1980

2/14/80 SOLAR MAX Ni/Cd
STANDARD BATTERY

5/19/83 INTELSAT V Ni/H₂
GEO

4/4/83 STS-3 Li-BCX
ASTRONAUT EQUIPMENT

4/7/84 LDEF LITHIUM & OTHERS
EXPOSURE TO SPACE

1990

10/18/89 GALILEO HOURS Li/SO₂/
WITH THERMAL BATTERY
FOR JUPITER PROBE

APPLICATIONS - FIRST SPACE MISSIONS

1990	4/25/90	HST NASA LEO	Ni/H ₂
	6/10/90	LEASAT Super Ni/Cd	GEO
	1/25/94	CLEMENTINE LUNAR MAPPING	SPV Ni/H ₂
	1/25/94	TUBSAT-B STORE MESSAGES	2 Cell CPV
1995	5/1995	CENTAUR 28V, 250AH LAUNCH VEHICLE	Li-SOCl ₂
	5/5/97	IRIDIUM-1 LEO 34 TO DATE	50Ah SPV
	NOV 97	FLIGHT EXP WAKESHIELD	Na/S
2000			



**EVOLUTION OF
NI-CD BATTERIES
IN SPACE**

NI-CD SPACE BATTERY EVOLUTION

	1958-69	1970-79	1980-89	1990-97
Technology	3-6 Ah Cells Pellon GTM Seals	5-20 Ah Cells Teflonation Ceramic Seals NASA Std Cells	NASA 50 Ah E-I Process Lt Wt Designs Passivation	Super Ni-Cds Pellon 2536
Performance	2-5% DOD < 1000 cycles Leaks Const. I Charge	10-20% DOD NASA VT	>10 Years GEO 40K Cycles LEO	'MATURE'
Manufacturers	Gould Gulton Saft Sonotone	EPI G.E.. Gulton Saft	EPI G.E./Gates Saft Sanyo	EPI Hughes Saft Sanyo Acme



**EVOLUTION OF
NI-H₂ BATTERIES
IN SPACE**



NI-H₂ SPACE BATTERY EVOLUTION

	1958-69	1970-79	1980-89	1990-97
Technology		35-50 Ah IPV E-I Aq. Process Back to Back(C) Recirculating(AF)	E-I Alc. Process 100 Ah	CPV & SPV 120 Ah 26% KOH
Performance		LEO 25% DOD 2000 Cycles Polar 40% DOD 5 years	40K Cycles LEO 10 YEARS GEO	50-100K LEO CYCLES
Manufacturers		EPI Yardney ERC SAFT GE	EPI Hughes JCI Saft Gates	EPI Hughes JCI Saft

KEY EVENTS IN SPACE BATTERY HISTORY

	1958-69	1970-79	1980-89	1990-97
NI-CD	'59 EXPLORER-6 (CYLINDRICAL) '62 ARIEL-1 LEO (PRISMATIC) '63 SYNCOM2 GEO		'80 SOLAR MAX NASA 20 AH STD '82 LANDSAT -D STD 50 Ah	'90 LEASAT GEO SUPER NI-CD
NI-H₂		'77 NTS-2 & AF FIRST IPV USE	INTELSAT 5 IPV GEO	'90 HUBBLE IPV '94 CLEMENTINE SPV '94 TUBSAT CPV
LITHIUM			'83 STS- LI-BCX '89 GALILEO Li-SO ₂	'95 CENTAUR '96 PATHFINDER



NASA MISSIONS TODAY



NEAR TERM NASA MISSIONS - GSFC

<u>LAUNCH DATE</u>	<u>MISSION NAME</u>	<u>MISSION TYPE</u>	<u>NO. BATS</u>	<u>NO CELLS/BAT</u>	<u>CELL CAPACITY</u>	<u>CELL TYPE</u>
11/97	TRMM	LEO	2	22	50Ah	EPI-SUPER NI-CD
12/97	TRACE/SMEX	LEO/SS	1	22	9Ah	EPI- SUPER NI-CD
?/97	ACE	LIBATION	1	18	12Ah	NI-CD
5/98	LANDSAT-7	LEO	2	17	50Ah	EPI - AXIAL Ni-H ₂
6/98	EOS-AM	LEO	2	54	50Ah	EPI-RE Ni-H ₂
7/98	GOES-L	GEO	2	28	12Ah	GATES / SAFT NI-CD
9/98	WIRE/SMEX	LEO	1	22	9Ah	EPI-SUPER NI-CD
?/99	IMAGE	LEO	1	22	21Ah	CS SUPER NI-CD
?/00	MAP	FULL SUN	1	11/2CELL	23Ah	CPV EPI-J RE NI-H ₂



NEAR TERM NASA MISSIONS - JPL

<u>LAUNCH DATE</u>	<u>MISSION NAME</u>	<u>MISSION TYPE</u>	<u>NO. BATS</u>	<u>NO CELLS/BAT</u>	<u>CELL CAPACITY</u>	<u>CELL TYPE</u>
1996	MGS	MARS ORB	2	11/2CELL	23Ah	CPV EPI-J RE NI-H ₂
1996	MPF	LANDER	1	18	40Ah	AG/ZN RECHARGE
1996	MPF	ROVER	3	3	12Ah	LI-SOCL ₂ 'D'
1997	CASSINI	PROBE	3	13	8Ah	LI-SO ₂
1998	NEW MIL DS-1		1	11/2CELL	12Ah	SAME AS MSTI-3
1998	NEW MIL DS-2		2	4	2Ah	LI-SOCL ₂ FLAT PLATE
1998	MARS SURVEYOR/98		2	11/2CELL	16Ah	NI-H ₂
1999	STARDUST		2	11/2CELL	16Ah	NI-H ₂
1999	STARDUST SAMP. RET		3	13	8AH	LI-SO ₂



NEAR TERM NASA MISSIONS - MSFC

<u>LAUNCH</u> <u>DATE</u>	<u>MISSION</u> <u>NAME</u> <u>TYPE</u>	<u>NO.</u> <u>BATS</u>	<u>NO</u> <u>CELLS/BAT</u>	<u>CELL</u> <u>CAPACITY</u>	<u>CELL</u> <u>TYPE</u>
1998	AXAF LEO	3	22 CELLS	40 Ah	EPI IPV NI-H ₂

**THE FUTURE OF
BATTERIES IN SPACE**

POTENTIAL NASA SPACE MISSIONS / APPLICATIONS

NASA MISSIONS

JPL

MARS LANDER AND ROVER -2001
MARS LANDER AND ROVER -2003
MARS SAMPLE RETURN MISSION - 2005
CHAMPOLION MISSION - 2003
SOLAR PROBE - 2005

GSFC

SATELLITE SERVICING TOOLS
LIBATION POINT SPACRAFT
(MAP-2000,NGST 2007)
GEO SPACECRAFT(GOES)
LEO SPACECRAFT(EOS)

JSC

SHUTTLE APPLICATIONS

AIR FORCE MISSIONS

LEO

NPOESS -2007
Surveill. Platforms
SBIRS Low

GEO

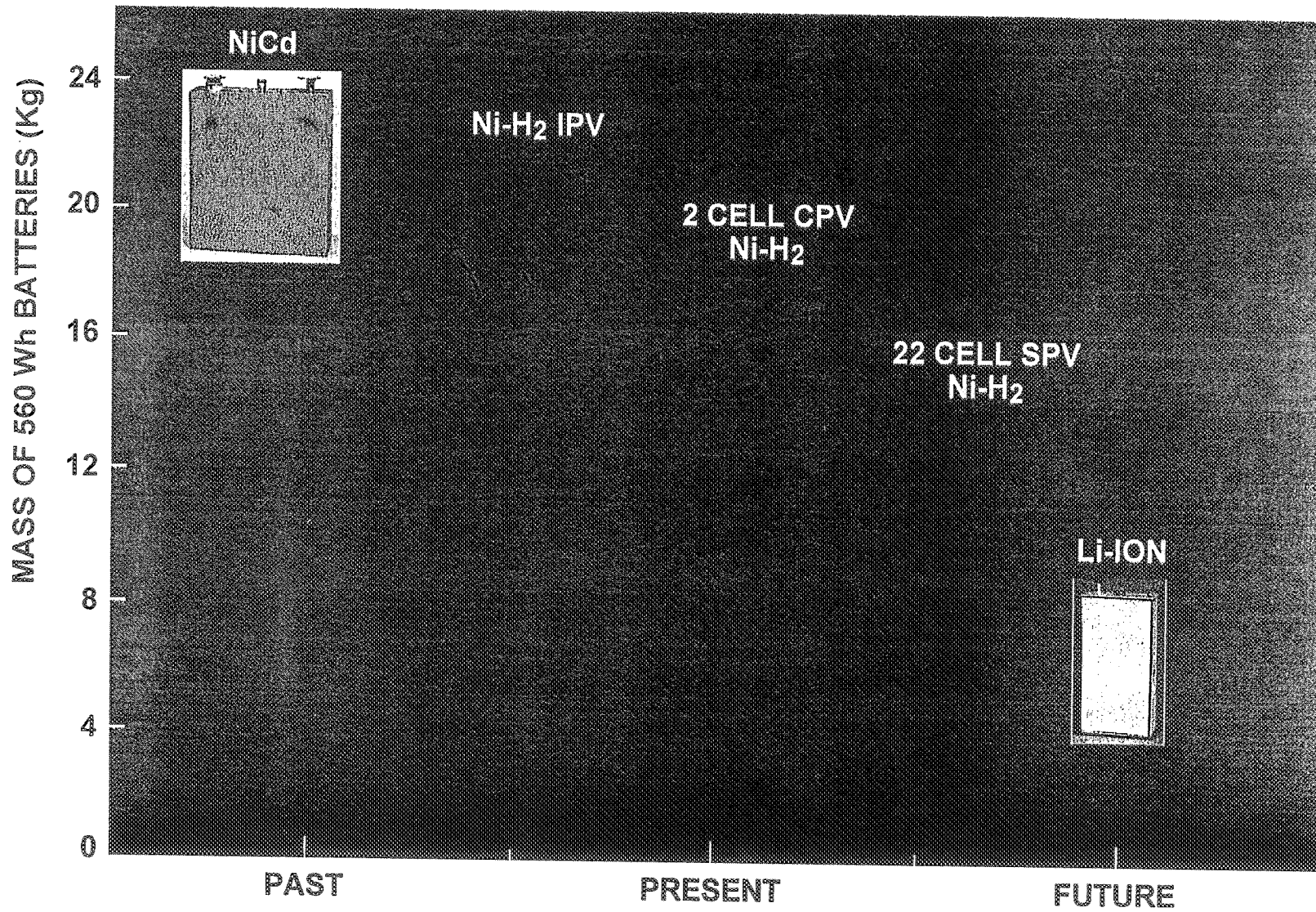
Milsatcom - 2002

DSP

AIRCRAFT

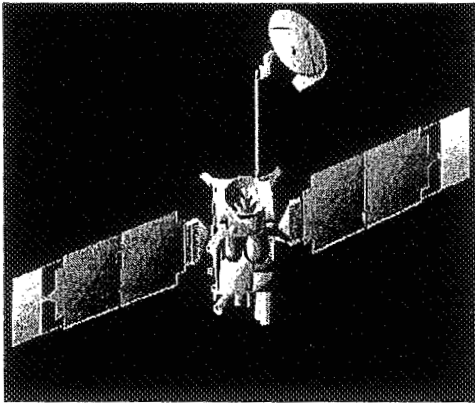
AVIATION 2001
UAVs- 2002

EVOLUTION OF FLIGHT BATTERIES

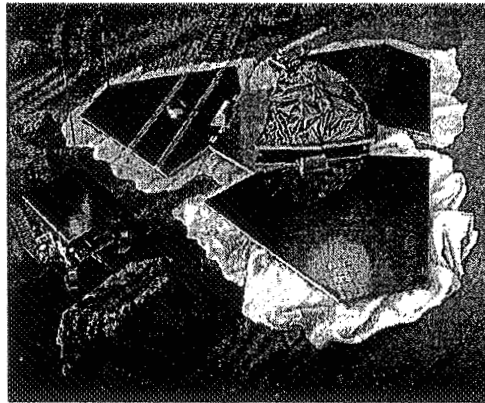


POTENTIAL NASA APPLICATIONS

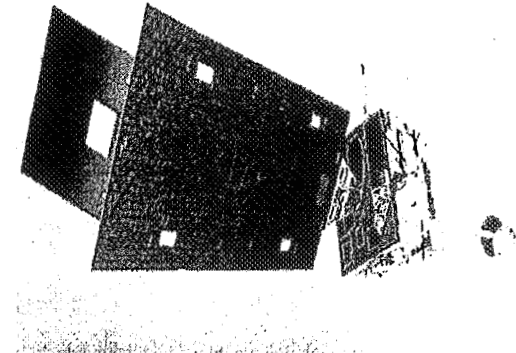
Planetary Orbiters



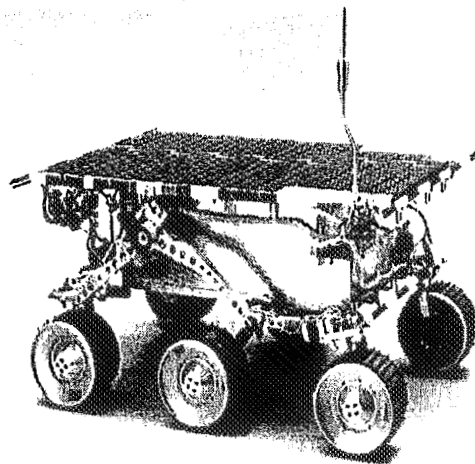
Planetary Lander



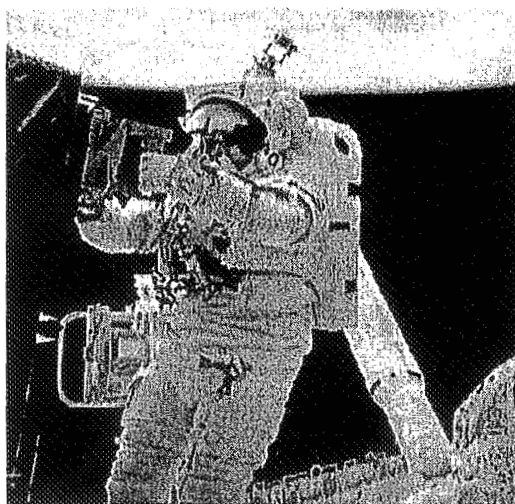
GEO Spacecraft



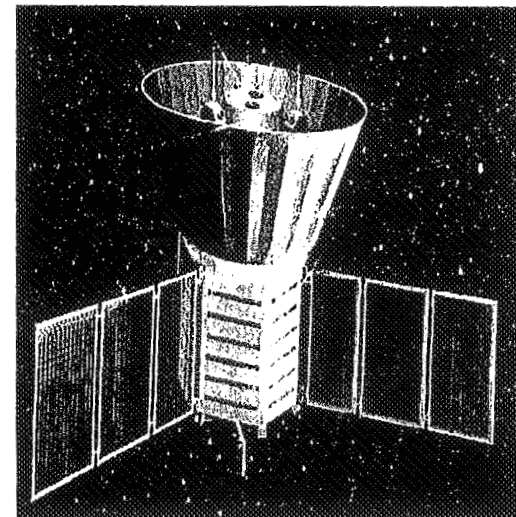
Planetary Rover



Astronaut Equipment



LEO Spacecraft



TECHNOLOGY PROGRESSION

1992

100 mAh
< 200 cycles

Anode Mat.
Electrolyte
Cat. Mat.
Separator
Binder

1996

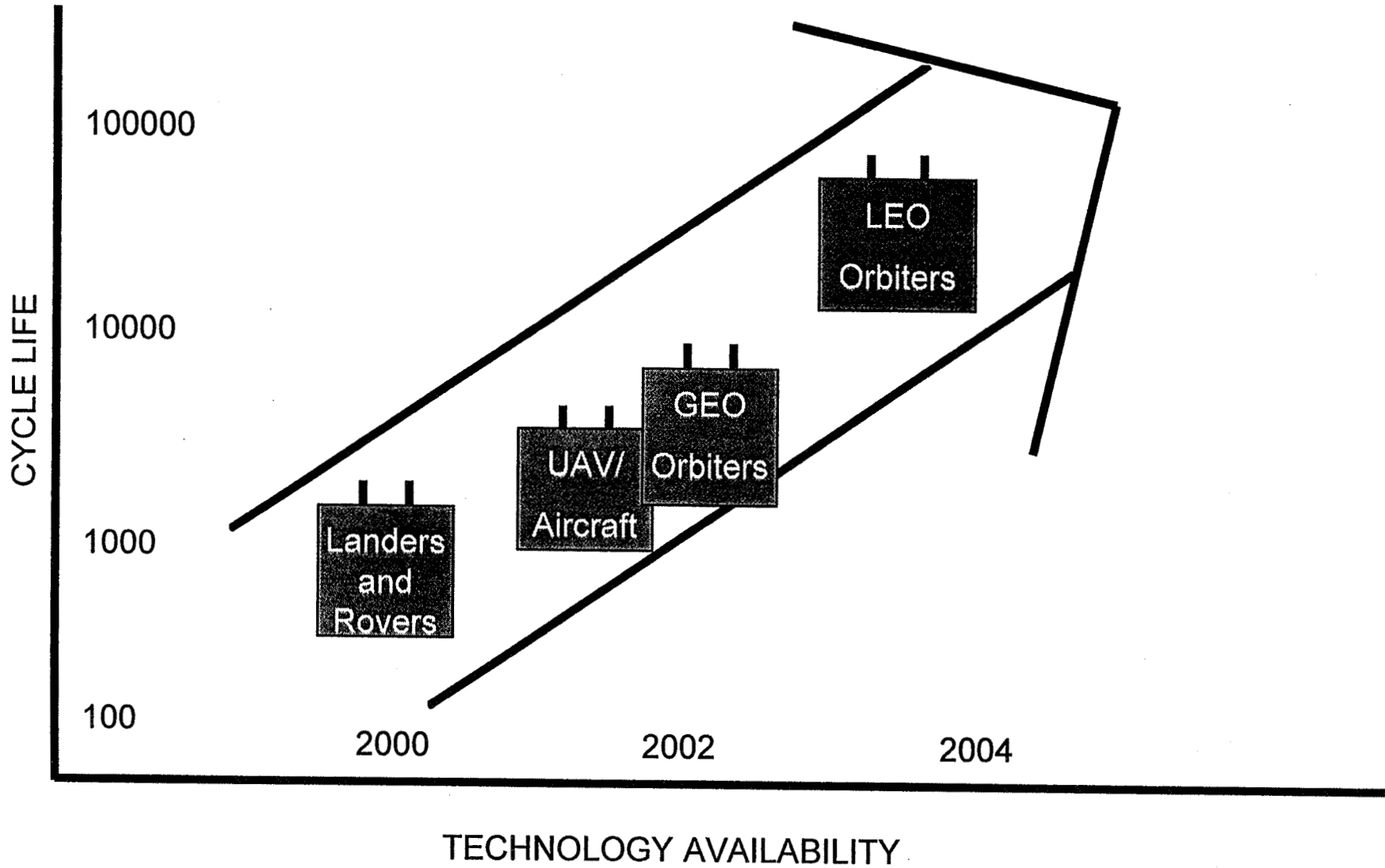
1-20 Ah Cells
100 Wh/kg
500 cycles

LONG LIFE
Cell Design
Battery Design
Manufacturing
Database
Charge Control

2003

28-270V
10-100 Ah
100 Wh/kg
2000 GEO &
30,000 LEO
CYCLES

TECHNOLOGY DEMONSTRATION MILESTONES



PROGRAM OBJECTIVES OF NASA / AF LI-ION PROGRAM

- **DEVELOP ADVANCED LITHIUM ION CELLS AND SMART BATTERIES FOR AEROSPACE AND DOD APPLICATIONS**
- **ESTABLISH U.S. PRODUCTION SOURCES**
- **DEMONSTRATE TECHNOLOGY READINESS FOR:**
 - **SATELLITE SERVICING TOOLS BY 1999**
 - **ROVERS AND LANDERS BY 2000**
 - **LIBATION POINT MISSIONS BY 2000**
 - **GEO MISSIONS BY 2001**
 - **MILITARY TERRESTRIAL APPLICATIONS BY 2001**
 - **LEO MISSIONS BY 2003**



TECHNOLOGY CHOICES FOR FUTURE MISSIONS

NEAR TERM (>2000):

LI-ION LIQUID ORGANIC ELECTROLYTE CELLS

- 1-20Ah CELL SIZES
- >1000 CYCLES
- SUPERIOR LOW TEMPERATURE PERFORMANCE
- COMMERCIAL APPLICATIONS USE
- LEVERAGE OF FUNDS SEVERAL PROGRAMS

LONG TERM MISSIONS (>2007)

LI - ION POLYMER

- HIGHER SPECIFIC ENERGY
- ADAPTABILITY TO SEVERAL CONFIGURATIONS

TECHNOLOGY APPROACH TO NASA / AF LI-ION PROGRAM

**DEVELOP ADVANCED ELECTRODE MATERIALS AND ELECTROLYTES TO
ACHIEVE IMPROVED LOW TEMP. PERFORMANCE AND LONG CYCLE LIFE**

**OPTIMIZE CELL DESIGN TO IMPROVE SPEC. ENERGY, CYCLE LIFE AND
SAFETY**

**ESTABLISH MANUFACTURING PROCESSES TO ENSURE PREDICTABLE
PERFORMANCE**

DEVELOP AEROSPACE LITHIUM ION CELLS IN 10, 20, 50, AND 200 AH SIZES

DEVELOP BATTERIES IN 28, 100 AND 270 V CONFIGURATIONS

DEVELOP ELECTRONICS FOR SMART BATTERY MANAGEMENT

DEVELOP A PERFORMANCE DATABASE FOR VARIOUS APPLICATIONS

**DEMONSTRATE TECHNOLOGY READINESS FOR VARIOUS NASA AND AIR
FORCE MISSIONS**

SUMMARY

THIS PAPER INCLUDED:

**A CHRONOLOGICAL HISTORY OF BATTERY FLIGHT
FROM 1959 TO THE PRESENT**

**A LIST OF THE NEAR TERM FLIGHT MISSIONS FROM
1997-2000**

**A PLAN FOR AN INTERAGENCY (NASA / AF) PROGRAM
TO DEVELOP LI-ION BATTERIES FOR PLANETARY,
AVIATION, LEO AND GEO MISSIONS FROM 2000-2003**

Page intentionally left blank

Battery System Management

Optimized Electrokinetic Control in Galvanic, Electrolytic, and Storage Operating Modes

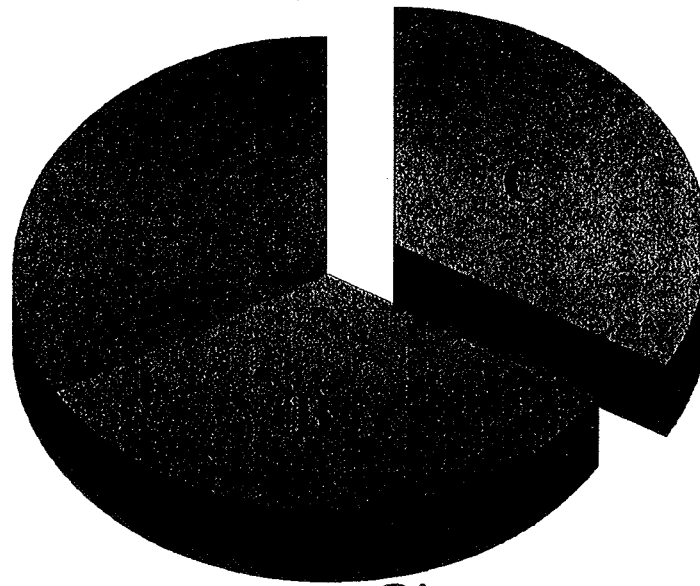
Floyd Williamson ZAE Research, Inc.
555 Sparkman Dr. Suite 450 Huntsville, AL 35816
205-890-0507 / FAX 205-890-0857 email: flw@hiwaay.net

Battery System Management

$$\text{Reliability} = A - B - C$$

Cell Physics

Determines
Inherent
Reliability



Discharge control

Historically, the
missing element

Charge control

Presently degrades
system reliability

Faraday's law:

$$m = \frac{sMt}{nF}$$

Theoretical capacity:

$$Q_T = x(nF)$$

Coulombic efficiency:

$$Q_P/Q_T$$

Tafel equation:

$$i = i_o \exp \left(\frac{\alpha_a F}{RT} \eta_s \right)$$

Total charge passed:

$$Q = \int_0^t I dt$$

The potential developed across the cell is equal to:

$$V = \eta_s (\text{anode}) + \eta_c (\text{anode}) + IR - \eta_c (\text{cathode}) - \eta_s (\text{cathode})$$

The current density:

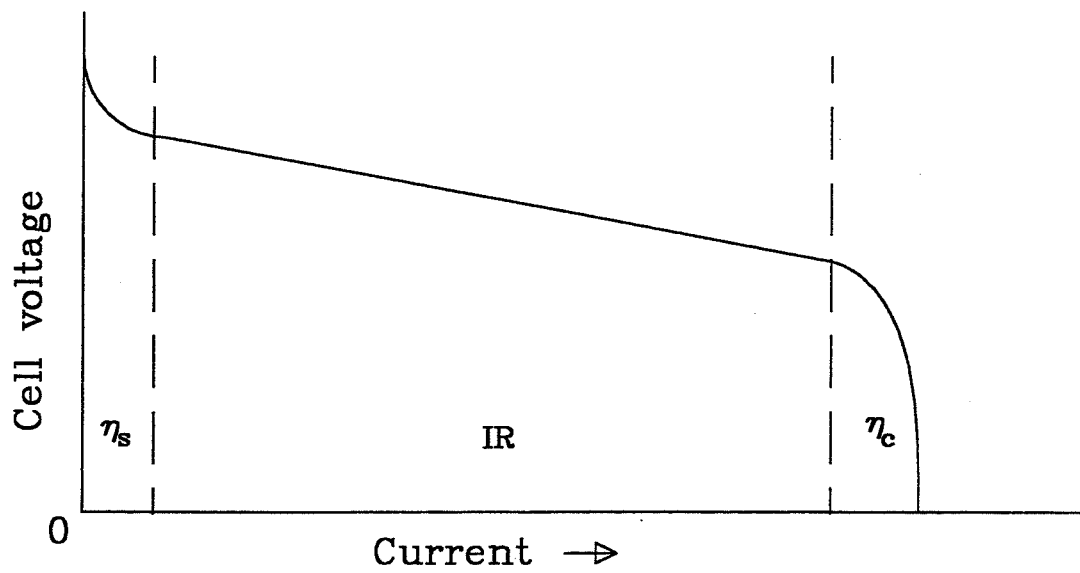
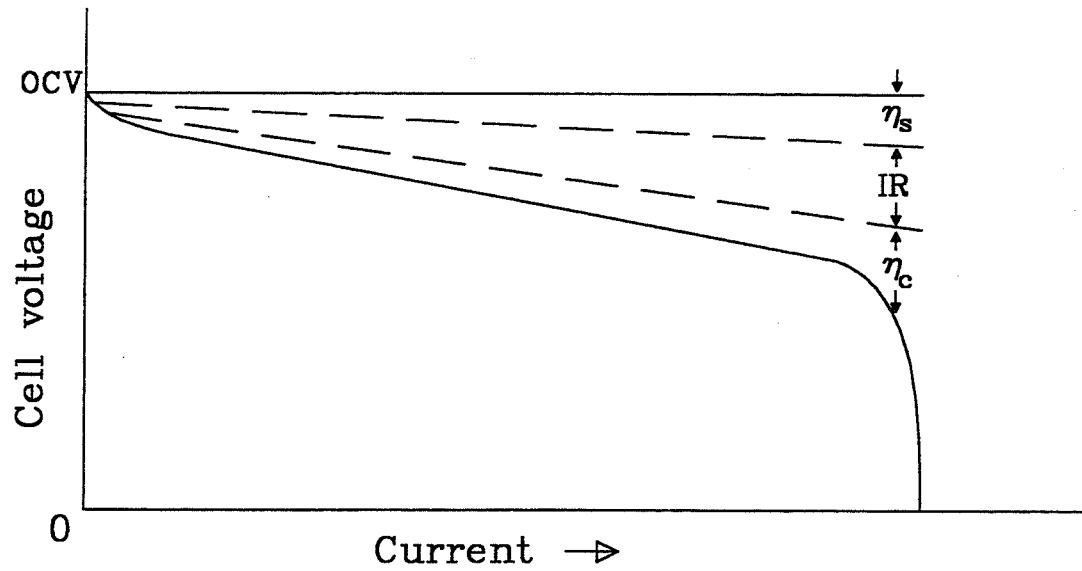
$$i = f(\eta_s, c_i) + C \frac{d\eta_s}{dt}$$

The effective capacitance C_s (Stern capacitor) of the double layer structure per the equation:

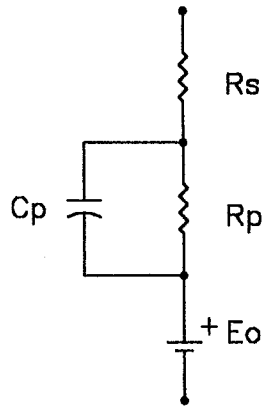
$$\frac{1}{C_s} = \frac{1}{C_h} + \frac{1}{C_{gc}}$$

Important concepts

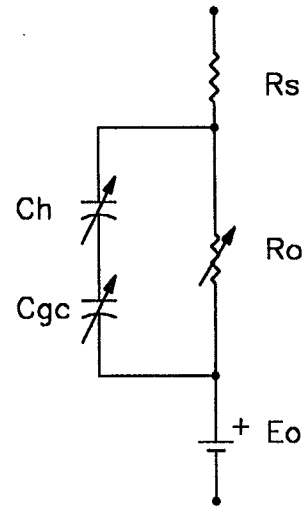
- **Tafel equation** shows the exponential relationship between current and activation overpotential.
- **Ions** respond exponentially to the application of DC currents.
- **Exchange current** is the measure of freedom from kinetic limitations.
- **Overpotentials** (polarization) act to impede the electric field that is driving the reaction rate.



Two views of discharge polarization.

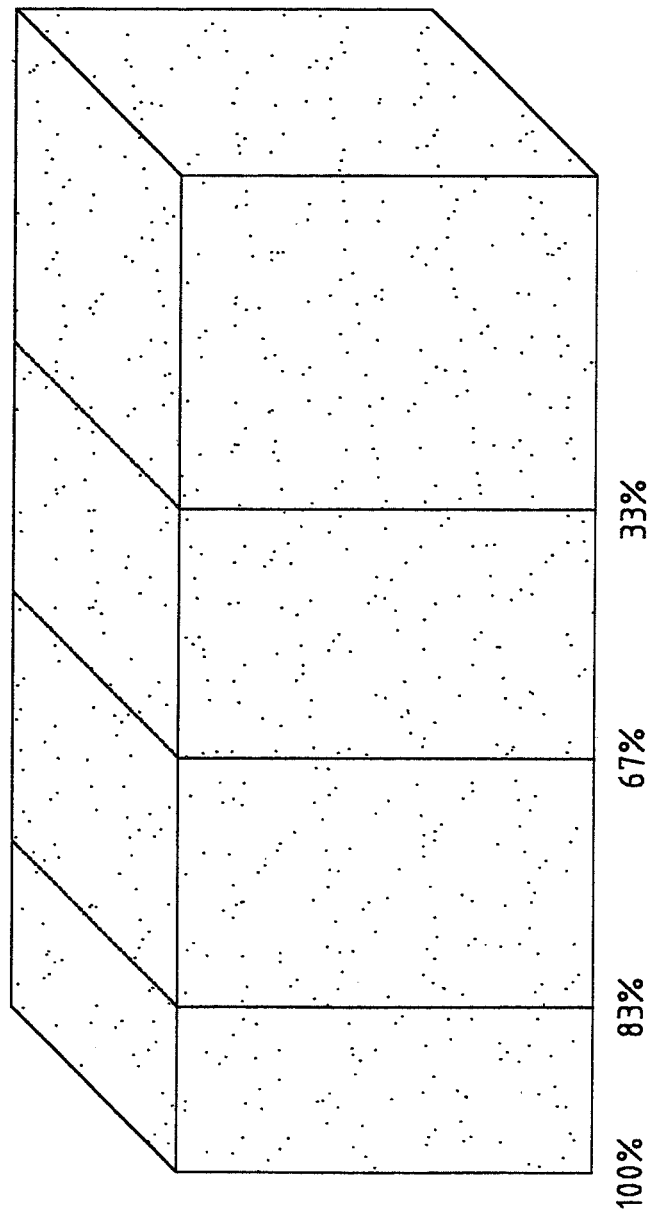
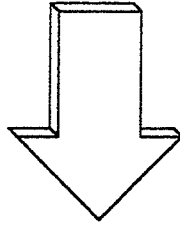


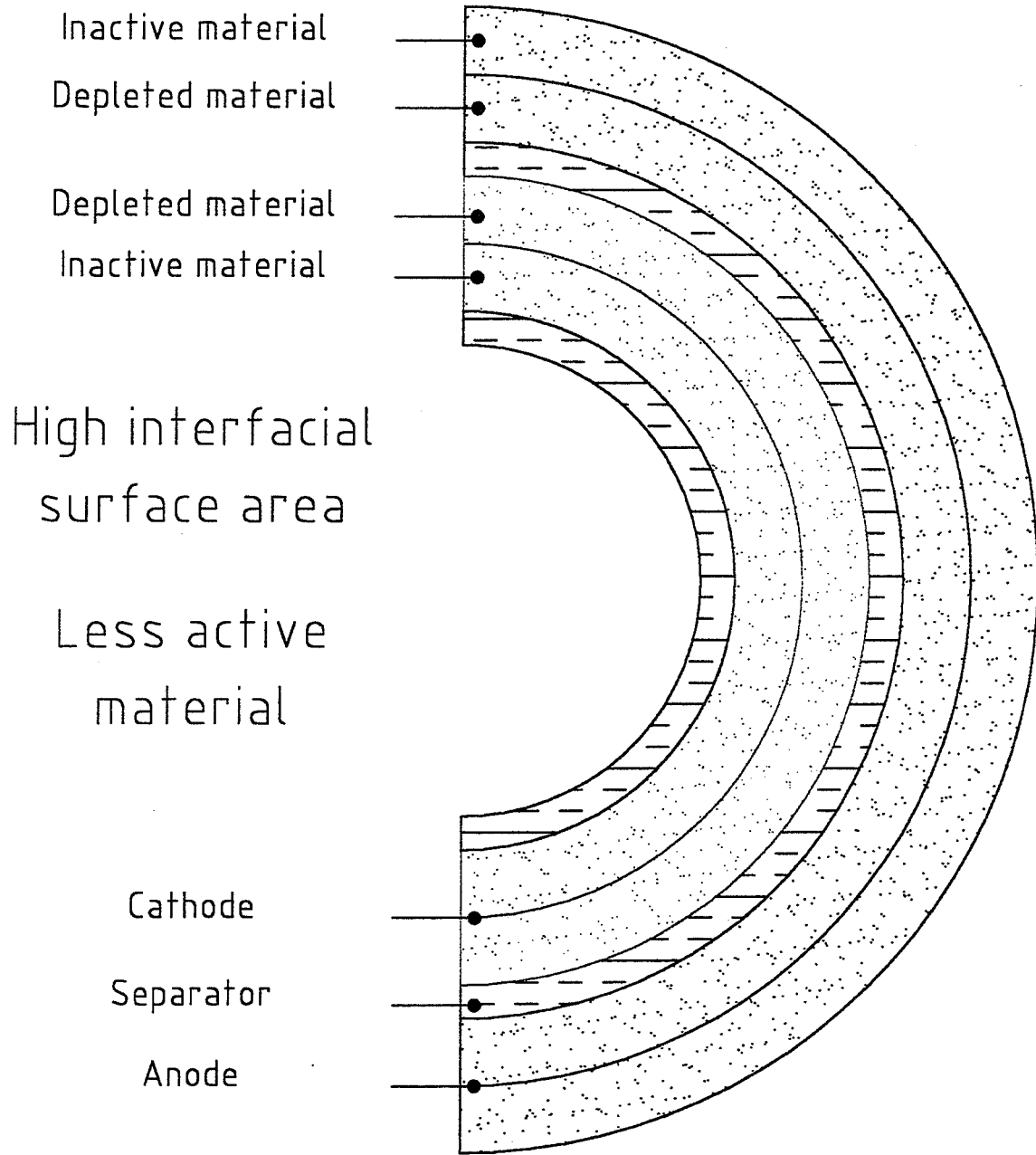
Simplistic



Realistic

Equivalent Circuit Diagrams – Electrochemical cell



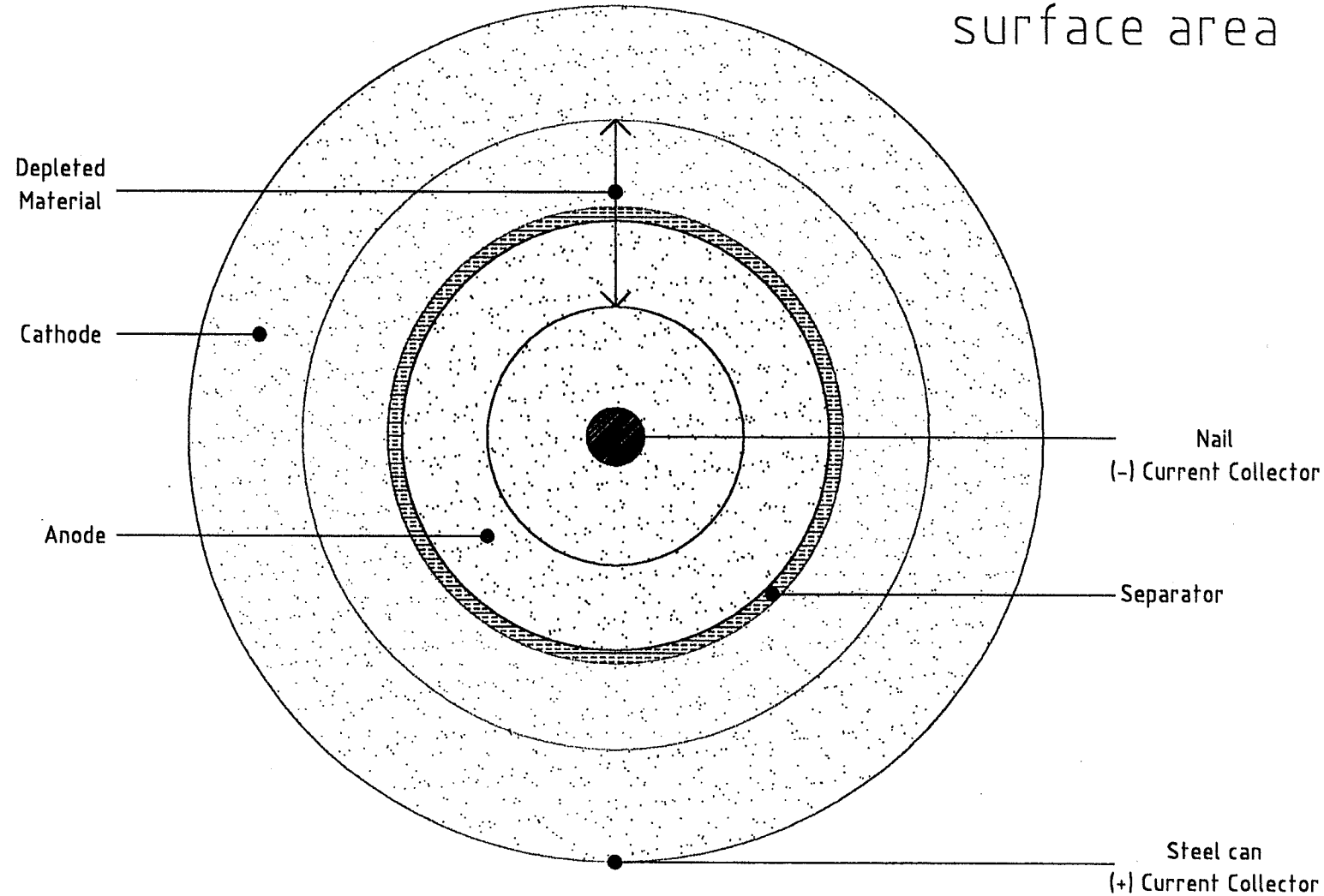


Cross-sectional view of spiral wound cell

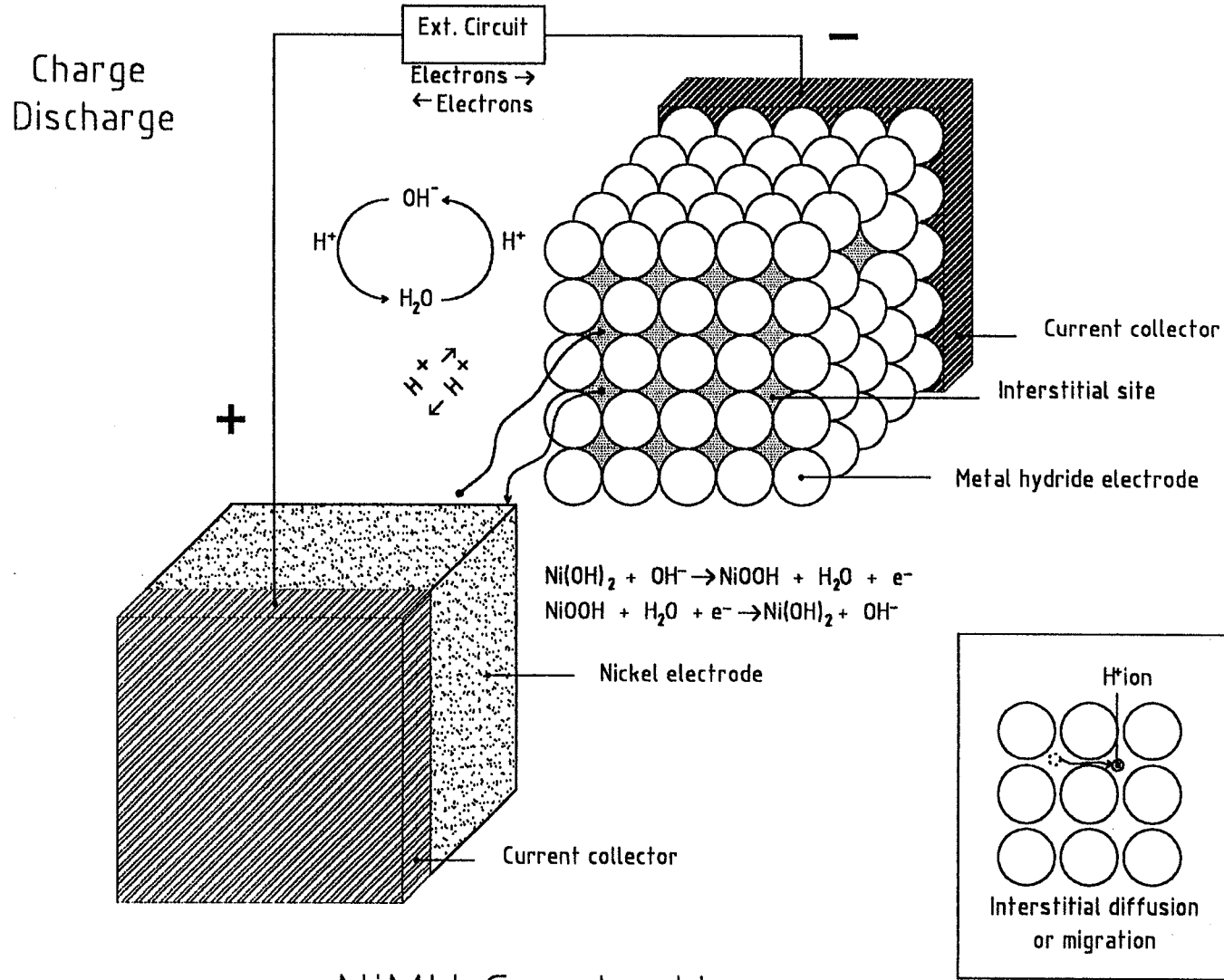
Large surface area

Large material mass

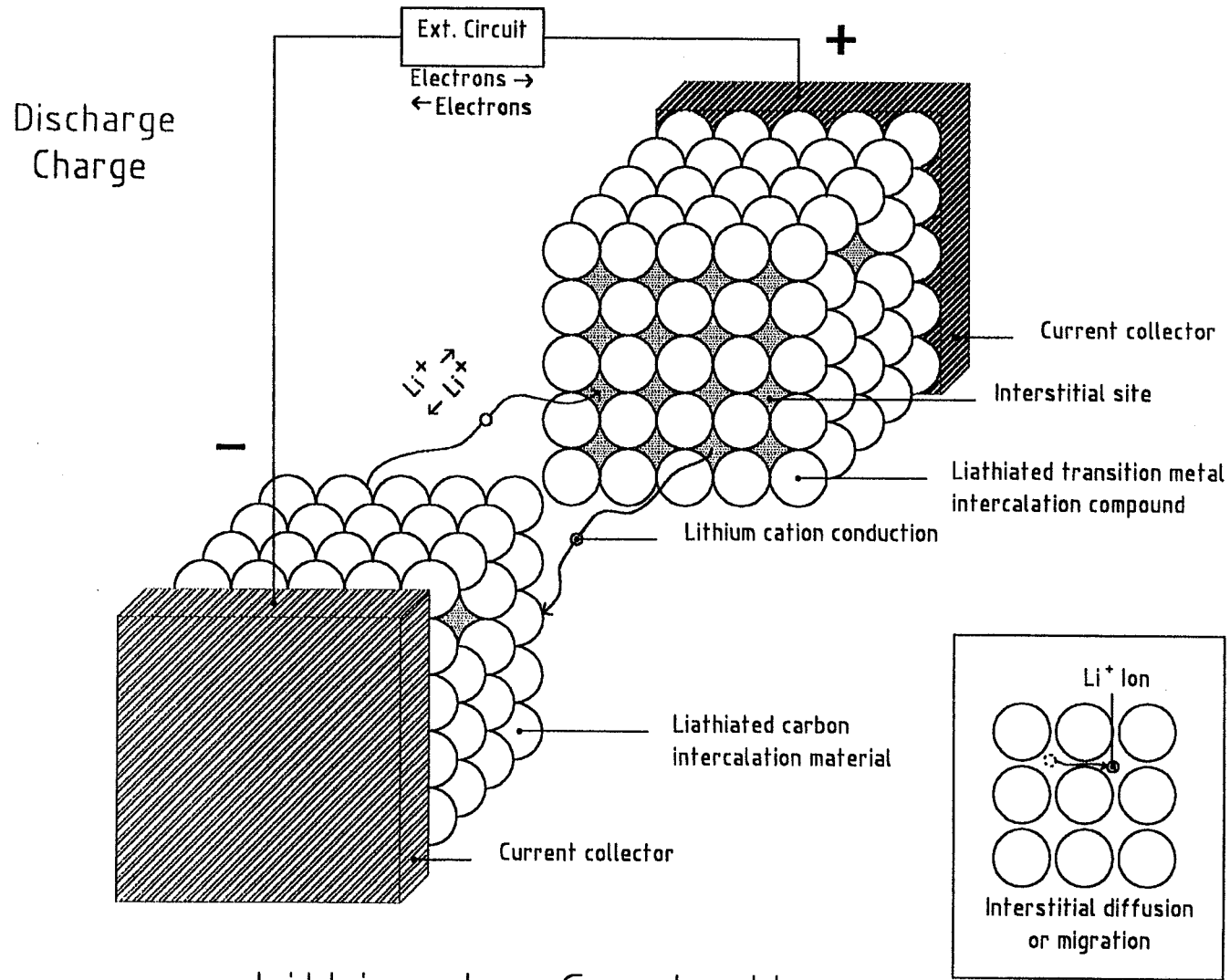
Small interfacial surface area



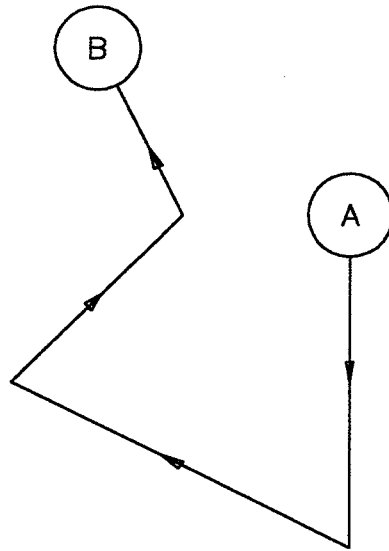
Cross-sectional view of a battery



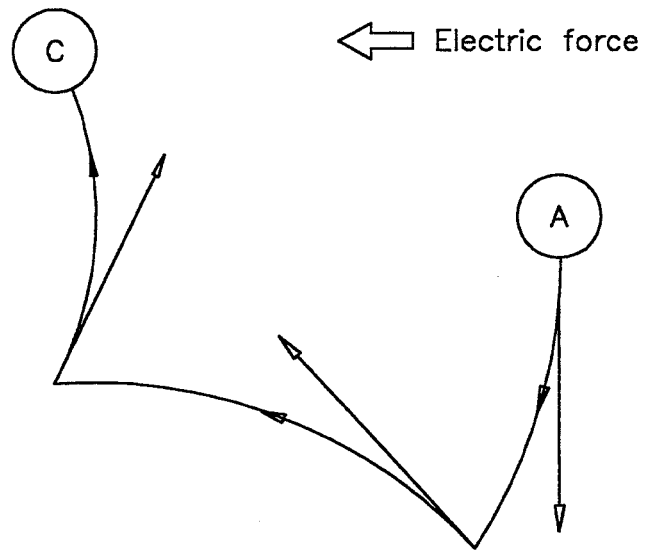
NiMH Conduction



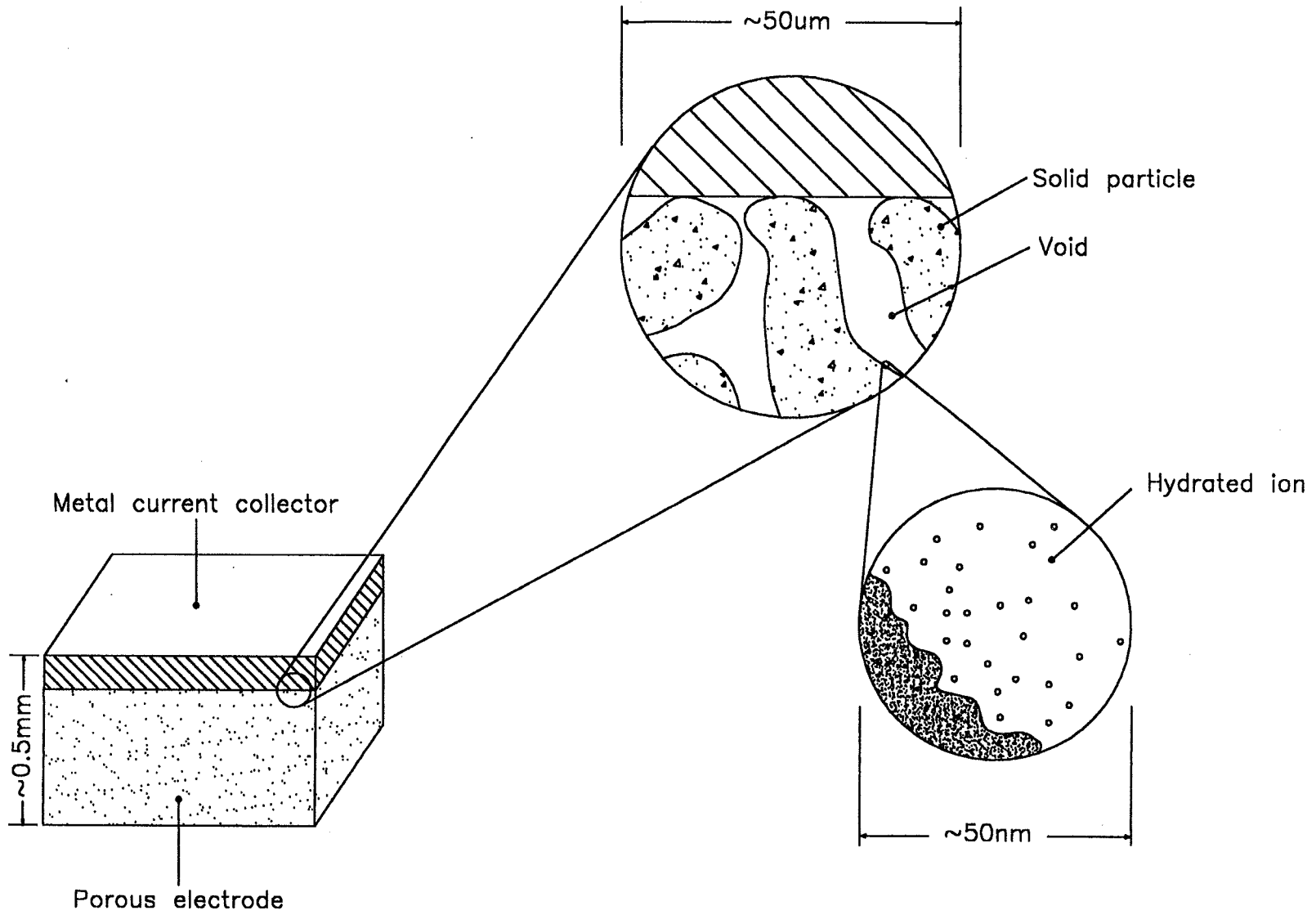
Lithium Ion Conduction



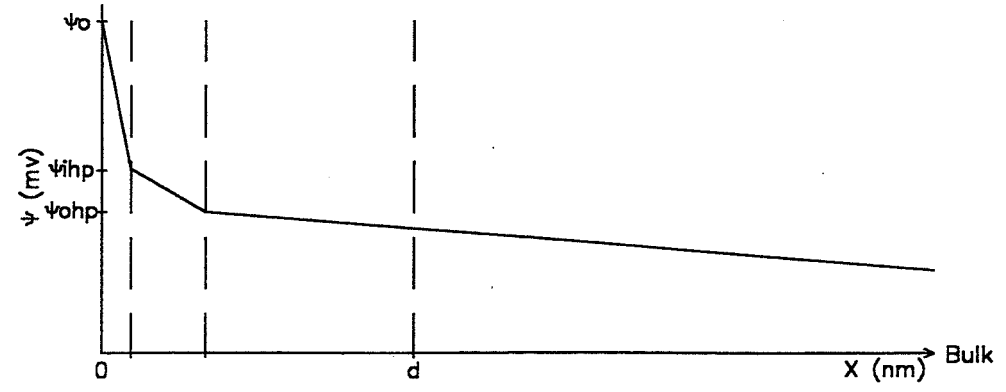
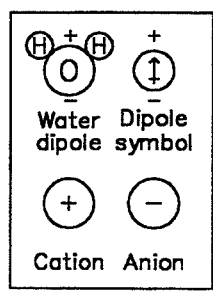
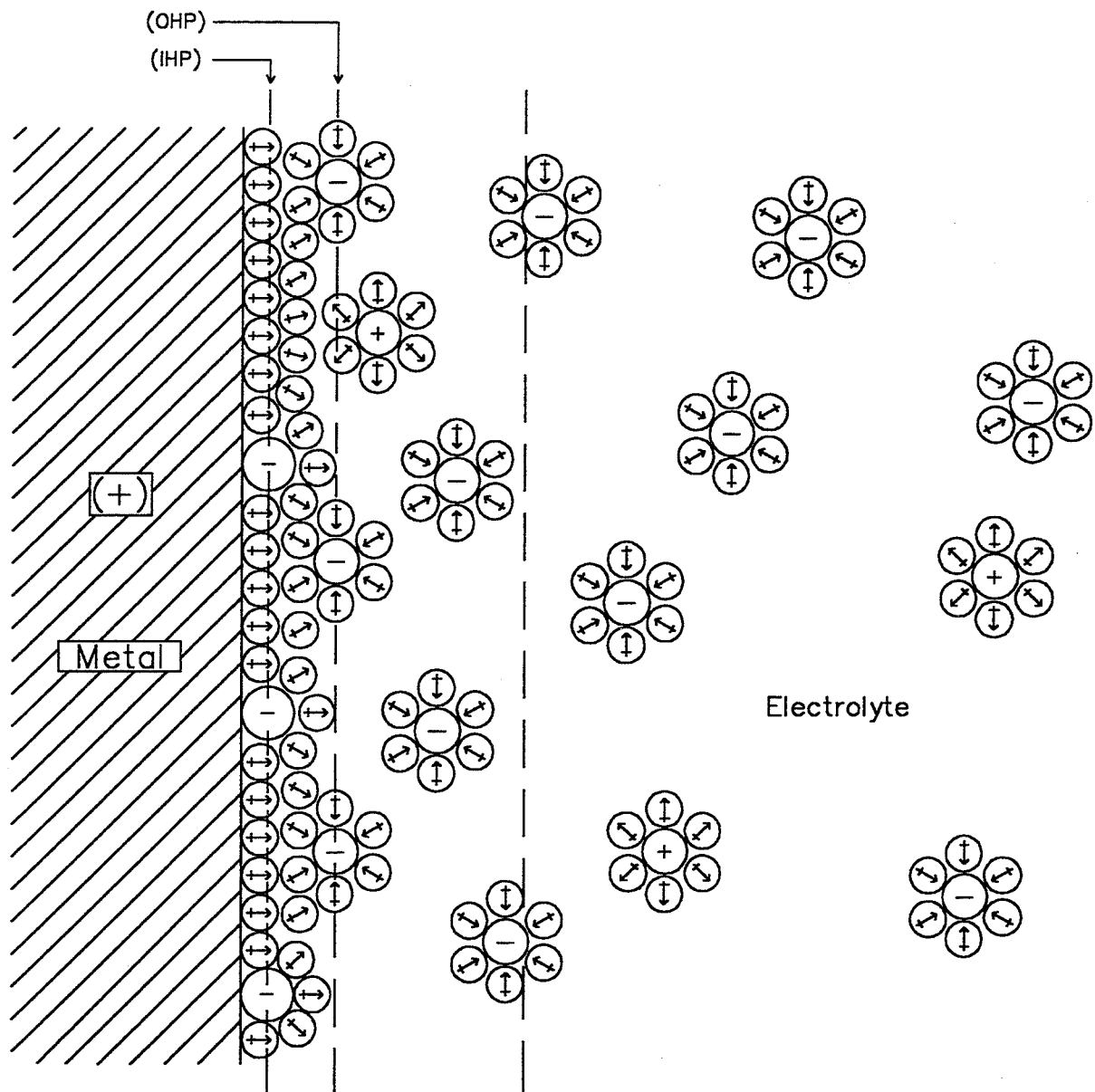
Random movement of particle with no electric field applied



Random movement of particle under influence of a DC electric field.



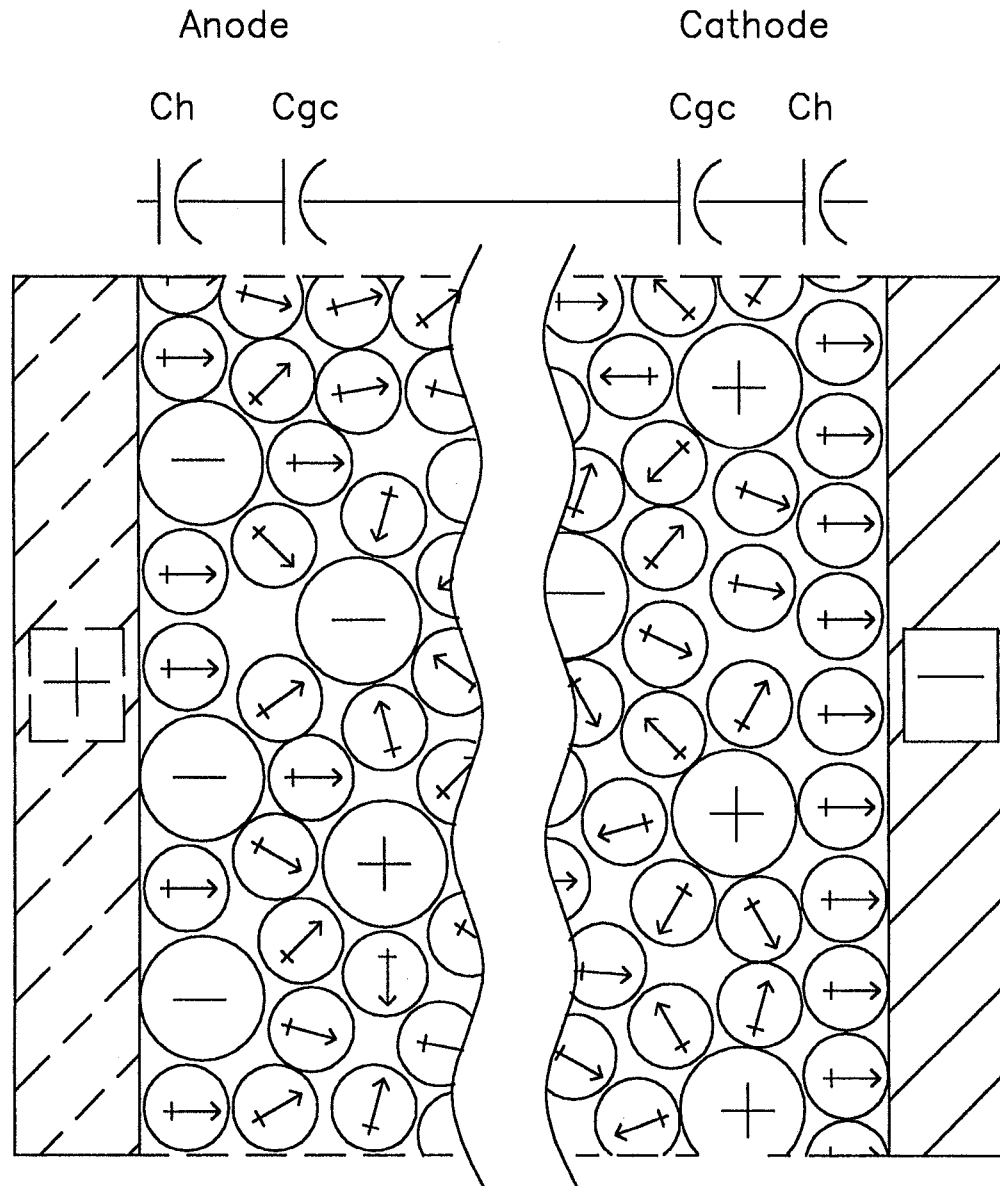
POROUS ELECTRODE



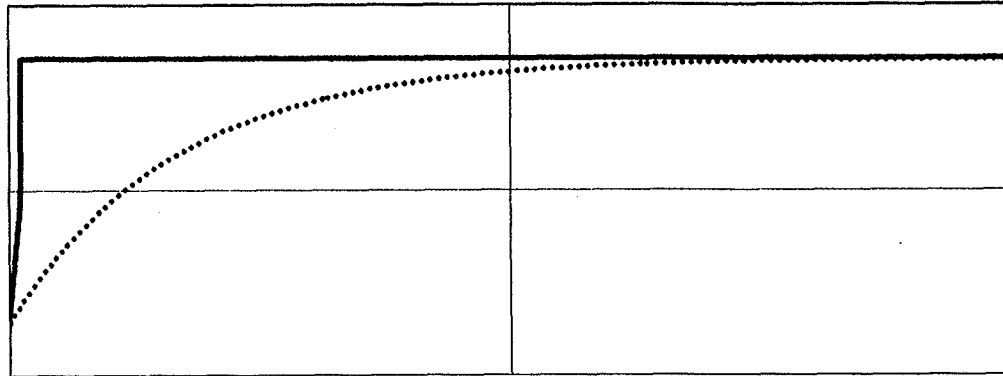
Dynamic nature of the electrical double layer

Electrical Double Layer (EDL)

- IHP on the order of 1 nm.
- OHP on the order of 3 nm.
- Typical capacitance $10\mu\text{F}/\text{cm}^2$ to $50\mu\text{F}/\text{cm}^2$.
- 100 mV across 1 nm yields 100×10^6 V/m.
- The potential is a kinetic resistance.
- Outside the Helmholtz layer the reactant species are too distant from surface to react.

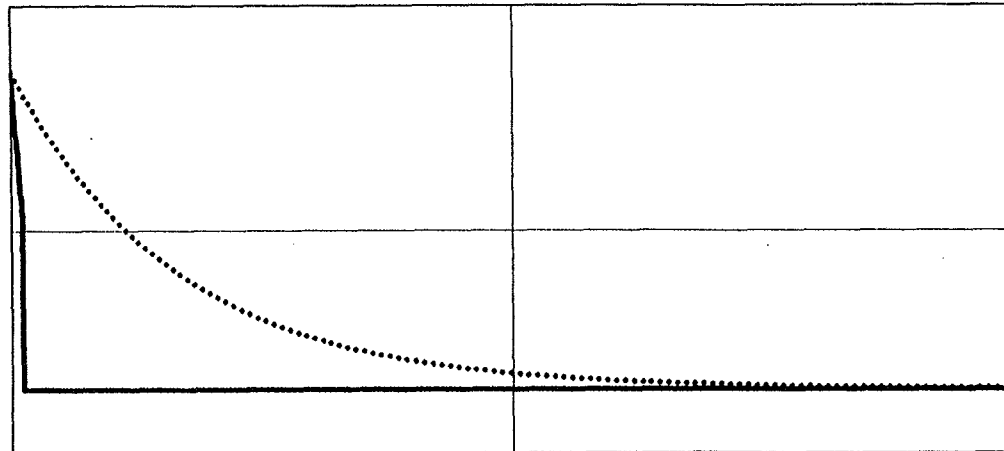


Electrical double layer showing effective capacitance.



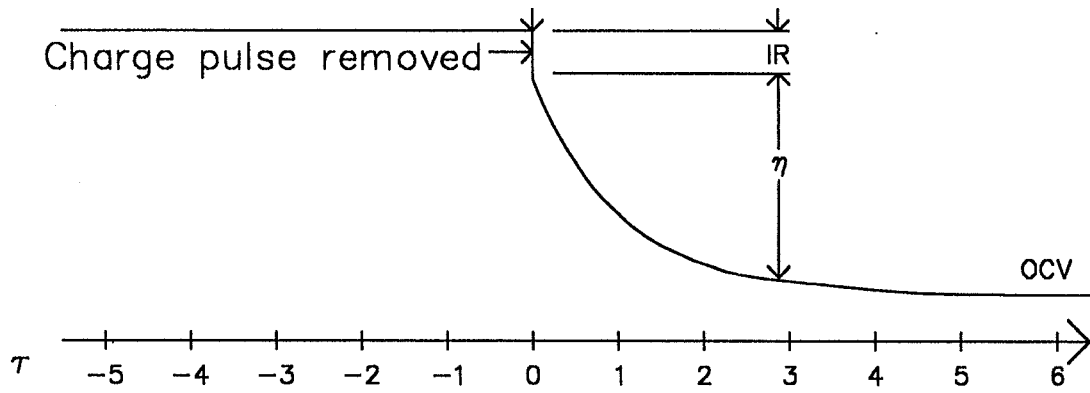
— Current
..... ions

Charge pulse



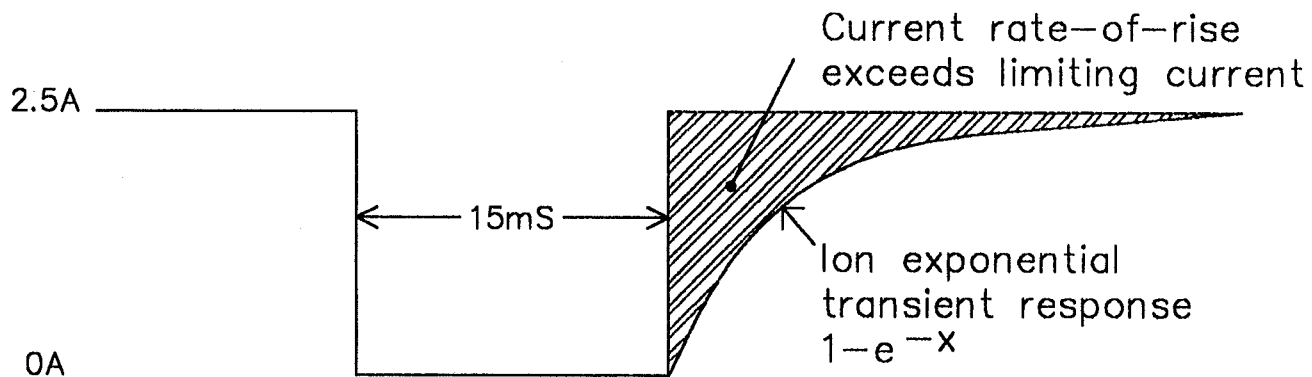
— Current
..... ions

Depolarization pulse

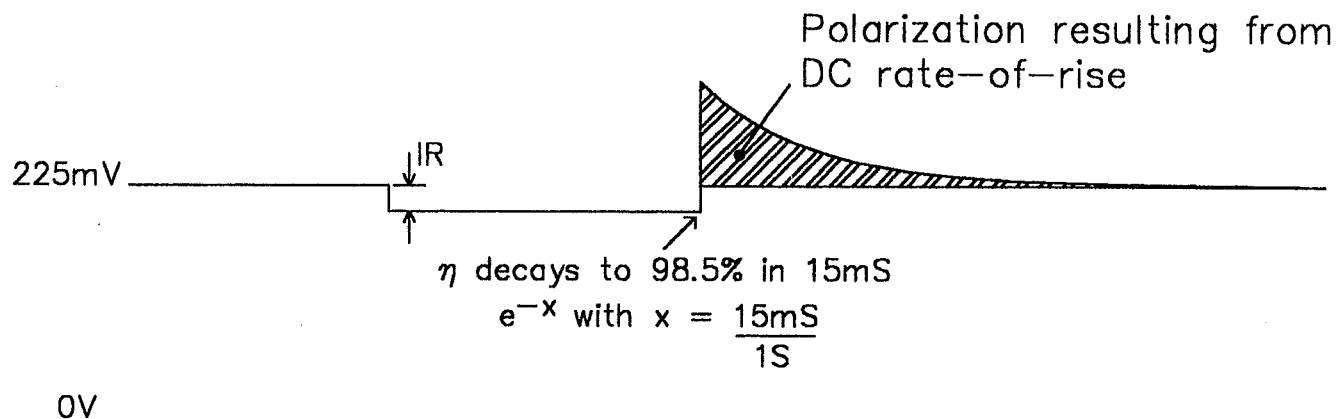


τ	0	1	2	3	4	5	6
η	100%	36.8%	13.5%	5%	1.8%	0.7%	0
Field Strength ⊕ $\eta = 100\text{mV}$	$100 \times 10^6\text{V/m}$	$36.8 \times 10^6\text{V/m}$	$27 \times 10^6\text{V/m}$	$5 \times 10^6\text{V/m}$	$1.8 \times 10^6\text{V/m}$	$0.7 \times 10^6\text{V/m}$	0
Field Strength ⊕ $\eta = 300\text{mV}$	$300 \times 10^6\text{V/m}$	$110 \times 10^6\text{V/m}$	$40.5 \times 10^6\text{V/m}$	$15 \times 10^6\text{V/m}$	$5.4 \times 10^6\text{V/m}$	$2.1 \times 10^6\text{V/m}$	0

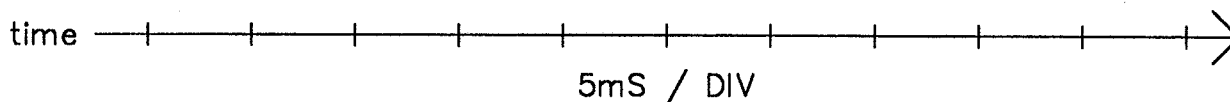
EDL (IHP) field strength based on η



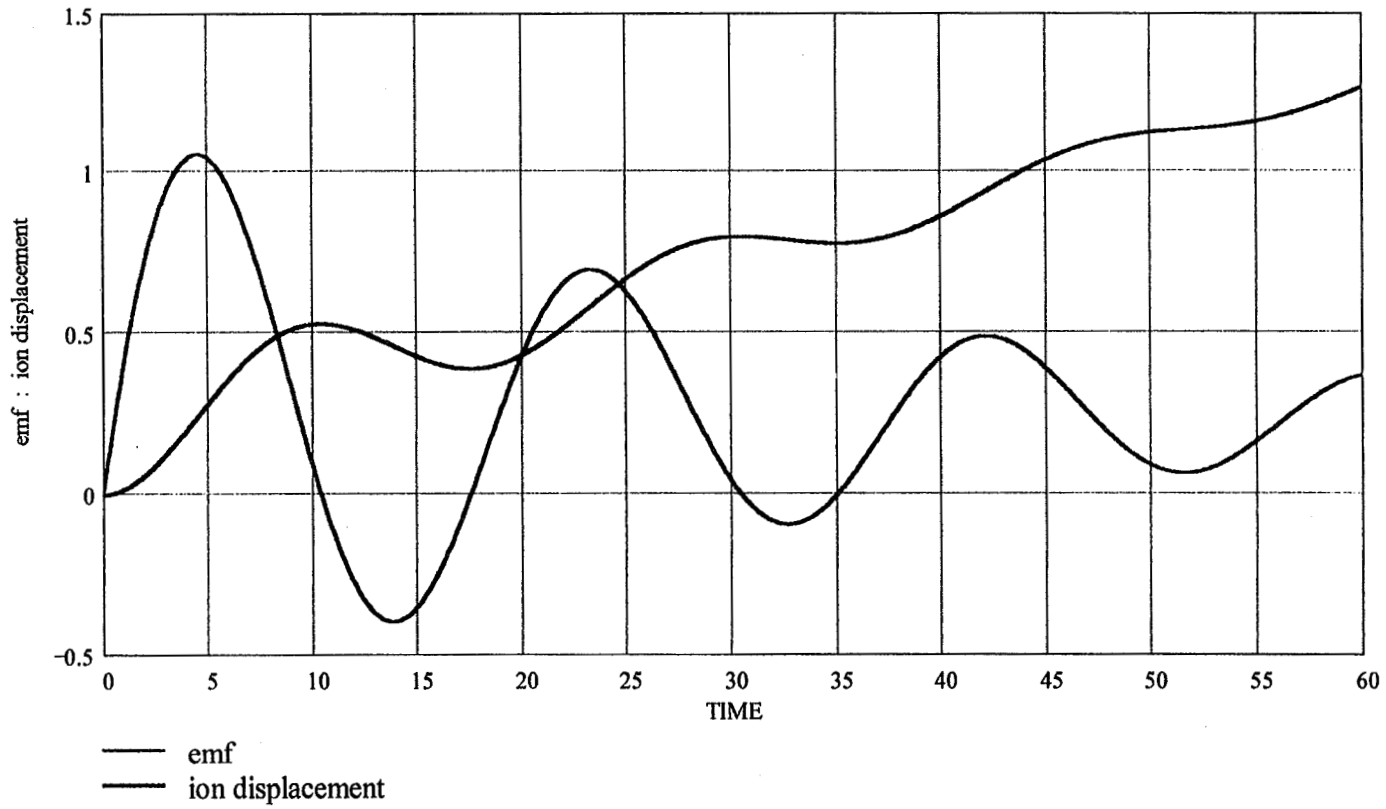
1 second charge pulse with 15mS depolarization pulse



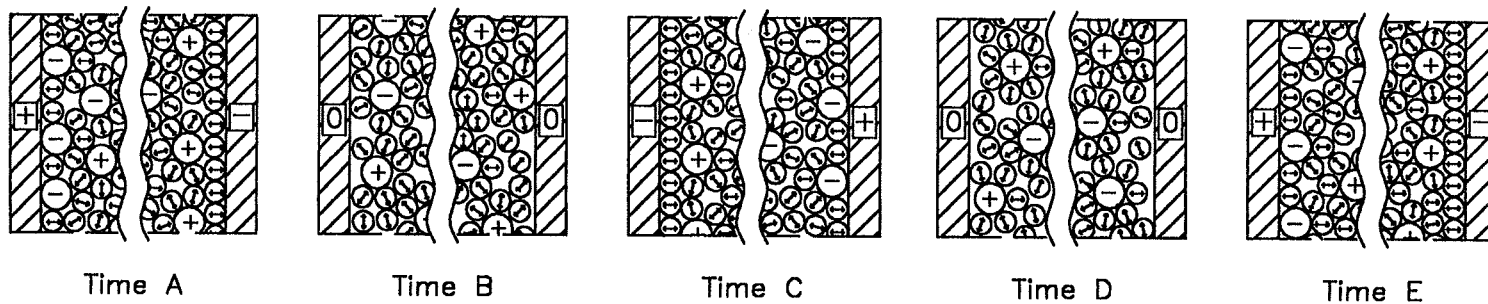
EDL voltage caused by the charge current



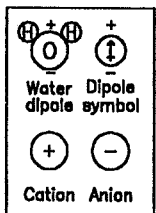
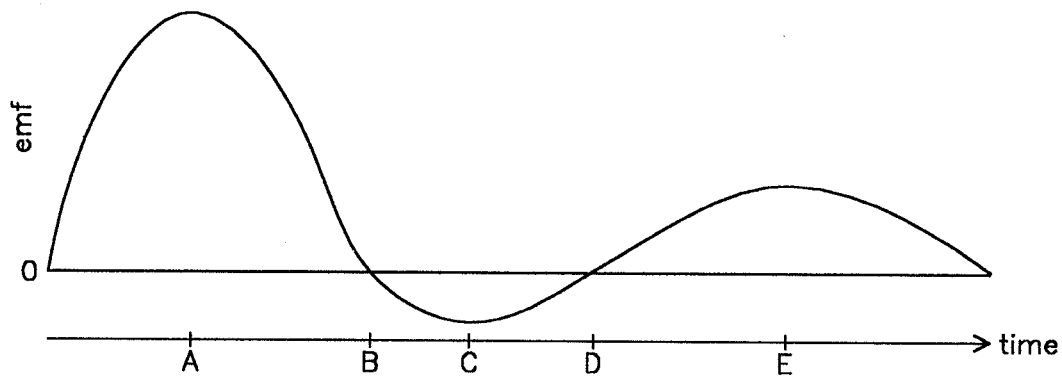
EDL with 1 second time constant



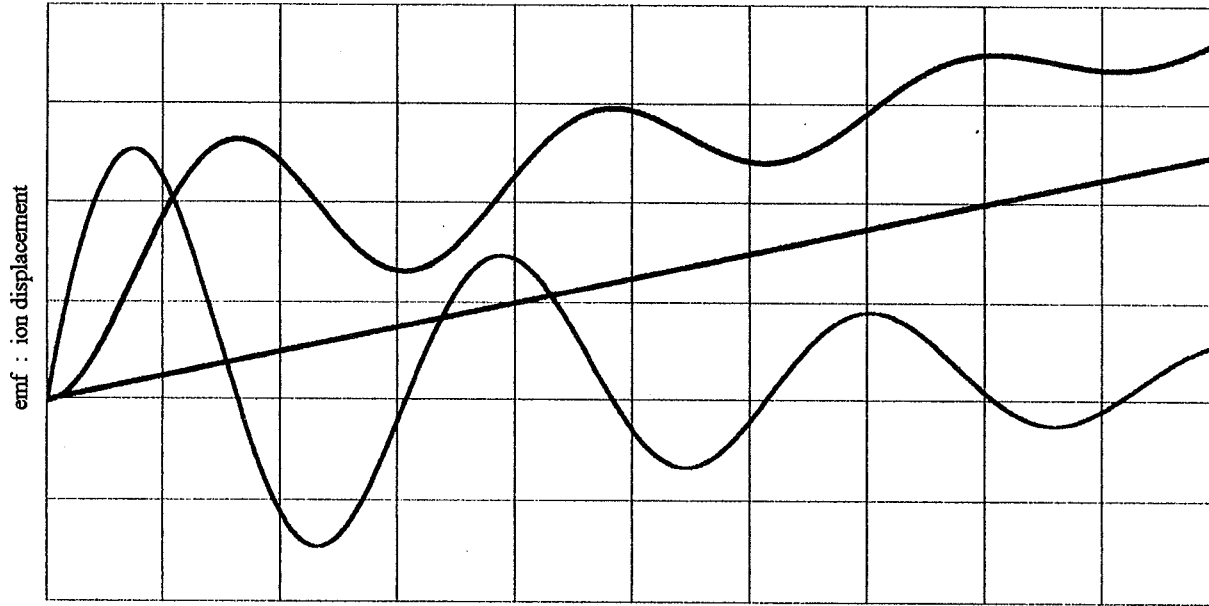
Ideal ECpulseTM waveform



Electrical double layer at each time interval

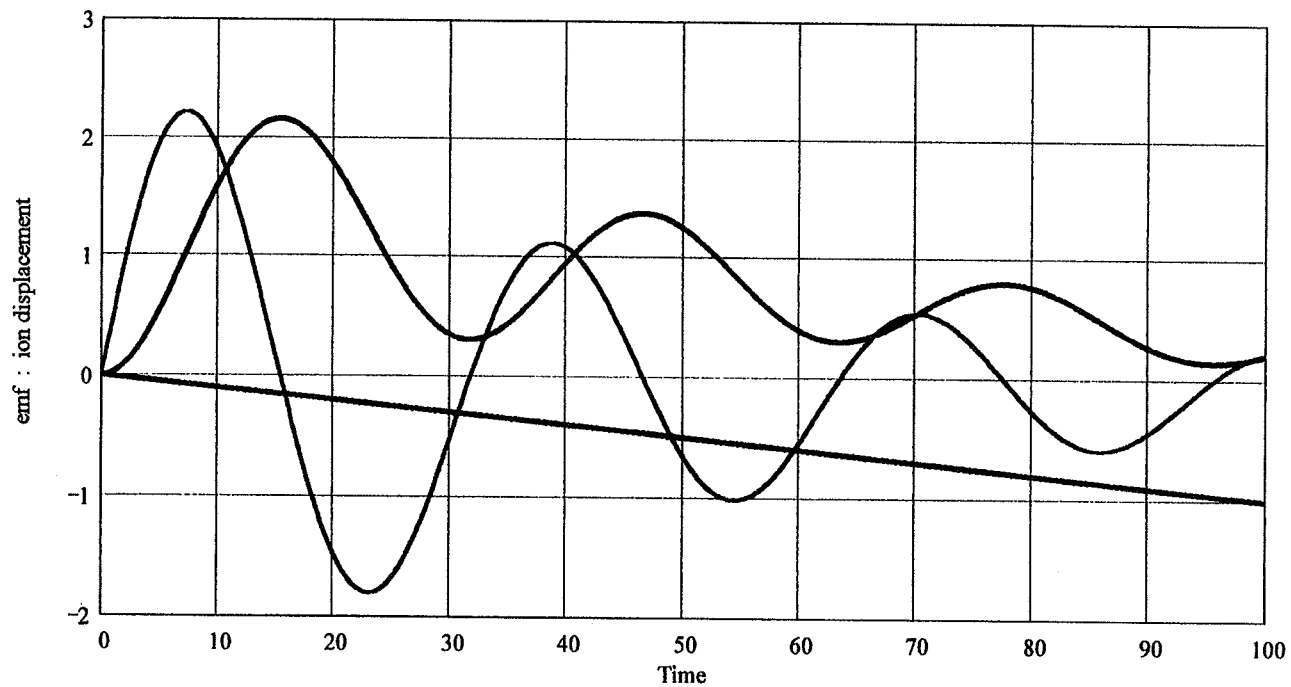


Electrical double layer reversal with ECpulseTM.



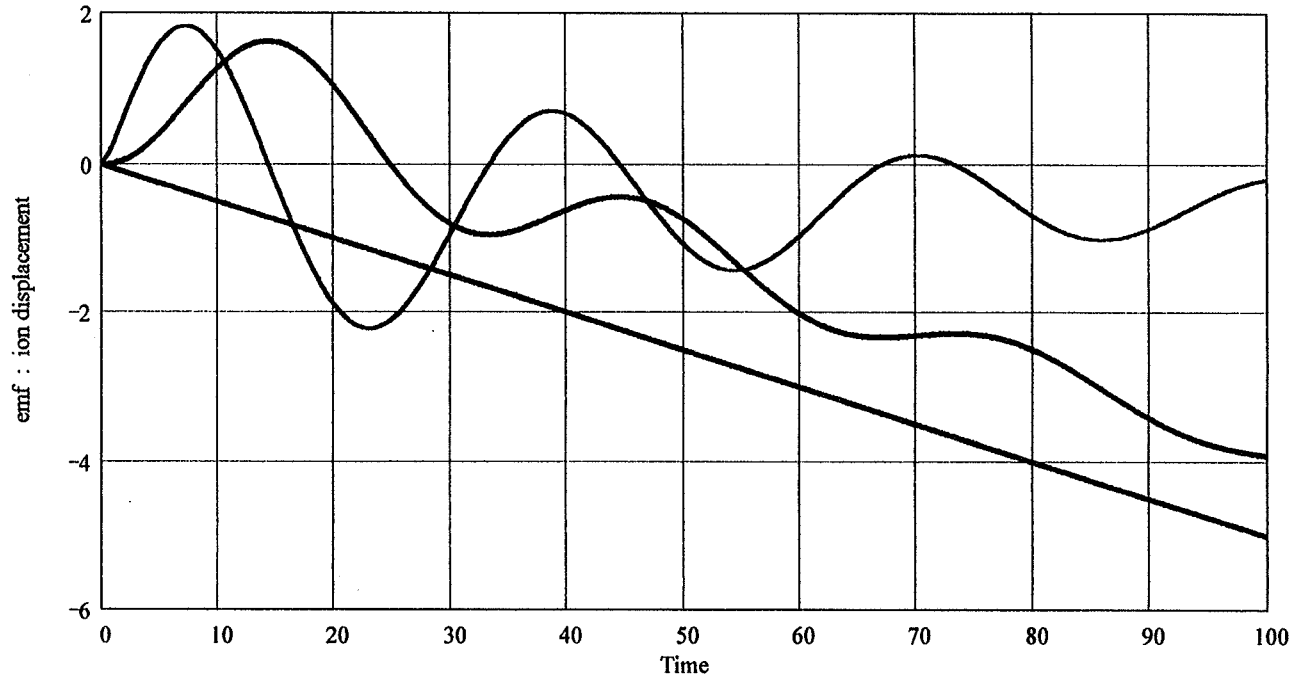
- ECpulseTM EMF
- ECpulseTM ion displacement
- DC ion displacement - PRIOR ART

ECpulseTM versus DC



- ECpulseTM EMF w/ -0.1 A DC offset
- ECpulseTM ion displacement
- DC ion displacement w/ -0.1A DC load

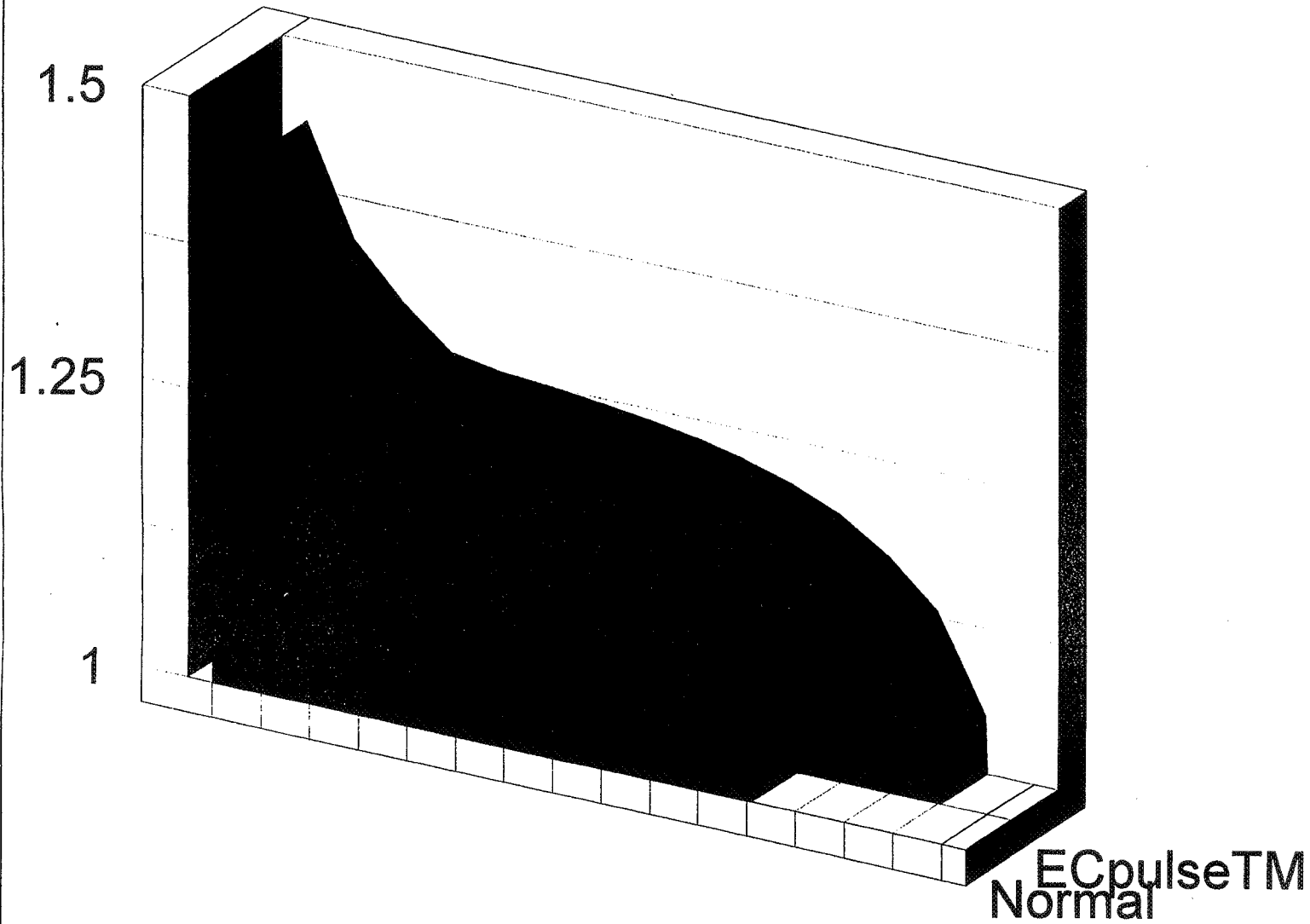
ECpulseTM versus DC

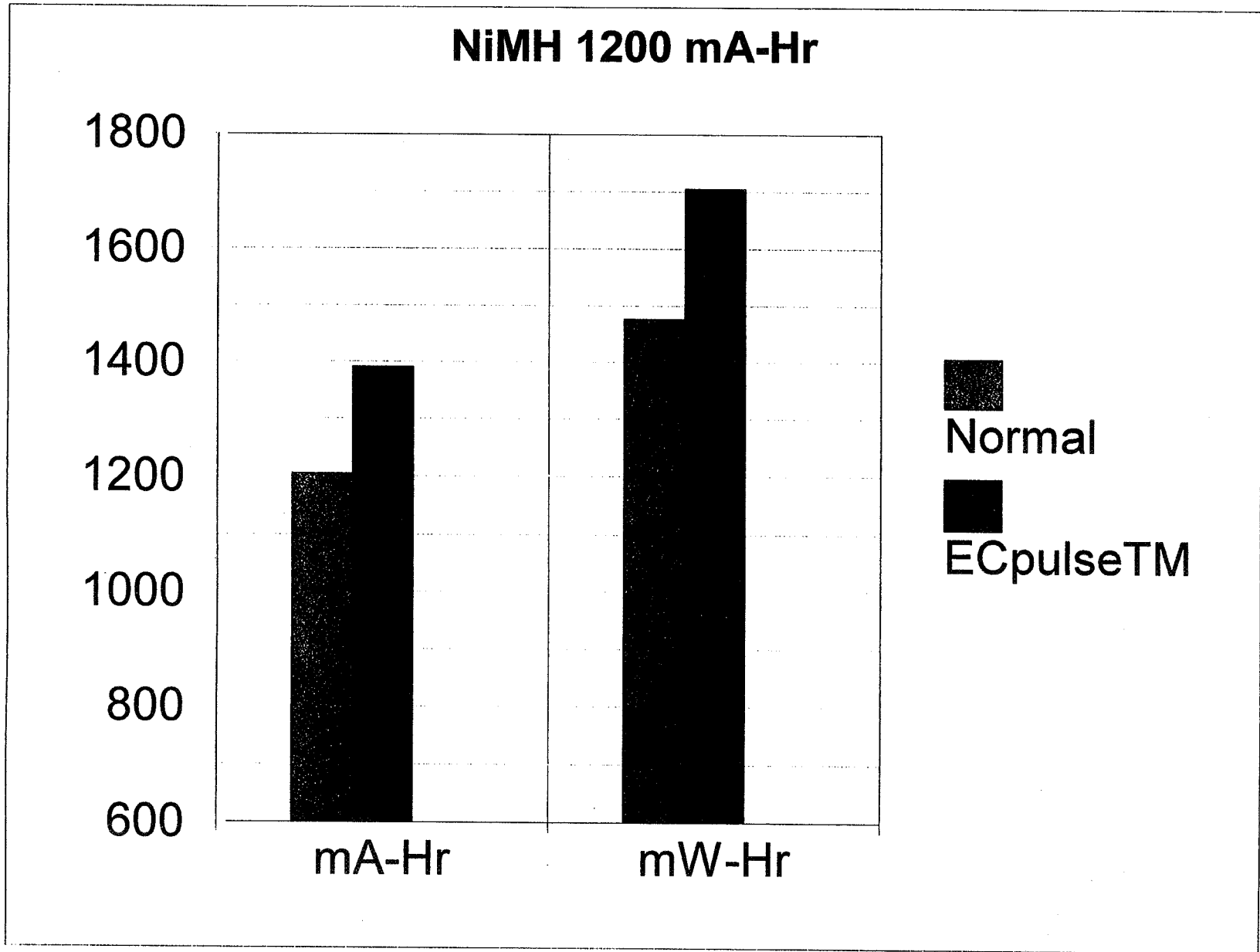


- ECpulseTM EMF w/ -0.5 A DC offset
- ECpulseTM ion displacement
- DC ion displacement w/ -0.5 A DC load

ECpulseTM versus DC

NiMH 1200 mA-Hr Discharge





Advanced Lithium-Ion ENergy Technology

**Ricky J. Roberson
Greg Tyler**

Huntsville Integrated Voltaic Equipment

(HIVE)

HIVE Goals:

1. Develop modular, scalable Li-Ion support technology applicable to any aerospace mission:

- **low to high voltages**
- **low to high currents**
- **high reliability/redundancy**

2. Produce an integrated prototype Li-Ion power supply to meet NASA ProSEDS mission requirements:

- **120 V DC, 3 Ah nominal**

3. Implement Li-Ion technology in another important aerospace project:

- **YOURS**

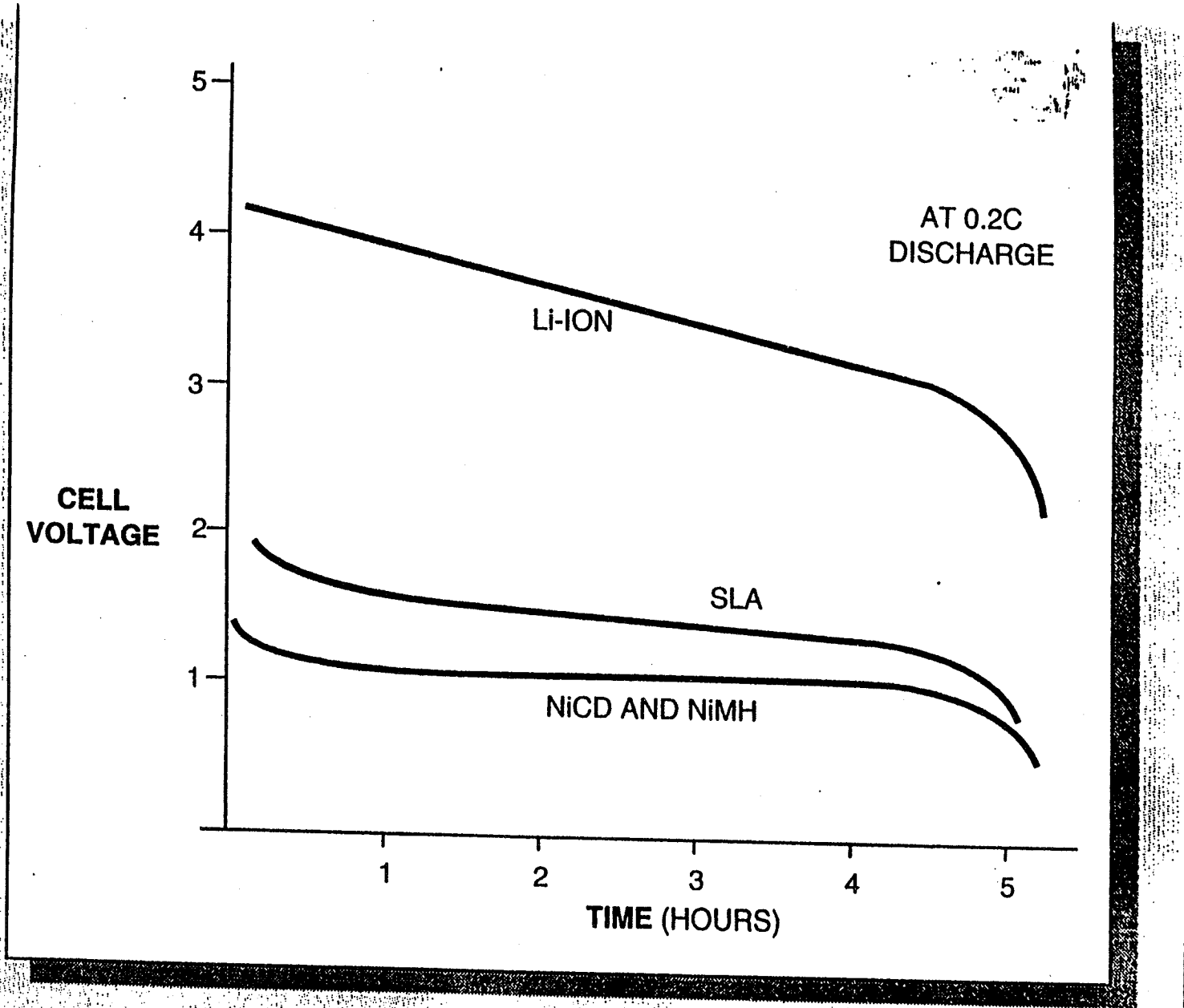
TABLE 1—TYPICAL BATTERY-TYPE CHARACTERISTICS¹

Battery characteristics	SLA	NiCd	NiMH	Li-Ion
Energy density (Whr/kg)	30	40	60	90
Energy density (Whr/l)	60	100	140	210
Operating cell voltage (V)	2.0	1.2	1.2	3.6 (average)
Discharge profile	Slightly sloping	Flat	Flat	Sloping
No. of recharge cycles ²	500	1000	800	1000
Self-discharge (%/month)	3	15	20	6
Internal resistance	Low	Lowest	Moderate	Highest
Discharge rate (C) ³	<5	<10	<3	<2

¹ These numbers are representative and may differ because of advances in technology and vendor implementations.

² Defined as the battery's achieving 80% of its initial charge capacity on recharge.

³ C=nominal capacity.

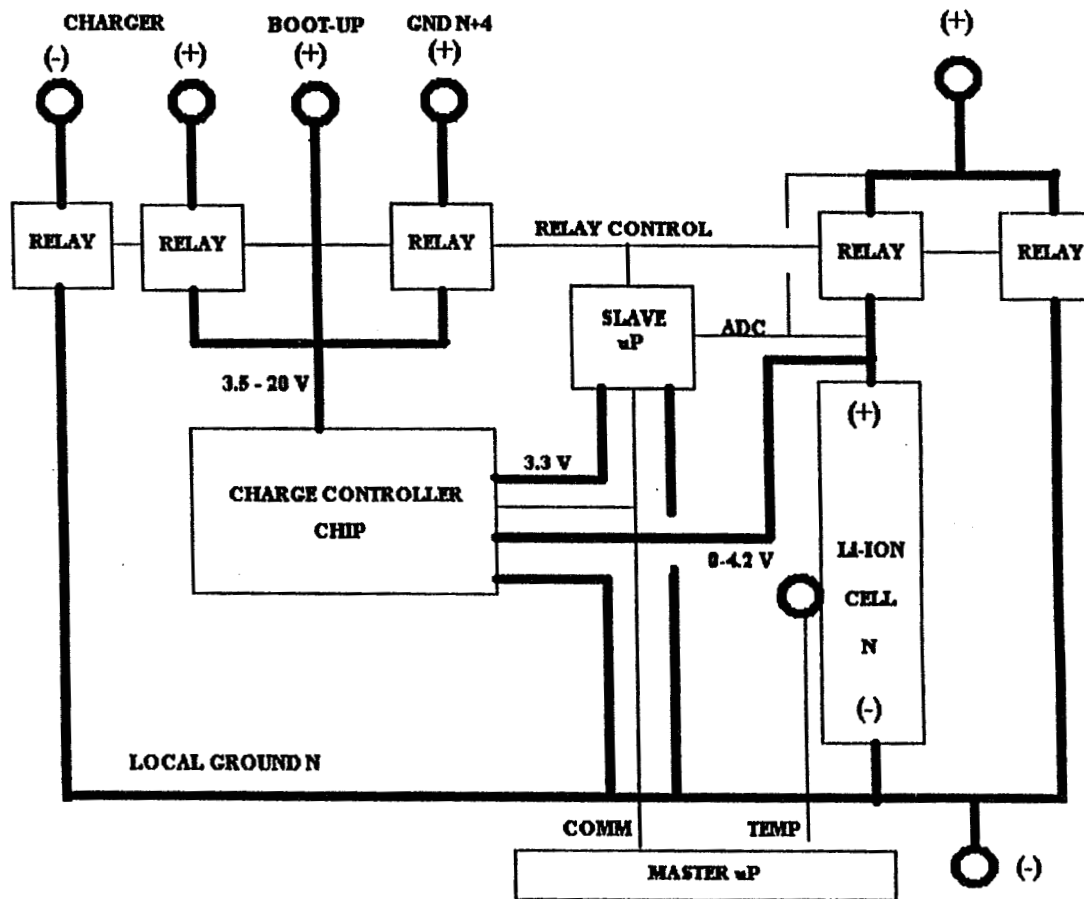


Each of the four major battery chemistries has a different discharge curve (NiCd and NiMH are similar) at a discharge rate of 0.2C

HIVE Li-Ion Electronic Integration Approach:

- **Use off-the-shelf 18650-size Li-Ion cells**
- **Avoid constant-voltage regulators to minimize capacity waste**
- **Stack Li-Ion cells to achieve required high voltages**
- **Isolate Li-Ion cells in stack from each other with solid-state relays (SSRs)**
- **Provide SSR-controlled alternate path for current flow around any given cell**
- **Implement microprocessor voltage/temp monitoring and SSR switching control**
- **Power local cell control electronics from upstream cells in stack**
- **Utilize redundant isolated Li-Ion cells to power electronics at top of stack**
- **Switch out unneeded cells from stack for controlled system discharge**
- **Switch out all cells from stack for individual cell recharge**

HIVE Li-Ion Electronic Integration Approach:



HIVE Major Electronic Component Selection:

- **Battery Cell:** Moli Energy ICR-18650 Li-Ion
- **Temperature Sensor:** Dallas Semiconductor DS1820
- **Charger Control Chip:** Maxim MAX846A
- **Slave Microprocessor:** National Semiconductor COP8ACC
- **Relay:** International Rectifier PVN012
- **And a variety of supporting capacitors, resistors, etc.**

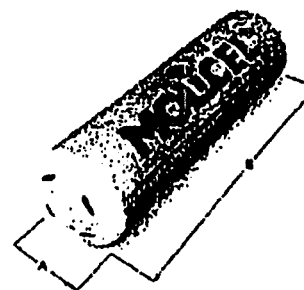
Hive Parts List:

PART	PART #		
1	LITHIUM ION BATTERY CELL	18650	
2	TEMPERATURE SENSOR	DS1820	
3	INTEGRATED CIRCUIT - BATTERY CHARGER	MAX848A	
4	MICROPROCESSOR	COP8ACC	
5	CRYSTAL - 4MHZ	X405	
6	OPTORELAY	PVN012	
7	OPTORELAY	PVN012	
8	OPTORELAY	PVN012	
9	OPTORELAY	PVN012	
10	OPTORELAY	PVN012	
11	TRANSISTOR	ZTX749	
12	DIODE	FR301CT1	
13	RESISTOR - POWER - 0.15 OHM 3W 1%	43F0.15	POWER
14	RESISTOR - SMT - 680 OHMS 5%	P680VCT	ZETEX
15	RESISTOR - SMT - 400K 1%	P402KFCT	VSET
16	RESISTOR - SMT - 1M 5%	P1.0MVCT	
17	RESISTOR - SMT - 10K 5%	P10KVCT	
18	RESISTOR - SIP - 8 PIN ISO 10K 2%	750-83-R10K	RESET
19	RESISTOR - SIP - 10 PIN ISO 560 OHM 2%	750-103-R560	ISET
20	RESISTOR - SIP - 6 PIN ISO 1M 2%	750-83-R1MEG	LED
21	RESISTOR - SIP - 6 PIN ISO 180K 2%	750-83-R180K	ADC 20-3
22	RESISTOR - SIP - 10 PIN BUS 100K 2%	750-101-R100K	ADC 5-2
23	CAPACITOR -		ADC
24	CAPACITOR -		VSET
25	CAPACITOR - 4.7UF 16V TANT	P2036	ISET
26	CAPACITOR - 4.7UF 35V TANT	P2063	BATT
27	CAPACITOR - 10UF 16V TANT	P2038	COP8
28	CAPACITOR - 22UF 35V TANT	P2101	RESET
29	CAPACITOR - 0.1UF CERAMIC	P4887	MAX
30	CAPACITOR - 0.01UF CERAMIC	P4904	CS+
31	CAPACITOR - 0.01UF CERAMIC	P4904	ZETEX
32	CAPACITOR - 0.01UF CERAMIC	P4904	CCI
33	CAPACITOR - 33PF CERAMIC	P4843	CCV
34	CAPACITOR - 33PF CERAMIC	P4843	XTAL
35	HEADER-4 PIN	S1311-04	XTAL
36	HEADER-7 PIN	S1311-07	GROUND
37	CONNECTOR-4 PIN	WM3102	PWR/COMM
38	CONNECTOR-7 PIN	WM3105	GROUND
39	SOCKET		PWR/COMM

MOLICEL®PRELIMINARY
INFORMATIONPRODUCT DATA SHEET
MODEL ICR-18650
HIGH ENERGY
LITHIUM-ION RECHARGEABLE BATTERY

NOMINAL SPECIFICATIONS

Nominal Voltage	3.7 V
Capacity	1500 mAh
Energy	5.6 Wh
Weight	42 grams
Energy Density Volumetric Gravimetric	325Wh/l 132 Wh/kg



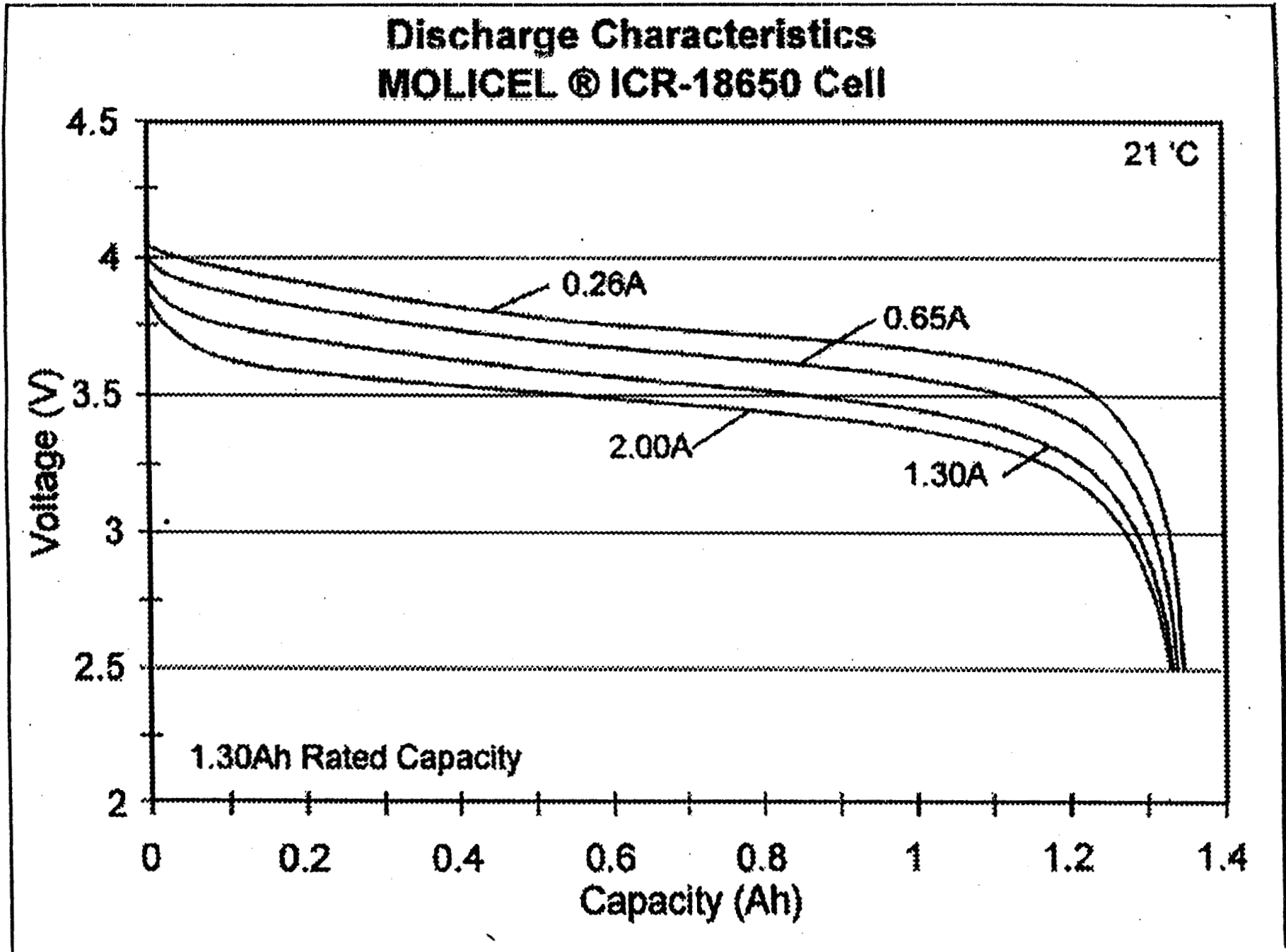
A: 18.3mm B: 65mm

OPERATING SPECIFICATIONS

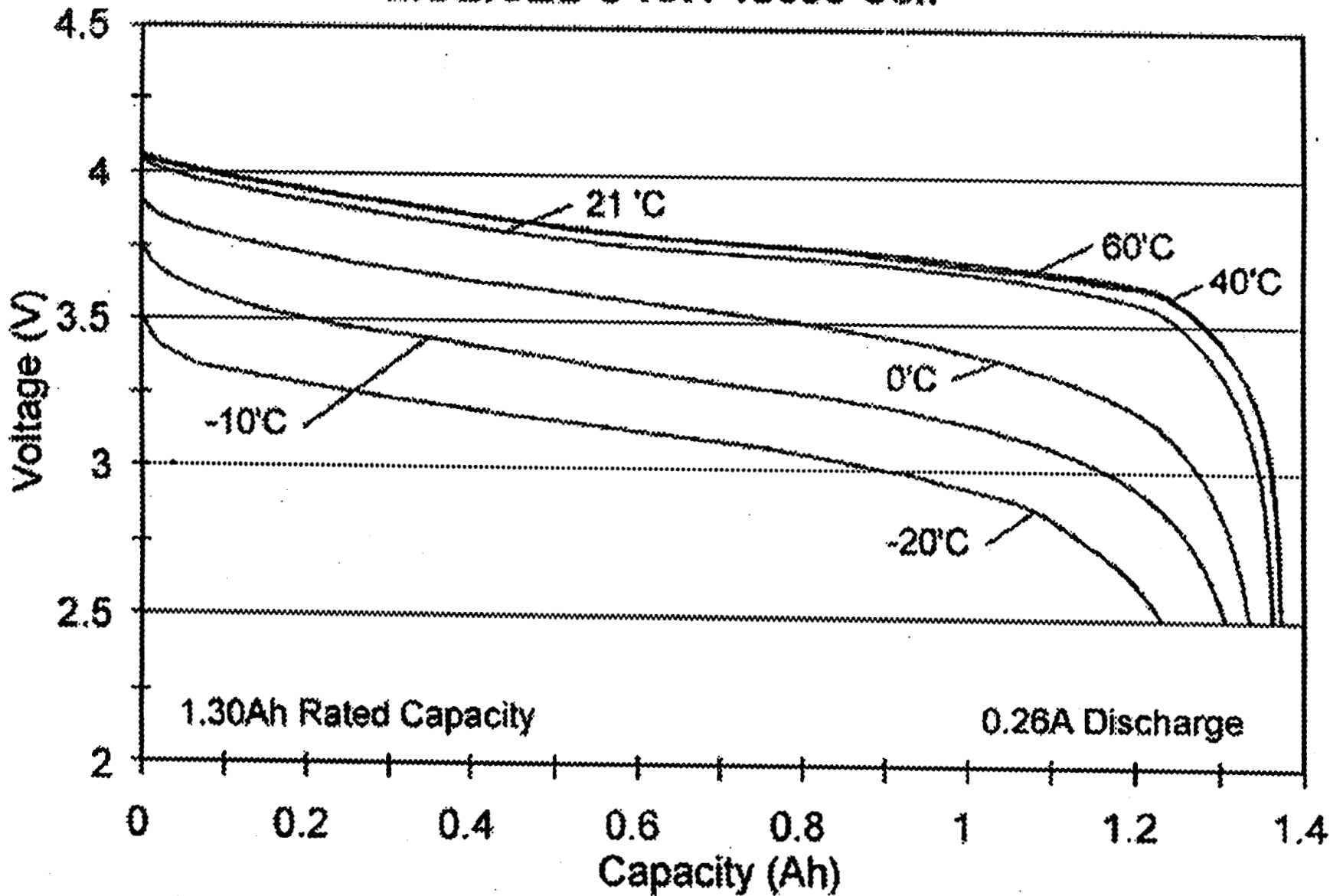
Operating Voltage	4.2 V to 3.0 V
Charge Voltage	4.2 V
Cutoff Voltage	2.5 V
Temperature Range Discharge Charge	-20°C to 60°C 0°C to 45°C
Maximum Discharge Current (Continuous)	3.0 A
Maximum Charge Current	1.5 A

STORAGE SPECIFICATIONS

Temperature Range	-20 °C to 60°C
Recommended Voltage Range	4.2 V to 2.5 V



Discharge Characteristics MOLICEL® ICR-18650 Cell



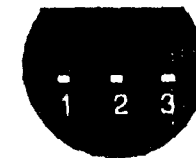
DALLAS
SEMICONDUCTOR

DS1820 1-Wire™ Digital Thermometer

FEATURES

- Unique 1-Wire™ interface requires only one port pin for communication
- Multidrop capability simplifies distributed temperature sensing applications
- Requires no external components
- Can be powered from data line
- Zero standby power required
- Measures temperatures from -55°C to $+125^{\circ}\text{C}$ in 0.5°C increments. Fahrenheit equivalent is -67°F to $+257^{\circ}\text{F}$ in 0.9°F increments
- Temperature is read as a 9-bit digital value.
- Converts temperature to digital word in 200 ms (typ.)
- User-definable, nonvolatile temperature alarm settings
- Alarm search command identifies and addresses

PIN ASSIGNMENT

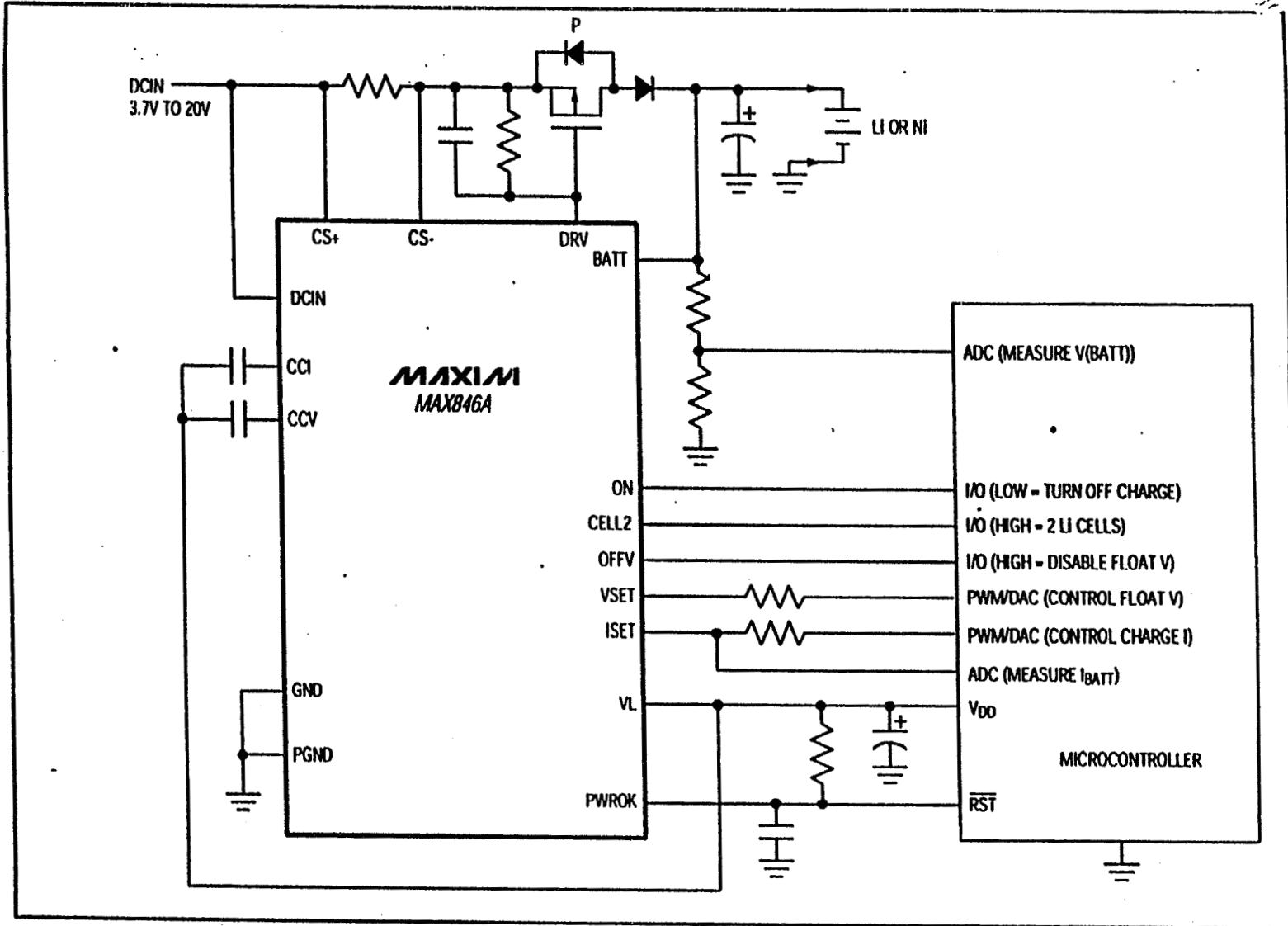


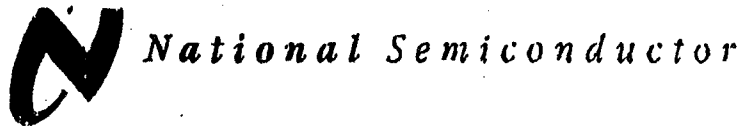
BOTTOM VIEW

DS1820
PR35 PACKAGE
See Mech. Drawings
Section

MAX846A

Battery-Charger System





March 1997

COP8ACC7 8-Bit One-Time Programmable (OTP) Microcontroller with High Resolution A/D Conversion

General Description

The COP8ACC7 is a member of the COP8™ 8-bit OTP microcontroller family. It is pin and software compatible to the mask ROM COP8ACC5 product family. (Continued)

Key Features

- Analog Function Block for high resolution A/D including
 - Analog comparator with seven input muxes
 - Constant Current Source and $V_{CC/2}$ Reference
 - 16-bit capture timer (upcounter) clocked from CKI with auto-reset on timer start-up
- Quiet design (reduced radiated emissions)
- 4096 bytes on-board OTP EPROM with security feature
- 128 bytes on-board RAM

Additional Peripheral Features

- Idle Timer
- One 16-bit timer with two 16-bit registers supporting:
 - Processor Independent PWM mode
 - External Event counter mode
 - Input Capture mode
- Multi-Input Wake-Up (MIWU) with optional interrupts (4)
- WATCHDOG and clock monitor logic
- MICROWIRE/PLUS serial I/O with programmable shift clock polarity

I/O Features

- Memory mapped I/O
- Software selectable I/O options (Push-Pull Output, Weak Pull-Up Input, High Impedance Input)
- High current outputs

- Schmitt Trigger inputs on ports G and L
- Packages: 28 DIP/SO with 23 I/O pins
20 SO with 15 I/O pins

CPU/Instruction Set Features

- 1 μ s instruction cycle time
- Eight multi-source vectored interrupt servicing
 - External Interrupt
 - Idle Timer T0
 - Timer T1 associated interrupts
 - MICROWIRE/PLUS
 - Multi-Input Wake Up
 - Software Trap
 - Default VIS
 - A/D (Capture Timer)
- Versatile and easy to use instruction set
- 8-bit Stack Pointer (SP) - stack in RAM
- Two 8-bit Registers Indirect Data Memory Pointers (B and X)

Fully Static CMOS

- Low current drain (typically < 5 μ A HALT current)
- Two power saving modes: HALT and IDLE
- Single supply operation: 2.7V to 5.5V
- Temperature ranges: 0°C to +70°C, -40°C to +85°C

Development System

- Emulation device for COP8ACC5
- Real time emulation and full program debug offered by MetaLink development system

Applications

- Battery Chargers
- Appliances

Smart Battery Charging with COP8ACC

National Semiconductor
Application Note 1075
Sayeed Rahman
May 1997

TABLE 1. Clock Speed vs Resolution, Conversion Time, and Achievable Accuracy

Clock Speed	Resolution	Conversion Time	Achievable Accuracy
10 MHz	12 Bits	0.410 ms	±2.0 LSB
10 MHz	8 Bits	0.026 ms	±1.0 LSB
5 MHz	13 Bits	1.640 ms	±2.5 LSB
4 MHz	10 Bits	0.260 ms	±1.5 LSB
2 MHz	11 Bits	1.300 ms	±1.5 LSB
1 MHz	12 Bits	4.100 ms	±1.5 LSB
1 MHz	10 Bits	1.025 ms	±1.0 LSB
1 MHz	8 Bits	0.260 ms	±1.0 LSB

MOSFET Photovoltaic Relay

Series PVN012

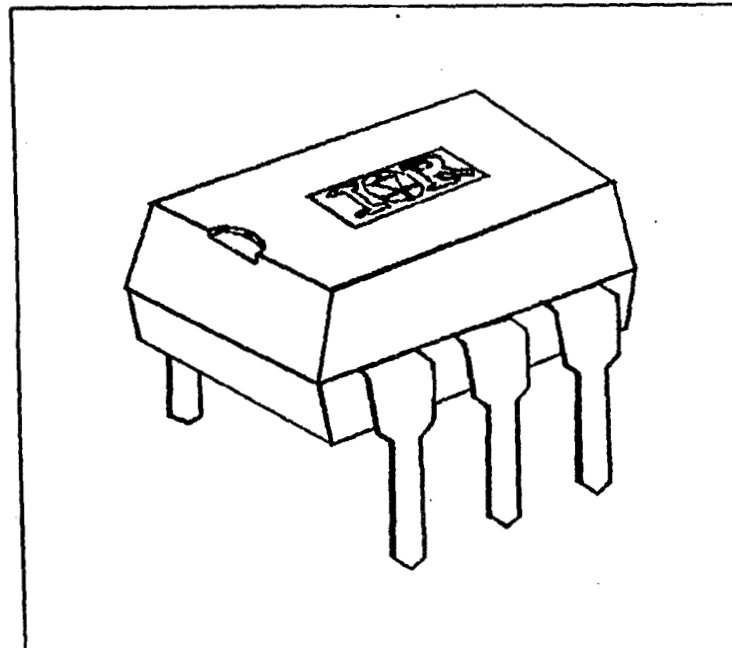
Microelectronic

Power IC Relay

Single Pole, Normally Open, 0-20V, 2.5A AC/ 4.5A DC

PVN012 Features

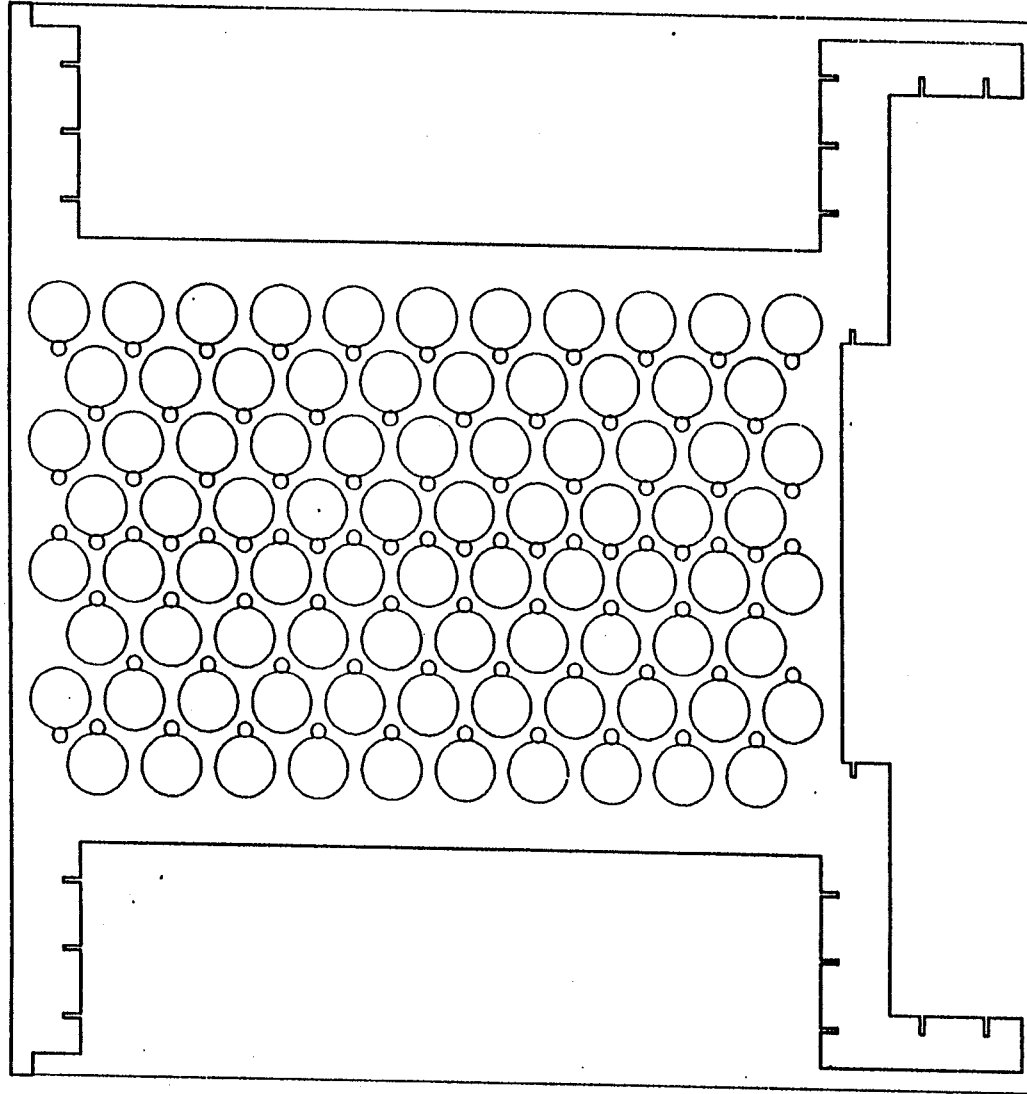
- 100m Ω On-Resistance ■
- GenV HEXFET output ■
- Bounce-free operation ■
- 2.5 - 4.5 Amp capacity ■
- Linear AC/DC operation ■
- 4,000 V_{RMS} I/O isolation ■
- Solid-State reliability ■
- UL recognized and CSA certified ■



HIVE Li-Ion Mechanical Integration Approach:

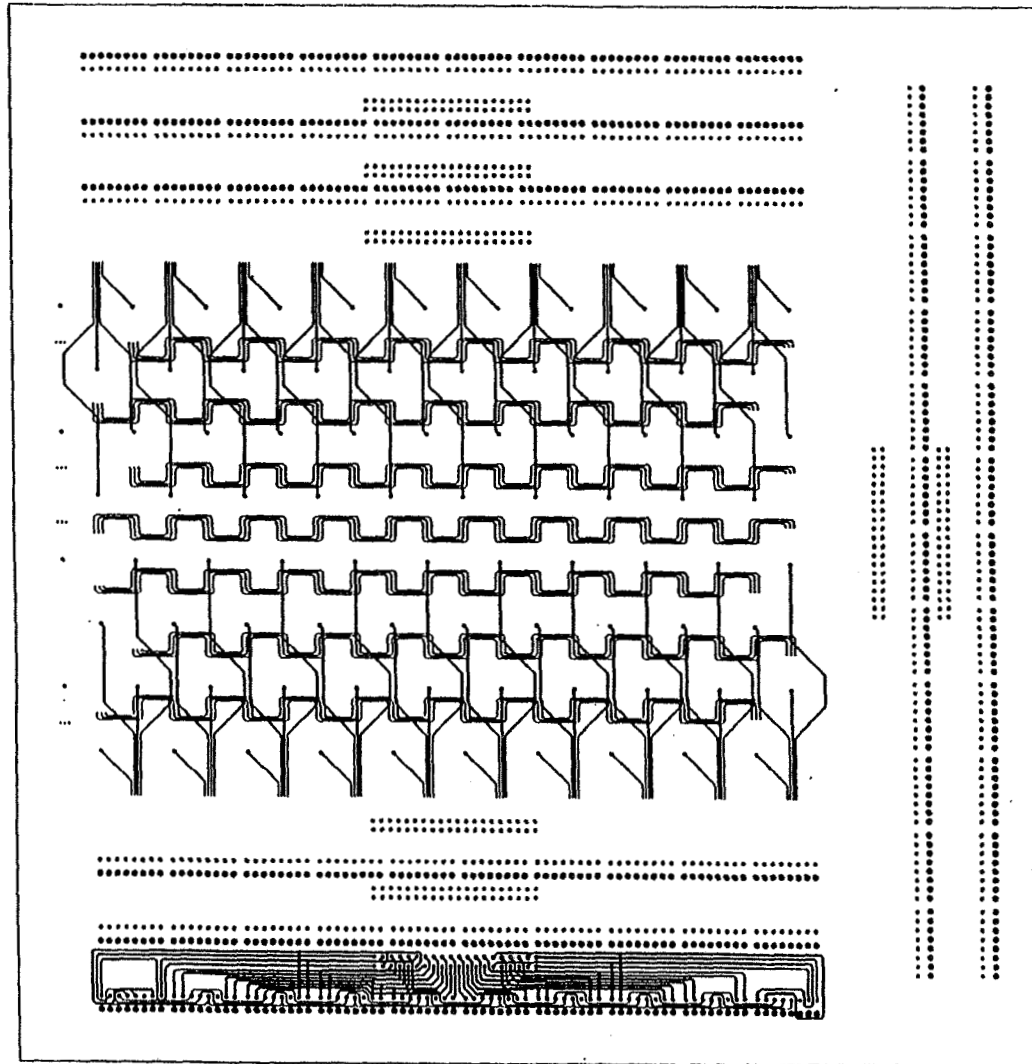
- **Prepare single epoxy "honeycomb" structure to hold Li-Ion cells**
- **Sandwich "honeycomb", Li-Ion terminals between two circuit boards**
- **Size charger/control circuitry to fit between these "power" boards**
- **Assemble via modular charger/control boards plugged into "power" boards**
- **Utilize through-hole, allowing repeated uP reprogramming / reinsertion**
- **Encase assembly within lexan plastic shell**

HIVE Li-Ion Honeycomb Support Structure:



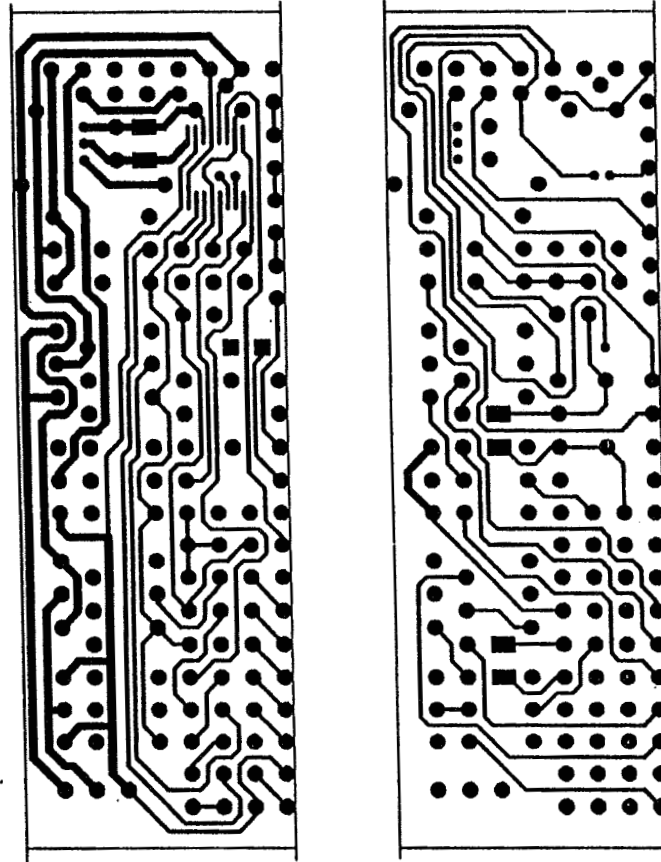
Size = 12 x 12 inches square; 2.5 inches high

HIVE Power Board Layout:



Size = 12 x 12 inches

HIVE Li-Ion Charger/Control Circuit:

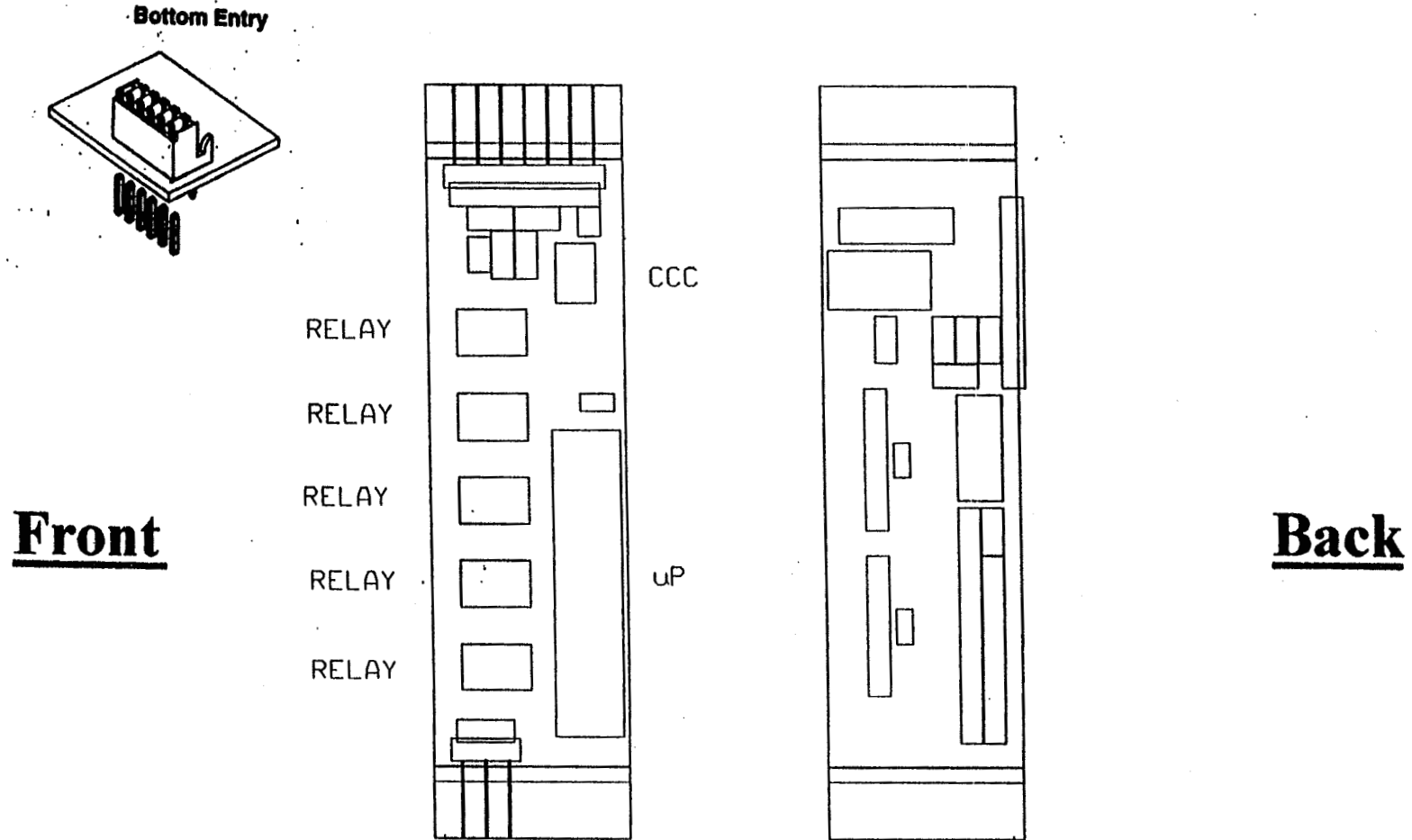


Front

Back

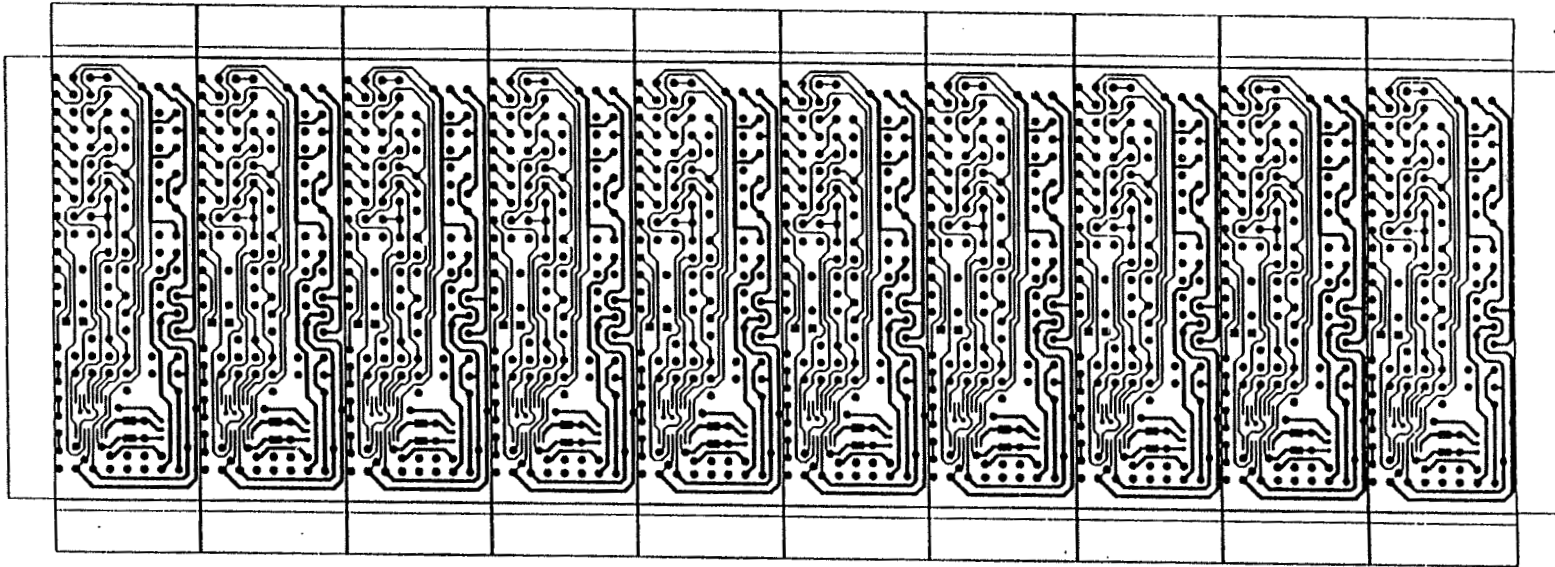
Size = 2.50 inches high by 0.85 inches wide

HIVE Li-Ion Charger/Control Circuit Parts Placement:

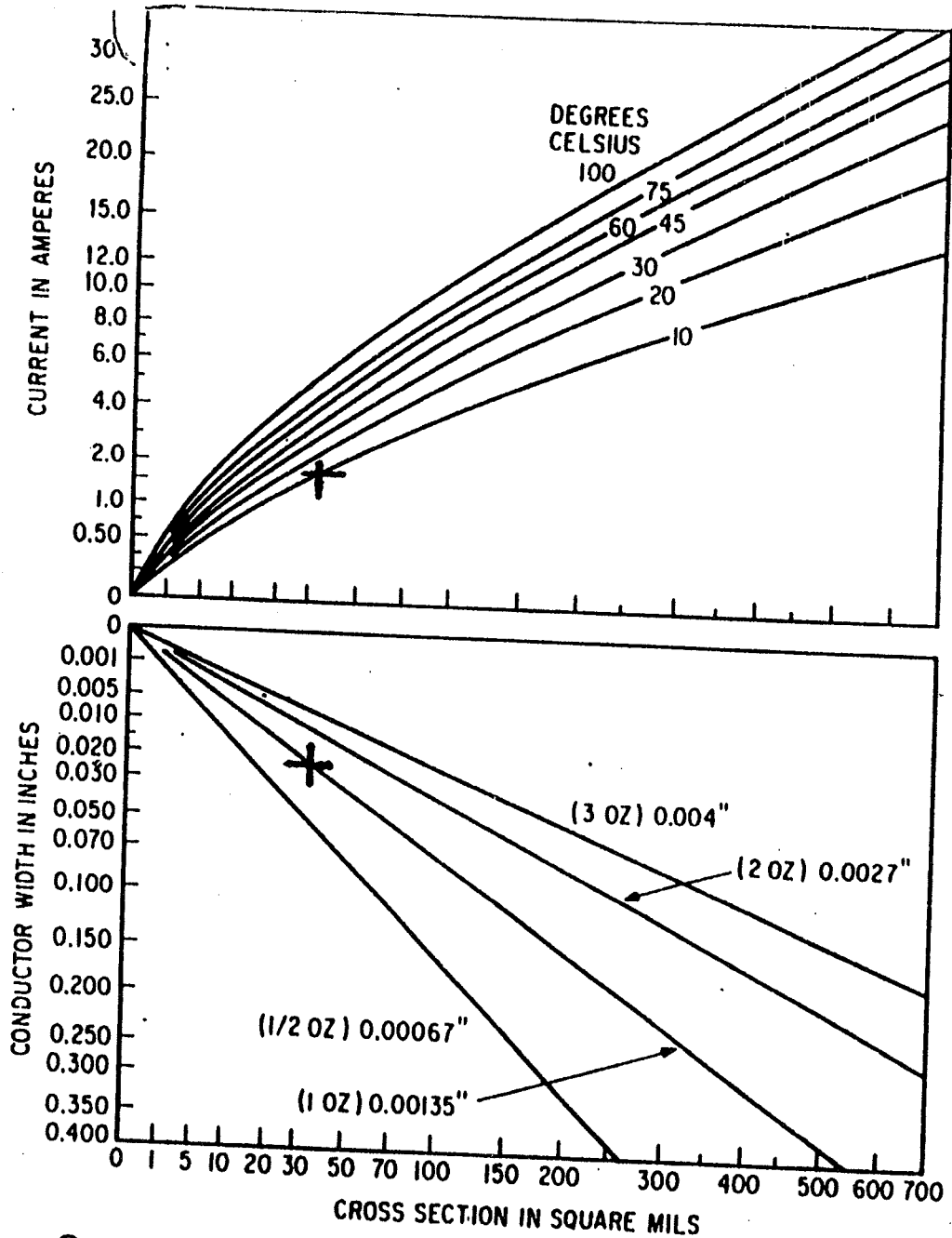


Size = 2.50 inches high by 0.85 inches wide

HIVE Li-Ion Charger/Control Module:



Size = 2.50 inches high by 9.00 inches wide (qty 6)
or 2.50 inches high by 10.70 inches wide (qty 2)



Current-carrying capacity of copper traces as a function of ...

	VOLTAGE BETWEEN CONDUCTORS (VDC or peak VAC)	CONDUCTOR SPACING (inches)
UNCOATED BOARDS <i>0-10,000 feet altitude</i>	0-150	.025
	151-300	.050
	301-500	.100
	500 +	.0002 in./V
UNCOATED BOARDS <i>Above 10,000 feet</i>	0-50	.025
	51-100	.060
	101-170	.125
	171-250	.250
	251-500	.500
	500 +	.0010 in./V
CONFORMALLY COATED BOARDS <i>Any altitude</i>	0-30	.010
	31-50	.015
	51-100	.020
	101-300	.030
	301-500	.060
	500 +	.00012 in./V

Minimum conductor spacing as a function of interconductor potential. (MIL-STD-275C)

Specs Sheet for Redco™ Phenolic (High Pressure Laminates)

Redco Phenolic (High Pressure Laminates)									
Nema Grade	Units	ASTM	XXX	LE	CE		G-5	G-9	G-10
Micarta® Grade			254	221	51F33	400	259-2	H12426	H22033
Base material			Paper	Fine weave fabric	Medium weave fabric	Medium weave fabric	Glass cloth	Glass cloth	Glass cloth
Resin			Phenolic	Phenolic	Phenolic	Phenolic	Melamine	Melamine	Epoxy
Color			Tan	Tan	Natural	Black	Gray	Gray	Green
Density	lb./cu.in.		049	048	050	051	074	074	057
Water absorption (1/8" thick)	percent	D229	0.4	0.7	1.1	1.1	0.4	0.2	0.05
Hardness	Rockwell "M"	D229	110	100	105	109	115	120	115
Tensile (with grain)	psi	D229	15,000	14,000	13,000	13,000	40,000	45,000	50,000
Compressive (flatwise)	psi	D229	36,000	38,000	37,000	45,000	65,000	65,000	50,000
Flexural (flatwise with grain) (1/8" thick)	psi	D229	20,000	22,000	19,000	21,000	50,000	55,000	60,000
Bonding strength (1/2" thick)	lb.	D229	1,200	1,800	2,000	2,200	1,800	2,300	2,600
Impact strength (Izod, edgewise with grain)	ft.lb./in. notch	D732	0.5	1.5	1.8	1.7	10.0	13.0	10.0
Shear (flatwise) (1/8" thick)	psi	D229	7,000	11,000	10,000	15,000	30,000	-	-
Dielectric strength	vpm	D229		350	200	--	300	--	550

HIVE ProSEDS Point Design Solution:

Power: Dual 0-120 V DC, 1.5 A busses

Energy: 500+ Whr

Weight: 19 pounds / 8.5 kilograms

Volume: 0.25 cubic feet / 7.0 liters

Size: 12x12x3 inches / 30x30x8 cm

Ratios: 60 Whr/kg for integrated power system

72 Whr/liter for integrated power system

Features: Individual voltage / temp monitoring on each of 84 Li-Ion cells
Digital data storage / dump of complete discharge / recharge cycle
Integrated non-metallic structure minimizes weight and volume
Integrated control electronics for both charging and discharging
Independent, adjustable power bus voltages
Advanced voltage regulation minimizes energy capacity waste

HIVE Future Efforts:

- **Build/program/test prototype outlined here**
- **Generate flight certification/documentation for components**
- **Design/build/flight-qualify “Mod 2” unit with NASA/MSFC oversight on reliability/redundancy**
- **Investigate DC/DC converter modules to increase output currents**
- **Implement mods allowing structure "stacking" to increase output currents**
- **Develop ongoing joint partnership efforts with other potential users/projects**

Page intentionally left blank

PERFORMANCE OF NICKEL-CADMIUM BATTERIES ON THE GOES I-K SERIES OF WEATHER SATELLITES

Sat P. Singhal
Computer Sciences Corporation

Walter G. Alsbach
Jackson & Tull

Gopalakrishna M. Rao
NASA/Goddard Space Flight Center

Abstract

The US National Oceanic and Atmospheric Administration (NOAA) operates the Geostationary Operational Environmental Satellite (GOES) spacecraft (among others) to support weather forecasting, severe storm tracking, and meteorological research by the National Weather Service (NWS). The latest in the GOES series consists of five spacecraft (originally named GOES I-M), three of which are in orbit and two more in development. Each of five spacecraft carries two Nickel-Cadmium batteries, with batteries designed and manufactured by Space Systems Loral (SS/L) and cells manufactured by Gates Aerospace Batteries (sold to SAFT in 1993). The battery, which consists of 28 cells with a 12 Ah capacity, provides the spacecraft power needs during the ascent phase and during the semi-annual eclipse seasons lasting for approximately 45 days each. The maximum duration eclipses are 72 minutes long which result in a 60 percent depth of discharge (DOD) of the batteries. This paper provides a description of the batteries, reconditioning setup, DOD profile during a typical eclipse season, and flight performance from the three launched spacecraft (now GOES 8, 9, and 10) in orbit.

INTRODUCTION

The US National Oceanic and Atmospheric Administration (NOAA) operates the Geostationary Operational Environmental Satellite (GOES) spacecraft (among others) to support weather forecasting, severe storm tracking, and meteorological research by the National Weather Service (NWS). The latest in the GOES series consists of five spacecraft (originally named GOES I-M), three of which (GOES 8, 9, and 10) are now

in orbit. National Aeronautics and Space Administration (NASA) is responsible for procurement, launch, and checkout of these spacecraft before turning them over to NOAA for operational use. They were built by Space Systems Loral (SS/L) with components from many vendors.

A key element in overall mission success is the successful operation of the battery system. These spacecraft carry two Nickel-Cadmium (Ni-Cd) batteries designed and manufactured by SS/L with cells manufactured by Gates Aerospace Batteries

(sold to SAFT in 1993). The battery, which consists of 28 cells with a 12 ampere-hour (Ah) capacity each, provides the spacecraft power needs during the ascent phase and during the semi-annual eclipse seasons lasting for approximately 45 days. The maximum duration eclipses are 72 minutes long which result in a 60 percent depth of discharge (DOD) of the batteries.

This paper provides a description of the batteries including the design and manufacturing process through acceptance testing and pre-launch preparation (References 1-4). Results are also provided from life cycle testing at the Naval Surface Warfare Center, Crane (Reference 5). The tests used battery packs prepared from cells out of the batch manufactured for spacecraft use. We also provide on orbit performance data from ascent phase, reconditioning, and from the eclipse seasons for the three spacecraft in orbit.

SPACECRAFT

The GOES 8, 9 and 10 spacecraft are three-axis stabilized geostationary satellites. Their dry mass is 977 kg and the nominal main bus power is 1150 W. They carry two main scientific instruments (Imager and Sounder) and a number of other measuring devices. During sunlight, they are powered by a single wing, two-panel solar array (SA). The SA has an output of 1300 W at beginning of life (BOL) Equinox and 1050 W at end of life (EOL) Summer Solstice. During eclipse, two 12 Ah Ni-Cd batteries with 28 cells each sustain the spacecraft. Power transfer from the batteries to the spacecraft bus is achieved through diode coupling. The power control unit (PCU) is the principal element for management and control of spacecraft primary power. The power control electronics (PCE) consists of the PCU, one

sequential shunt unit, and four electro-explosive device (EED) extension units. Key features of the PCE are as follows:

- a. Provides functions required for the primary bus.
- b. Provides direct energy transfer of SA power to the power distribution bus.
- c. Regulates and limits the voltage of the primary power bus to 42 ± 0.5 V dc during sunlight operation.
- d. Minimizes primary bus ripple and voltage transients by use of SA regulation and primary bus filtering.
- e. Allows flexibility of battery-charge control to optimize battery energy balance, thermal control.
- f. Maintains minimum battery temperature control through use of thermistors and heaters in the associated batteries.
- g. Includes provisions for individual battery reconditioning.
- h. Provides fail-safe and redundant actuation control of spacecraft EED (pyrotechnics) functions.
- i. Eliminates single-part failure criticality by use of circuit redundancy, protective functions, fault protection of spacecraft heater loads, and alternate mode operation selectable by command.
- j. Permits operational flexibility and status monitoring of key subsystem parameters by command and telemetry functions.

Redundancy Provisions. Power conditioning functions use both active and commandable redundancies. Commandable redundancy is provided for the following PCE functions:

- a. Battery discharge control
- b. Battery temperature control
- c. Voltage telemetry monitors

- d. Battery relay commanding
- e. Battery charge control
- f. EED ignition control (3 levels)
- g. Battery reconditioning control

Some important functions for the battery control are listed below.

Battery Charge Control. The battery charge control configuration provides capability of up to eight discrete battery charge rates. Battery charge current is supplied by six charge control arrays located on the SA wing. Within the PCU, charge control array sections A, B, and C are connected through relays and isolating diodes to battery 1. A similar arrangement is provided for charge control arrays D, E, and F for battery 2.

Battery Temperature Control. The battery temperature control circuitry provides dual modes to connect and disconnect the heater. A total of four battery temperature controls are provided, one for each half of each battery. Automatic control of minimum battery temperature* at $5(2) \pm 1$ °C is provided by heaters integrated with each battery assembly and separate temperature controllers in the power control unit. A precision thermistor on each battery provides temperature feedback to these controllers. Manual override allows the heaters to be switched on or off by command.

* Value in parenthesis for GOES 8 only.

Battery Reconditioning. Individual reconditioning of each battery is provided by command. A parallel group of resistors mounted external to the power control unit provide the reconditioning load.

Commanded Load Control. Application of power to individual loads is through an on/off control input to each load dc/dc

converter and by direct power bus switching of non-electronic loads (heaters).

Eclipse Load Controller. The GOES PCU contains redundant load controller functions. Each load controller monitors the SA current and the shunt current. Each primary power bus load (excepting command functions) is connected to and disconnected from the primary bus by command. In addition, power is automatically removed from sunlight loads upon eclipse entrance and automatically restored upon eclipse exit. Command override of this automatic function is provided.

BATTERY DESIGN DESCRIPTION

The battery subsystem of the GOES spacecraft consists of two assemblies, each containing 28 series-connected cells with a nominal capacity of 12 Ah and weighing approximately 12.9 kg each. Battery cell design has been guided by the life and reliability requirements of a 5-year geosynchronous satellite application and incorporates features that reduce the effects of unavoidable Ni-Cd cell degradation modes. Figure 1 shows one of the two batteries (S/N 206) used on GOES-9.

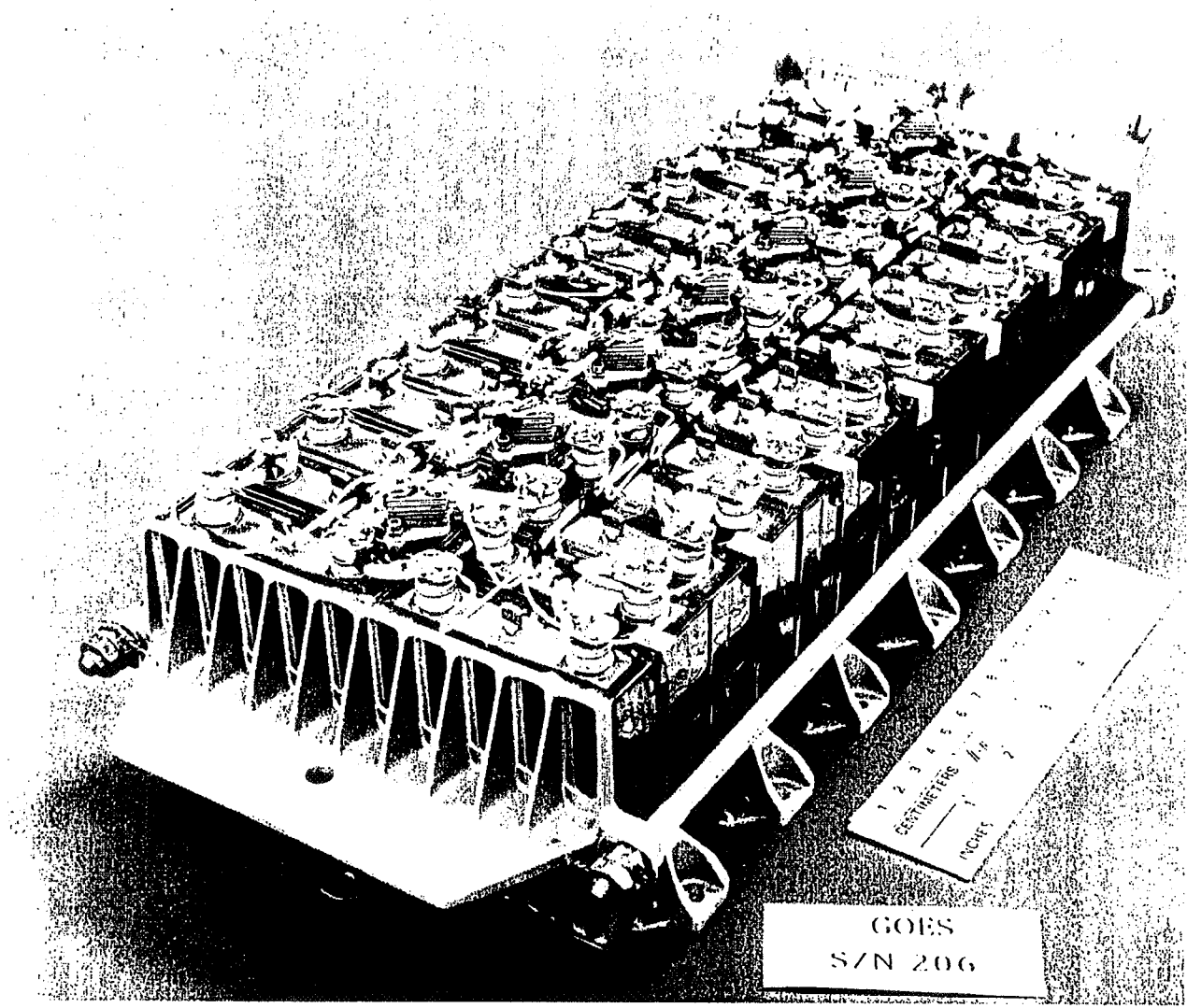


Figure 1. 12 Amp-hour NiCd Battery (S/N 206) used on the GOES-9 Spacecraft

Electrical Design. The nominal capacity of each battery assembly is 12 Ah. The 60% DOD design limit for maximum duration eclipse operation represents load capabilities of 409 W at BOL and 398 W at five years, based on average cell discharge voltages of 1.245 and 1.22 V, respectively, and a 1.0 V loss in the PCU. The 28 cells in series provide compatibility with charge voltage limits and deliver typical discharge voltages of 32.4 to 36.0 V.

Reconditioning. Reconditioning of the batteries during the one-month period preceding each eclipse season is required to maximize subsequent voltage performance and consequently minimize DOD.

Circuit Reliability. Circuit reliability within the battery is achieved by redundancy in wiring. Series connection between cells is provided by two parallel-connected, stranded copper wires soldered to the cell terminal lugs. Battery power connections are made to the terminals at the end of the cell series string by four redundant wires leading to the battery power connector.

Telemetry. The battery wiring harness design includes provision for telemetry of 28 individual cell voltages and battery temperatures. Additionally, overall battery voltage and current signals can be sensed.

Mechanical Design. The structural and mechanical design of the GOES battery is optimized to efficiently perform two important functions:

- a. Cell support and restraint
- b. Battery to equipment platform mounting.

Cell Support and Restraint. The basic mechanical design approach involves the restraint of two rows of 14 cells between

two endplates, with each group of four cells supported by a rib structure. The key component to the battery design is the concept of supporting four cells on one rib, and compressing seven of these subassemblies between two endplate/tie-rod assemblies. The design of the rib positively holds the corners of the prismatic cells in place. The compression force exerted by the endplates on the cells is controlled by the torque applied by the two tie rods. The cells are pre-loaded to 40 lbf/in² in this manner. The end plates are designed to withstand a nominal cell overcharge pressure of 75 lbf/in² with minimal deflection. The endplates also provide mounting flanges for supporting the two connectors. The endplates are machined from heat-treated 7075-T73 aluminum, which alleviates stress corrosion issues, and the tie rods are titanium. The cell support ribs are cast from A357-T61 aluminum.

Thermal Design. The thermal design of the GOES battery is such that temperature control is both passive and active. The passive control is primarily conductive through the cell support ribs, and the active control is via resistive heaters mounted on the same ribs. The seven aluminum ribs are sized to effectively conduct the heat dissipated by the four adjacent battery cells to the equipment platform of the spacecraft. The design is such that temperature gradients are only 3 °C. The ribs also have a mounting flange for the resistive heater elements. These flanges are centrally located such that an even distribution of heat throughout the battery assembly is achieved at times when the heaters are activated. The seven heaters are sized to dissipate the required heat for thermal control. Temperature sensing for each battery is accomplished by four precision wafer thermistors located on the battery assembly. Battery flatness is maintained within 0.020 inch during

assembly to allow for uniform thermal contact with the spacecraft. A silicone thermal grease is used between the battery and equipment platform on the GOES spacecraft to further reduce gradients and contact resistance.

Cell Design Summary. The Ni-Cd cell is designed to maximum margins for a greater than 5-year orbital lifetime. The prismatic Ni-Cd cells are packaged in a thin wall (0.012 in) 304L stainless steel container. A low profile terminal seal/cover configuration is used with double ceramic alumina-to-metal seals. Eleven positive and 12 negative plates are used. The specified negative-to-positive electrochemical capacity ratio is 1.70:1. This ratio ensures that the cells will remain positive limited during the 5-year mission. The positive electrode group has a theoretical electrochemical capacity of 15.6 \pm 1.2 Ah and the negative group 26.4 \pm 3.6 Ah. Active material loading is 1.25 \pm 0.06 and 1.55 \pm 0.065 Kg/m² for the positive and negative plates, respectively. The negative plates are treated with Teflon to reduce cadmium migration and increase the quantity of electrolyte used within the cell. The balance of positive and negative loading, electrochemical capacity ratio, and negative plate treatment enhance long-term cell performance required for the 5-year GOES mission. Non-woven Pellon 2536 nylon filament material approximately 0.007-0.009 inch thick is used for the separator. Weight concentration of 31% potassium hydroxide electrolyte provides for the transport of ions between the electrodes. This combination is being used for sealed Ni-Cd cells operated over the temperature range of 0 to 30 °C. Carbonate and nitrate levels are maintained at less than 2.0 g/l and 1.0 mg/l, respectively.

Interfaces. The battery interfaces are rigidly controlled during battery assembly. The

battery mounting surface and mounting hole pattern are controlled within close tolerances for an assembly of this type. Flatness of the battery is maintained within 0.020 inch, and the mounting hole pattern is drilled within 0.020 inch. Two electrical connectors are provided on the battery assembly. The power connector is an eight-socket connector through which the battery is charged and discharged. Four bus wires each are connected to the positive and negative terminals. The second connector is a 50-socket connector. Through this connector the interface is provided for individual cells voltage sensing, thermistor measurement, and heater bus.

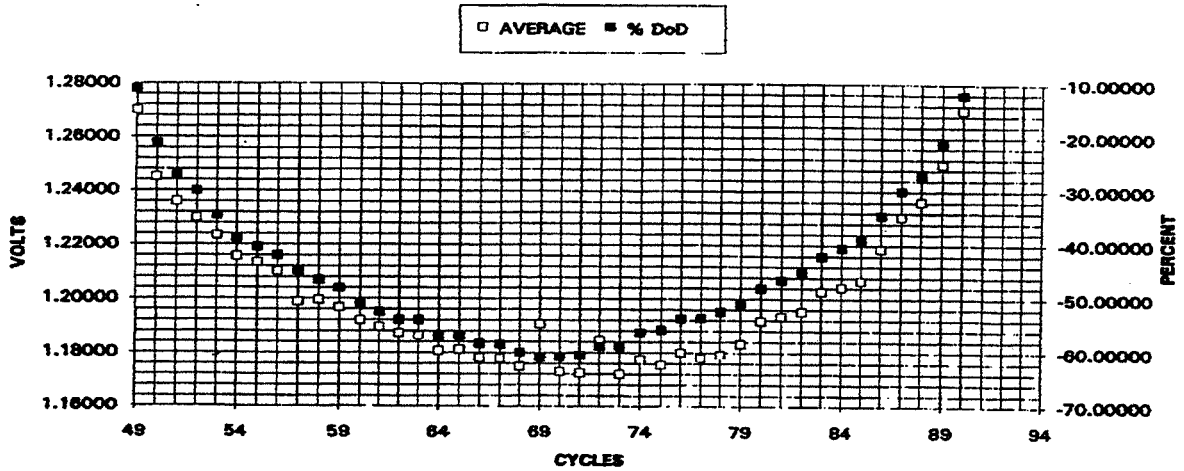
Battery and Cell History. The following designations refer to the flight batteries.

Spacecraft	Battery Serial Number
GOES-I	204, 203
GOES-J	205, 206
GOES-K	207, 208

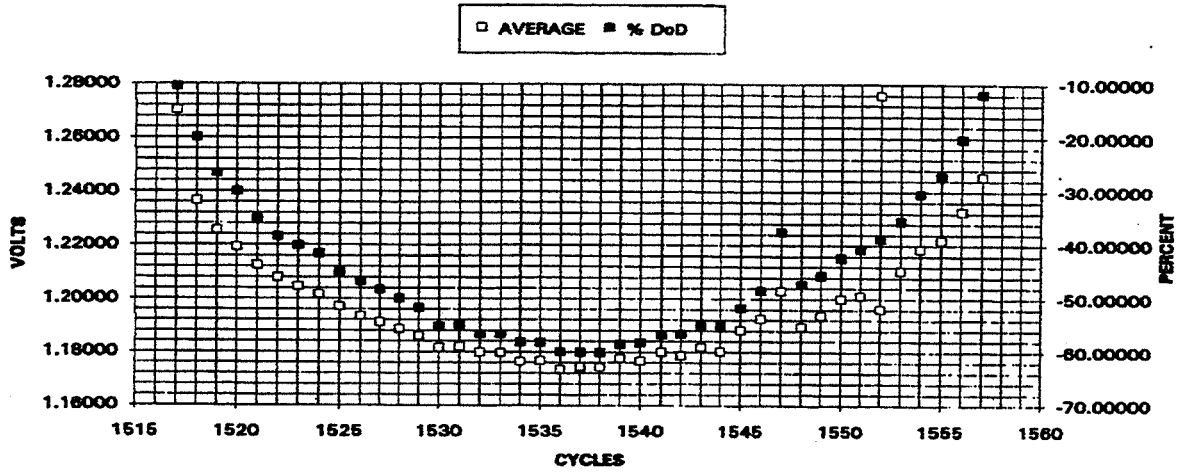
Life-test. As with most NASA spacecraft, life-testing was started at Crane Naval Surface Warfare Center. A pack of cells for each satellite is undergoing real time or accelerated life-test. The test conditions are close to those in orbit with a 6.0 A discharge rate (equivalent to C/2) and 0.9 A charge rate followed by a trickle charge period. Before entering a shadow period a reconditioning cycle is run. The cycles shown are (Figures 2-4):

GOES I. Shadow Periods 2, 12, and 25;
GOES J. Shadow Periods 2, 9, and 25;
GOES K. Shadow Periods 1 and 10.

6227B SHADOW 2, AVERAGE CELL VOLTS



6227B SHADOW 12, AVERAGE CELL VOLTS



6227B SHADOW 25, AVERAGE CELL VOLTS

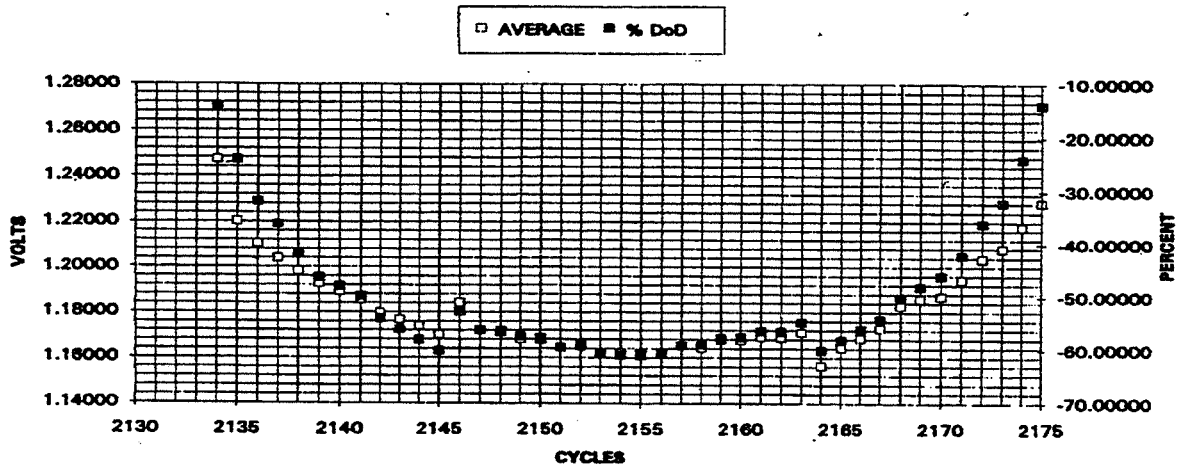
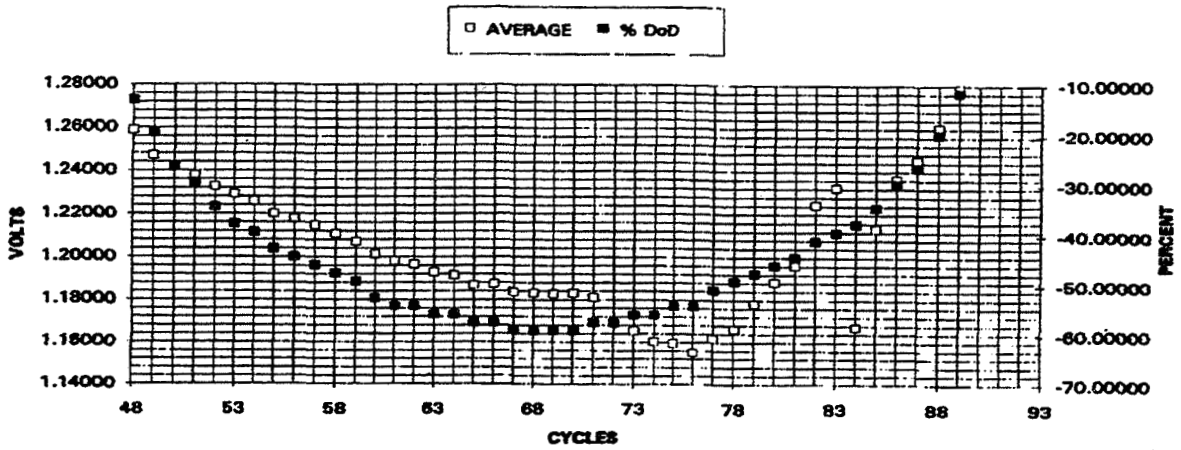
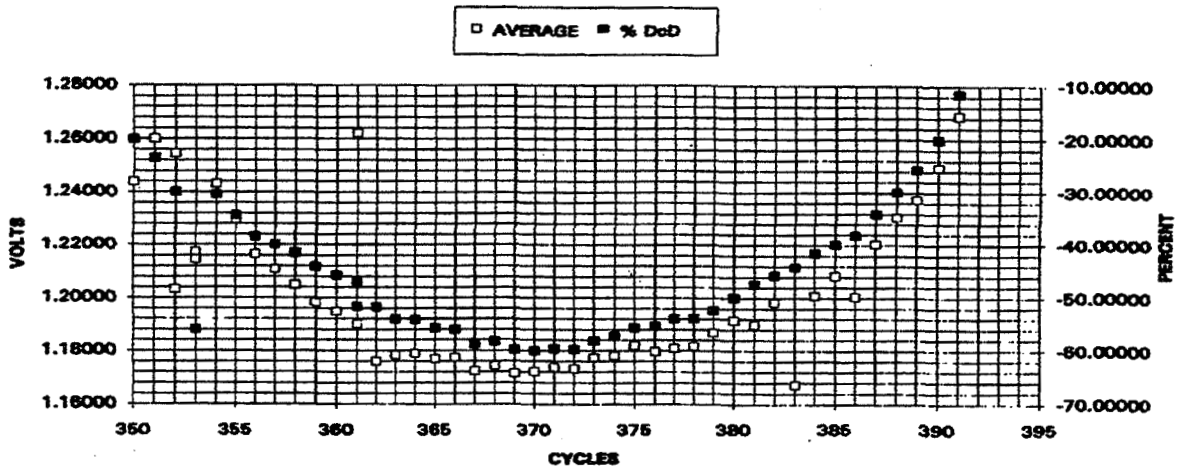


Figure 2. Battery DOD and Average Cell Voltages for Battery Pack 6227B (GOES-8) during shadow Periods 2, 12, and 25

**6227C SHADOW 2, AVERAGE CELL VOLTS,
VOLTAGE LIMIT LOW CYCLES 72 -96**



6227C SHADOW 9, AVERAGE CELL VOLTS



6227C SHADOW 25, AVERAGE CELL VOLTS, 72% DoD

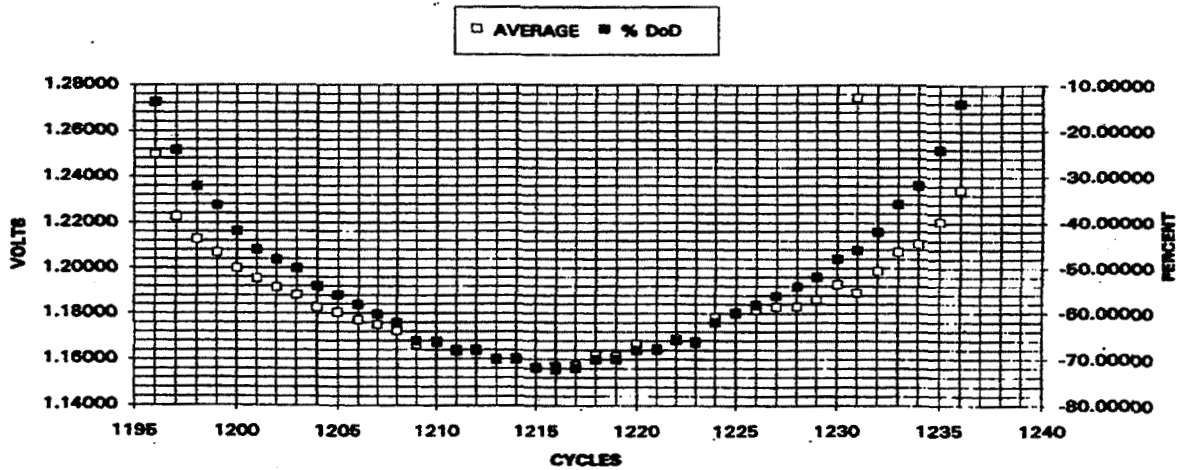
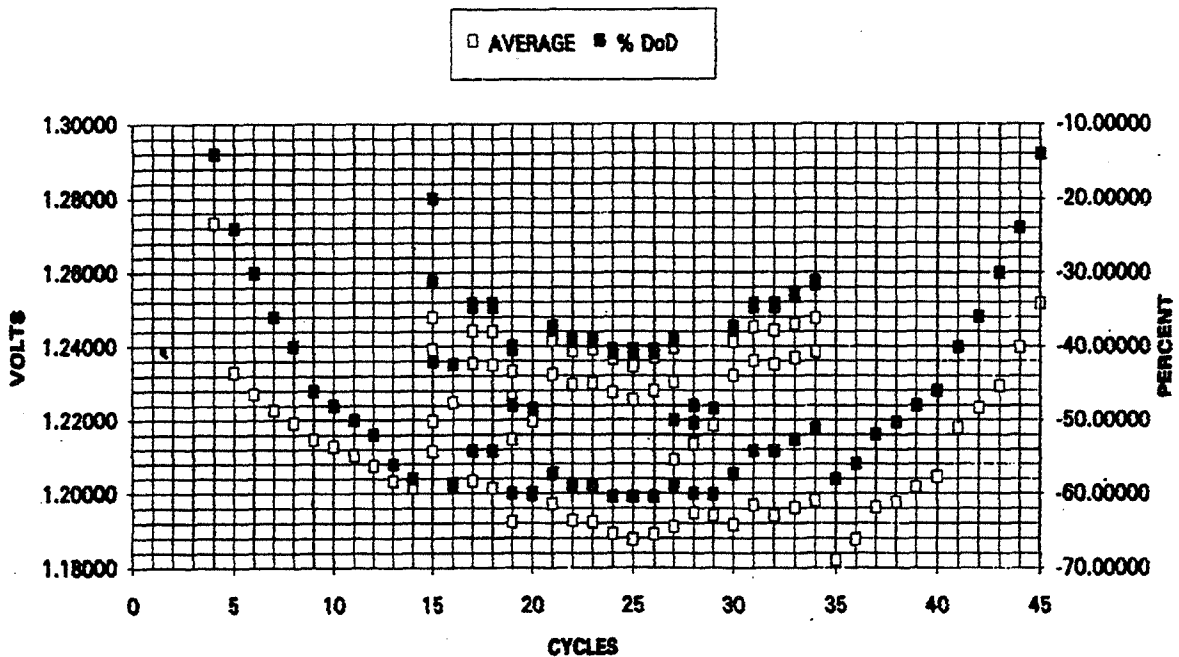


**Figure 3. Battery DOD and Average Cell Voltages for Battery Pack 6227C
(GOES-9) during Shadow Periods 2, 9, and 25**

**GOESK SHADOW 1, AVERAGE CELL VOLTS
TWO STEP DISCHARGE**



**GOESK SHADOW 10, AVERAGE CELL VOLTS
TWO STEP DISCHARGE**

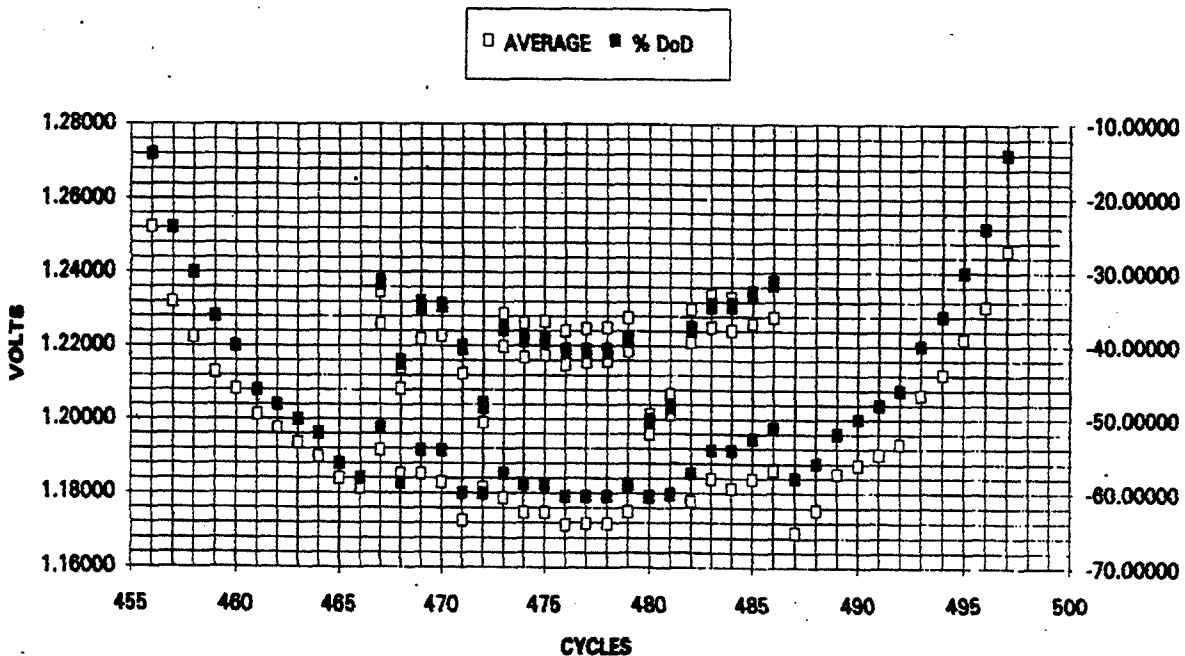


Figure 4. Battery DOD and Average Cell Voltages for Battery Pack GOESK (GOES-10) during Shadow Periods 1, and 10

All curves show nominal behavior and are within specification. There is also good agreement with the recorded flight data. Please note that shadow period 25 corresponds to 12.5 years of mission, which is more than twice the specified lifetime.

Manufacturing. The cells used for this battery were manufactured by Gates from 1989 to 1993, designated as lot # 5 with serial numbers 12AB31 and 12AB35. Based on an original 9 Ah design, they were name-plated as 12 Ah cells with specified acceptance capacity at 12.6 Ah. Out of the 500 originally manufactured cells 20 were taken into a 500 cycle test to address problems in two Aerospace Alerts. One alert from 1985, reported problems of negative electrode failure; and other, from 1988, reported problems in the hot gas sinter process and with the Pellon 2536 separator.

Storage. The cells were put in dry storage in a controlled environment

Acceptance Testing. The basic acceptance testing consists of seven steps (listed below), some of which were repeated until required results were achieved.

1. Reconditioning
2. Voltage Recovery
3. Capacity(20 °C): 12.8 Ah at 1.51 V max
4. Capacity(10 °C): 12.0 Ah at 1.52 V max
5. Capacity(0 °C): 11.5 Ah at 1.54 V max
6. Conditioning (20 °C): 12.8 Ah at 1.51 V
7. Voltage Recovery

Specified key values and acceptance test results for the GOES-I, -J, and -K batteries are listed in Table 1.

Table 1. Cell Acceptance Data for GOES-I, -J, -K Batteries.

Step	Requirement	GOES-I 9/20/88 - 5/20/90	GOES-J 7/16/90 - 7/6/92	GOES-K 6/7/93 - 5/11/94
3. Capacity at 20 °C Max Voltage Capacity	< 1.51 V > 12.8 Ah	< 1.485 V 12.8 Ah - 13.5 Ah	< 1.490 V 12.8 Ah - 13.2 Ah	< 1.479 V 11.9 Ah - 12.9 Ah
4. Capacity at 10 °C Max Voltage Capacity	< 1.52 V > 12.0 Ah	< 1.510 V 13.0 Ah - 14.3 Ah	< 1.514 V 13.4 Ah - 14.5 Ah	< 1.52 V 12.0 Ah - 13.1 Ah
5. Capacity at 0 °C Max Voltage Capacity	< 1.54 V > 11.5 Ah	< 1.530 V 12.7 Ah - 13.8 Ah	< 1.515 V 12.7 Ah - 14.3 Ah	< 1.53 V 12.1 Ah - 13.0 Ah
6. Conditioning at 20 °C Max Voltage Capacity	< 1.51 V > 12.8 Ah	< 1.485 V 12.8 Ah - 13.5 Ah	< 1.485 V 12.8 Ah - 13.5 Ah	< 1.469 V 11.8 Ah - 13.2 Ah
7. Voltage Recovery	> 1.145 V	N/A	N/A	> 1.190 V

BATTERY OPERATION

The two 12 Ah rated Ni-Cd batteries connected to the primary bus via redundant diodes and relays are designed for operation at a 60% maximum DOD for the mission. Criteria for battery management, including power subsystem design features to implement the same, are discussed below.

Functions provided for each battery by the power subsystem to monitor, control, and protect the batteries are as follows:

- a. Battery voltage monitors
- b. Individual cell voltage monitors
- c. Battery charge current monitors
- d. Battery discharge current monitors
- e. Battery temperature monitors
- f. Battery heater status monitors
- g. Battery relay status monitors
- h. Battery reverse current monitors
- i. Battery relay control commands
- j. Battery charge rate control commands
- k. Battery reconditioning controls
- l. Battery charge voltage limiting
- m. Thermostatically controlled battery heaters

Pre-launch and Launch. During the pre-launch and launch phases of the mission, the spacecraft is kept on external power until approximately 4 minutes before launch. Should a launch hold of more than 10 minutes be encountered while the spacecraft is on internal power, consideration should be given to recharging the batteries before continuing with the launch operation.

Battery Charge Control. Batteries can be charged in either a continuous or sequenced mode. The primary consideration on the

following recommended battery charge control implementation is to minimize battery stress while providing adequate charge return to ensure energy balance. This objective is satisfied using the lowest practical charge rate in the sequenced mode to minimize average battery temperature. The methodology recommended has been flight proven on previous SS/L programs and verified by life cycle testing.

General Configuration Control. The electrical power subsystem permits considerable flexibility in battery charge management. Charge power is derived from the SA using two identical groups of three charge control arrays. Group 1 consists of arrays A, B, and C; group 2 of arrays D, E, and F. The typical current output of these arrays is summarized in Table 2 for various conditions.

Table 2. Battery Charge Array Current

Season/Life	Charge Control Array Module		
	A, D	B, E	C, F
Vernal Equinox			
BOL	0.99	0.33	0.33
EOL	0.91	0.30	0.30
Autumnal Equinox			
BOL	0.97	0.32	0.32
EOL	0.89	0.30	0.30
Summer Solstice			
BOL	0.86	0.29	0.29
EOL	0.80	0.27	0.27
Winter Solstice			
BOL	0.93	0.31	0.31
EOL	0.87	0.29	0.29

Two basic charge modes are available. First, with the normal recommended synchronous orbit sequenced mode, current is applied to

the two batteries in an alternating fashion in an approximately 10-minute cycle. Any combination of the six charge arrays can be switched between the batteries. Alternately, any combination of arrays A, B, and C can be used for battery 1 and any combination of arrays D, E, and F for battery 2. Second is the continuous charge mode. In this mode only the latter arrangement is practical.

For one time only, a maximum DOD of 70% would be allowed for a battery temperature maintained between 5 °C and 25 °C. This maximum DOD, if approached, allows no margin for contingencies. To provide such a margin, a mission goal for maximum DOD should not exceed 60%.

Normal Eclipsed Orbits Charge Control.

Battery charge control performance is evaluated by use of the following telemetry provided for each battery:

- a. Battery voltage
- b. Individual cell voltages
- c. Charge current
- d. Battery temperature
- e. Battery heater status

The 110% charge return at the full rate, followed by trickle charge until the next eclipse, ensures sufficient recharge for all eclipse cycles.

Battery Temperature Control. Battery temperature profiles are largely governed by the battery charge profiles. Thermostatically controlled 19.5 watt battery heaters are provided to maintain the minimum battery temperature* above +4 (1) °C. These heaters are designed to cycle on at +5 (2) ±1 °C and off at +9 (5) ±1 °C. Heater operation is controlled by a precision thermistor in each battery in conjunction with level detectors and relay drivers within the PCU. This function can be overridden by command to

either turn the battery heater on or off regardless of battery temperatures. The intended use of this override function is to provide manual heater control in the event of a failure in the automatic heater control.

* Values in parenthesis for GOES 8 only.

Battery Reconditioning. To maximize battery discharge voltage during each eclipse, both batteries are reconditioned prior to the start of each eclipse season. These reconditioning cycles are performed as close as possible to the next solar eclipse to obtain the maximum benefit.

ON-ORBIT PERFORMANCE

First of the GOES series I-M spacecraft was launched on April 13, 1994, and was renamed GOES 8 after achieving nominal operational orbit. The next two were launched on May 23, 1995 (GOES 9) and April 25, 1997 (GOES 10). The batteries provide spacecraft power needs from just before launch to the time of partial SA deployment soon after launch (the outer panel is deployed approximately ten days later providing full power). The batteries also shoulder the power needs during eclipses, any maneuvers causing loss of solar power, and whenever the power produced falls short of the spacecraft needs. The sections below discuss battery performance during these various phases. Specific data is generally provided for GOES 10. However, data from GOES 8 and GOES 9 is also included whenever this data was useful to establish trends.

Ascent phase Battery Performance

The batteries on the GOES spacecraft provide power to the primary bus starting a few minutes before launch when the spacecraft is switched to internal power. This first round of battery support is completed when the SA is partially deployed approximately 1.5 hours after launch. During the next few days, the batteries provide the spacecraft power needs during special events such as the magnetometer boom and full SA deployment phase and the dipole estimation phase. Also depending upon the time in orbit before the Apogee Maneuver Firing No. 1 (AMF #1), the batteries provide support during several eclipses lasting approximately 15 minutes each.

For all cases when the batteries experienced a non-zero discharge current, data was

retrieved from the archives at 5.12 second intervals. The charge removed during discharge (D) from the batteries was then calculated as an integral of the discharge current over time, i.e.,

$$D \text{ (Ah)} = \int I \text{ dt.}$$

The integral is evaluated numerically by using current values at 5.12 sec intervals. The DOD is then given as a percentage fraction of the nameplate capacity (C_0) of the batteries (12 Ah each for a total of 24 Ah for the system). Thus

$$\text{DOD} = 100 * D \text{ (Ah)} / C_0$$

gives the DOD value for the individual battery or the system as a whole depending on the values of the current and capacity used above.

Table 3 lists all times during the ascent phase when the batteries on the GOES-K spacecraft were subjected to discharge. The maximum DOD was recorded during the Magnetometer boom and SA deployment phase; corresponding battery discharge currents are shown in Figure 5.

Table 3. GOES-10 Battery Discharge History from Launch to Early On-orbit

Date	DOY	Time Range	Event	Max Dis I		Max DOD (%)
				Battery 1	Battery 2	
4/25/97	115	05:43 - 07:08	Launch to Partial SA deploy	4.0	4.1	20.6
4/25/97	115	18:33 - 18:47	Transfer Orbit Eclipse #1	4.4	5.2	9.5
4/26/97	116	07:11 - 07:25	Transfer Orbit Eclipse #2	5.4	5.9	10.2
4/26/97	116	19:48 - 20:03	Transfer Orbit Eclipse #3	5.7	6.0	12.7
4/29/97	119	16:50 - 17:30*	Apogee Maneuver Firing #2	1.6	1.3	4.0
5/04/97	124	23:14 - 00:01	Mag Boom & SA Deploy	4.5	4.7	26.0
5/05/97	125	18:03 - 18:30	Dipole Estimation	7.1	7.4	22.7

* Intermittent discharge currents (up to 0.6 A) from 17:30 to 18:00.

GOES-10 Mag Boom and SA Deploy Sequence

1997/124/23:00:00-1997/125/00:10:00
ALL POINTS RETRIEVED
SatPol Singhal (EPS)

Page: wbatdis_1 SC10 (TEST1)
Wed, 29-Oct-1997 21:46:25
Minor Frame Quality: 100.00%

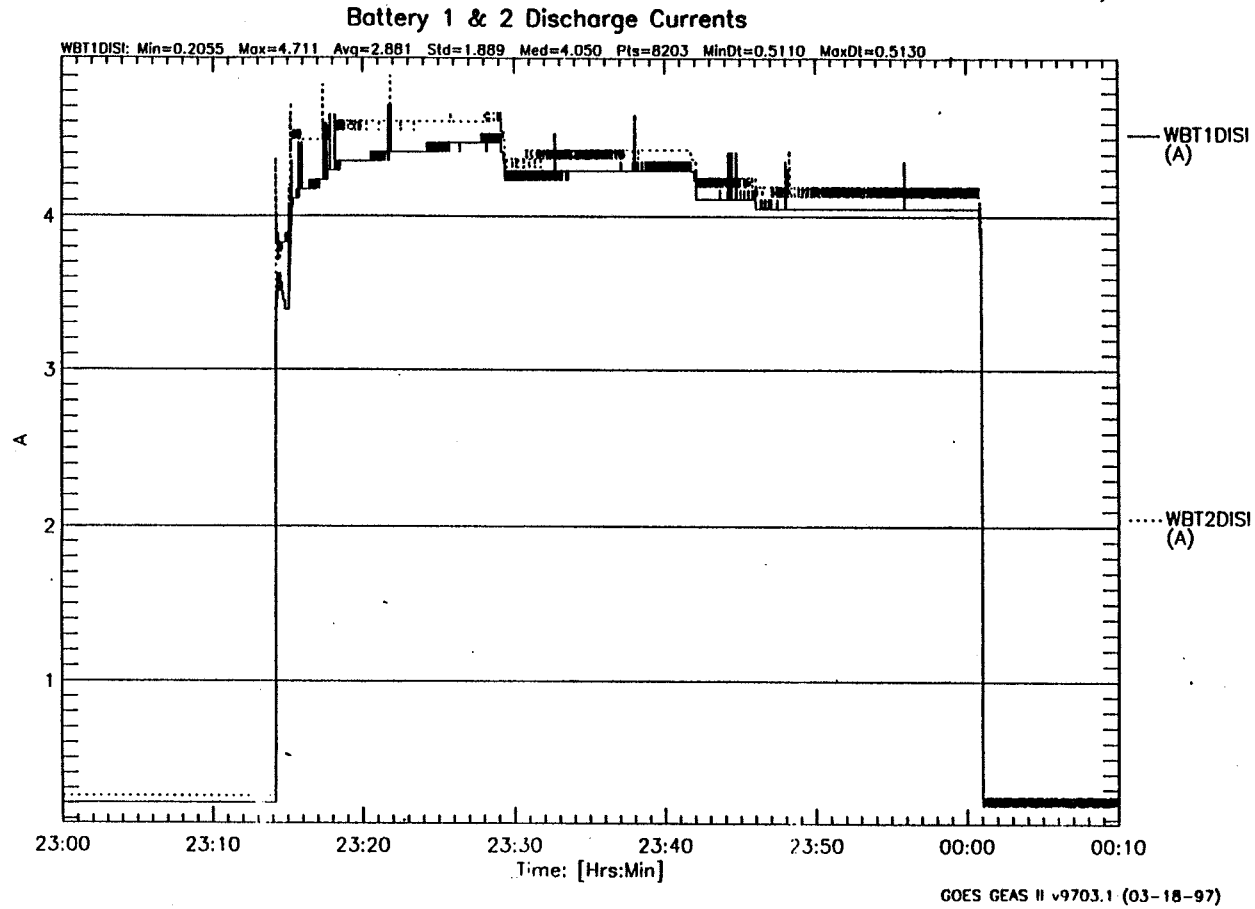


Figure 5. Battery Discharge Currents During the Magnetometer Boom and full Solar Array Deployment Phase for the GOES-10 Spacecraft.

Battery Reconditioning

Spacecraft Batteries are reconditioned prior to the start of each eclipse season. The batteries are individually reconditioned by use of the following sequence after verifying that the other battery is connected to the spacecraft bus.

- a. Turn off battery charging
- b. Open battery discharge relay number 2
- c. Inhibit the battery under voltage protection
- d. Turn on battery reconditioning

The 139.6 ohm resistive load is connected across the battery, resulting in an initial C/48 (0.25 A) reconditioning discharge rate. The individual cell voltages of the selected battery are monitored throughout the reconditioning discharge period. When the first cell voltage reaches 0.5 ± 0.1 V, the reconditioning discharge is terminated. Figure 6 shows the battery reconditioning circuitry.

On-orbit reconditioning has been performed prior to 7 eclipse seasons for GOES-8, and 5 eclipse seasons for GOES-9. The batteries on GOES-10 were not reconditioned prior to the fall 1997 eclipse season.

Charge removed from the batteries during reconditioning was calculated using a different approach than that described earlier. During reconditioning, the nominal discharge current has a value of 0.25 A (C/48 rate). However, the step size for the discharge current telemetry is 0.06 A, too coarse to show discharge current changes as the battery voltage changes. Since the battery is being discharged by connecting it to a constant resistor (139.6 Ohms), the discharge current is given by the use of Ohm's law

$$I = V/R$$

and the charge removed as an integral of battery voltage, i.e.,

$$D (\text{Ah}) = (1/R) \int V dt$$

In addition, since the reconditioning process continues for 60 - 65 hours, the voltage data for integration is sampled at 1-minute intervals at the beginning and end of the process (where the voltage is changing comparatively rapidly) and at 5-minute intervals during the middle 48 hour period.

Figure 7 shows the performance of GOES-8 battery 1 during its first reconditioning cycle (Fall 1994). The reconditioning was terminated when cell 12 voltage dropped to a value of 0.5 V. Corresponding data for battery 2 is shown in Figure 8.

Table 4 compares the results from all reconditioning cycles to date: seven for GOES-8 and five for GOES-9. The data show that the battery capacity has improved with time. The table also shows the end of discharge (EOD) battery voltage for each case.

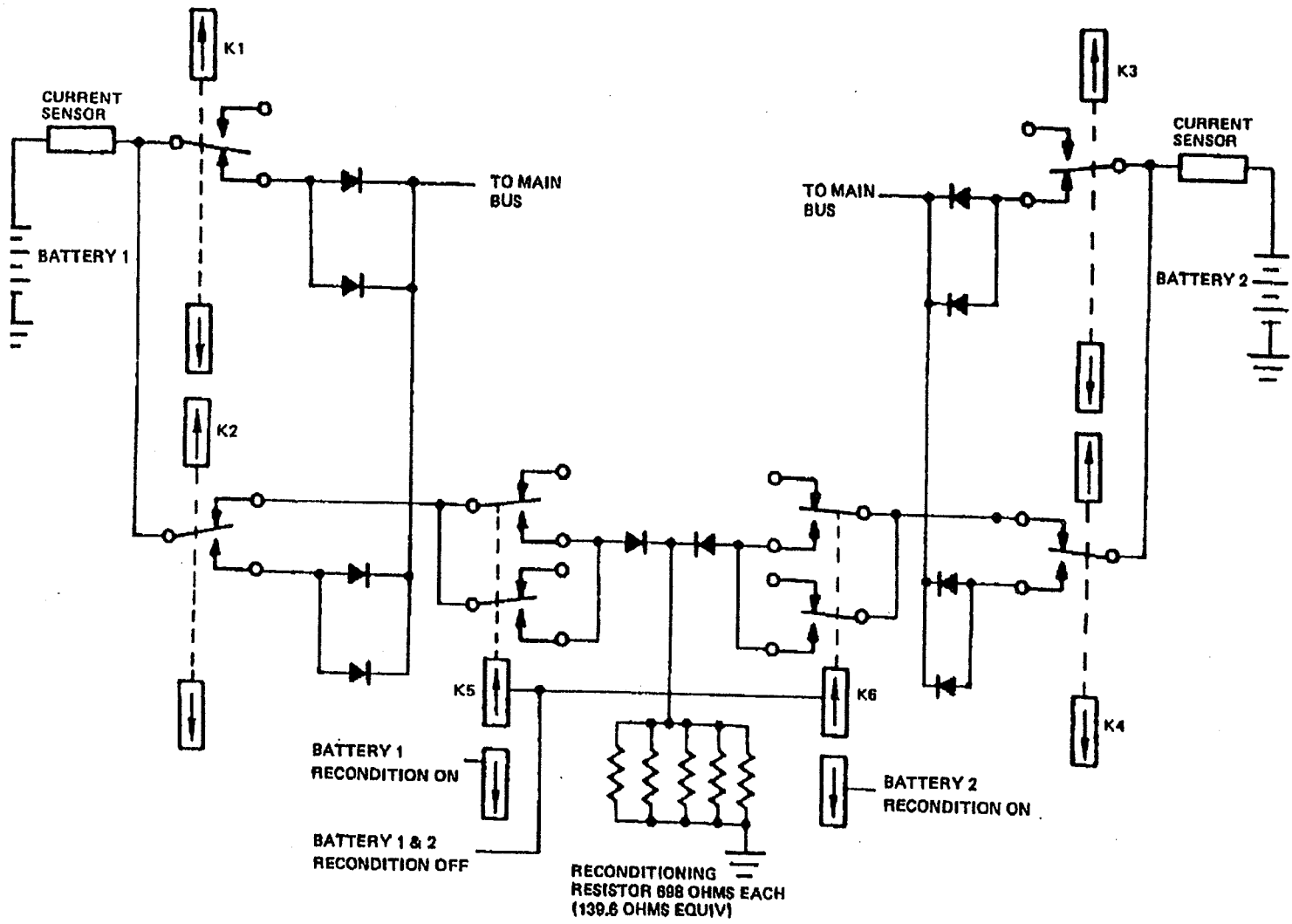


Figure 6. Battery Reconditioning Circuitry

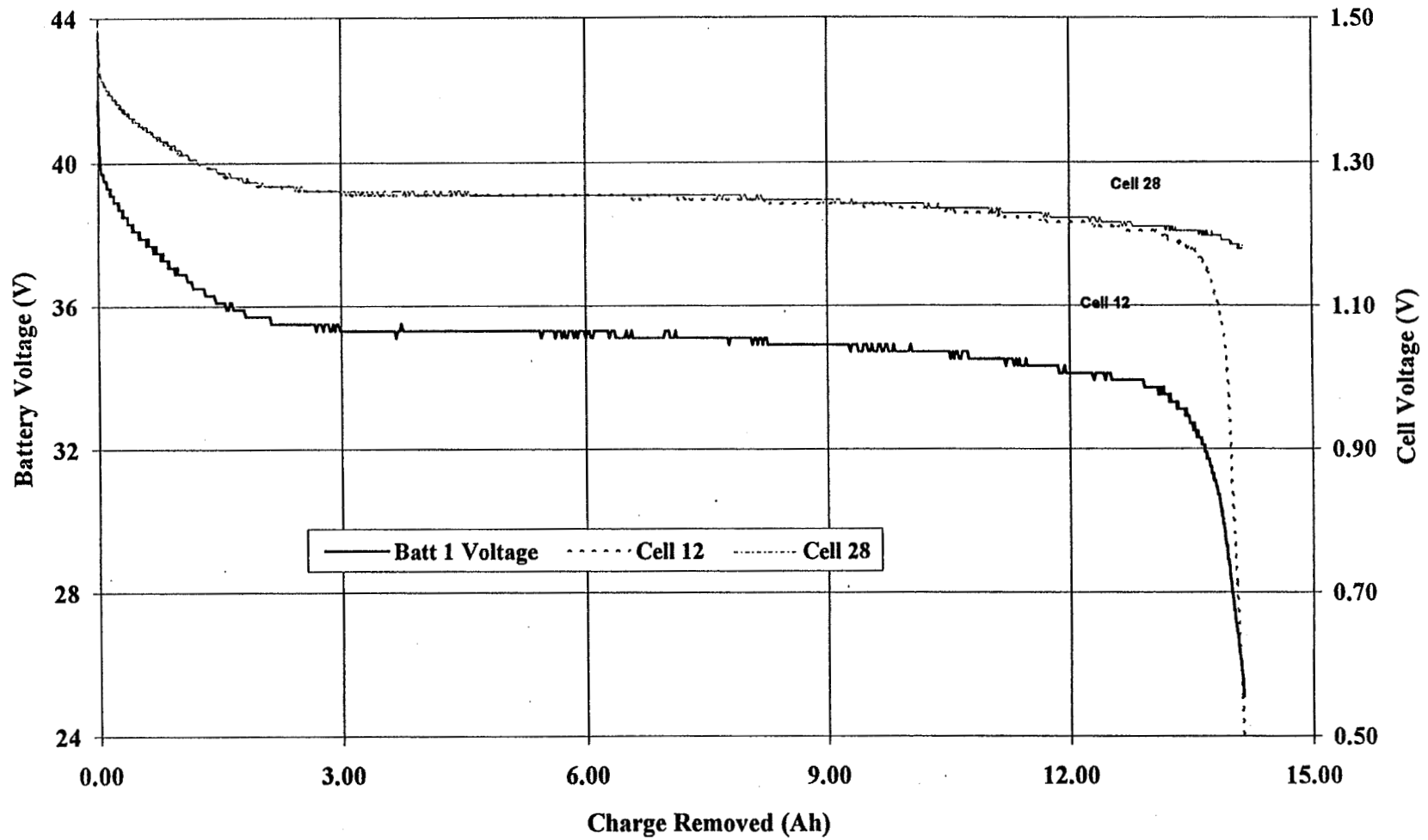


Figure 7. GOES-8 Fall 1994 Battery 1 Reconditioning: Battery and Cell Voltages for the Weakest (Cell 12) and Strongest (Cell 28) Cells as a Function of Charge Removed from the Battery.

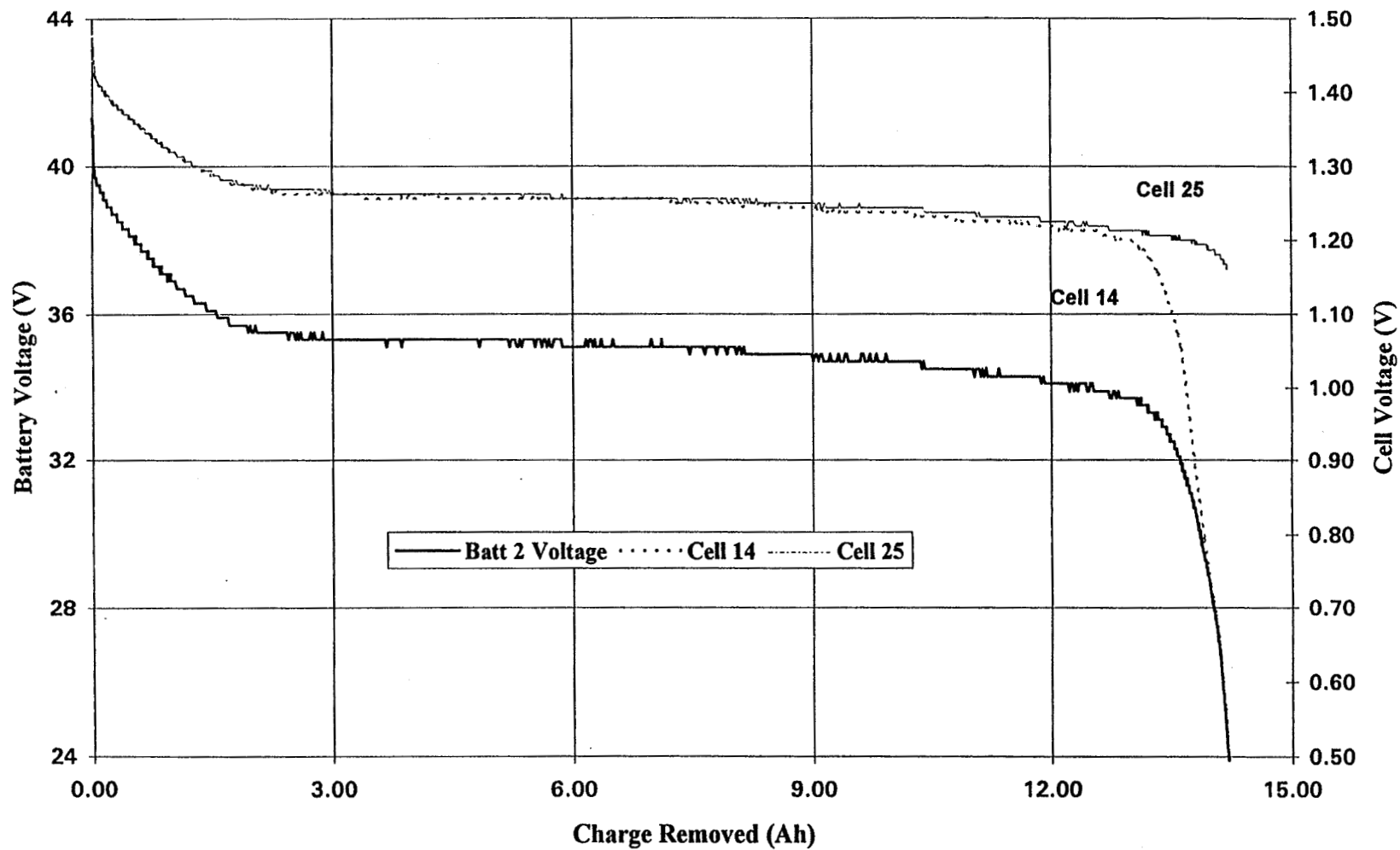


Figure 8. GOES-8 Fall 1994 Battery 2 Reconditioning: Battery and Cell Voltages for the Weakest (Cell 14) and Strongest (Cell 25) Cells as a Function of Charge Removed from the Battery.

Table 4. Battery Reconditioning Results for GOES-8 and -9.

		GOES-8		GOES-9	
		Ah Removed	EOD Voltage	Ah Removed	EOD Voltage
Fall 1994	Battery 1	14.14	25.1		
	Battery 2	14.21	23.9		
Spring 1995	Battery 1	15.25	19.7		
	Battery 2	15.41	19.1		
Fall 1995	Battery 1	15.32	20.3	14.06	22.9
	Battery 2	15.60	19.7	13.82	27.5
Spring 1996	Battery 1	15.89	18.1	15.23	18.9
	Battery 2	15.92	18.3	15.14	19.7
Fall 1996	Battery 1	15.57	19.3	15.30	19.3
	Battery 2	15.73	18.9	15.31	20.1
Spring 1997	Battery 1	16.00	16.3	15.77	17.7
	Battery 2	16.09	17.1	15.60	19.5
Fall 1997	Battery 1	15.68	18.9	15.40	18.7
	Battery 2	15.69	19.5	15.26	19.7

Battery Performance During The Eclipse Seasons

The GOES spacecraft experience the loss of solar power during the semi-annual eclipse seasons that last approximately 45 days each centered on the Vernal and Autumnal equinox. The duration of the eclipses vary from a few minutes to a maximum of 72 minutes on or near the equinox. We have analyzed the eclipse data for all 13 eclipse seasons (7 for GOES-8, 5 for GOES-9, and one for GOES-10) and found it to be consistent and predictable. We provide details of the latest (Fall 1997) eclipse season below along with some statistical data from the previous cases.

Figure 9 shows the daily battery DOD during the Fall 1997 eclipse season for GOES-10. The figure shows the DOD for batteries 1 and 2 and for the battery system as a whole. As the eclipse duration gets longer, the batteries are discharged for a longer period resulting in almost a linear increase in the battery DOD. The DOD curve, as shown, is not smooth because of the active load management that had to be performed to stay within the 60 % DOD limit. Operationally, we have the so-called "20-minute" rule that was imposed after a power amplifier failure on GOES-8. The uplink carriers from the ground station to the spacecraft provide extra heating to the power amplifiers during the eclipse but result in a higher DOD that would exceed the 60% limit during the longer eclipses. A balance is struck between the two requirements by keeping the carriers up during the eclipse except during the central portion of the season when the carriers are brought down at the start of the eclipse and then brought up 20 minutes before the end of the eclipse. During the central seven days of the eclipse

season, this 20-minute rule was further modified to a 10-minute rule. In addition, the Attitude and Orbit Control Subsystem (AOCS) team kept both Earth Sensors operating during the eclipse season except for the days when the power engineer required one of them to be turned off to avoid excessive drain on the batteries.

Figure 10 shows the total DOD for the battery system for all three spacecraft for the Fall 1997 season. The data for GOES-8 and -9 also show the effects of the power management by modifying the times for the uplink carriers. However, other aspects of active power management are evident only for the GOES-10 spacecraft since this was the first eclipse season for it.

Figure 11 shows the battery discharge currents for Day of Year (DOY) 266 (September 23, 1997) for the three spacecraft. The eclipse times are separated by 2-hour intervals reflecting the fact that the three spacecraft are geostationary at 75 degrees W (GOES-8), 105 deg W (GOES-10), and 135 deg W (GOES-9) longitude. The figures show a sharp rise in the discharge currents near the end of the eclipse due to the uplink carriers (approximately 90 Watt increase in power consumption).

Figures 12 through 14 show the battery minimum voltage versus DOD for batteries 1 and 2 for GOES-8, -9, and -10 respectively. GOES-10 data shows larger spread between the battery voltages at the same DOD (encountered before and after the maximum duration eclipse), probably reflecting the fact that these batteries had not gone through reconditioning, as mentioned earlier. Figure 15 shows the battery minimum versus DOD data for all 6 batteries together. The results clearly indicate that the batteries are behaving as a family.

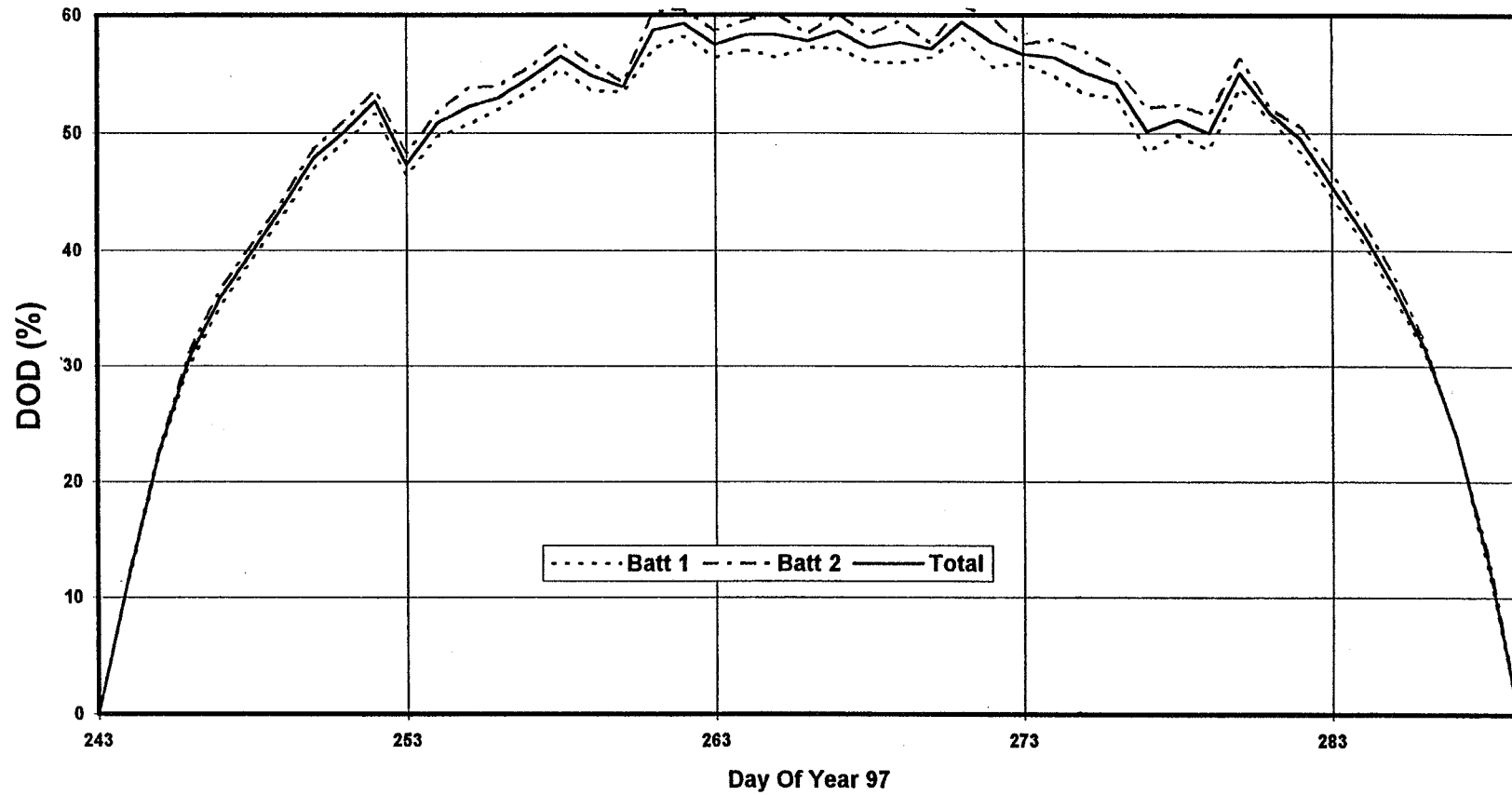


Figure 9. GOES-10 Battery Depth of Discharge (DOD) During the Fall 1997 Eclipse Season.

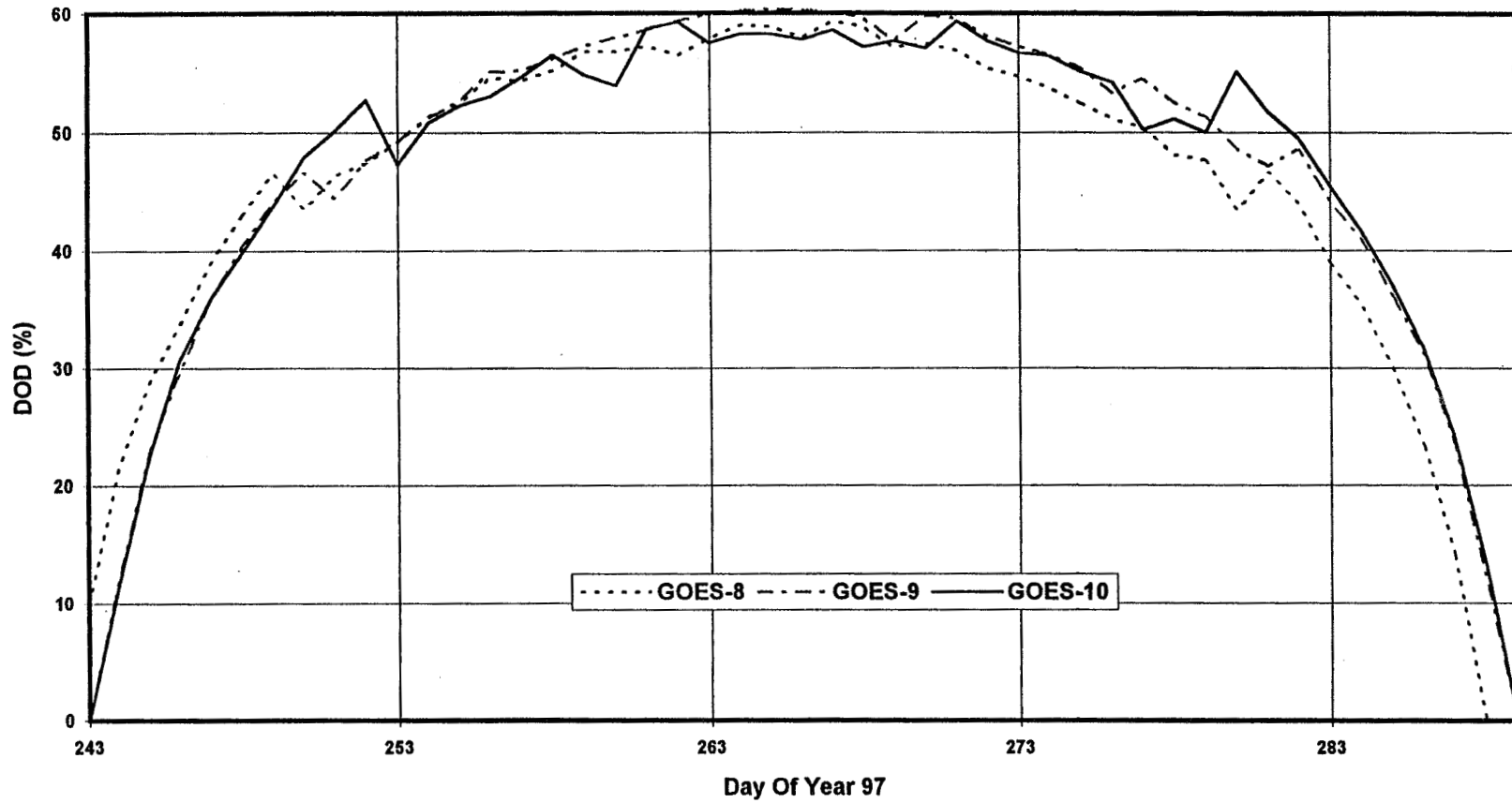
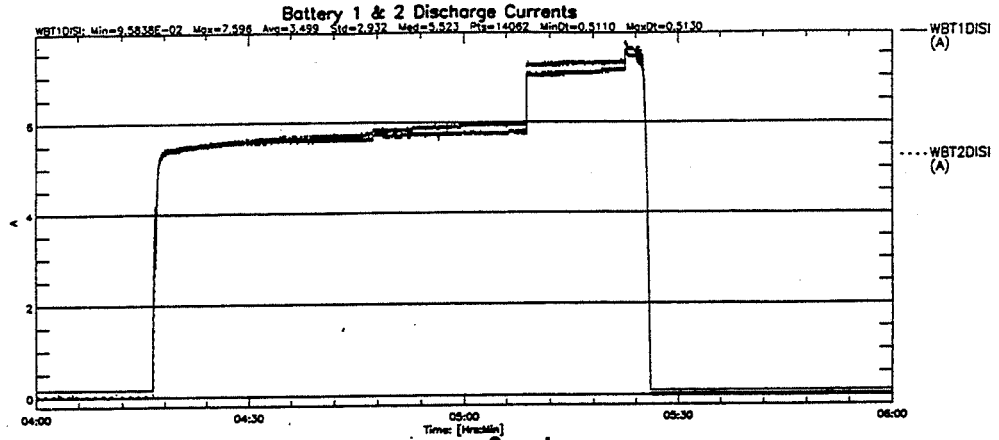


Figure 10. Battery Depth of Discharge (DOD) During the Fall 1997 Eclipse Season for GOES-8, GOES-9, and GOES-10.

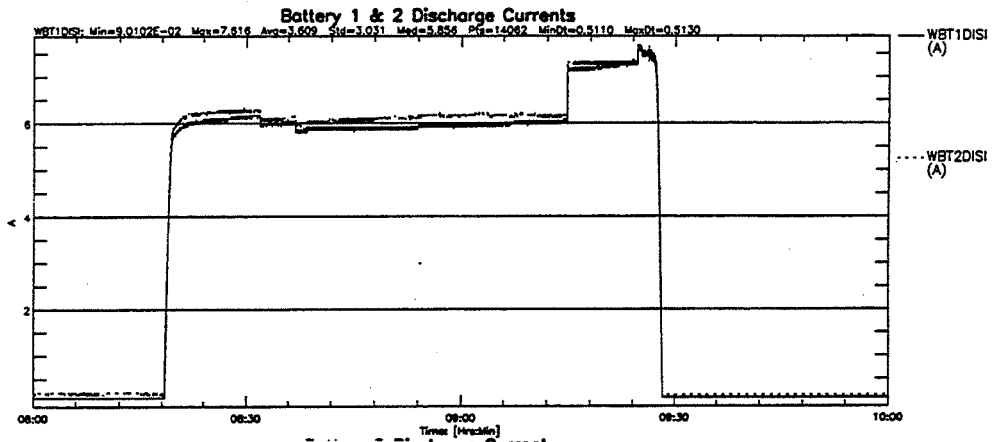
1997/266/04:00:00-1997/266/06:00:00
 ALL POINTS RETRIEVED
 SatPal Singhal (EPS)

Page: wbatdis_ SC08 (TEST1)
 Tue, 4-Nov-1997 10:17:13
 Minor Frame Quality: 100.00%



1997/266/08:00:00-1997/266/10:00:00
 ALL POINTS RETRIEVED
 SatPal Singhal (EPS)

Page: wbatdis_ SC09 (TEST1)
 Tue, 4-Nov-1997 10:17:51
 Minor Frame Quality: 100.00%



1997/266/06:00:00-1997/266/08:00:00
 ALL POINTS RETRIEVED
 SatPal Singhal (EPS)

Page: wbatdis_ SC10 (TEST1)
 Tue, 4-Nov-1997 10:18:08
 Minor Frame Quality: 100.00%

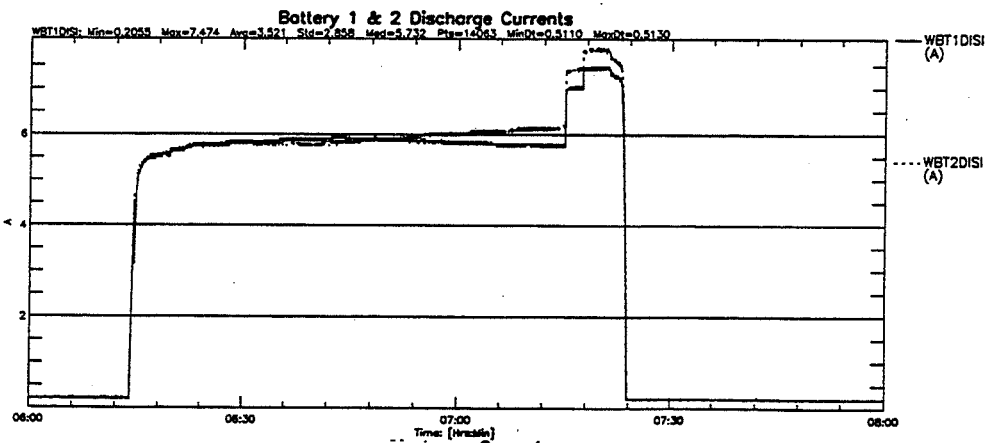


Figure 11. Battery Discharge Currents During the eclipse on Day 266 (September 23) of the Fall 1997 Eclipse Season for (a) GOES-8, (b) GOES-9, and (c) GOES-10.

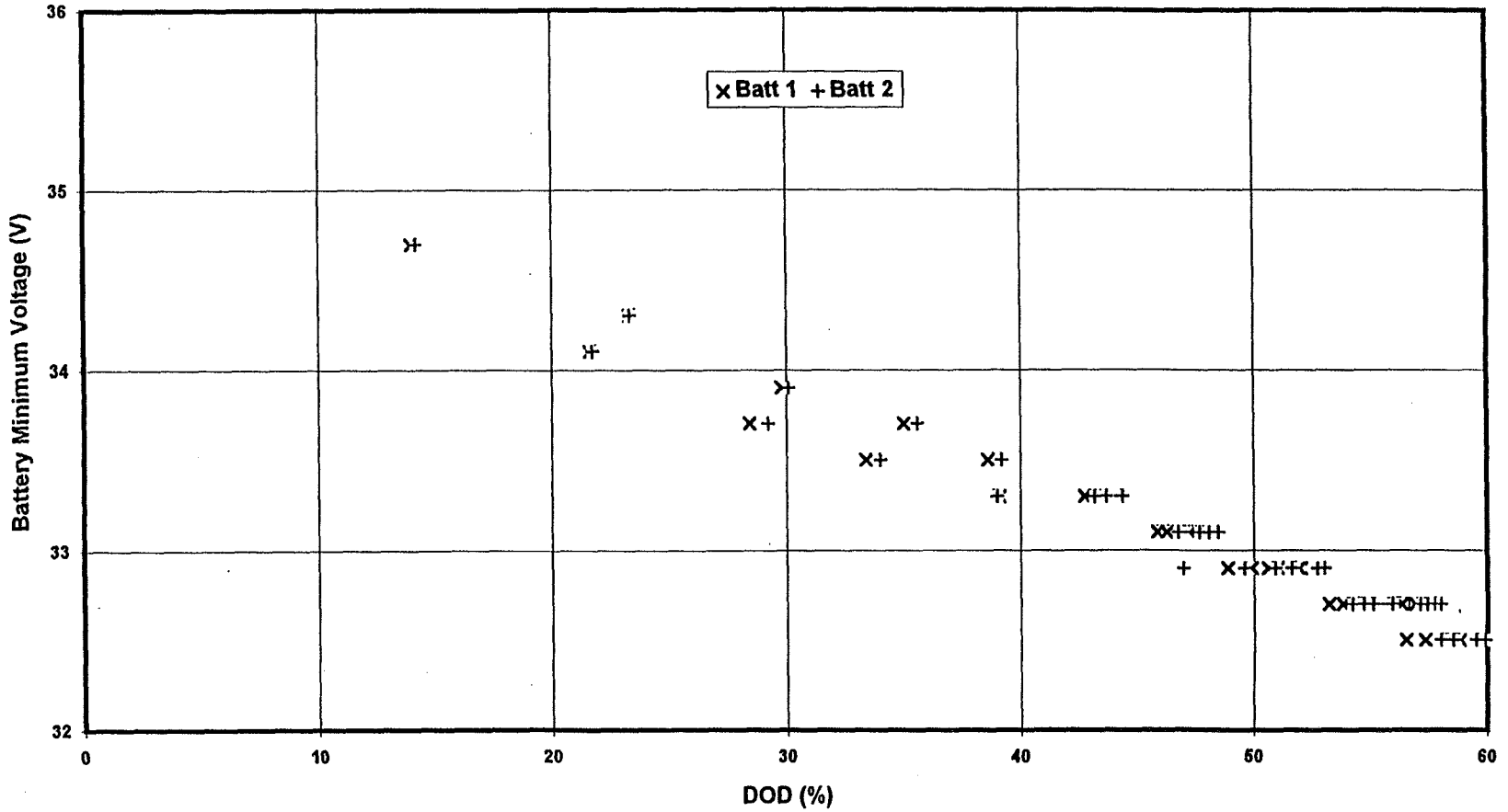


Figure 12. Battery Minimum Voltage as a Function of Battery Depth of Discharge (DOD) During the Fall 1997 Eclipse Season for GOES-8.

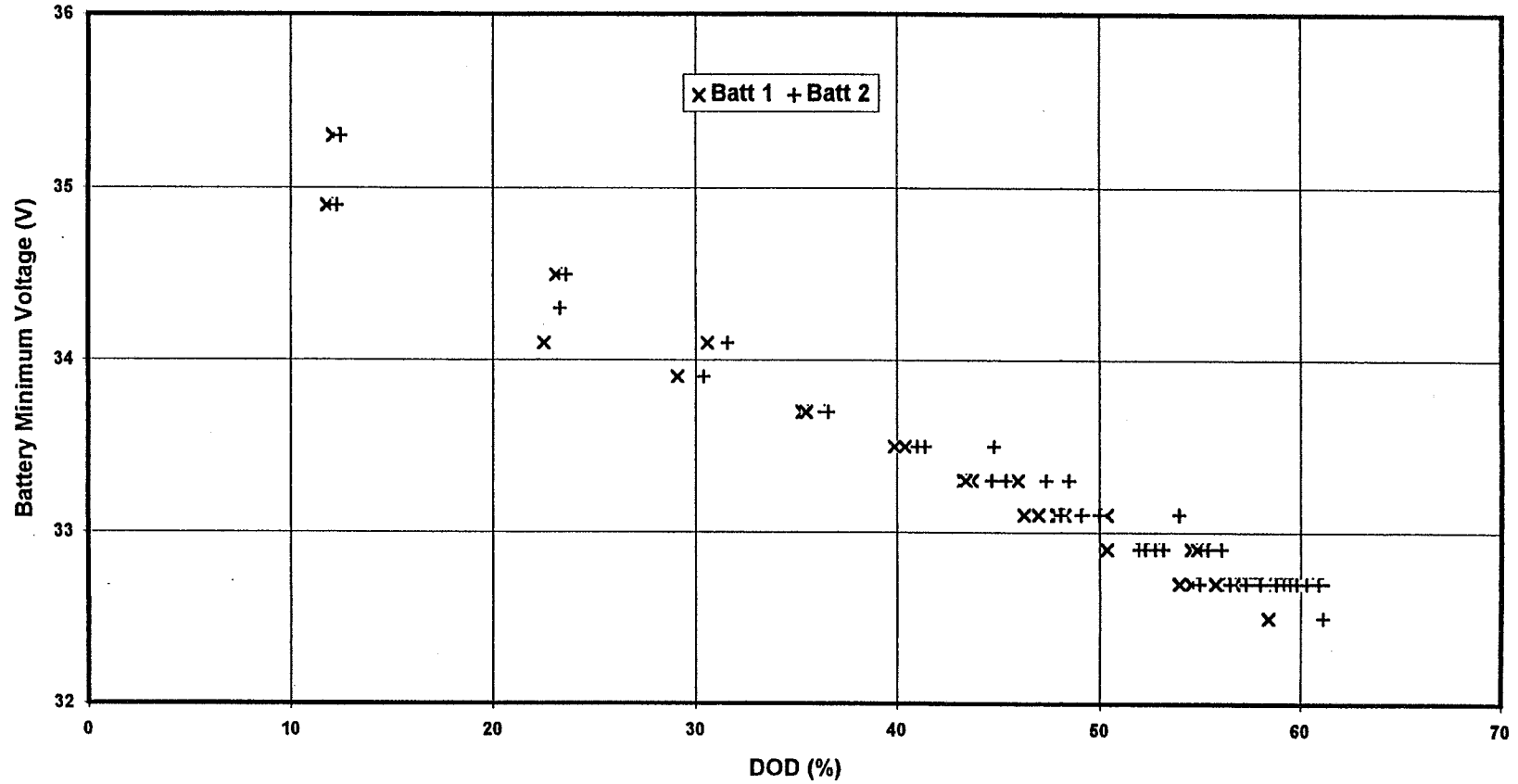


Figure 13. Battery Minimum Voltage as a Function of Battery Depth of Discharge (DOD) During the Fall 1997 Eclipse Season for GOES-9.

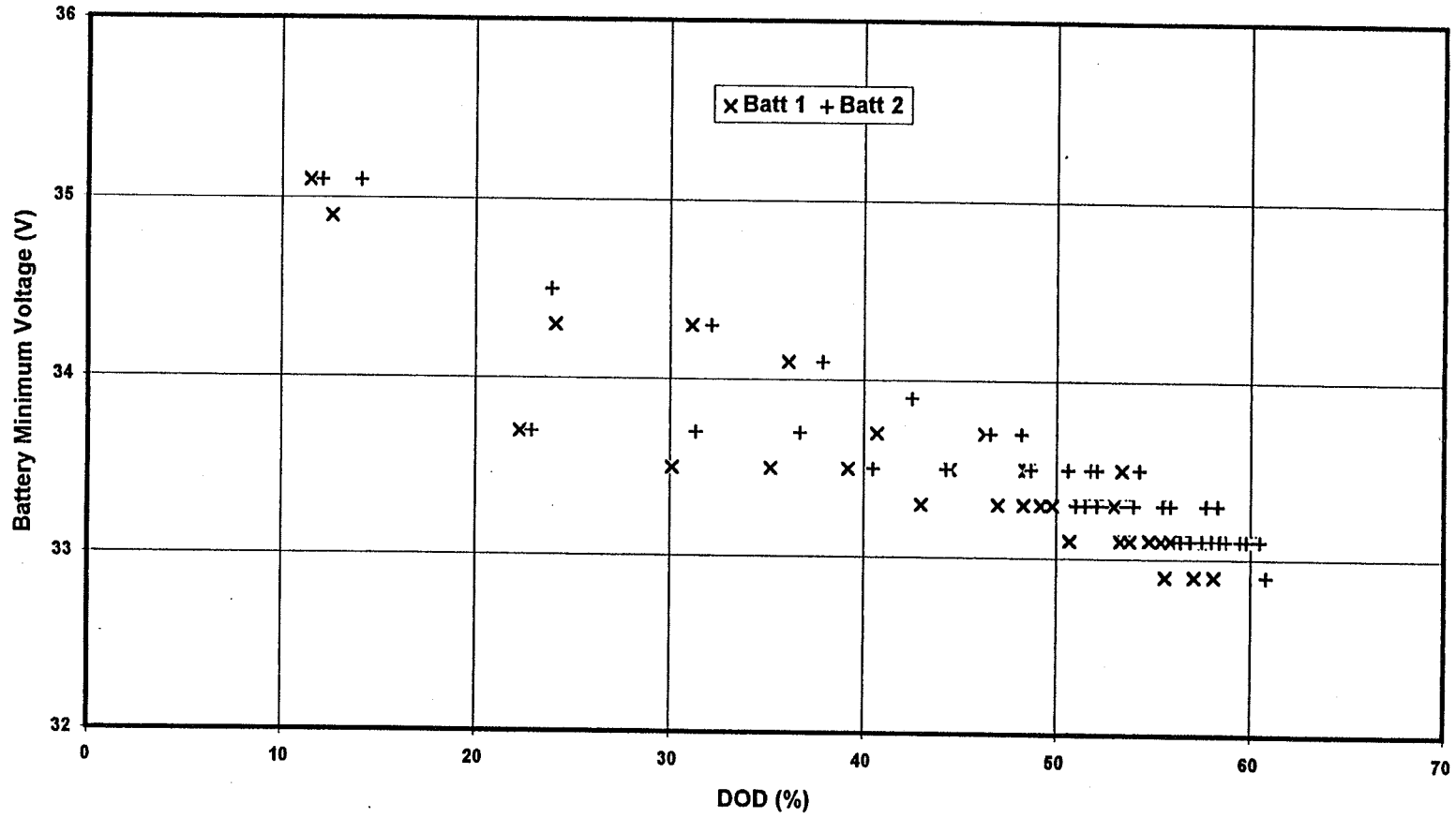


Figure 14. Battery Minimum Voltage as a Function of Battery Depth of Discharge (DOD) During the Fall 1997 Eclipse Season for GOES-10.

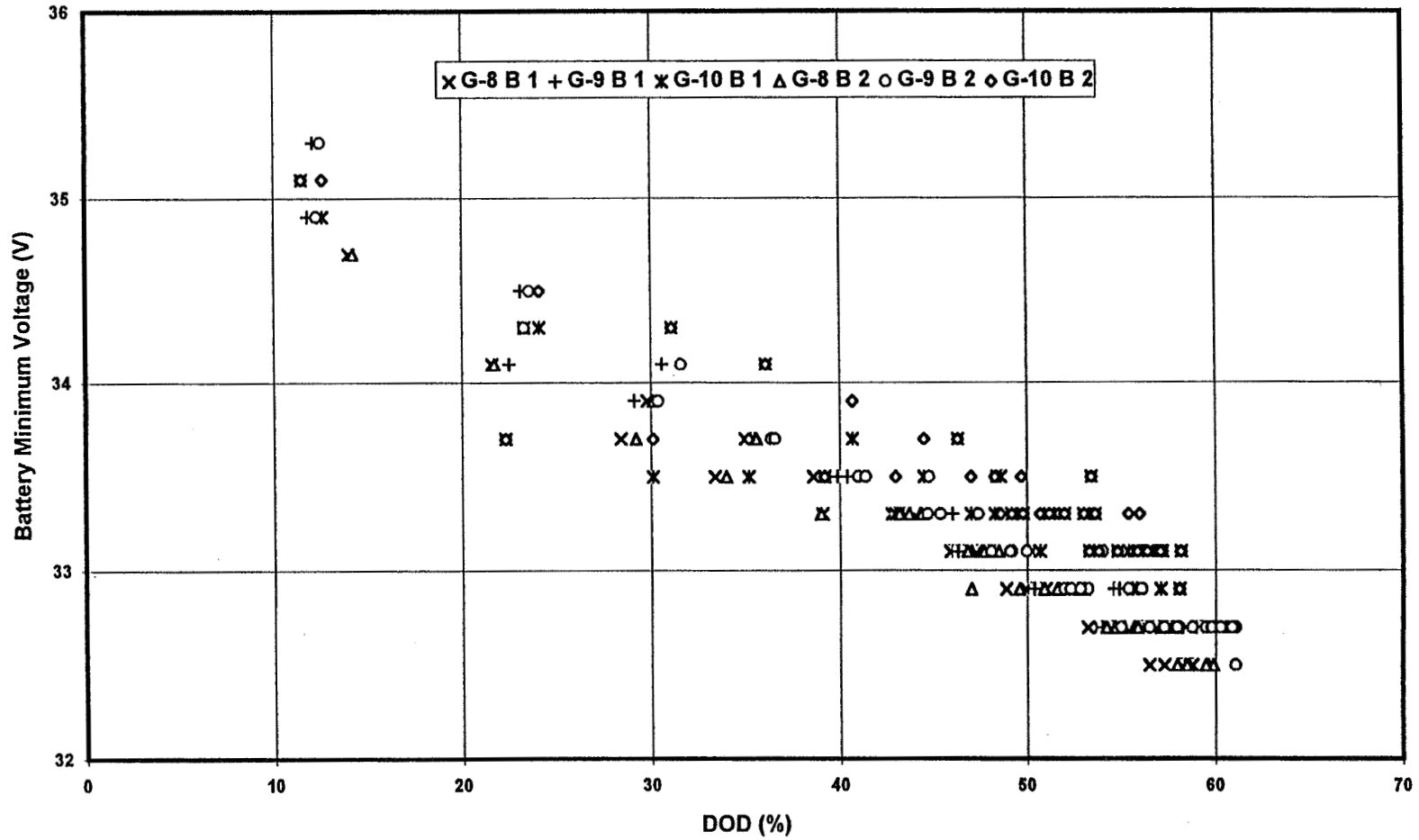


Figure 15. Battery Minimum Voltage as a Function of Battery Depth of Discharge (DOD) During the Fall 1997 Eclipse Season for all 6 Batteries on the GOES-8, -9, -10 Spacecraft.

During the Fall 1997 eclipse season, the minimum battery voltages recorded were 32.5 V, 32.5 V, and 32.9 V (both batteries) for GOES 8, 9, and 10 respectively. The minimum cell voltages recorded for the three spacecraft were: 1.160 V (Battery 1) and 1.161 V (Battery 2) for GOES-8; 1.161 V (both batteries) for GOES-9; and 1.174 V (Battery 1) and 1.186 V (Battery 2) for GOES-10.

The battery temperatures ranged from approximately 0 °C to 9 °C for GOES-8, 1 °C to 12 °C for GOES-9, and 2 °C to 13 °C for GOES-10. Daily peaks in the battery

temperatures were observed near the end of the discharge cycle while the minimums were recorded a few hours before the end of charge cycle, as expected.

Table 5 lists the minimum battery voltages during all of the eclipse seasons encountered by the three spacecraft. As expected, the minimum battery voltages get lower with the aging of the batteries but they seem to have leveled off at 32.5 Volts. The battery temperatures have stayed in the same range for all eclipses (values as indicated above for the latest eclipse season).

Table 5. Minimum Battery Voltages During the Eclipse Seasons

	GOES-8		GOES-9		GOES-10	
	Battery 1	Battery 2	Battery 1	Battery 2	Battery 1	Battery 2
Fall 1994	33.3 V	33.3 V				
Spring 1995	33.1 V	33.1 V				
Fall 1995	32.7 V	32.7 V	33.1 V	33.1 V		
Spring 1996	32.5 V	32.5 V	32.9 V	32.7 V		
Fall 1996	32.7 V	32.5 V	32.7 V	32.7 V		
Spring 1997	32.5 V	32.5 V	32.7 V	32.7 V		
Fall 1997	32.5 V	32.5 V	32.5 V	32.5 V	32.9 V	32.9 V

SUMMARY AND CONCLUSIONS

On-orbit performance of the batteries on GOES 8, 9, and 10 spacecraft indicates that the batteries are performing within specifications and results behave as a family. In addition, the battery capacities to date have shown improvement and indicate a leveling off at approximately 16 Ah under the C/48 discharge conditions. Ground test data indicate that the batteries will meet power requirements for the spacecraft mission life of 5-7 years.

ACKNOWLEDGMENTS

The authors wish to thank NASA for support of this work under contracts NAS 5-32590 and NAS 5-32600. They also wish to thank the following individuals for their help during preparation of this paper: Mr. Steve Hall (Naval Surface Warfare Center, Crane) for life cycle test data, Mr. Ron Hudak (SS/L) for activation and acceptance test data, Dr. Milt Phenneger (CSC), and Mrs. Cheryl Singhal for review of the paper.

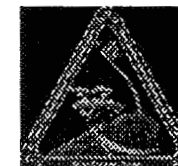
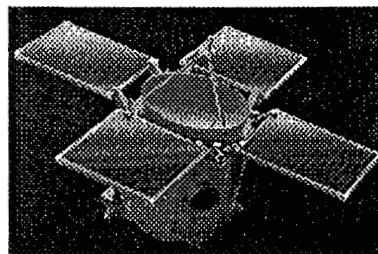
REFERENCES

1. GOES I-M Databook, DRL 101-08, GSFC Specification S-480-21A, SS/L, Palo Alto, CA.
2. GOES Program, Spacecraft Operations Handbook (SOH), Volume III (Rev G, August 1995), Spacecraft Description, SS/L, Palo Alto, CA.
3. GOES I-M Electrical Power Subsystem CDR, WDL-TR 11088, NAS5-29500.
4. Nickel Cadmium Battery Cell Lot 5 500 Cycle Test Final Report, GOES PCC TM PWR 3336

5. Harry Brown, Steve Hall, and Gopal Rao, Review of Ni-Cd Tests at Crane, presented at the 1997 NASA Aerospace Battery Workshop.

ACRONYMS

Ah	Ampere hour
AMF	Apogee Maneuver Firing
AOCS	Attitude and Orbit Control Subsystem
BOL	Beginning of Life
DOD	Depth of Discharge
DOY	Day of Year
EED	Electro-Explosive Device
EOD	End of Discharge
EOL	End of Life
GOES	Geostationary Operational Environmental Satellite
NASA	National Aeronautics and Space Administration
Ni-Cd	Nickel-Cadmium
NOAA	National Oceanic and Atmospheric Administration
NWS	National Weather Service
PCE	Power Control Electronics
PCU	Power Control Unit
SA	Solar Array
SS/L	Space Systems Loral



Near Earth Asteroid Rendezvous

Flight Battery Performance

1997 NASA Aerospace Battery Workshop

Jason E. Jenkins - JHU Applied Physics Laboratory

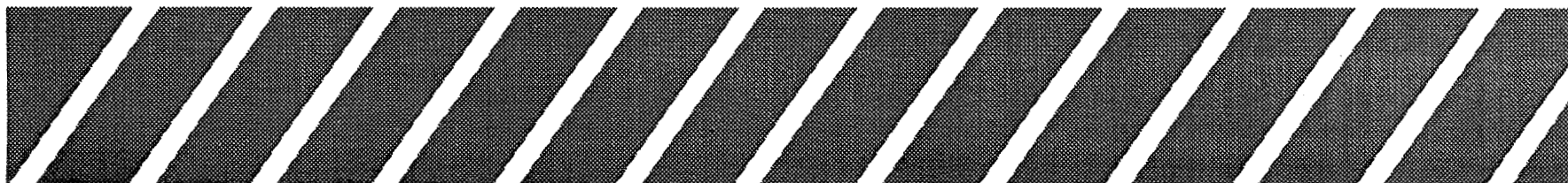
Jason.Jenkins@jhuapl.edu

Jeff W. Hayden - Eagle Picher Industries, Inc.

Jeff.Hayden@kktv.com

David F. Pickett - Eagle Picher Industries, Inc.

aaaa_energy_enterprises@msn.com



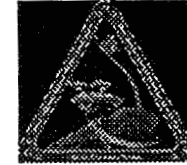
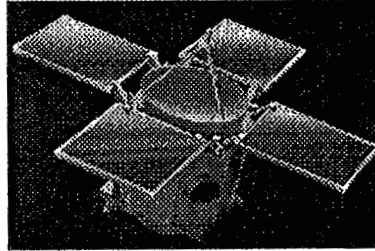
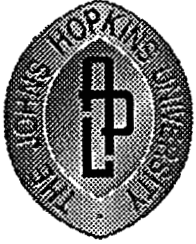


1997 NASA Battery Workshop NEAR Flight Battery Performance



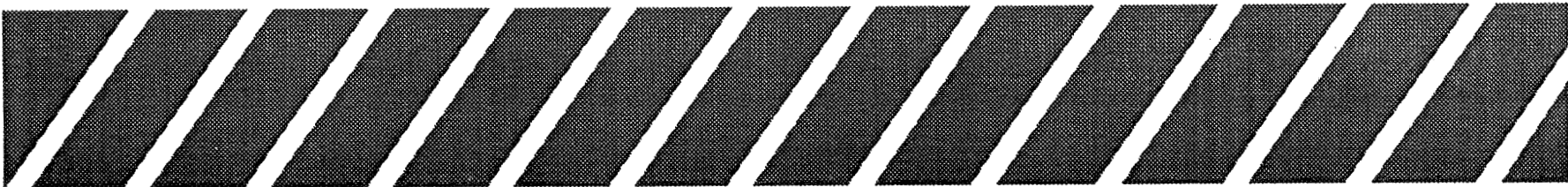
Presentation Outline

- ◆ Background & Flight Observation
 - Jason Jenkins - JHU/Applied Physics Laboratory
- ◆ Mission Simulation Tests
 - Jeff Hayden - Eagle-Picher Industries, Inc.
- ◆ Explanation of Events
 - David Pickett - Eagle Picher Industries, Inc.



Background & Flight Observations

Jason E. Jenkins - JHU Applied Physics Laboratory
Jason.Jenkins@jhuapl.edu



1997 NASA Battery Workshop
NEAR Flight Battery Performance



System Description



- ◆ **System / Mission Design**
 - DET power system architecture
 - Battery isolated from main bus by redundant linear regulated chargers and discharge diodes
 - Mission design allows solar-only baseline operation after launch
- ◆ **Battery Charging**
 - Ground commanded 2-level constant current charge control (C/20 & C/75) with concurrent 8-level VT limit (Modified NASA levels 0-7)
 - Over-temperature, over/under-voltage protection in autonomy software

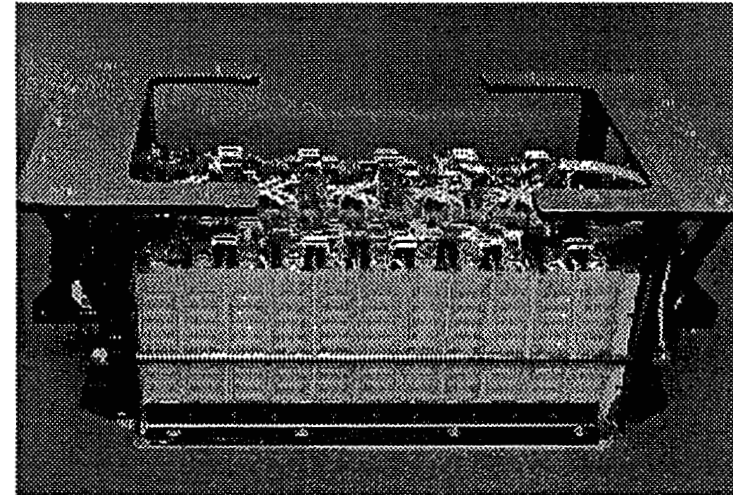


1997 NASA Battery Workshop NEAR Flight Battery Performance



Battery Description

- ◆ Battery Design
 - 22-Cell, 9-Ah TOMS-EP heritage Super NiCd™
 - Radiative thermal interface with thermostatically controlled heaters
 - Flight telemetry: stack/half-stack voltage, charge/discharge current, temperature



1997 NASA Battery Workshop
NEAR Flight Battery Performance



Battery Activity Overview

- ◆ NEAR launched February 18, 1996
 - 15.5% Launch DOD
 - Recharged at C/20 - VT5
 - Maintained at C/75 - VT5 trickle
- ◆ Four *Thermal Bias* modes in preparation for Mathilde observation Apr 25 - June 27, 1997
 - Unexpected I-V performance observed
 - Ground tests initiated on NEAR life-test cells at EPI
- ◆ Ground tests confirm no loss of capacity performance after extended trickle charge storage

NASA Battery Workshop, Huntsville,AL Nov 18-20, 1997



1997 NASA Battery Workshop NEAR Flight Battery Performance



Thermal Bias Regime

- ◆ Thermal bias intended to top-off battery and raise temperature to survive heater disablement during Mathilde observation
 - Start from C/75 - VT5 trickle charge
 - Raise VT limit to VT7 (highest available per system design)
 - Raise charge rate to C/20
 - Hold for 4.3 Hours
 - Lower charge rate to C/75
 - Lower VT limit to VT5
- ◆ Thermal bias regime performed 4 times on flight battery



1997 NASA Battery Workshop NEAR Flight Battery Performance



Flight Thermal Bias Observations

- ◆ First Thermal Bias (Shamtily 3A) performed in flight April 25, 1997 (14 months into mission)
 - Starting C/75-VT5 trickle charge was VT5 limited
 - ❖ Actual trickle charge current $\sim C/100$
 - With raised limits, current spiked to .21A quickly decreasing to .15A with voltage reaching VT7
 - Voltage stayed at VT7 with current gradually increasing to .35A over 4.3 h.
 - C/75-VT5 trickle charge following thermal bias did not reach VT5 limit.



1997 NASA Battery Workshop NEAR Flight Battery Performance

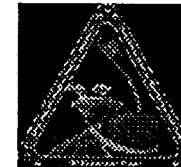


Flight Thermal Bias Observations (continued)

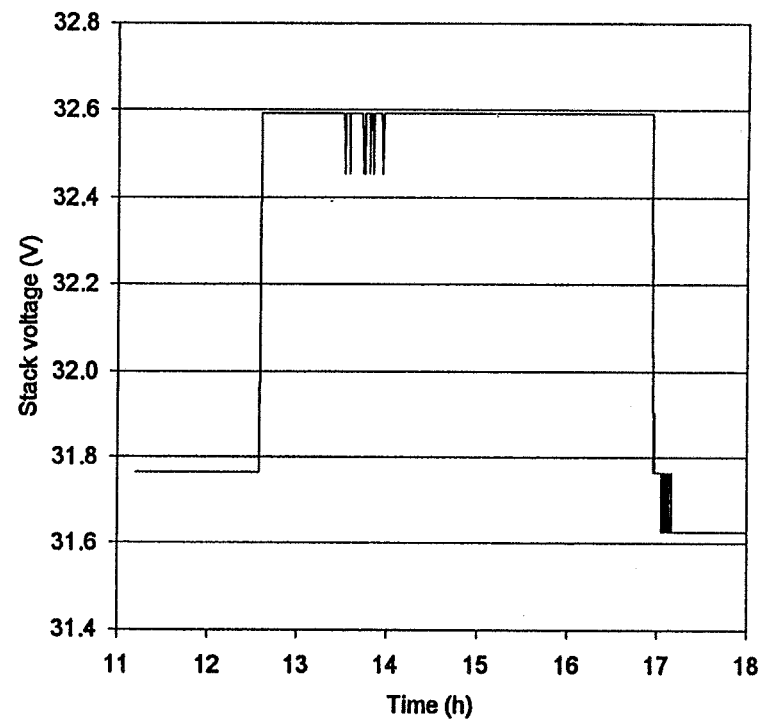
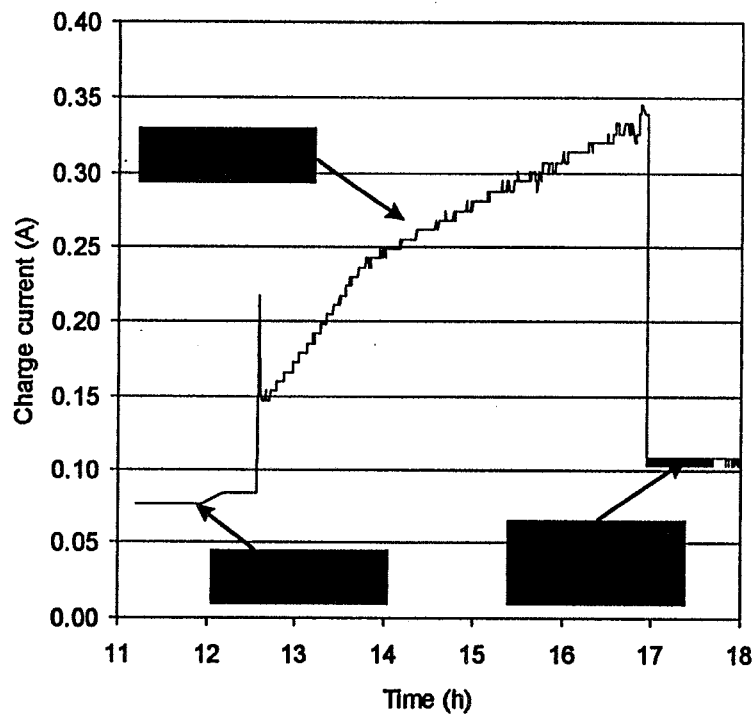
- ◆ Ground Test Regime commenced May 15, 1997
- ◆ Thermal bias repeated 3 additional times with similarly observed behavior
 - Shamtilly 4 - May 21, 1997
 - Shamtilly 5 - May 30, 1997
 - Mathilde Encounter - June 27, 1997



1997 NASA Battery Workshop NEAR Flight Battery Performance



Thermal Bias 1 (Shamtilly 3A) April 25, 1997



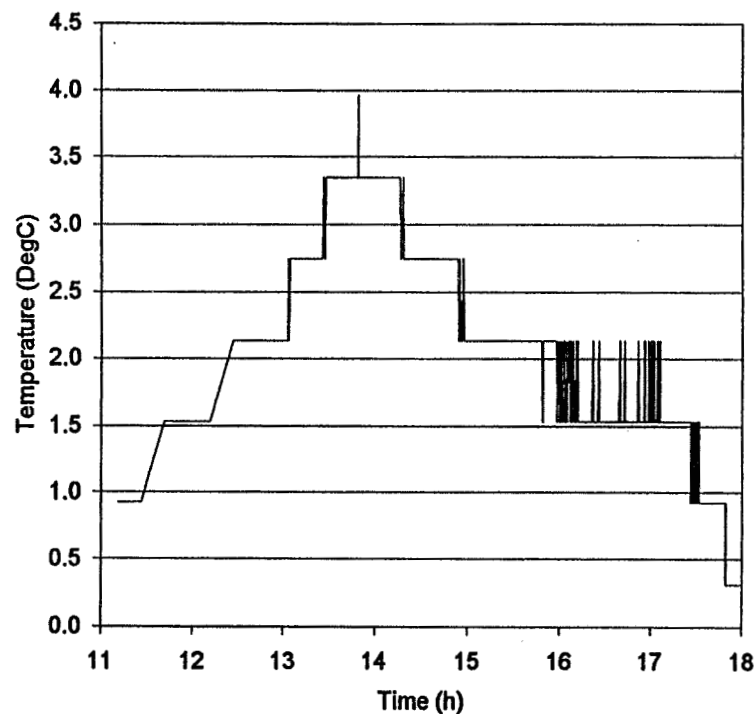
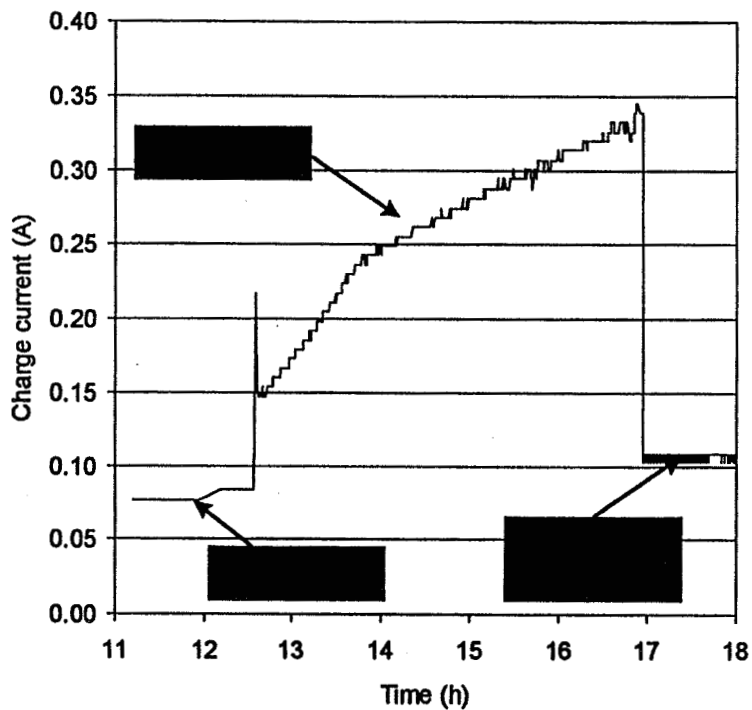


1997 NASA Battery Workshop NEAR Flight Battery Performance



Thermal Bias 1 (Shamtilly 3A)

April 25, 1997 (continued)



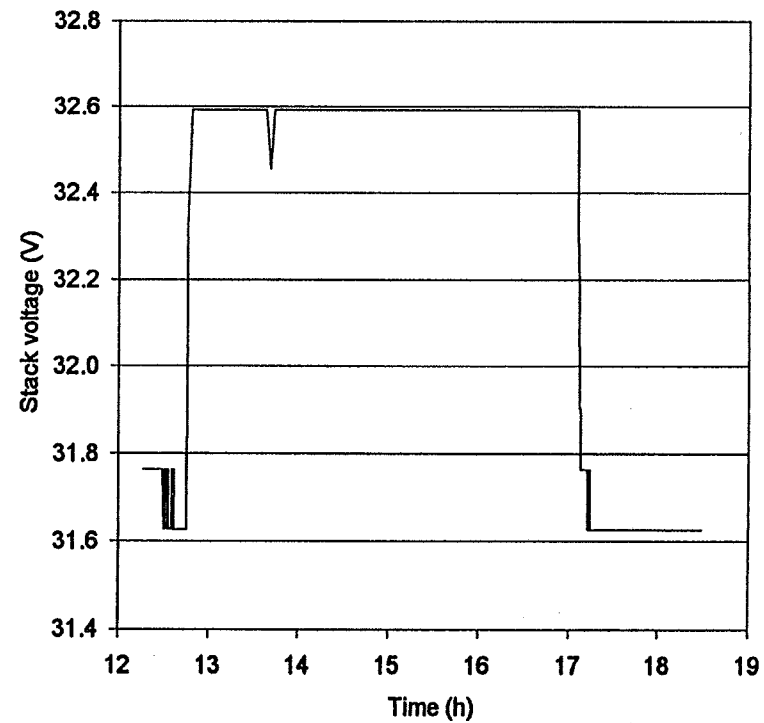
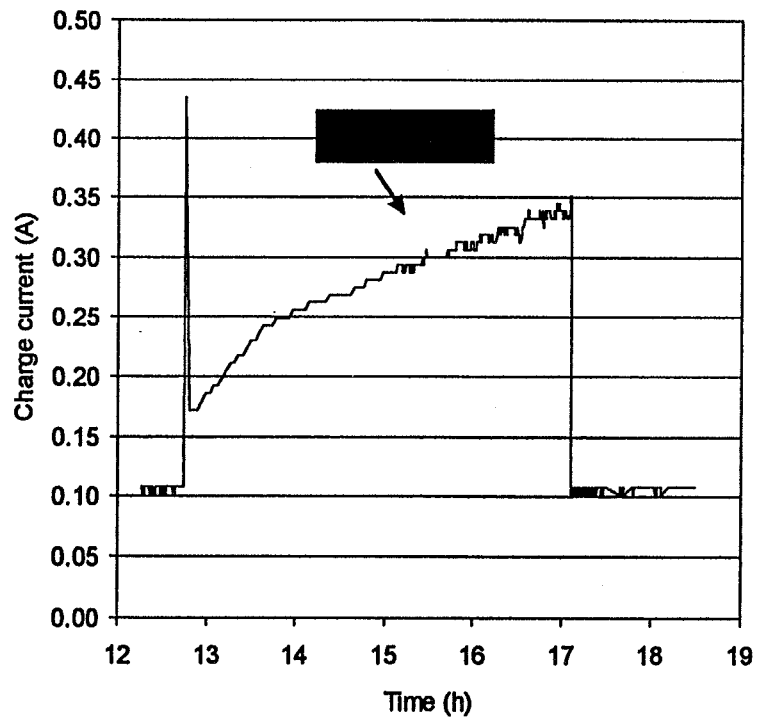


1997 NASA Battery Workshop NEAR Flight Battery Performance



Thermal Bias 2 (Shamtilly 4)

May 21, 1997

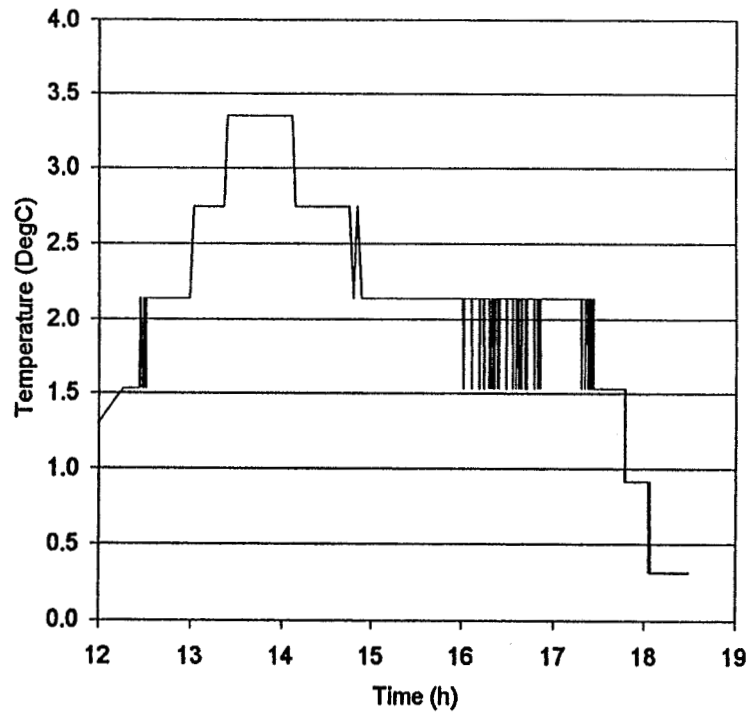
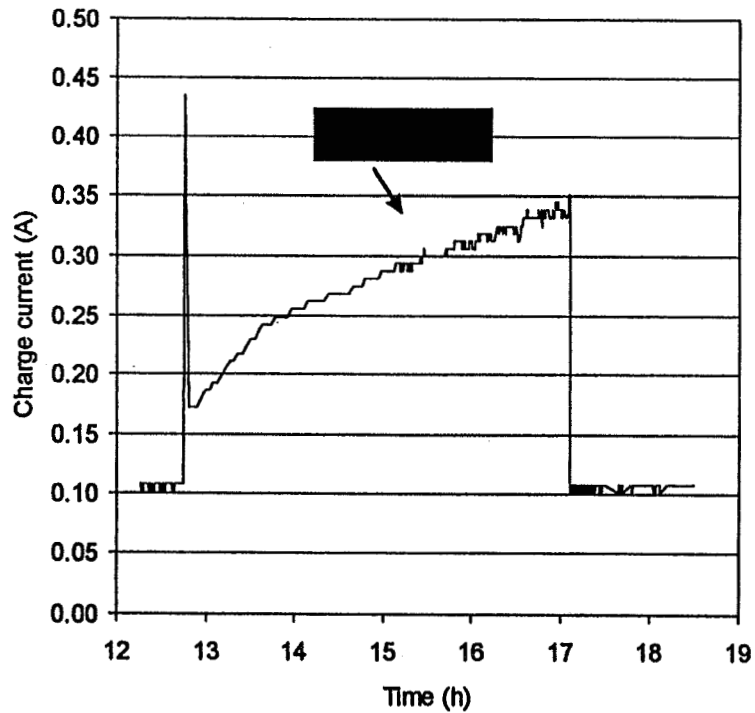




1997 NASA Battery Workshop NEAR Flight Battery Performance

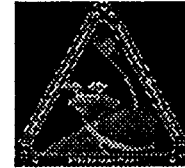


Thermal Bias 2 (Shamtilly 4) May 21, 1997 (continued)



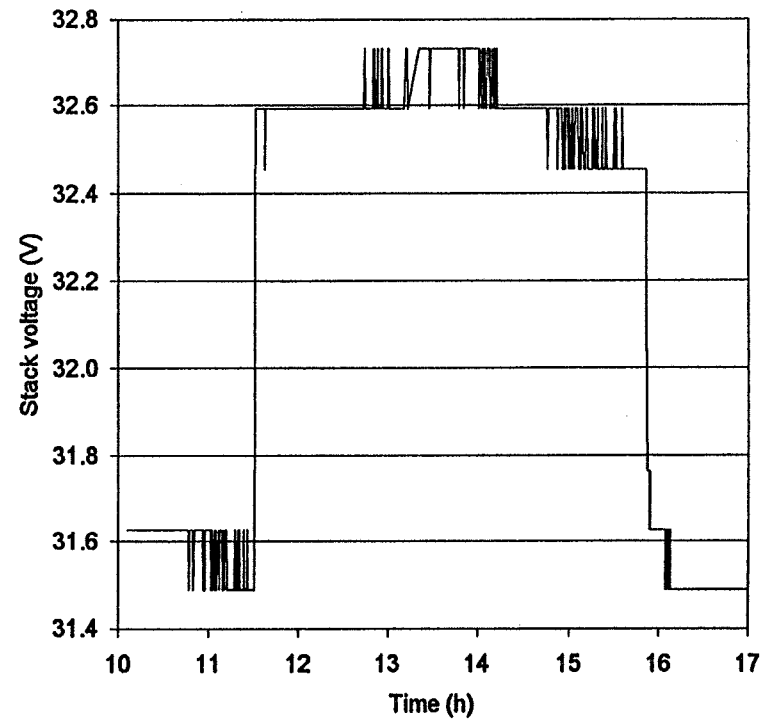
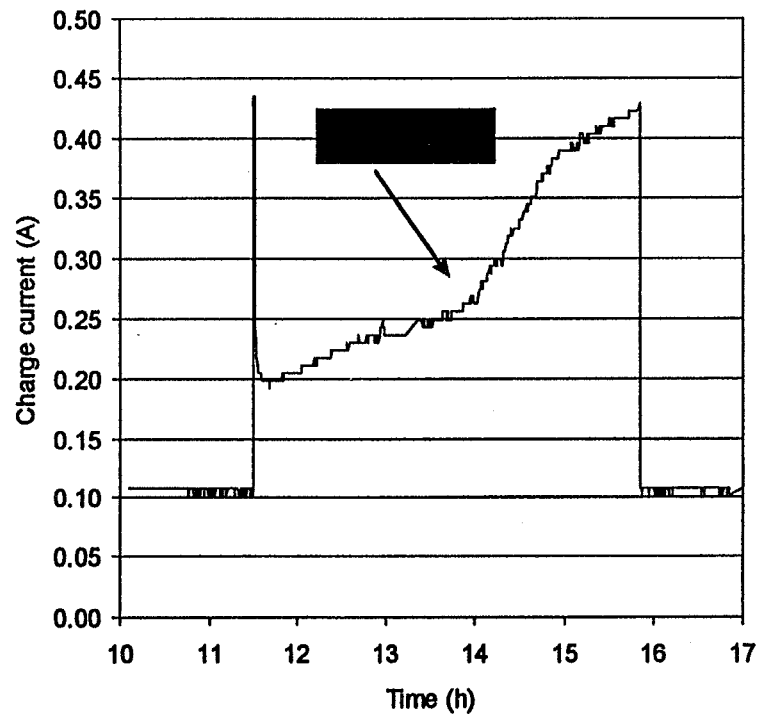


1997 NASA Battery Workshop NEAR Flight Battery Performance



Thermal Bias 3 (Shamtilly 5)

May 30, 1997



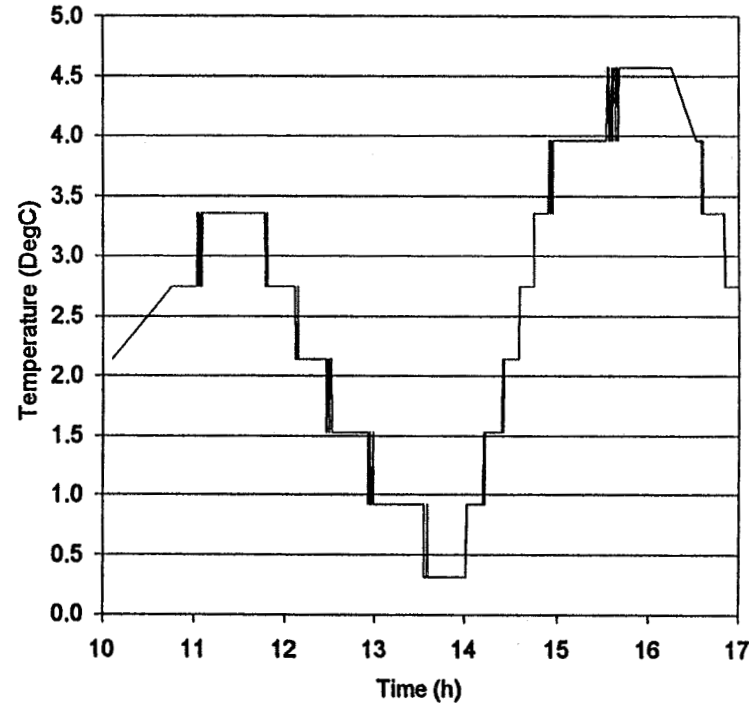
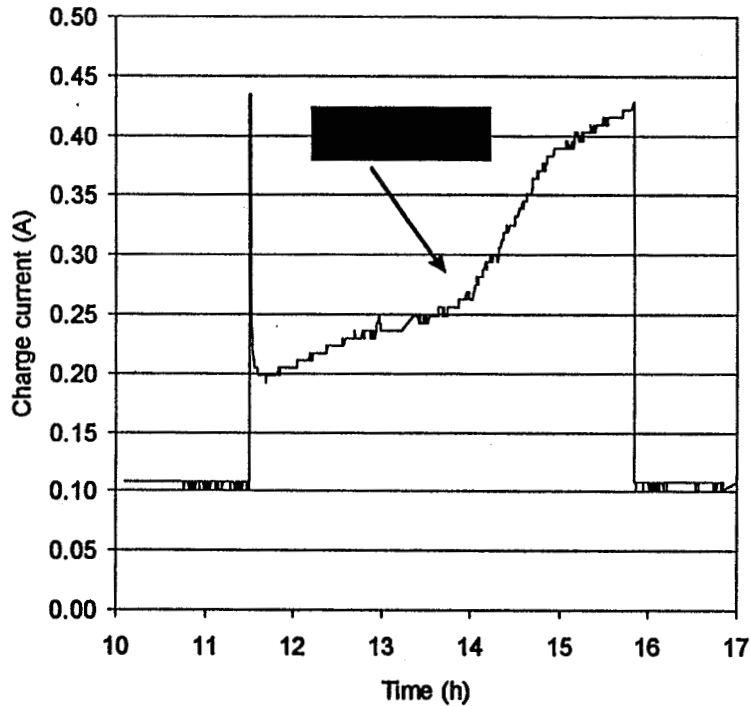


EAGLE EPICHER
POWER SYSTEMS DEPARTMENT

1997 NASA Battery Workshop NEAR Flight Battery Performance



Thermal Bias 3 (Shamtilly 5) May 30, 1997 (continued)



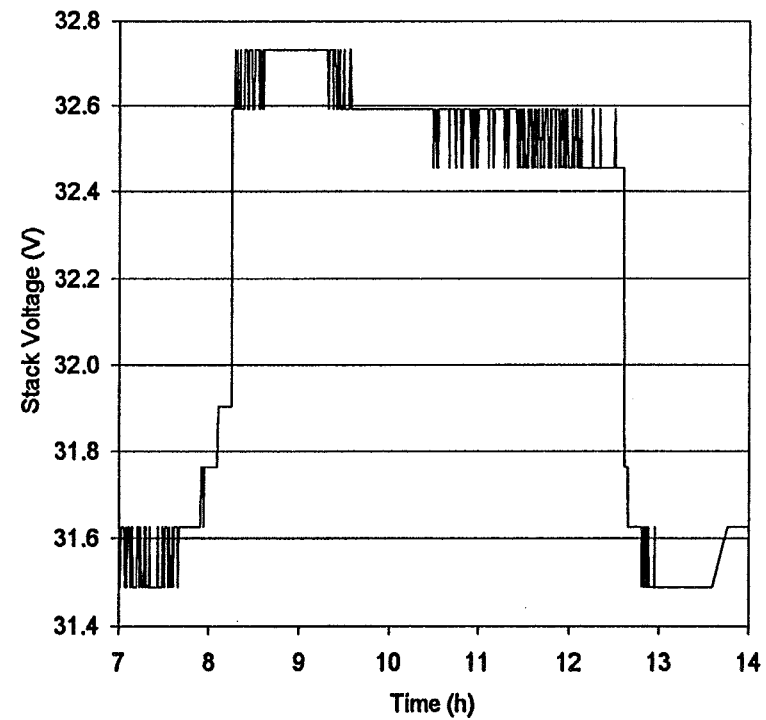
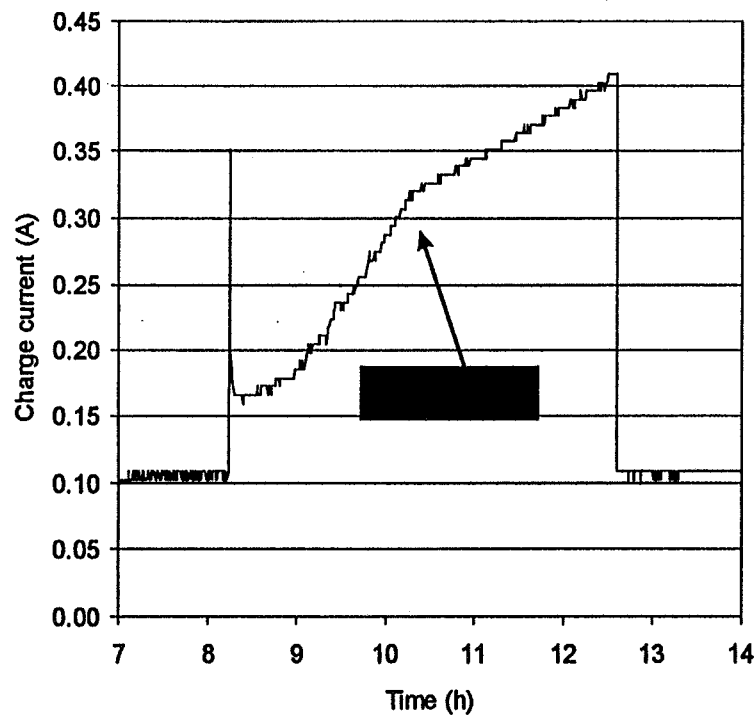


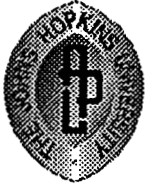
1997 NASA Battery Workshop NEAR Flight Battery Performance



Thermal Bias 4 (Mathilde Encounter)

June 27, 1997

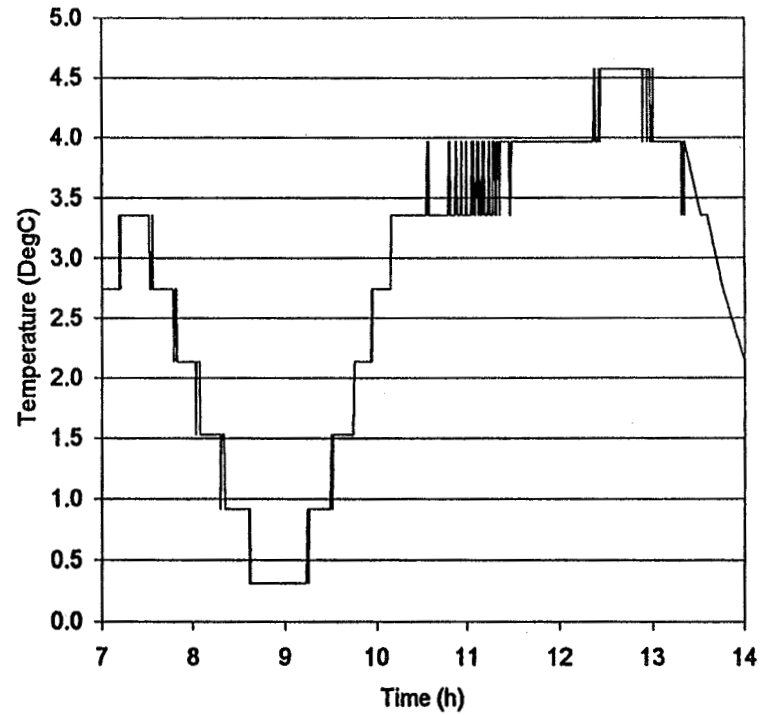
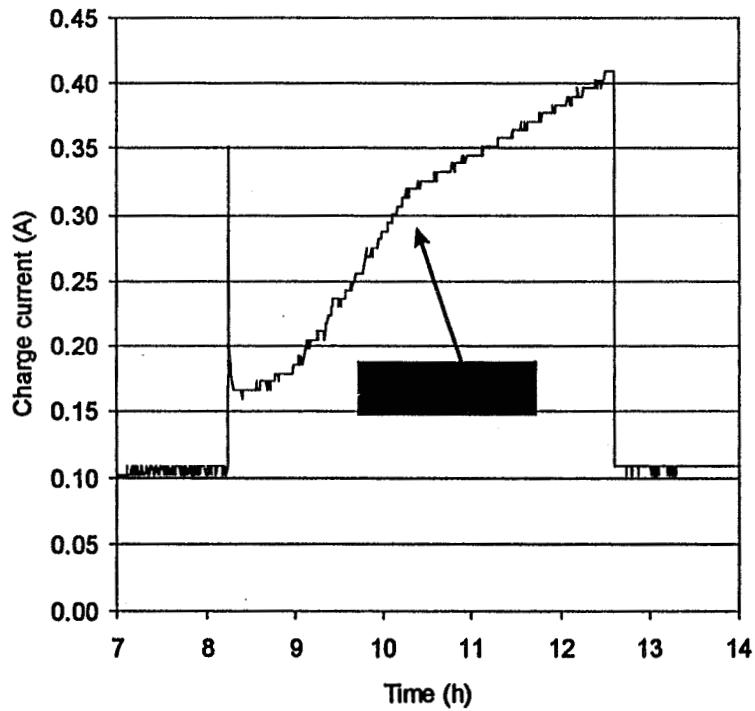


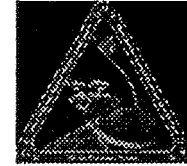
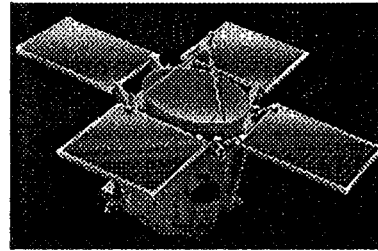
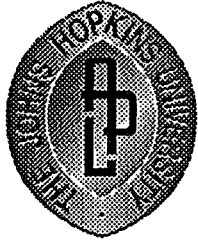


1997 NASA Battery Workshop NEAR Flight Battery Performance



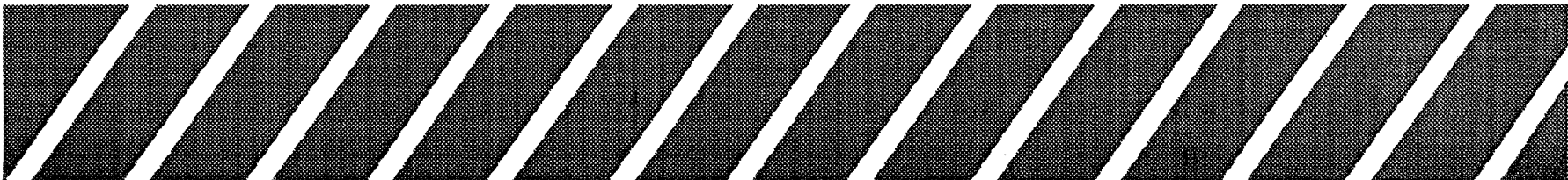
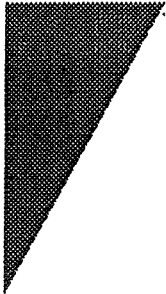
Thermal Bias 4 (Mathilde Encounter) June 27, 1997 (continued)





Mission Simulation Test

Jeff W. Hayden - Eagle Picher Industries
Jeff.Hayden@kktv.com





1997 NASA Battery Workshop NEAR Flight Battery Performance



Spacecraft Cruise Simulation

November 30, 1995 through May 15, 1997

◆ Trickle Charge

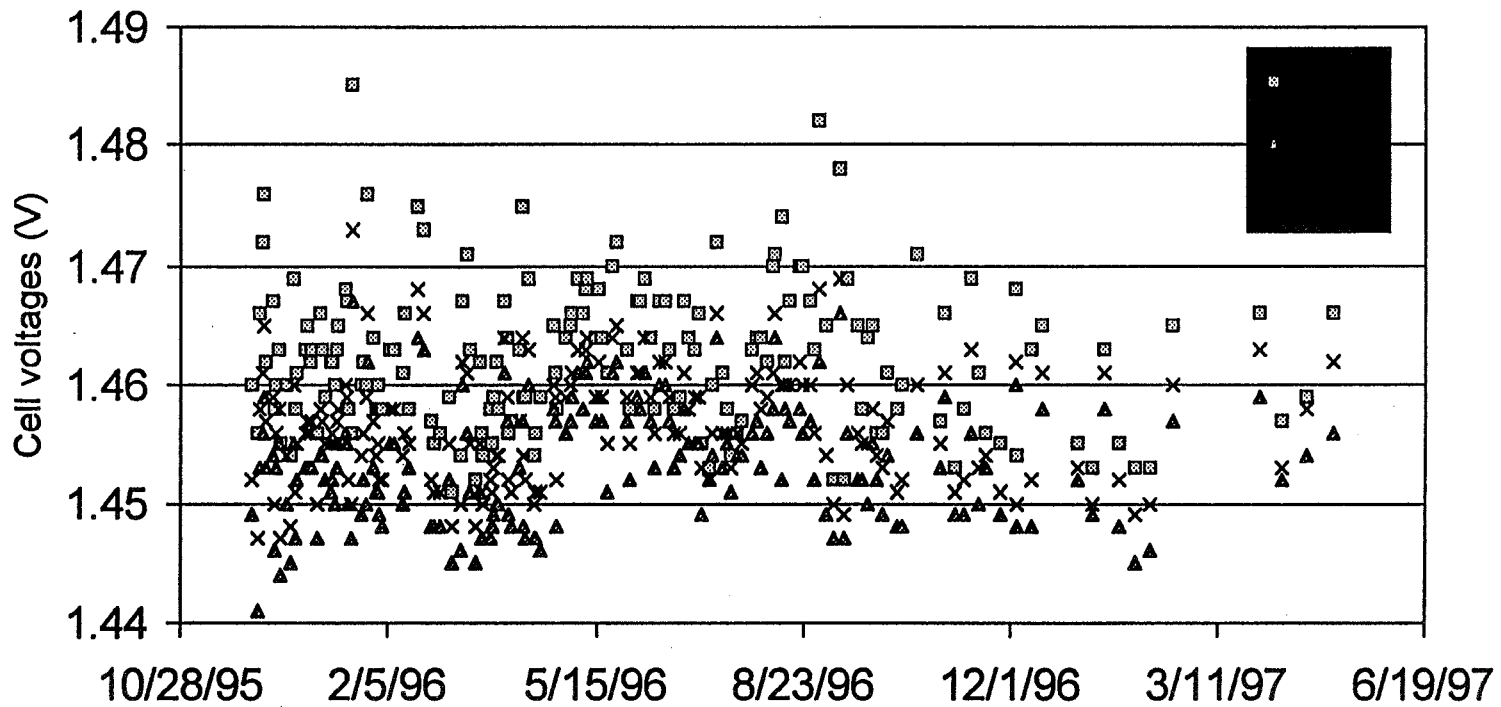
- Test cells were selected from the NEAR flight lot
 - ◆ 9-Ah 18964EC-9 Super NiCd™ Cell Lot 2
- Nine cells were assembled into a battery for the trickle charge portion of the test
- The nine cell battery was trickle charged at +5 degrees Celsius with 0.140 A



1997 NASA Battery Workshop NEAR Flight Battery Performance



Cruise Simulation at EPI





1997 NASA Battery Workshop NEAR Flight Battery Performance



Test Battery Reconfiguration



- ◆ The original nine-cell battery was reconfigured into 2 four-cell batteries, with the 9th cell set aside
 - Battery 1 consists of four cells: serial numbers 5, 46, 70, and 73
 - Battery 2 consists of four cells: serial numbers 9, 36, 37 and 50



1997 NASA Battery Workshop NEAR Flight Battery Performance



Battery 1 Capacity Measurement May 15, 1997

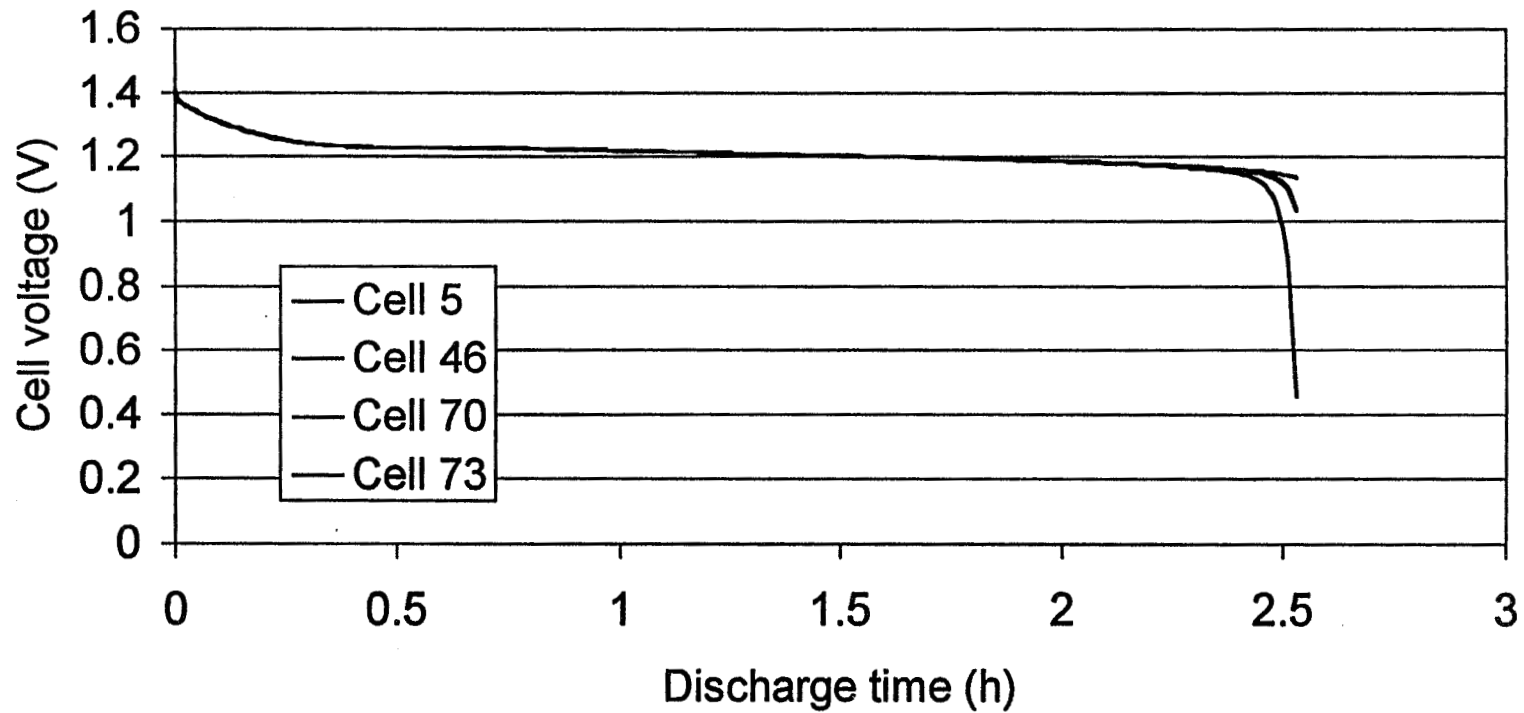
- ◆ Returned to a trickle charge at .12 A
 - Temperature, current, and voltage stabilized
- ◆ Discharged at C/2 (4.5 A) until the first cell reached 0.5 V
 - Battery temperature at 5 degrees Celsius
- ◆ Battery 1 delivered 11.4 Ah after being on trickle charge for 17.5 months
 - End-of-discharge voltages were as follows:



1997 NASA Battery Workshop NEAR Flight Battery Performance



Battery 1 Capacity Discharge 11.4 Ah





1997 NASA Battery Workshop NEAR Flight Battery Performance



Battery 2 Thermal Bias Simulation

- ◆ Returned to a trickle charge at .12 A
 - Temperature, current, and voltage stabilized
- ◆ Trickle charged at 0.12 A constant current with a voltage clamp at VT 5 or 5.792V for 2 weeks
 - The voltage clamp was not reached



1997 NASA Battery Workshop NEAR Flight Battery Performance

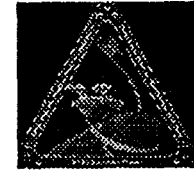


Battery 2 Thermal Bias Simulation (Continued)

- ◆ The VT 5 clamp was raised to VT 7 and the current clamped at .45 Amps for 4.3 Hours
 - The current initially spiked to about 0.44 Amps
 - The current fell to about 0.37 Amps before it began to slowly increase
 - The entire spike event lasted about 13 minutes
 - The current increased over a 17 minute period until the 0.45 Current clamp was reached



1997 NASA Battery Workshop NEAR Flight Battery Performance



Battery 2 Thermal Bias Simulation (Continued)

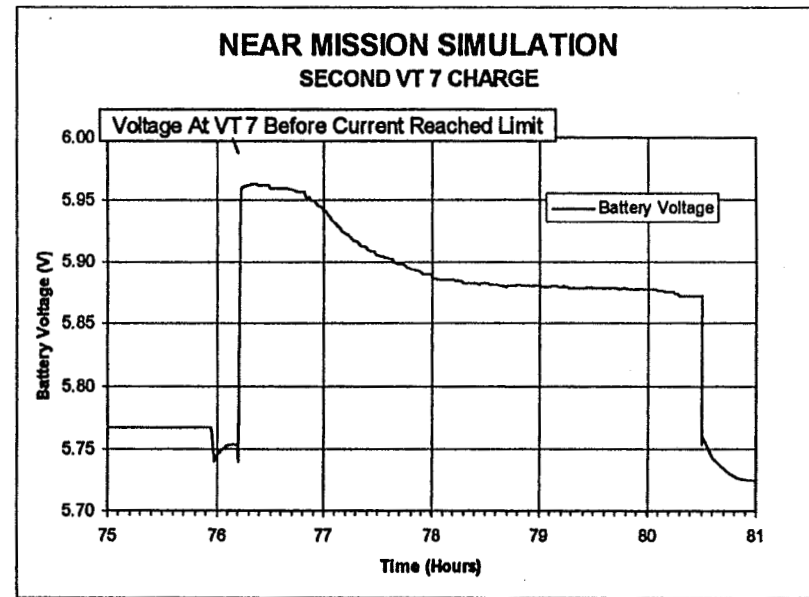
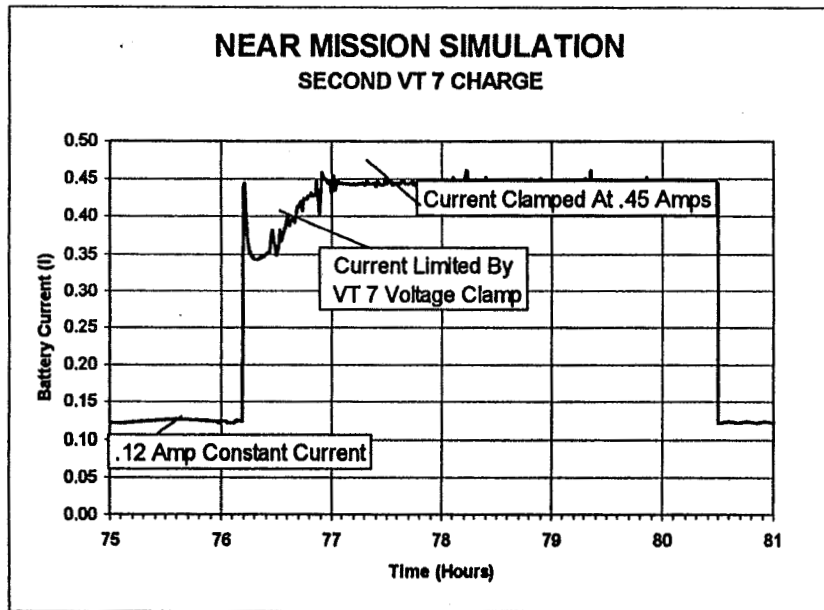
- ◆ After 4.3 Hours the VT7 level was reduced to VT5 and the current maintained at 0.12 A
- ◆ The thermal bias simulation was repeated 3 additional times before the battery was discharged



1997 NASA Battery Workshop NEAR Flight Battery Performance



2nd Thermal Bias Simulation

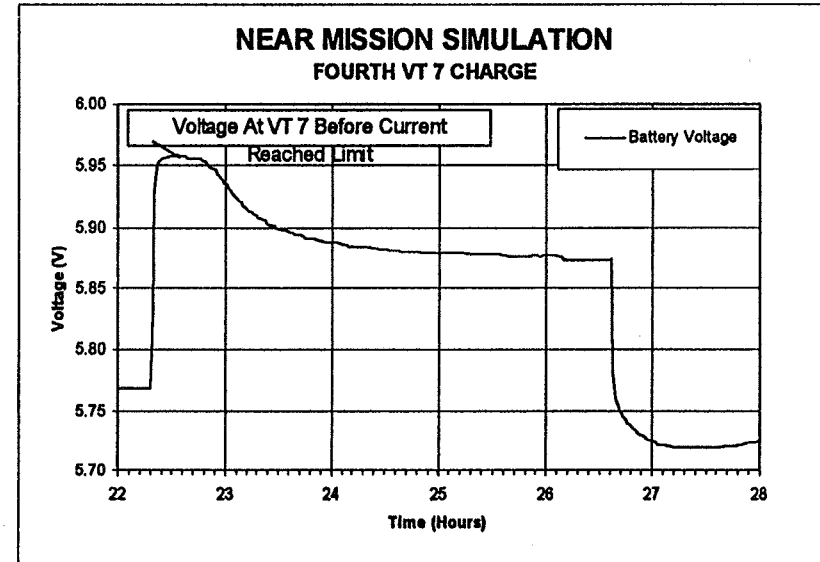
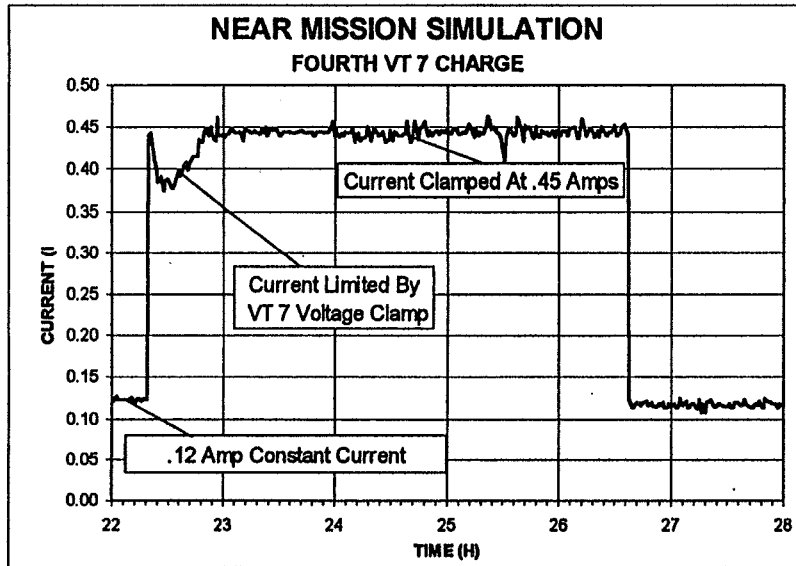




1997 NASA Battery Workshop NEAR Flight Battery Performance



4th Thermal Bias Simulation



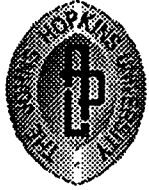


1997 NASA Battery Workshop NEAR Flight Battery Performance

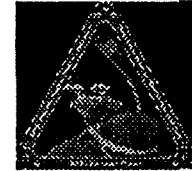


Battery 2 Capacity Measurement June 6, 1997

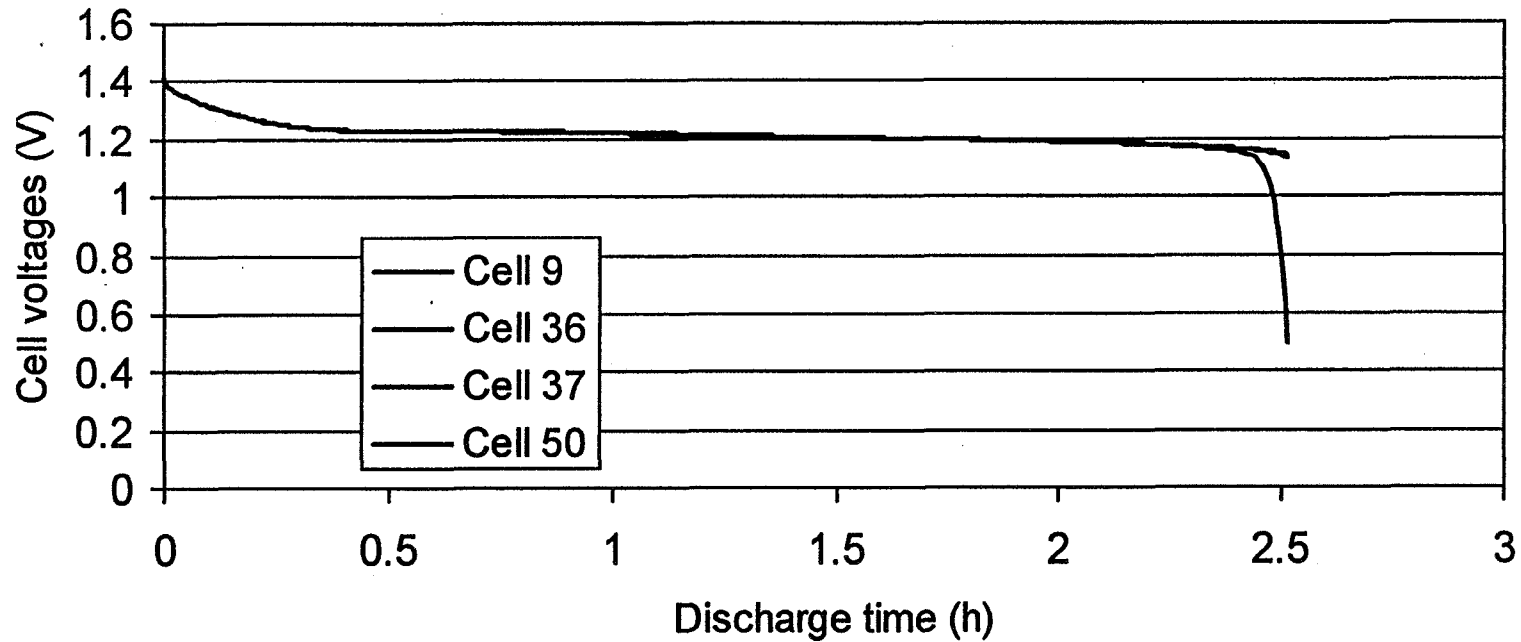
- ◆ Discharged at C/2 (4.5 A) until the first cell reached 0.5 V
 - Battery temperature at 5 degrees Celsius
- ◆ Battery 2 delivered 11.2 Ah after being on trickle charge for 17.5 months and boost-charged at the C/20-VT7 level four times



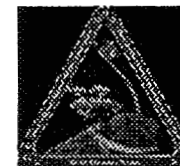
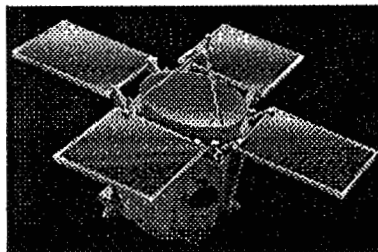
1997 NASA Battery Workshop NEAR Flight Battery Performance



Battery 2 Capacity Discharge 11.2 Ah



NASA Battery Workshop, Huntsville, AL Nov 18-20, 1997



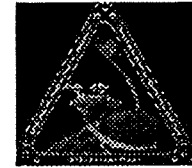
Explanation of Events

David F. Pickett - Eagle Picher Industries
aaaa_energy_enterprises@msn.com





1997 NASA Battery Workshop NEAR Flight Battery Performance



Battery on Trickle Charge

- ◆ Very little, if any, active material is being converted
- ◆ Cells are at their oxygen gassing potential
 - All current is being used to generate oxygen which is recombined by the cadmium electrode.
 - Generation and recombination rate vary according to trickle charge current.
- ◆ Cells are not at same state-of-charge as they would be if charged at a higher rate (say C/20)



EAGLE P ICHER
POWER SYSTEMS DEPARTMENT

1997 NASA Battery Workshop NEAR Flight Battery Performance



VT7 Level Imposed

- ◆ Cells now accept more current from charging circuit
- ◆ A current spike results from nonfaradaic charging (capacitive or whatever)
- ◆ Spike decays after physical charging of electrode surface subsides.
- ◆ Electrodes in cell begin accepting faradaic charge
 - Gassing
 - Active material conversion



1997 NASA Battery Workshop NEAR Flight Battery Performance



VT7 Level Imposed (continued)

- ◆ Electrodes are accepting charge with positive electrode limiting.
- ◆ Cells most likely will not reach hydrogen gassing potential (unless one or more cells out of balance) because of voltage clamp
- ◆ As upper voltage clamp is reached acceptance decreases
- ◆ VT5 level is imposed once the VT7 time interval has timed out at 4.3 hours



1997 NASA Battery Workshop NEAR Flight Battery Performance



VT5 Level Resumed

- ◆ Battery now reverts back to trickle charge mode
- ◆ Post VT7 voltage reduced due to removed polarization during overcharge.

Page intentionally left blank



1997 NASA AEROSPACE BATTERY WORKSHOP



**CRANE CELL TESTING
SUPPORT OF
Goddard Space Flight Center**
Steve Hall and Harry Brown
NAVSURFWARCENDIV Crane
Gopalakrishna Rao
NASA Goddard Space Flight Center



AEROSPACE BATTERY CELL TESTING



- Verification Of Secondary Cells
- Objective and Benefit

To verify the quality and reliability of aerospace battery cells and batteries for NASA flight programs and to design the battery/cell for upcoming NASA spacecraft.



GSFC LEO PROGRAMS

PROJECT	PACK	TYPE	Ah	ORBIT		°C	K CYCLE
				CHG TYPE	DoD		
NICKEL CADMIUM							
SWAS	6016F	SUPER	21	MISSION/A	VAR	5	12
POES	0040P	SAFT/F	40	MISSION/B		5	6
POES	0041P	SAFT/F	40	STRESS/B		20	6
POES	0042P	SAFT/F	40	STRESS/B		20	1
XTE	0052T	SUPER	50	MISSION/A		14.4	13
TRMM	0053T	SUPER	50	MISSION/A		17	12
TRMM	6151T	SUPER	50	MISSION/A		25	10
TRMM	6152T	SUPER	50	MISSION/A		17	0
NICKEL HYDROGEN							
LANDSAT	3050H	EPI	50	MISSION/A	20	5	10
HST	3600H	EPI	93	MISSION/C	11	-5	27
HST	3601H	EPI	93	MISSION/C	11	-5	27

Chart above shows LEO orbit packs cycling at Crane associated with GSFC flight programs. There is a total of 11 project packs currently cycling. Nine of these are mission simulation regimes and the remaining two are in a 40% DoD stress test regime.

Pack 6016F is a variable DoD cycling regime. The DoD changes every 30 days with a 7 day trickle charge between changes. This sequence is 5, 20, 10, 25, 5, 10, 5, 20 and 10 percent depth of discharge and is repeated until the end of life.

Charging techniques vary for each pack and are listed below:

- A. Constant current with a V/T to a C/D ratio then trickle charge.
- B. Constant current with a V/T.
- C. Constant current to specific voltage then trickle charge.



GSFC GEO PROGRAMS

PROJECT	PACK	TYPE	Ah	ORBIT	MAX DoD	°C	SHADOW
GOES	GOES1	SAFT/G	12	REAL	60	5	4
GOES	GOESK	SAFT/G	12	ACCEL	60	10	10
GOES	G027B	SAFT/G	12	ACCEL	60	5	9
TDRSS	6232E	SAFT/F	40	ACCEL	50	5	23

ALL GOES PACKS ARE SEQUENTIALLY CHARGED
SAFT/G = CELLS FROM GAINESVILLE
SAFT/F = CELLS FROM FRANCE

The GOES packs, are cycled according to a 42 day GEO, with a maximum DoD of 60%. Except for GOES1 the orbits are accelerated time (six shadows per year) at 5 or 10 degree centigrade. All packs are sequential recharge at .9 amp (six minutes on, six minutes open circuit) with V/T to a specified per-cent of ampere-hour out of previous discharge. Then sequentially trickle charge at .3 amp (six minutes on, 6 minutes open circuit) with V/T for remainder of the twenty-four hour cycle.

The TDRSS pack 6232E was fabricated by TRW similar to the flight battery configuration. This included wrapping each cell in a layer of fiberglass, inserting thermal shims between cells and bonding the cells to the shims with RTV, and compressing the pack to a mechanical pre-load similar to the flight pack (63 psi). The cells are cycled according to a 45 day accelerated GEO cycling regime (12 hour orbit) with a maximum DoD 50%. Pack temperature is controlled by a cold plate.



DISCONTUNUED LEO PACKS



PROJECT	PACK	TYPE	Ah	ORBIT	DoD	°C	K CYCLE
TOMS	6090T	SUPER	9	STRESS	50	20	20
SAMPEX	0090B	SUPER	9	MISSION	12	5	18
SWAS	6015F	SUPER	21	STRESS	50	20	13
HQ	6140S	SAFT/F	40	STRESS	40	20	20
NOAA	NOAA1	SAFT/G	47		VAR	5	5

PACK	COMMENTS
6090T	LOW EODV ,CHARGE CROSSOVER DIVERGENCE 138 MV
0090B	CHARGE CROSSOVER DIVERGENCE 148 MV
6015F	EOC DIVERGENCE 132 MV
6140S	EOC DIVERGENCE 65 MV, LOW EODV, HI C/D, C-4 INTERNALLY SHORTED
NOAA1	C-2 INTERNALLY SHORTED

SAFT/G = CELLS FROM GAINESVILLE
SAFT/F = CELLS FROM FRANCE

Pack 6090T at start of cycling repaired leaky pressure fitting connector on cell 5. Cell 5 removed on cycle 4150 because of high charge voltage and sent to Comsat Labs for DPA.

Pack 0090B on cycle 4110 repaired leaky pressure fitting connector on cell 5. Cell 5 removed on cycle 7171 because of high charge voltage and sent to Comsat Labs for DPA. After completing 8000 cycles cell 1 pressure gradually increased over a period of 400 cycles. Several reconditioning cycles were performed in attempt to control pressure. Recharge trip was then changed from 104 to 100 percent on cycle 11,454 and pressure returned to nominal.

Pack 6015F. Charge divergence began after 10000 cycles and gradually increased though-out life.

Pack 6140S These cells were designated as the standard design aerospace nickel-cadmium cell and were from of lot 196 .

NOAA1 Cells 1 through 8 are lot 6 cells and were from packs 0648N and 0649N. Cells failed because of charge divergence after completing over 2900 cycles. Cells 9 through 17 were 42 Ah Mars Observer cells. The purpose of the test was to investigate the effects of divergence in a battery pack containing more than 10 cells.




DISCONTINUED GEO PACKS

PROJECT	PACK	TYPE	Ah	ORBIT	DoD	°C	SHADOW
GOES	6227B	SAFT/G	12	REAL sequential	60	5	25
GOES	6227C	SAFT/G	12	ACCEL sequential	60	0	34

PACK	COMMENTS
6227B	COMPLETED MISSION
6227C	COMPLETED MISSION

SAFT/G = CELLS FROM GAINESVILLE
SAFT/F = CELLS FROM FRANCE

Pack 6227B was a real time test but after completing the mission requirements of 13 shadow periods it was changed to accelerated orbit similar to pack 6227C.

Packs were cycled according to a 42 day GEO regime with a maximum of 60% DoD. The orbit was accelerated time at 0 or 5 degree centigrade.

They were sequential recharge at .9 amp (six minutes charge, six minutes open circuit) with V/T of 1.482 v/c to 115% or 1.508 v/c to 120% of ampere-hour out of previous discharge. Then sequentially trickle charge at .3 amp (six minutes charge, 6 minutes open circuit) with V/T for remainder of the twenty-four hour cycle.

Packs were discontinued after completing mission requirements and special mission unique test.



HQ PROGRAMS

PACK	TYPE	Ah	ORBIT	DoD	°C	K CYCLE
NICKEL CADMIUM						
6091T	SUPER	9	MISSION	31	5	19
6106M	MAGNUM	10		VAR	0	17
6122M	MAGNUM	10	STRESS	40	20	19
0106M	MAGNUM	21		VAR	0	13
0121M	MAGNUM	21	STRESS	40	20	13
6506M	MAGNUM	50		VAR	0	17
6522M	MAGNUM	50	STRESS	40	20	18
NICKEL HYDROGEN						
5009M	HUGHES	48	STRESS	60	10	15

Packs with DoD identified as variable (VAR) are being cycled as follows:
 The first 2000 cycles DoD was 10 per-cent. The next 2000 cycles DoD was increased to 25 per-cent. Then DoD increased to 50 per-cent for 2000 cycles. This sequence is repeated until the end of life.



MAGNUM PACKS

PACK	Ah	% DoD	CHG RATE	V/T	% C/D	DIVERGENCE		AVG
TEMP						CROSS	EOC	EODV
6106M 0°C	10	10	C	1.440	108-109	28	3	1.214
		25	C	1.460	104-106	32	8	1.181
		50	C	1.480	102-103	26	6	1.134
6506M 0°C	50	10	C	1.420	101-102	3	1	1.206
		25	C	1.440	102-103	4	1	1.166
		50	C	1.460	102-103	7	2	1.137
0106M 0°C	21	10	.5C	1.420	112-113	8	2	1.226
		25	.5C	1.460	112-113	6	2	1.177
		50	C	1.480	107-108	6	2	1.090
6122M 20°C	10	40	.8C	1.454	108-112	4	4	1.127
6522M 20°C	50	40	.8C	1.454	108-112	4	4	1.128
0121M 20°C	21	40	.8C	1.445	110-120	7	2	1.127

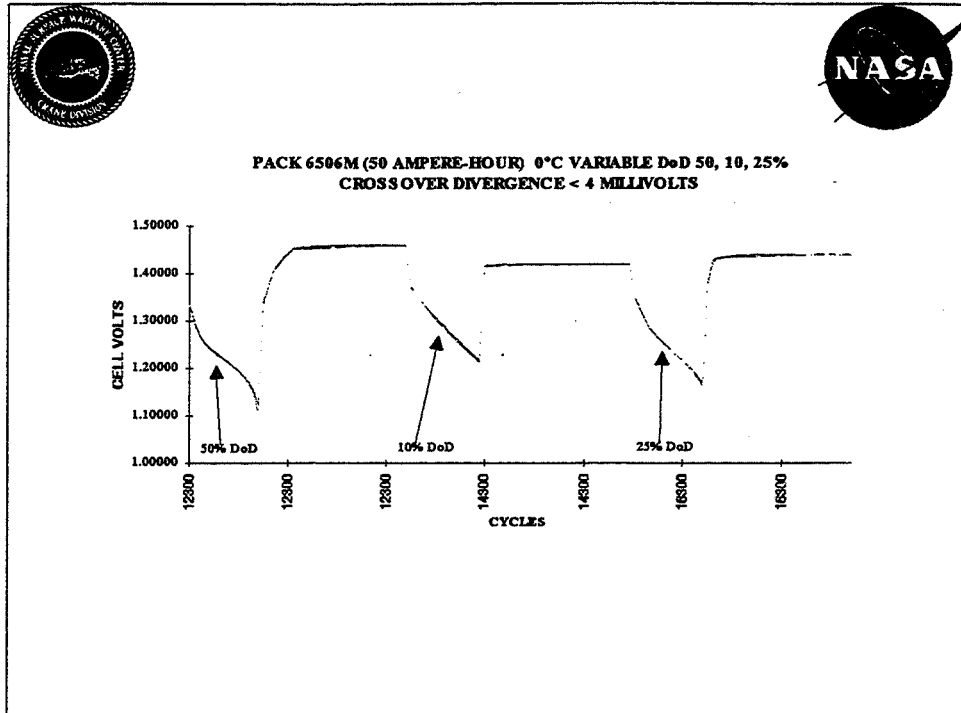
Due to the anomalous capacity and voltage performance of Super and Magnum cells have experienced at low temperatures (-10 to 5° C). A program was initiated to test a sampling of these cells at either a particular mission profile or at low temperature with variable DoD's.

The C/D ratio given in chart is the normal operating range for the cycle life of pack.

The 10 and 50 Ah cells are cycled with the same parameters the only difference being the voltage limits for 10 Ah pack 6106M is 20 millivolts higher at all levels.

Recharges were higher for the second sequence of 10% DoD

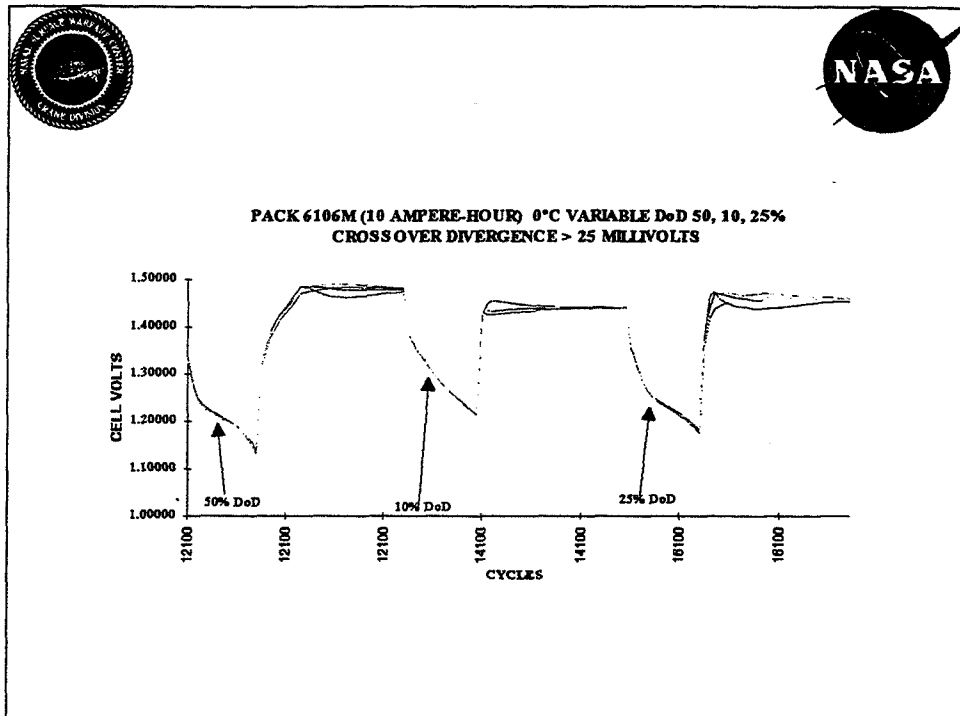
Packs 0106M and 0121M (21 Ah cells) recharges are higher than other packs for the same voltage limit. This is true for both test regimes.



Plots shows each of the six cells of the pack during a full charge and discharge cycle at 50, 10 and 25 depth of discharge . There is very little charge divergence(4 millivolts) in pack.

Crossover occurs when the charging regime is changing from constant current to a constant potential.

The voltage limit on the 50 Ah pack 6506M was decreased by 20 millivolt (1.420 volts) after 900 cycles into the second sequence of the 10% DoD test. This was done because of recharges above 119%. This resulted in no increase in the end of charge divergence or significantly decreasing the end of discharge voltages.



Plots shows each of the six cells of the pack during a full charge and discharge cycle at 50, 10 and 25 depth of discharge. Charge divergence varies from 26 to 32 millivolts.

Crossover occurs when the charging regime is changing from constant current to a constant potential.

The voltage limit for the 10 Ah pack 6106M was increased by 20 millivolts (1.500 volts) for approximately 1700 cycles. This occurred around 4600 cycles and during the 50% DoD test. This increase in voltage did not improve charge voltage divergence or significantly improve end of discharge volts. The 50%DoD was returned to the 1.480 volt level after this sequence.



COMMENTS ON PERFORMANCE

- Divergence is greater at crossover
- Pack 6106M (10 Ah) divergence six times higher than 6506M (50 Ah)
6106M (10 Ah) voltage limit are 20 mv higher all DoD's
- Stress packs 6122M (10 Ah) and 6522M (50 Ah) divergence < than 5 mv

Crossover occurs when the charging regime is changing from constant current to a constant potential.

The 10 Ah pack 6106M divergences is six times greater than the 50 Ah pack 6506M. All testing parameters are the same except 6106M voltage level is set 20 millivolts higher than 6506M.

Their sister packs in the 20 °C 40% stress regime testing parameters are identical. However their C/D's and end of discharge voltages are very similar.



COMMENTS ON C/D

- Recharges were 4-8% higher for the second sequence of 10% DoD
- The 10 Ah packs 0106M and 0121M C/D's higher for same voltage value

Recharges were 4 to 8 percent higher on the second sequence of 10 % DoD. The 10 ampere-hour packs C/D's were 5-10 percent higher for the same voltage level when compared to the 21 and 50 ampere-hour packs.



HUBBLE CAPACITY CHECKS

- Yearly capacity checks were performed only on 3601H for the first 3 years

Pack Shunted With 1.2 Ohms To .2 Volts Any Cell

- After 46 months capacity checks were initiated for both packs.

Packs were discharged at C/6 to .9 volts any cell prior to shunt period.

Packs 3600H capacity increasing by 2.7% and 3601H by 1.1 and 4.3% each period.

Flight batteries experiencing the same capacity increase.

The ten cells used in these two packs were manufactured by Eagle-Picher Industries, Inc. (EP) for the Hubble Space Telescope (HST) project and are from the Flight Module 1 and Flight Module 2 lots. The cells from pack 3600H are from lot FM1. The cells from pack 3601H are from lot FM2 which is the same lot as the cells that have been in orbit on the HST spacecraft since April 24, 1990.

Both packs followed the same set of parameters except pack 3601H which was reconditioned after each yearly shadow period. A resistor of 1.2 ohm was placed across pack until any cell reached .2 volts.

This procedure was changed after 46 months. Both packs are now reconditioned as described below:

Charge 9.3 amp for 10 hours

Charge 4 amp for 14 hours

Discharge 15 amp to .9 volts first cell

Shunt pack with 1.2 ohms to .2 volts first cell

Sequence performed a total of five cycles.

The capacity growth during capacity checks is similar to increase's experience by the flight battery.

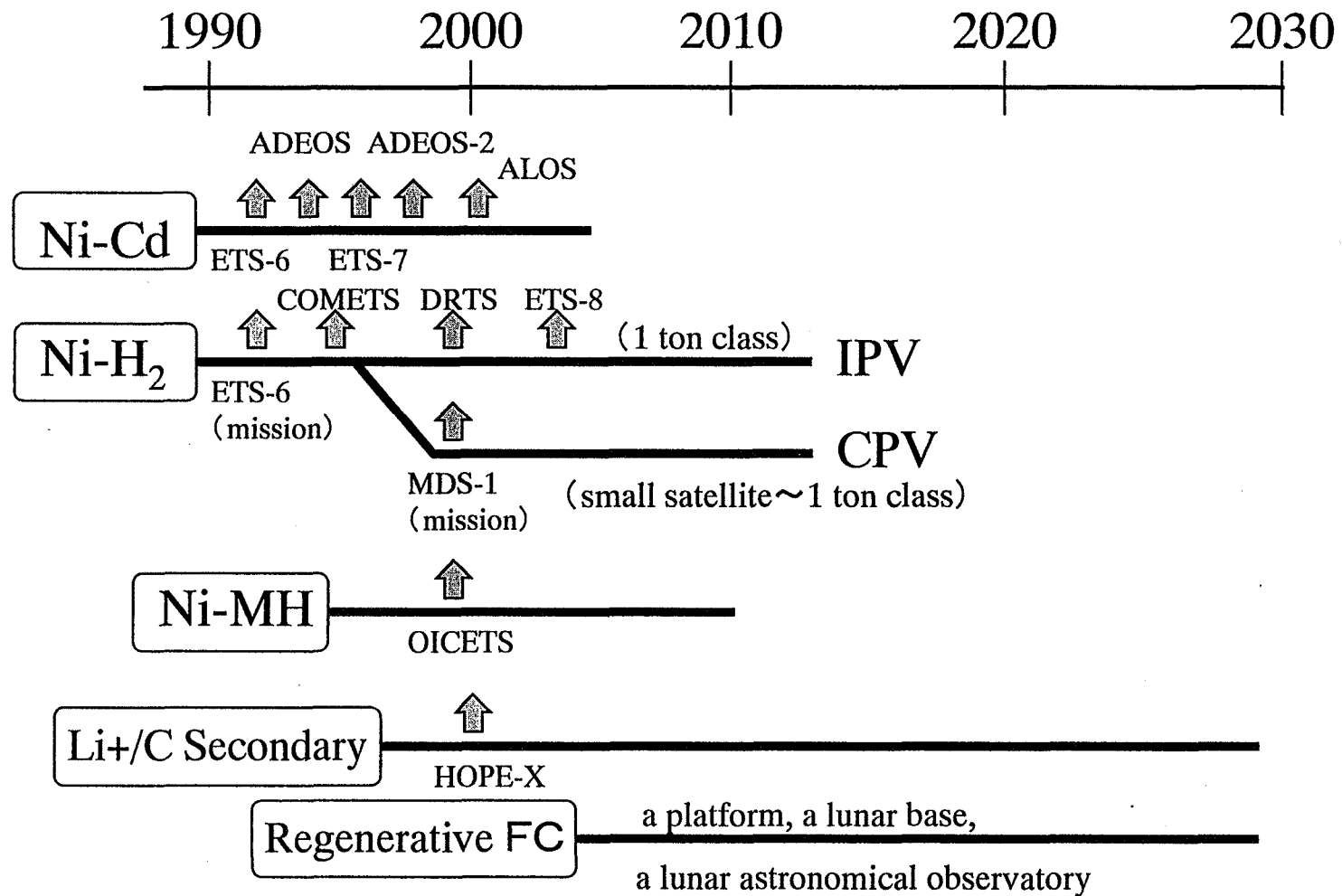
Status of Nickel Metal Hydride Cell Development

Y. Sone, H. Kusawake, K. Koga, and S. Kuwajima

Office of Research and Development
Electronic and Information Technology Laboratory
National Space Development Agency of Japan
(NASDA)

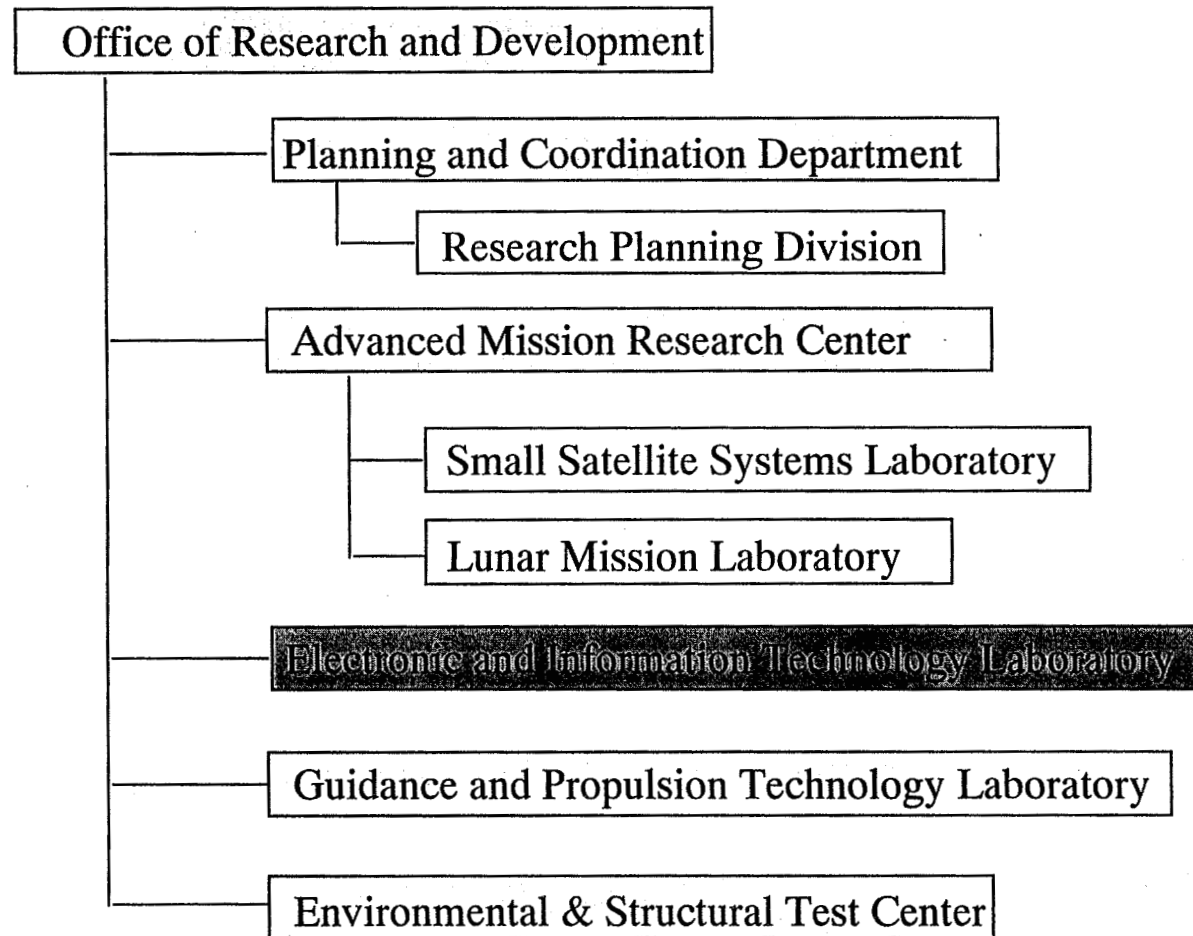


Development of Space Batteries at NASDA





Organization for the NASDA Battery Development





Electronic and Information Technology Laboratory

Major study activities

-LIDAR Technology Demonstration Satellite
(LIDAR : Light Detection and Ranging)

-High Performance Batteries

-Solar Cell

-Communication and Data Handling

-Optical Inter-Satellite Communication

-Remote Sensing Technology



Development of Ni-MH Cells

NASDA has been developing Space Ni-MH Cells on the contract with SANYO Electric Co. Ltd.

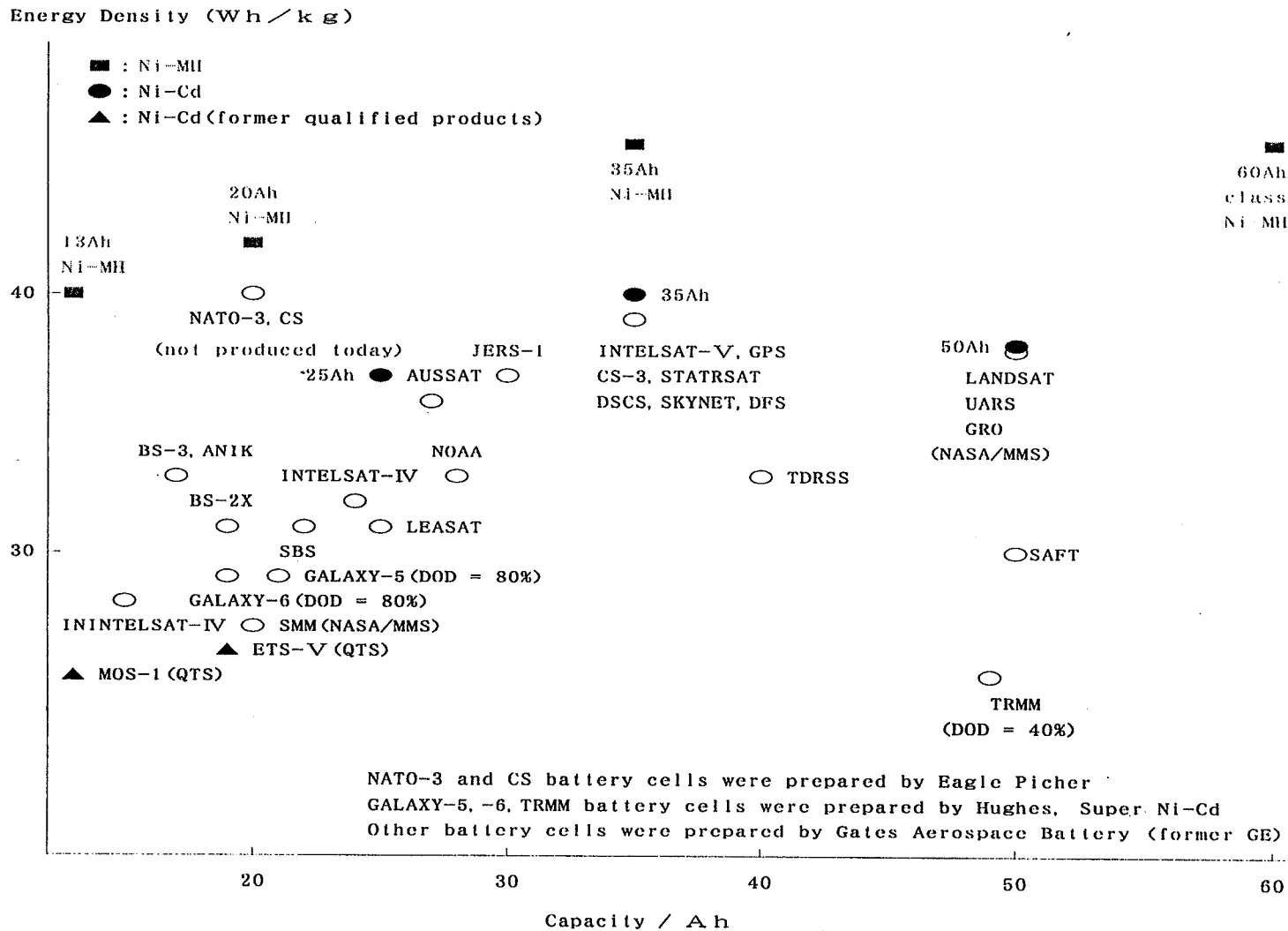
1st manufactured cell showed initial capacity of over 35 Ah and specific energy density of about 50 Wh/kg (about 860 g of weight).

Ni-MH cell was decided to be used for Optical Inter-orbit Communication Engineering Test Satellite (denoted as OICETS) which will be launched in 2,000.

In this report, we are going to show the stable charge/discharge performance of Ni-MH cells, and its applicability to OICETS.



Comparison of the Energy Density of Space Battery Cells



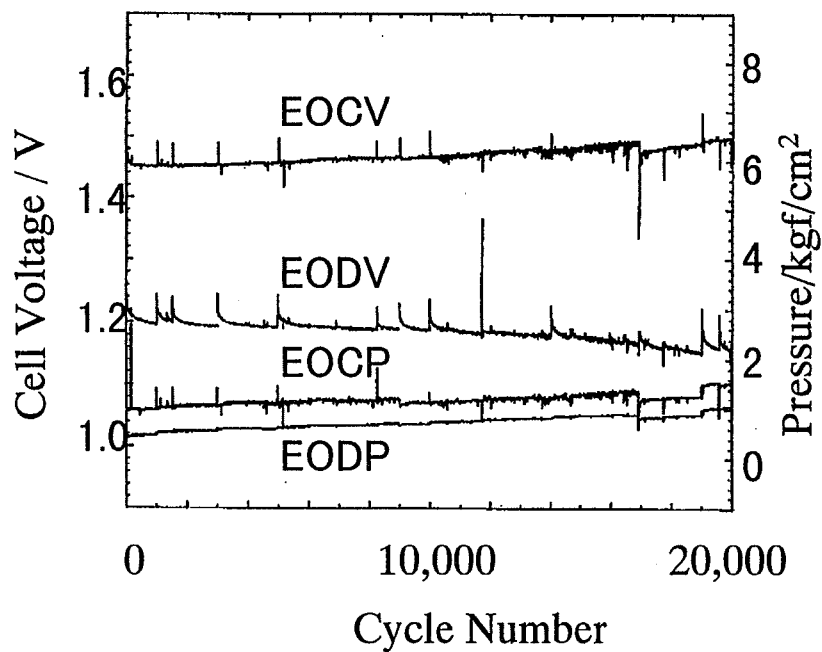


Requirement for the 35 Ah Ni-MH cell

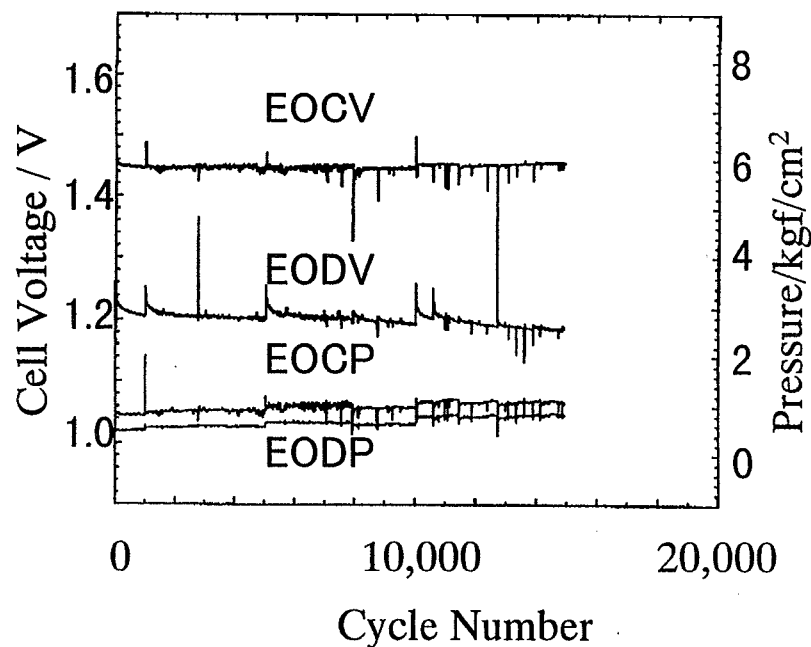
Test Mode	1	2
Charge	0.3 C, 52.5 min	0.48 C, 52.5 min
Discharge	0.5 C, 30 min	0.8 C, 30 min
Depth of Discharge	25%	40%
Recharge Ratio	1.05	1.05
Requirement	20,000 cycles	10,000 cycles



Life Cycle Test with DOD = 25 %



BBM in FY1992

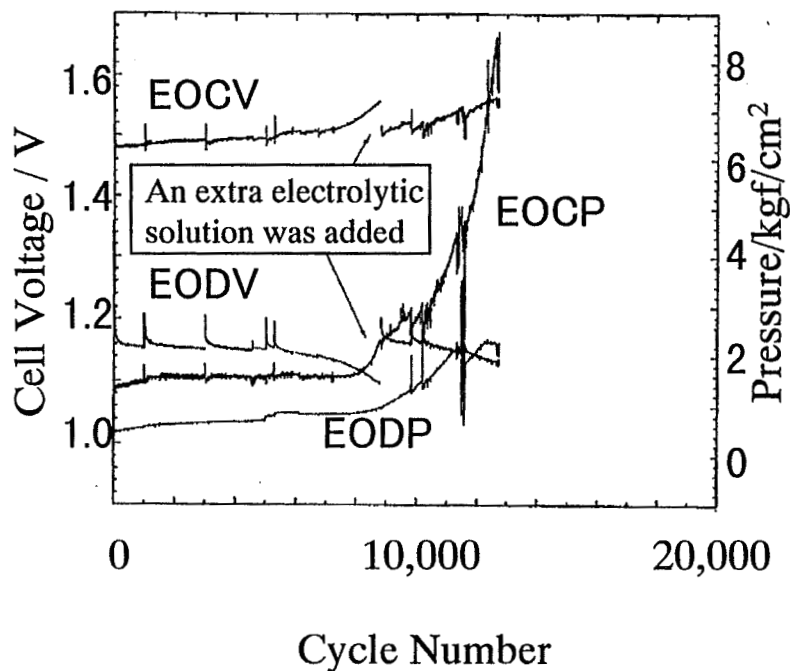


BBM in FY1993

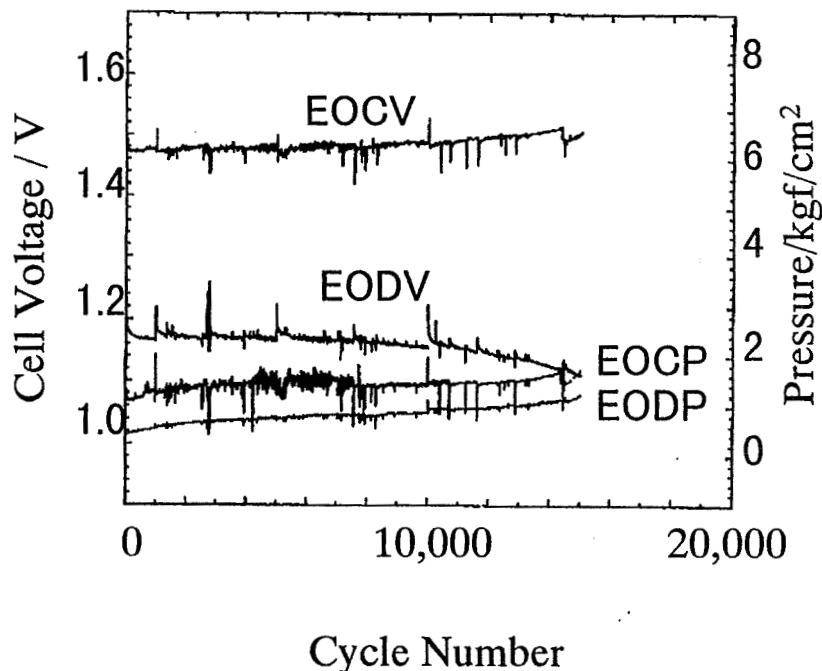
The amount of electrolytic solution was increased, while the space between electrodes was decreased.



Life Cycle Test with DOD = 40 %



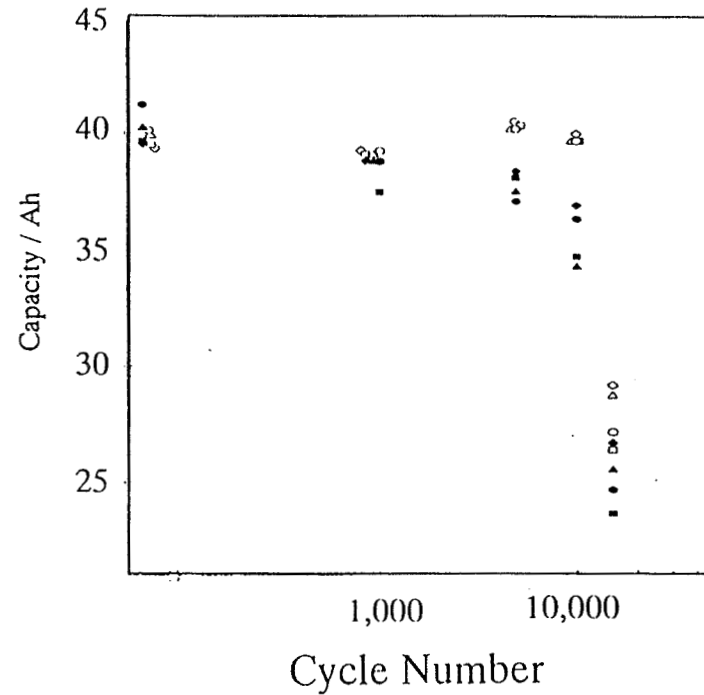
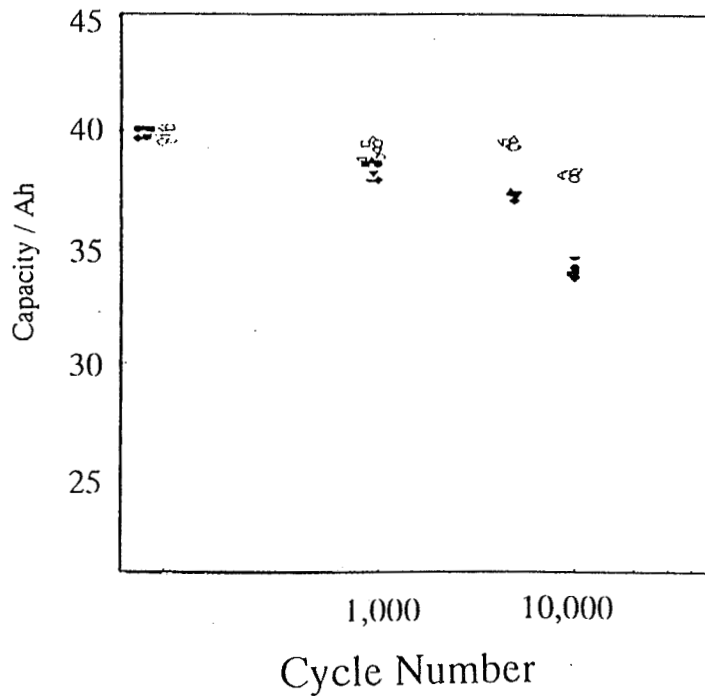
BBM in FY1992



BBM in FY1993

The amount of electrolytic solution was increased, while the space between electrodes was decreased.

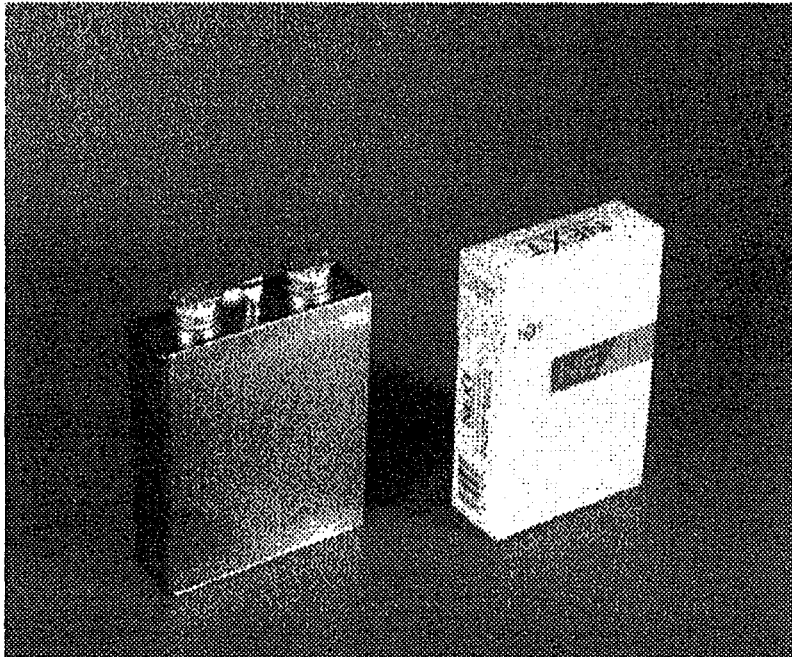
The capacity of the calls designed in FY1993 shows very stable performance. It revealed to have more than 10,000 life cycles with DOD=40%.





13 Ah Ni-MH Cell for OICETS

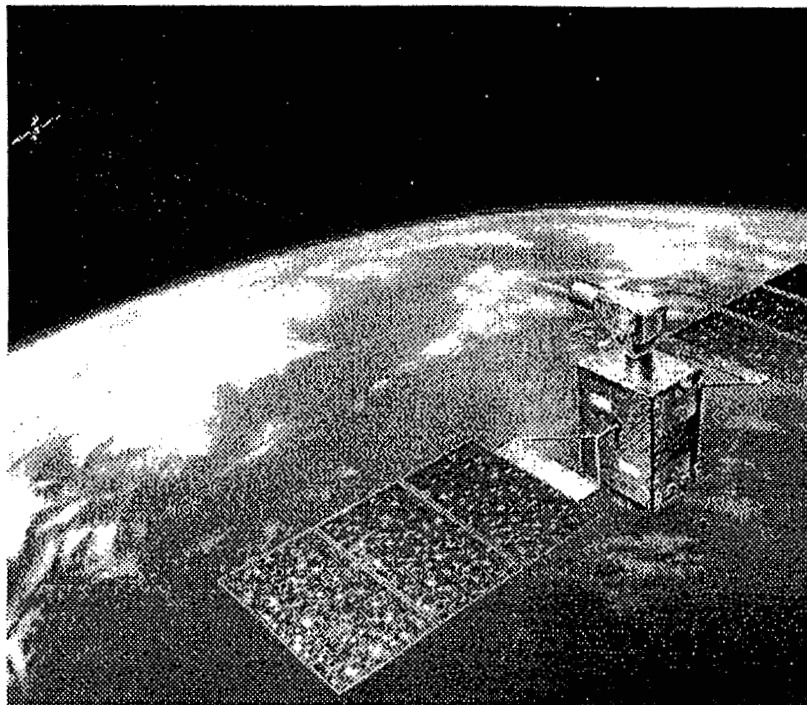
After the life cycle tests of 35 Ah cells designed in FY1993, 13 Ah Ni-MH cell for OICETS, which is scheduled to be launched in 2,000, was designed and qualified for the space use.



Nominal Capacity	13Ah
Required Life Cycles	20,000@DOD=25% 10,000@DOD=40%
Weight	less than 390 g
Energy Density	more than 40 Wh/kg



'Optical Inter-orbit Communication Engineering Test Satellite'



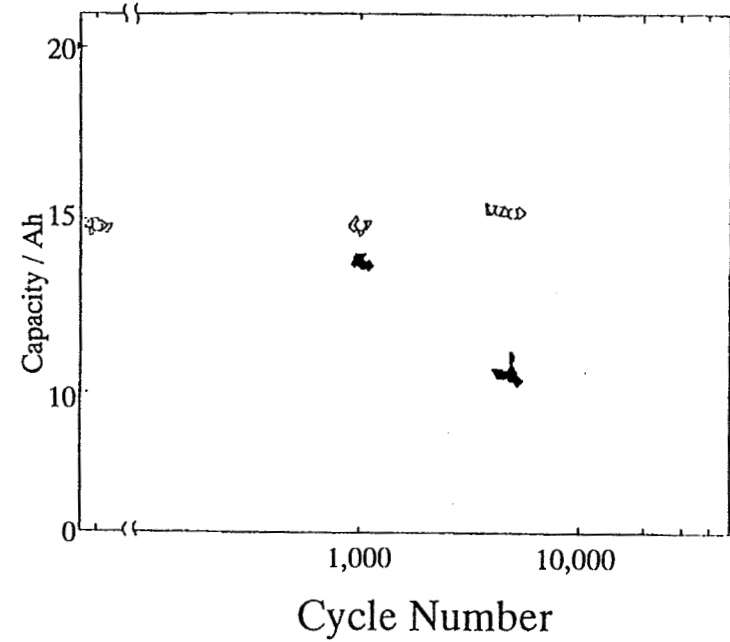
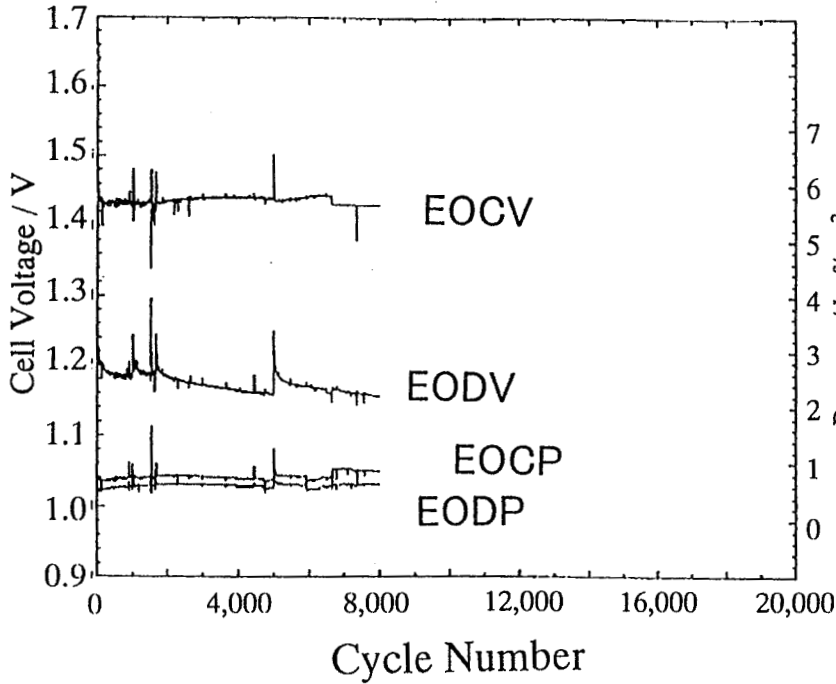
OICETS is a denotation of 'Optical Inter-orbit Communication Engineering Test Satellite.' This satellite is going to make an optical contact with ARTEMIS from ESA.

The successful development of Ni-MH cells enhanced us to use it for this satellite.



The Performance of 13 Ah Ni-MH EM Cells

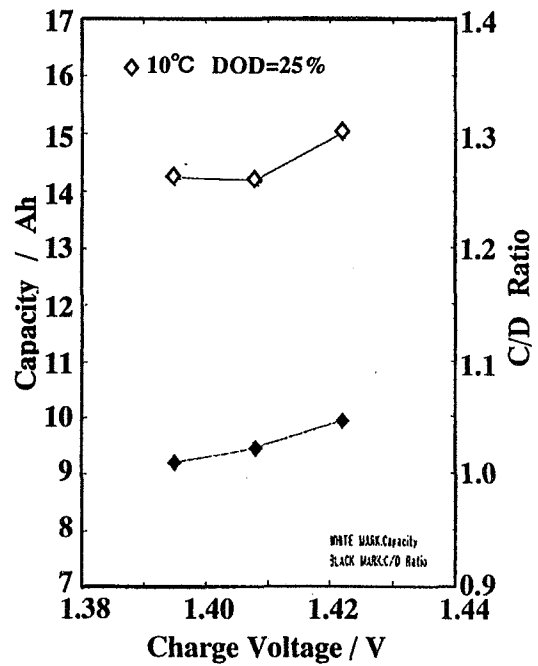
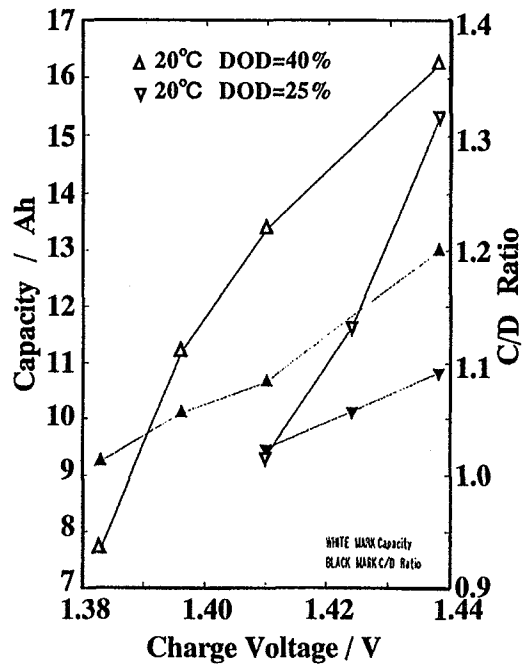
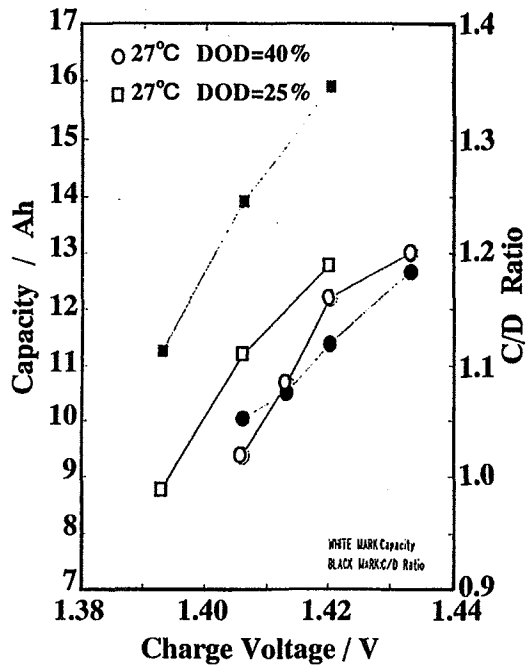
The trend data of 13 Ah Ni-MH cells (EM) are shown during the cycle tests with DOD = 40%. We could observe very stable performance of these type of cells. Now, the life cycle tests of QT cells are also being measured. The same type of stable performance of QT cells as that of EM ones is observed.

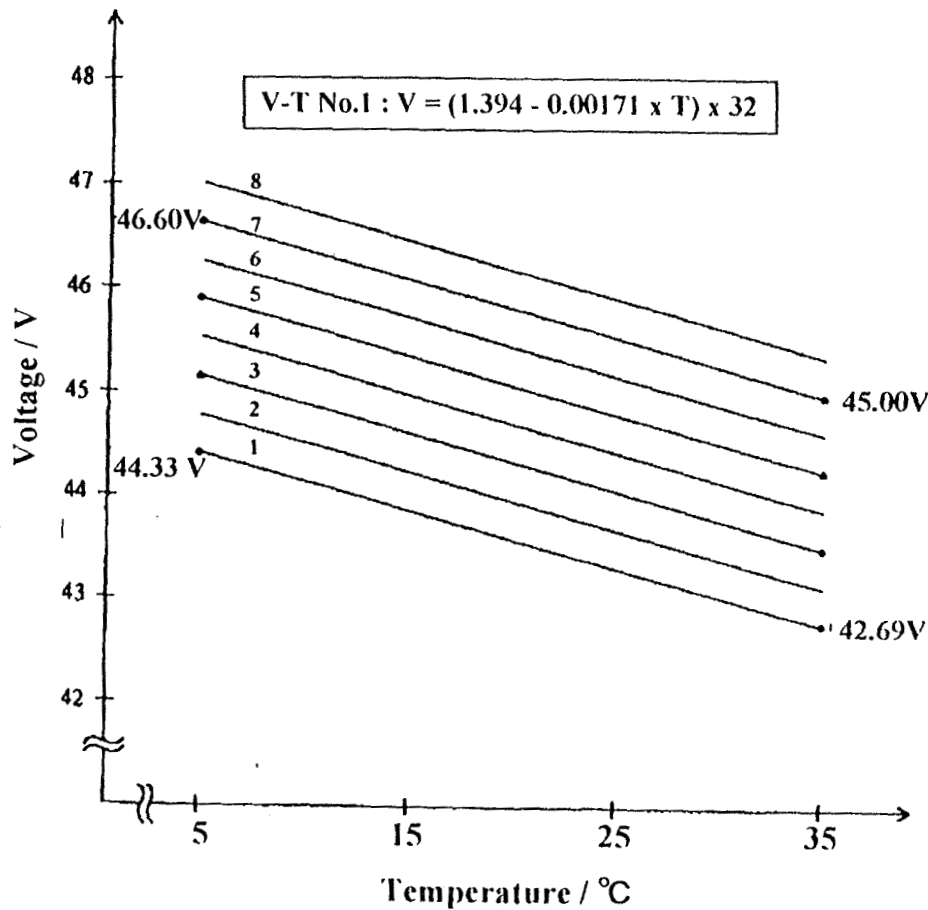




The relationship between C/D Ratio and Capacity

The following figures shows the relationship between C/D ratio and capacity of 13 Ah Ni-MH cells. These results revealed the best C/D ratio for N-MH is 1.05 when the DOD.





Using the relationship between C/D ratio and capacity, V-T curves for OICETS were prepared. The line No. 5 will be used in the case of DOD=25%. The line No. 7 will be used in the case of DOD=40%. The lines of No. 1-4 would be used if 'short-circuit' happened to one of the cells.



The renewal designed 35 Ah Ni-MH Cells

Aiming at the prolonged life and lightweight cell, we re-designed the 35 Ni-MH cell.

The main difference from the standard cell is as follows.

Design	standard	prolonged life	lightweight
NEG/POS ratio	1.95	1.95	1.61
Separator	Nylone	Polypropylene	Polypropylene
Electrolyte / g	92.2	106.03	106.03 (TBD)

The Ni-MH cells were manufactured and the life cycle performance were measured.

Through the measurement using 35 Ah Ni-MH cells, we confirmed the stable performance of this type of cells with the life cycle more than 20,000 with the DOD=25%.

These stable performance enhanced us to prepare 13 Ah cells for OICETS.

Now, the life cycle tests for 13 Ah cells are continued. The trend data suggests the satisfactory performance of 13 Ah cells.

Page intentionally left blank

Battery Systems
for
X-38 Crew Return Vehicle (CRV)
and
Deorbit Propulsion Stage (DPS)

NASA Aerospace Battery Workshop 1997

Outline

- Introduction
- Objectives/Approach
- Requirements/Groundrules
 - Common
 - 28V
 - 270V
- Design Trades/Solutions/Redundancy Plan/Margins
 - 28V DPS
 - 28V CRV
 - 270V CRV
- Envelope/Size/Mass
- Interfaces
- Deviations from OPS CRV

Top Level CRV Requirements

- Provide for the safe return of ISS crew of zero to 6 in case
 - emergency return of ill or injured crew person
 - ISS can not maintain critical systems, pressure, attitude, or is contaminated
 - Shuttle is not available to return crew
- Crew return without pressure suits
- On-orbit lifetime of 3 years
- 700 nautical miles of cross range
- Land lander
- Separation time from ISS < 3 minutes
- Planned return mission time is 3 hours maximum
- Contingency return mission time is 9 hour maximum



CRV Advantages over Soyuz

- Returns a crew of six with wider size tolerances
- Has 700 nmi of cross range
 - Lifting body aerodynamics
 - Electromechanical Actuators for flight surface control
 - 2 flaps, 2 rudders
- Soft, precise land landing at many more sites
 - Gliding parafoil
 - Electric motors power winches to control the chute
- 3 year on-orbit life
- Potentially refurbishable

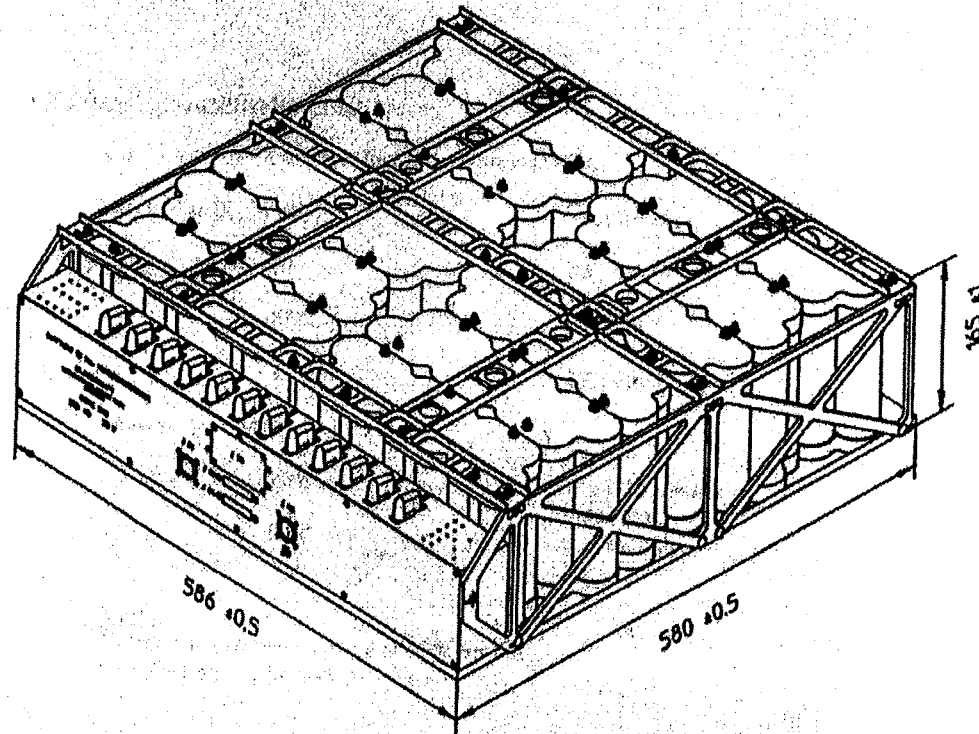
Unique Approach to X-38 Program

- Design, Build, and Test in small increments for rapid feedback
 - Pallet Drops (parachute weight tests)
 - Dog House Drop (parachute drop test with a vehicle-like shape)
 - V-131 (X-24 aero shape with fixed surfaces dropped from a B52)
 - V-132 (same shape with EMA controlled surfaces)
 - V-133 (20% bigger, again B52 dropped)
 - V-201 (Shuttle launched, 5/00, unmanned return test)
 - V-202 (Ariane launched, 3/02, unmanned return test)
- No prime contractor (except for Deorbit Propulsion Stage) thru V-202
- Later, a prime contractor will build operational CRVs for ISS

Battery Objectives and Approach

- Provide safe battery designs for lowest volume and cost, and within schedule
- Take advantage of less complex reqts for V201 vs OPS CRV to simplify design and reduce cost
- Use only existing commercial cell designs as building blocks for larger battery
- Derive battery designs from the ASTRO-SPAS design which is the largest lithium battery design with Shuttle flight experience
- Place maximum amount of battery energy on DPS
- DPS battery is non rechargeable
- CRV batteries are rechargeable

FRIWO SILBERKRAFT
Technical Data of Space qualified Lithium-SO₂ Batteries



Requirements and Groundrules

- Common to all batteries
 - 1 failure tolerant for mission success and to a critical hazard
 - 2 failure tolerant to a catastrophic hazard
 - Compliant to “Manned Space Vehicle Battery Safety Handbook” JSC-20793
 - 9 year useful life (5 for storage, 1 in transit, 3 on-orbit)
 - Capacity gauge circuit to track %Ah remaining with 1% resolution
 - Gauge draws < 50 microA (<2 Ah over 4 years) from the battery
 - Refurbishable by replacing battery strings
 - Capable after vibration to 14 grms

Requirements and Groundrules (cont.)

- 28 V High Energy Density Battery (Wh/L)
 - 28.9 kWh over a continuous 9 hour period for Crew Return Vehicle
 - Avionics 2.2 kW for 9 hours
 - ECLSS 0.9 kW for 9 hours
 - RCS 1.0 kW for 1 hour
 - 7.0 kWh over a continuous 7 hour period for Propulsion Module
- 270 V High Power Density Battery (W/L)
 - 4 kWh over a 25 minute period for EMAs, then Winches
 - EMAs peak at 100 kW (400A) for 80ms every 2s for 15 minutes
 - Baseline load is 8.91 kW (33A) for 15 minutes
 - Winch peak is 50 kW (200A) for 5s at end of 10 minutes
 - Baseline load is 4.05 kW (15A) for 10 minutes

DPS Battery Requirements

- Performance
 - 29.4 kWh at 28 +5V, -4V at 7 hour rate after
 - 3 years on-orbit while at 0 to 30C (14 days for V201)
 - Minimum capacity = 1050 Ah
 - Average Power = 4.2 kW
 - Peak Power = 5.5 kW for <1 minute
 - Vacuum exposure for 3 years (14 days for V201)
 - Non-operating exposure range -31C to 72C
 - Use high energy density commercial lithium primary cell design
 - Compliant with NASA RP 1353 “Primary Battery Design and Safety Guidelines Handbook”
- Operation
 - Expired batteries replaced on ground, if CRV/PM returned via Shuttle
 - A rechargeable 28V battery on CRV is used for monthly check-outs

Li Cell Characterization Approach

- Released an SOW to determine feasibility of candidate cell designs
- Schedule (finish by Dec 97) and cost (<\$25K) restraints
- Response from vendors;
 - Friwo-Silberkraft; test both SO₂ and MnO₂ for \$24.9K
 - WGL: only willing to sell their BCX DD-cells, Crane did testing, \$24.6K
 - YTP: test SOCl₂ DD-cell in two phases \$22.4K and \$22.3K
 - Eagle Picher: wanted too much (\$62K) with using existing cells
 - Centaur: no formal bid yet
 - Ultralife: can not support schedule
 - Bluestar, PCI, and BEI: no bid or no response

SOW for Li Cell Characterization for Manned Spacecraft

- Purpose - Determine performance and safety of a candidate building block cell
- Design - Consider only existing cell designs with very minor modifications
- Manufacture - Build enough (26 minimum) cells to support verification tests
- Performance tests
 - Cell capacity at 3 rates and 2 temperatures
 - Cell Vibration of BOL and EOL cells (14.1 grms at 0.16 g²/Hz)
 - Acceptance tests (leakage, weight, dimensions, OCV, CCV, X-ray)
- Safety tests
 - Cell voltage reversal at 3 rates and 2 temperatures
 - Cell short circuit at 2 rates and max temperature
 - Cell charging with and without diode protection
 - High temperature exposure and heat-to-vent
- Cell Pressure Analysis to determine pressure vs temperature at all states of charge
- Deliverables - Test report with complete cell drawings to establish configuration control

Lithium Cell Design Trades

Company	Chemistry	Cell	Mass, lbs	Volume, cu.in.	Remarks
Friwo-Silberkraft	SO2	G62	643.10	16,618.15	Proven battery design, highest volume
Friwo-Silberkraft	MnO2	M25	629.80	11,870.08	Same batt design, Li-MnO2 cell
Wilson Greatbatch	BCX II	DD	435.09	8,869.92	Vendor will only do cell work
Yardney	SOCl2	IRDD-3H	525.20	10,050.67	High temp DD cell, experienced vendor

Li/MnO₂ cell has some advantages

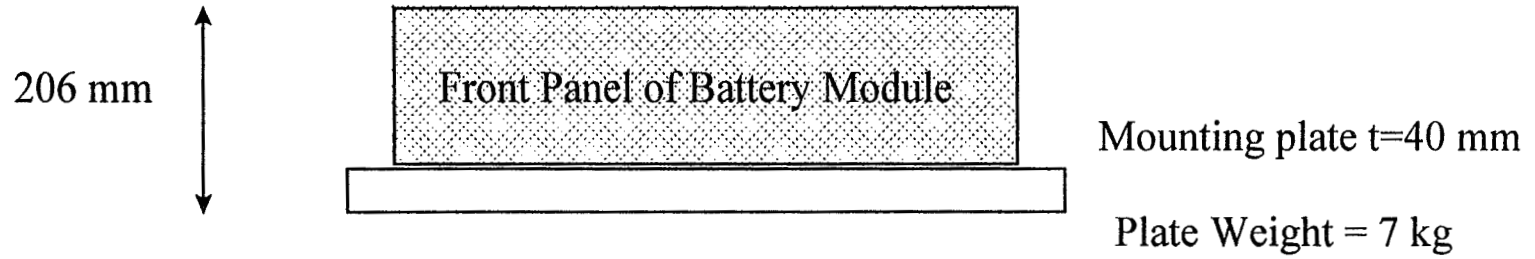
- less hazardous than BCX or SOCl₂ options
- NCR may not be required for internal short hazard
- only chemistry w/o voltage delay issue
- acceptable volume

Design Solutions/Redundancy Plan/Margins

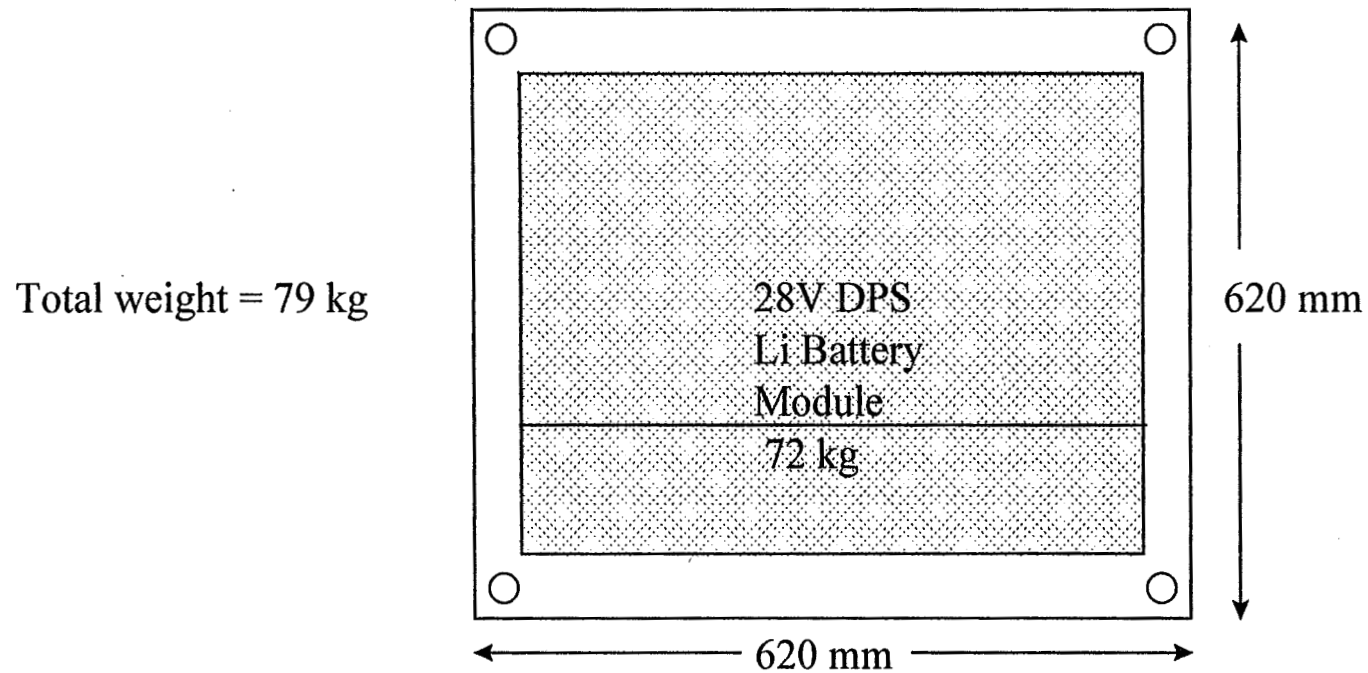
- 28V DPS Battery Point Design
 - Using reference Cell: Li/MnO₂ 32Ah cell (P/N M25) from Friwo-Silberkraft, Germany
 - Battery String = 12 cells in series
 - Battery Module = 12 strings in parallel
 - Flight Battery Set = 4 Battery Modules
 - Voltage: Open Circuit = 38V, Closed Circuit = 24-33V
 - Capacity starting at 0C = 1536 Ah vs 1050Ah required
 - Redundancy Plan: 3 modules needed, 4 flown
 - Margin after one module fails: 9.7%
 - Capacity gauge circuit in each module
 - Battery mounting plate for each module

Envelope/Size/Mass

- Battery module Size w/ Battery Mounting Plate
 - 586.5 mm wide 620 mm wide
 - 580.5 mm deep 620 mm deep
 - 166 mm tall 206 mm tall
 - 72 kg 79 kg



DPS will require 4 battery modules like below



Interfaces

- Structural
 - BMP to be designed by DPS contractor
 - Built by battery vendor
- Electrical
 - Power - Pair of 8 AWG stud post connectors for +, -
 - Data from Capacity Gauge (8 wires, RS-422)
 - CHG: need +5V for wake-up from avionics, switched off during sleep mode
 - TXD: output battery data to avionics every 1.7s
 - CTS, RXD: inputs for GSE only to calibrate, modify, inspect parameters
 - data output: 16 byte packet (%Ah remaining, voltage, current, temperature)
 - Serial output data format: 9600 baud, 8-bit, no-parity, 1 stop bit
 - Each of the 4 lines has a dedicated return line
- Thermal
 - Starting battery temp: 0 to 30C
 - Non operating exposure: -31C to 72C
 - Generates an average 840W of heat during discharge

CRV 28V Battery Requirements

- Performance
 - 7.2 kWh at 28 + 5V, - 4V
 - Average power = 3.6 kW
 - Peak power = 7.2 kW for seconds?
 - Minimum Capacity = 258Ah at 2 hr rate after 36 cycles
 - Self-discharge <1% per day
 - Stowed in cabin, capable of vacuum exposure non-operating
 - Temperature range at start of operation = 10C to 45C
 - Non-operating temperature = -40C to 55C
- On-Orbit Operation
 - 1 hour discharge every month over 3 years (over 1 year for V201)
 - Recharge in 4 hrs from 4.2 kW max at 120V or 28V (28V only for V201)
 - Unavailability time < 5 hours/month including 1 hour check-out (99.3%)
 - Top-off continuously from 40 W max at 120V or 28V (28V only for V201)

NiMH Cell Design Trades

28V MV Battery Cell Design	258 Ah Capacity, Ah	# of cells	mass, lbs	volume, cu.in.
Sanyo NiMH HS-35S	37.00	184.00	493.05	78,217.30
Sanyo NiMH HS-50S	53.00	138.00	531.30	86,940.00
Sanyo NiMH HR-4/3FAU	3.50	2,208.00	411.71	75,288.38
Toshiba NiMH TH-3500	3.40	2,208.00	355.40	67,154.11

Smaller NiMH cells are used in point design because

- more Wh/L and less memory effect than any NiCd
- more quickly available and less costly than large prismatic NiMH cells
- proven on EMU Helmet Lights on STS-82 and STS-86

NiMH Cell Characterization Approach

- Awarded a SOW to determine abuse tolerance of best 2 candidate cells
 - Toshiba TH-3500 3.398 Ah at C/2 over 100 cycles
 - Sanyo HR-4/3FAU 3.503 Ah at C/2 over 100 cycles
- Above cell designs have demonstrated highest Wh/L in our testing
- Schedule (finish by Jan 97) and cost <\$15K

NiMH Cell Abuse Tolerance Testing On-going

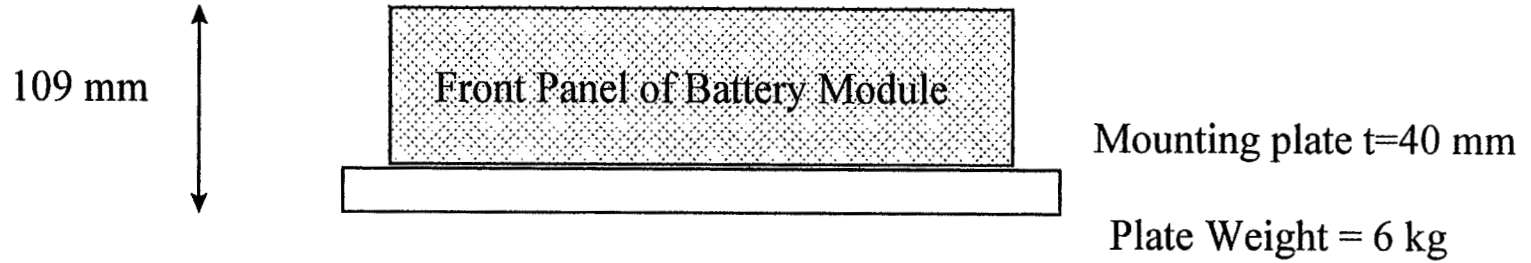
- Purpose - Determine safety of a candidate building block cell
- Design - Consider only existing cell designs with very minor modifications
- Manufacture - Build enough (43 minimum) cells to support verification tests
- Performance tests
 - Cell capacity at C/2 with 2C pulses at RT
 - Cell Vibration
 - Acceptance tests (leakage, weight, dimensions, OCV, CCV)
- Safety tests
 - 100% Cell voltage reversal on 3 cells
 - Cell short circuit with 23 cells in series
 - Cell overcharging tolerance
 - High temperature exposure and heat-to-vent

Design Solutions/Redundancy Plan/Margins

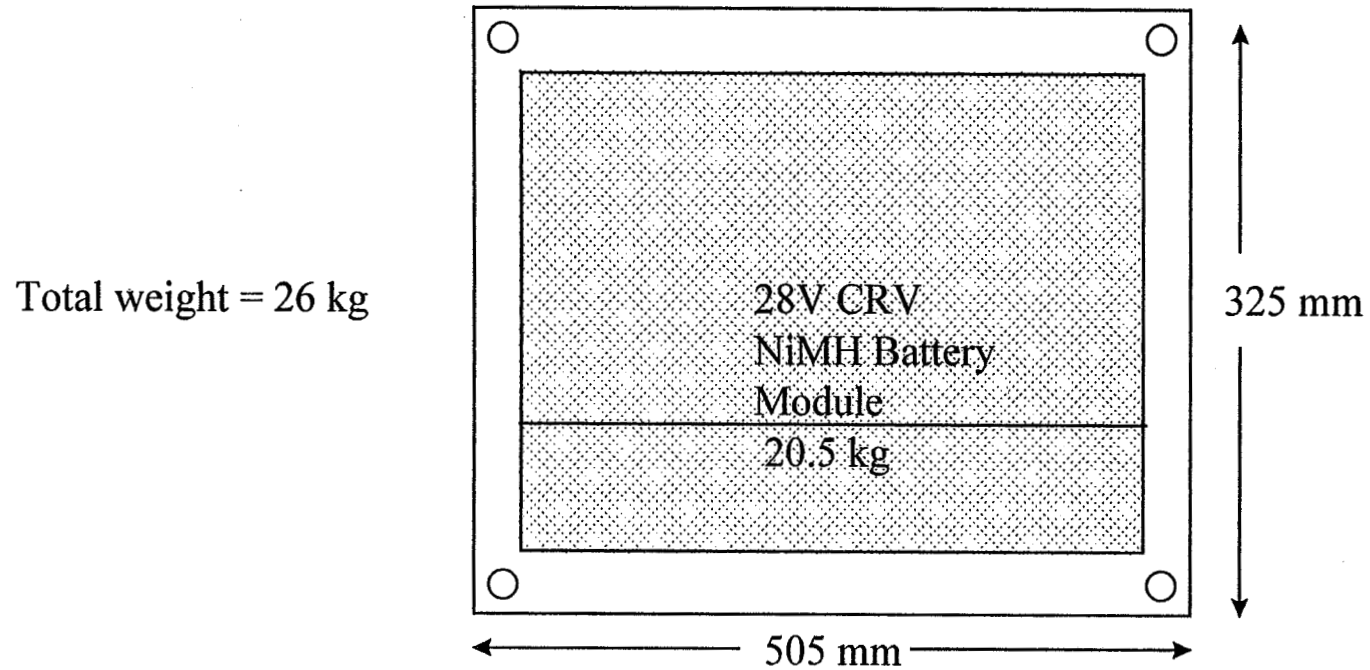
- 28V CRV Battery Point Design
 - Reference Cell: NiMH 3.4Ah cell (P/N TH-3500) from Toshiba, Japan
 - Battery String = 23 cells in series
 - Battery Module = 12 strings in parallel
 - Flight Battery Set = 8 Battery Modules
 - Voltage: Open Circuit = 31V, Closed Circuit = 24-31V
 - Capacity starting at 10C = 316 Ah vs 258Ah required
 - Redundancy Plan: 7 modules needed, 8 flown
 - Margin after one module fails: 7.4%
 - Capacity gauge circuit in each module
 - Charger circuit in each module accepting 28V input
 - Battery mounting plate for each module

Envelope/Size/Mass

- **Battery module Size** **w/ Battery Mounting Plate**
 - 465 mm wide 505 mm wide
 - 284 mm deep 325 mm deep
 - 79 mm tall 109 mm tall
 - 20.5 kg 26 kg



CRV will require 8 battery modules like below



Interfaces

- Structural
 - BMP to be designed by JSC
 - Built by battery vendor
- Electrical
 - Power - Pair of 12 AWG stud post connectors for +, -
 - Data from Capacity Gauge (8 wires, RS-422)
 - CHG: need +5V for wake-up from avionics, switched off during sleep mode
 - TXD: output battery data to avionics every 1.7s
 - CTS, RXD: inputs for GSE only to calibrate, modify, inspect parameters
 - data output: 16 byte packet (%Ah remaining, voltage, current, temperature)
 - Serial output data format: 9600 baud, 8-bit, no-parity, 1 stop bit
 - Each of the 4 lines has a dedicated return line
- Thermal
 - Starting battery temp: 10 to 40C
 - Non operating exposure: -31C to 55C
 - Average heat generation during discharge = 180W, during charge = 720W

CRV 270V Battery Requirements

- Performance
 - 270 +60/-20V during discharge, 360-367V during charge
 - Average power = 1.651 kW, Peak Power = 100 kW during 80 ms
 - Minimum Capacity = 14.68 Ah after
 - 36 five minute discharge cycles once a month
 - Self-Discharge < 0.2% per day
 - Outside cabin, vacuum exposed for 3 years (14 days for V201)
 - Commercial lead acid cells
- On-orbit Operations
 - 5 minute discharge every month over 3 years (over 1 year for V201)
 - Recharge in 4 hrs from 4 kW max at 120V (GSE charging only for V201)
 - Unavailability time < 5 hours/month, including check-out (= 99.3%)
 - Top-off continuously from 20 W max at 120V (GSE charging only for V201)
 - GSE charging on pad no earlier than T-10 days

High Power Cell Design Trades

<u>Cell Design</u>	<u>1C Cap. (A-h)</u>	<u>Total # cells</u>	<u>Battery mass (#)</u>	<u>Battery volume (cu.in.)</u>
Hawker Cyclon D	1.90	1920	1052.6	14744.5
Hawker Cyclon Tall D	3.70	1280	1073.1	14852.7
Hawker Cyclon X	3.90	1280	1427.1	19800.7
EPS NiCd Cs EPP-1750CS	1.65	3690	613.7	7296.7
EPS Ni-MH Cs EMP-2200CS	2.00	3690	602.4	7335.0
Sanyo NiCd D N-4000DRL	4.00	2214	1022.9	14719.1
Sanyo NiCd Cs N-1700SCR	1.70	3936	654.6	8581.7
Bolder 9/5 Cs	1.20	2880	727.4	10147.9

Hawker Cyclon Tall D cells used in point design because

- Vacuum exposure tolerance of Cyclon cell has been demonstrated by test
- Crimp seals of NiCd and NiMH cells are untested at vacuum
- NiCd, NiMH require too many cells in series

Cyclon Tall D-cell Performance and Abuse Tests

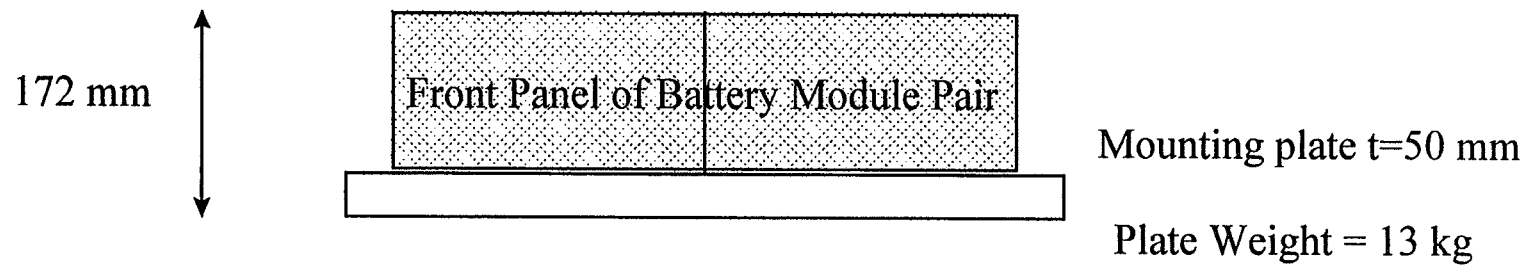
- Purpose - Determine performance and safety of a candidate building block cell
- Performance tests
 - Capacity cycling - 36 cycles with CRV peak profile while at 10, 25, and 40C
 - 12V battery capacity cycling
 - Discharge - crude CRV profile
 - Charge - CV with 1A current limit
 - Cell Vibration
 - Acceptance tests (leakage, weight, dimensions, OCV, CCV)
 - 2 months exposure to 80C w/ and w/o vacuum
 - < 0.2% mass loss in both cases
- Safety tests
 - 100% voltage reversal on 12 V battery - benign vent
 - Short circuit with 15 cells in series at 90A - no vent
 - 12V battery overcharging tolerance - benign vent
 - High temperature exposure and heat-to-vent - benign

Design Solutions/Redundancy Plan/Margins

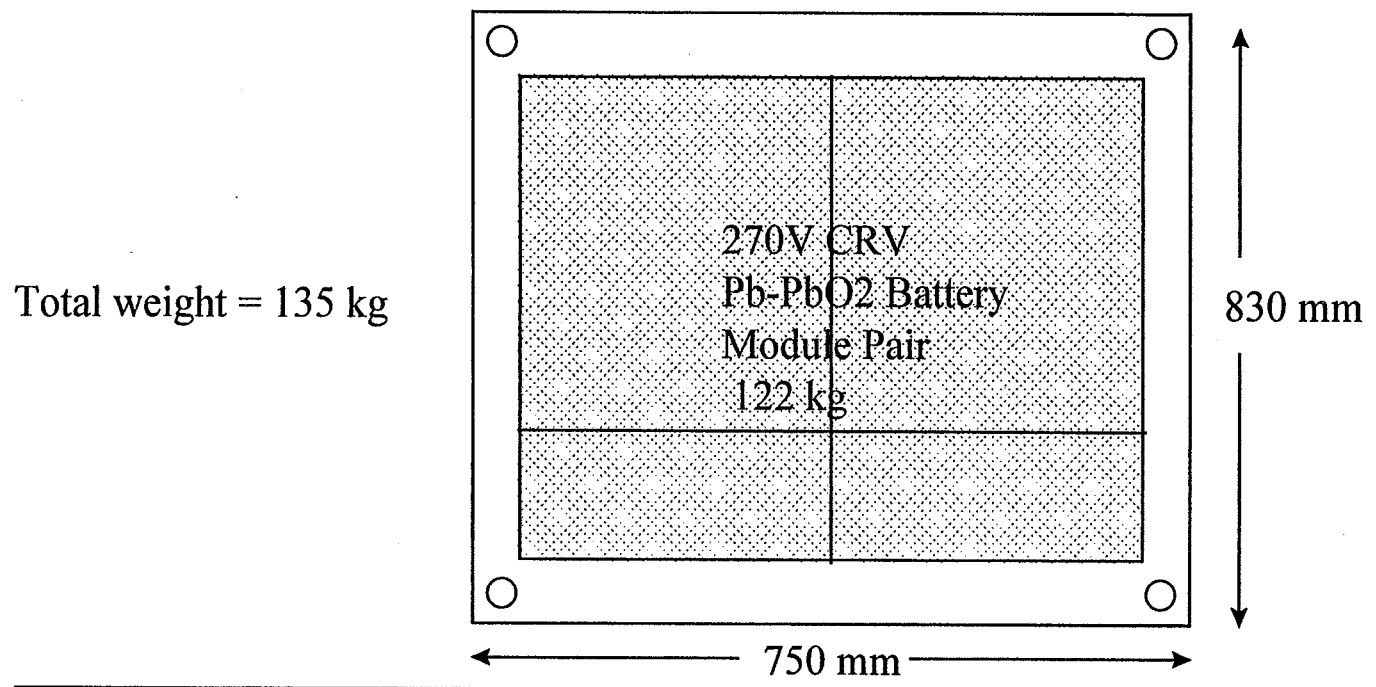
- 270V CRV Battery Point Design
 - Reference Cell: Lead acid 2.5 Ah cell (P/N Cyclon Tall D) from Hawker Energy Products, MO
 - Battery String = 32 cells in series
 - Battery Module = 5 strings in series
 - Flight Battery Set = 8 Battery Modules
 - Voltage: Open Circuit = 342V, Closed Circuit = 250-320V
 - Capacity starting at 0C = 20 Ah vs 14.68Ah required
 - Redundancy Plan: 7 modules needed, 8 flown
 - Margin after one module fails: 19.2%
 - Capacity gauge circuit in each module
 - Charger circuit in each module accepting 120V input
 - One battery mounting plate for two modules side by side

Envelope/Size/Mass

- 2 battery module size w/ Battery Mounting Plate
 - 680 mm wide 750 mm wide
 - 760 mm deep 830 mm deep
 - 122 mm tall 172 mm tall
 - 122 kg 135 kg



CRV will require 8 battery modules like below



Interfaces

- Structural
 - BMP to be designed by JSC
 - Built by battery vendor
- Electrical
 - Power - Pair of 8 AWG stud post connectors for +, -
 - Data from Capacity Gauge (8 wires, RS-422)
 - CHG: need +5V for wake-up from avionics, switched off during sleep mode
 - TXD: output battery data to avionics every 1.7s
 - CTS, RXD: inputs for GSE only to calibrate, modify, inspect parameters
 - data output: 16 byte packet (%Ah remaining, voltage, current, temperature)
 - Serial output data format: 9600 baud, 8-bit, no-parity, 1 stop bit
 - Each of the 4 lines has a dedicated return line
- Thermal
 - Starting battery temp: 10 to 50C
 - Non operating exposure: -31C to 60C

Deviations from OPS CRV

- Friwo proposes M25 lithium cell design vs M62
 - unproven shutdown separator = possible NCR for internal short
 - M25 is current production line
- waive NHB5300.4 guidelines for solder, PWB, etc, use high quality commercial standard
- Life requirements reduced
- MIL-W-22759 wire inspection by RIFT lab waived except on 270V system
- Clean room requirements waived

Lithium-Ion Focused Session

Page intentionally left blank

Improved Li/BCX Primary Cells for Space Applications

D. M. Spillman, N. M. Waite, M. F. Pyszczek, E. S. Takeuchi

Wilson Greatbatch Ltd.
10,000 Wehrle Drive
Clarence, New York 14031

Abstract

Li/BCX (bromine chloride in thionyl chloride) primary cells have been qualified for flight aboard the space shuttle for over fifteen years. These cells provide high energy density while maintaining an excellent safety record. Recently, changes to the electrolyte have resulted in an improved Li/BCX II system with a lower self-discharge rate. The use of low molarity electrolytes in programs unique to NASA have improved the safety hazards tolerance of these cells while maintaining or increasing their energy density.

Introduction

Wilson Greatbatch Ltd. develops and manufactures lithium cells and battery packs for the medical, space, industrial and commercial markets. Many applications still require the use of lithium primary batteries with a high energy density. This is especially true for space applications.

During the past fifteen years, the Li/BCX (bromine chloride in thionyl chloride) primary battery system has been qualified for flight aboard the space shuttle. The excellent safety record of the system, high open circuit voltage of 3.9 volts, good low temperature performance, specific energy of 472 Wh/kg and energy density of 1,035 Wh/L make it an attractive power supply for a variety of applications (1, 2, 3). Presently, Li/BCX C, D and DD cells are qualified power sources for the video cameras, cassette tape data recorders, hand warmers in gloves, helmet lights, AN/PRC-112 survival radio and extravehicular mobility unit/personal life support system used in every shuttle flight.

The Li/BCX system exhibits excellent voltage retention when stored for several years at room temperature. Data will be presented to show that advances made to the Li/BCX II system have improved the self-discharge previously observed. In addition, the restart capability and energy density of the system have been maintained or improved, particularly at lower discharge rates. In programs unique to NASA, the use of lower molarity electrolytes has been investigated and shown to enhance cell safety. Li/BCX II cells are now tolerant to a fifty milliohm short-circuit at room temperature and can be exposed to temperatures as high as 140°C without leaking. Despite the reduced salt concentration used in the electrolyte, the high, moderate and low rate discharge capacity goals of the various programs were still achieved.

Chemistry and Design Features

All cells were spirally wound and contained in stainless steel cases and lids that have corrosion resistant glass-to-metal seals. Battery grade lithium was laminated onto metal grids to form the anode current collector assembly. The cathode current collector assembly was fabricated by sheeting a mixture of carbon black and polytetrafluoroethylene binder onto expanded metal. The separator was a nonwoven glass fiber paper. The two electrodes and the separator were wound together and inserted into the stainless steel case. The anode lead was then welded to the case, resulting in a case negative configuration, and the cathode lead was welded to the positive pin

feedthrough in the header. The BCX and BCX II electrolytes were prepared by forming a suitable electrolyte salt in-situ in the bromine chloride in thionyl chloride solution. After filling with the BCX or BCX II catholyte, cells were hermetically sealed by welding a stainless steel ball over the fill hole.

Characteristics of the Li/BCX System

The Li/BCX system offers several features which make it the power system of choice for several space applications. In addition to having a good safety record and high proven reliability, the system offers a power density as high as 95 W/l and has an energy density of 1035 Wh/l. Additionally, cells are rated for operation at temperatures in the range -55°C to 72°C. When necessary, modifications to the system allow for operation at temperatures approaching -100°C. Historically, the Li/BCX system has been characterized by a self-discharge rate of 3-15%/year.

To fully characterize the Li/BCX system, a large number of D cells were built and stored at room temperature for several years. After initially testing fresh cells under loads ranging from 0.5 ohms to 3010 ohms, additional cells were periodically removed from storage after 6, 12, 24 or 36 months and fully discharged under the same spectrum of loads. As shown in Figure 1, the mid-life operating voltage of the Li/BCX system remained stable even after three years of room temperature storage, varying by less than 200 millivolts. Furthermore, cells discharged under a 1 ohm load maintained a mid-life operating voltage of over 3.0 volts.

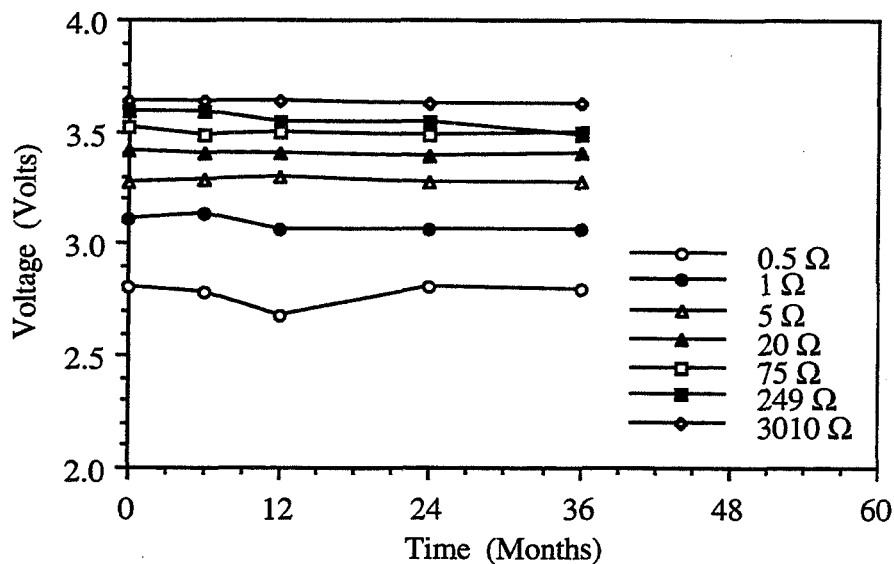


Figure 1: Voltage retention of Li/BCX D cells at 50% depth of discharge.

The capacity retention of Li/BCX D cells over a three year period is shown in Figure 2. The 2.0 volt discharge capacity was measured and recorded for cells that were discharged after 0, 6, 12, 24 or 36 months of room temperature storage. When discharged under loads ranging from 5 ohms to 249 ohms, fresh cells generally provided 13.5 to 15.0 Ah. Over the three year storage period, the cell capacity declined to about 11.0 to 12.0 Ah, representing a yearly self-discharge rate of approximately 9%. As expected, fresh cells that were discharged under a considerably heavier load of 1 ohm or 0.5 ohms provided less capacity due to increased cell polarization. Cells discharged under a 3010 ohm load, however, also provided lower capacity.

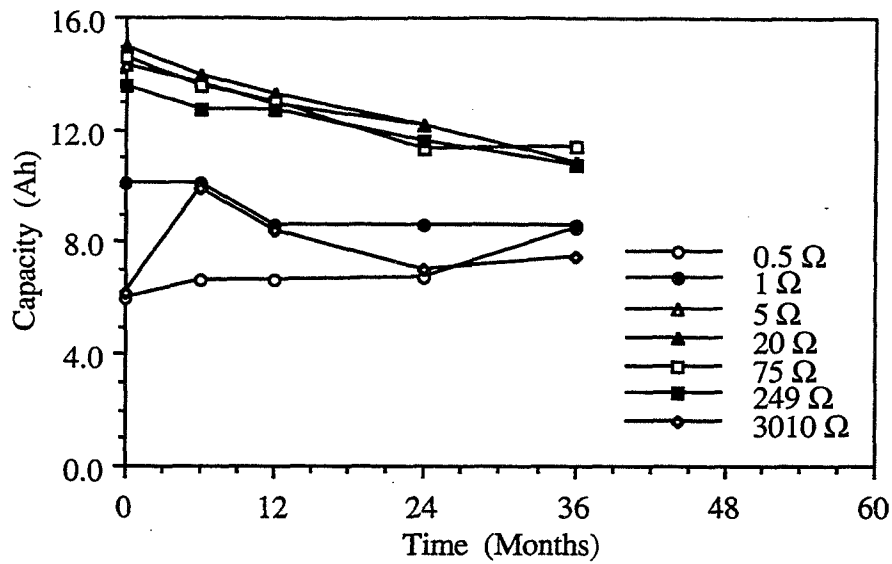


Figure 2: Capacity retention of Li/BCX D cells to 2.0 volts.

Microcalorimetry, in which cell heat dissipation is measured under load or on open circuit voltage, has proven to be a useful tool in estimating the lifetime of Li/BCX cells (4). Recently, modifications and improvements to the electrolyte have resulted in the development of BCX II cells which are characterized by lower self-discharge as measured via microcalorimetry and confirmed via discharge test. As shown in Figure 3, when stored at room temperature over a four year period, Li/BCX II D cells exhibited approximately forty percent of the heat dissipation that Li/BCX D cells exhibited. This manifests itself in a much slower degradation in open circuit voltage as shown in Figure 4. While the open circuit voltage of Li/BCX D cells decreased from 3.95 volts to 3.67 volts over a period of eighteen months, the open circuit voltage of Li/BCX II D

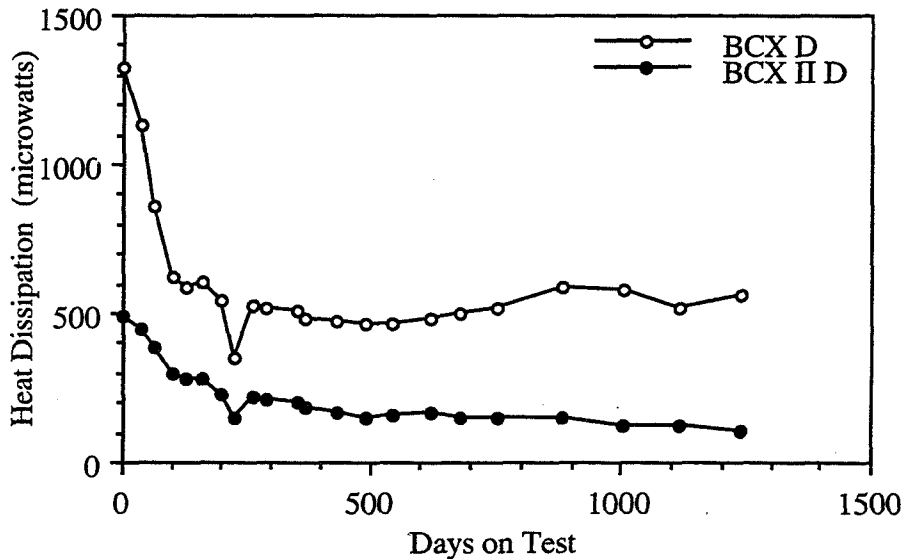


Figure 3: Heat dissipation of Li/BCX D and Li/BCX II D cells.

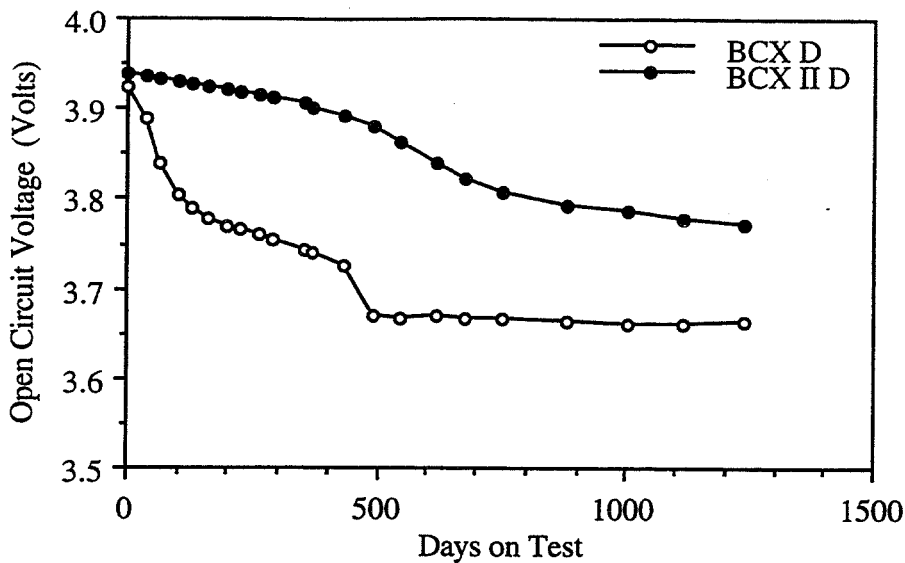


Figure 4: OCV stability of Li/BCX D and Li/BCX II D cells.

cells remained at or above 3.75 volts after four years.

Complementing the microcalorimetry results are discharge results for fresh Li/BCX D and Li/BCX II D cells. In Figure 5, the 2.0 volt discharge capacity obtained for cells tested at room temperature under loads ranging from 0.5 ohms to 3010 ohms is shown. Discharge capacity for the Li/BCX system and the Li/BCX II system is comparable under loads ranging from 0.5 ohms to 20 ohms. At 75 ohms and 249 ohms, discharge capacity is higher for the Li/BCX II system, validating the data obtained via microcalorimetry. Discharge tests under a 3010 ohm load remain in

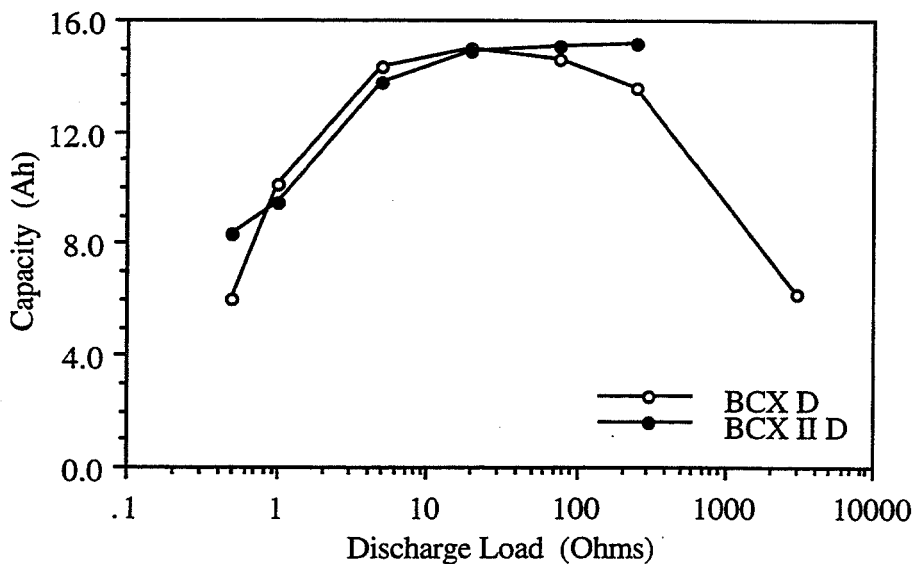


Figure 5: Comparison of discharge capacity to 2.0 volts for fresh cells.

progress; however, capacity obtained to date with the Li/BCX II system has already surpassed that previously obtained with the Li/BCX system.

Voltage delay is a common occurrence associated with liquid cathode primary lithium cells. The phenomenon is attributed to increased thickness of the lithium passivation layer which results in increased cell impedance. During application of a discharge load, the cell voltage may be initially depressed before recovering to a steady-state value. The voltage delay phenomenon becomes more pronounced when cells are stored at elevated temperature or for long periods of time and subsequently discharged at low temperature and high current.

Comparisons were made of the room temperature voltage delay characteristics of Li/BCX D and Li/BCX II D cells discharged under a 4 ohm load. The results are shown in Figures 6 through 9 for fresh cells and for cells previously discharged to 10%, 30% and 60% depth of discharge, respectively. For fresh cells, as shown in Figure 6, little difference existed between the voltage of Li/BCX and Li/BCX II cells.

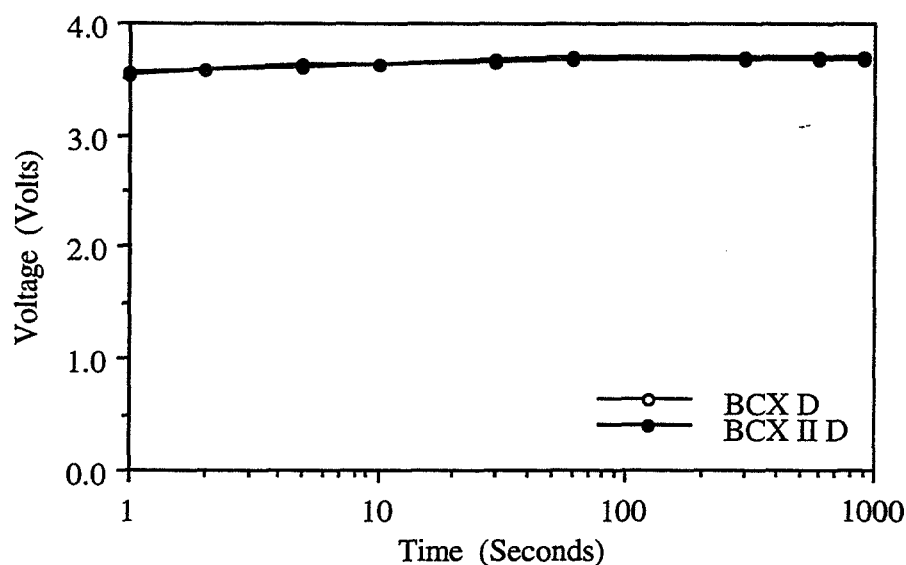


Figure 6: Room temperature voltage delay of fresh cells under 4 ohm load.

As shown in Figure 7, differences in voltage began to emerge at 10% depth of discharge. The Li/BCX II D cells exhibited a slightly higher voltage during the first five minutes of discharge; however, the voltage of both systems remained above 3.0 volts following application of the discharge load. In Figure 8, significant differences existed between the two systems at 30% depth of discharge. Whereas the voltage of Li/BCX II D cells remained above 3.0 volts, that of the Li/BCX D cells was depressed below 2.0 volts for the initial thirty seconds of the test and did not reach 3.0 volts during the first fifteen minutes of discharge. When restarted after 60% depth of discharge, Li/BCX D cells remained between 2.3 volts and 2.6 volts for the initial fifteen minutes of the test. Although the Li/BCX II D cell voltage declined below 2.0 volts during the initial ten seconds of test, it surpassed the voltage of the Li/BCX system within thirty seconds and ultimately recovered to above 3.0 volts within five minutes.

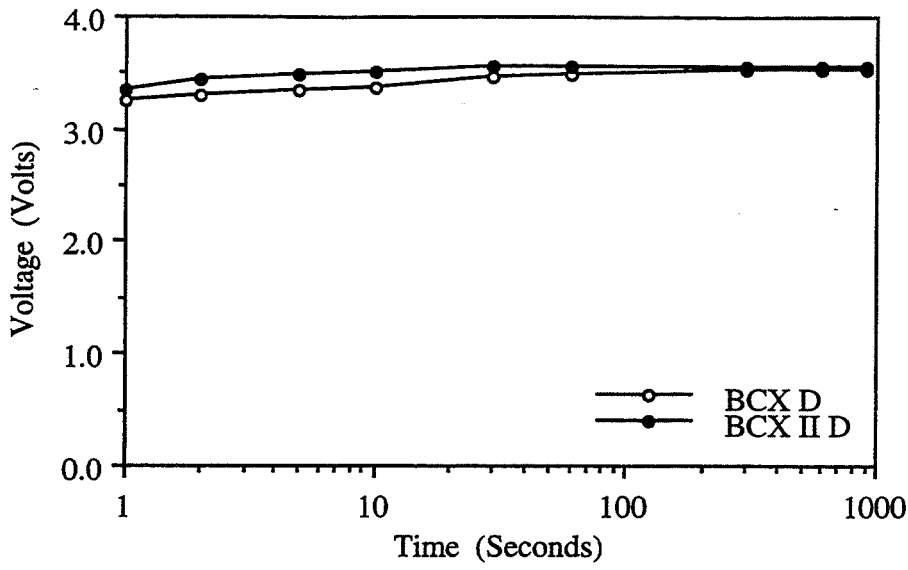


Figure 7: Room temperature voltage delay under 4 ohm load of cells at 10% depth of discharge.

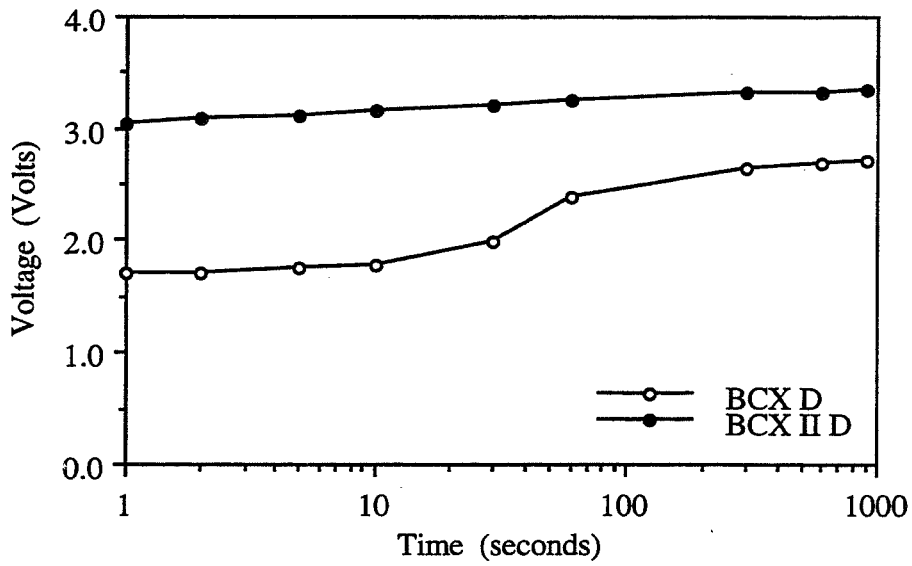


Figure 8: Room temperature voltage delay under 4 ohm load of cells at 30% depth of discharge.

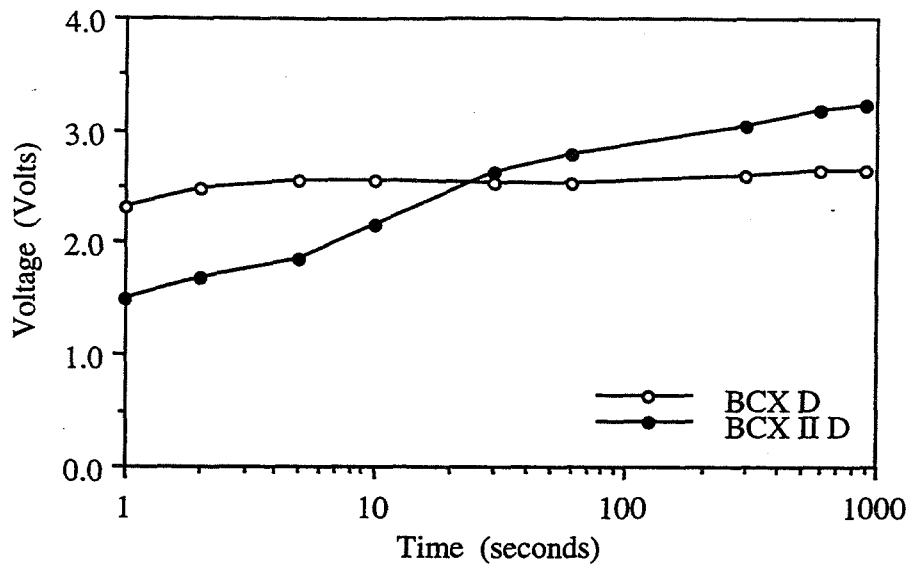


Figure 9: Room temperature voltage delay under 4 ohm load of cells at 60% depth of discharge.

Improved Cells for Space Applications

Wilson Greatbatch Ltd. and NASA have embarked on a series of development efforts aimed at maintaining or increasing the rate capability, capacity and temperature tolerance of Li/BCX cells while increasing the short-circuit hazards tolerance (5, 6, 7). To achieve these objectives, low molarity Li/BCX II cells including 0.6 M Li/BCX II C cells, 0.4 M Li/BCX II D cells and 0.6 M Li/BCX II DD cells were developed for present and future applications.

A primary goal for the next generation of cells is to be tolerant of a fifty milliohm external short-circuit while maintaining internal continuity and not having cells leak, vent or rupture. Short-circuit tests were conducted on low molarity Li/BCX II cells at room temperature using the designated angle iron as specified in NASA document number EP5-83-025 Rev. G. The test results are presented in Table 1. The 0.6 M Li/BCX II C cell exhibited a peak current of up to 22.5 amps and a peak temperature as high as 85.5°C. The 0.4 M Li/BCX II D cell and the 0.6 M Li/BCX II DD cell exhibited peak currents of 22.0 amps and 33.3 amps, and peak temperatures of 86.5°C and 100.0°C, respectively. None of the 0.6 M Li/BCX II C cells or the 0.4 M Li/BCX II D cells leaked, vented or ruptured as a result of these tests; however, a few of the 0.6 M Li/BCX II DD cells were observed to leak or vent mildly at the glass to metal seal.

Table 1. Fifty Milliohm Short-Circuit Tolerance of Low Molarity Li/BCX II Cells.

	Peak Current (Amps)	Peak Temp. (°C)	Physical Changes
0.6 M C Cell	19.2 - 22.5	59.0 - 85.5	None
0.4 M D Cell	16.0 - 22.0	77.0 - 86.5	None
0.6 M DD Cell	26.0 - 33.3	85.2 - 100.0	Mild Vent

The temperature tolerance of low molarity Li/BCX II C, D and DD cells was determined by exposing fresh cells, cells discharged to 2.0 volts or lower, and cells subjected to a fifty milliohm short-circuit test to temperatures in the range of 100°C to 160°C at 10°C exposure intervals. The test results are reported in Table 2. The temperature tolerance of all three types of cells was maintained at or above 100°C, nearly 30°C above the maximum temperature rated for use. The 0.6 M Li/BCX II C cells were tolerant to 140°C without leaking at the glass-to-metal seal.

Table 2. Temperature Tolerance of Low Molarity Li/BCX II Cells.

	Minimum Leakage Temperature
0.6 M C Cell	140°C
0.4 M D Cell	125°C
0.6 M DD Cell	100°C

The specific attributes of the Li/BCX and Li/BCX II systems make them attractive for use in a number of space applications. Accordingly, NASA may use the same cell for a variety of applications and each application may require that a specific capacity be obtained under a particular test regime. When designed, each type of cell may be required to meet minimum capacity requirements under various discharge loads. This allows the cell to be used interchangeably among the various programs and applications.

The capacity requirements for the 0.6 M Li/BCX II C cell are shown in Table 3. When discharged at room temperature under a 6 ohm load, cells are expected to provide a mean discharge capacity of 4.0 Ah. When discharged under a 10 ohm or 75 ohm load, cells are expected to provide a capacity of 5.0 Ah and 6.0 Ah, respectively. The low molarity cell provided 4.94 Ah, 5.38 Ah and 7.24 Ah to 2.0 volts when discharged under a 6 ohm, 10 ohm or 75 ohm load, satisfying the various program requirements.

Table 3. 0.6 M Li/BCX II C Cell Capacity Summary.

Discharge Load (Ohms)	Requirement (Ah)	Achieved (Ah)
6	4.00	4.94
10	5.00	5.38
75	6.00	7.24

The 2.0 volt capacity requirements for the 0.4 M Li/BCX II D cell and for the 0.6 M Li/BCX II DD cell are shown in Tables 4 and 5 along with the capacity achieved. The 0.4 M Li/BCX II D cells provided 10.0 Ah and 12.3 Ah when discharged at room temperature under a 10 ohm or 20 ohm load, satisfying the program requirements of 10.0 Ah. The 0.6 M Li/BCX II DD cell was required to provide 22.0 Ah at room temperature when discharged under a 1.5 ohm load, 25.0 Ah when discharged under a 2.5 ohm load and 27.0 Ah when discharged under a 10 ohm load. The data provided in Table 5 indicate that these objectives were achieved. The mean capacity delivered to 2.0 volts was recorded as 28.7 Ah, 32.3 Ah and 35.6 Ah, respectively.

Table 4. 0.4 M Li/BCX II D Cell Capacity Summary.

Discharge Load (Ohms)	Requirement (Ah)	Achieved (Ah)
10	10.0	10.0
20	10.0	12.3

Table 5. 0.6 M Li/BCX II DD Cell Capacity Summary.

Discharge Load (Ohms)	Requirement (Ah)	Achieved (Ah)
1.5	22.0	28.7
2.5	25.0	32.3
10.0	27.0	35.6

Development of the Li/BCX II system coupled with the use of low molarity electrolytes has led to the development of improved lithium primary cells for future space missions. As shown in Table 6, the specific energy and energy density of DD cells has been increased from 472 Wh/kg and 1035 Wh/l to 560 Wh/kg and 1256 Wh/l, an improvement of more than 18.5%. Additionally, the self-discharge rate of the system is projected to decrease from 3-15%/year to 1-3%/year, further improving the reliability and attractiveness of the system.

Table 6. DD Cell Capacity Comparison.

	1.14 M Li/BCX DD Cell	0.6 M Li/BCX II DD Cell
Specific Energy	472 Wh/kg	560 Wh/kg
Energy Density	1035 Wh/l	1256 Wh/l
Self-Discharge	3-15%/Year	1-3%/Year

Conclusions

The Li/BCX primary system offers stable voltage and high capacity after several years of storage. Recent improvements to the system have led to lower heat dissipation, resulting in a more stable open circuit voltage, a lower self-discharge rate and improved voltage delay characteristics. Low molarity Li/BCX II C, D and DD cells have been developed to meet the requirements of future space applications. The short-circuit hazards tolerance of these cells has been improved and the temperature tolerance has been maintained. The specific energy and energy density of low molarity Li/BCX II cells have been increased while the self-discharge rate is projected to decrease markedly.

References

1. C. C. Liang, P. W. Krehl and D. A. Danner, *Journal of Applied Electrochemistry*, 11, 563 (1981).
2. R. M. Murphy, P. W. Krehl and C. C. Liang, in *Proceedings of 16th Intersociety Energy Conversion Engineering Conference*, p. 97 (1981).
3. P. W. Krehl and C. C. Liang, *Journal of Applied Electrochemistry*, 13, 451 (1983).
4. E. S. Takeuchi, S. M. Meyer, and C. F. Holmes, *Journal of Electrochemical Society*, Vol. 137, No. 6, p. 1665 (1990).
5. P. J. Size, E. S. Takeuchi, *Lithium D-Cell Study, Final Report*, March 1993 (contract number NAS9-18395).
6. D. M. Spillman, N. M. Waite, E. S. Takeuchi, *NASA Flight C Cell Development Program, Final Report*, April 1996 (purchase order number T-5789T).
7. D. M. Spillman, N. M. Waite, E. S. Takeuchi, *NASA Flight DD Cell Development Program, Final Report*, October 1997 (purchase order number T-3193V).

Acknowledgment

This work was partially funded by NASA, Johnson Space Center, under contract/purchase order numbers NAS9-18395, T-5789T and T-3193V. The authors would like to thank Mr. Bob Bragg for his useful comments and discussion related to achieving the various program objectives.

Development of Ultra Low Temperature, Impact Resistant Lithium Battery for the Mars Microprobe

H. Frank, F. Deligiannis, E. Davies, B. V. Ramakumar and S. Surampudi

Electrochemical Technologies Group, Jet Propulsion Laboratory

4800 Oak Grove Dr., Pasadena, California

and

P. G. Russel and T. B. Reddy

Yardney Technical Products, Inc.,

82, Mechanic St., Pawcatuck, CT

ABSTRACT

The requirements of the power source for the Mars Microprobe, to be backpacked on the Mars 98 Spacecraft, are fairly demanding, with survivability to a shock of the order of 80,000 g combined with an operational requirement at -80°C . Development of a suitable power system, based on primary lithium-thionyl chloride is underway for the last eighteen months, together with Yardney Technical Products Inc., Pawcatuck, CT. The battery consists of 4 cells of 2 Ah capacity at 25°C , of which at least 25 % would be available at -80°C , at a moderate rate of C/20. Each probe contains two batteries and two such probes will be deployed. The selected cell is designed around an approximate 1/2 "D" cells, with flat plate electrodes. Significant improvements to the conventional Li-SOCl₂ cell include : a) use of tetrachlorogallate salt instead of aluminate for improved low temperature performance and reduced voltage delay, b) optimization of the salt concentration, and c) modification of the cell design to develop shock resistance to 80,000 g. We report here results from our several electrical performance tests, mission simulation tests, microcalorimetry and AC impedance studies and Air gun tests. The cells have successfully gone through mission-enabling survivability and performance tests for the Mars Microprobe penetrator.



Development of a Ultra- Low Temperature, Impact-Resistant Li primary Battery for Mars Microprobe

**Harvey Frank, Frank Deligiannis, Evan Davies,
Kumar Bugga and Rao Surampudi**

and

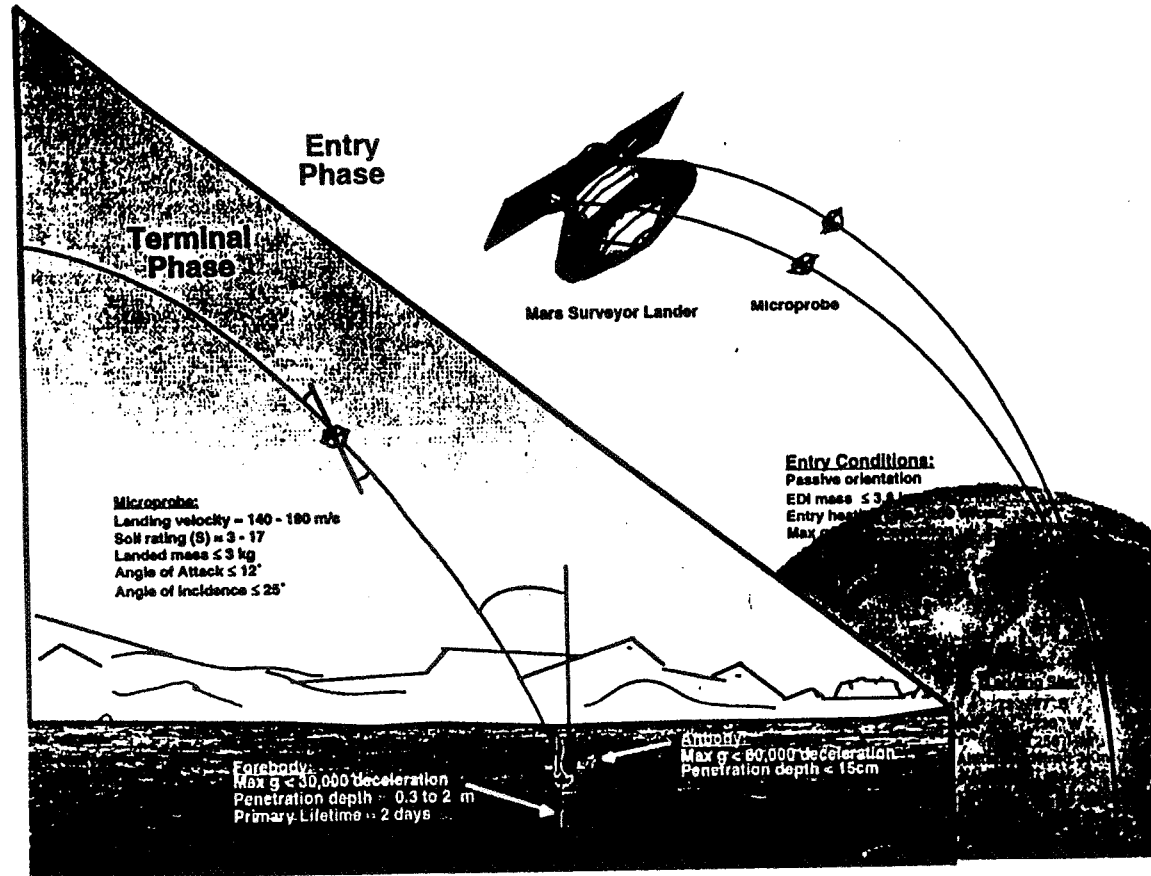
**Phil Russel and T. B. Reddy
Yardney Technical Products**

Nov. 18, 1997

**NASA Aerospace Battery Workshop
November 18-20, 1997, Huntsville, AL**



Mars Microprobe - Mission Description 1





SCIENCE OBJECTIVES



- **Acceleration data during entry and descent**
- **Atmospheric pressure data**
- **Soil temperature data**
- **Soil water content - spectrometer and electromechanical drill incorporated in the forebody.**



Mars Microprobe - Mission Description 2

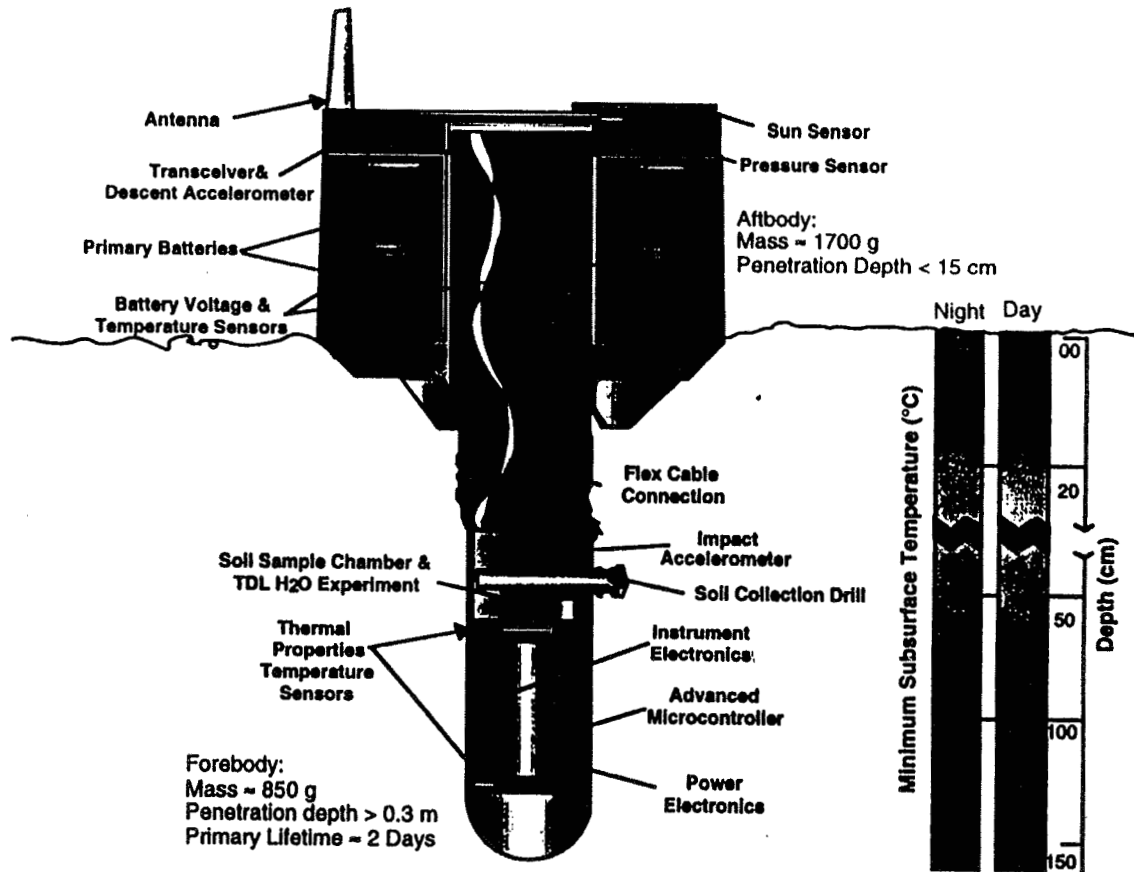


Figure 1-7: Landed Configuration

Mars Microprobe Battery Objective

- Demonstrate flight like hardware that meets performance requirements after representative impact test in representative thermal environment
 - 6 - 12 volts
 - 2 year life
 - 2 A-hr capacity RT
 - 0.5 A-hr capacity at -80°C
 - Survive impact 200 m/sec
 - Load profile attached



BACKGROUND



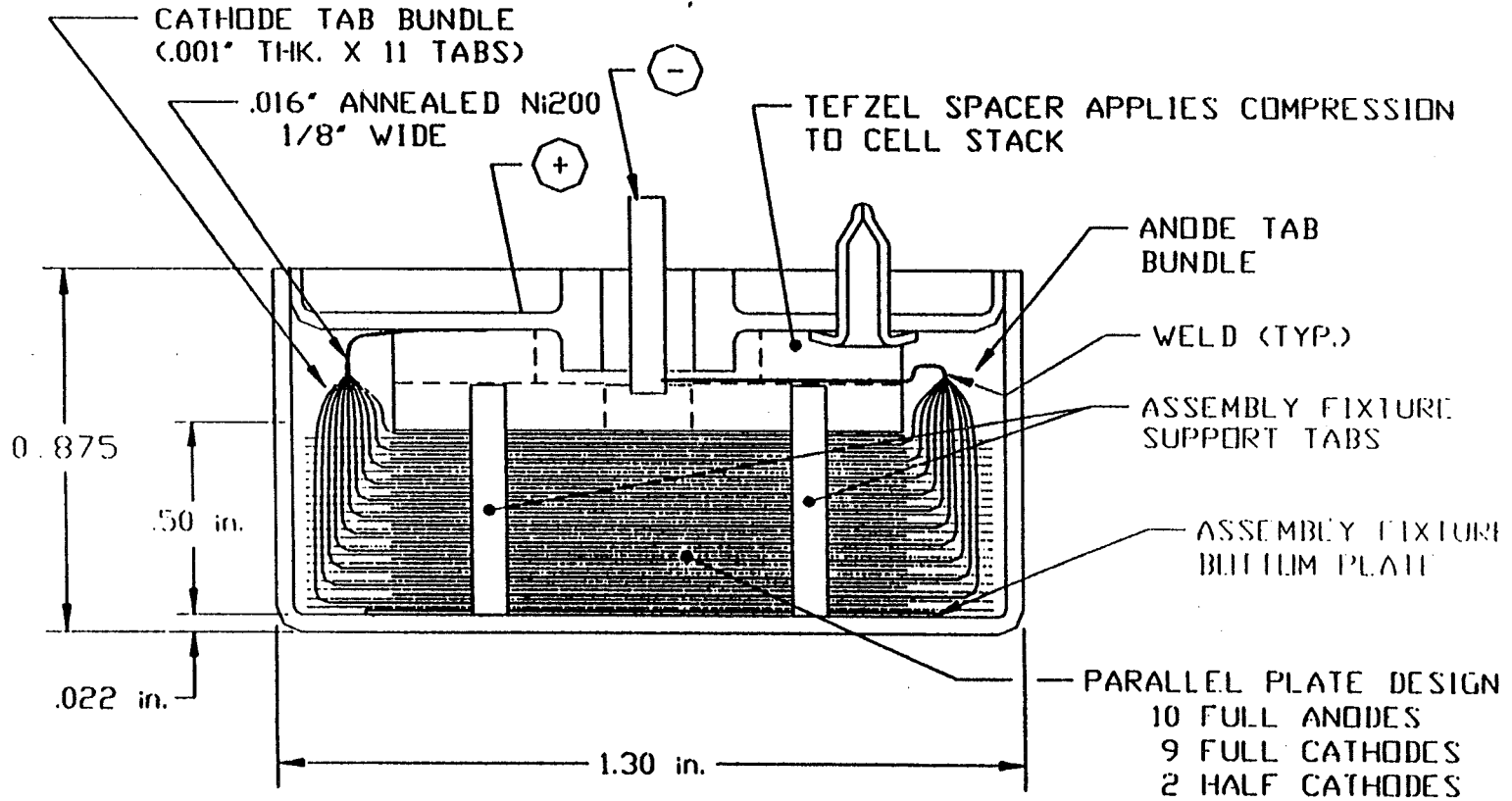
- **Li-SOCl₂ is the most suitable system from the polarization curves and discharge tests at -80°C.**
- **Lithium tetrachlorogallate gave improved discharge and voltage delay characteristics compared to tetrachloroaluminate.**
- **Lower salt concentrations (0.5 M vs. 1.0 M) improve electrolyte conductivity.**
- **Pancake (flat-plate) design in sliced “D” cell.**



MARS MICROPROBE CELL



VERTICAL CROSS-SECTION OF THE FINAL 2 Ah CELL DESIGN



TOPICS

- Microcalorimetry and AC Impedance
- Battery Motor Tests
- Voltage Delay
- Impact Testing
- Accelerated Storage
- Special Topics
 - Inspections
 - Installation and Wiring
 - Safety
 - Prior Issues
- Schedule
- Assessments

LOAD PROFILES

REQUIRED LOADS (ORIGINALLY)

- Descent: first 10 min @ -40 °C
 - 8 mA -4 min, 13 mA -4 min, 30 mA -2 min
- Surface Operations for next 6 hrs
 - Sleep mode: 1 mA, -60 to 80 °C
 - Science pulses: 33 mA, -60 to -80°C, each 1/2 hr
 - Drill: 88 mA, 10 min, -40 °C, TBD time
 - H₂O Heater: 605 mA, 20 min, -60 °C, TBD time
 - Transmit: 176 mA, 15 min, -80 °C, TBD time

NEW REQUIREMENTS FOR SURFACE OPS

- H₂O Calib, 605 mA, 2 min, -60°C, TBD time
- Transmit: Highest Power, 15+min, -60 to -80 °C

MICROCALORIMETRY

OBJECTIVE

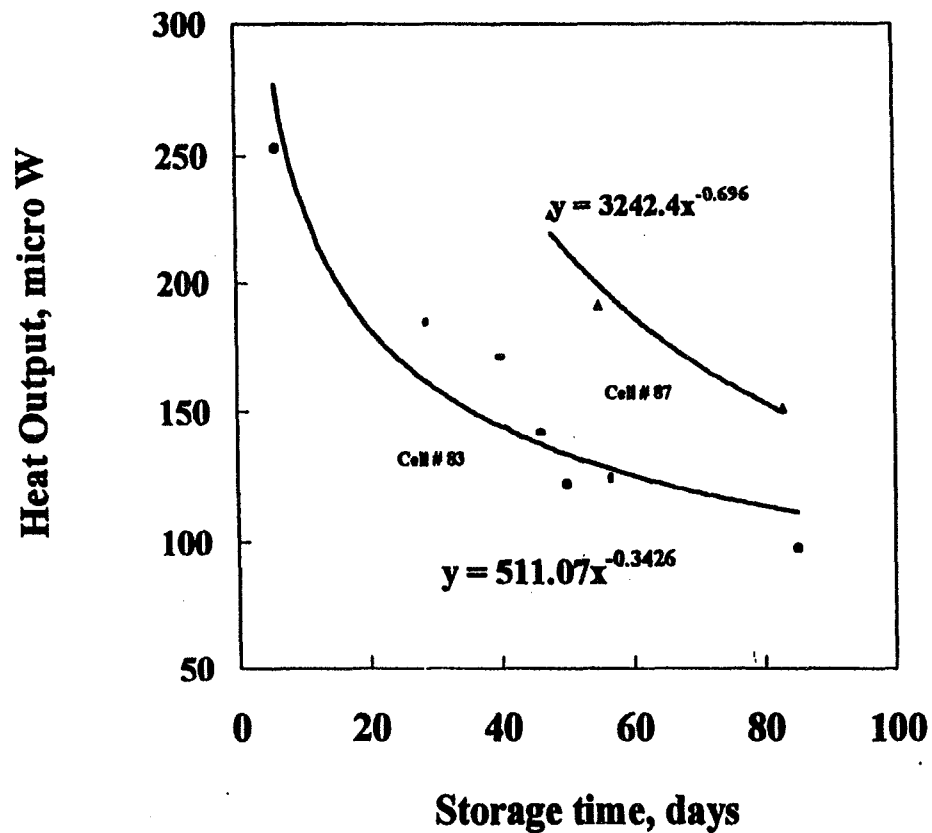
- **Predict capacity loss of cells for 2 year stand @ RT.**
- **Determine effect of temperature on capacity losses.**
- **Obtain 'acceleration factor' for elevated temperature storage tests.**

APPROACH

- **Measure heat from cell from cells using microcalorimeter, periodically during storage.**
- **Measure heat from cells over a range of temperatures.**
- **Analyze data to make predictions.**



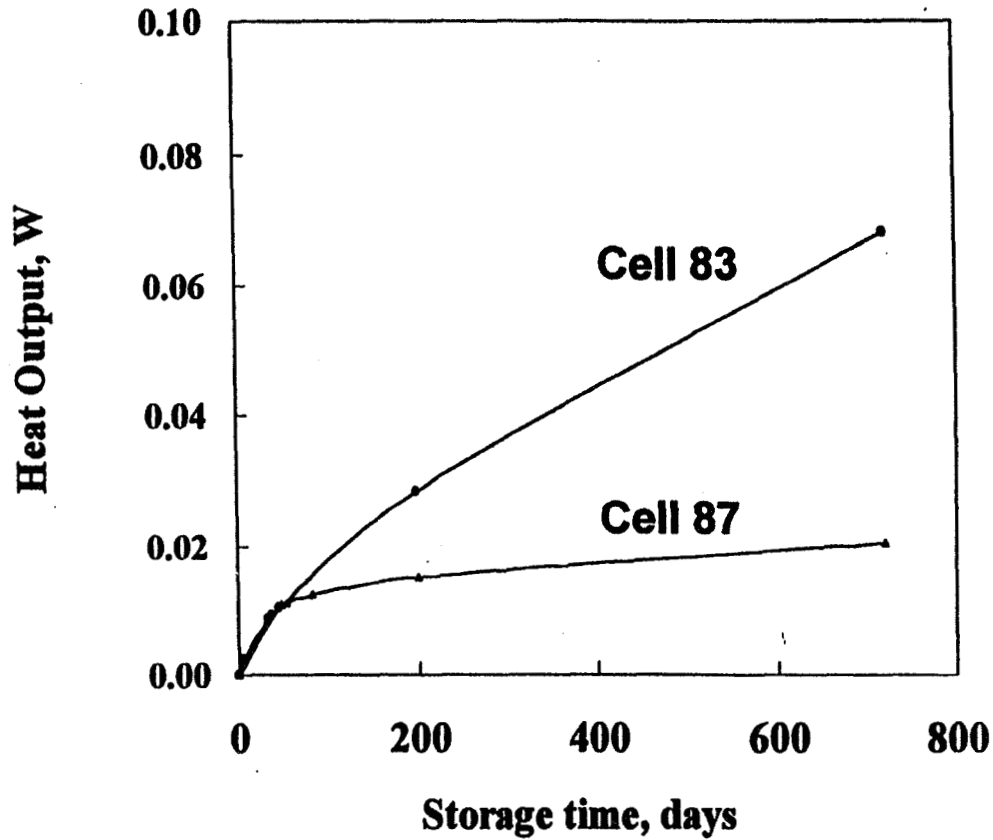
Observed Cell Heat Output During Storage



- Exponential decay in corrosion rate during storage



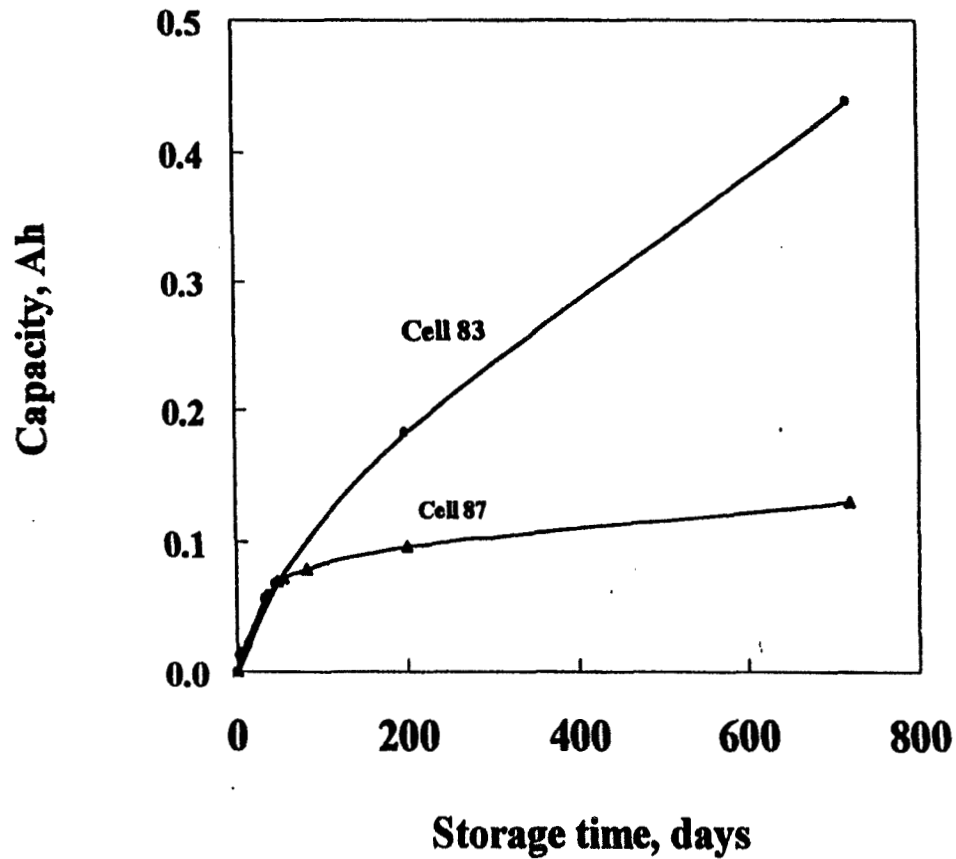
Predicted Cumulative Heat Output Over 2 Years



- Predicted based on extrapolation of experimental data

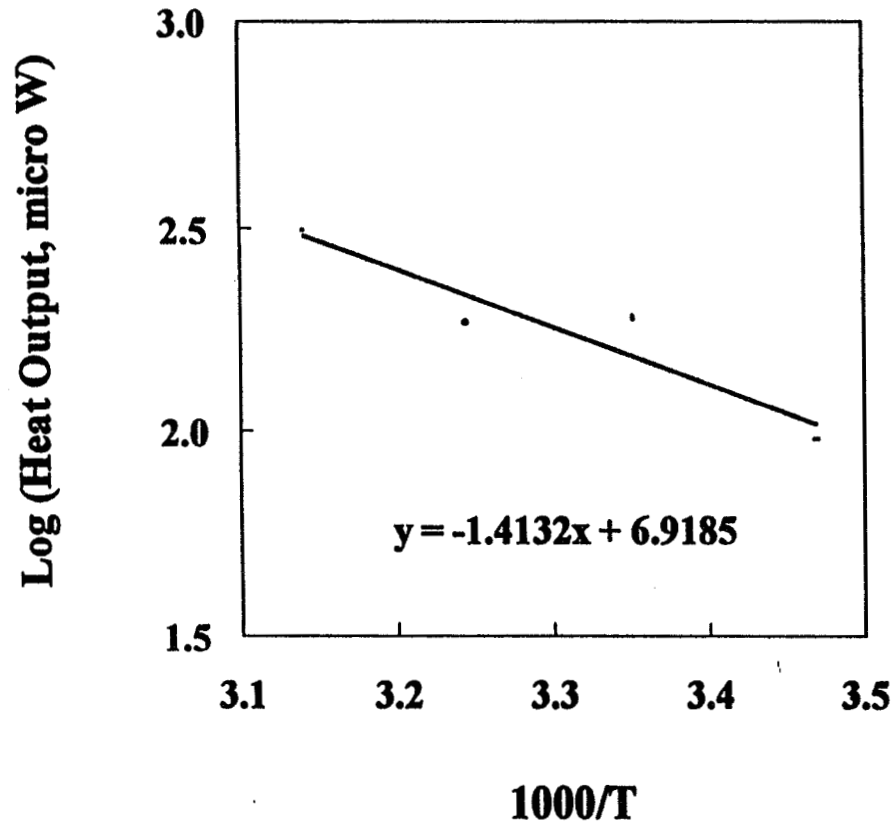


Predicted Capacity Loss During Storage at RT



- Calculated based on a thermoneutral voltage of 3.72 V

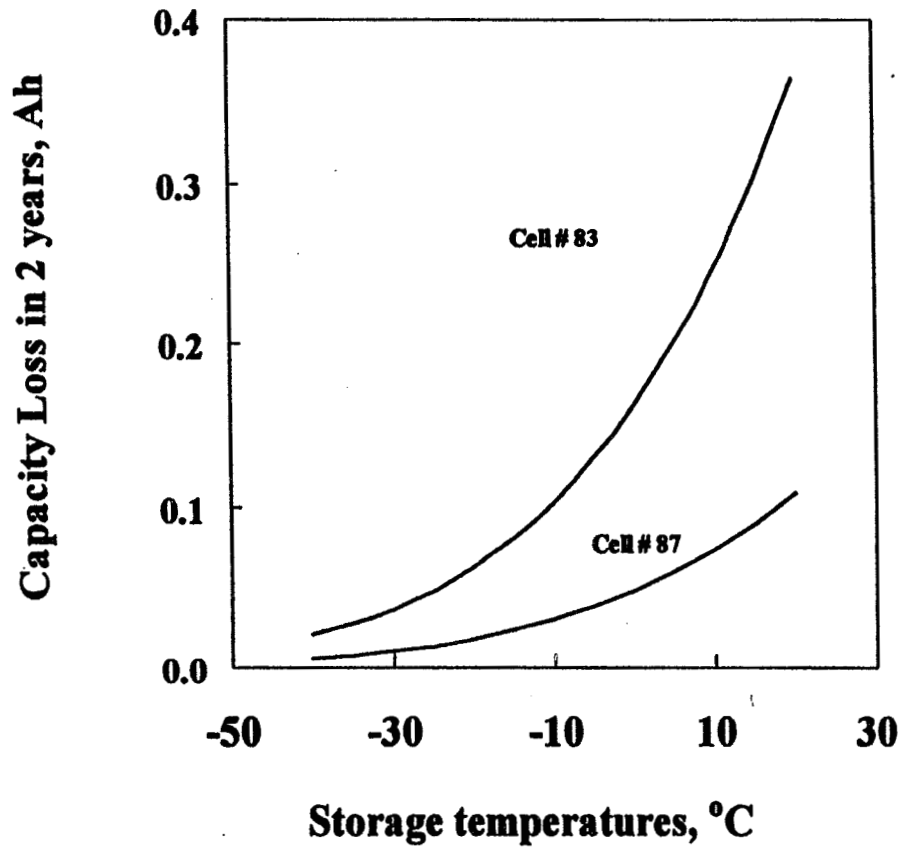
Arrhenius Plot of Li Corrosion (Self Discharge)



- Activation Energy : 1.64 kcal/mole



Predicted Capacity Loss vs. Storage Temperature



- Lower storage temperature desired.



ELECTROCHEMICAL IMPEDANCE SPECTROSCOPY

OBJECTIVE

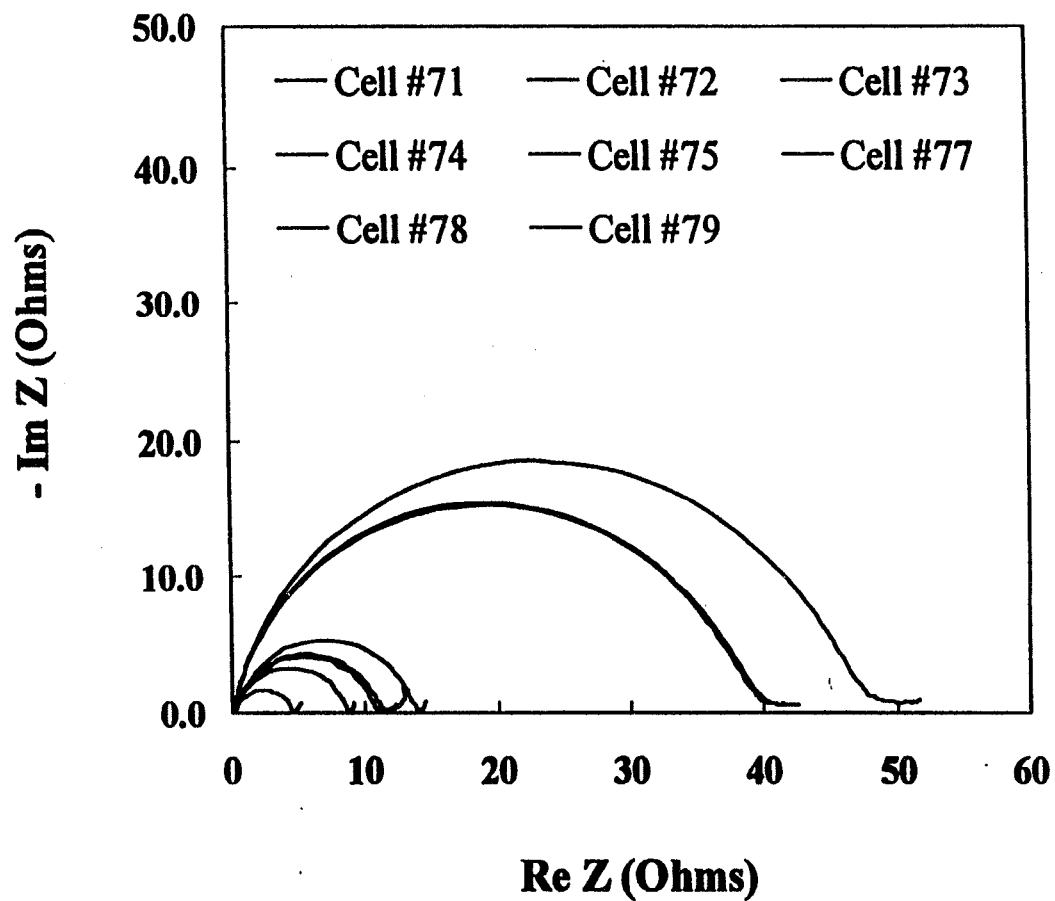
- **Examine variations in the cell construction and or workmanship non-destructively.**
- **Examine the (lithium) interfacial conditions that would impact stability (life) and voltage delay.**
- **Detect signs of cell degradation during stand.**

APPROACH

- **Establish baseline impedance spectra of the cells.**
- **Establish correlations, if any, with the life and voltage delay characteristics.**



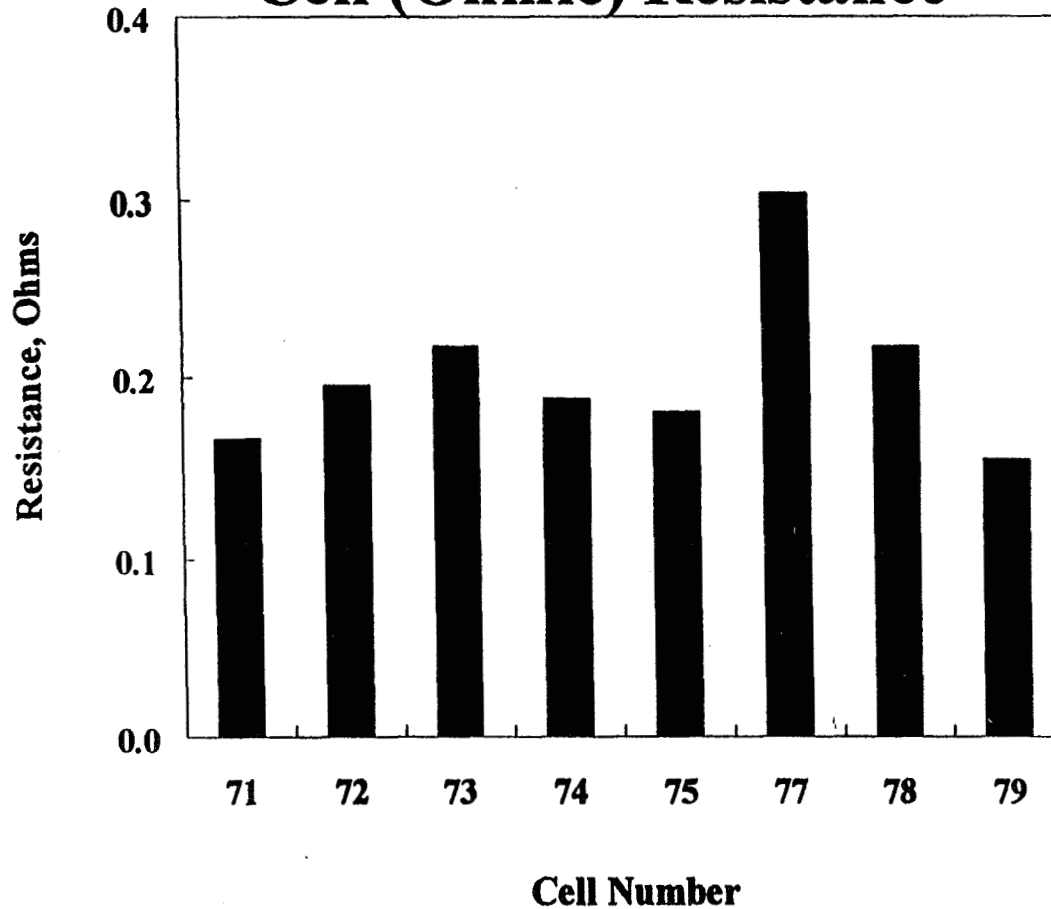
Impedance Spectra of Fresh Cells



- **Film Resistance varies from cell to cell.**



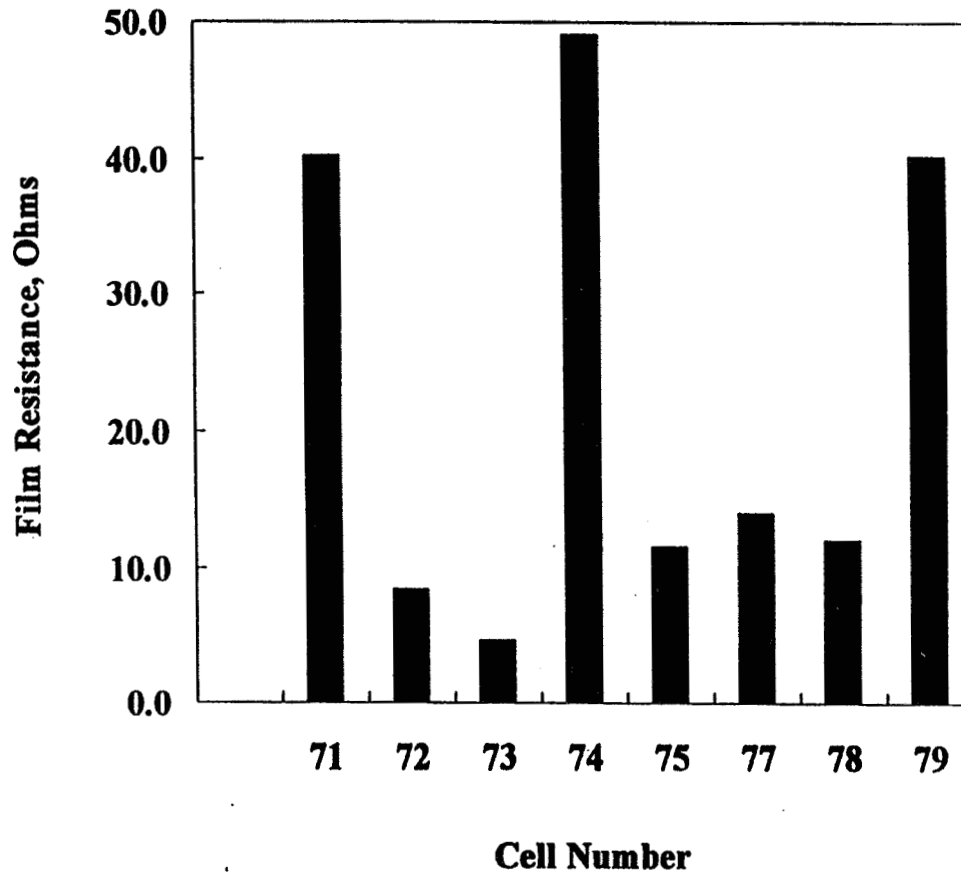
Cell (Ohmic) Resistance



- Cell Resistance 150-210 mΩ; consistent with the mOhm measurement after film voltage delay.



Film Resistance

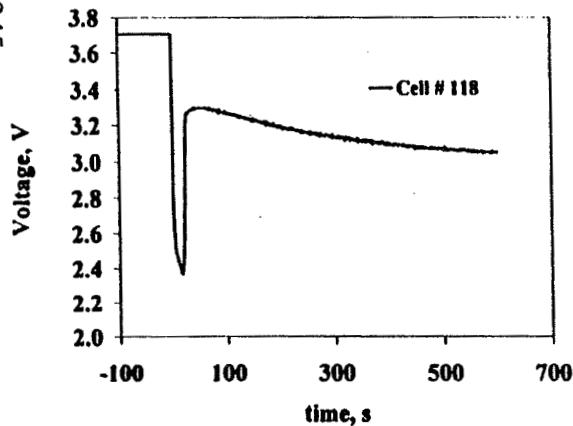


- Film resistance varies from 5-40 Ω .

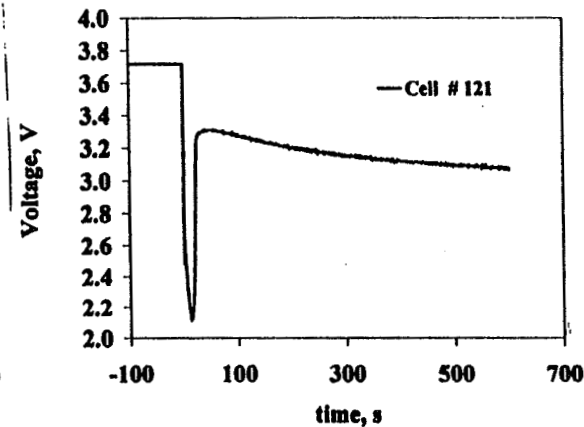
VOLTAGE DELAY

(EXPLORATORY DATA ON YTP 2 AH CELLS)

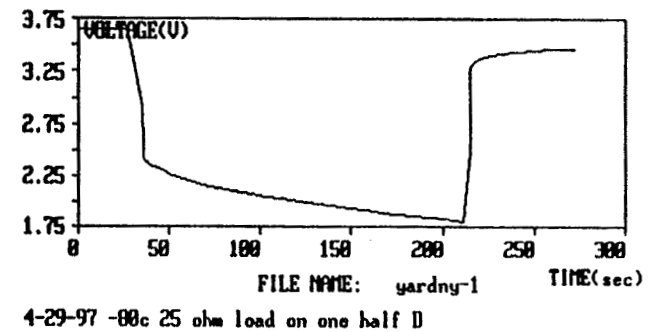
Delay at 100 mA at -40 C



Delay at 100 mA at -40 C



Delay at -80 C



- Delay appears significant but not excessive @ moderate currents @ -40 to -60 degrees C
- Delay could pose problems at moderate currents @ -80 degrees C

VOLTAGE DELAY

CONCLUSIONS

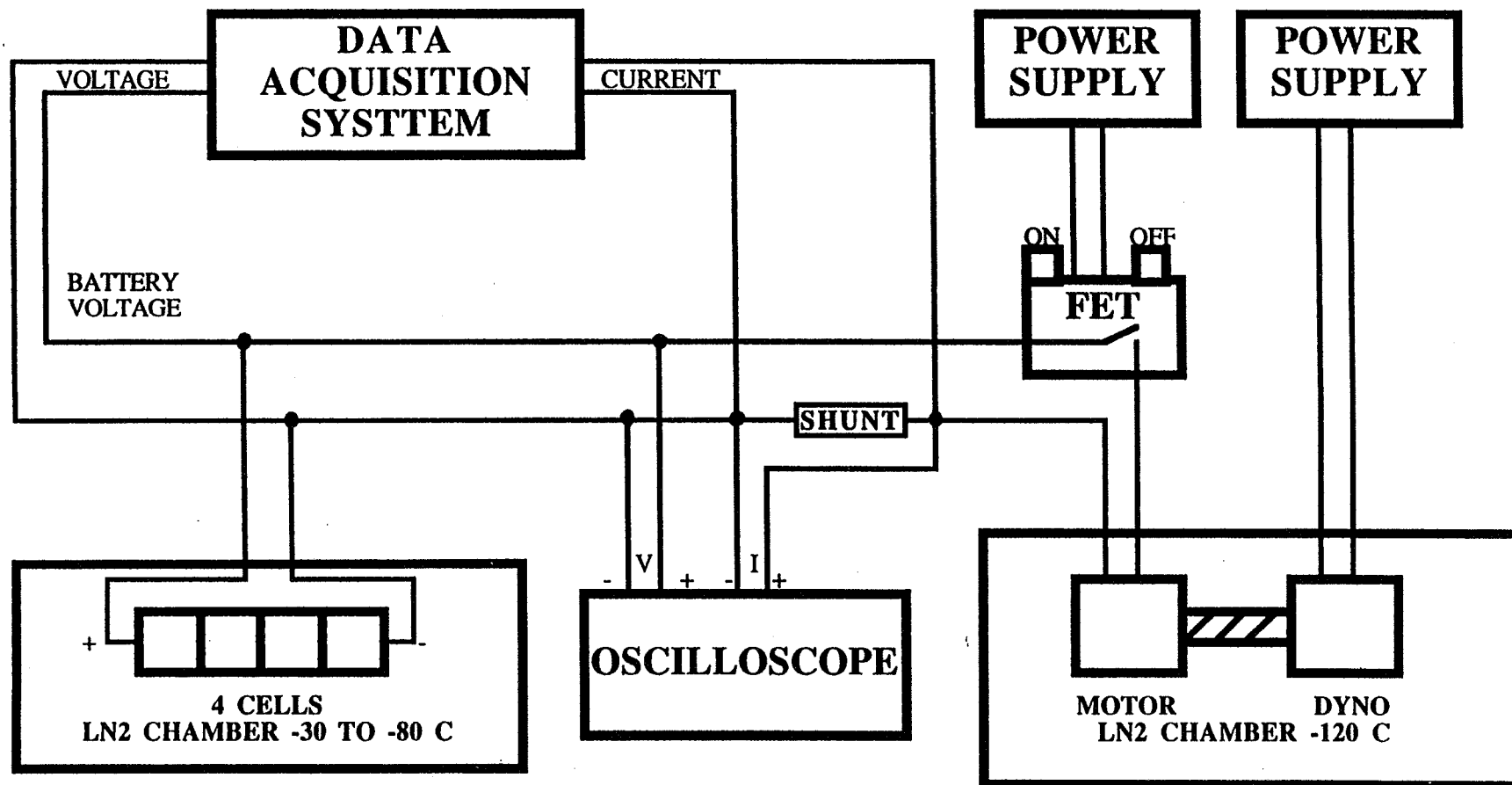
- Voltage depression from delay is significant but not excessive at moderate loads @ -40 to -60 degrees C
 - Can meet early descent loads with adequate voltage @ temps to -60 degrees C
- Voltage depression from delay is appreciable at moderate loads @ -80 degrees C
 - Can meet Initial transmit load but with little margin
 - May incorporate short conditioning discharge prior to transmit @ -80 degrees C
- No voltage depression from delay later in profile @ -60 degrees C for H2o Expt @ 605 mA, and even high new transmit to 1A.

BATTERY - MOTOR TESTS

OBJECTIVES

- DETERMINE CAPABILITY OF BATTERY @ -30 TO -80 degrees C TO RUN DRILL MOTOR @ -120 degrees C
- DETERMINE TRANSIENT MOTOR START AND OPERATIONAL MOTOR CURRENTS AND VOLTAGES
- DETERMINE TRANSIENT MOTOR STALL AND STEADY MOTOR STALL CURRENTS AND VOLTAGES.

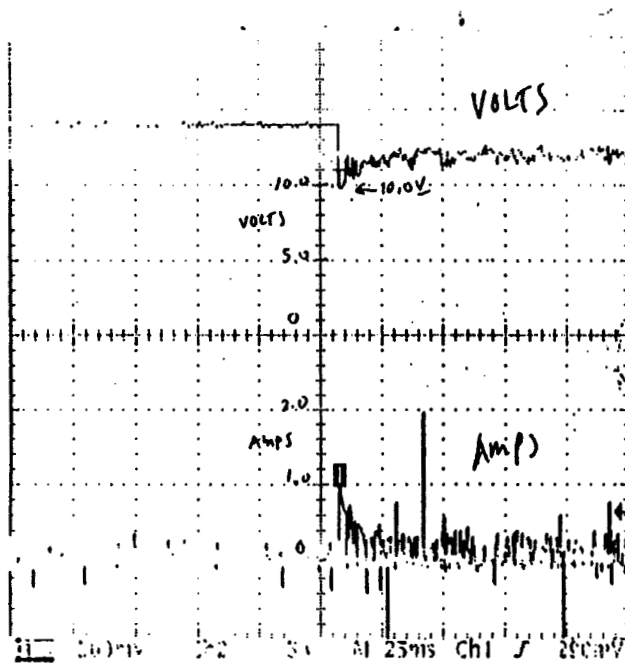
DS2 BATTERY/MOTOR TEMP TEST



- Scope triggers by motor start and records transient voltage and current
- Dyno set for 1 inch-lb to simulate drill
- Motor shaft frozen for stall
- DAS records steady state voltage and current

BATTERY MOTOR TESTS

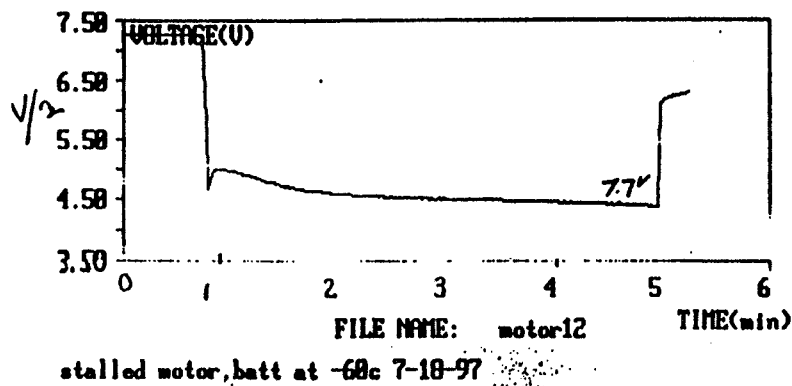
(Sample - Transient Start @ -60 degrees C)



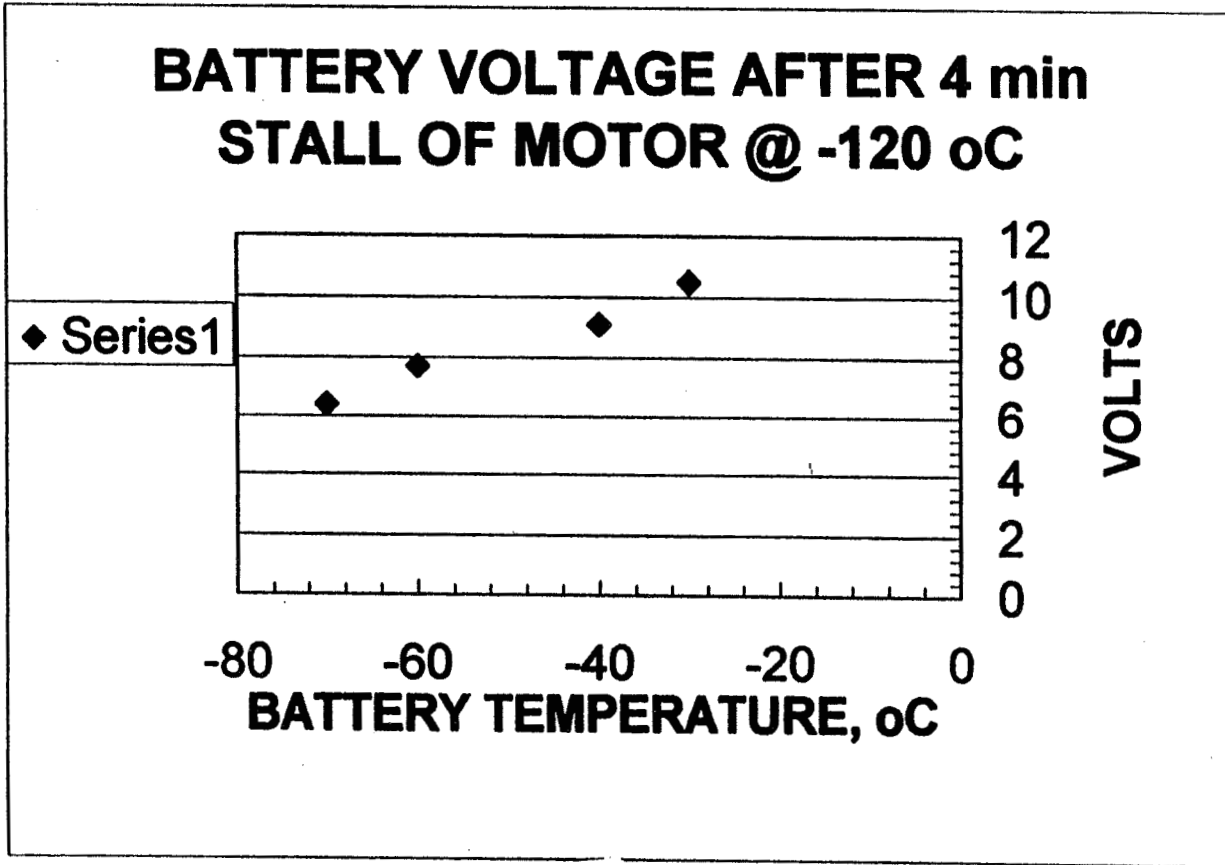
- Scope trace @ -60 degrees C
- Peak current near 1A and Min V near 10.0 V
- Lasts only 25 ms
- Current quickly tapers to near 70 mA
- Similar results from -30 to -70 degrees C

BATTERY MOTOR TESTS

Sample - Stall Run @ -60 degrees C



- DAQ trace @ -60 degrees C for 4 min.
- Start spike noted
- Voltage near 7.7 V @ 390 mA
- Similar results from -30 to -70 degrees C



BATTERY MOTOR TESTS

Summary/Conclusion

•STARTING CHARACTERISTICS

- Current near 1 A for 25 ms
- Minimum voltage decreases with temp (8V @ -70 degrees C, 4V @ -80 degrees C)

•RUN CHARACTERISTICS

- Currents near 70mA
- Voltages relatively stable for at least 10 min
- Voltage level declines with temp (10V @ -70 degrees C, 4V @ -80 degrees C)

•STALL CHARACTERISTICS

- Currents near 400 mA
- Voltages relatively stable for 4 min
- Voltage level declines with temp (7.7 V @ -60 degrees C)

•BATTERY CAN OPERATE DRILL AND STALL @ -60 Degrees with margin

IMPACT TESTING

OBJECTIVE

- Demonstrate capability of battery:
 - Withstand 200 m/sec impact shock
 - Deliver required electrical loads at minimum temperatures

APPROACH

- Install cells in probe assemblies
- Fire assembly into target with airgun
- Retrieve assembly and conduct discharge tests in accord with mission profile and temp.

IMPACT TESTING

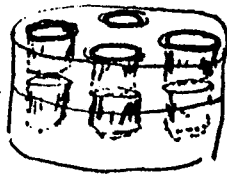
TEST ITEMS

- Two cell types

- Old: GTM + Cover with fill port in center as terminal
- New: New GTM + Thicker cover with pin in center & fill tube on side
- Electrode stacks + electrolyte same for old and new types

- Two cell configurations in probe

OLD



2 LAYERS OF
FOUR CELLS

NEW



1 LAYER OF
EIGHT CELLS

IMPACT TESTING

OVERVIEW

TEST NO.	DATE	CELL TYPE	NO CELLS	PROBE TYPE	AOA	HIGHLIGHT
36	3/13/97	OLD	4	21	10 degrees	All got GTM cracks and leaks, 3 functioned
38	4/4/97	OLD	2	11	NA	Both got GTM cracks and leaks, both functioned
42	5/29/97	OLD	8	11	+2	All got GTM cracks and leaks, 1 opened, 7 functioned
50	8/28/97	NEW	8	11	-15	No cracks, no leaks, 1 rented, 1 bulged, 7 functioned
53	10/29/97	NEW	7	11	+2	No cracks, no leaks, 7 functioned

AIRGUN TEST # 42

OVERVIEW

- 8 cells, old design, 1 layer config
- No venting
- But all cells had small cracks & slow leaks in GTM
- 1 cell developed “open” condition”
- Remaining 7 cells delivered good output @ -80 °C

Significance

- * One layer configuration appears best
- * Old GTM-Seal assembly inadequate
- * Cells survived and functioned (with leaks)
- * “Open” due to faulty pin weld

AIRGUN TEST #42

DISCHARGE TEST RESULTS

•Descent Load Tests @ - 40 degrees C

Had computer problems

Best estimates below

611 ohm.....3.3 - 3.5 V

61 ohm.....3.2 - 3.4 V

10 ohm.....3.2 - 3.3 V

•Discharge Load Tests @ - 80 degrees C

<u>Cell #</u>	<u>Ah</u>
71.....	0.75
72.....	0.36
73.....	0.64
74.....	0.87
75.....	0.80
77.....	0.85
78.....	0.82
79.....	0.01 (Opened)

AIRGUN TEST # 53

OVERVIEW

- 7 cells as 4 and 3 cell batts, new seal design, 1 layer config
- Improved external wiring
- No leaks and no venting
- 4 cell batt delivered good output on profile, also delivered high power transmit of 10 W @ -60 °C
- 1 bad cell in 3 cell batt limited output but this batt operated on constant load @ -80 °C

SIGNIFICANCE

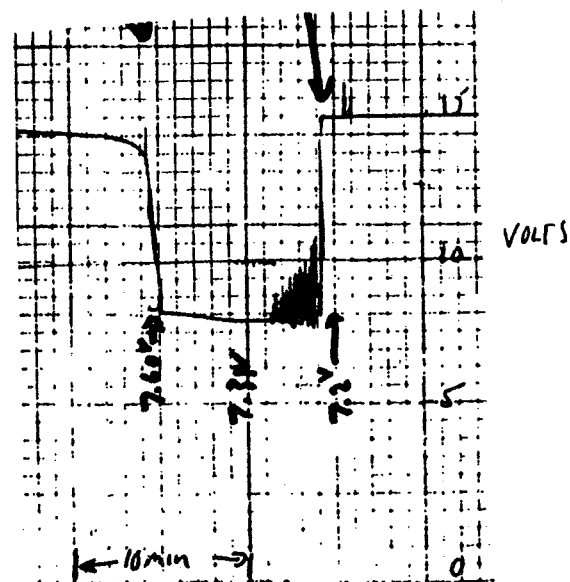
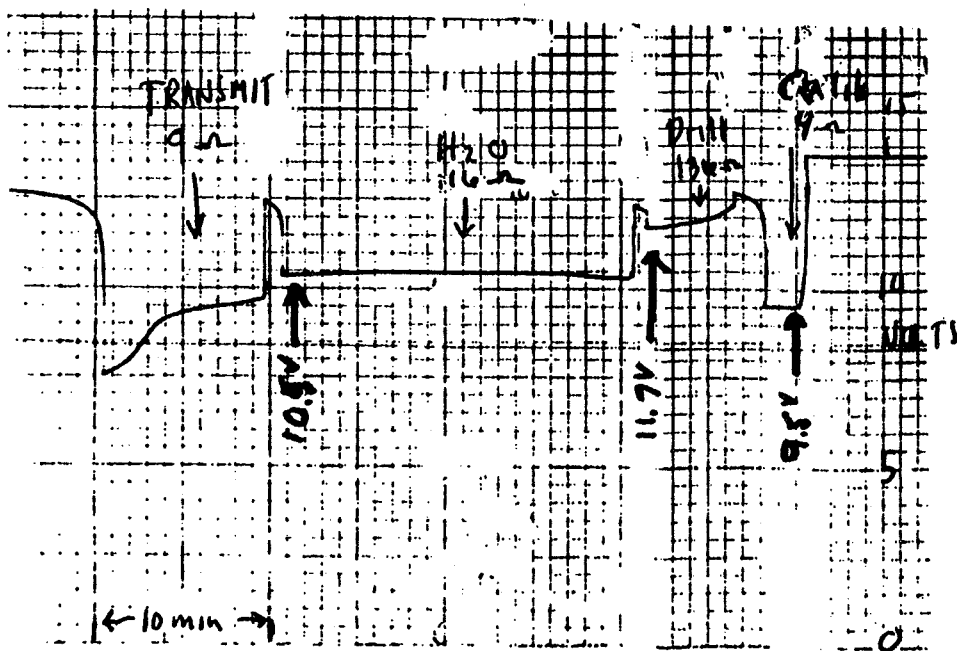
- New seal design again withstood shock
- External wiring mods appear to have eliminated shorts
- Must investigate cause for bad cell in 3 cell batt

AIRGUN TEST # 53

MISSION PROFILE TEST

$T = -60^{\circ}\text{C}$

$T = -80^{\circ}\text{C}$



GRAPHIC CONTROLS CORPORATION BUFFALO, NEW YORK

9280-0764

ACCELERATED STORAGE

OBJECTIVE

- Project performance after 2 years storage.
- Support microcalorimetric projections.

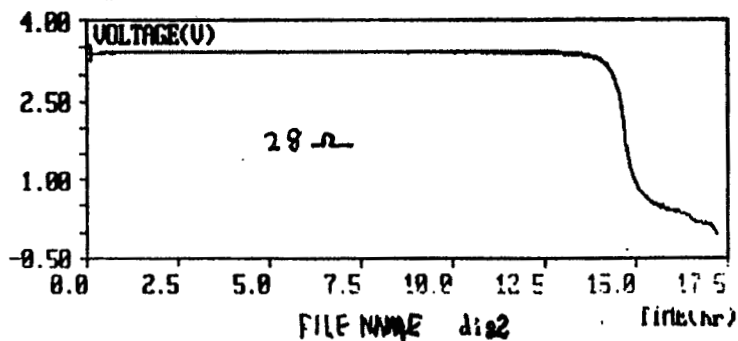
APPROACH

- Store some cells at ambient temperature.
- Store additional cells at elevated temperature.
- Periodically remove and test cells.
- Compare actual with projected capacities
- Also examine trends in voltage delay.

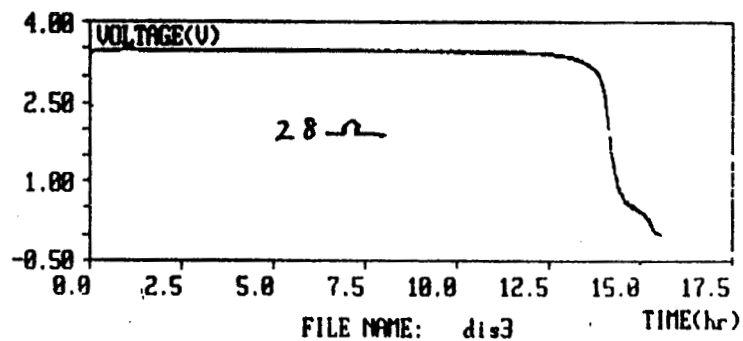
ACCELERATED STORAGE

CAPACITY TESTS @ RT

1 month @ RT



1 month @ 50 degrees C



No measurable loss in capacity at 50 degrees C

ASSESSMENT 1

- Favorable Project for meeting 2 year shelf life
 - 78-93% capacity retention after 2 yrs @ RT
 - Improved retention at lower temps
 - Accelerated tests consistent with projections.
- Battery can successfully operate drill motor
 - Sustain 1 A surge starting current
 - Run motor > 10 min @ temp < -60 degrees C
 - Sustain 1 A surge stall current
 - Run motor > 4 min @ temp < -60 degrees C

ASSESSMENT 2

•VOLTAGE DELAY

- Effects present but not excessive for planned moderate initial loads @ -40 to -60 degrees C
- Limits maximum initial load especially at very low temperatures, - 80 degrees C

•IMPACT SURVIVABILITY

- New GTM-cover design eliminated cracking and leaks and external wiring mods eliminated external shorting
- Several cells delivered good post impact perf and a battery met profile and 10 W
- Must determine cause for one “low” cell in Airgun #53
- Successful repeat run would help ensure meeting qual



Acknowledgement

This work was carried out at the Jet Propulsion Laboratory, California Institute of Technology under contract with National Aeronautics and Space Administration and in collaboration with Yardney Technical Products, Inc.,.

Development of 20 to 50-Ah Li-Ion Cells for Aerospace Applications

Lynn Marcoux and Gregg Bruce

**1997 NASA Aerospace Battery Workshop
18 November 1997**



Development of 20 to 50-Ah Li-Ion Cells for Aerospace Applications



Topics

- o Programmatics**
- o Component Evaluation Development**
- o 20-Ah Prismatic Cells**
- o 20-Ah Cylindrical Cells**
- o Current Activities**

Development of 20 to 50-Ah Li-Ion Cells for Aerospace Applications



Program Highlights

- o Initiated in 1991 and funded at \$US 3,019k, funded 50:50 USAF:DND (DIPP)**
- o Major corporate support initiated in 1996**
- o Emphasis is on 20 to 50-Ah cells with deliverables in 1997 and 1998**
- o Focus on LiCoO₂ positive electrodes for performance for spacecraft application**
- o Parallel development of cell chemistry and cell design**
- o Both prismatic (wound) and cylindrical designs being evaluated**
- o 20-Ah Cells delivered to USAF/NASA May 1997**
 - > 100 Wh/kg**
 - > 500 cycles above 75% Q_{initial}**
- o 50-Ah cells scheduled for delivery May 1998**



Component Development Activities

- o Component development at BATC for the most part involves evaluation of existing materials in C cells

- o Positive electrode materials evaluated to date include
 - $\text{Li}_x\text{Mn}_y\text{O}_z$ (Riedel-de Haën, BATC, Cyprus, Kerr McGee, JEC, MaxPower)
 - LiCoO_2 (Honjo, Seimi, Cyprus, FMC, JEC)
 - LiNiO_2 (Seimi)

- o Near term plans for positive electrode material improvement
 - $\text{LiCo}_x\text{Ni}_y\text{O}_z$ supplied by Westaim, FMC, Honjo

- o Negative electrode activities have included both evaluation of commercial carbons in C cells and developmental materials in Li/C button cells

- o Commercial Carbon materials evaluated
 - Lonza, KS6, KS15, KS44, KS75, SFG15, SFG44
 - Conoco XP Petroleum Coke
 - Nippon Carbon LK-702, LK-201
 - Osaka Gas MCMB



Electrolyte Studies - Rate Capability/Low Temperature

- o LiCoO₂ vs. graphite in C cells suspended unprotected in the thermal chamber**
- o All tests at room temperature ended the charge step with 1.5 hr CVC**
- o Low temperature tests included charge at low temperature**
- o All tests at low temperature ended the charge step with 2.5 hr CVC**
- o All tests carried out between 4.1 V and 3.0 V**
- o For rate study all tests carried out with symmetrical charge and discharge rates (C/10 charge, C/10 discharge)**
- o After a charge or discharge step under low temperature conditions the cell was held for 4 hours at rest to allow for the cell to reach equilibrium temperature**

Development of 20 to 50-Ah Li-Ion Cells for Aerospace Applications



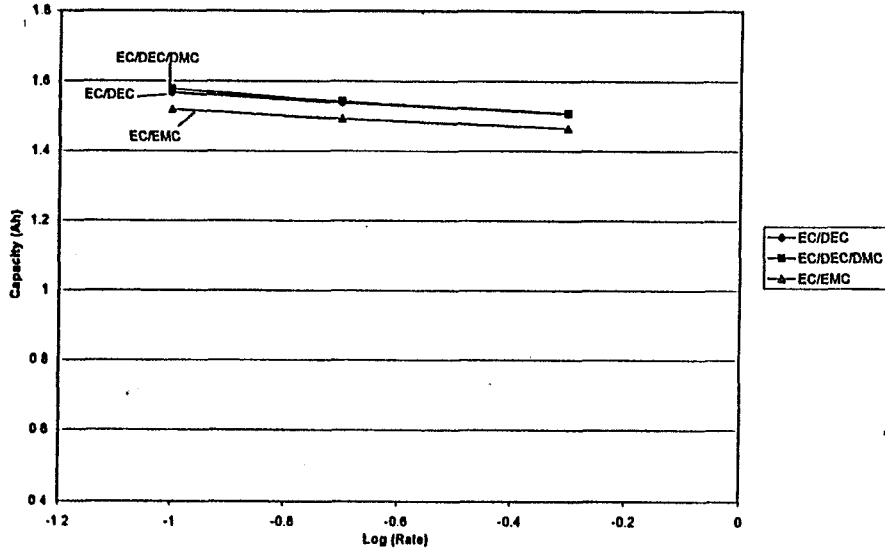
1997 NASA Aerospace Battery Workshop

-270-

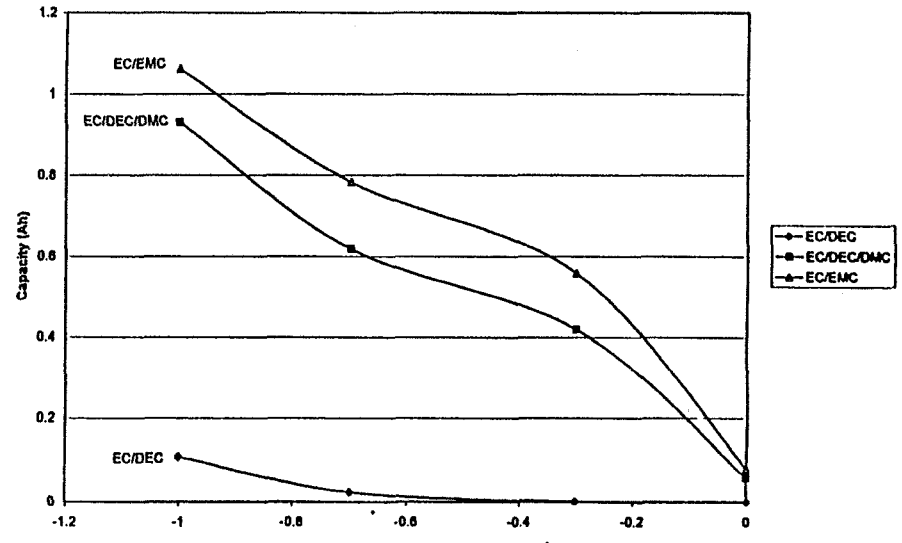
Lithium-Ion Focused Session

Capacity vs. Log Rate (C) at Various Temperatures with Various Electrolytes

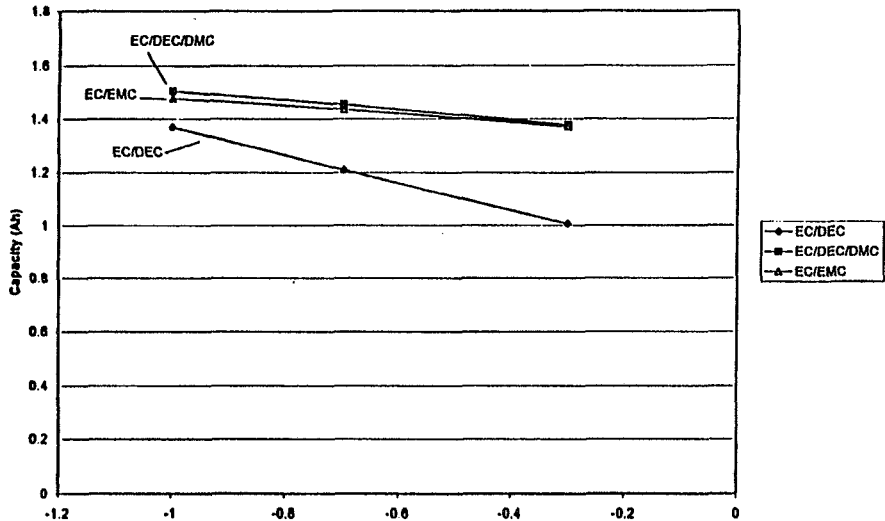
Electrolyte Study: Room Temp



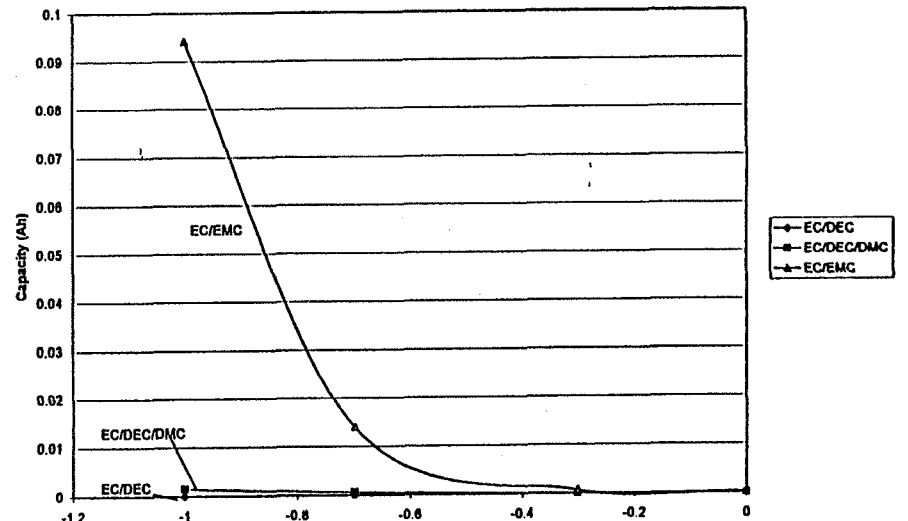
Electrolyte Study: -20 C



Electrolyte Study: 0 C



Electrolyte Study: -40 C



Development of 20 to 50-Ah Li-Ion Cells for Aerospace Applications



20-Ah Prismatic Cell - First Iteration

- o **Welded stainless steel enclosures**
 - Selected welded design (tooling cost, design freedom)
 - 0.027" 304 stainless steel
 - 2.69 x 12.9 x 10.9 cm (1.06" x 5.08" x 4.29")
 - Packing efficiency = 90-95%
- o **Electrode dimensions**
 - Positive, 600 x 8.80 x 0.017 cm
 - Negative, 630 x 9.10 x 0.011 cm
- o **Standard penetrations**
 - 2 GTM seals (0.090" Mo pin)
 - Fill tube
- o **Tig welded cap/can**
- o **Safety Features**
 - Celgard 2300™
 - Excess carbon capacity
 - Wide separator margin (2 x 0.25")
 - Taped tabs
 - 235 psi rupture disk
 - 2 x 0.065" Pos-Neg electrode margins



20-Ah Prismatic Cell Design - Second Iteration

o Results of mass analysis of first generation prismatic cells

- Cap/can	229 g	26%
- Electrolyte	216 g	24%
- Positive electrode	260 g	29% (78% active)
- Negative electrode	143 g	16% (47% active)
- Other	40 g	5 %

o Mass reduction strategy

- Reduce case thickness to 0.017" (from 0.027")
- Reduce electrolyte mass to 180 g
- Increase active material loadings
- Explore higher capacity graphites
- Projected specific energies of 105-115 Wh/kg
- Consider cylindrical designs

Development of 20 to 50-Ah Li-Ion Cells for Aerospace Applications



Cell Capacity, Mass and Cycle Life Data

Cell Id.	Cell Mass, g	Capacity, Ah	Specific Energy, Wh/kg	Comments
P002	862	23.4	97.9	768 cycles, 78% Q_{init} .
P005	836	20.2	87.0	300 cycles to 75% Q_{init} .
P009	848	22.9	97.4	351 cycles, 67% Q_{init} .
P010	858	21.5	90.2	433 cycles to 84% Q_{init} .
P023	815	23.7	105	0.017" case, 103 cycles to 95% Q_{init} .
P025	837	24.2	104	0.017" case, high cap. C 169 cycles to 83% Q_{init} .
P027	842	24.8	106	0.017" case, high cap. C 350 cycles to 83% Q_{init} .

Development of 20 to 50-Ah Li-Ion Cells for Aerospace Applications

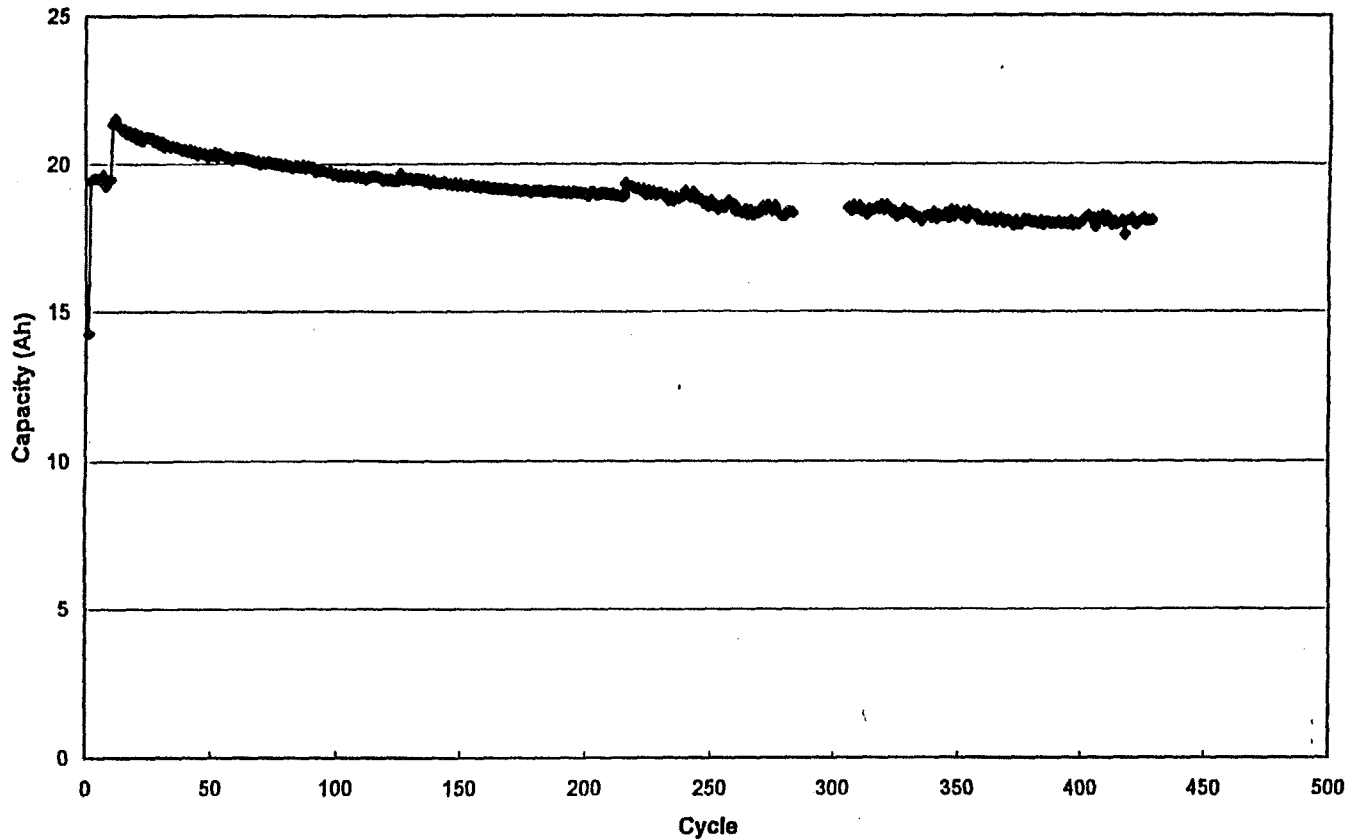


1997 NASA Aerospace Battery Workshop

-275-

Lithium-Ion Focused Session

Cell P010 - Capacity vs. Cycle No. @ 100% DOD, C/5 Rate



Development of 20 to 50-Ah Li-Ion Cells for Aerospace Applications

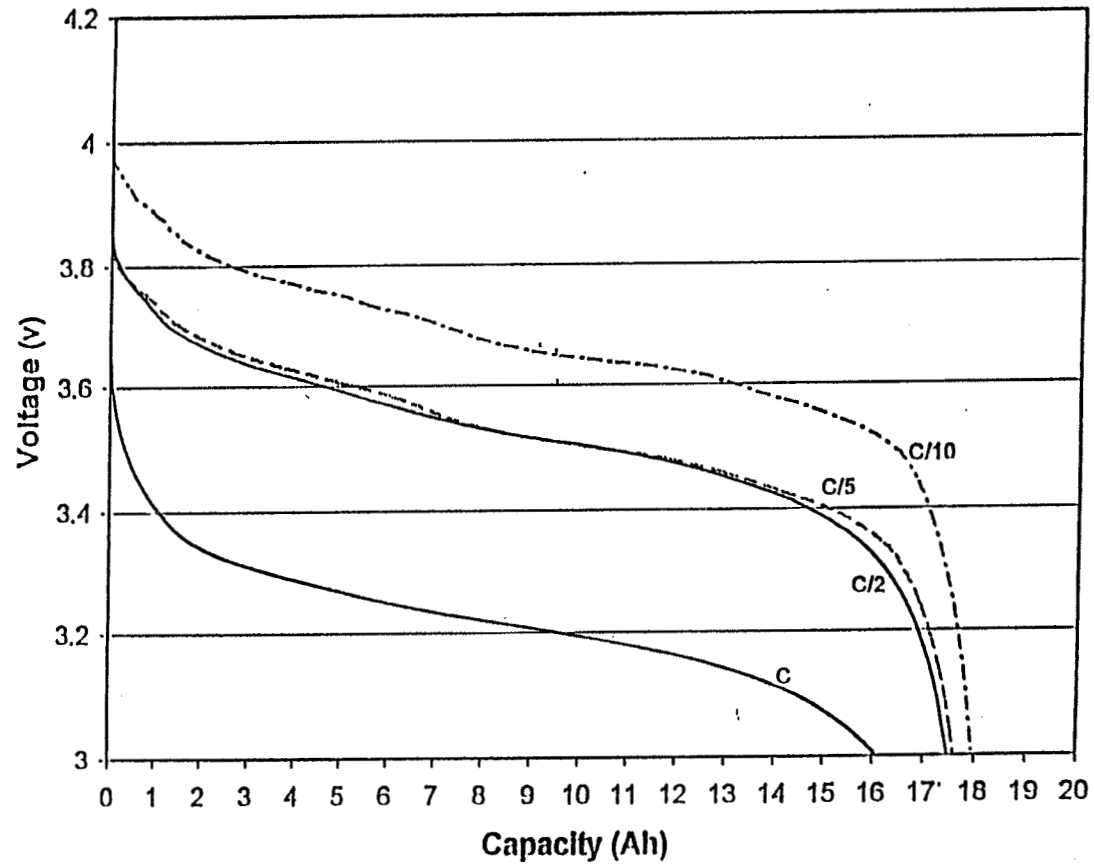


1997 NASA Aerospace Battery Workshop

-276-

Lithium-Ion Focused Session

Performance - Rate Capability, 100% DOD, Room Temp



Development of 20 to 50-Ah Li-Ion Cells for Aerospace Applications



Energy and Charge Efficiency - Cell P003

Cycle #	Discharge		Charge				Eff (Ah) %	Eff (Wh) %	% CVC
	AH	WH	AH (CC)	WH (CC)	AH (CV)	WH (CV)			
15	20.918	75.304	19.205	74.426	1.788	7.238	99.643	92.212	8.517
25	20.73	74.627	19.121	74.104	1.676	6.778	99.678	92.267	8.059
50	20.33	73.189	18.916	73.357	1.454	5.863	99.804	92.387	7.138
75	20.091	72.328	18.828	73.051	1.298	5.229	99.826	92.397	6.449
100	19.911	71.678	18.613	72.319	1.273	5.127	100.126	92.552	6.401
150	19.58	70.49	18.467	71.8	1.166	4.686	99.730	92.161	5.939
200	19.386	69.79	18.251	71.027	1.207	4.856	99.630	91.971	6.203
225	19.171	69.017	17.787	69.457	1.389	5.604	99.974	91.948	7.243

- o Assuming all energy inefficiency results from resistive losses implies a cell resistance of 35 mΩ
- o Actual cell resistances (1000 Hz and d.c. polarization) yield cell resistances of 30-50 mΩ depending on dod and cycle no.
- o System mass implications
 - Thermal management (radiator size)
 - Array size



Conclusions and Future Plans (Prismatic Cells)

- o Wall thickness of enclosure reduced from 0.027" to 0.017"**
- o Electrolyte reduced to 180g from 200g**
- o Build more cells with MCMB and LK-702 positives and fully characterize performance**
 - Various rates and charging regimes**
 - Various temperatures**
- o Fully characterize safety**
- o Prismatic vs cylindrical cycle life?**

Development of 20 to 50-Ah Li-Ion Cells for Aerospace Applications



First Iteration 20-Ah Cylindrical Cell - Design Features

- o Standard Drawn Can**
 - HU-3830
 - SS 304
 - 0.019"
 - 3.50" dia, 2.50" height

- o Penetrations identical to prismatic design except for GTM**
 - Two different types
 - Both pins 0.125" Mo or Ta
 - Ta pin is flattened, drilled and threaded (2-56)

- o Electrode dimensions**
 - Positive, 1300 x 4.40 x 0.017 cm
 - Negative, 1330 x 4.70 x 0.011 cm

- o Project performance 97 Wh/kg (LK-702)**
 - Measured Performance 109 Wh/kg

Development of 20 to 50-Ah Li-Ion Cells for Aerospace Applications



Cell Capacity, Mass and Cycle Life Data

Cell Id.	Cell Mass, g	Capacity, Ah	Specific Energy, Wh/kg	Comments
C002	839	27.3	117	High cap. C, 446 cycles to 76% $Q_{init.}$
C004	799	25.9	117	376 cycles to 76% $Q_{init.}$
C006 to C024	738 ± 18	24.0 ± 0.7	110 ± 2	Delivered to USAF
C033	791	24.1	110	560 cycles to 70% $Q_{init.}$
C034	787	23.8	109	710 cycles to 72% $Q_{init.}$
C037	802	24.7	111	133 cycles to 92% $Q_{init.}$
C039	806	25.6	114	286 cycles to 89% $Q_{init.}$

Development of 20 to 50-Ah Li-Ion Cells for Aerospace Applications

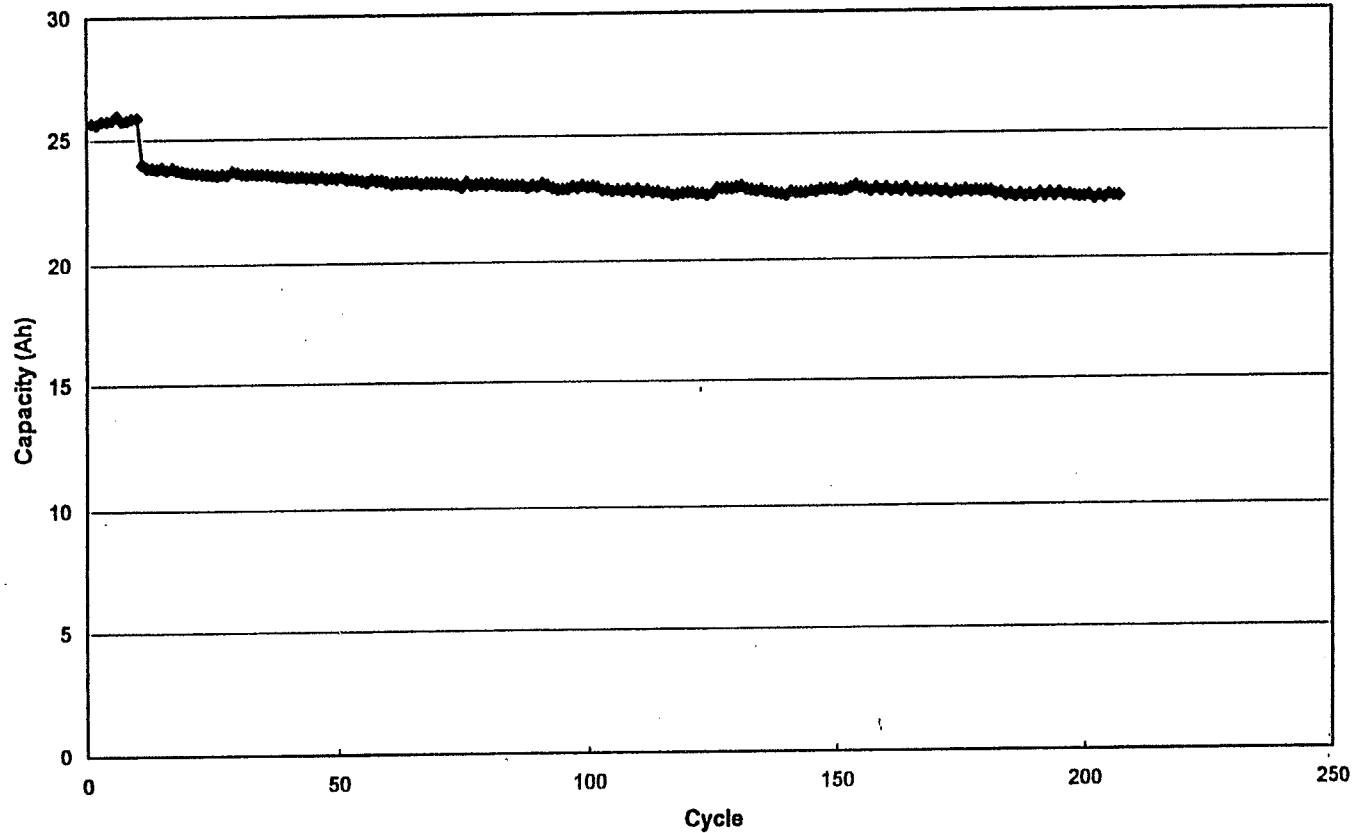


1997 NASA Aerospace Battery Workshop

-282-

Lithium-Ion Focused Session

Cell C004 Capacity vs. Cycle No. @ 100% DOD, C/5 Rate



Development of 20 to 50-Ah Li-Ion Cells for Aerospace Applications

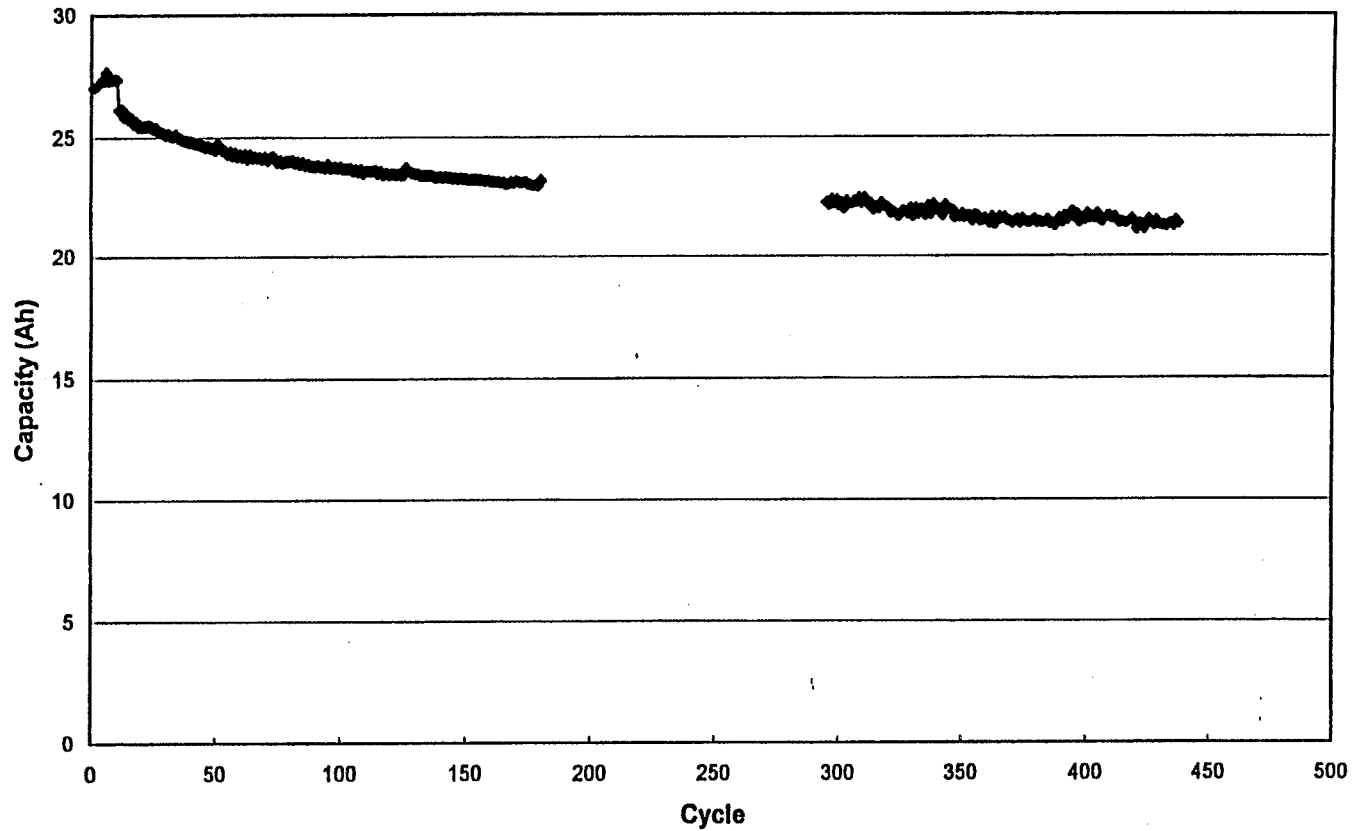


1997 NASA Aerospace Battery Workshop

-283-

Lithium-Ion Focused Session

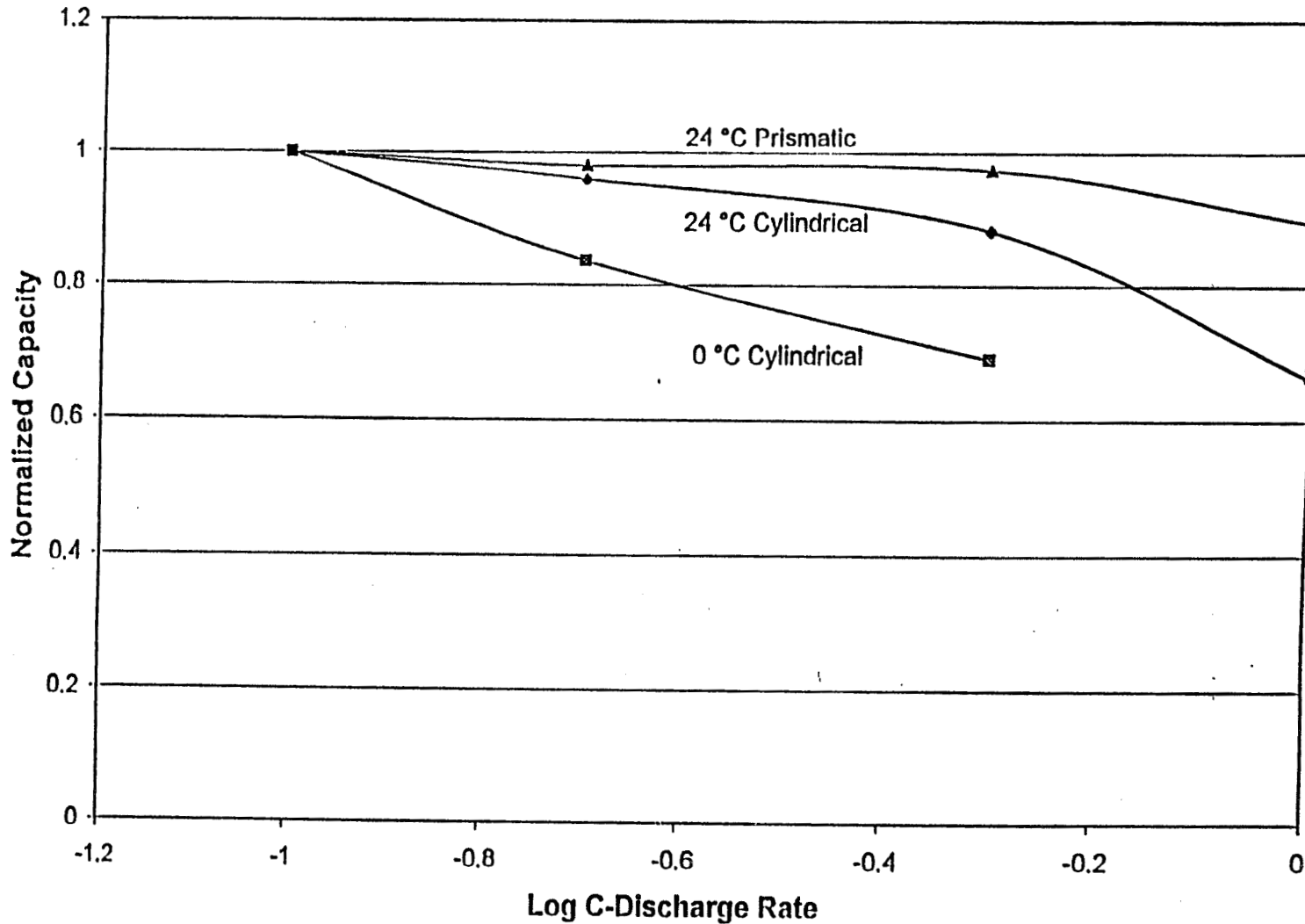
Cell C002 Capacity vs. Cycle No. @ 100% DOD, C/5 Rate



Development of 20 to 50-Ah Li-Ion Cells for Aerospace Applications



Capacity vs. Rate for Cylindrical and Prismatic Cells



Development of 20 to 50-Ah Li-Ion Cells for Aerospace Applications



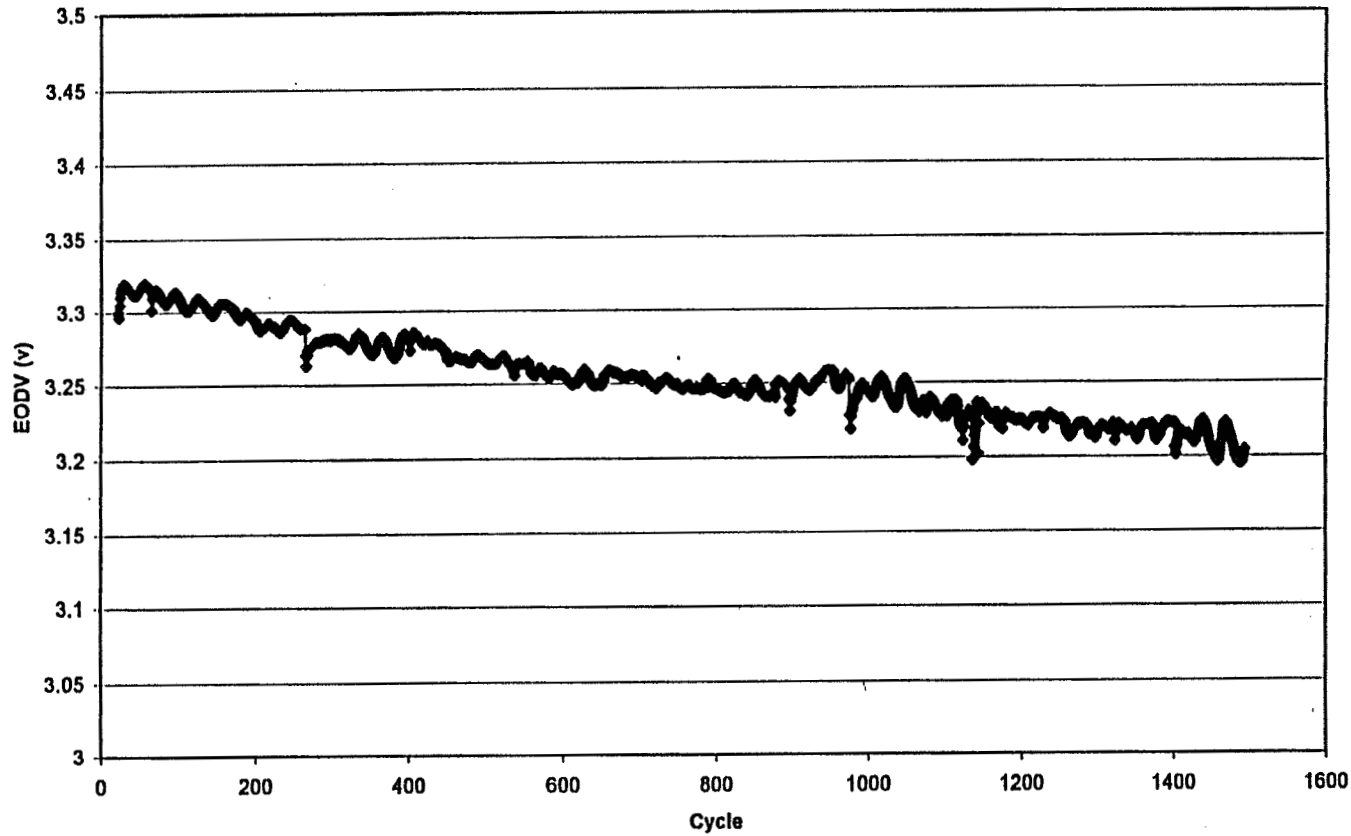
20-Ah Cylindrical Cells - Accelerated LEO Test

- o Two cells tested at 25 °C**
- o 12 Min. discharge at c rate (20 A)**
- o 36 Min. Charge**
 - Constant current to 4.05 V**
 - Constant current to end of charge period**
- o Over 1500 cycles > 3.00 V to date**

Development of 20 to 50-Ah Li-Ion Cells for Aerospace Applications



20-Ah Cylindrical Cells - Accelerated LEO Test





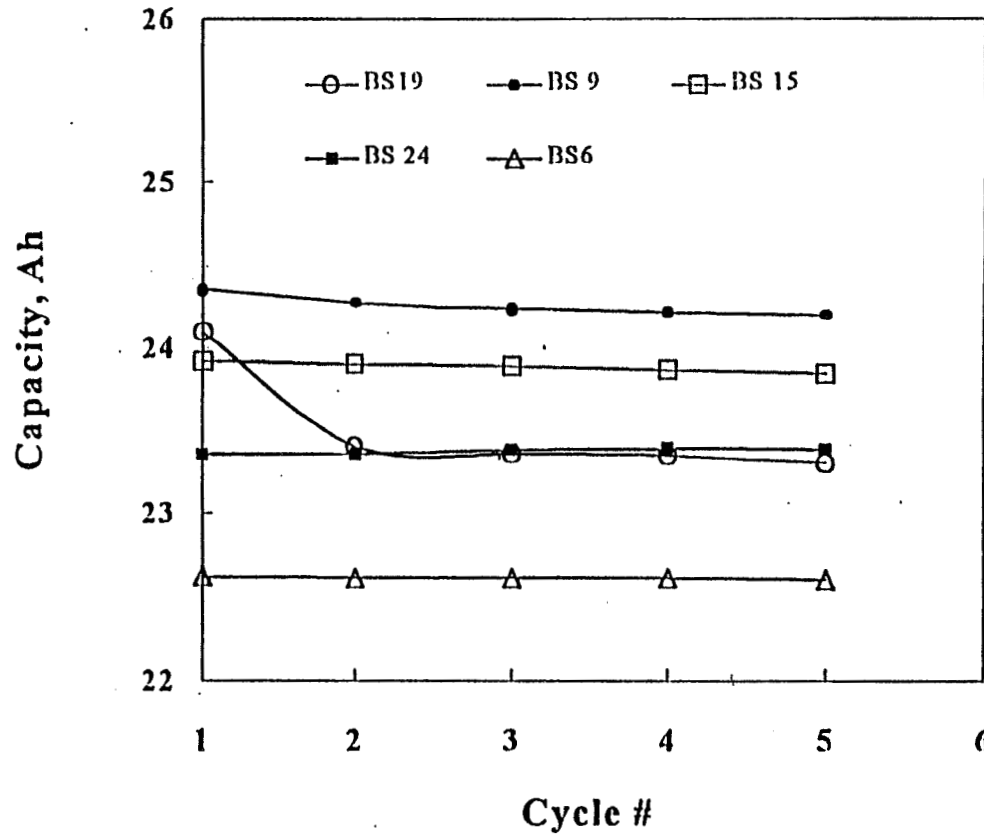
Performance - Safety/Abuse Tests

- o Short-Circuit (0.050 ohm), safe no fire/vent. Max temperature 85°C. Cell was cycled after test**
- o Oven test (150°C, 2 hours) violent vent/fire**
- o Overcharge 50-Ah, 4.66V safe no fire/vent**
- o Overcharge test to 100-Ah, 56-Ah, 4.68V fire/vent**
- o Forced over-discharge (50-Ah) safe no fire/vent**
 - Cell charged after this abuse test showed no capacity, acting as a resistor**
 - Cell disassembly revealed copper plating through the separator**

Development of 20 to 50-Ah Li-Ion Cells for Aerospace Applications



JPL Test Results (S. Surampudi & K. Bugga) Conditioning Cycles (C/10 charge, C/5 discharge)



1997 NASA Aerospace Battery Workshop

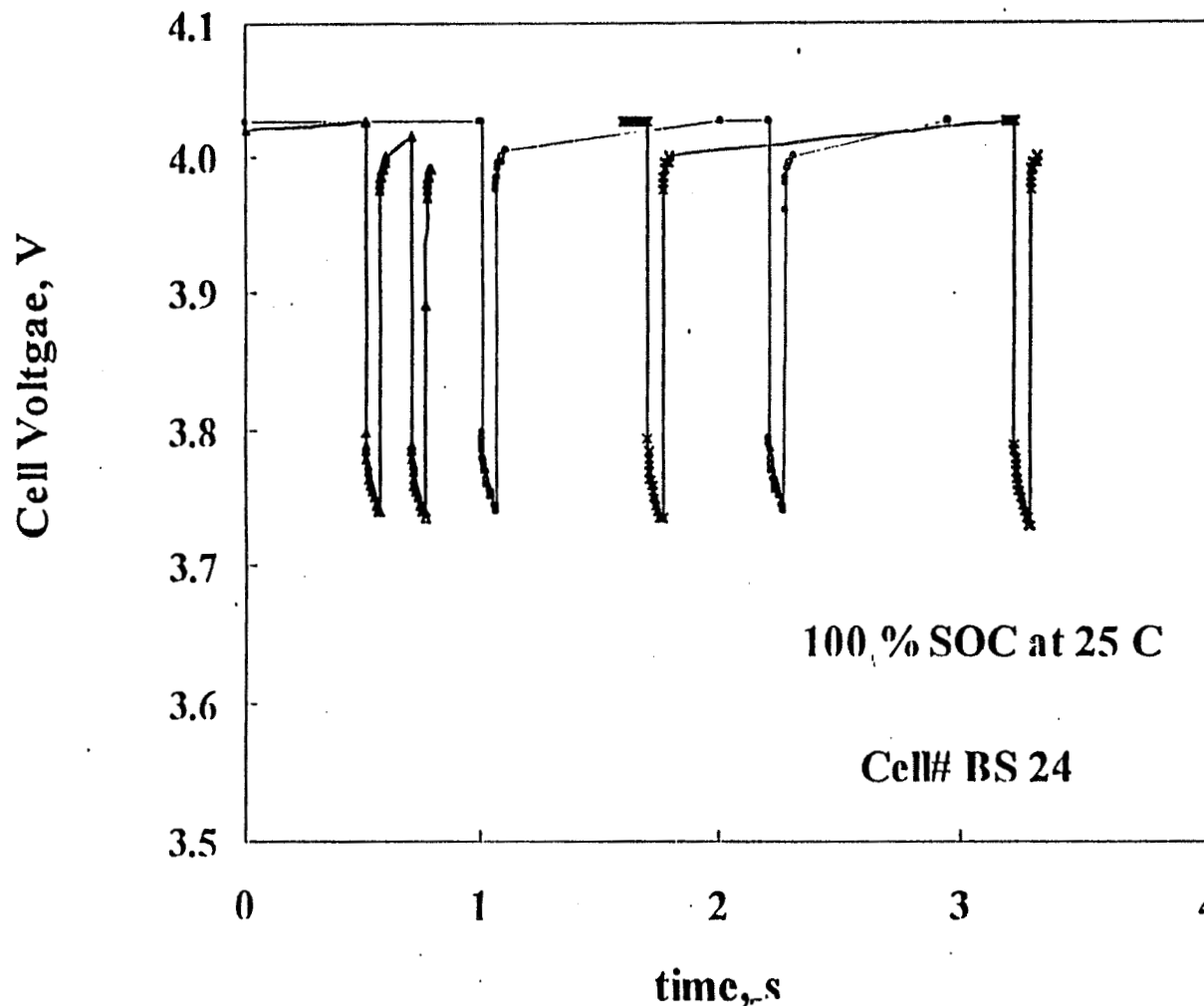
-288-

Lithium-Ion Focused Session

Development of 20 to 50-Ah Li-Ion Cells for Aerospace Applications



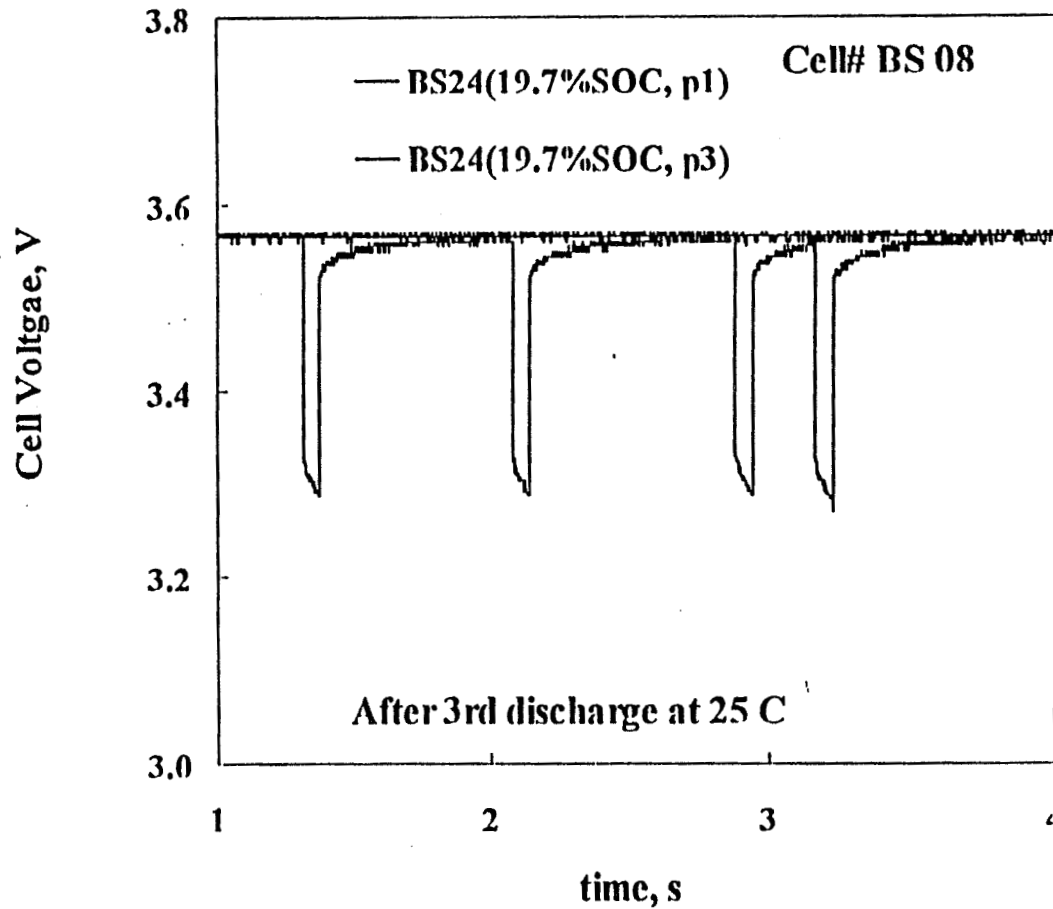
JPL Test Results (S. Surampudi & K. Bugga)
60 A, 120 msec Pulses at Room Temp. & 100% SOC



Development of 20 to 50-Ah Li-Ion Cells for Aerospace Applications



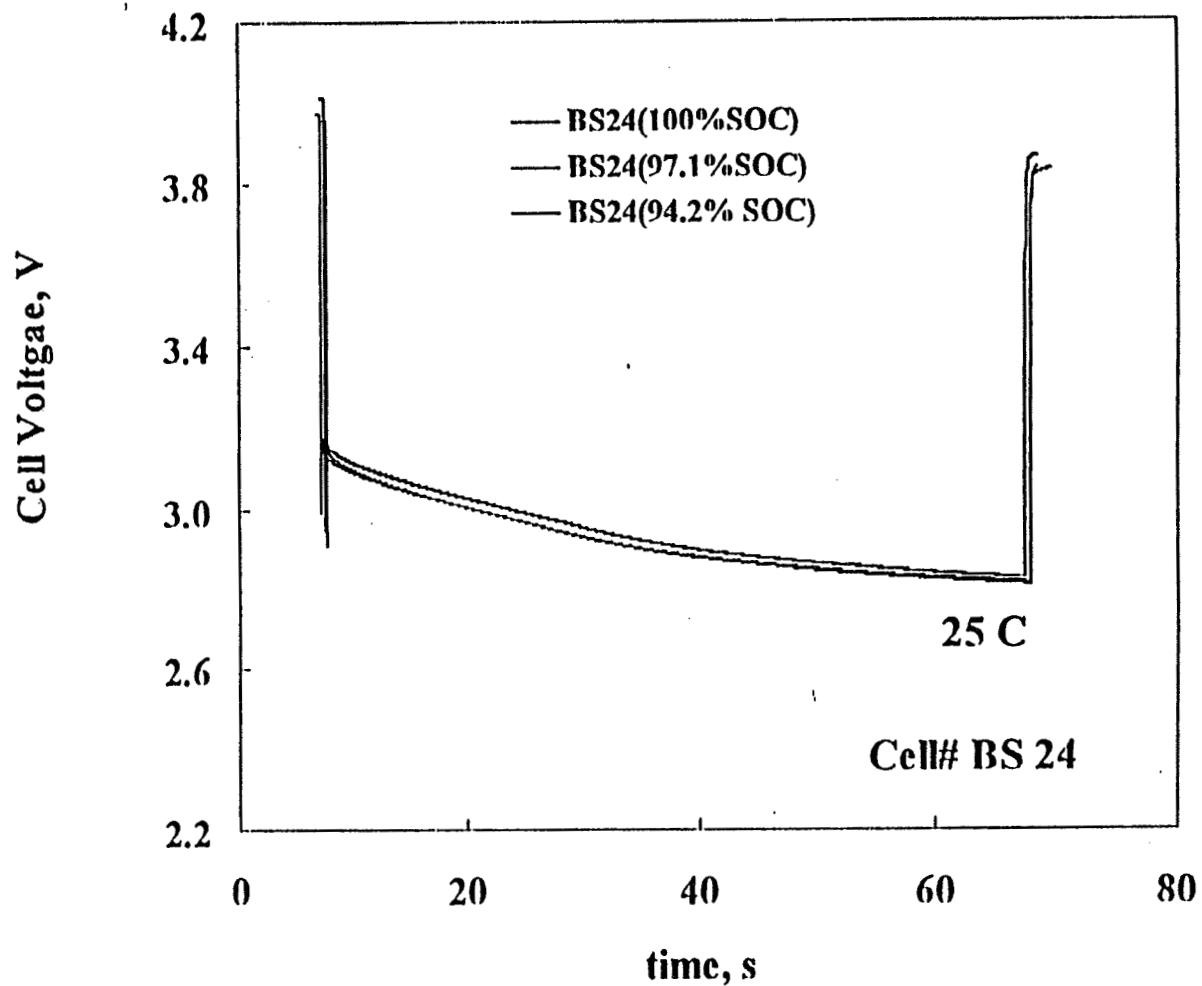
JPL Test Results (S. Surampudi & K. Bugga) 60 A, 120 msec Pulses at Room Temp. & 20% SOC



Development of 20 to 50-Ah Li-Ion Cells for Aerospace Applications



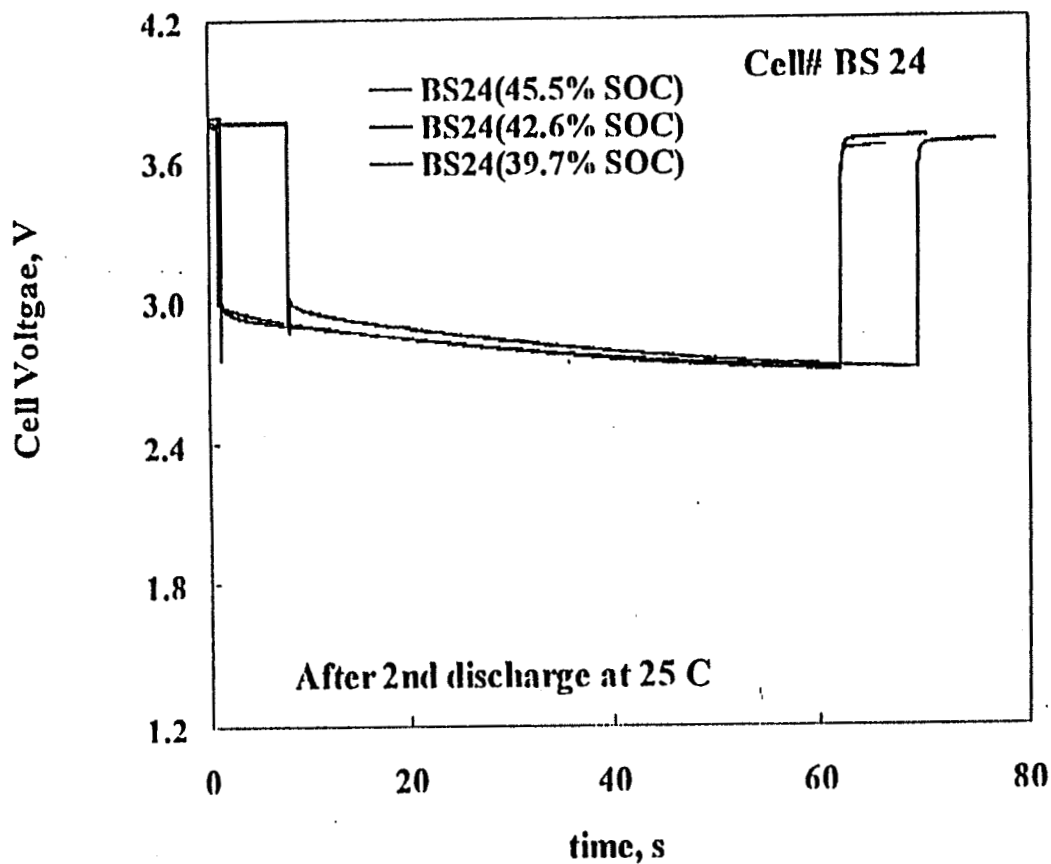
JPL Test Results (S. Surampudi & K. Bugga) 40 A, 60 sec Pulses at Room Temp. & 100% SOC



Development of 20 to 50-Ah Li-Ion Cells for Aerospace Applications



JPL Test Results (S. Surampudi & K. Bugga) 40 A, 60 sec Pulses at Room Temp. & 40% SOC





First Iteration 20-Ah Cylindrical Cells - Conclusions

- o Overall high rate capability of present cylindrical design is poor with respect to power**
- o As expected the low temperature performance of the design is also poor**
- o To date the safety of this design does not appear to be an overriding issue with possible exception of the high temperature oven test and extended overcharge**
- o Larger diameter lower pressure rupture disc will be added safety feature**
- o Change length to diameter aspect ratio to improve high rate and low temperature performance**

Development of 20 to 50-Ah Li-Ion Cells for Aerospace Applications



Near Term Plans

- o **Continue present activities**
 - Continue component development/improvement (carbon)
 - Continue design development/improvement (safety features, current collection)
 - Fabricate and test next generation 20-Ah prismatic and cylindrical cells (Lot 1 in formation)
 - Complete fabrication of Lot 1 50-Ah cells
 - Safety and abuse tests
 - Cycle life tests (including accelerated GEO testing)

- o **Develop pre-pilot scale (40, 50-Ah cells/week) production capability (May '98)**
 - Present capability is 10, 20-Ah cells /week
 - Capital expenditure of \$CDN 2.5 million

- o **Initiate scale-up (to 100-Ah) design analysis**
 - Cell Model (current density, aspect ratio, thermal, resistance)
 - Compare cylindrical vs. prismatic
 - Determine scale up limits

Development of 20 to 50-Ah Li-Ion Cells for Aerospace Applications



Next Generation of 20-Ah Cylindrical Cells

- o Pursue new design with better rate/low temperature capability**
- o Standard Hudson Tool and Die can**
 - HU-3570, 0.019" 304SS, 2.625" diameter, 4.5" length**
- o Penetrations similar to previous designs except for GTM**
 - GTM is larger and Ta pin (0.187") is flattened and treaded (4-40)**
- o Electrode dimensions**
 - Positive, 660 x 8.80 x 0.017 cm**
 - Negative, 680 x 9.10 x 0.011 cm**
- o Projected performance**
 - 110 Wh/kg (LK-702), 127 Wh/kg (MCMB)**
 - 220 Wh/l (LK-702), 240 Wh/l (MCMB)**
- o First lot of cells presently undergoing formation**

Development of 20 to 50-Ah Li-Ion Cells for Aerospace Applications

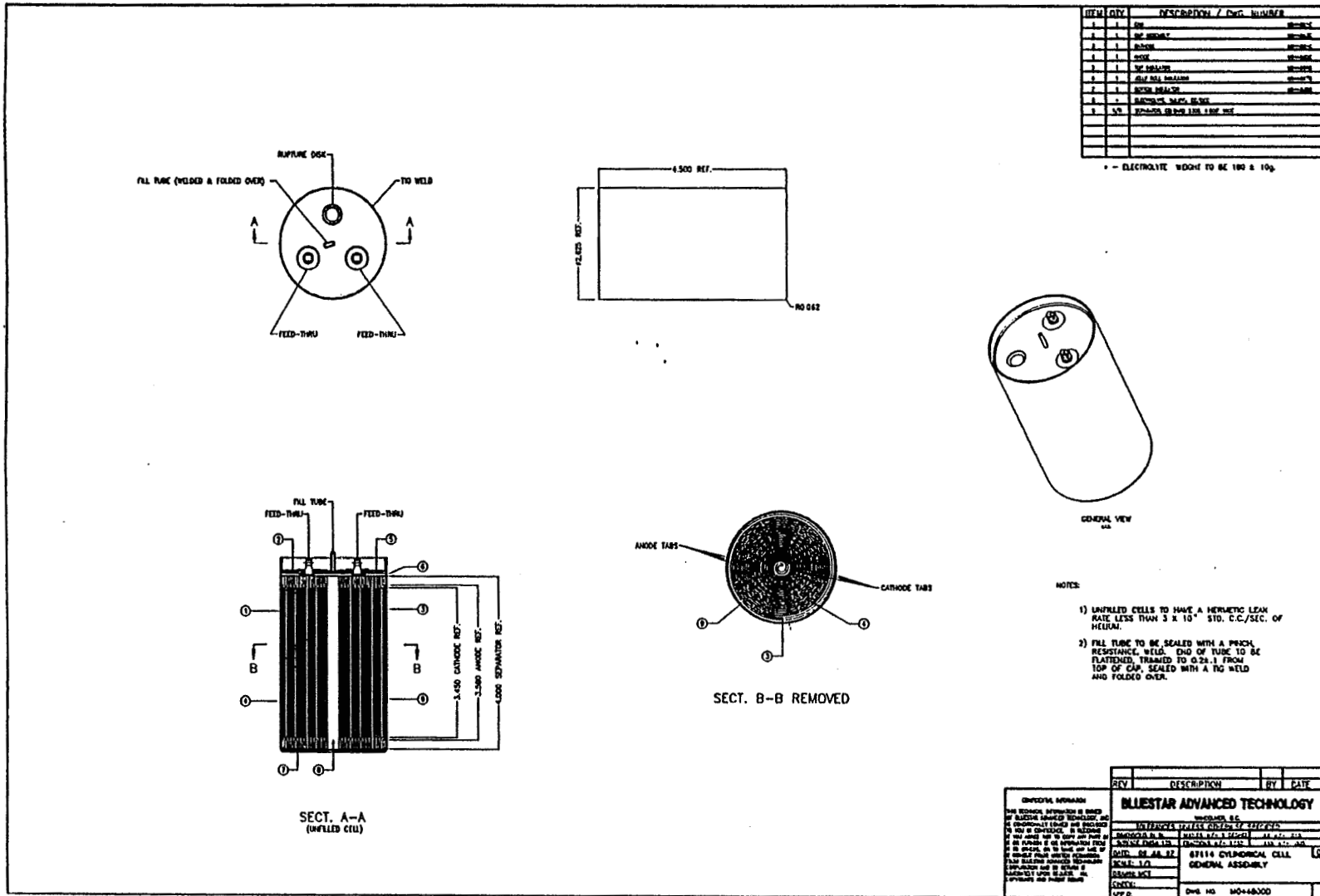


Next Generation of 20-Ah Cylindrical Cells - Cell Design

1997 NASA Aerospace Battery Workshop

-296-

Lithium-Ion Focused Session





50-Ah Cylindrical Cell Design Features

- o Standard Hudson Tool and Die drawn can**
 - SS 304
 - 0.019"
 - 2.56" dia, 7.09" height

- o Penetrations similar to previous designs except for GTM**
 - GTM is larger and Ta pin (0.187") is flattened, drilled and treaded (4-40)
 - Investigate lower pressure rupture disc

- o Electrode dimensions**
 - Positive, 675 x 16.1 x 0.017 cm
 - Negative, 690 x 16.4 x 0.011 cm

- o Projected performance**
 - 117.7 Wh/kg (LK-702), 125.6 Wh/kg (MCMB)
 - 278.1 Wh/l (LK-702), 319.6 Wh/l (MCMB)

Page intentionally left blank

EAGLE EP PICHER
Technologies Division

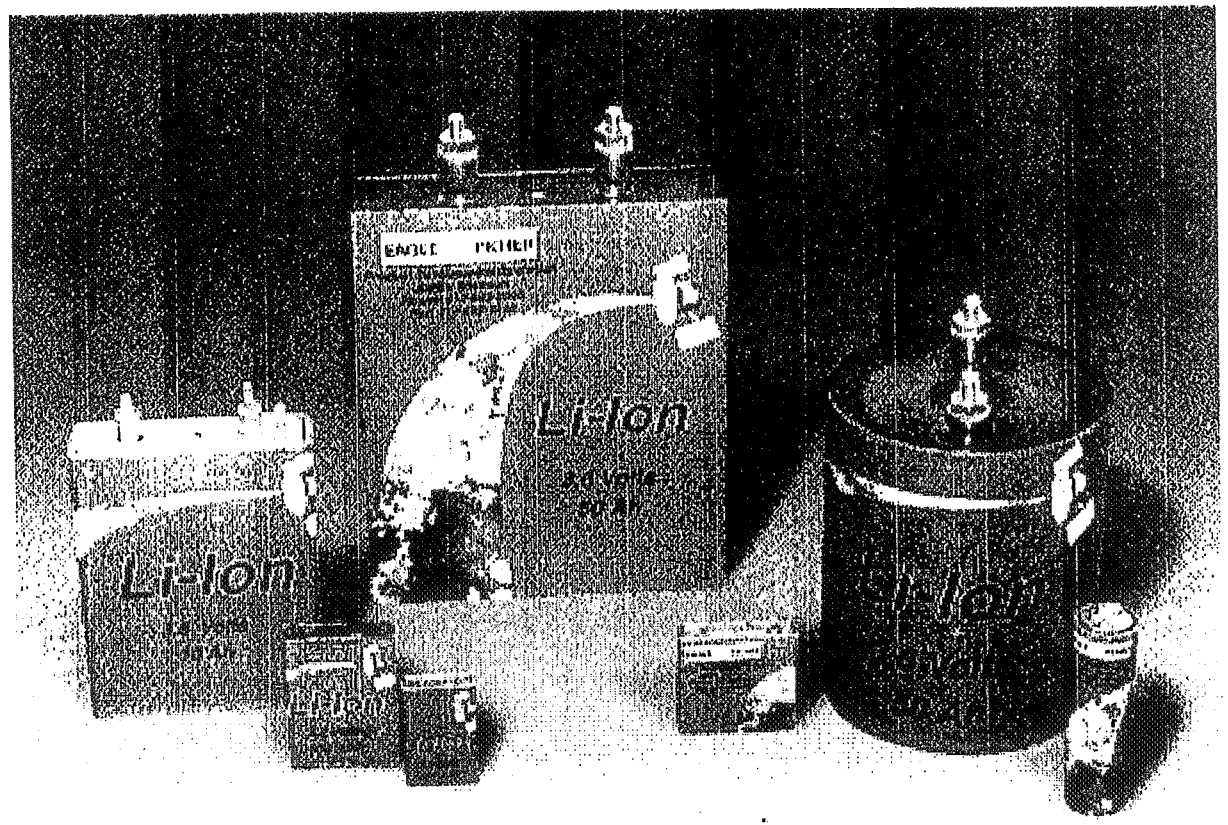
FEDERAL
SYSTEMS
DEPARTMENT

Rechargeable Lithium-Ion Battery Development at Eagle-Picher Industries

Chad Kelly
Advanced Electrochemical Systems Group
Federal Systems Department
Eagle-Picher Industries, Inc.
Joplin, Missouri 64802

EAGLE EPICHER
Technologies Division

FEDERAL
AVIATION
ADMINISTRATION
DEPARTMENT

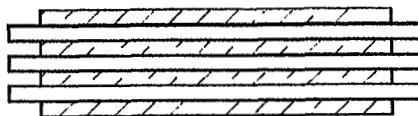


EAGLE EPICHER
Technologies Division

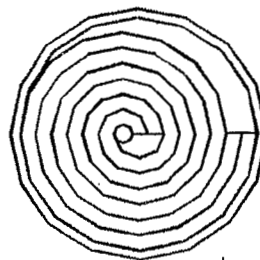
CELL CONFIGURATIONS

FEDERAL
SYSTEMS
DEPARTMENT

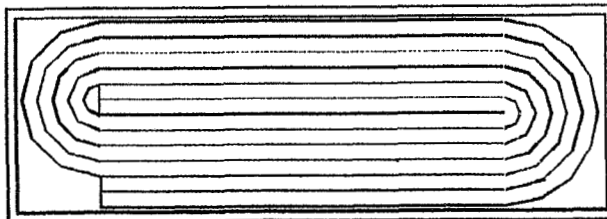
STACKED



SPIRAL WOUND



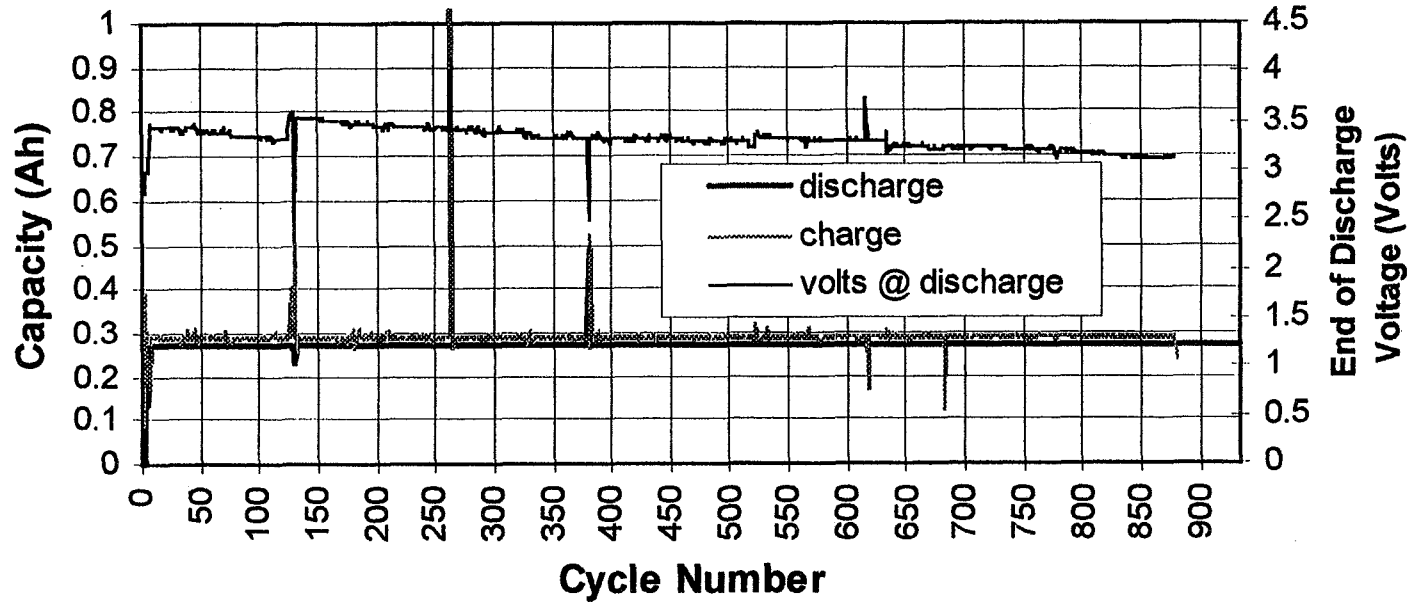
FOLDED



- Three configurations of electrodes
 - ◆ stacked - prismatic
 - ◆ spiral wound - cylindrical
 - ◆ pseudo spiral - prismatic
- Cell case materials
 - ◆ stainless steel
 - ◆ Surlyn coated aluminum bags
 - ◆ Aluminum



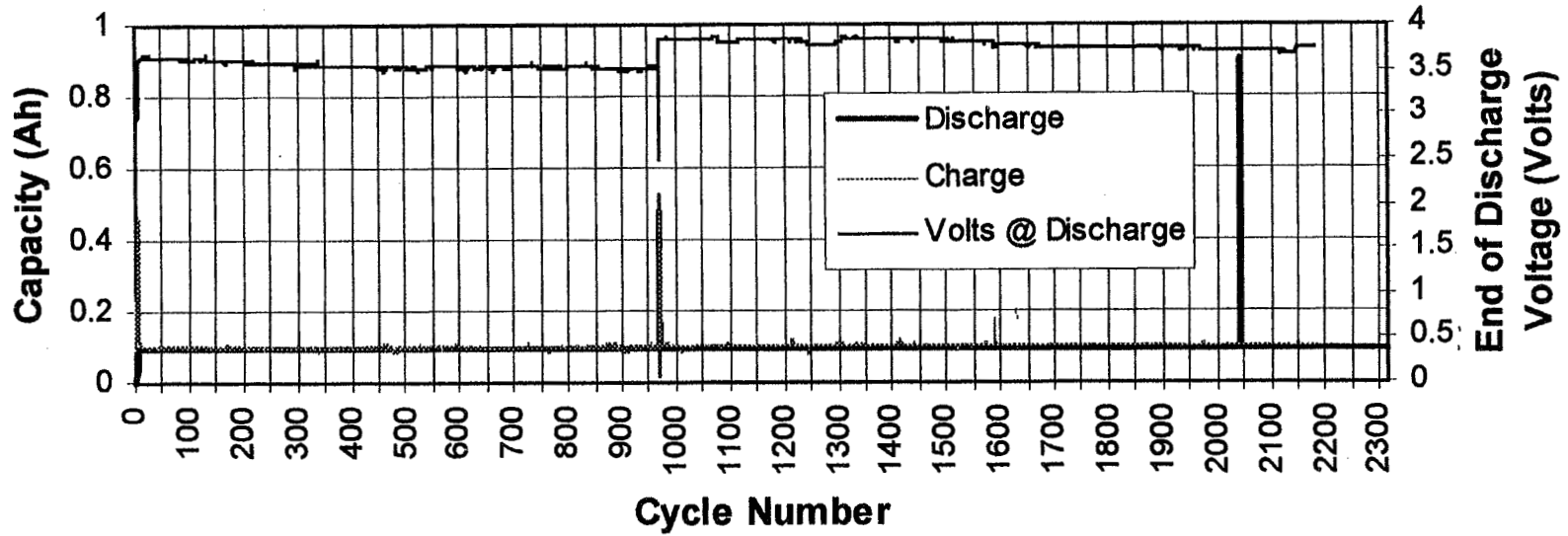
Spiral-Wound Cell (700mAh) at 42% DOD -4 Celcius at C/5



EAGLE P P ICHER
Technologies Division

FEDERAL
SYSTEMS
DEPARTMENT

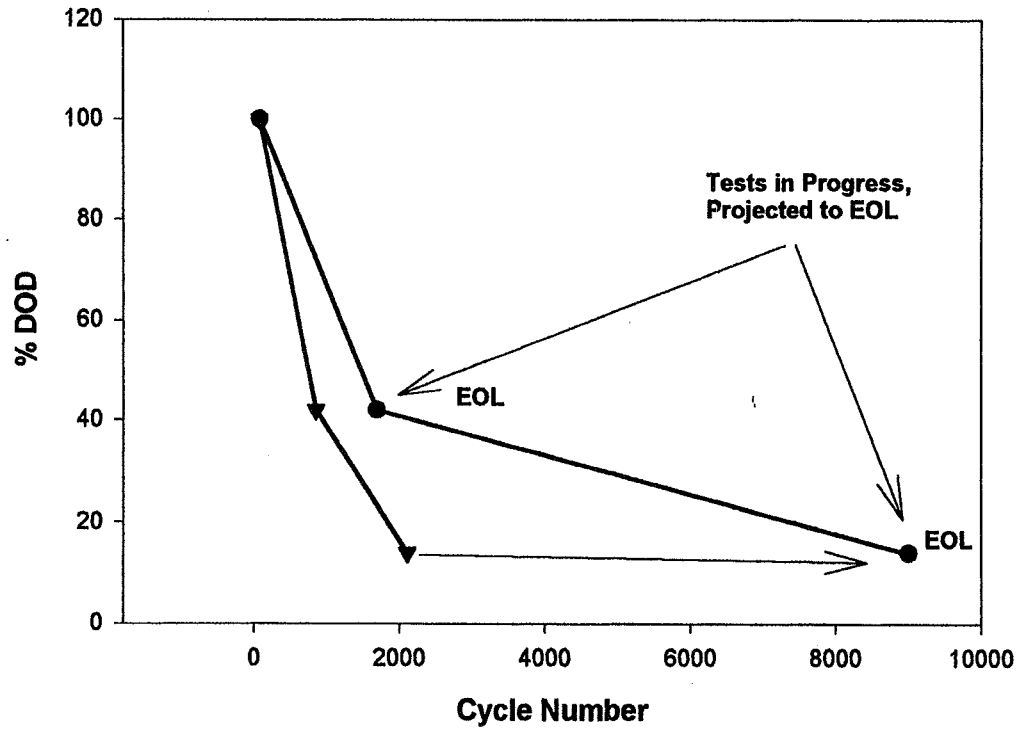
**Spiral-Wound Cell (700mAh) at 14% DOD
-4 Celcius at C/5**



EAGLE EPICHER
Technologies Division

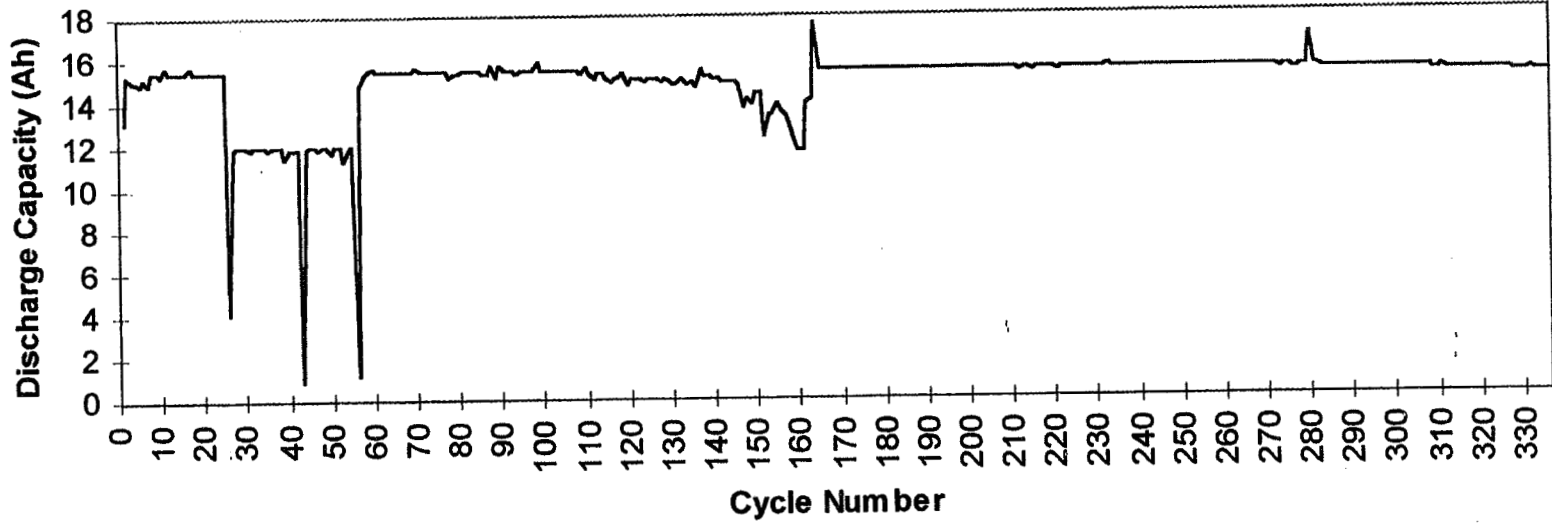
FEDERAL
SYSTEMS
DEPARTMENT

Cycle Life Characteristics of June 96' Li-ion Technology (700mAh cell)



EAGLE P P ICHER
Technologies Division

FEDERAL
SYSTEMS
DEPARTMENT





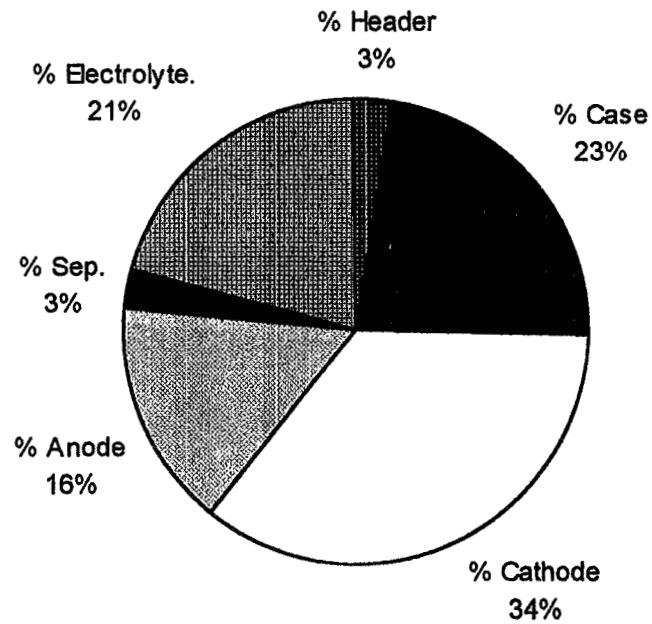
28 Volt-15 Ah Prototype Eagle-Picher Battery
Preliminary Cell Capacity Performance

Cell Number	Discharge Capacity (Ah)		
2239701	14.31	Mean Capacity 14.275 Ah Standard Deviation 22.8 mAh COV 0.15% % Variation 0.49%	
2249701	14.28		
2249702	14.28		
2259701	14.28		
2259702	14.27		
2259703	14.24		
2259704	14.28		
2259705	14.25		

EAGLE EPICHER
Technologies Division

FEDERAL
SYSTEMS
DEPARTMENT

15 Ah Cell Weight Attributes



EAGLE EPICHER
Technologies Division

FEDERAL
SYSTEMS
DEPARTMENT

Lithium-Ion Current Capabilities	
Rate Capability	C (4C Pulse)
Temperature	-20°C ---> 30°C
Cycle Life	>350 @ 100% DOD >1000 @ 42% DOD >2300 @ 14% DOD
Wh/Kg	>70 @ C >100 @ C/10
Wh/l	>235
Shelf Life	Test in Progress
Cell Sizes	20 mAh - 100 Ah
Designs	Prismatic Stack Spiral Wound Psuedo Spiral Wound

Page intentionally left blank

Evaluation of 20 Ah Li Ion Cells

*Marshall Smart, B. V. Ratnakumar, C. K. Huang and S. Surampudi
Electrochemical Technologies Group, Jet Propulsion Laboratory
4800 Oak Grove Dr., Pasadena, CA*

*Carole Hill and Dan Radzykewycz
Air Force Research Lab, Albuquerque, NM*

*R. A. Marsh
Air Force Research Lab, Dayton, OH*

ABSTRACT

Lithium ion cells of 20 Ah capacity were fabricated by Bluestar Advanced Technology Corporation, Canada under a developmental contract from US Air Force. In this paper, we report our studies on the evaluation of these cells under various test conditions. These include generic test conditions such as discharges and charges at different temperatures to understand the rate-limiting processes in the discharge/charge processes as a function of temperature, and cycle life under standard cycling conditions (100 % DOD) at ambient temperature. In addition, tests are being done to ascertain the performance of the cells in the Mars 2001 Lander application, which includes pulse testing of the cells at 60 A and 40 A loads for 100 mS and 1 min., respectively at different states of charge and temperatures, and cycling at low temperature at partial depths of discharge.



EVALUATION OF 20 Ah LITHIUM ION CELLS (BLUESTAR)

Marshall Smart, Kumar Bugga

Chen-Kuo Huang and Rao Surampudi

Electrochemical Technologies Group, JPL

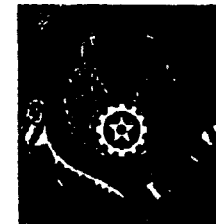
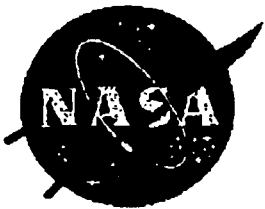
and

Carol Hill, Dan Radzykewycz and R. A. Marsh

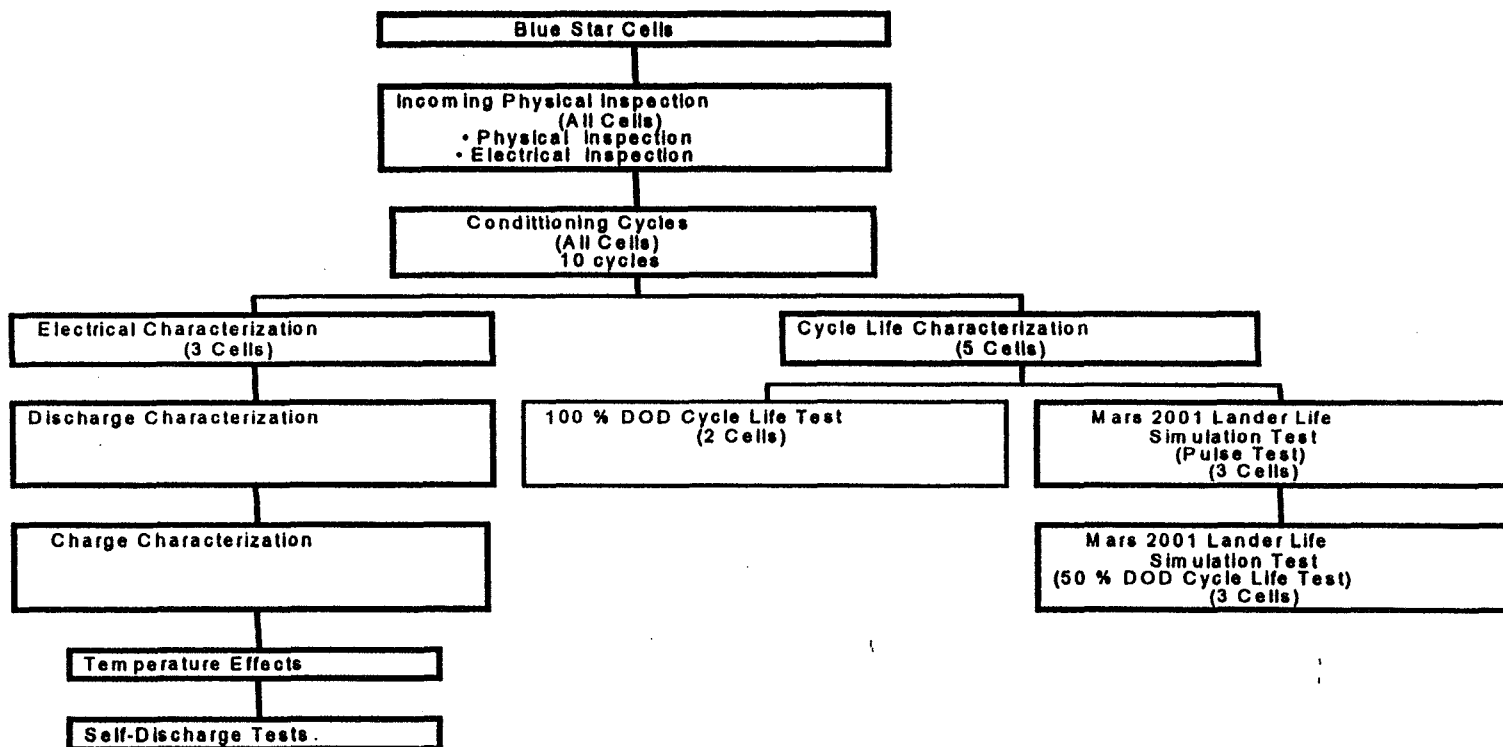
Air Force Research Laboratory

November 18, 1997

**NASA Aerospace Battery Workshop
November 18-20, 1997, Huntsville, AL**

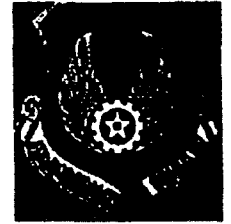


Blue Star Lithium-Ion Testing Flow Chart

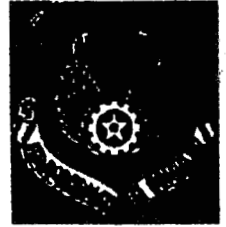




Characterization Tests

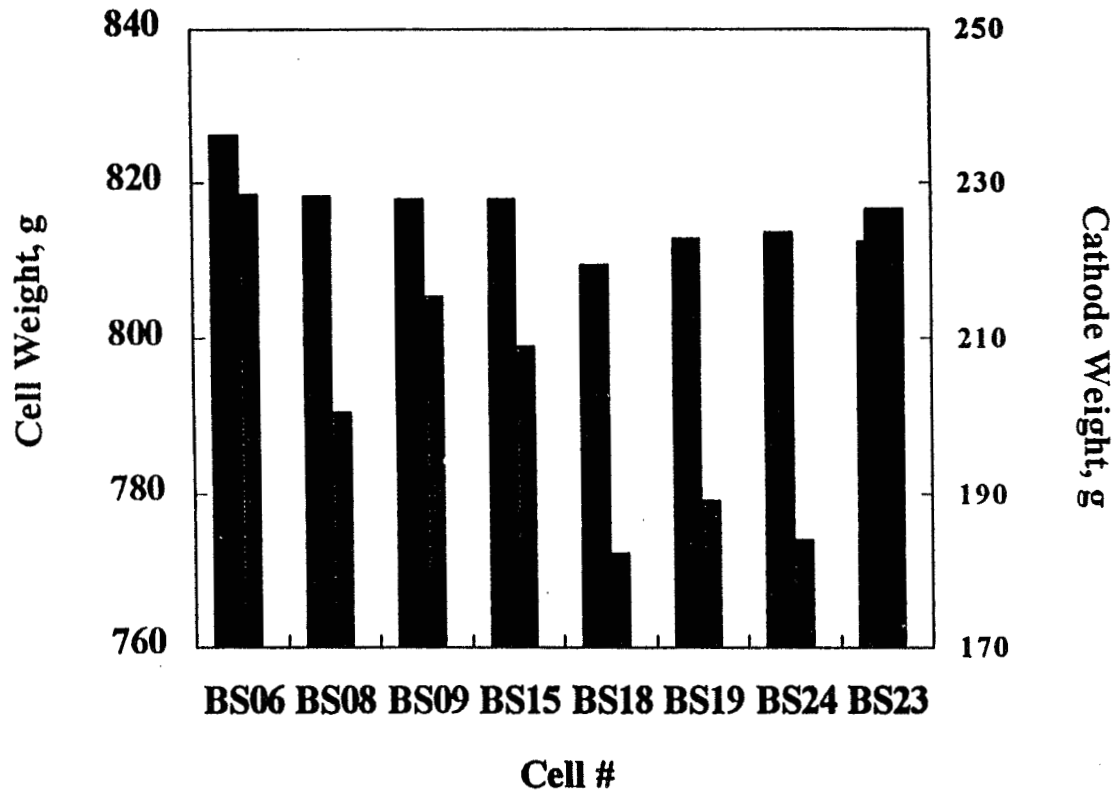


Temp.	Charge Rate			Discharge Rate		
	C/10	C/5	C/2	C/10	C/5	C/2
20°C	x			x		
	x				x	
	x					x
0°C		x		x		
	x			x		
	x				x	
-20°C		x		x		
	x			x		
	x				x	
-30°C			x	x		
	x				x	
	x					x
RT/-20°C		x		x		
	x			x		
	x				x	
(Charge at room temp. and discharge at -20° for 5 cycles)						
• Self-discharge at 20°C will be performed as described below.						
50°C	x			x		
	x				x	
	x					x
		x		x		
			x	x		
• Self-discharge at 50°C will be performed as described below.						

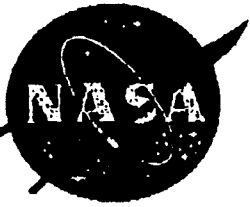


Weight Distribution

Weights of 20 Ah (Blue Star) Li Ion Cells

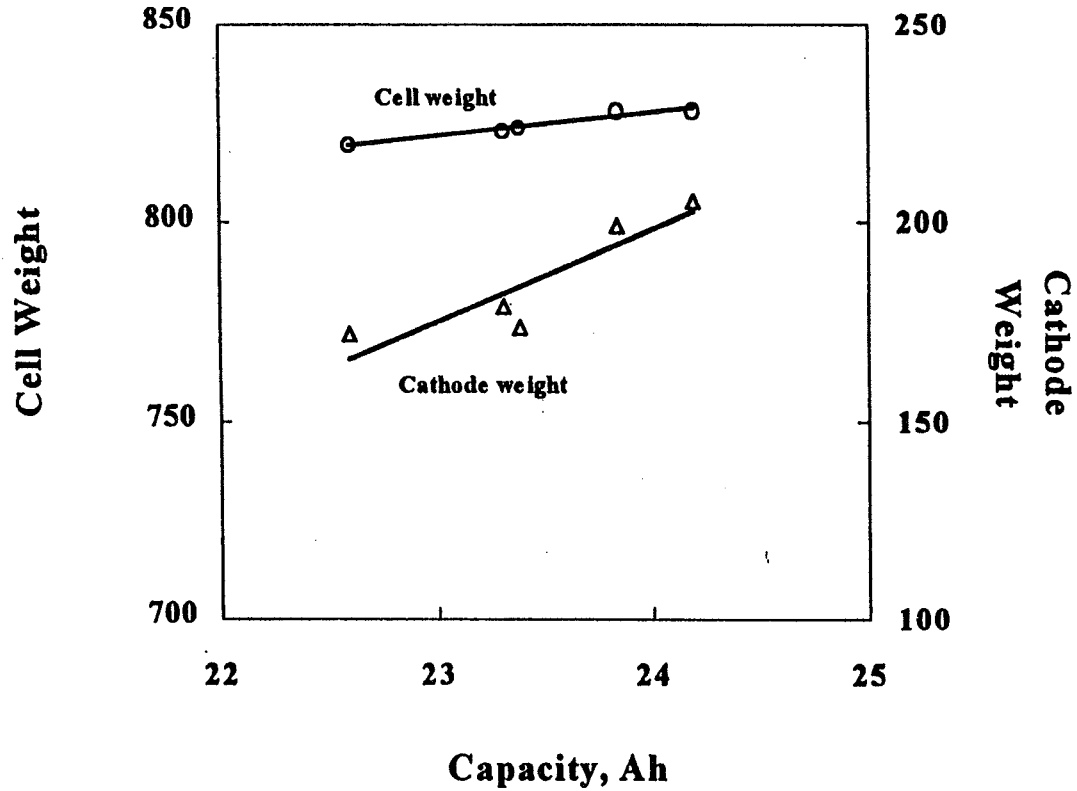


- Cell weight more consistent among the cells compared to the cathode weight.

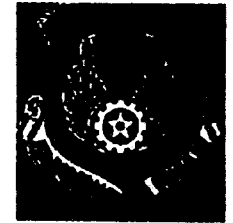


Weight vs. Capacity

20 Ah (Blue Star) Li Ion Cells

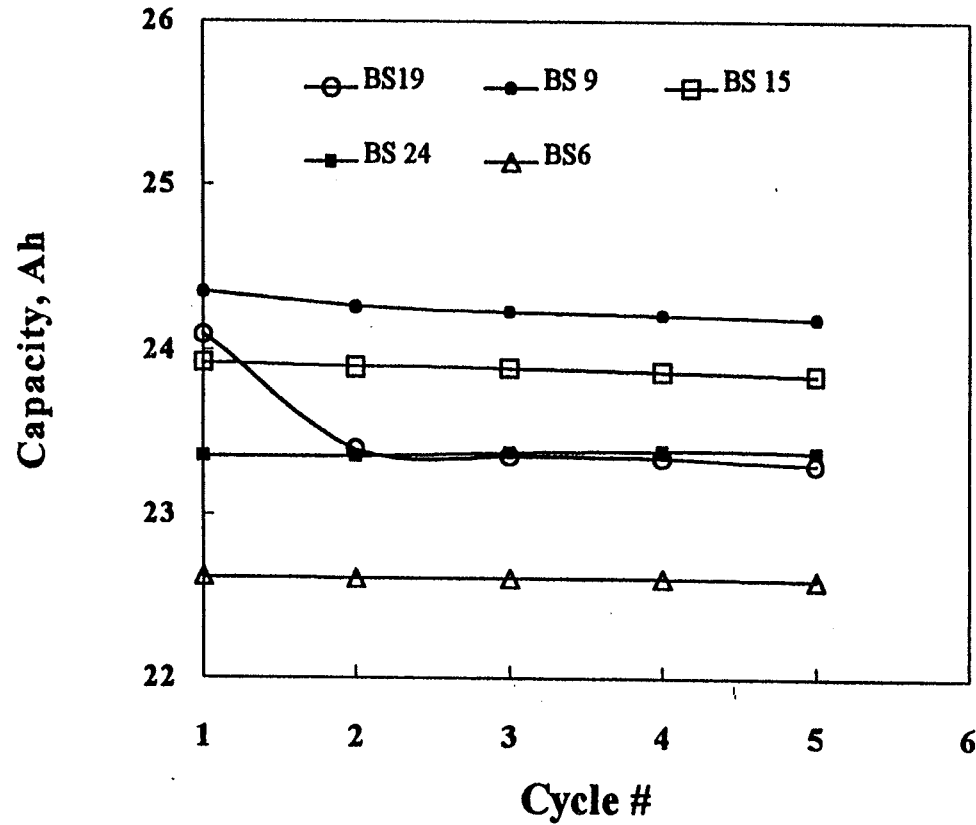


- Capacity increase with increasing cathode weight.

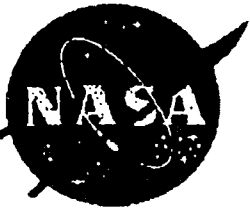


Conditioning Cycles

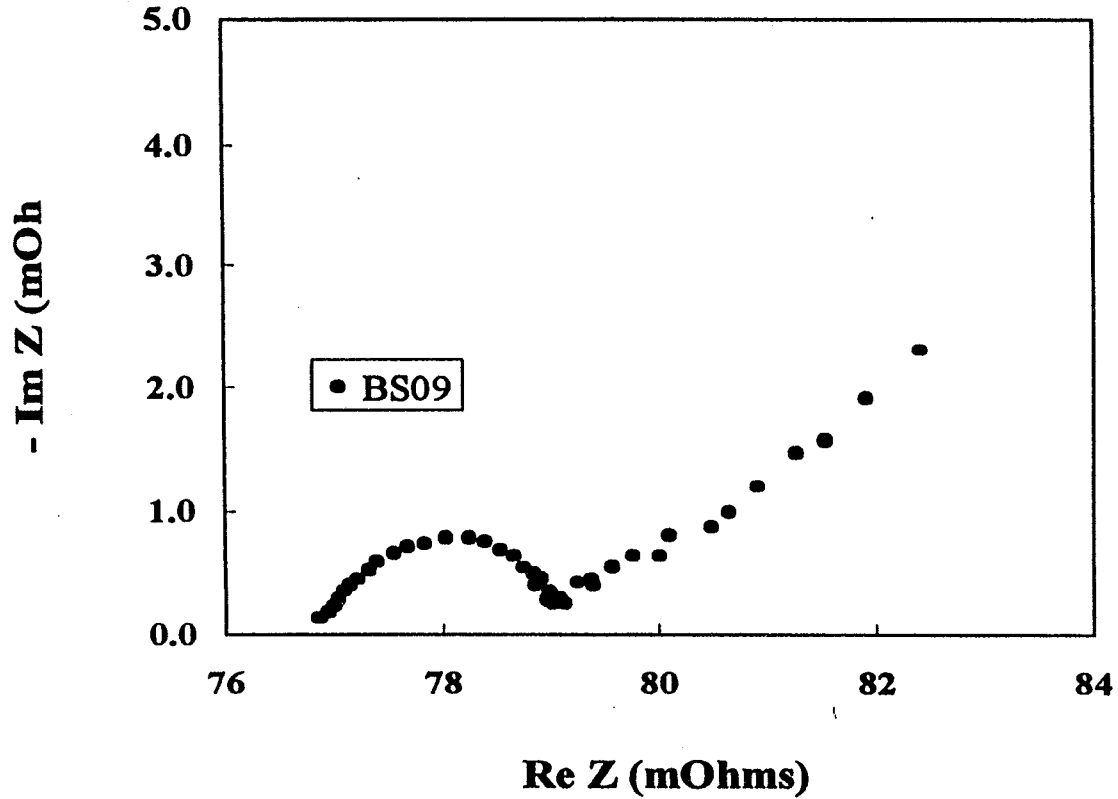
Conditioning Cycles of 20 Ah (Blue Star) Li Ion Cells



- Cell capacity around 23 Ah



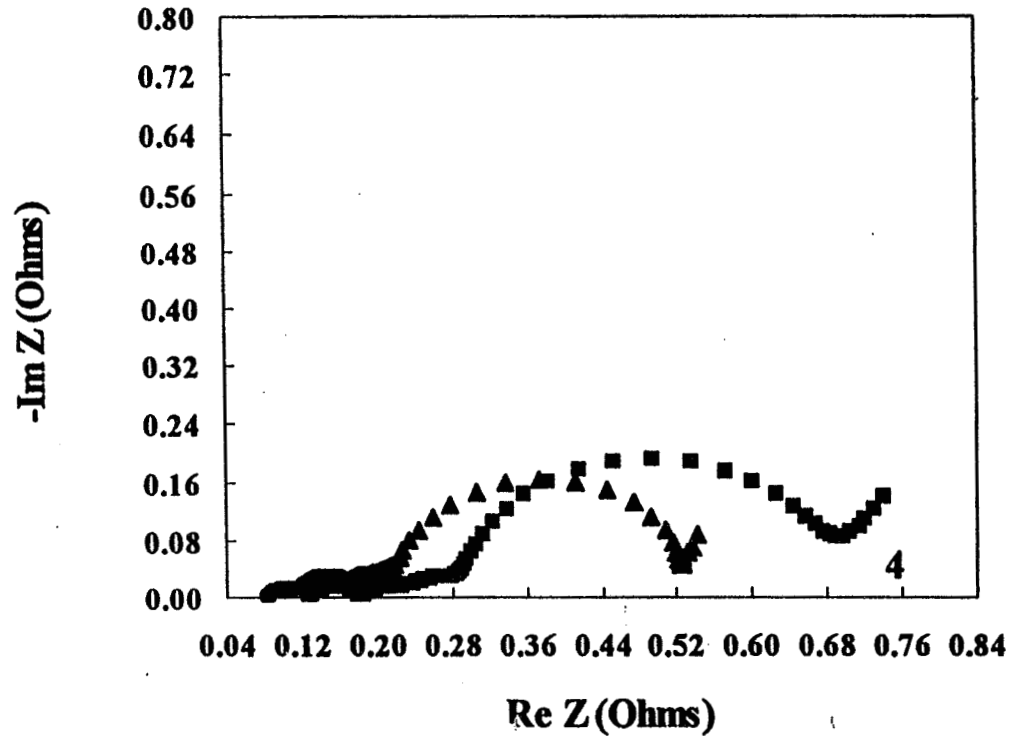
AC IMPEDANCE OF 20 Ah CELL



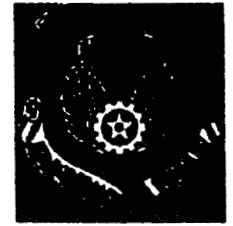
- Impedance reflective of a slow charge transfer process followed by diffusion.



EIS of JPL Experimental Li Ion Cells

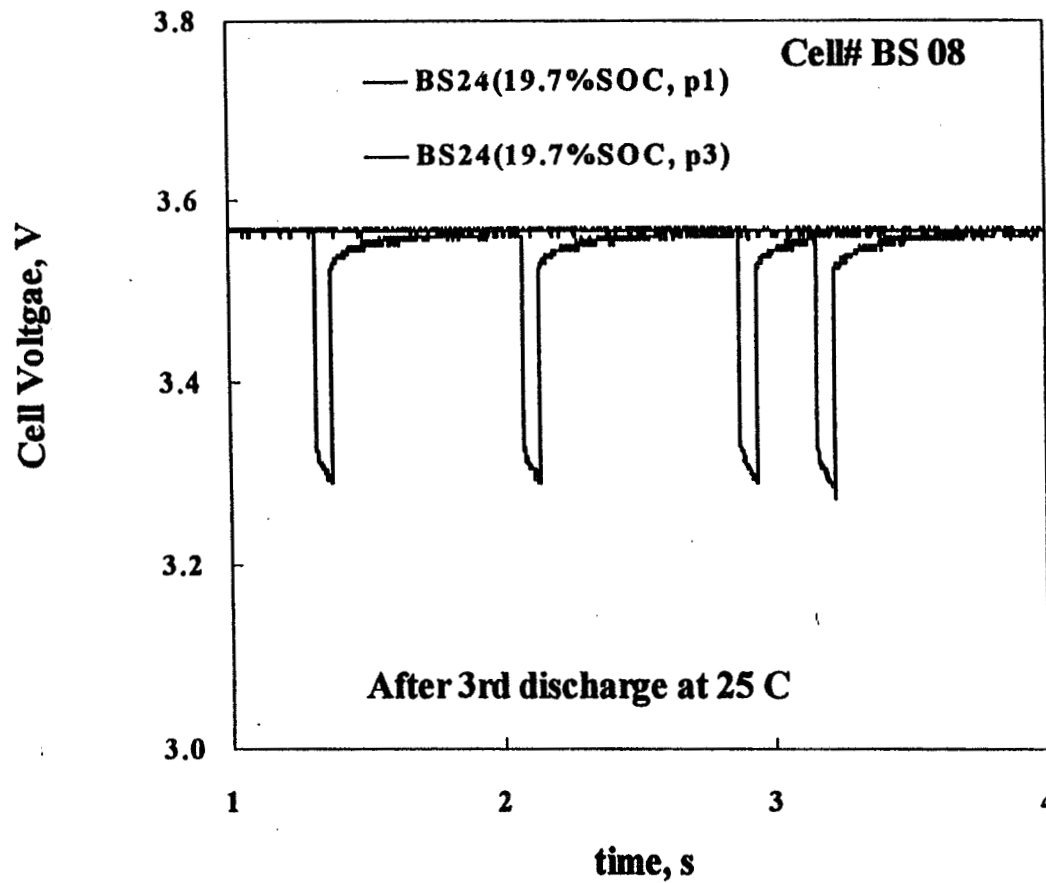


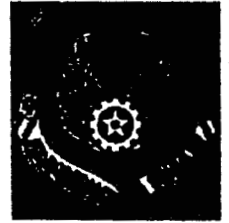
- Cathode impedance dominant portion of the total cell Impedance.



Pulses at 60 A at 25°C

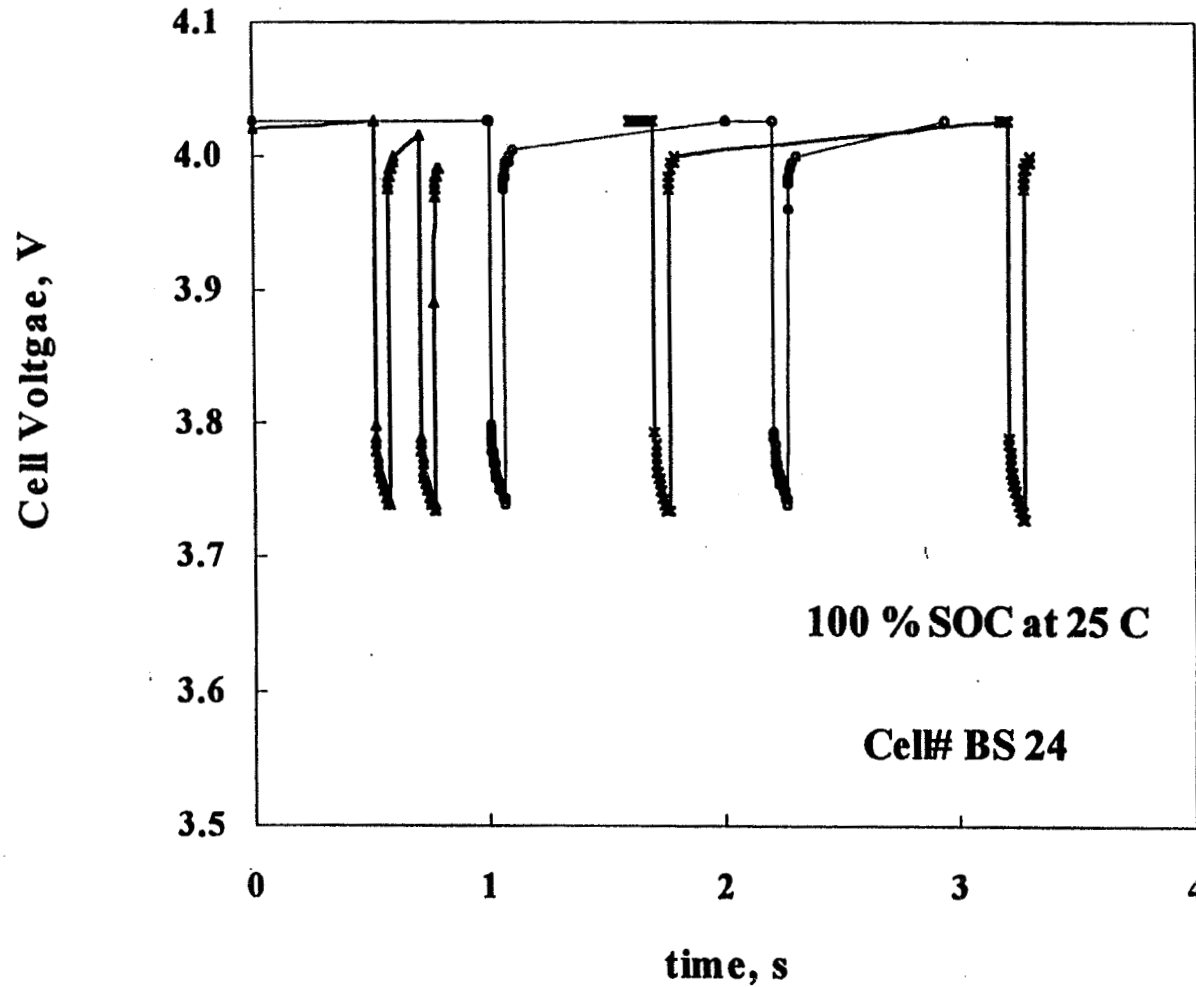
Pulsing of Blue Star 20 Ah Cell at 60 A (120 mS)

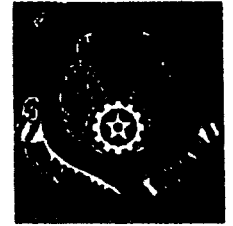




Pulses at 60 A at 25°C

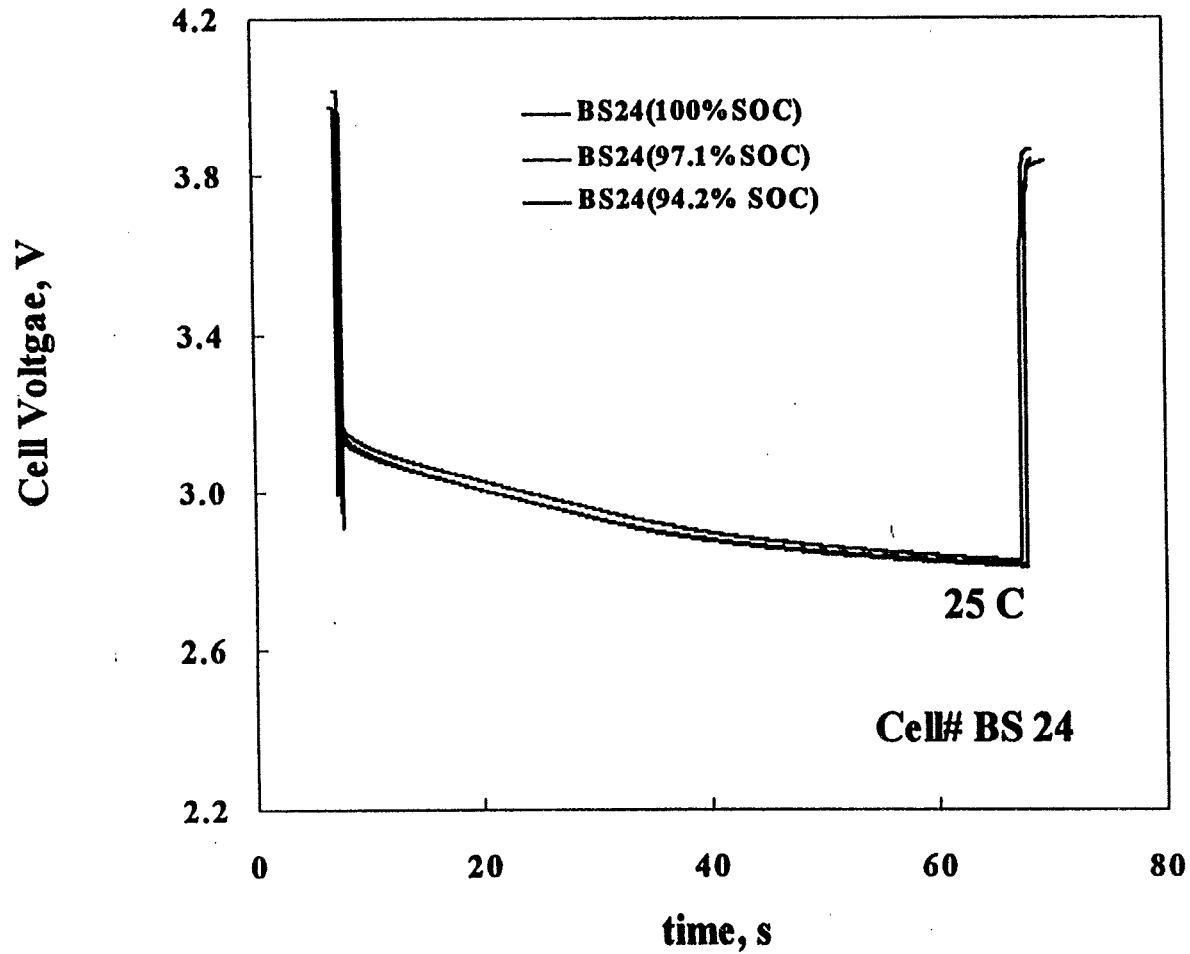
Pulsing of Blue Star 20 Ah Cell at 60 A (120 mS)





Pulses at 40 A at 25°C

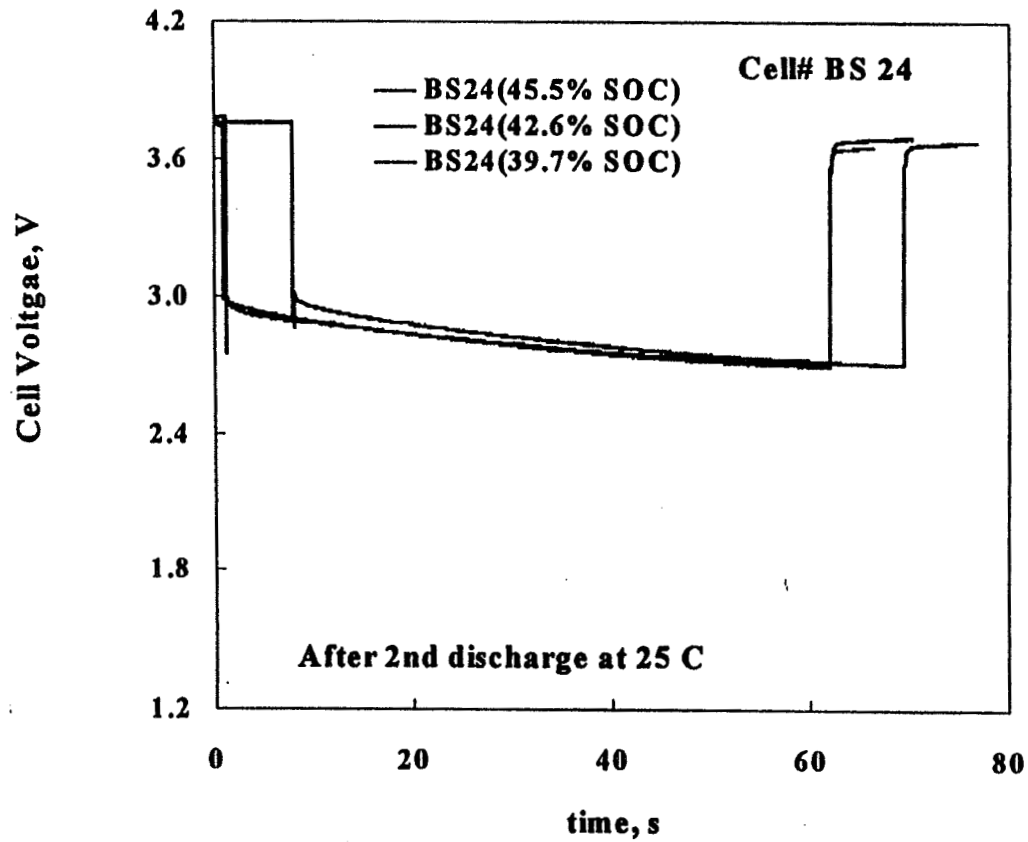
Pulsing of Blue Star 20 Ah Cell at 40 A (60 S)





Pulses at 40 A at 25°C

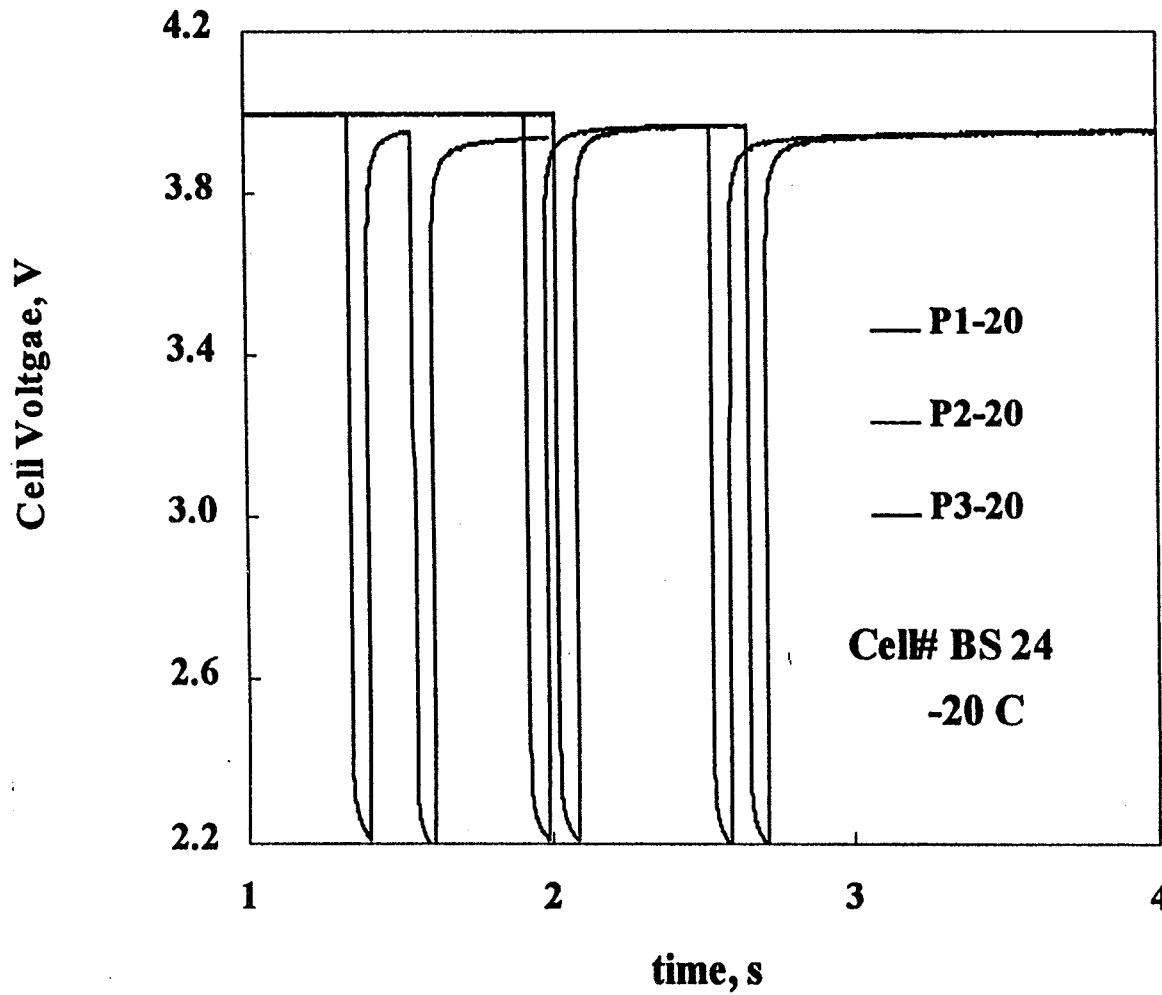
Pulsing of Blue Star 20 Ah Cell at 40 A (60 S)

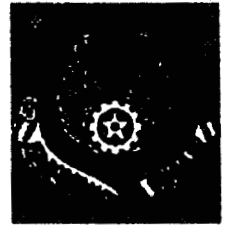




Pulses at 60 A at -20°C

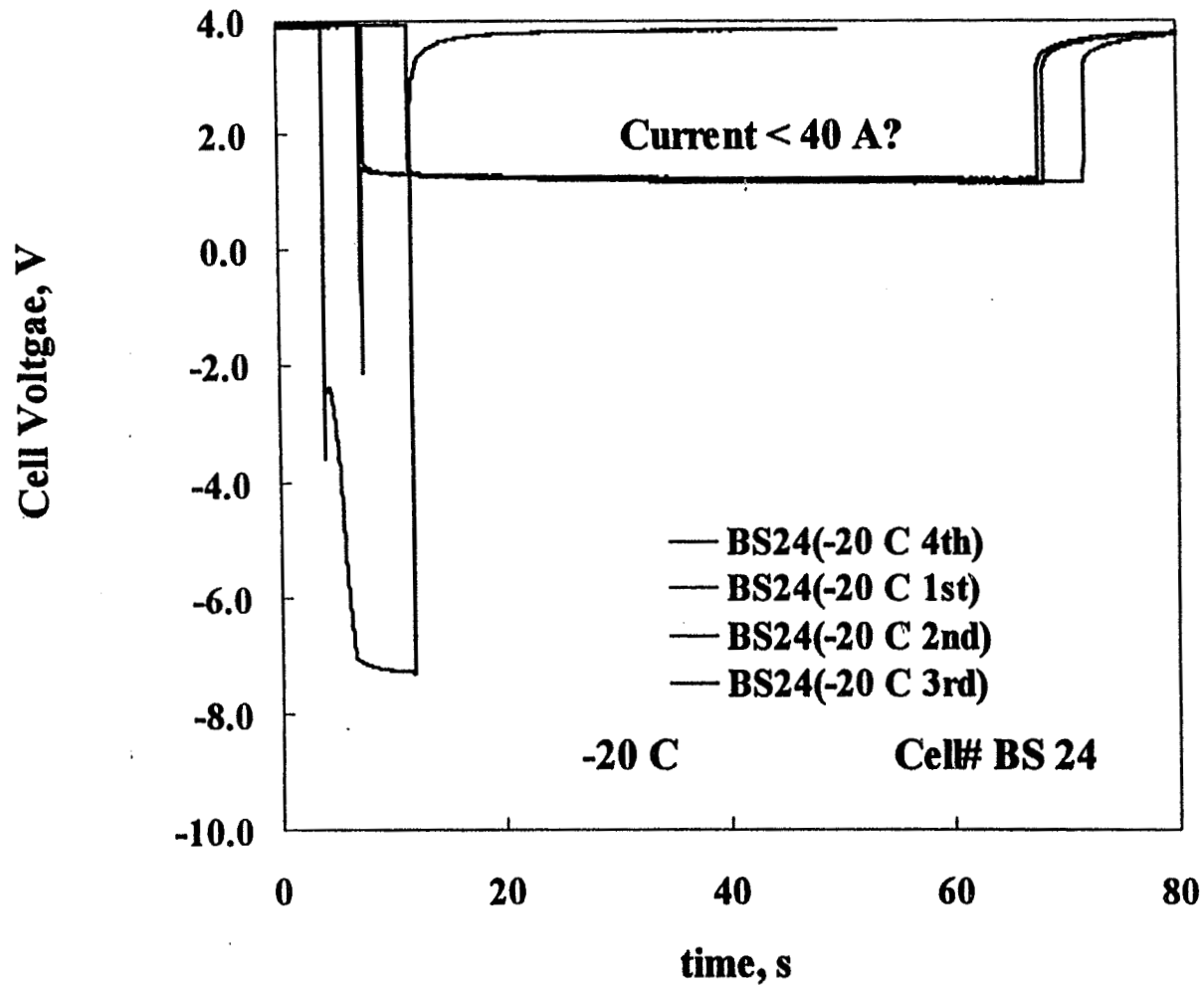
Pulsing of Blue Star 20 Ah Cell at 60 A (120 mS)





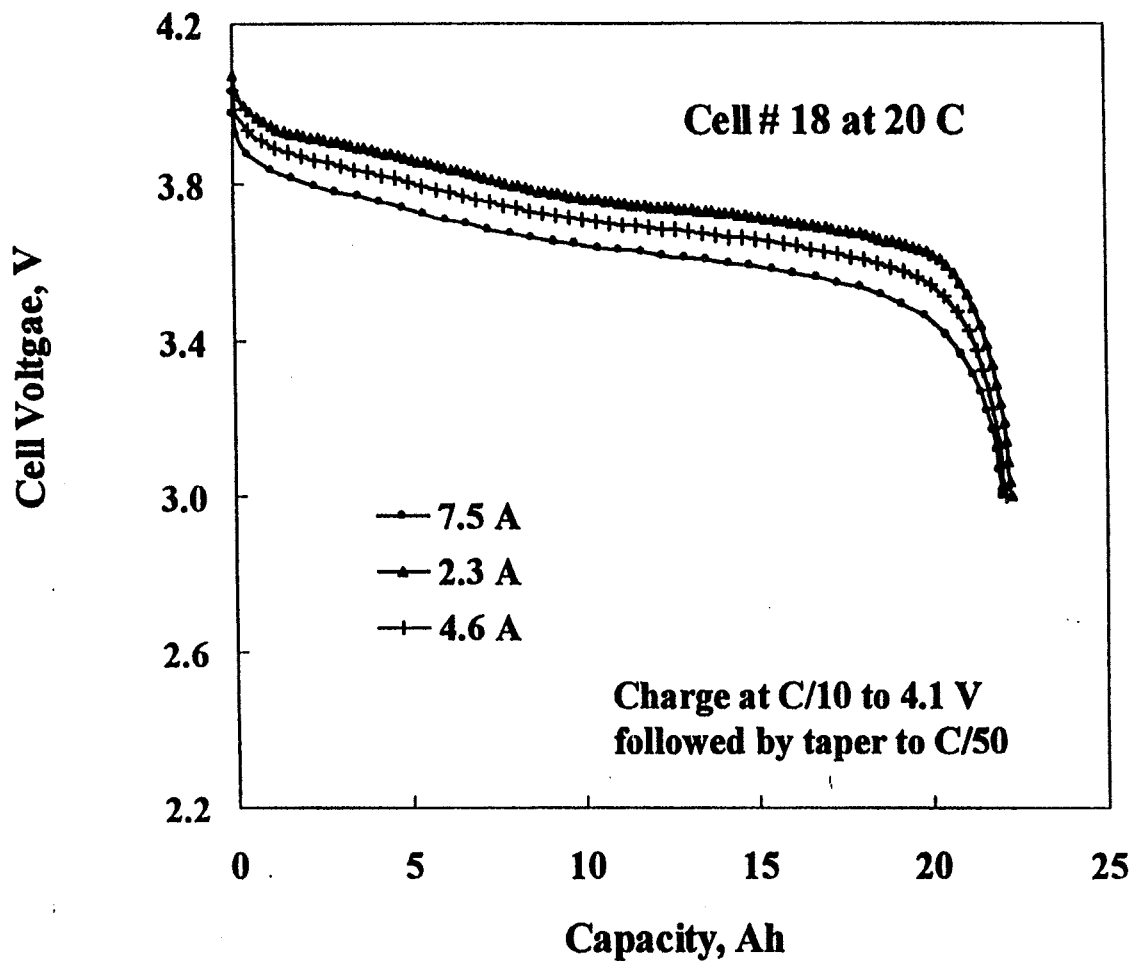
Pulses at 40 A at -20°C

Pulsing of Blue Star 20 Ah Cell at 40 A (60 S)





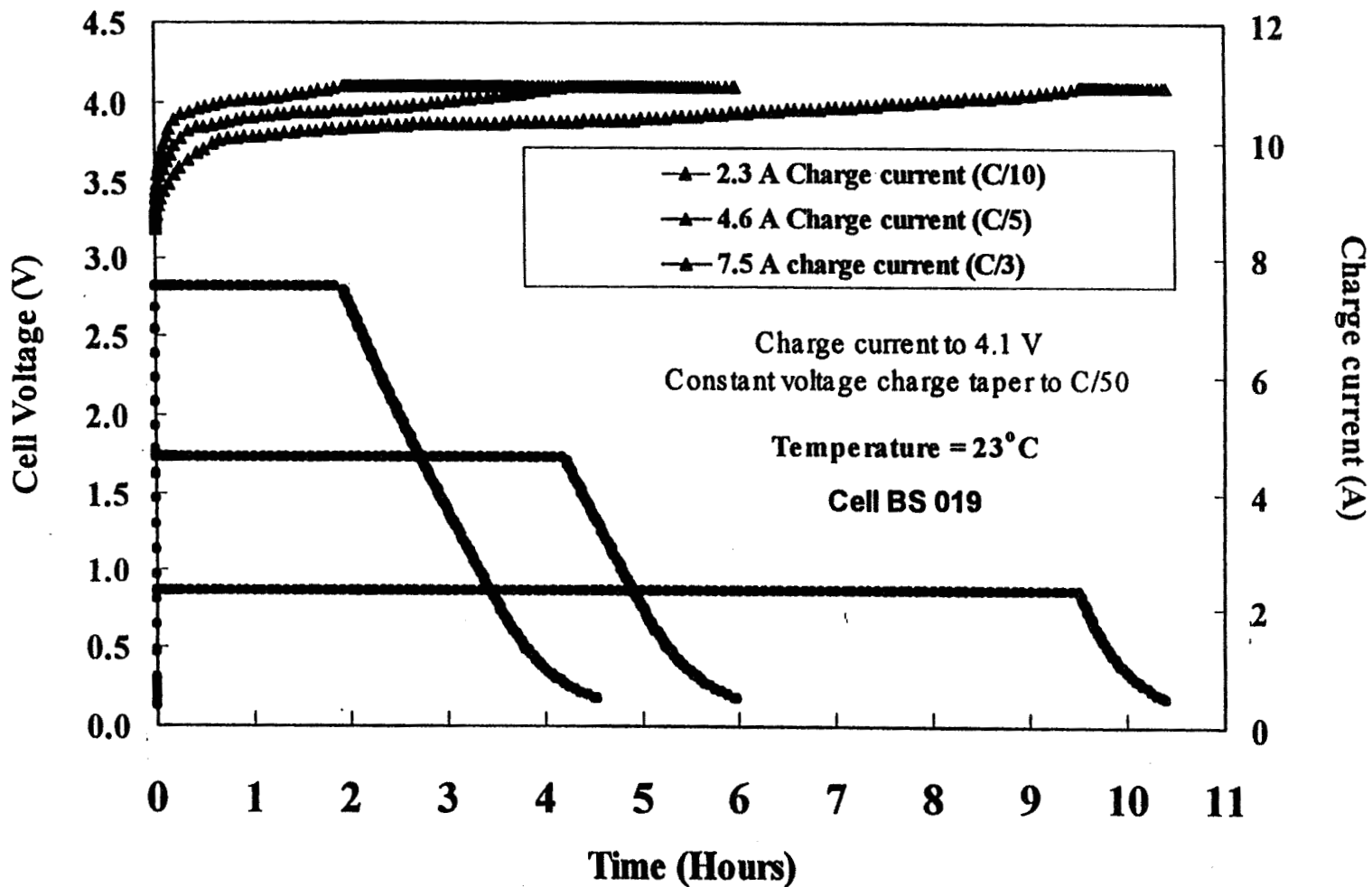
Discharge at 25°C



- Nearly 100 % utilization at C/3 discharge rate.

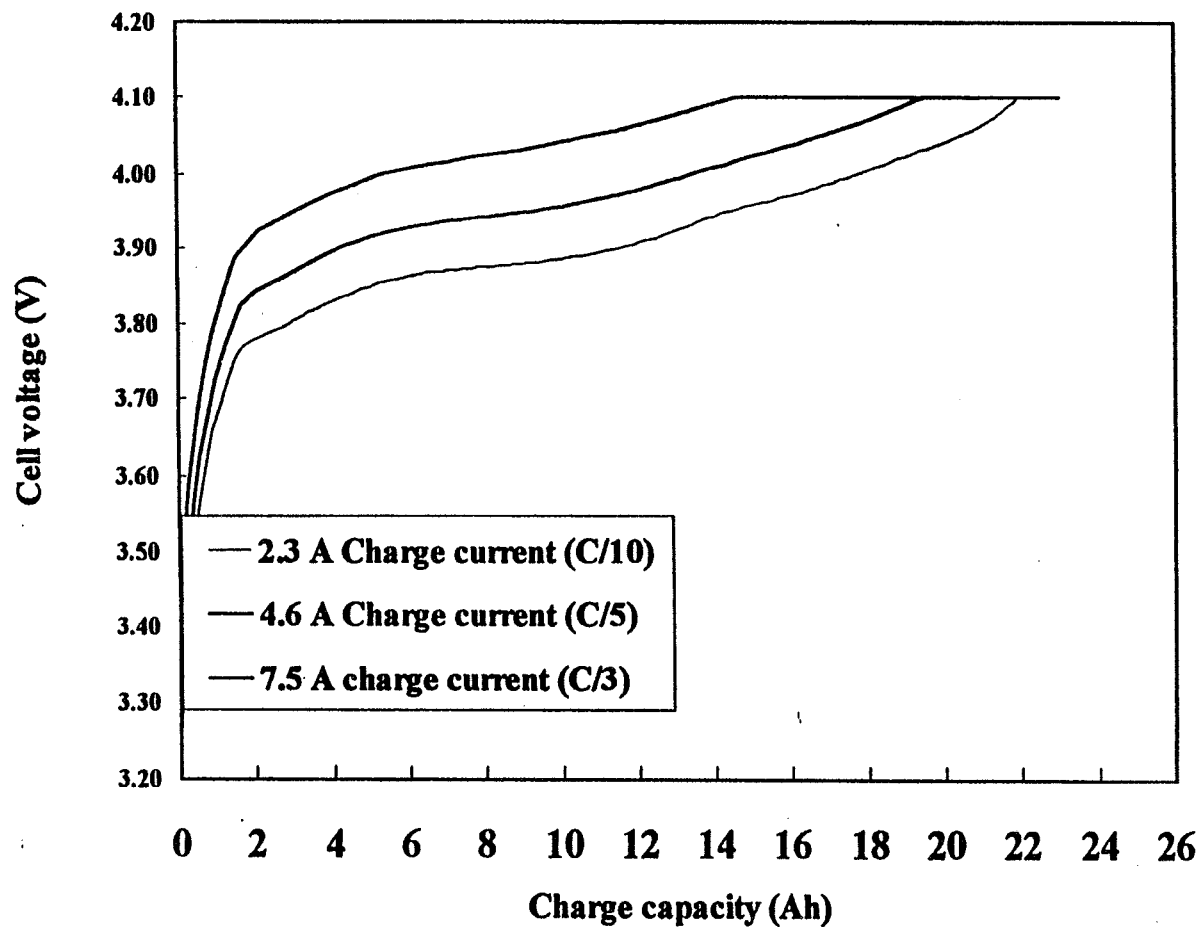


Charge at 25°C





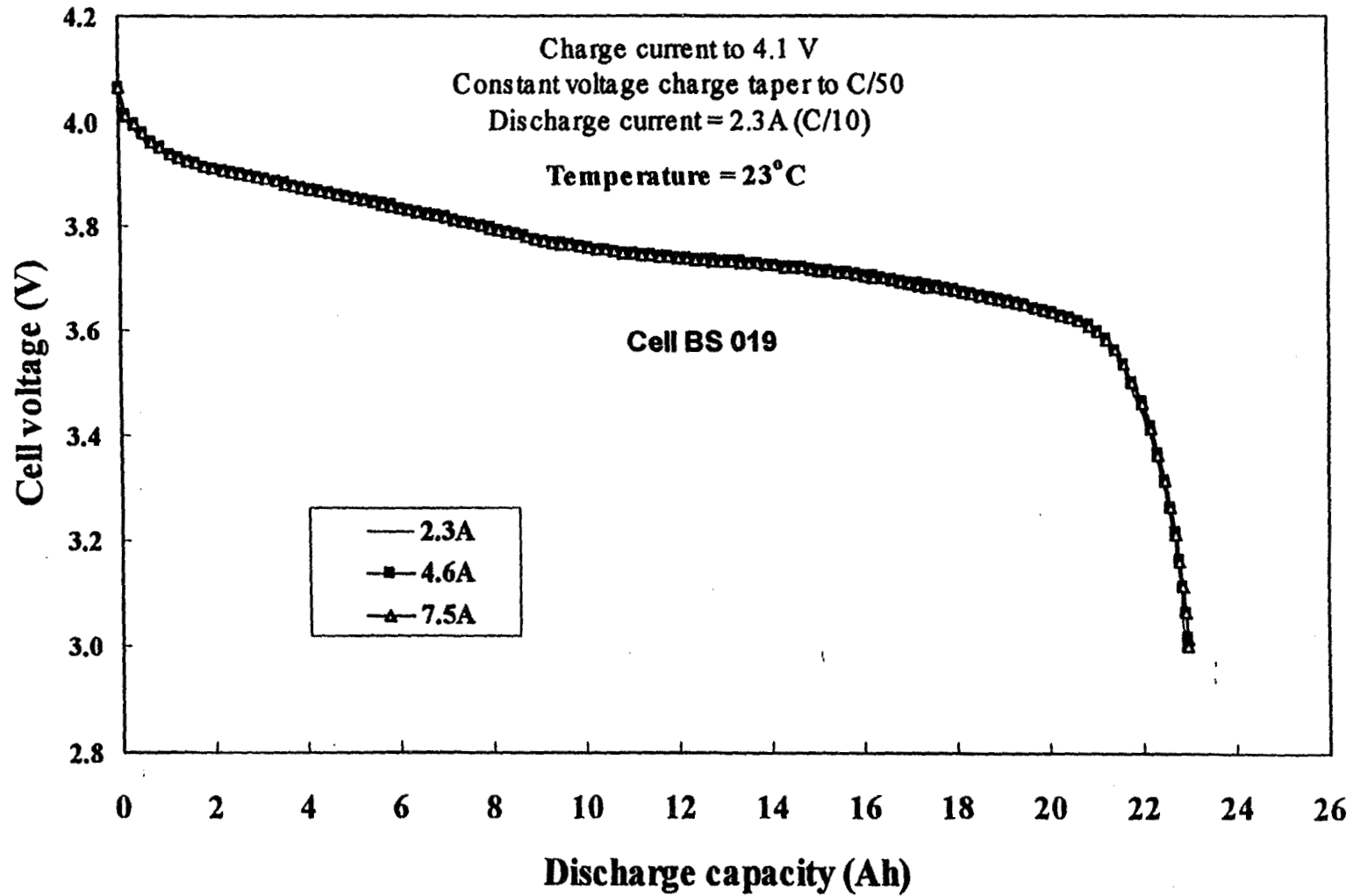
Charge at 25°C



- Above 2/3 capacity in constant current mode at highest rate tested, i.e., C/3/



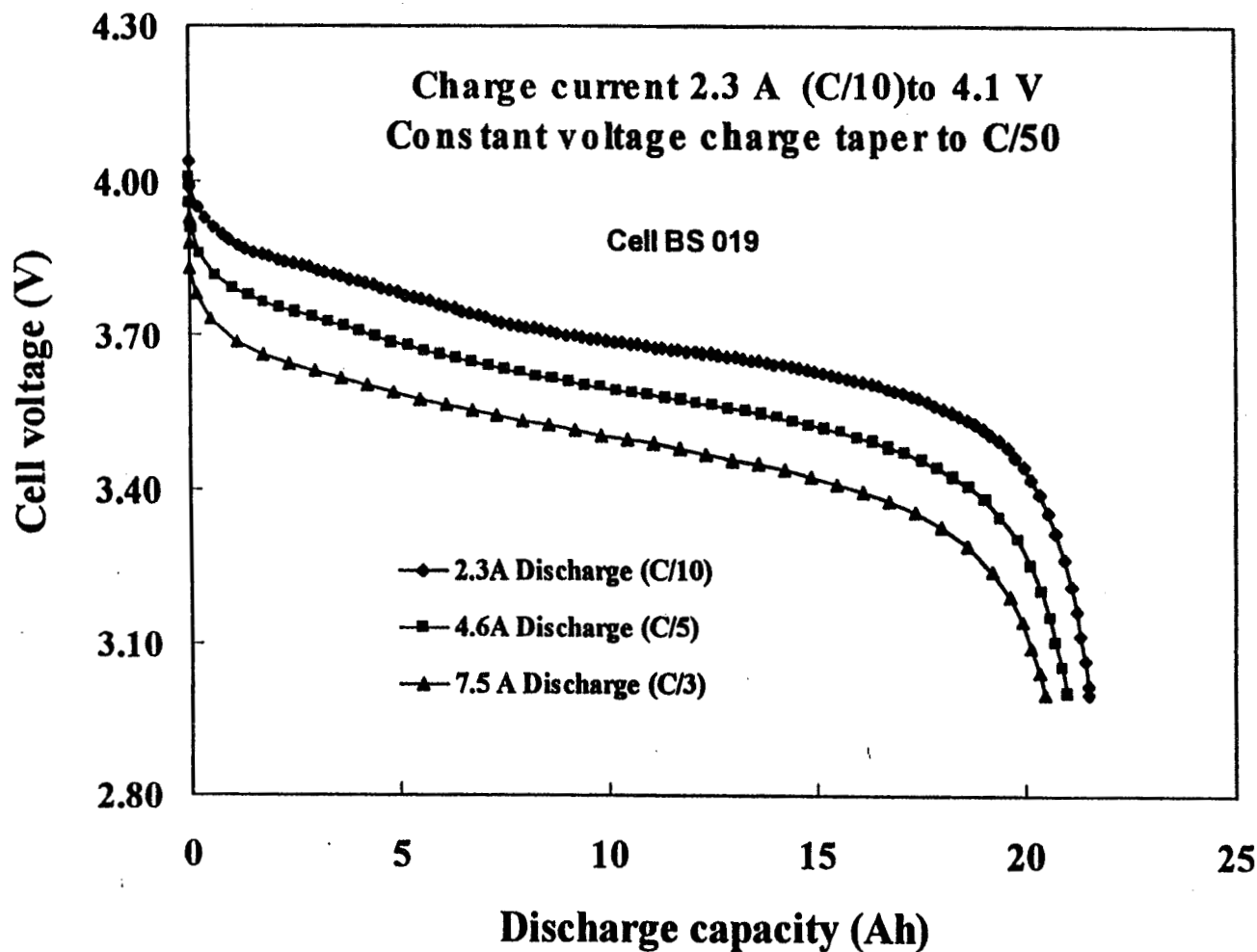
Charge at 25°C



- Nearly 100 % charge input in 3 hours of charging.



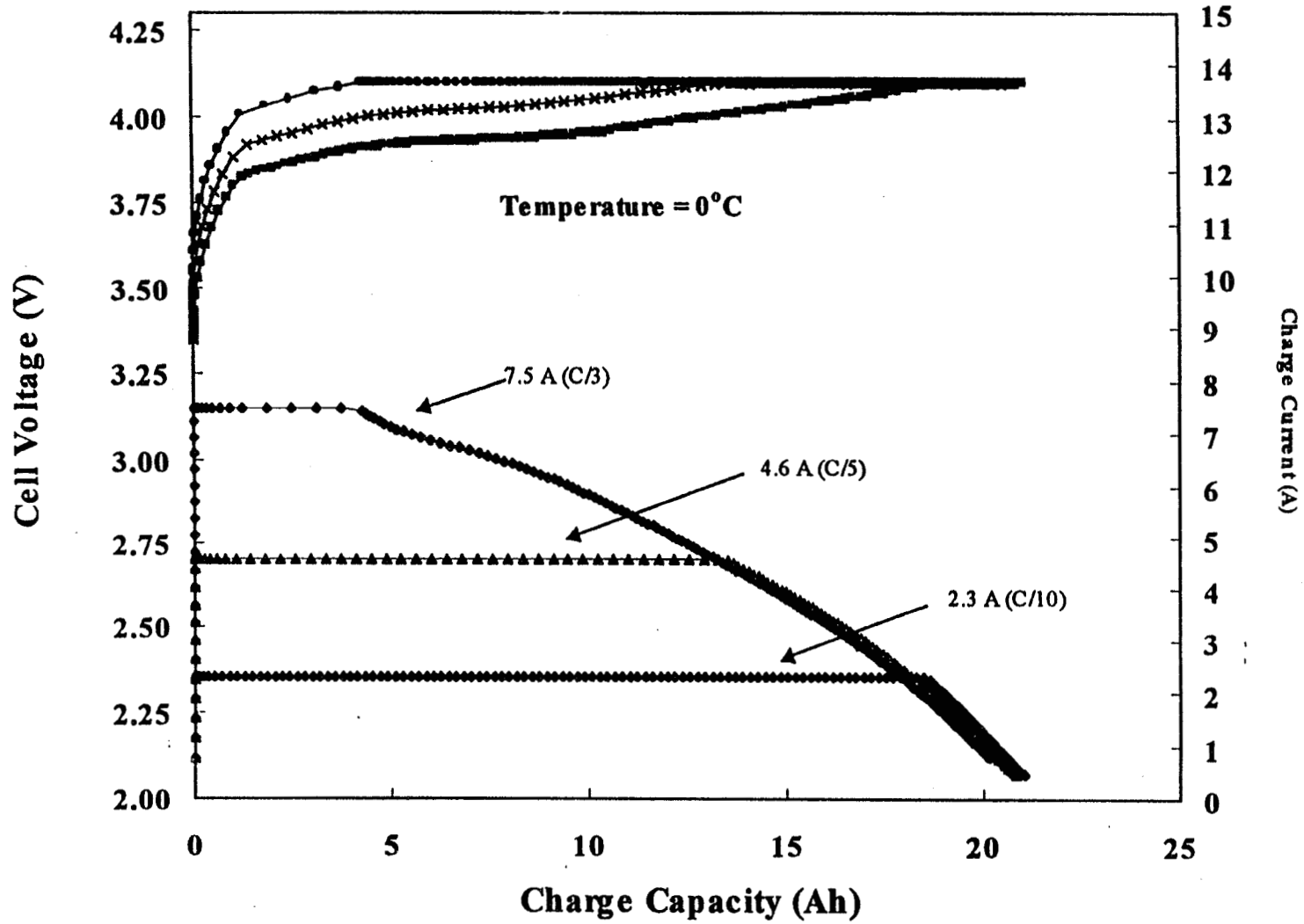
Discharge at 0°C

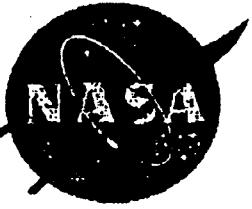


- Nearly 90 % capacity realized at C/3 discharge rate at 0 °C

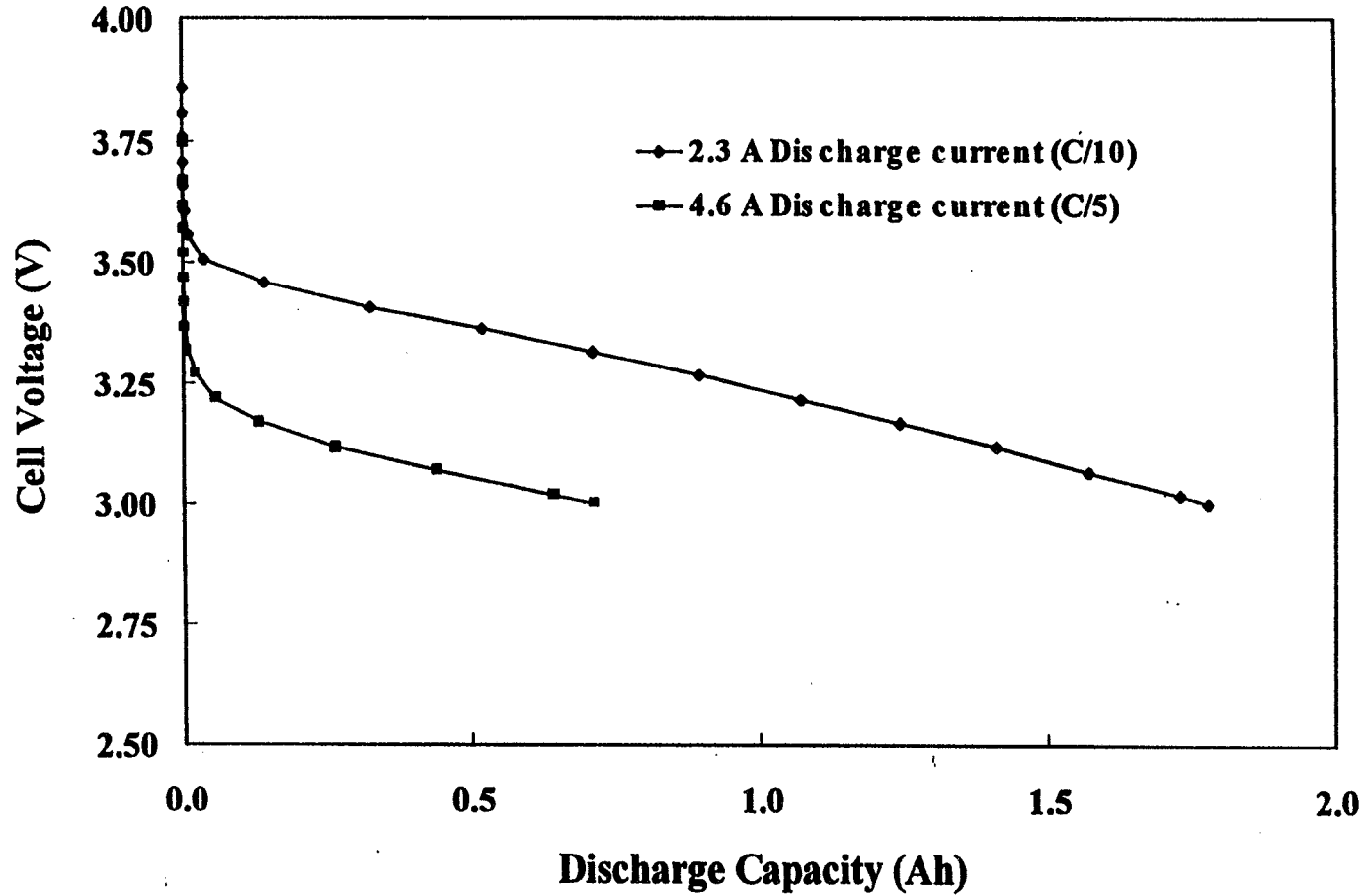
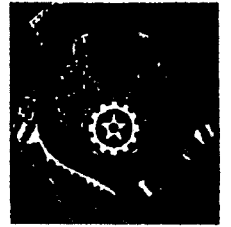


Charge Profiles at 0°C





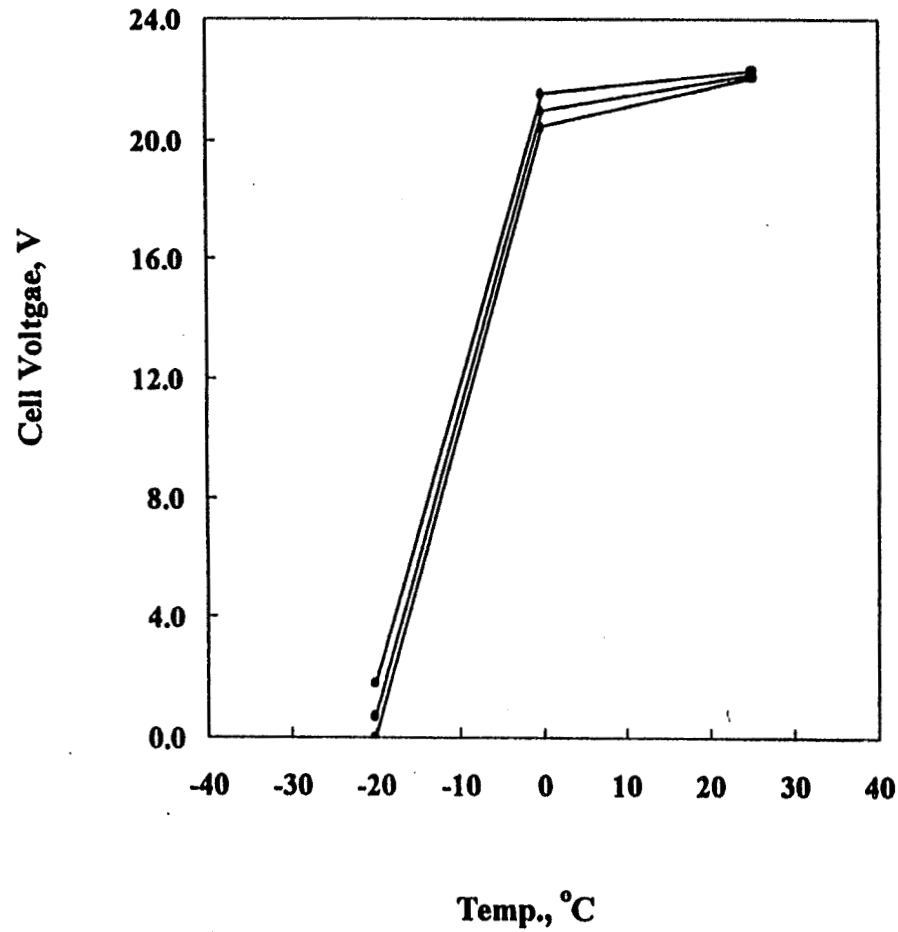
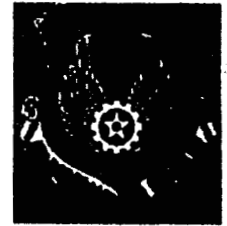
Discharge at -20°C



- Poor Performance at -20°C



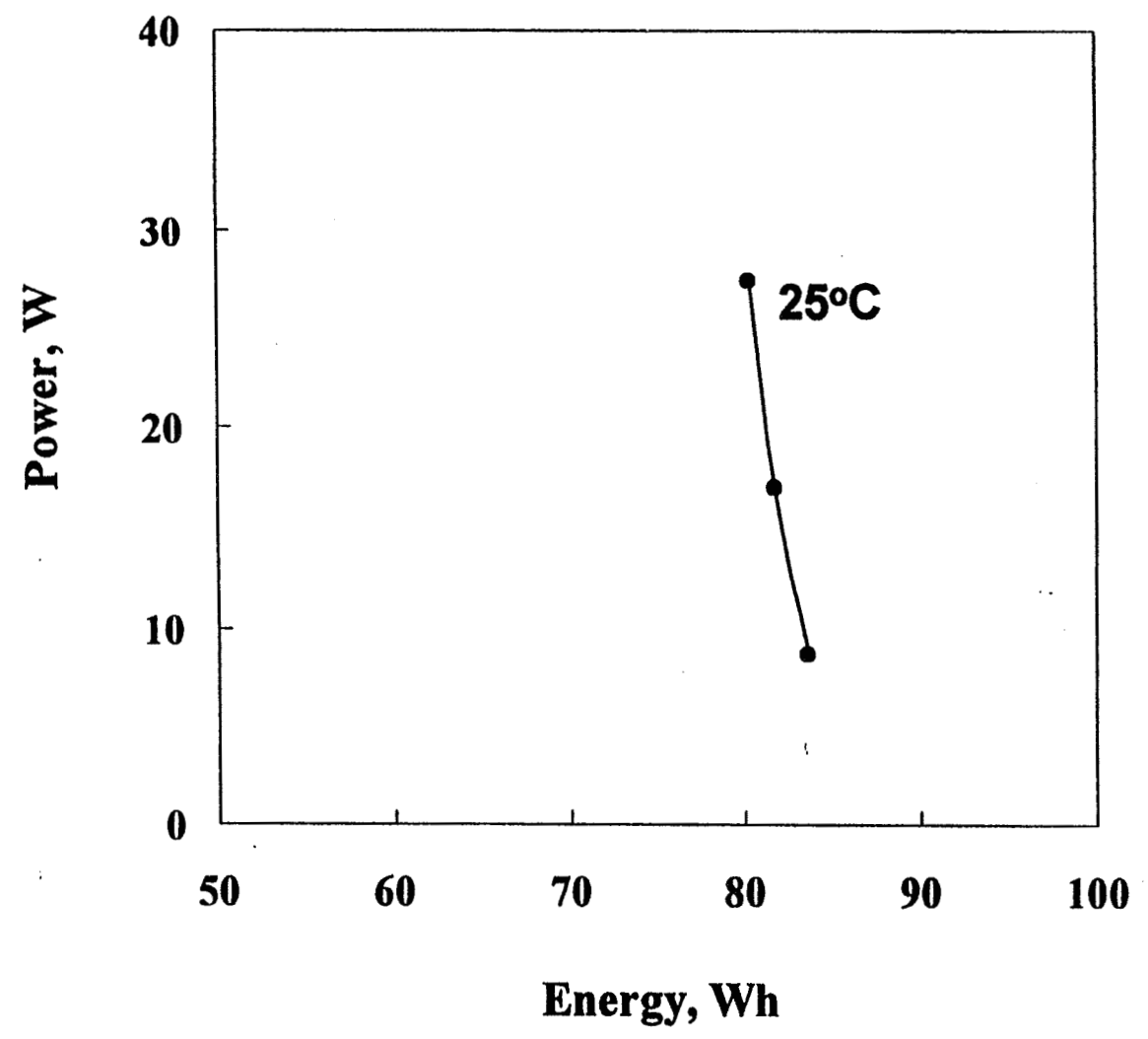
Capacity vs. Temperature



- Poor performance at -20°C

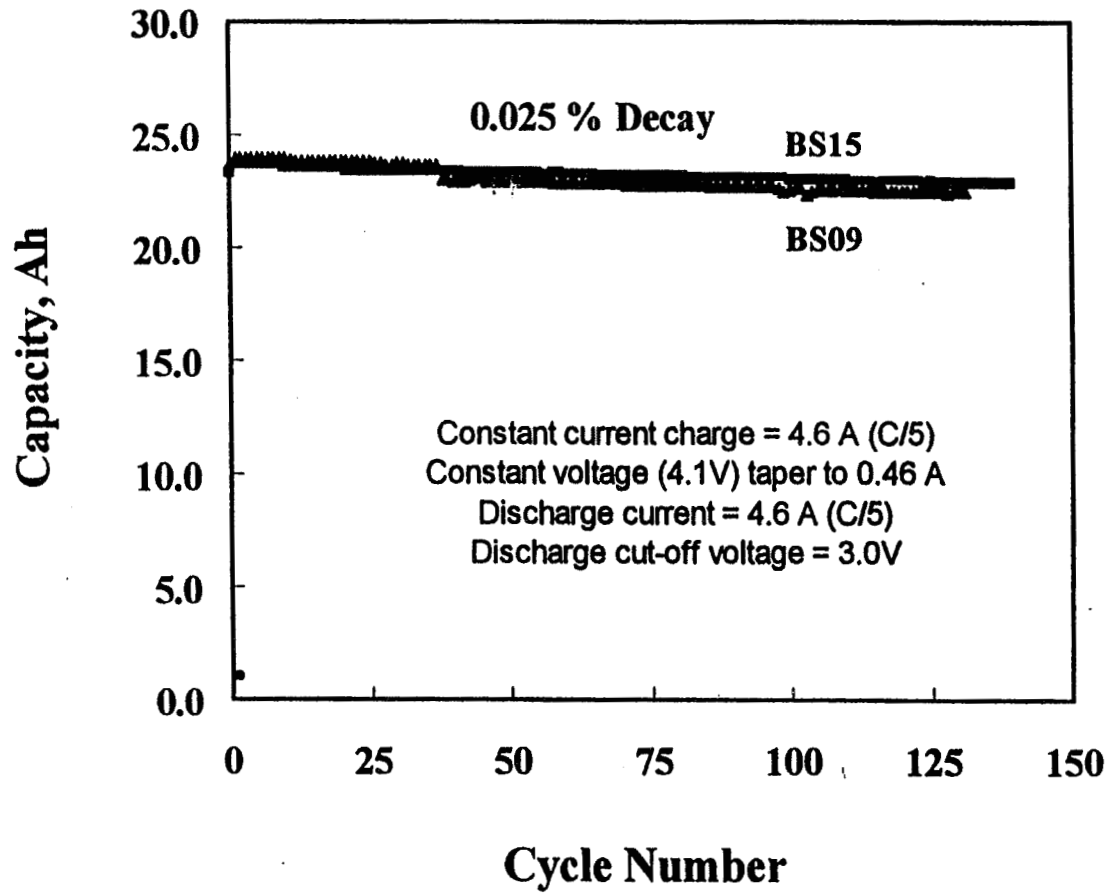


Ragone Plot





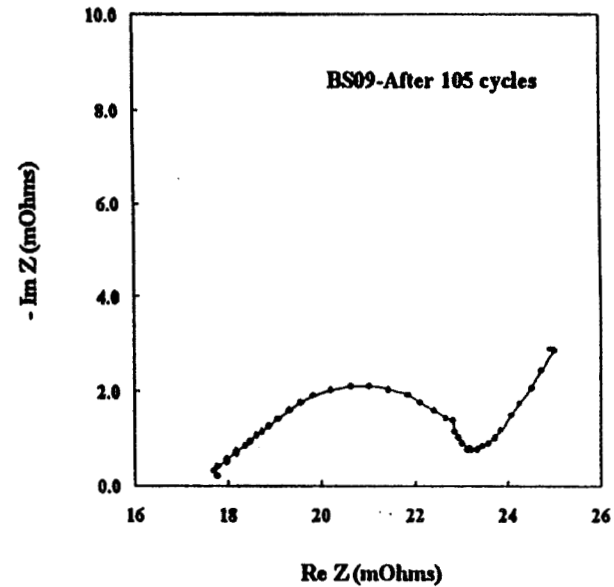
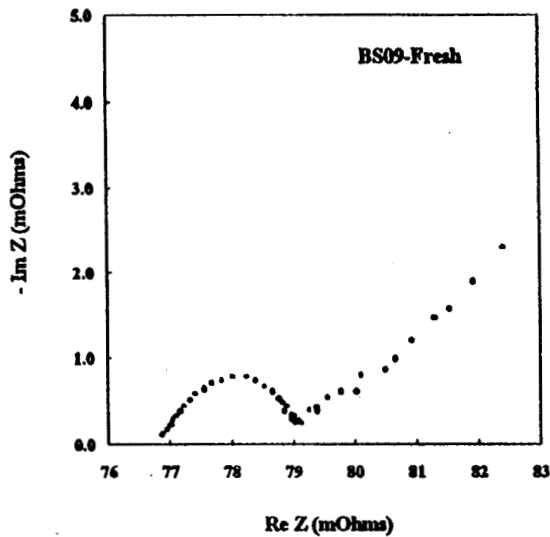
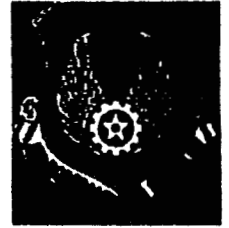
Cycling (100% DOD) at 25°C



- Capacity fade 0.025 % per cycle.



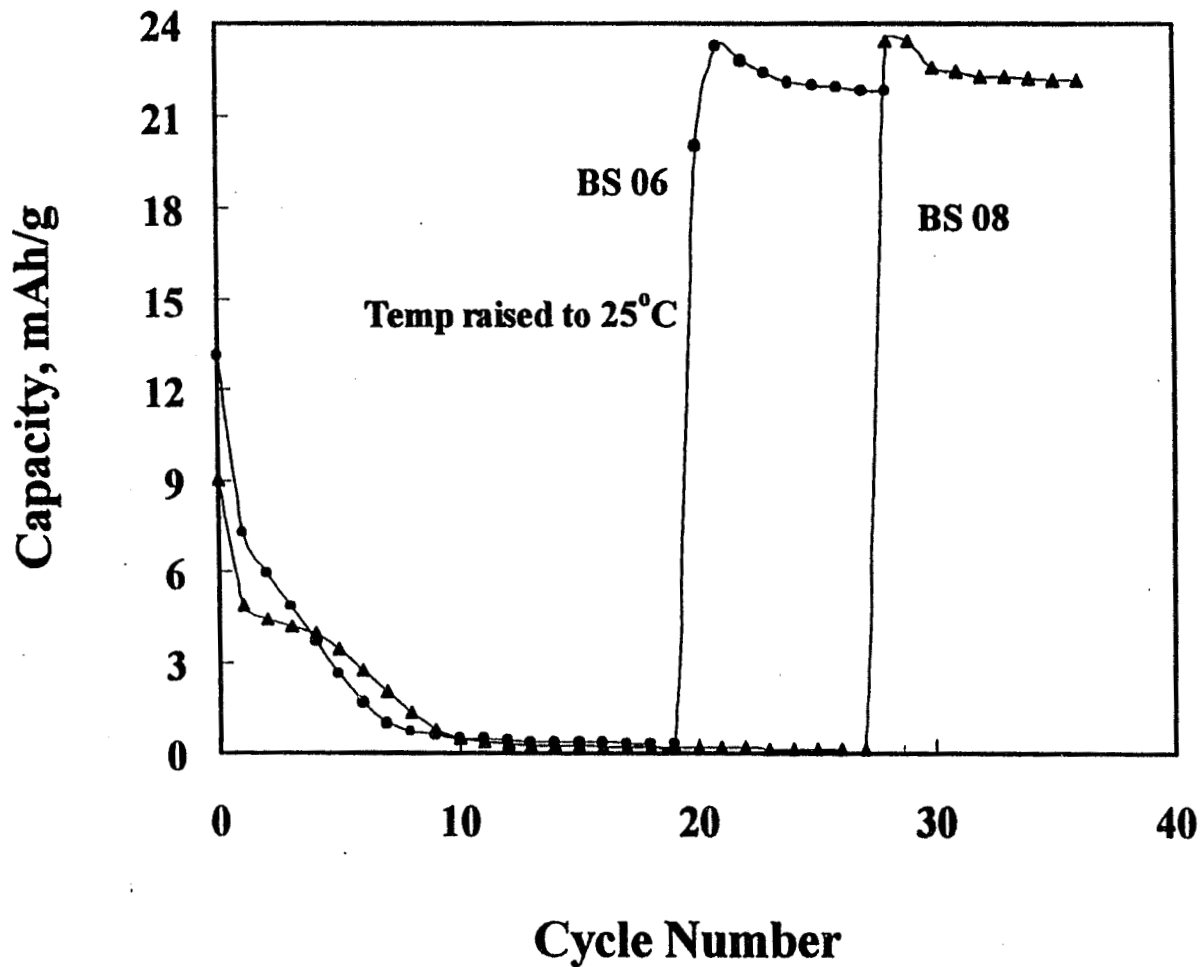
EIS During Cycling



- Marginal increase in the charge transfer (Faradaic) impedance
- Additional charge transfer polarization.
- Decrease in the series (Ohmic) resistance.



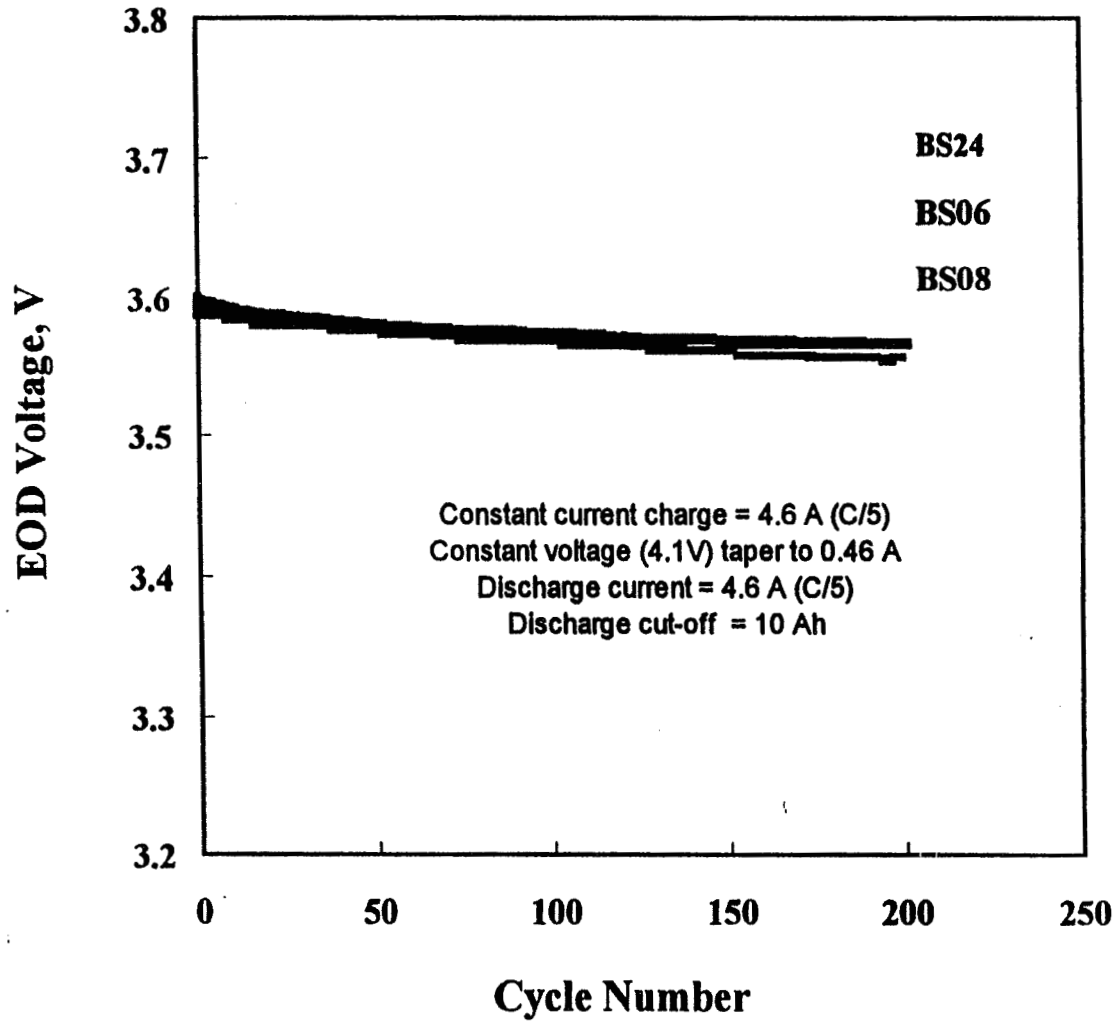
Cycling at 50% DOD at -20°C- Mars 2001 Lander



- Performance at -20°C inadequate.



Cycling at 50% DOD at 0°C- Mars 2001 Lander



- Depression in the EOD Voltage : 0.2 mV/cycle.



SUMMARY



- **Bluestar 20 Ah cells have so far shown good cycle life characteristics both at 100 % and 50 % DOD, which encouraging from the Mars 2001 mission point of view.**
- **Charge and discharge characteristics are fairly good at moderate rates.**
- **Low temperature performance needs to be improved to enable the Mars Exploratory missions.**



Acknowledgement

This work was carried out at the Jet Propulsion Laboratory, California Institute of Technology under contract with National Aeronautics and Space Administration and in collaboration with the Air Force Research Laboratory. The cells were fabricated by Bluestar under Air Force contract.

The Li-ion Battery Qualification Programme for STRV-1d

Vijay V. Thakur

Space Power Laboratory

Defence Evaluation and Research Agency, UK.



Overview

- ◆ Mission background
- ◆ Battery requirements
- ◆ Qualification programme details
- ◆ Test results
- ◆ Conclusion

STRV-1c&d mission background

- ◆ 100kg microsattellites in GTO as Ariane V piggyback
- ◆ Technology demonstration mission in high radiation orbit exposed to space environment from LEO to GEO
- ◆ Approximately 750 eclipses per year
- ◆ Fully regulated 28V bus, GaAs and InP solar arrays, NiCd primary battery
- ◆ Li-ion battery experiment (LIBE) on STRV-1d

LIBE mission objectives

- ◆ First flight of Li-ion battery in space
- ◆ Operate entire mission following LEOP with Li-ion battery
- ◆ Primary NiCd battery in 'standby' mode, autonomous switchover to NiCd in the event of a Li-ion battery performance anomaly
- ◆ Monitor battery voltage, individual cell voltages, battery temperature

Li-ion battery requirements

- ◆ Battery voltage : $17.0V \leq V_{\text{batt}} \leq 24.0V$
- ◆ Battery delivered energy : 46Wh @ 60% DoD
- ◆ Battery operating temperature : $-15^{\circ}\text{C} \leq T_{\text{batt}} \leq 45^{\circ}\text{C}$
- ◆ Battery total mass < 4.5kg, individual module dimensions < 175mm x 155mm x 40mm
- ◆ No effect on battery delivered energy due to 'sinusoidal' charge current
- ◆ Pulse discharge performance to be demonstrated
- ◆ ≥ 1000 life cycles at 46Wh discharge each with $V_{\text{eod}} > 17.0V$

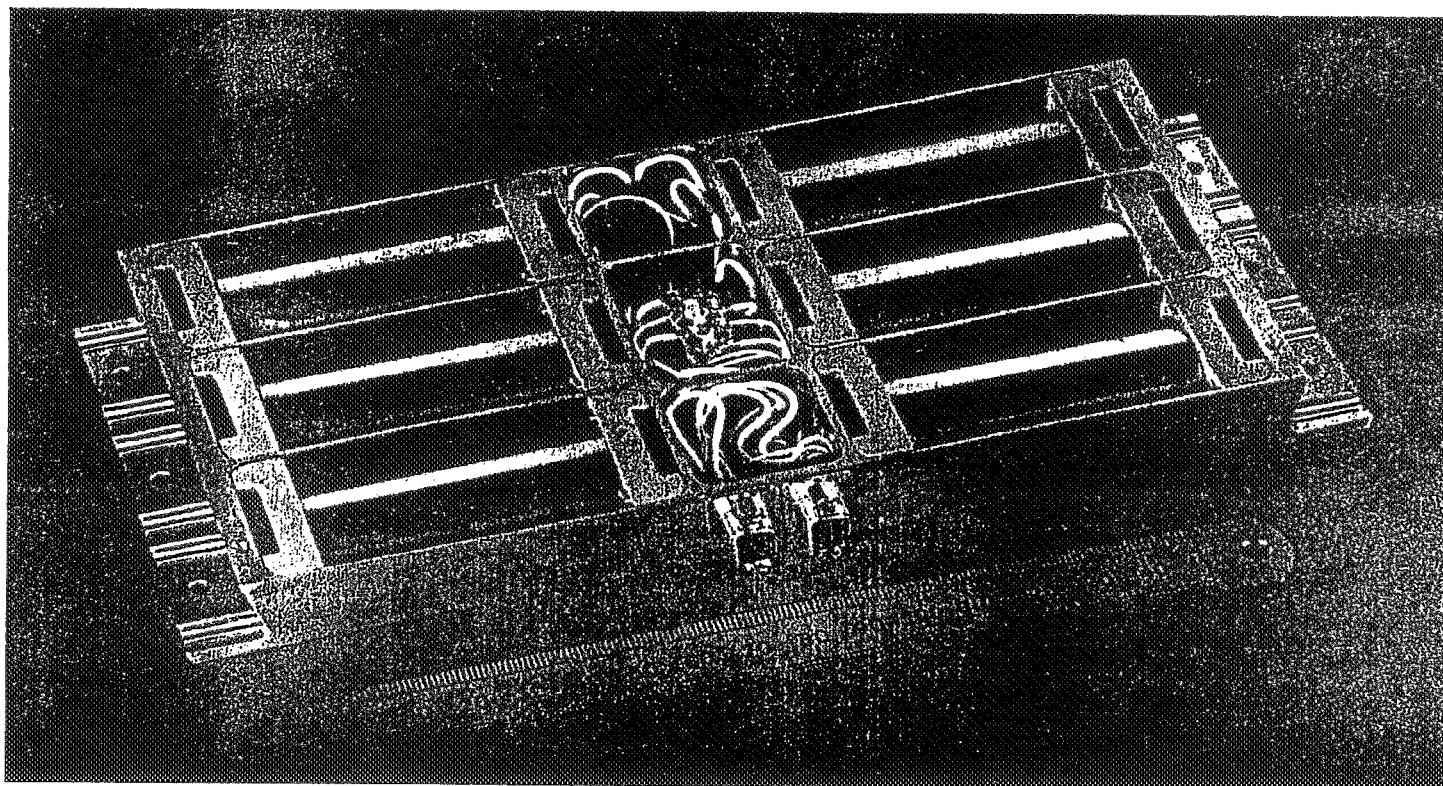
Qualification programme details

- ◆ Discharge performance (delivered energy) for C/5, C/2 and 2C discharge to 17.0V (ambient temp.)
- ◆ Discharge performance for C/5 discharge to 17.0V over temperature range $-15^{\circ}\text{C} \leq T_{\text{batt}} \leq 45^{\circ}\text{C}$ (15°C intervals)
- ◆ Discharge performance for sinusoidal charge current profile between 0mA and 600mA
- ◆ Pulse discharge performance for 2C pulses, 1sec 'ON', 9sec 'OFF'
- ◆ Life cycle test : charge at 1.08C to 24.0V, discharge at 0.6C to deliver 46Wh/cycle

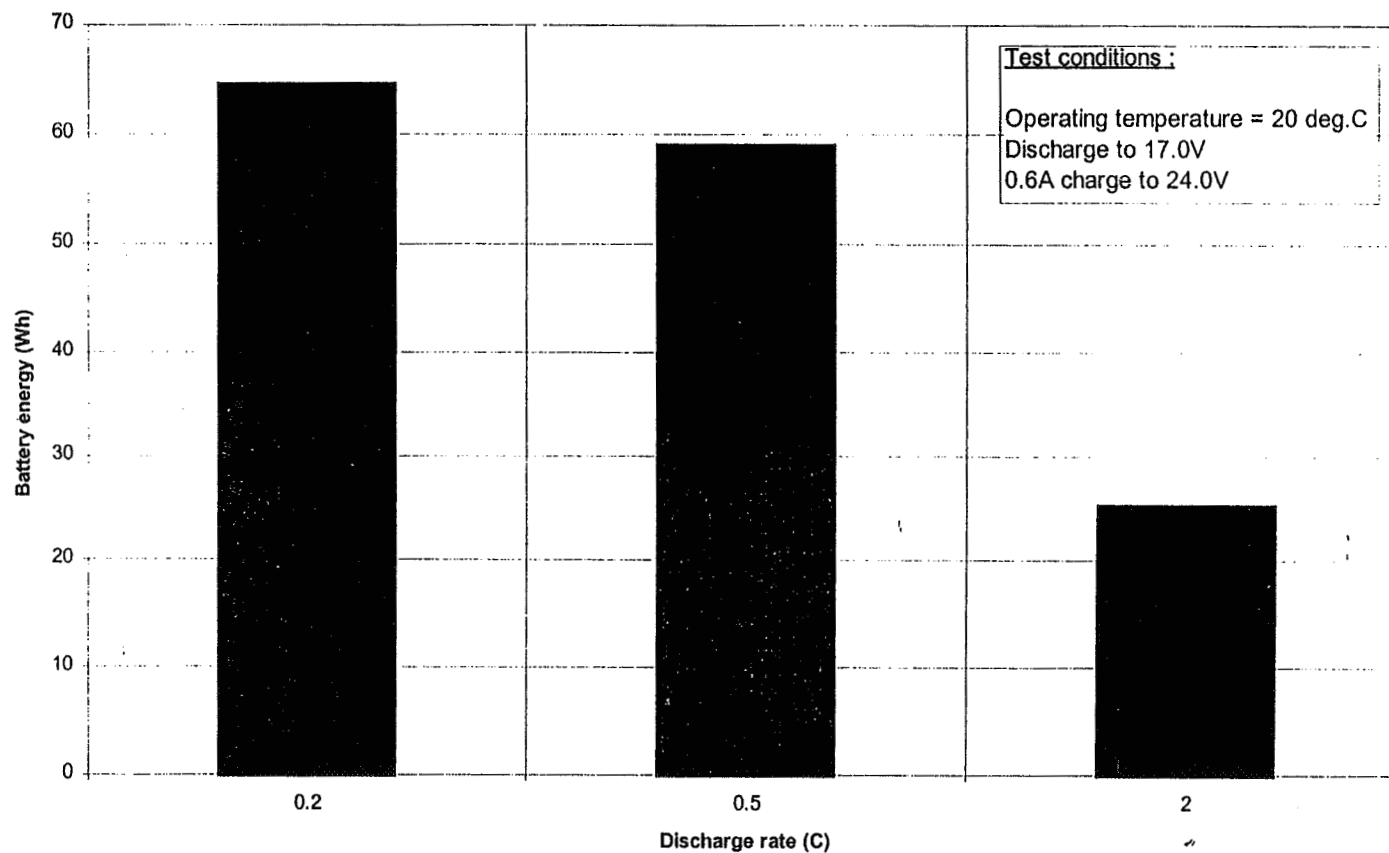
Li-ion battery physical parameters

- ◆ 12 x SONY 26650 cells, 2.7Ah nameplate capacity
 - ◆ Recommended cell operating values : $V_{eoc} = 4.2V$, $V_{eod} = 2.5V$
- ◆ Two battery modules in parallel, 6 series cells/pack
- ◆ Battery mass (total) : 1.74kg
 - ◆ 62.3Wh/kg (C/5 discharge, 100% DoD, 20°C)
- ◆ Battery volume (per module) : 183mm x 94mm x 31mm
 - ◆ 61.0Wh/l (C/5 discharge, 100% DoD, 20°C)

STRV-1d Li-ion battery module

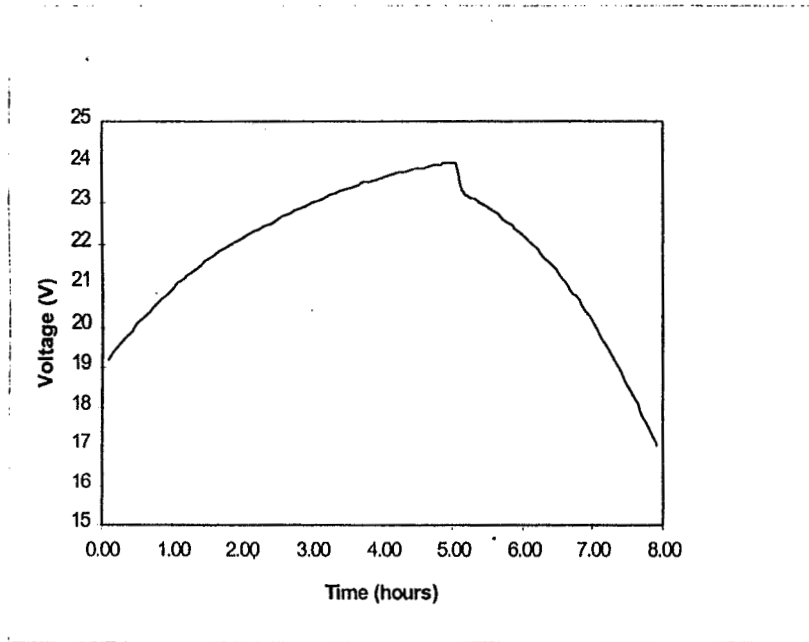


Discharge performance tests - delivered energy

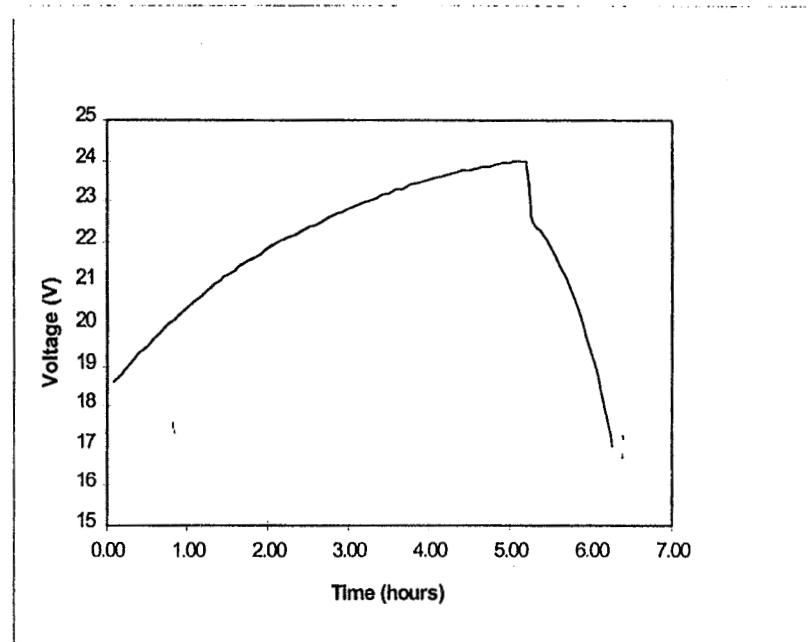


Discharge performance tests - battery voltages (1)

C/5 discharge

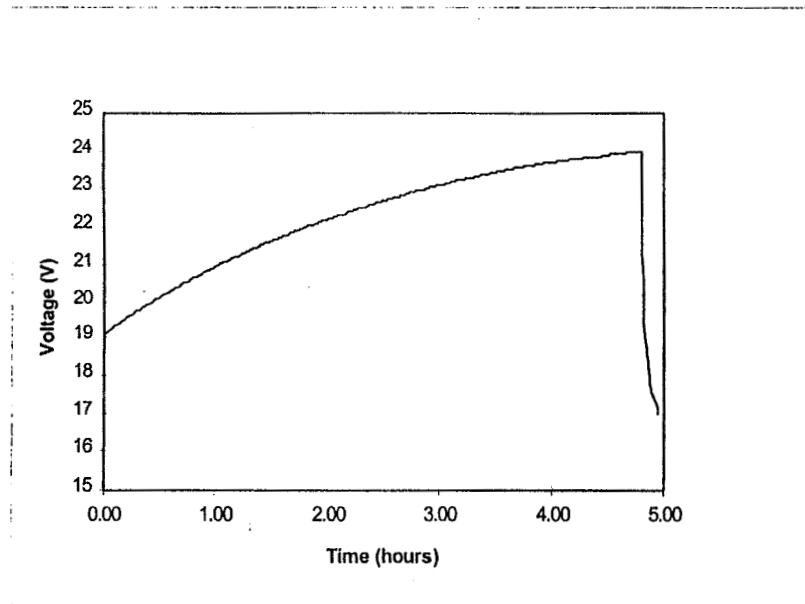


C/2 discharge

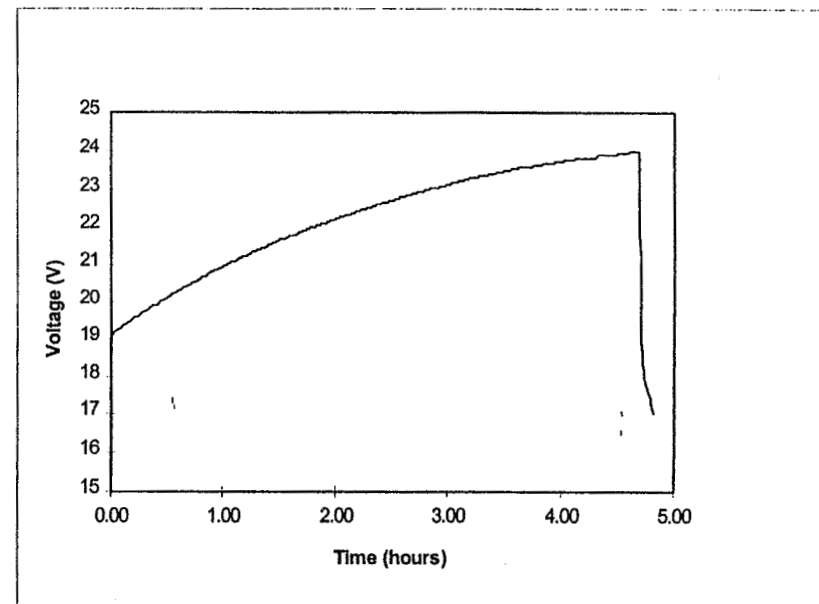


Discharge performance tests - battery voltages (2)

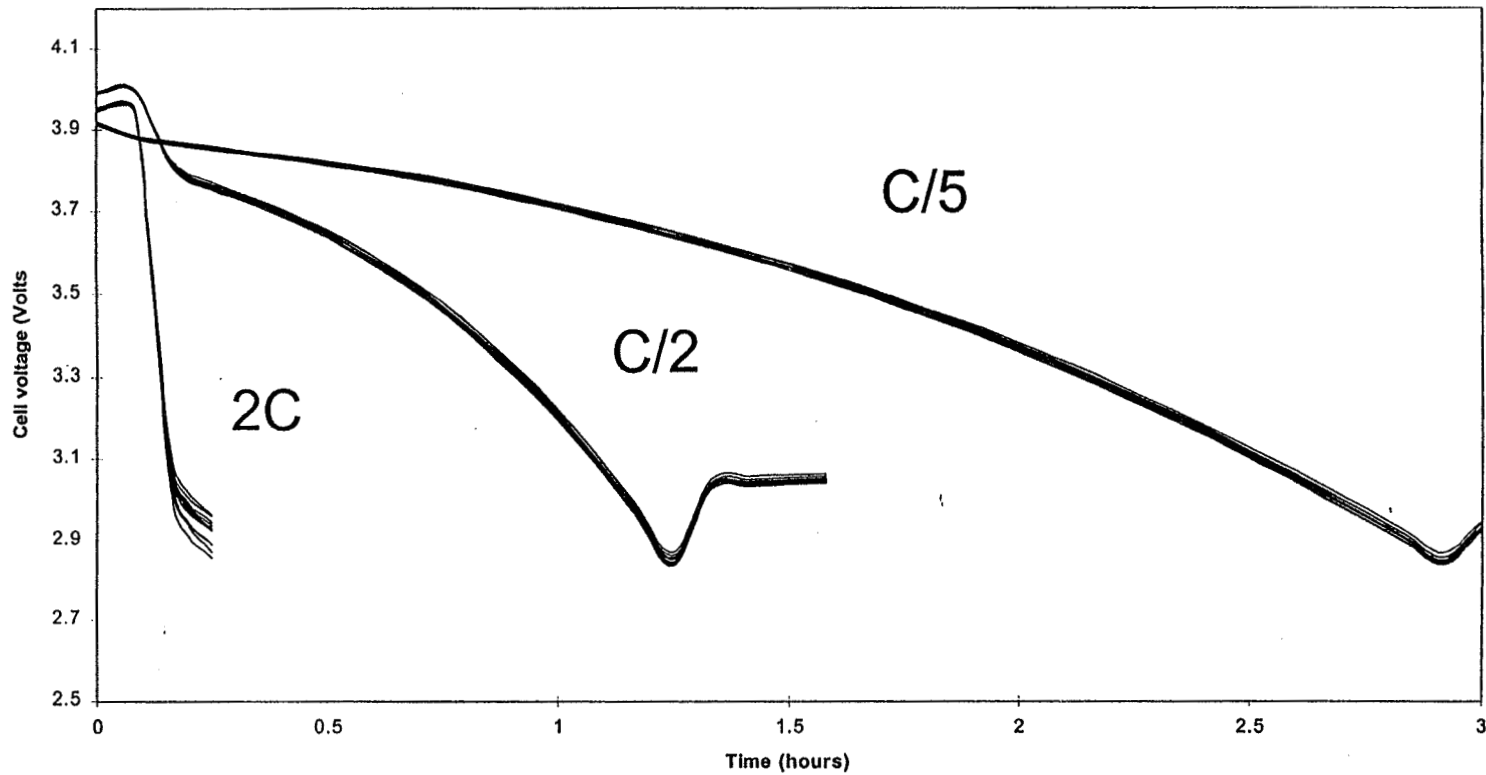
2C discharge - pack A



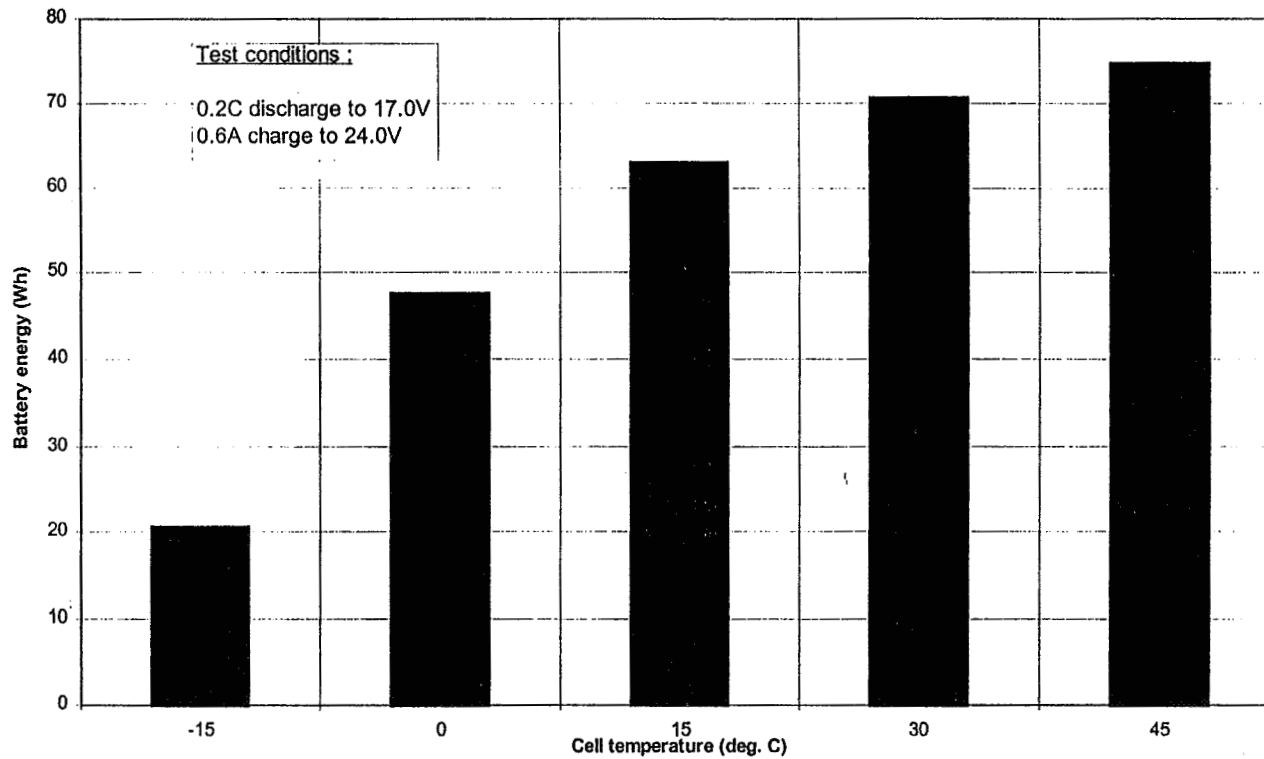
2C discharge - pack B



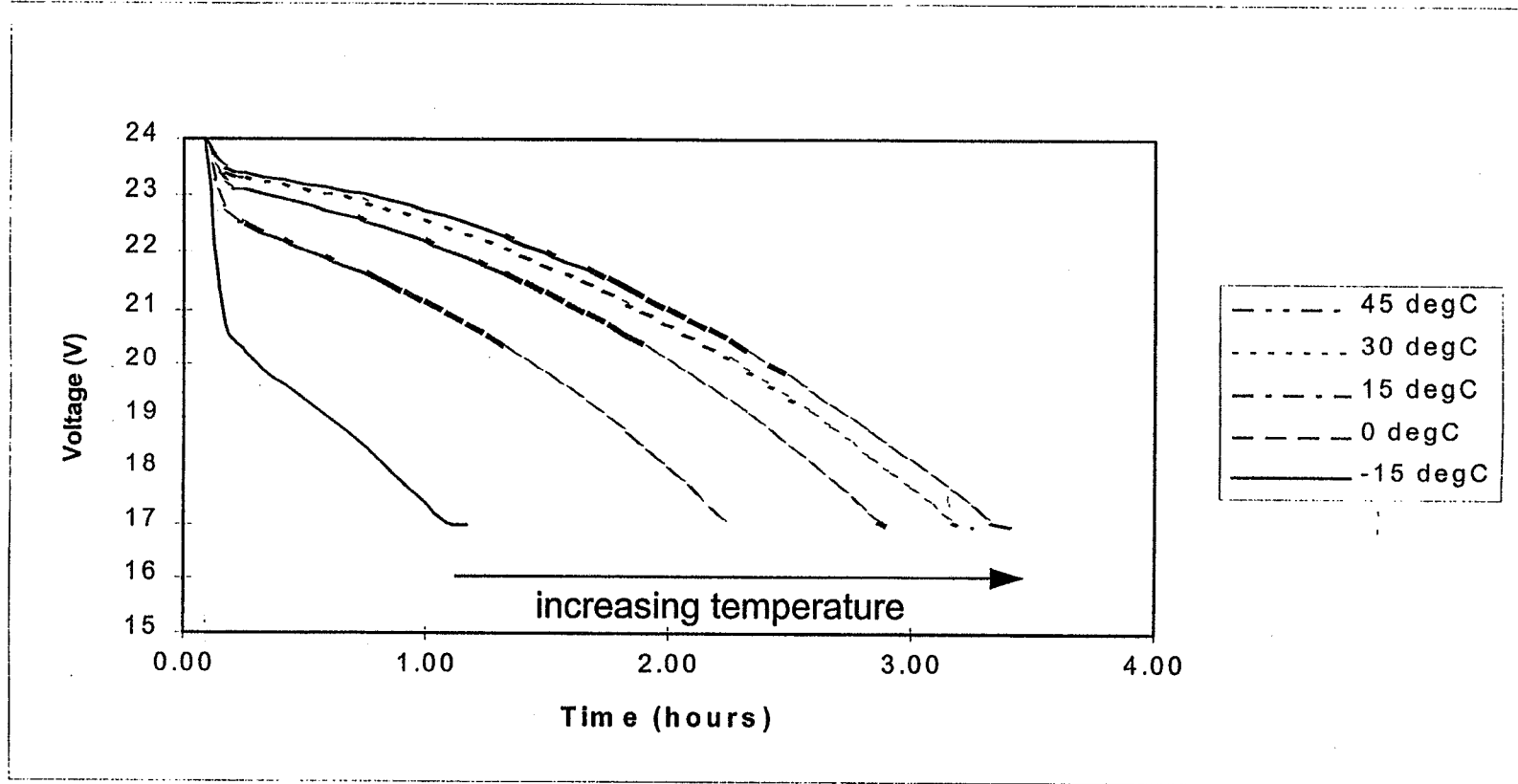
Discharge performance tests - Individual cell voltages during discharge



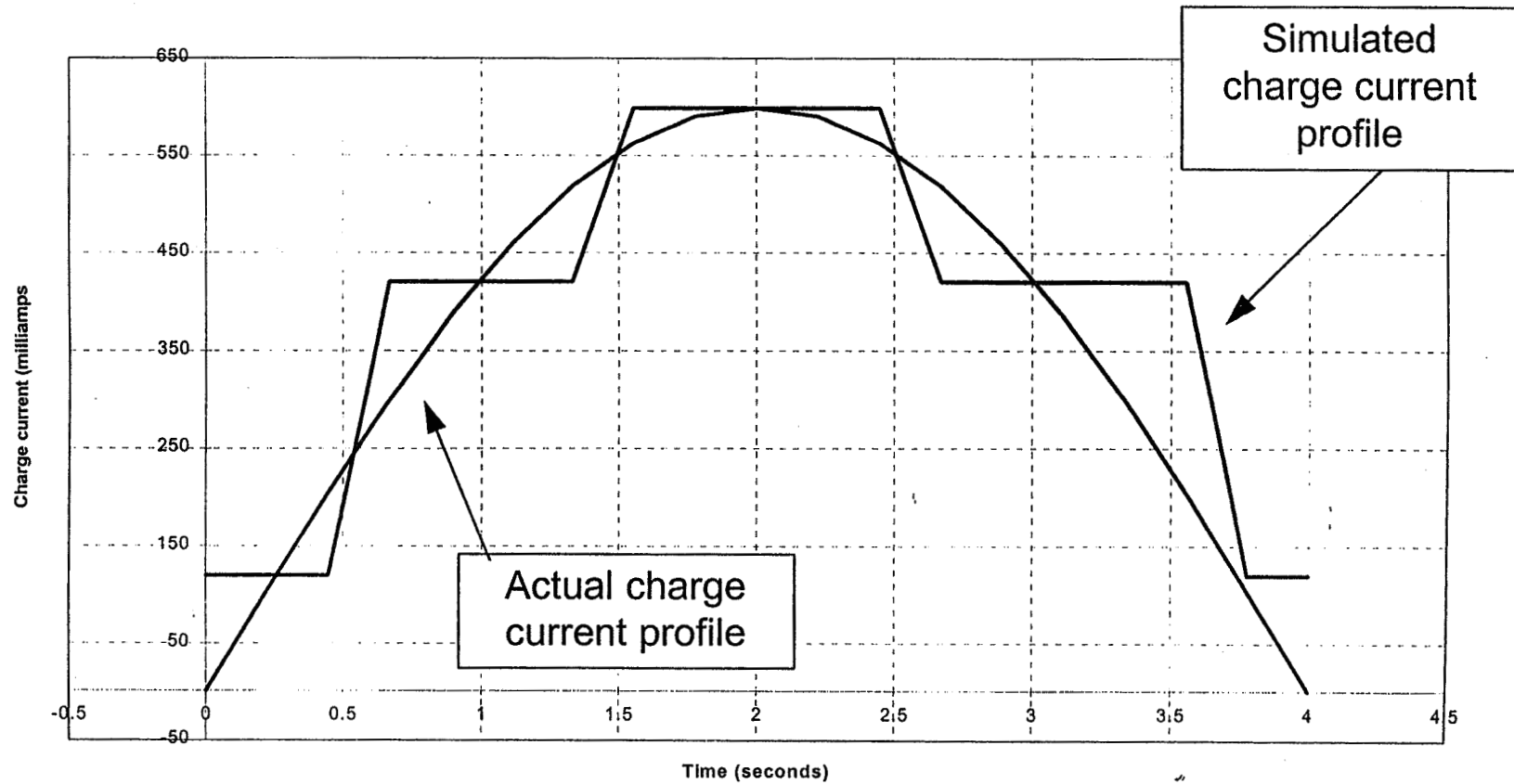
Temperature performance tests - delivered energy



Temperature performance tests - battery discharge voltage



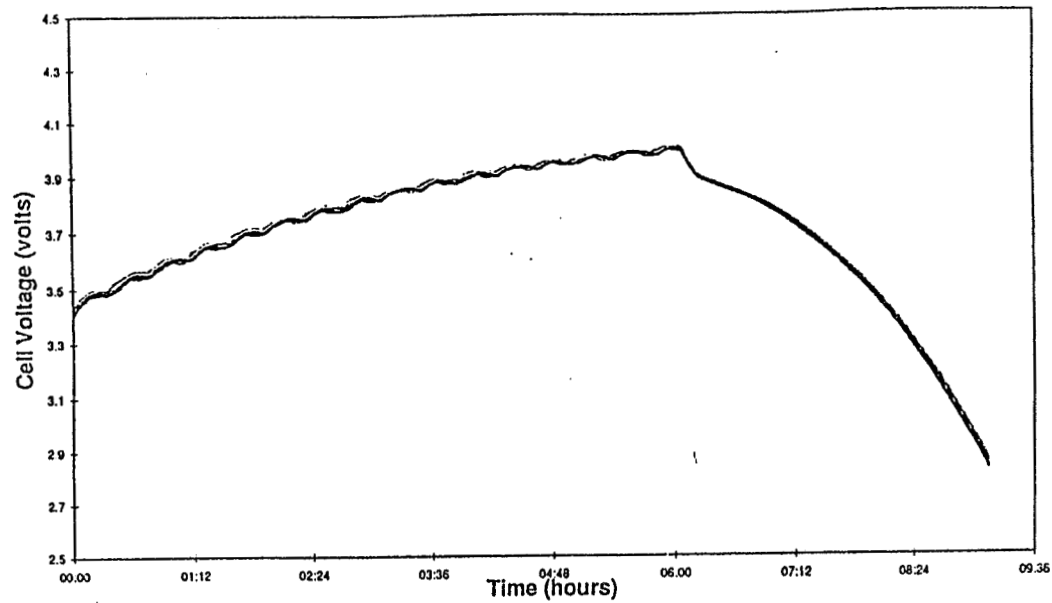
Sinusoidal charge current tests - current profiles



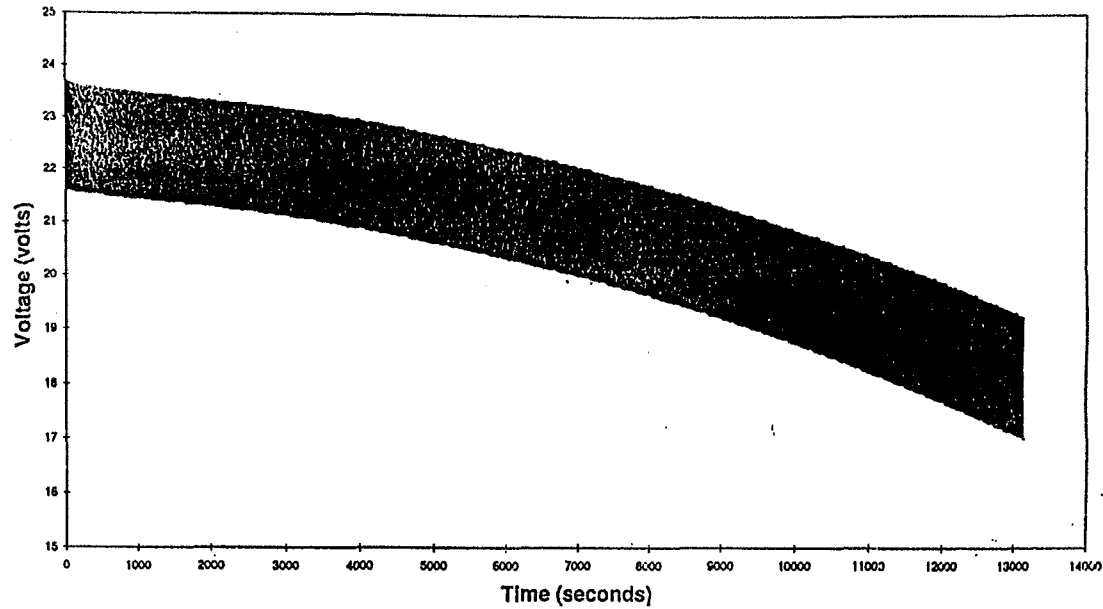
Sinusoidal charge current tests - energy delivered

Cycle	Battery delivered energy during discharge (Wh)
First sinusoidal charge	68.2
Second sinusoidal charge	68.3
Standard charge	66.6

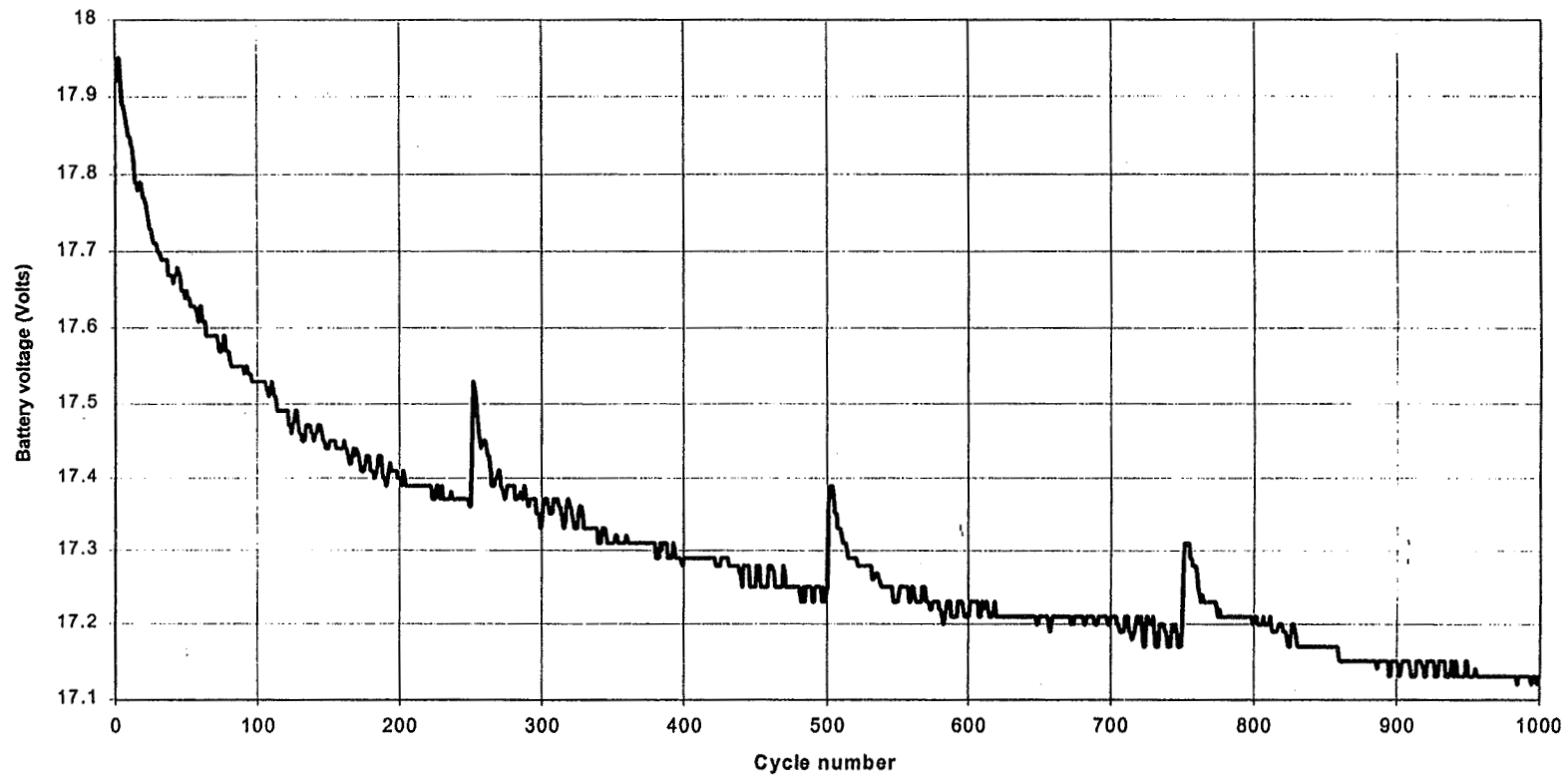
Sinusoidal charge current tests - battery voltages



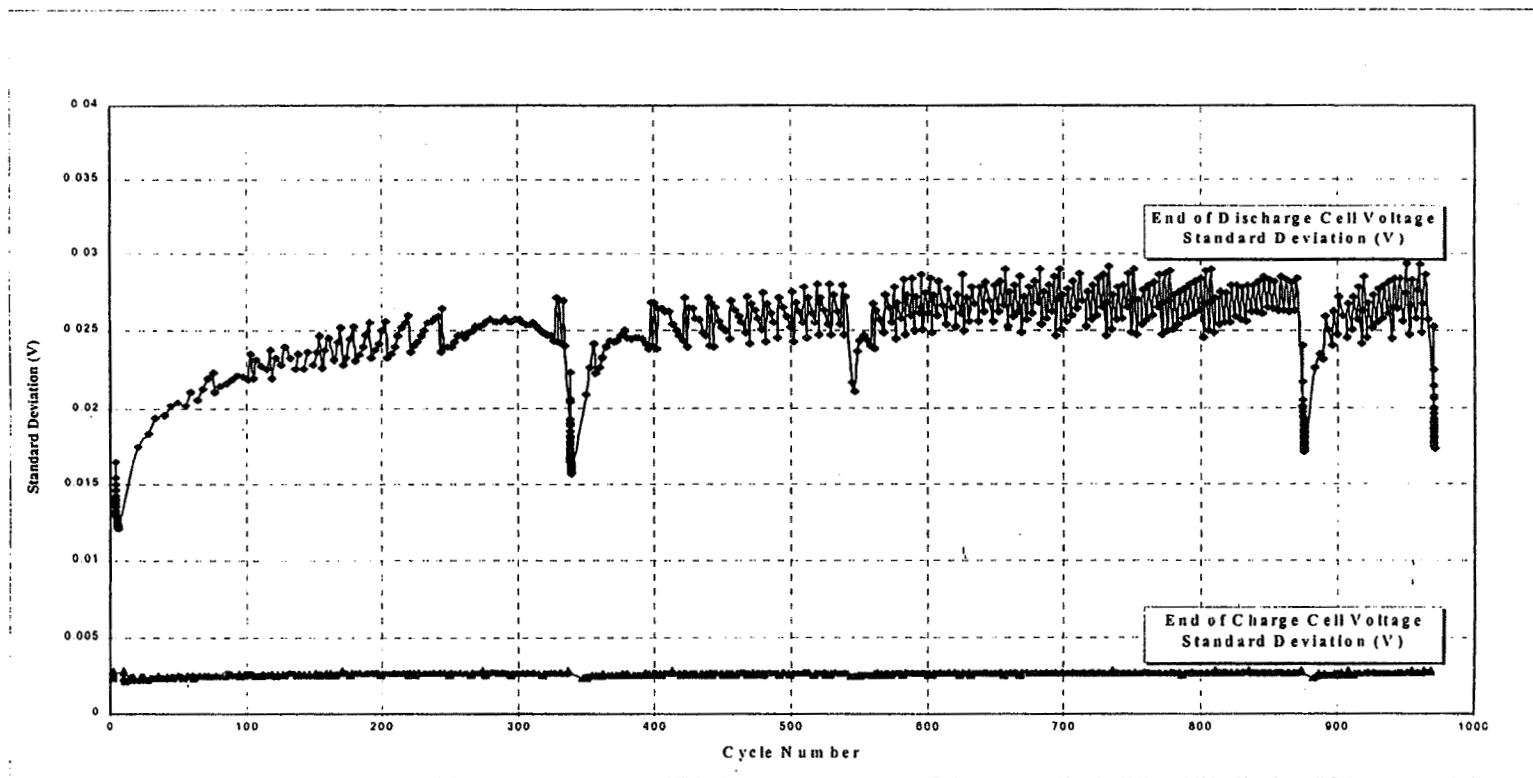
Pulse discharge performance tests - battery voltages



Life cycle test - battery voltages



Life cycle test - individual cell voltage spread



Test results summary

- ◆ Energy requirements met for C/5, C/2 rate, not for 2C rate
- ◆ Energy requirements met for $0^{\circ}\text{C} \leq T_{\text{batt}} \leq 45^{\circ}\text{C}$, not for -15°C
- ◆ No adverse affect of sinusoidal charge current profile on delivered energy
- ◆ > 1300 2C pulse discharges achieved
- ◆ 1000 cycles under life test conditions achieved
- ◆ Mass and volume requirements met except for x-axis dimension (acceptable in current spacecraft configuration)

Conclusions

- ◆ Required performance at 2C rate and -15°C can be met if V_{eod} operating limit reduced
 - ◆ $V_{eod} = 17.0V$ (2.83V/cell) is above manufacturer's limit of $V_{eod} = 15.0V$ (2.50V/cell)
- ◆ Pulse discharge and life performance meets STRV-1d requirements
 - ◆ life cycling to continue at new test facility, December 1997
- ◆ Capacity reduction vs. cycle life data still to be analysed
 - ◆ increasing recovery time result not yet explained

Acknowledgments

- ◆ Funding
 - ◆ British National Space Centre - ATS/3/3 programme
 - ◆ AEA Technology
- ◆ Engineering team (AEA Technology - Space and Defence Systems Group)
 - ◆ Mike Cooke (electrical design/ test programme manager)
 - ◆ Charlie McCarthy (mechanical design / modeling)
 - ◆ Carl Thwaite (test data analysis)

Page intentionally left blank

Rate Capability Analysis of Li-ion Cells

**Esther Sans Takeuchi and
Randolph A. Leising**

*Wilson Greatbatch Ltd.
10,000 Wehrle Drive, Clarence NY 14031*



Outline

Introduction

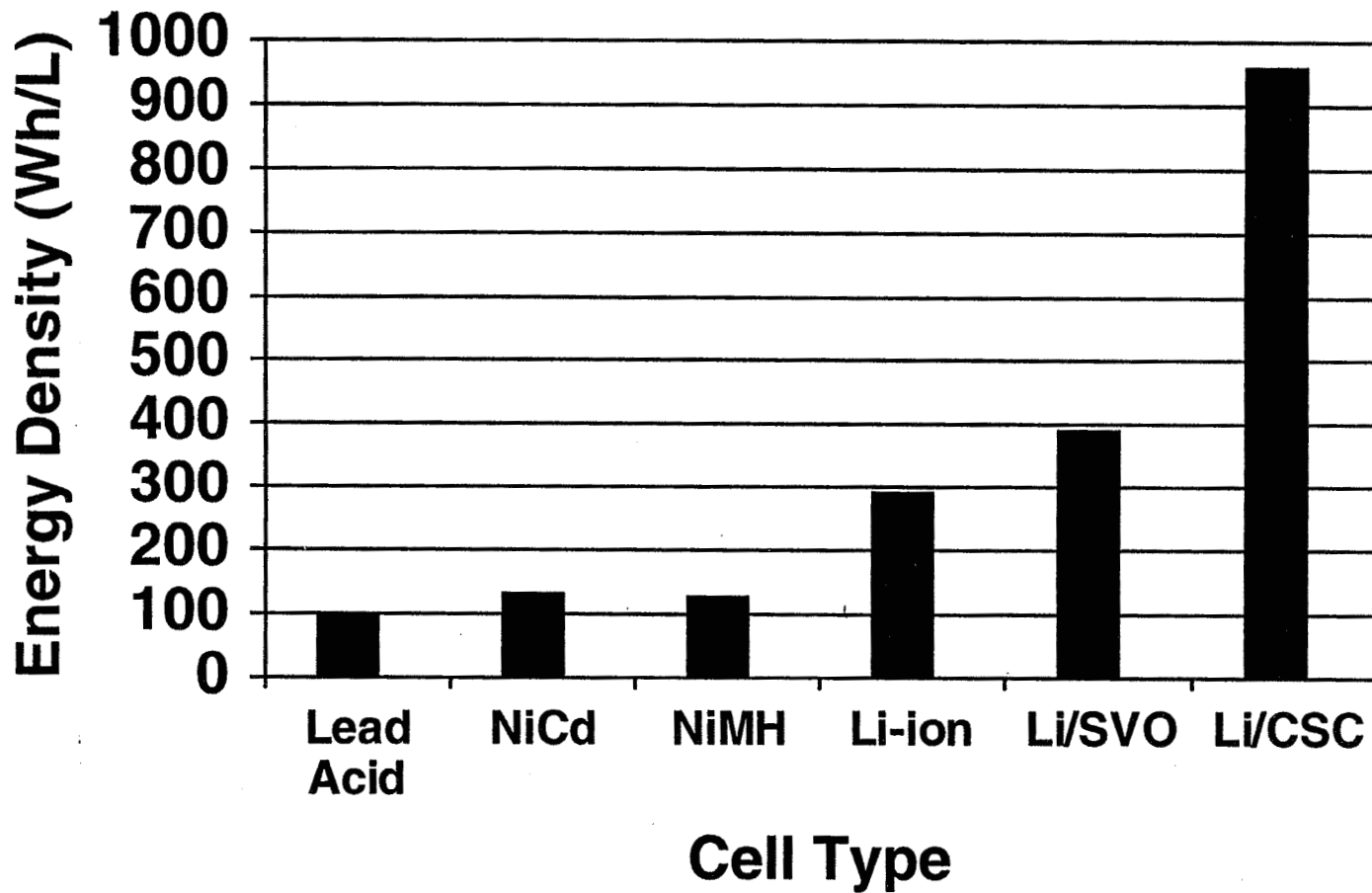
Results

- Specifications for WGL Li-ion Cells
- Safety Test Results
- Cycle Test Results
- High Rate Testing
 - Continuous Discharge
 - Pulse Testing

Summary



Energy Density Comparison for Primary and Secondary Batteries



WGL Li-ion Specifications

Energy Density

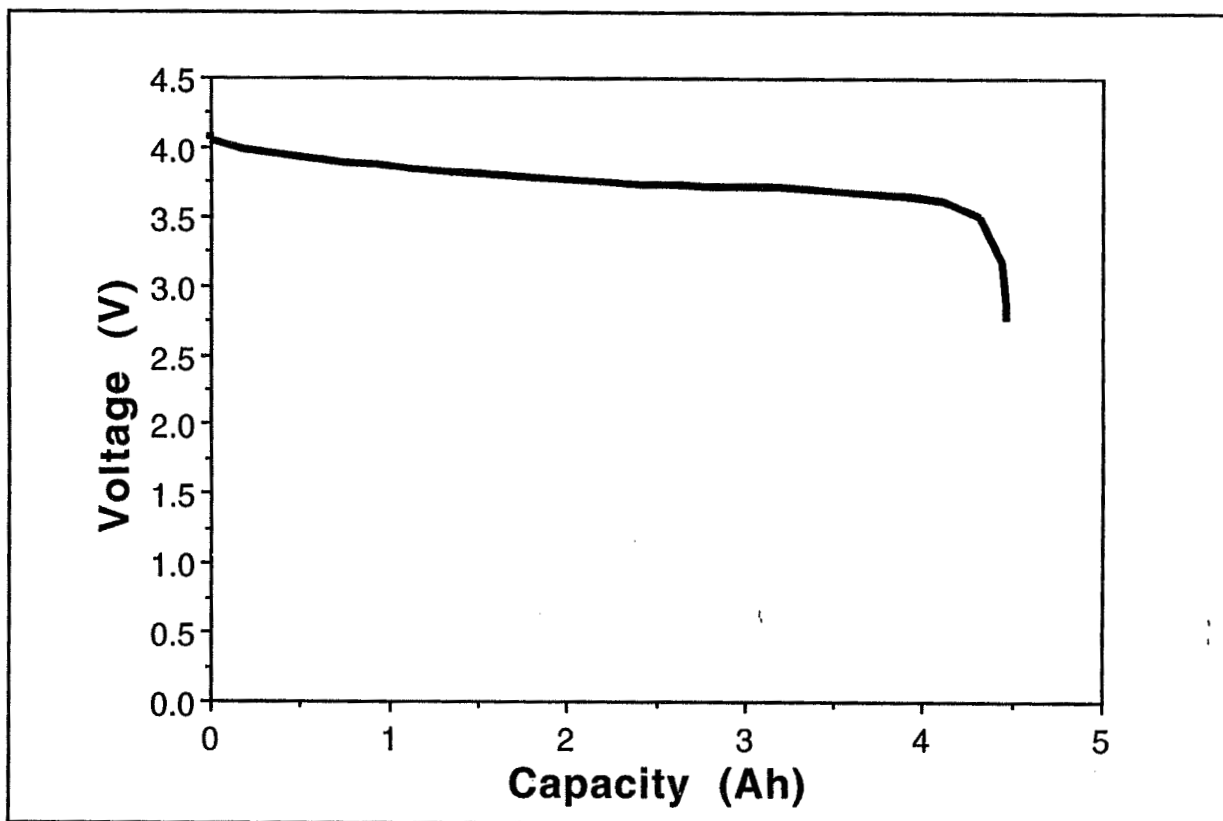
	Cell Size			
	AA	1/2C	C	D
Weight (g)	19	38	62	142
Volume (cc)	7.2	14.8	24.9	53.7
Capacity (Ah)	0.55	0.75	1.95	4.40
Wh/kg	107	73	116	115
Wh/L	283	188	290	303



WGL Li-ion Specifications

Voltage Profile

WGL D-Size Li-ion (750 mA Discharge)



WGL Li-ion Safety & Abuse Testing

- Short circuit testing (BOL) - no vent
- Short circuit testing after extended cycling - no vent
- Force overcharge testing - no vent
- Force overdischarge testing - no vent
- Shock test - no vent
- Max current/max temp - no vent
- Initiated DOT crush test - passed test



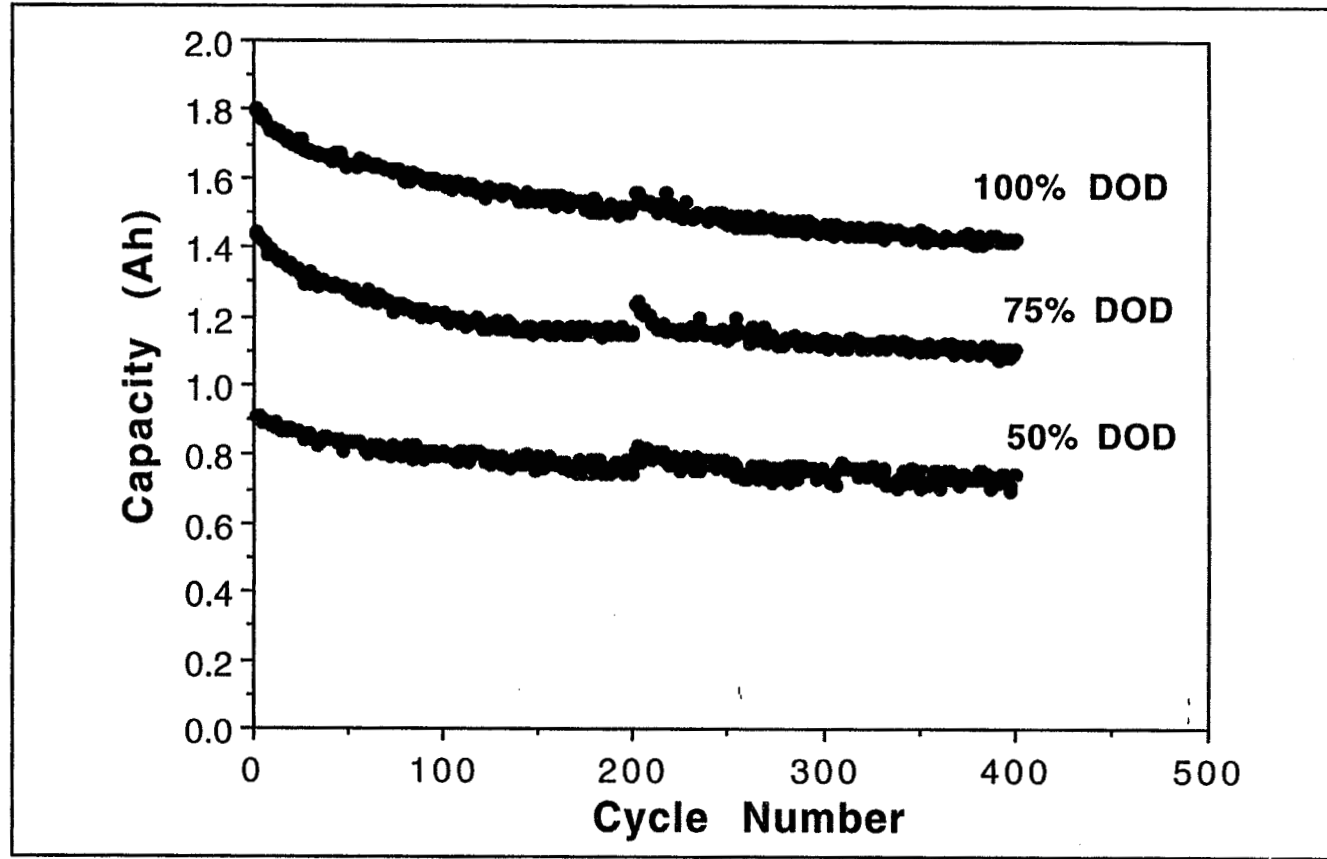
WGL Li-ion Performance Testing

- Cycle testing (25°C, 37°C, 50°C)
- High cycle number testing (%DOD)
- Rate capability (continuous discharge)
- High rate pulse discharge
- Storage/self discharge characterization



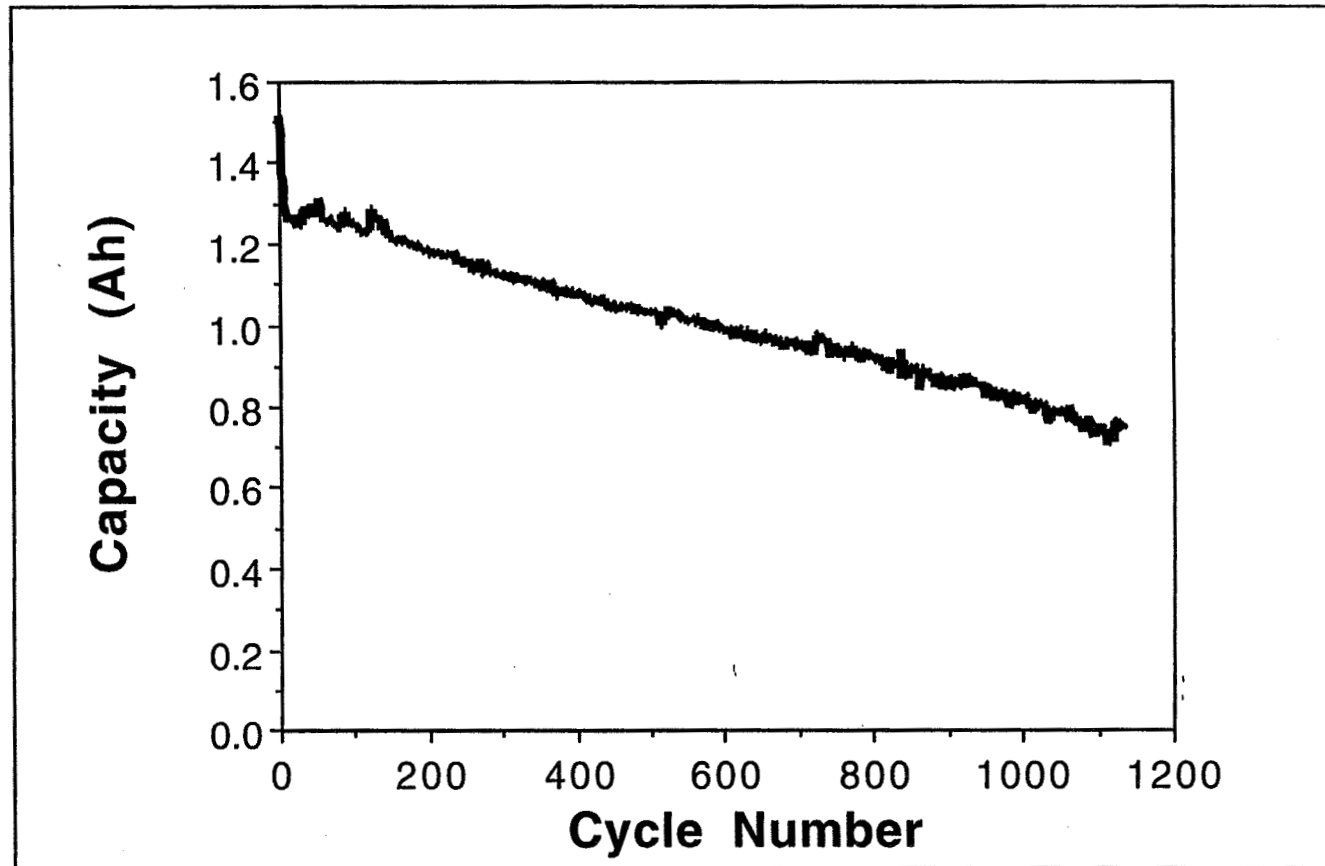
WGL Li-ion Cell Performance

WGL C-Size Li-ion (750 mA Discharge)



WGL Li-ion Cell Performance

WGL C-Size Li-ion (1.0 A Discharge)



Li-ion Rate Capability Testing

Accelerated Rate Test Procedure

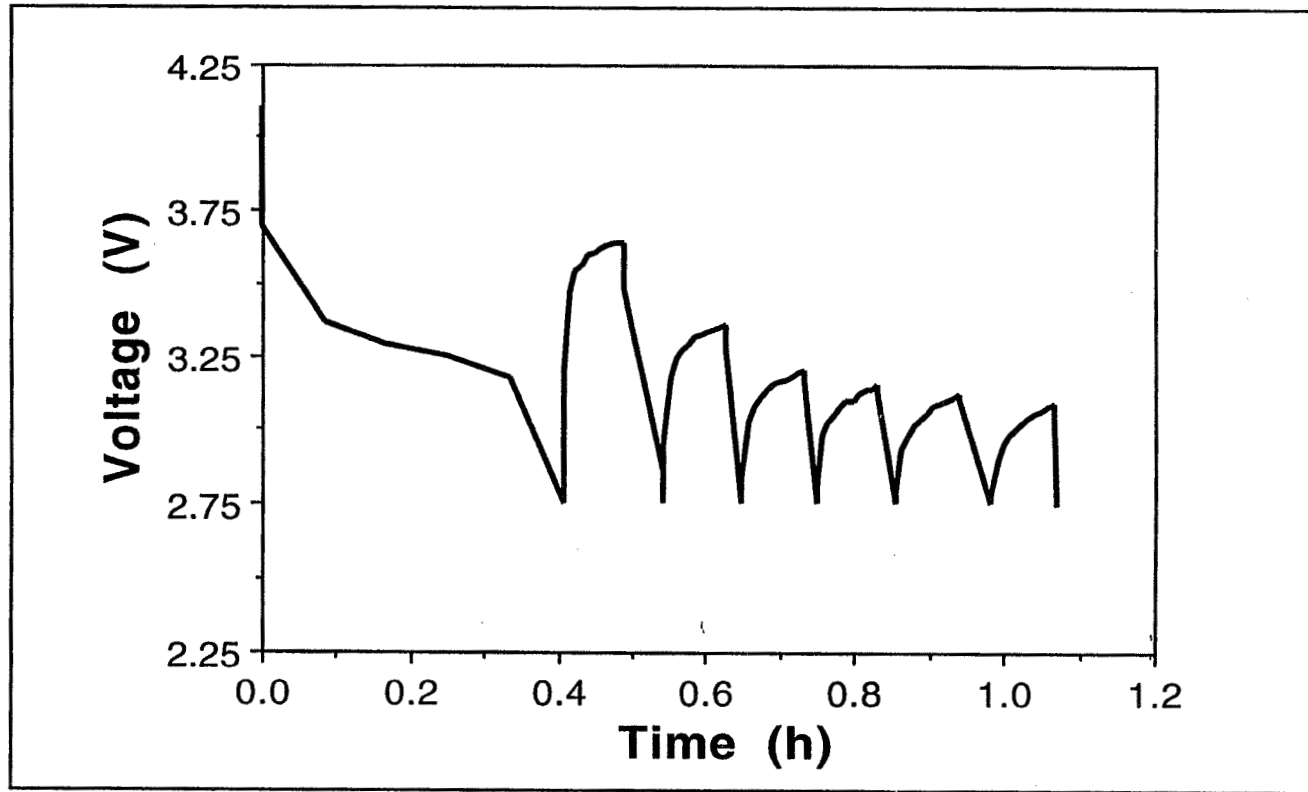
- Fully charge cell to +4.1 V
- Discharge cell at current densities of 8, 4, 2, 1, 0.5, 0.25 and 0.125 mA/cm² to +2.75 V without charge steps between discharge steps
- Allow cell to rest for 5 min between discharge steps

Doyle, M.; Newman, J.; Reimers, J. J. *Power Sources*, **1994**, 52, 211-216.



Li-ion Rate Capability Testing

Accelerated Discharge Rate Test Procedure
WGL C-Cell (8, 4, 2, 1, 0.5, 0.25, 0.125 mA/cm²)



Li-ion Rate Capability Testing

WGL C-Size Li-ion Accelerated Rate Data

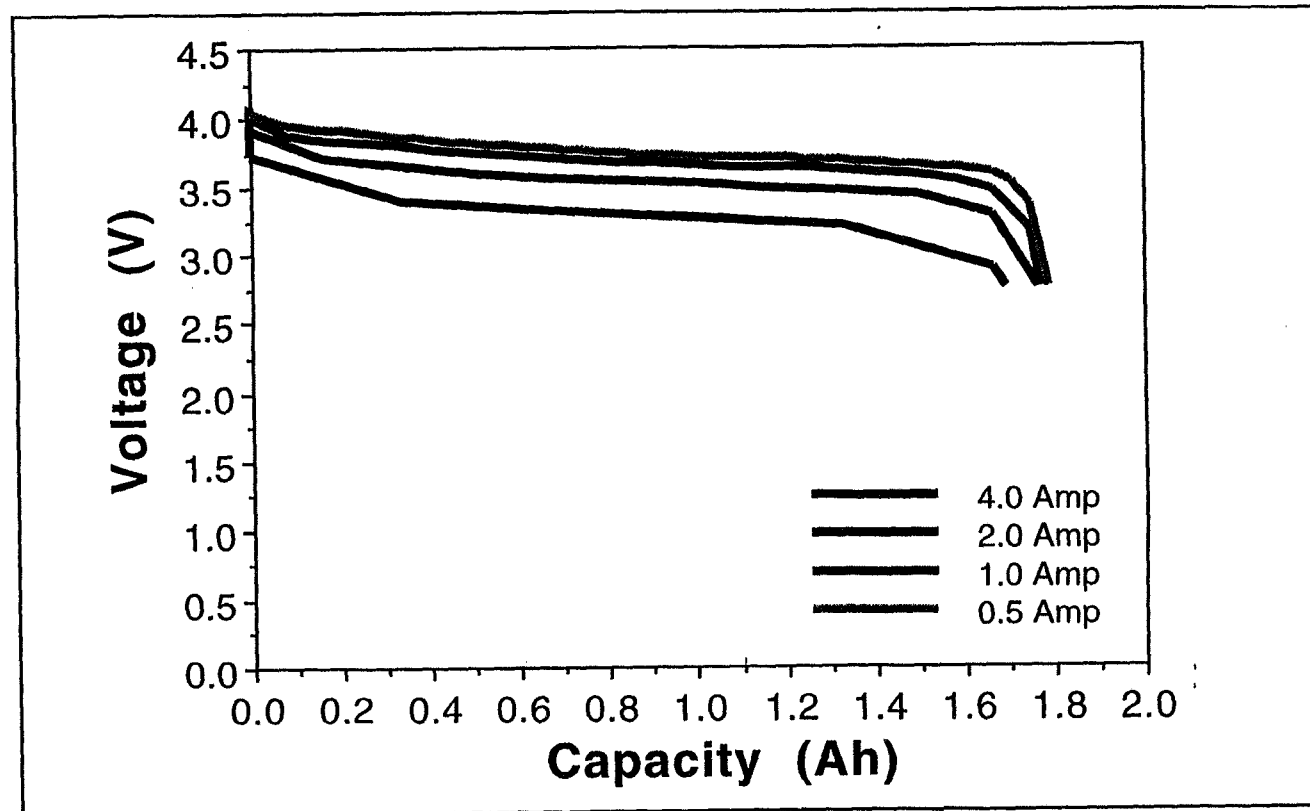
Discharge Current	Current Density	Capacity (% of Total)
----------------------	--------------------	-----------------------

4.0 A	8 mA/cm ²	1.62 Ah (92%)
2.0 A	4 mA/cm ²	1.72 Ah (98%)
1.0 A	2 mA/cm ²	1.74 Ah (99%)
0.5 A	1 mA/cm ²	1.76 Ah (99.2%)
0.25 A	0.5 mA/cm ²	1.76 Ah (99.5%)
0.125 A	0.25 mA/cm ²	1.76 Ah (99.9%)
0.062 A	0.125 mA/cm ²	1.76 Ah (100%)



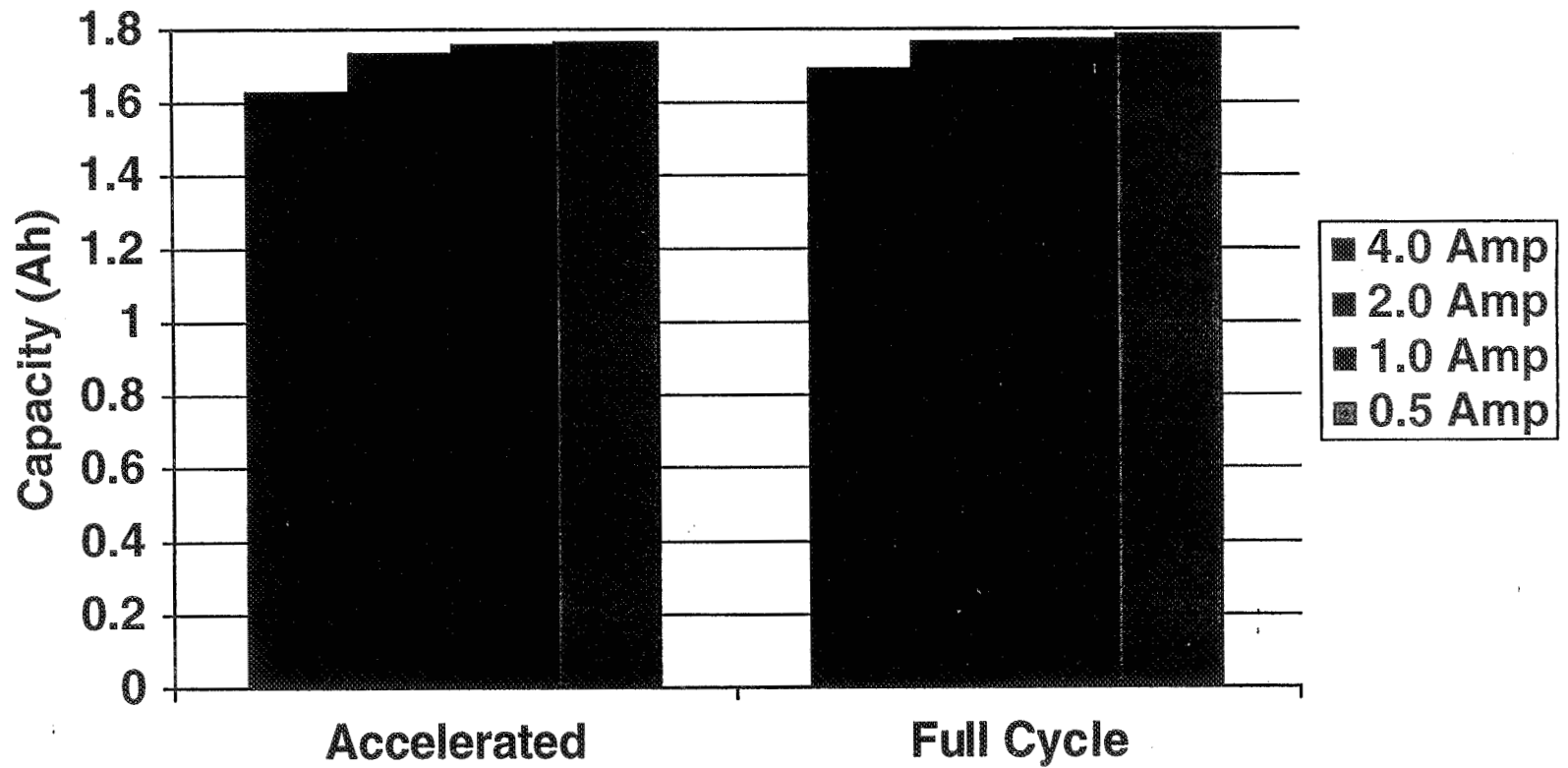
Li-ion Rate Capability Testing

WGL C-Cell Discharge Rate Test



Li-ion Rate Capability Testing

WGL C-Cell Discharge Rate Test Comparison



Li-ion Rate Capability Testing

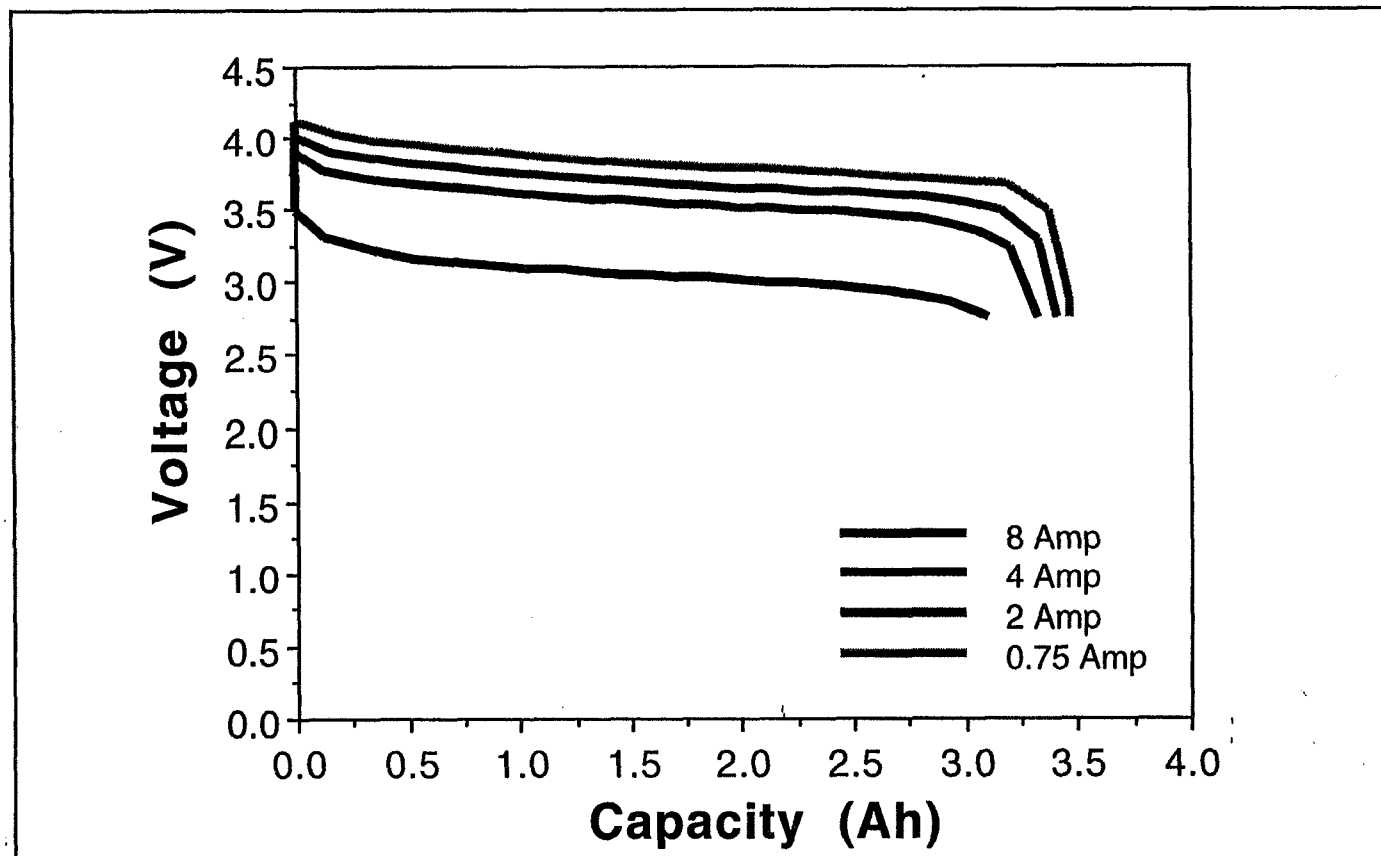
WGL D-Size Li-ion Accelerated Rate Data

Discharge Current	Current Density	Capacity (% of Total)
8.0 A	8 mA/cm ²	4.15 Ah (92%)
4.0 A	4 mA/cm ²	4.40 Ah (98%)
2.0 A	2 mA/cm ²	4.45 Ah (99%)
1.0 A	1 mA/cm ²	4.48 Ah (99%)
0.5 A	0.5 mA/cm ²	4.50 Ah (99%)
0.25 A	0.25 mA/cm ²	4.51 Ah (100%)



Li-ion Rate Capability Testing

WGL D-Cell Discharge Rate Test



Li-ion Rate Capability Testing

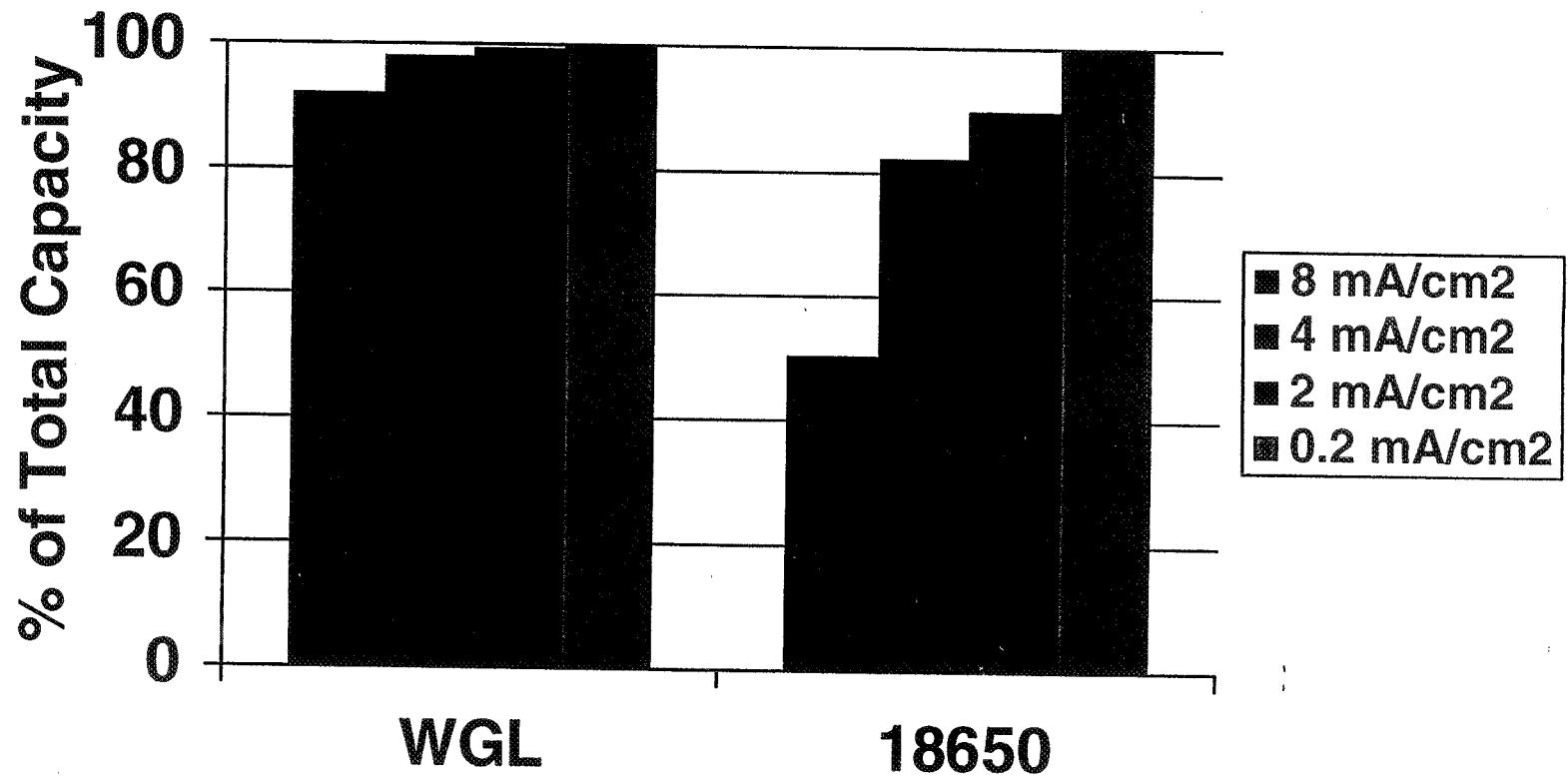
WGL D-Size Accelerated Charge Rate Data

Charge Current	Current Density	Capacity (% of Total)
4.0 A	4 mA/cm ²	0.49 Ah (11%)
2.0 A	2 mA/cm ²	3.09 Ah (70%)
1.0 A	1 mA/cm ²	3.72 Ah (84%)
0.5 A	0.5 mA/cm ²	4.08 Ah (92%)
0.25 A	0.25 mA/cm ²	4.35 Ah (98%)
0.125 A	0.125 mA/cm ²	4.43 Ah (100%)



Li-ion Rate Capability Testing

WGL C-Cell vs Commercially Available Li-ion 18650



Li-ion High Rate Pulse Testing

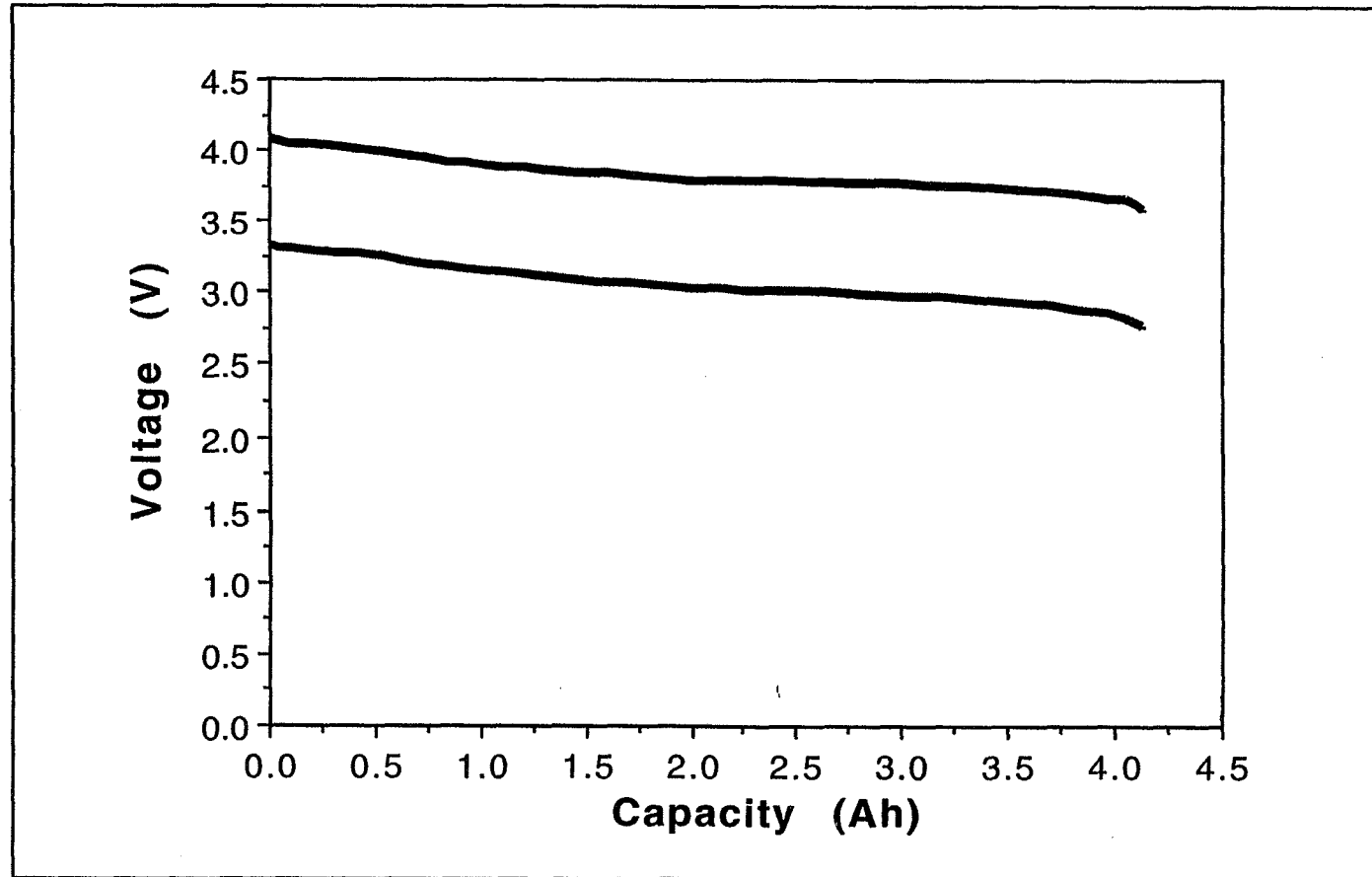
WGL C and D-Size Li-ion Cells

Cell	Voltage at 50% DOD		
	Prepulse V	Pulse V	RDC
C-Size	3.81	3.42	0.10
D-Size	3.81	3.04	0.10



Li-ion High Rate Pulse Testing

WGL D-Size Li-ion (10 Amp/2 sec Pulses)



Summary

- WGL has developed cylindrical, hermetically-sealed Li-ion batteries in the AA, 1/2C, C & D sizes
- WGL Li-ion cells display high cycle life under a variety of test regimes
- An accelerated rate test was used to evaluate the rate capability of Li-ion cells
- WGL Li-ion cells provide high rate capability compared to commercially available Li-ion cells



Page intentionally left blank

Nickel-Hydrogen Session

Page intentionally left blank



MARS PATHFINDER BATTERY PERFORMANCE

**B. OTZINGER, D. PERRONE, S. DAWSON, T. VALDEZ
S. SURAMPUDI , R. EWELL, M. SHIRBACHEH,**

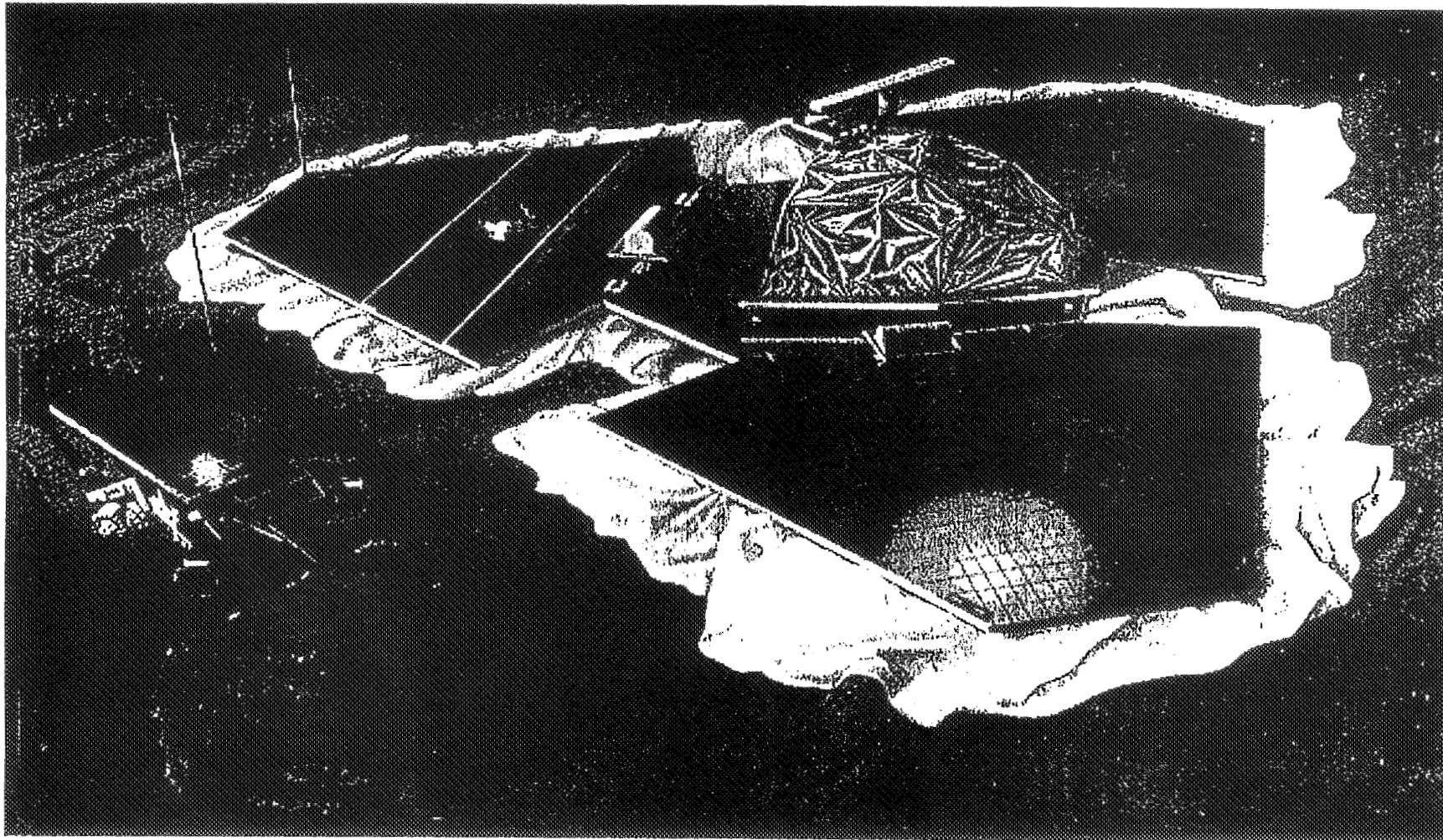
**NASA BATTERY WORKSHOP
HUNTSVILLE, ALABAMA
NOVEMBER 18-20, 1997**

OUTLINE

- **MISSION REQUIREMENTS**
- **BATTERY DESIGN FEATURES**
- **BATTERY OPERATIONAL OVERVIEW**
- **BATTERY PERFORMANCE**
 - **PRELAUNCH**
 - **CRUISE**
 - **EDL**
 - **MARS OPERATIONS**
- **SUMMARY AND CONCLUSIONS**



MARS PATHFINDER LANDER



1997 NASA Aerospace Battery Workshop

-391-

Nickel-Hydrogen Session

ELECTROCHEMICAL TECHNOLOGIES GROUP

MPF Ag-Zn BATTERY



MPF BATTERY SPECIFICATIONS

- **VOLTAGE** 27 V
- **CAPACITY** 40 Ah
- **RATE CAPABILITY** 1-5 A
- **PULSE CAPABILITY** 40 A FOR 40 MSEC
- **CYCLE LIFE** 40
- **WET LIFE** 14 MONTHS
- **WEIGHT** 15 KG
- **DIMENSIONS** 9.8" x 7.4" x 7.4"

KEY CELL DESIGN FEATURES

- **Robust separator system - 5 layers of cellophane and 2 layers of polymer membrane.**
To achieve long calendar and cycle life
- **Triple redundant case-to-cover seal including basic ultrasonic seal.**
To prevent electrolyte leakage
To improve safety
- **Large cell plate area - approximately 200 square inches.**
Low temperature operation
For enhanced pyro-firing
- **Unique leak-free cell vent valves.**
For inverted battery operation
allow gas venting under off-limit operation
- **Minimal free electrolyte**
For inverted battery operation

KEY BATTERY DESIGN & PROCESS FEATURES

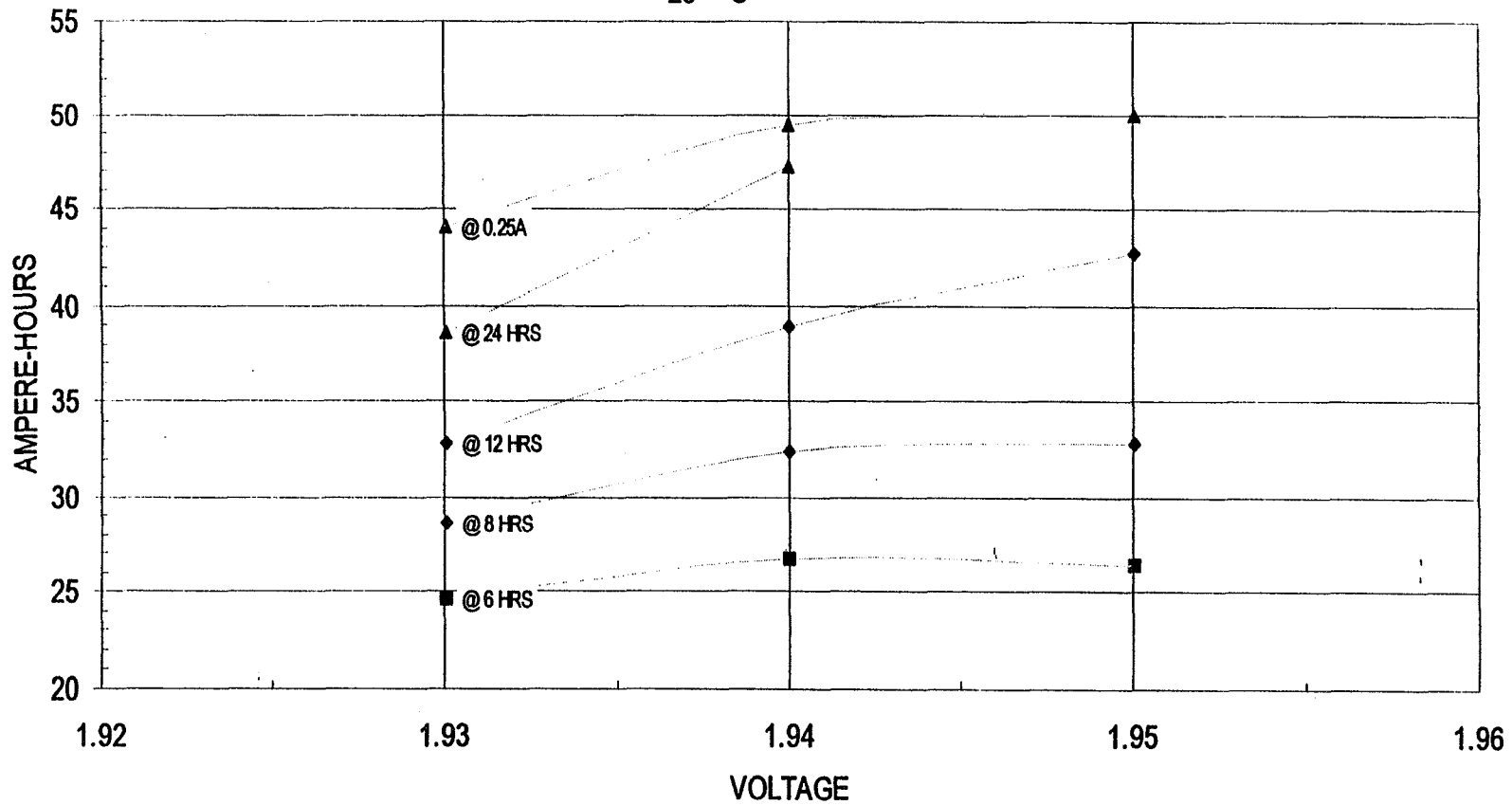
- **Titanium fabricated battery case with sealable cover and gasket.**
Light weight construction
gas and electrolyte containment
- **Battery vent valve and pressurization port.**
Redundant valve to protect cells from electrolyte loss
- **Battery heater and two temperature sensors.**
Thermal management for charge control
- **Over-pot of cells, surface conformal coating, connector back side potting and electrolyte absorption system.**
Prevent ionic conductive paths
Improve safety
- **Cell Matching and selection**
Extend cycle life

KEY BATTERY OPERATING STRATEGIES

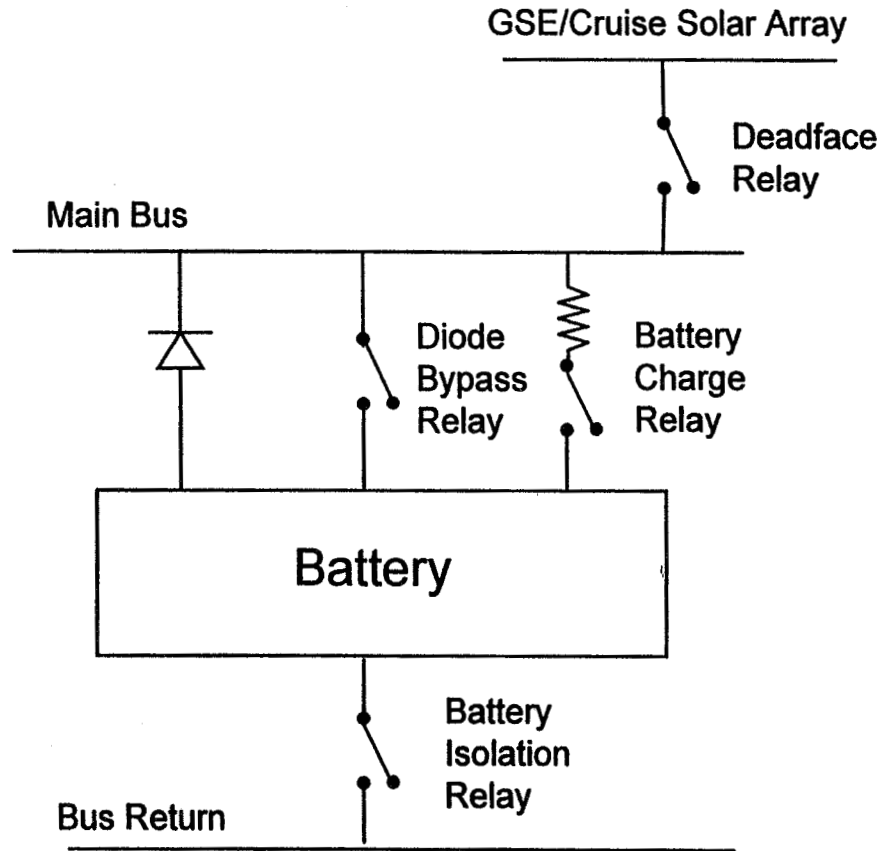
- **Battery was mounted inverted and maintained at 12 C during pre-launch and launch Phases**
- **Battery was partially discharged to 80% SOC and on open circuit stand, at -5 to 0 degrees C, during 7 Month cruise period.**
- **Battery was charged at end of cruise through 1.2 Ohm resistor to 0.2 A cut-off and 1.95 V / cell Ave.**
- **Battery was heated to 15 to 20 degrees C prior to all charges.**
- **Battery was charged during Mars operations without resistor to a selective shunt limiter controlled maximum voltage. Six voltage settings were available with 1.95 V / cell Ave., the nominal full charge selection.**
- **Battery was taper charged to a constant shunt limiter voltage, 1.95 V / cell Ave.. well below the 2 V. limit employed in constant current charging with same full charge result.**

BATTERY CAPACITY VS CHARGE VOLTAGE

MARS PATHFINDER -- 16 BST Ag-Zn CELLS WITH 2+5 SEPARATOR SYSTEM
CONSTANT VOLTAGE CHARGE CHARACTERISTIC FOR NEW CELLS WITH 4.5 AMPERE INRUSH AT
25 °C

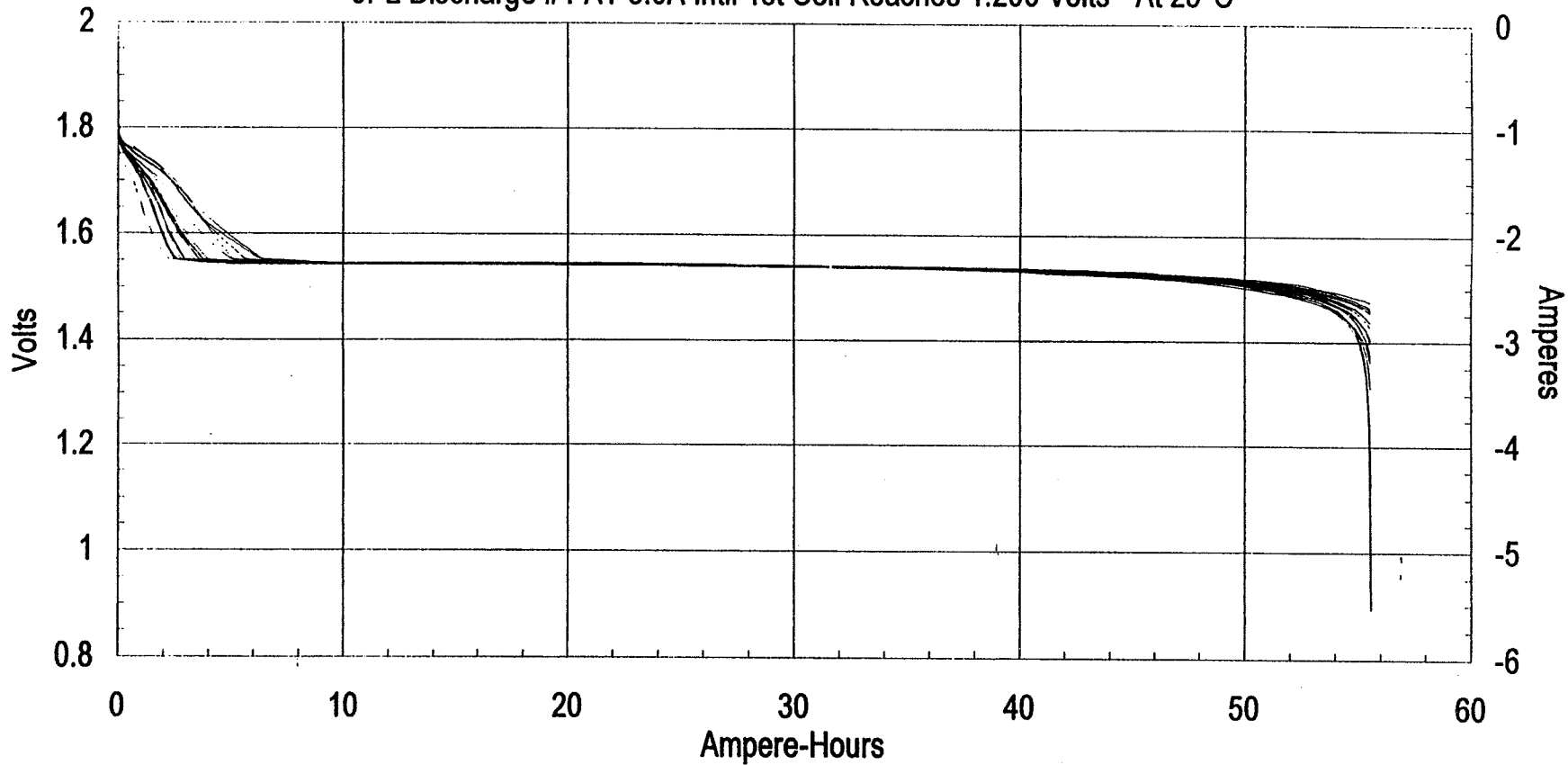


MARS Pathfinder Power System Configuration Relays



MPF BATTERY PRELAUNCH DISCHARGE

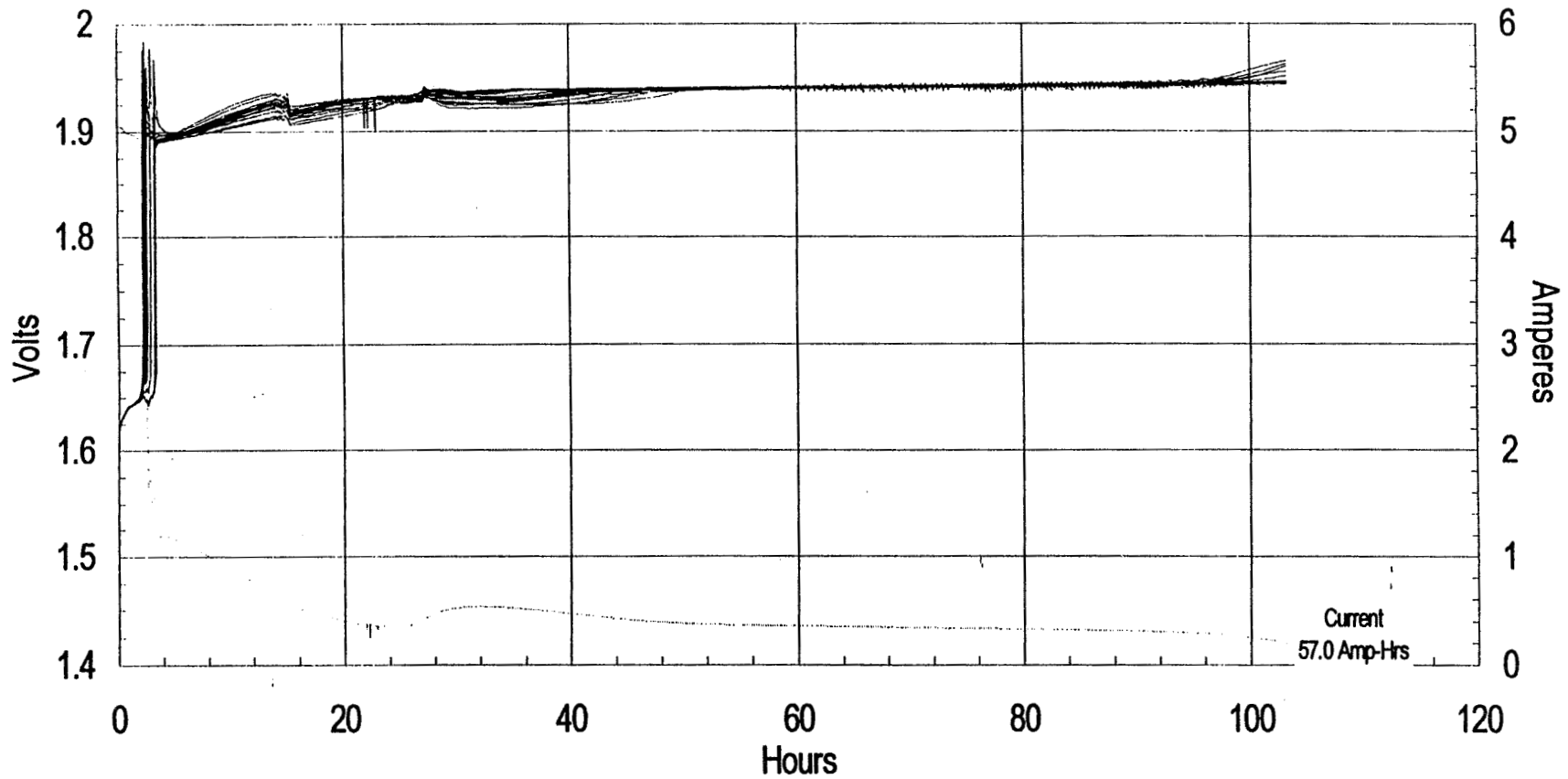
Mars Pathfinder -- BST 18 Cell 40 Ampere-Hour, Ag-Zn, Flight Battery
JPL Discharge #1 AT 3.0A Intil 1st Cell Reaches 1.200 Volts - At 25°C



MPF BATTERY PRELAUNCH CHARGE

Mars Pathfinder -- BST 18 Cell, 40 Ampere-Hour, Ag-Zn, Flight Battery

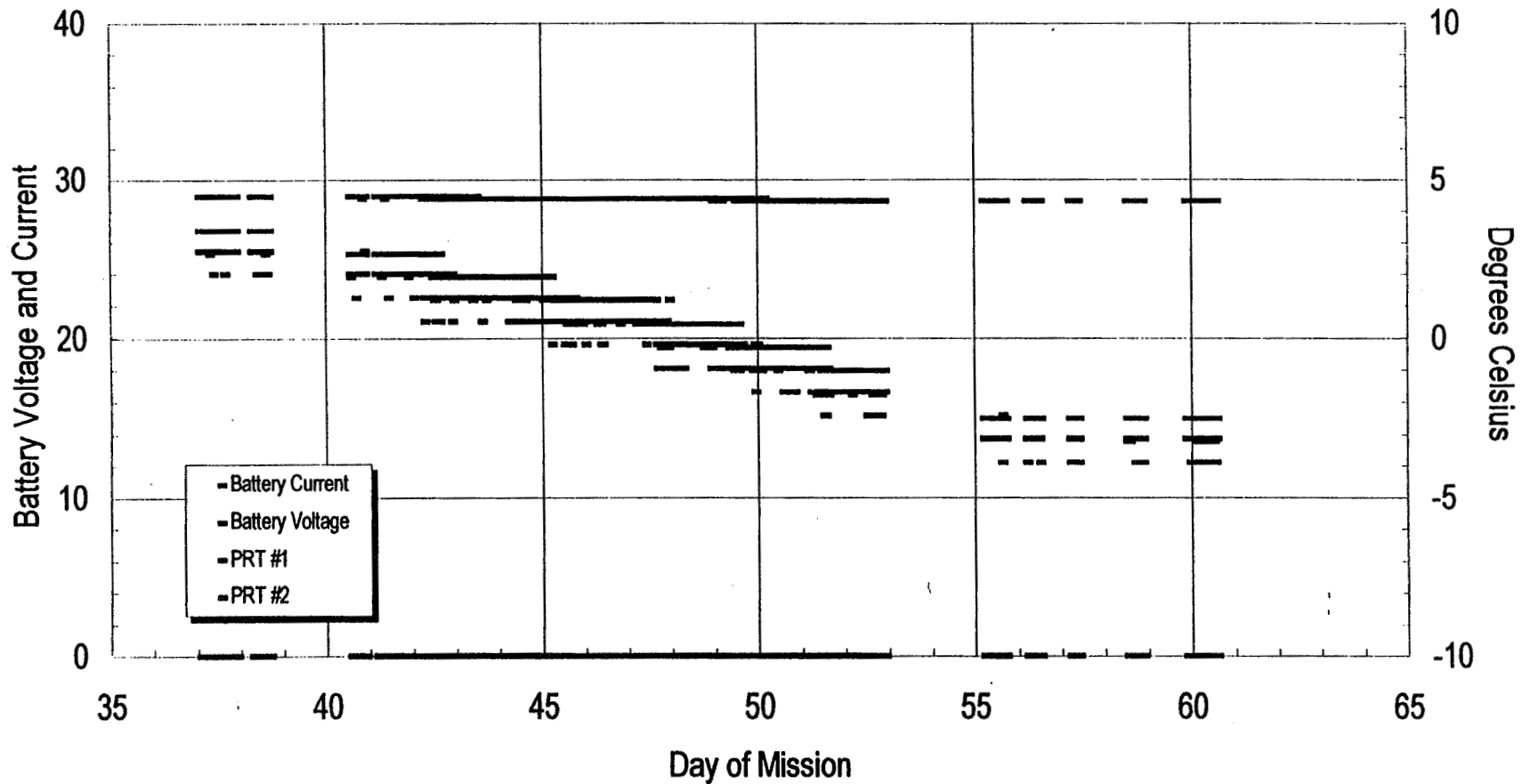
JPL Charge #2 AT 1.960 Volts Per Cell To A 0.2A Cut Off At 25°C - With 1.14 Ohm Resistor





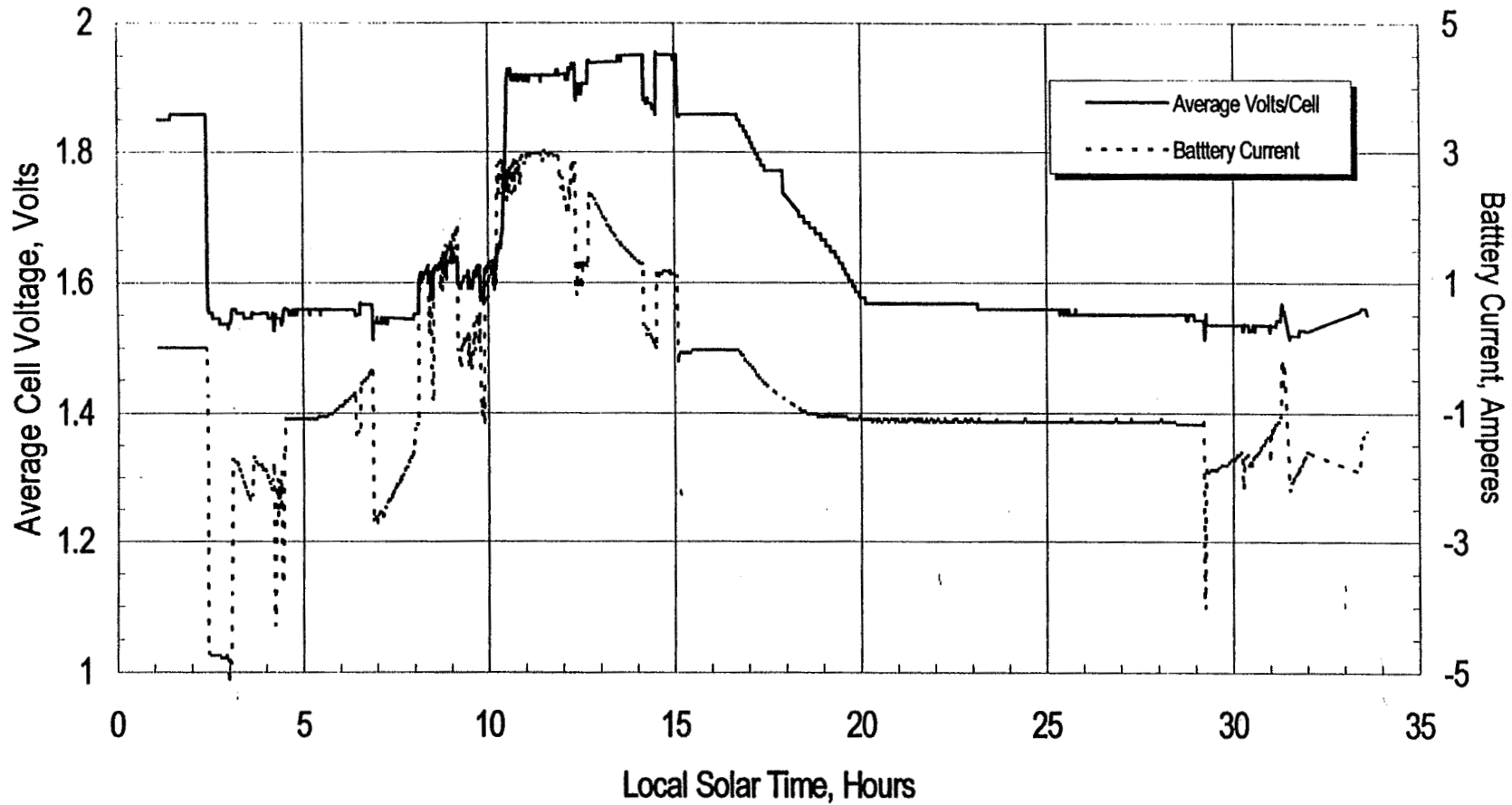
MPF BATTERY VOLTAGE AND TEMPERATURE DURING CRUISE

AgZn Battery Performance during Day 37 to 60 of Cruise



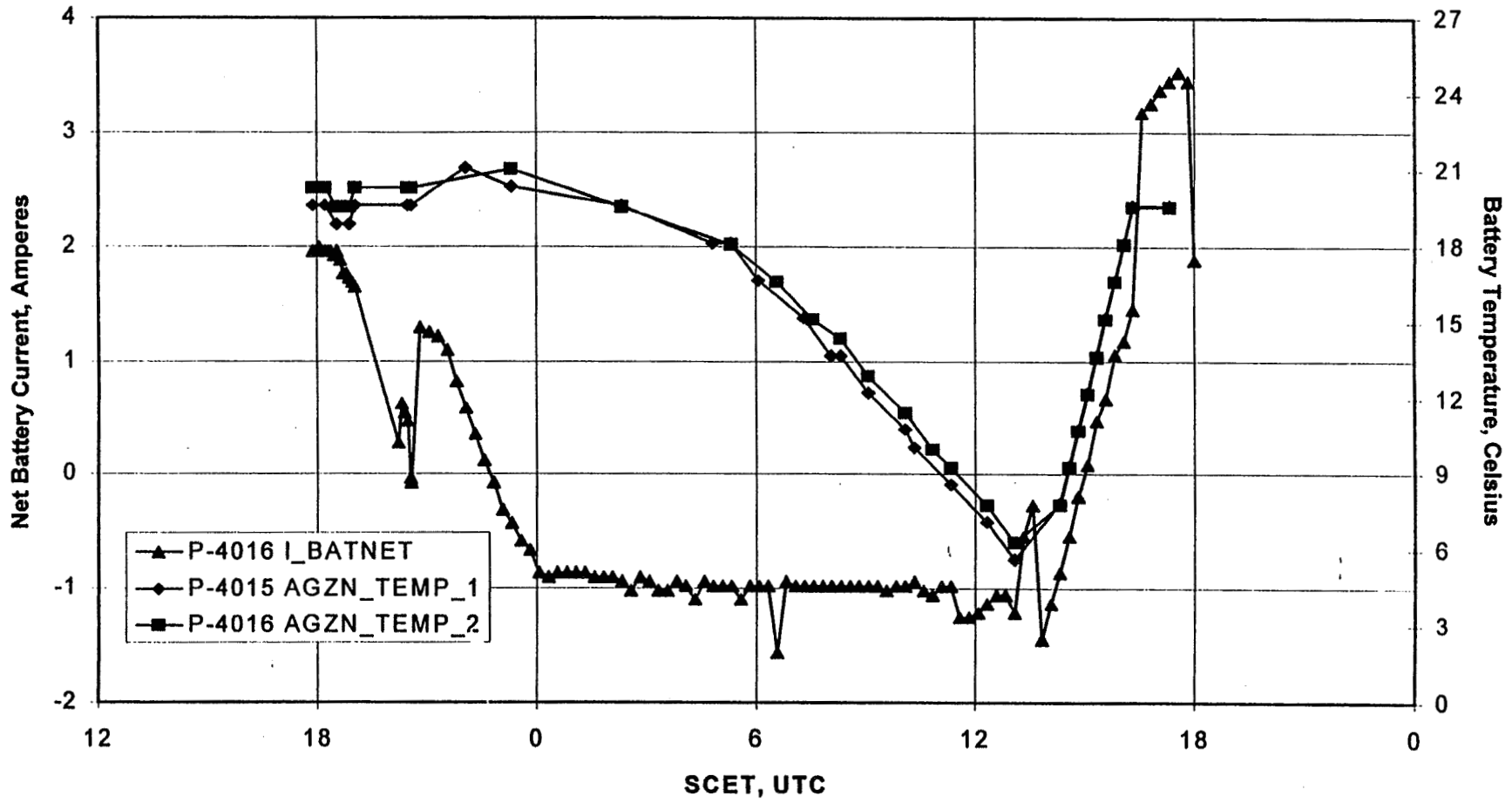
MPF BATTERY PERFORMANCE-EDL/SOL1

Mars Pathfinder Flight Battery - EDL and SOL 1



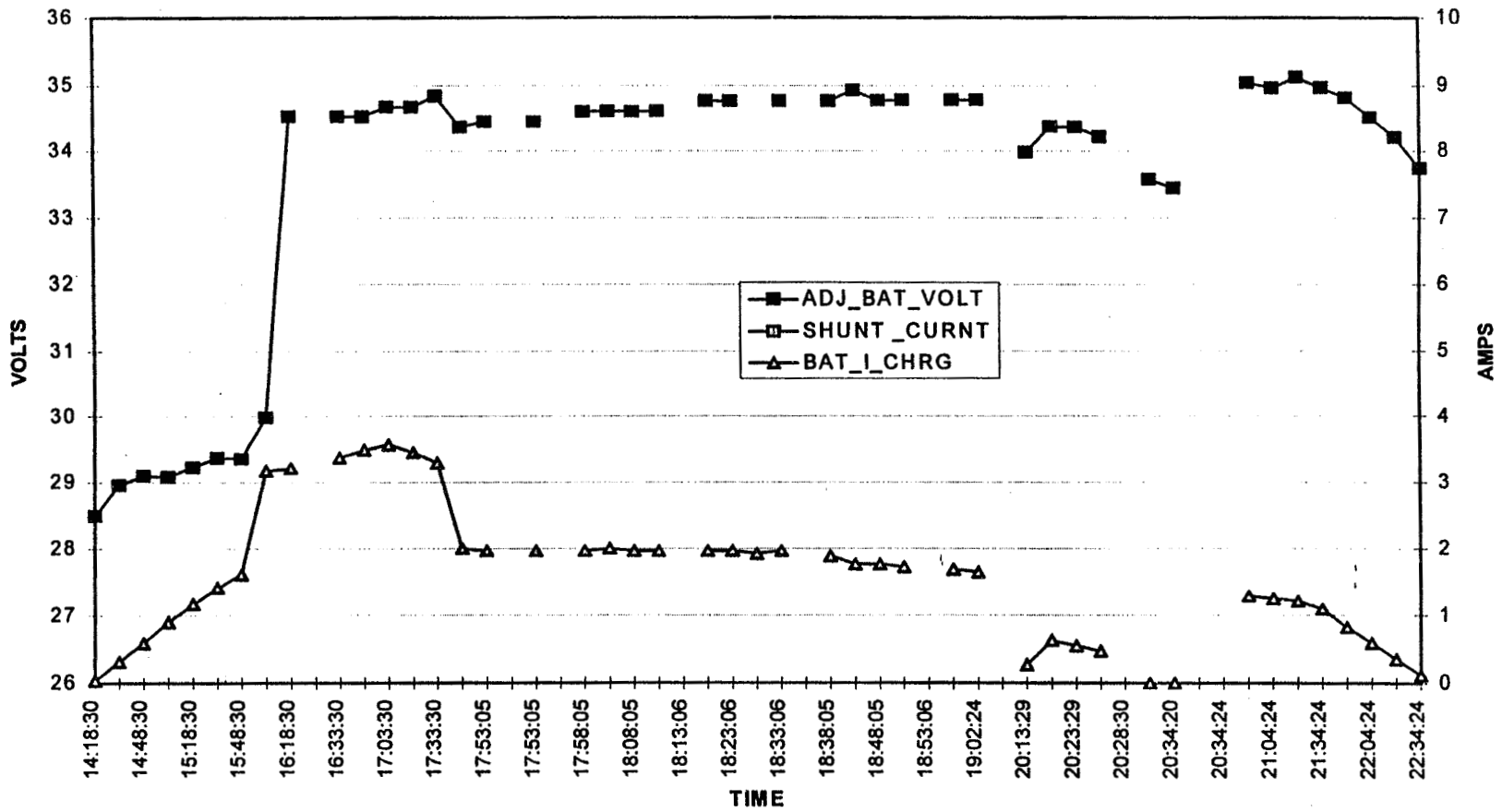
MPF BATTERY PERFORMANCE- SOL25

Flight Battery Sol 25 data



MPF BATTERY PERFORMANCE SOL-25

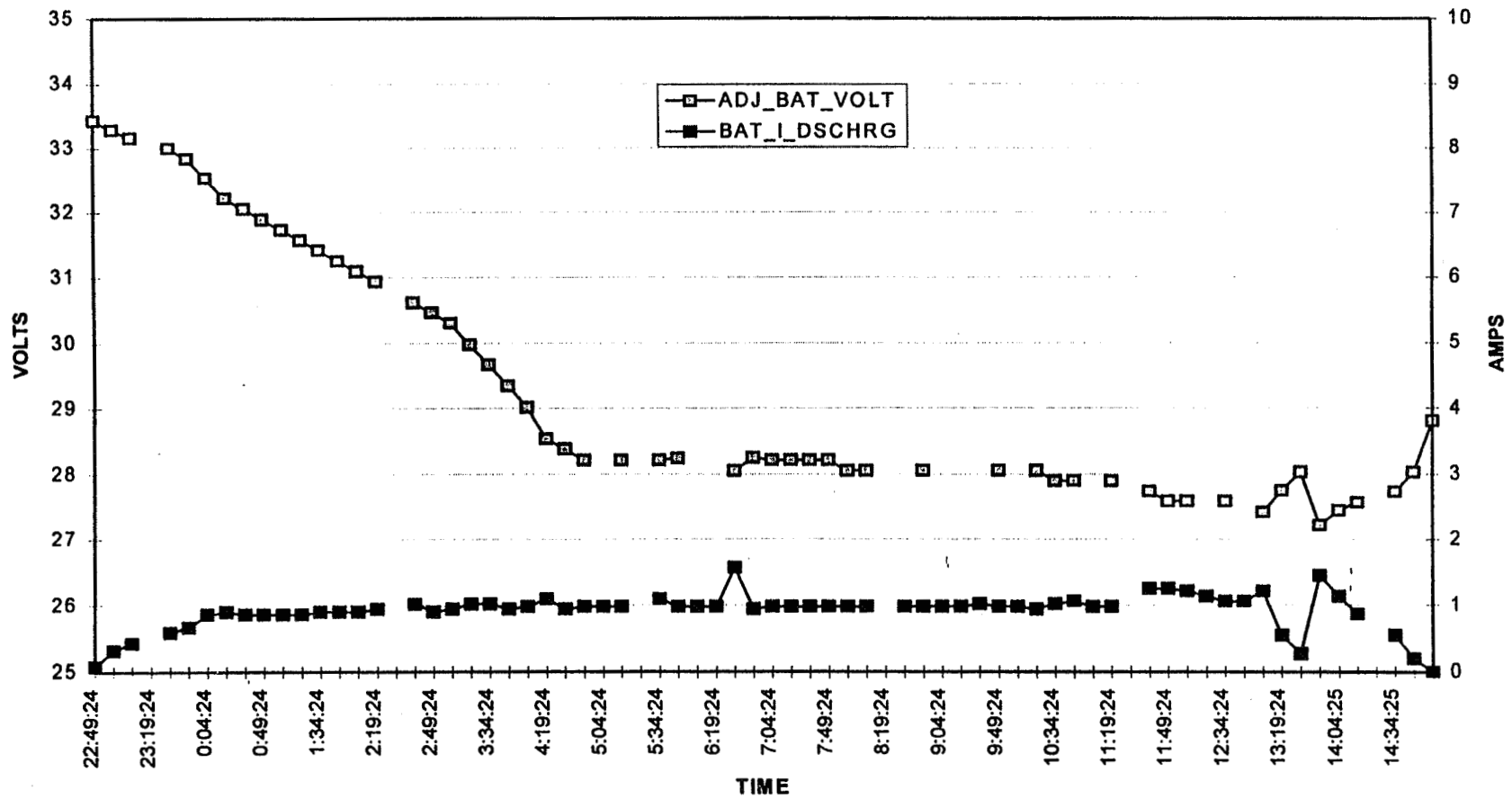
SOL #25 CHARGE





MPF BATTERY PERFORMANCE-SOL 25

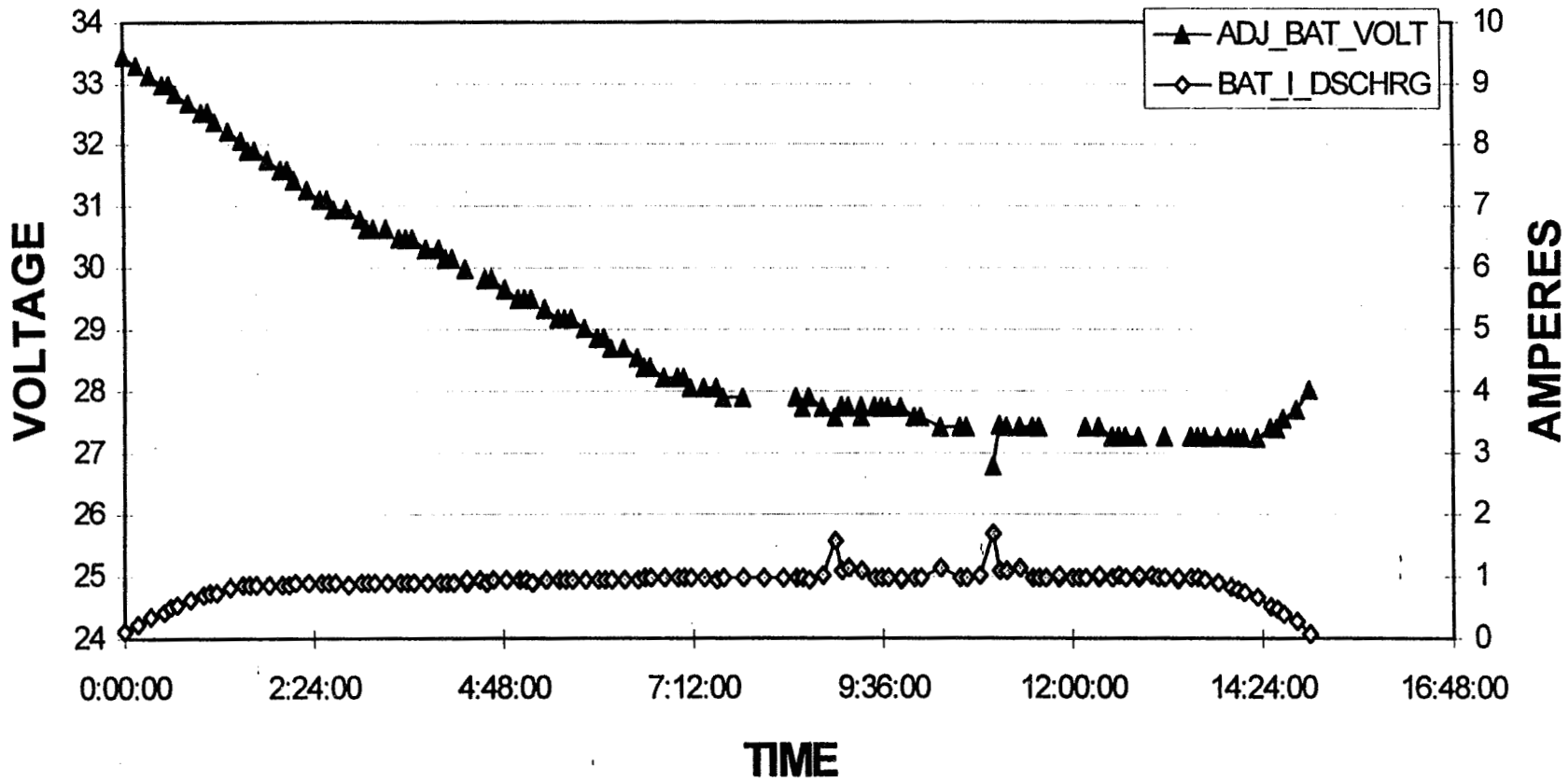
SOL #25 DISCHARGE





MPF BATTERY PERFORMANCE-SOL 68

SOL 68 DISCHARGE



SUMMARY AND CONCLUSIONS

- **The first use of a silver-zinc battery in a spacecraft application that called for extensive rechargeable operation after 12 months of active stand has proven to be very successful.**
- **BST has developed a silver-zinc battery with unique design features for the Mars Pathfinder mission.**
- **JPL has developed battery management strategies to meet the Mars Pathfinder mission requirements.**
 - Partial SOC at low temperature and open circuit stand was found to be the most effective method for insuring extensive cycle life following a long period of active storage
 - Silver-zinc battery charging at a reduced constant voltage was shown to provide full charge and a capability of supporting a large number of cycles.
 - Launch of an inverted silver-zinc battery was shown to be possible when a leak free cell vent valve is employed.
 - The use of a silver-zinc battery and shunt limiter in a direct energy transfer power system resulted in a very energy efficient design approach.



ACKNOWLEDGMENT

The work described here was carried out at the Jet Propulsion Laboratory,
California Institute of Technology, under contract with the
National Aeronautics and Space Administration.

Page intentionally left blank

CYCLE LIFE EXPECTATIONS FOR IPV NICKEL-HYDROGEN CELLS

**Lawrence H. Thaller
The Aerospace Corporation**

**Presented at
The NASA Aerospace Battery Workshop
Huntsville, AL
18-20 November, 1997**

Electronics Technology Center
Energy Technology Department



OUTLINE

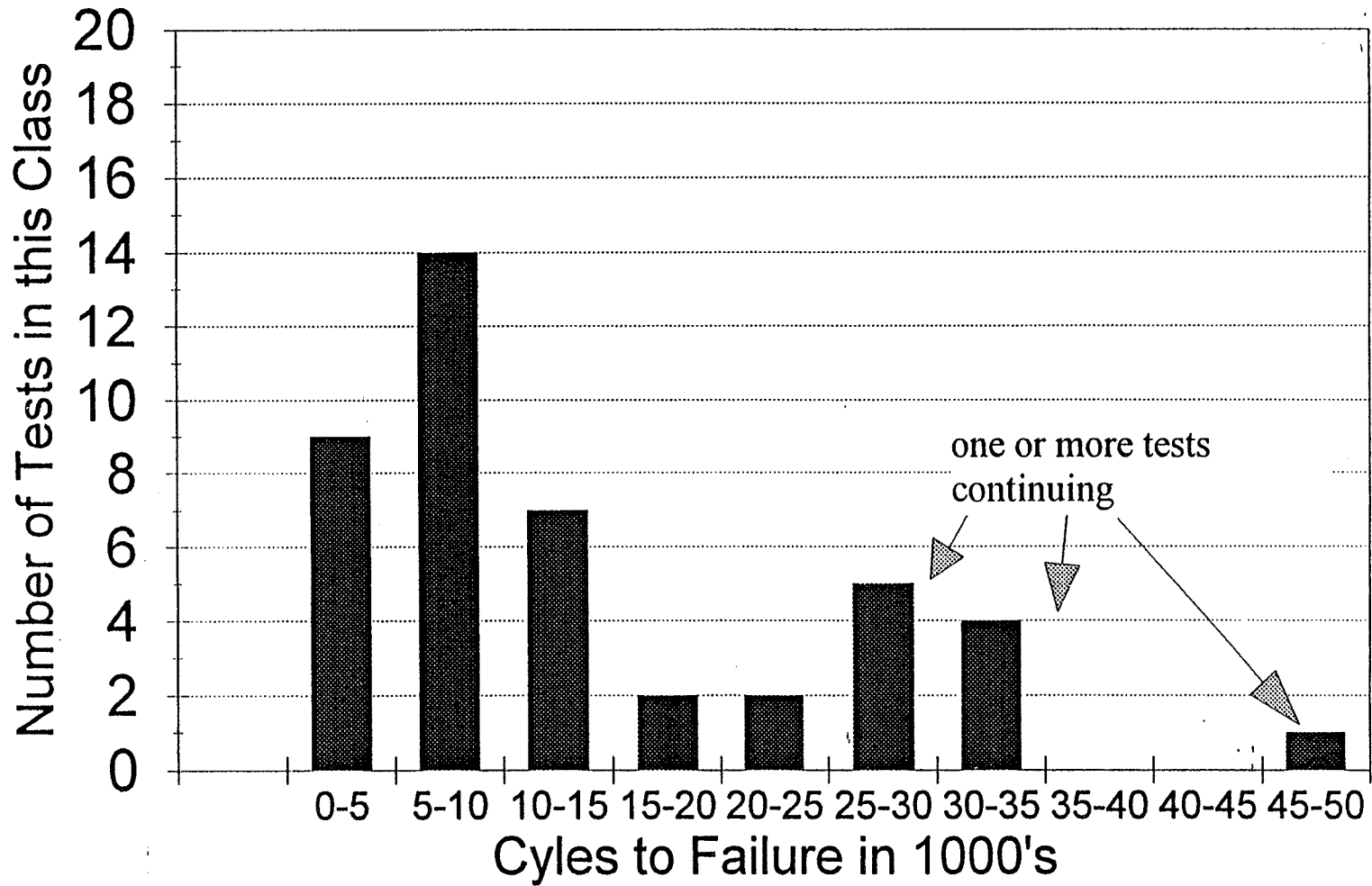
- Reasons For The Study
- Sources Of The Information Used In Study
- Types Of Information Used In Study
- Types Of Models Available To Interpret Data
- Focus Of The Study
- Initial Findings
- Classification Of Life Limiting Factors
- Assessing Significance Of Degradation Modes
- General Statements Concerning Expected Cycle Life

REASONS FOR THE STUDY

- IPV Nickel-Hydrogen Technology About 25 Years Old
- Several Significant Data Bases Have Been Developed
- Some Programs Interested In Longer Life Missions
- Some Programs Interested In Higher Energy Density
- Operation Of Nickel Electrode Better Understood
- DPA Studies Have Yielded Much Useful Information
- Results To Date Suggest Higher Useable Energy Densities Should Be Available Within Certain Restrictions
- A Valid Question Would Be - How Long Should IPV Nickel Hydrogen Cells And Batteries Last?

DATA BASE OF TESTS AT 60% DOD

Sources - AF, MM, NASA LeRC, NASA SSA



SOURCES OF INFORMATION USED IN STUDY

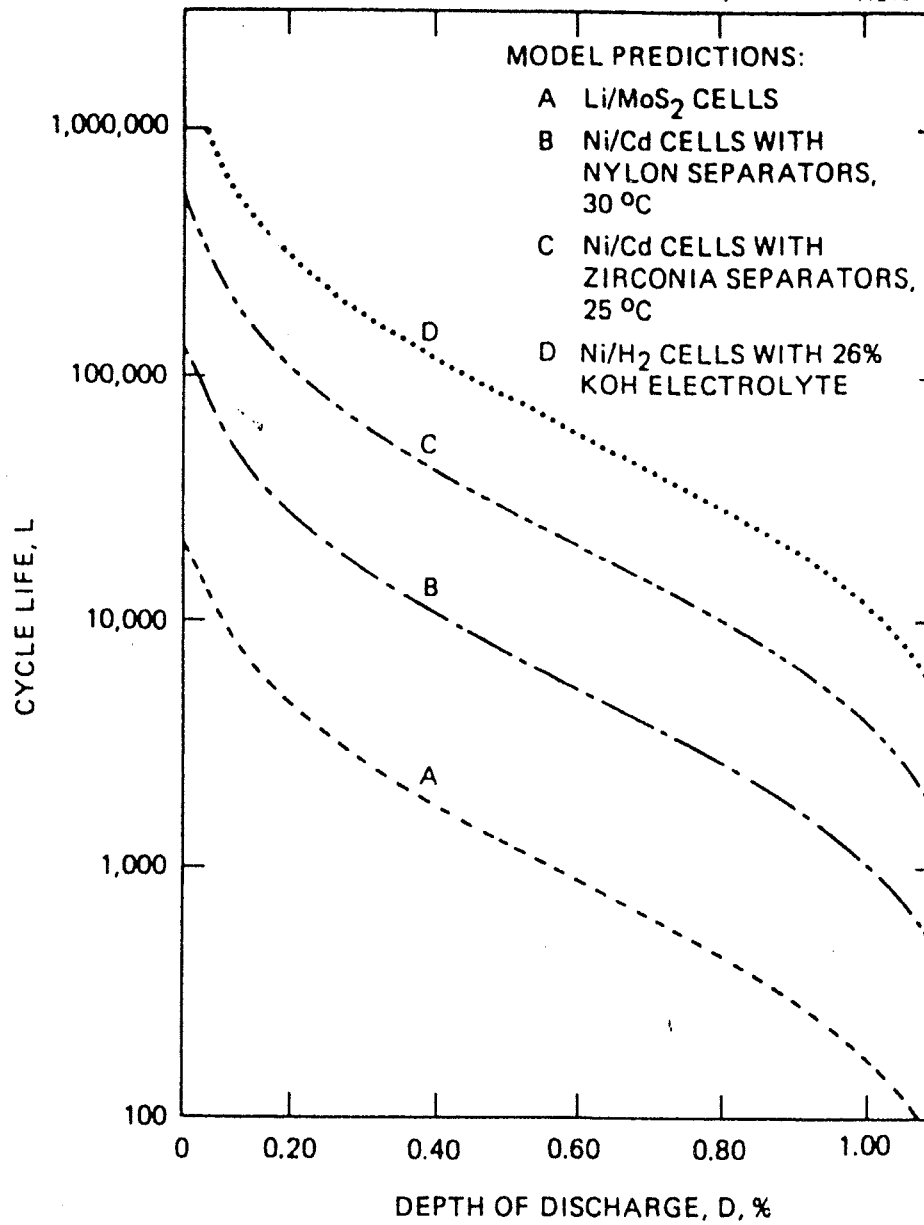
- Cycling Studies Conducted At LMA Denver Supported By Several Customers
- Cycling Studies Conducted At The Navy Facility At Crane Supported By Several Different Air Force Elements
- Cycling Studies Conducted At the Navy Facility At Crane And At The NASA Lewis Research Center Supported By The NASA Space Station Activity
- Cycling Studies Conducted At Several Locals Supported By The Battery Group At NASA Lewis
- The Open Literature and Private Communications Addressing Pertinent Issues Affecting Cycle Life And Degradation Modes

TYPES OF INFORMATION USED

- Capacity Retention As Cells Are Cycled
- Pressure Rise As Cells Are Cycled
- End Of Charge Voltage As Cells Are Cycled
- Temperature Effects On Cycle Life
- Electrolyte Concentration Effects On Cycle Life
- Cell Design Factors And Their Effect On Cycle Life
- Electrolyte Fill Amounts And Their Effect On Cycle Life
- A Review Of Manufacturing Difficulties That Are Common To This Technology
- The DPA Results Following Premature Cell Failure
- The Static And Dynamic Modeling Work At Aerospace

MODELS AVAILABLE TO HELP INTERPRETATION OF DATA

- Cycle Life Versus Depth Of Discharge Model
 - Suggests the relationship between cycle life and depth of discharge when the degradation mode is due to a slow wearout of the cell
- Static IPV Cell Model
 - Follows the affect of plate expansion, plaque corrosion, and gamma phase formation on the electrolyte requirements of the particular cell design
- Dynamic IPV Cell Model
 - Follows the mass transport requirements of a cell design as a function of electrolyte concentration and state of charge



FOCUS OF THE STUDY

- Information That Could Be Gleaned From Cell Tests That Cycled A Long Time
- Information That Could Be Gleaned From Cell Tests That Did Not Cycle For A Long Time
- Cell Tests That Were Conducted At High Stress Levels
 - Deep depths of discharge
 - High recharge ratios
 - High temperatures
 - High end of charge voltages

INITIAL FINDINGS

- In Reviewing The 60% DOD Data, The Cycle Life Was Found To Span The Range Of Less Than 1000 Cycles To Over 50,000 Cycle and Still Cycling
- The Wearout Model Could Not Be Used, One Had To Assume Inappropriate Cell Designs, Manufacturing, Or Charge Management Problems
- Cycling Problems Were Divided Between:
 - Cell design related issues
 - Manufacturing related issues
 - Charge management related issues

CELL DESIGN ISSUES

- 1997 IECEC Paper By Thaller Deals With This Issue
 - Cell Designs must take into account the changes taking place within a cell as it is cycled
 - In particular, changes that impact the electrolyte requirements are very important
 - These are plate expansion, plaque corrosion, gamma phase formation, and temperature gradients

MANUFACTURING ISSUES

- Most Of The Manufacturing Related Issues Are Associated With The Nickel Electrode
 - Sinter pore size and pore size distribution
 - Active material loading levels and distribution within the plaque
 - Activation procedures, storage procedures, and contaminants
- Most Of These Issues Are Reported In The Open Literature And Can Be Kept Under Control

RECENT FINDINGS REPORTED BY CRANE

- Cells cycled at 10°C always cycled longer than equivalent cells cycled at -5°C
- A recharge protocol that included a taper charge as the cells approached full charge always resulted in longer cycle lives compared to equivalent cells that were charged at a constant current to the same charge return ratio.
- Cells that were filled with 26% potassium hydroxide as the electrolyte always cycled longer than equivalent cells filled with 31% potassium hydroxide.
- The cause of failure of cells cycled to 60% DOD in all cases where failed cells were disassembled was always attributed to degradation of the nickel electrodes.

1997 IECEC Papers presented at the Hawaii meeting

INFORMATION GLEANED FROM DATA BASES

- Of the 23 packs where a failure was reported in the Air Force and NASA supported testing at the Navy facility at Crane, 22 were associated with either recharge ratios that were 1.05 or higher, or the end-of-charge voltage was above 1.55 Volts.
- Of the 21 failures reported in the testing carried out at NASA Lewis under Space Station sponsorship, 19 occurred in tests where the recharge ratio was 1.05 or above, while for the 18 tests where there has been no failure, the recharge ratio has been 1.04 or below. The tests that are still running have accumulated between 44,000 and 50,000 LEO cycles at 35% DOD.

CHARGE MANAGEMENT ISSUES

- Charge Management Was Found To Play An Important Part In The Cycle Life Of Test Carried Out At 60% DOD
 - High end of charge voltages can result in high rates of plaque corrosion and excessive oxygen formation within the pores of the nickel electrode.
 - NASA Lewis is testing cells with plaque material that has undergone a passivation process
 - Cycling to date has indicated a significant reduction in the corrosion rate estimated by the pressure rise with cycling

SIGNIFICANCE OF DEGRADATION MODES

- Plate Expansion
 - NASA supported work at Hughes (1980s) reports up to 80% plate expansion
 - Air Force funded testing on Pack 5402H showed an average of 6% plate expansion when DPAed after 42,000 40% DOD cycles (cell was removed from test prior to failure)
- Plaque Corrosion
 - NASA supported work at Hughes reported up to 50% corrosion of the nickel after about 40,000 at 80% DOD in an accelerated 45 minute LEO cycling test
 - Cell from Air Force Pack 5402H showed an average corrosion of about 22% when analyzed during the DPA studies

DPA studies on Air Force cell were carried out at Aerospace by G.To and M. Quinzio under the direction of Dr. Zimmerman

CONCLUDING REMARKS

- IPV Nickel-Hydrogen Cells Have The Potential For Extremely Long Cycle Lives
 - Current champion in terms of DOD and cycle life are cells manufactured by Eagle Picher under the direction of the design team at NASA Lewis
 - 50,000 LEO cycles at 60% DOD
- Deeper Depths Of Discharge Are Available If The Four Main Factors Resulting In Abbreviated Cycling Are Properly Addressed
 - Proper Cell Design
 - Proper Nickel Electrode Manufacture
 - Proper Charge Control
 - Proper Thermal Environment

Page intentionally left blank



Life Cycle Testing of Spaceflight Qualified Nickel-Hydrogen Battery Cells

Chris Fox, Jennifer Francisco, Kevin Ames, Ron Replinger

Power Subsystems Department

Joplin, MO 64802

(417) 623-8000

<http://www.epi-tech.com>

Cell Design Variable

EAGLE EPICHER
Technologies Division

- ◆ **Plaque**
 - Thickness
 - Porosity
 - Type
 - Dry Sinter vs Slurry
- ◆ **Electrolyte (KOH) Concentration**
 - 31% vs 26%
- ◆ **Separator Type**
 - Asbestos vs ZIRCAR® vs 2 ZIRCAR®
- ◆ **Electrolyte Management**
 - Wall Wick vs No Wall Wick vs Catalyzed Wall Wick vs PTFE
- ◆ **Cell Configuration**
 - COMSAT Design vs Mantech (Air Force)
 - IPV, CPV, DPV, SPV (5" and 10" diameter, batteries only)
 - 2.5", 3.5", 4.5", 5.5" diameter

IN-HOUSE NiH₂ LEO LIFE TEST SUMMARY

EAGLE P P ICHEP
Technologies Division

<u>Cell</u>	<u>Cell Type</u>	<u># of Cells</u>	<u>Regime</u>	<u>DOD</u>	<u># of Cycles</u>
RNH 50-15	IPV	19	ACC LEO	15%	127,770
RNH-80	IPV	1	ACC LEO	15%	117,908
RNH-50-15	IPV	1	ACC LEO	15%	112,903
RNH-76-3	IPV	5	ACC LEO	15%	108,015
RNH-76-9	IPV	1	ACC LEO	15%	96,866
RNH 30-1	IPV	10	RT LEO	30%	69,806
RNH 50-15	IPV	7	RT LEO	45%	56,880
RNH-76-3	IPV	7	RT LEO	45%	55,879
RNH-76-3	IPV	10	ACC LEO	15%	50,170
RNH-76-3	IPV	4	RT LEO	45%	35,179
RNHC 10-1	CPV	11	RT LEO	40%	17,897
RNHD 40-1	DPV	3	RT LEO	30%	8,004
RNHD 60-1	DPV	3	RT LEO	30%	5,225

RT = Real Time ACC = Accelerated

IN-HOUSE NiH₂ LEO LIFE TEST SUMMARY

EAGLE EPICHER
Technologies Division

<u>Cell</u>	<u>Cell Type</u>	<u># of Cells</u>	<u>Regime</u>	<u>DOD</u>	<u># of Cycles</u>
RNH-56-1	IPV	3	RT LEO	70	*15,100
RNH-56-1	IPV	3	RT LEO	70	*15,100
RNH-56-1	IPV	1	RT LEO	70	*15,100
RNH-56-1	IPV	4	RT LEO	70	*15,100
RNH-56-1	IPV	3	RT LEO	70	*12,900
RNH-56-1	IPV	4	RT LEO	70	*5,200
RNH-56-1	IPV	3	RT LEO	70	*800

<u>Battery</u>	<u>Cell Type</u>	<u># of Cells</u>	<u>Regime</u>	<u>DOD</u>	<u># of Cycles</u>
SAR-10013	IPV	27	RT LEO	12%	31,443

RT = Real Time

ACC = Accelerated

* = RLF Plaque

IN-HOUSE NiH₂ GEO LIFE TEST SUMMARY

EAGLE EPICHER
Technologies Division

<u>Cell</u>	<u>Cell Type</u>	<u># of Cells</u>	<u>Regime</u>	<u>DOD</u>	<u># of Seasons</u>
RNH 120-H	IPV	4	ACC GEO	75%	44
RNH-65-15	IPV	6	ACC GEO	56%	42
RNH-120-1	IPV	6	ACC GEO	100%	23
RNH-76-11	IPV	6	ACC GEO	57%	21
RNH-100-7	IPV	6	ACC GEO	57%	20
RNH 65-33	IPV	4	ACC GEO	70%	17

<u>Battery</u>	<u>Cell Type</u>	<u># of Cells</u>	<u>Regime</u>	<u>DOD</u>	<u># of Cycles</u>
SAR-10017	IPV	27	RT GEO	75%	*9
SAR-10017	IPV	27	ACC GEO	75%	*24

RT = Real Time ACC = Accelerated * = Complete

OFF-SITE NiH₂ LIFE TEST SUMMARY

EAGLE EPICHER
Technologies Division

<u>Cell Type</u>	<u># Cells</u>	<u>Type</u>	<u>Cell % DOD</u>	<u>Location</u>	<u># of Cycles</u>
RNH 30-1	14	LEO	13%	MSFC	53,200
RNH 100-1	8	LEO	40%	LMC	44,488
RNH 90-3	4	LEO	7%	MSFC	42,700
RNH 90-3	4	LEO	7%	MSFC	41,600
RNH 90-3	132	LEO	7%	MSFC	41,500
RNH 90-3	22	LEO	7%	MSFC	40,900
RNH 90-3	4	LEO	7%	MSFC	40,860
EP-26	6	LEO	60%	LMC	33,019
RNH 90-13	8	LEO	30%	MSFC	27,100
RNH 48-1	5	LEO	35%	MSFC	4,700
RNH 48-1	5	LEO	45%	MSFC	4,700
RNH 65-15	6	GEO	55%	TRW	42 Seasons
RNH 100-7	6	GEO	65%	TRW	20 Seasons
RNH-50-59	2	GEO	65%	LMC	19 Seasons
RNH 98-1	2	GEO	65%	TRW	02 Seasons
RNH 98-3	4	GEO	65%	TRW	02 Seasons

TERMINATED NiH₂ LIFE TESTS

<u>Cell Type</u>	<u># Cells</u>	<u>Type</u>	<u>Cell % DOD</u>	<u>Location</u>	<u># of Cycles</u>
RNH 35-3	14	LEO	13%	MSFC	49,815
EP	16	LEO	40	LMC	42,259
RNH-50-19	6	LEO	40	LMC	42,259
RNH-50-19	5	LEO	40	LMC	42,259
RNH-30-9	12	LEO	22	MSFC	27,250
EP	8	LEO	40	LMC	24,309
RNH-30-1	10	LEO	30	EPI	17,000
RNH-50-15	6	LEO	50	EPI	10,799
RNH-76-3	6	LEO	50	EPI	9,576
EP	8	LEO	60	LMC	9,499

ON-ORBIT NiH₂ IPV CELL HERITAGE

EAGLE EPICHER
Technologies Division

<u>CELL/ BATTERY</u>	<u>PROGRAM NAME</u>	<u>TOTAL CYCLES</u>	<u>DOD</u>
RNH-50-1	USAF	1,216	25%
RNH-35-1	NTS2	580	60%
RNH-30-1	IV FM6	1,305	80%
RNH-30-1	IV FM7	1,268	60%
RNH-30-1	IV FM8	1,233	60%
RNH-40-1	SPACENET FM1	1,214	60%
RNH-40-1	SPACENET FM2	1,172	60%
RNH-30-1	IV FM10	1,139	60%
RNH-30-1	G STAR FM1	1,057	60%
RNH-30-1	IV FM11	1,115	60%
RNH-35-1	ASC FM1	819	60%
RNH-30-1	IV FM12	1,092	60%
RNH-50-15	SATCOM FM1	1,078	60%
RNH-50-15	SATCOM FM2	1,032	60%
RNH-30-1	G STAR FM2	1,048	60%
RNH-40-1	SPACENET FM4	872	60%
RNH-30-1	IV FM13	855	60%

ON-ORBIT NiH₂ IPV CELL HERITAGE



<u>CELL/ BATTERY</u>	<u>PROGRAM NAME</u>	<u>TOTAL CYCLES</u>	<u>DOD</u>
RNH-35-1	PAN AM SAT FM#1	848	60%
RNH-30-1	G STAR FM3	778	60%
RNH-50-15	ASTRA 1A	804	60%
RNH-30-1	IV FM15	792	60%
RNH-30-3	G STAR FM4	629	60%
RNH-30-3	ITALSAT	615	60%
RNH-50-15	ASTRA 1B	604	60%
RNH-50-27	ANIK E F2	596	70%
RNH-40-7	ASC-2	594	70%
RNH-40-7	AURORA-2	582	70%
RNH-50-27	ANIK E F1	552	70%
RNH-78-1	TELECOM 2-A	533	80%
RNH-78-1	TELECOM 2-B	503	80%
RNH-50-15	INTELSAT K	489	60%

ON-ORBIT NiH₂ IPV CELL HERITAGE

EAGLE EPICHER
Technologies Division

<u>CELL/ BATTERY</u>	<u>PROGRAM NAME</u>	<u>TOTAL CYCLES</u>	<u>DOD</u>
RNH-50-27	SATCOM C4	521	60%
RNH-50-27	SATCOM C3	518	60%
RNH-78-1	HISPASAT 1A	466	60%
RNH-78-1	HISPASAT 1B	389	60%
RNH-50-27	TELSTAR 401(a)	277	70%
RNH-50-27	TELSTAR 401(b)	277	70%
RNH-76-11	MILSTAR DFS1	339	60%
RNH-50-27N	BS3N	302	70%
RNH-65-15	MILITARY (Classified)	226	70%
RNH-42-1	KOREASAT - 1	205	70%
RNH-45-7	TELSTAR 402R	192	70%
RNH-76-11	MILSTAR DFS2	182	60%

ON-ORBIT NiH₂ IPV CELL HERITAGE

EAGLE EPICHER
Technologies Division

<u>CELL/ BATTERY</u>	<u>PROGRAM NAME</u>	<u>TOTAL CYCLES</u>	<u>DOD</u>
RNH-42-1	KOREASAT - 2	165	70%
RNH-50-49	INMARSAT- 3 F1	145	70%
RNH-50-49	INMARSAT- 3 F3	82	70%
RNH-78-1	TELECOM 2C	175	80%
RNH-78-1	TELECOM 2D	114	80%
RNH-50-49	INMARSAT- 3 F2	107	70%
RNH-100-7	GE-1	106	80%
RNH-100-7	GE-2	71	70%
RNH-120-1	TEMPO-2	62	70%
RNH-120-1	TELSTAR 501	43	100%
RNH-50-49	INMARSAT- 3 F4	40	70%
RNH-40-15	GPS-IIR	1460	60%
RNH-100-7	GE-3	17	70%
RNH-100-7	ECHOSTAR-3	10	70%
RNH-120-1	APSTAR 2R	7	100%
RNH-40-15	GPS-2-28	34	60%

ON-ORBIT NiH₂ IPV BATTERY HERITAGE

EAGLE P ICHER
Technologies Division

<u>CELL/ BATTERY</u>	<u>PROGRAM NAME</u>	<u>TOTAL CYCLES</u>	<u>DOD</u>
SAR 10007 (RNH-35-3)	OLYMPUS	373	60%
SAR 10011 (RNH-30-3)	IV/TV SAT II	745	60%
SAR-10015 (RNH-90-3)	HST	41,410	9%
SAR 10009 (RNH-65-1-3)	EUTELSAT FM1	606	80%
SAR 10009 (RNH-65-1-3)	EUTELSAT FM2	574	80%
SAR 10009 (RNH-65-1-3)	EUTELSAT FM3	499	80%
SAR 10009 (RNH-65-1-3)	EUTELSAT FM4	450	80%

ON-ORBIT NiH₂ IPV BATTERY HERITAGE

EAGLE P P ICHEP
Technologies Division

<u>CELL/ BATTERY</u>	<u>PROGRAM NAME</u>	<u>TOTAL CYCLES</u>	<u>DOD</u>
SAR-10009 (RNH-65-1)	TURKSAT 1B	294	70%
SAR-10017 (RNH-78-1)	ORION F1	266	75%
SAR 10009 (RNH-65-1-3)	EUTELSAT FM6	221	80%
SAR-10041 (RNH-45-1)	ASIASAT 2	177	80%
SAR-10073 (RNH-50-57)	ECHOSTAR 101	169	70%
SAR-10057 (RNH-65-33)	TURKSAT 1C	121	80%

ON-ORBIT NiH₂ IPV BATTERY HERITAGE

EAGLE EPICHER
Technologies Division

<u>CELL/ BATTERY</u>	<u>PROGRAM NAME</u>	<u>TOTAL CYCLES</u>	<u>DOD</u>
SAR-10073 (RNH-50-57)	ECHOSTAR 102	106	70%
SAR-10057 (RNH-65-33)	NAHUEL 1A	71	70%
SAR-10041 (RNH-45-3)	INTELSAT 801	64	70%
SAR-10041 (RNH-45-3)	INTELSAT 802	35	70%
SAR-10041 (RNH-45-3)	INTELSAT 803	13	70%

ON-ORBIT NiH₂ CPV BATTERY & CELL HERITAGE

EAGLE EPICHER
Technologies Division

<u>CELL/ BATTERY</u>	<u>PROGRAM NAME</u>	<u>TOTAL CYCLES</u>	<u>DOD</u>
RNHC-6-1	TUBSAT-B (CPV)	624	15%
RNHC-10-1	ORBCOMM F1 (CPV)	14,335	20%
RNHC-10-1	ORBCOMM F2 (CPV)	14,335	20%
RNHC-10-1	MICROLAB F1 (CPV)	14,335	20%
RNHC-10-1	MSTI-3 (CPV)	8,200	30%
SAR-10037 (RNHC-10-1)	MSTI-2 (CPV)	20,571	20%
SAR-10027 (RNHC-6-1)	APEX (CPV)	17,734	20%
SAR-10061 (RNHC-20-1)	MGS (CPV)	92	30%

ON-ORBIT NiH₂ SPV BATTERY HERITAGE

EAGLE EPICHER
Technologies Division

<u>CELL/ BATTERY</u>	<u>PROGRAM NAME</u>	<u>TOTAL CYCLES</u>	<u>DOD</u>
JC-1	CLEMENTINE (SPV)	1,902	50%
SAR-10065	IRIDIUM 01 (SPV)	2,775	31%
SAR-10065	IRIDIUM 02 (SPV)	2,775	31%
SAR-10065	IRIDIUM 03 (SPV)	2,775	31%
SAR-10065	IRIDIUM 04 (SPV)	2,775	31%
SAR-10065	IRIDIUM 05 (SPV)	2,775	31%
SAR-10065	IRIDIUM 06 (SPV)	2,141	31%
SAR-10065	IRIDIUM 07 (SPV)	2,141	31%
SAR-10065	IRIDIUM 08 (SPV)	2,141	31%
SAR-10065	IRIDIUM 09 (SPV)	2,141	31%
SAR-10065	IRIDIUM 10 (SPV)	2,141	31%
SAR-10065	IRIDIUM 11 (SPV)	2,141	31%
SAR-10065	IRIDIUM 12 (SPV)	2,141	31%
SAR-10065	IRIDIUM 13 (SPV)	1,839	31%
SAR-10065	IRIDIUM 14 (SPV)	1,839	31%
SAR-10065	IRIDIUM 15 (SPV)	1,839	31%
SAR-10065	IRIDIUM 16 (SPV)	1,839	31%
SAR-10065	IRIDIUM 17 (SPV)	1,839	31%

ON-ORBIT NiH₂ SPV BATTERY HERITAGE

EAGLE P P ICHER
Technologies Division

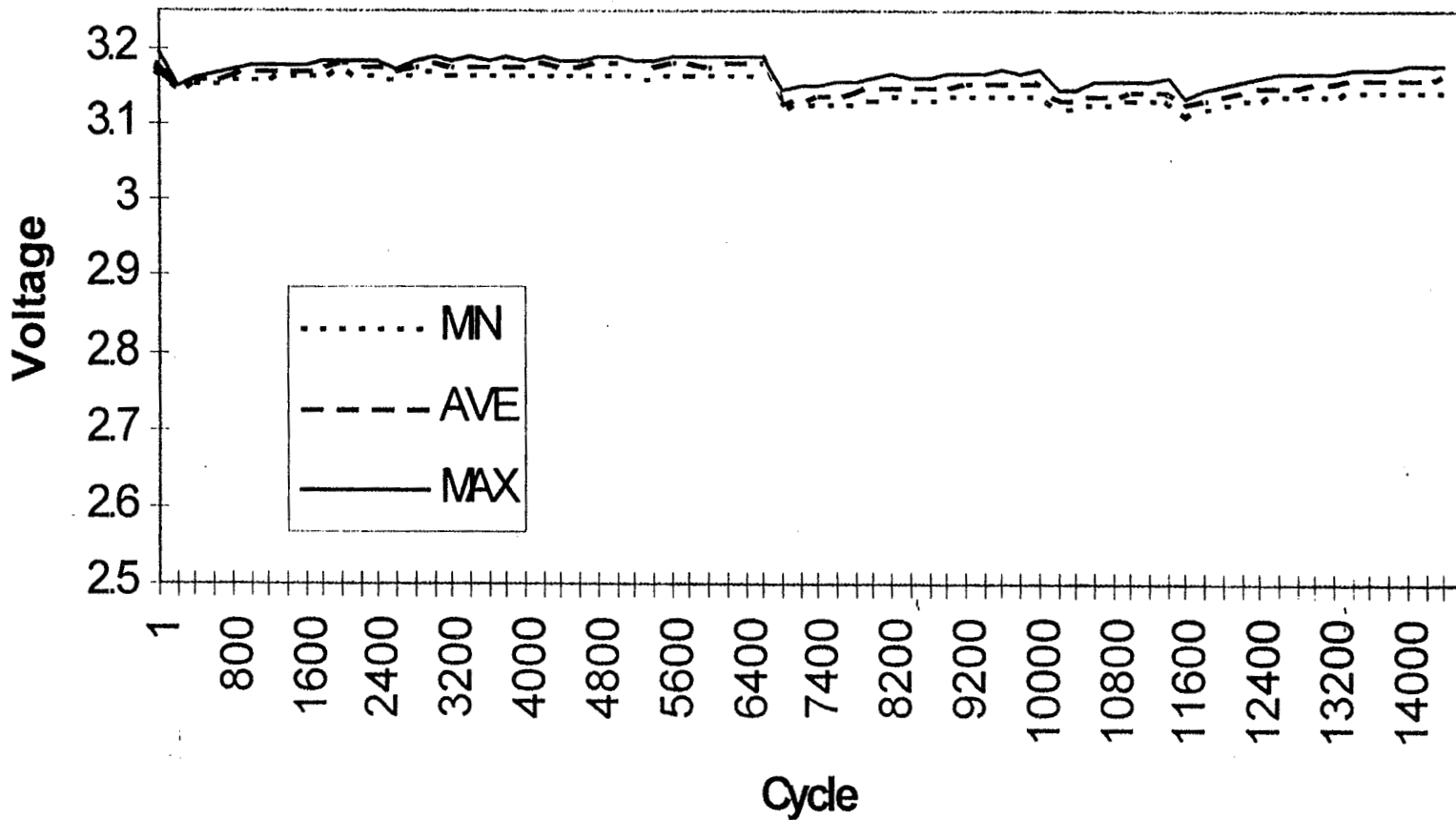
<u>CELL/ BATTERY</u>	<u>PROGRAM NAME</u>	<u>TOTAL CYCLES</u>	<u>DOD</u>
SAR-10065	IRIDIUM 18 (SPV)	1,234	31%
SAR-10065	IRIDIUM 19 (SPV)	1,234	31%
SAR-10065	IRIDIUM 20 (SPV)	1,234	31%
SAR-10081	IRIDIUM 21 (SPV)	1,234	31%
SAR-10081	IRIDIUM 22 (SPV)	1,234	31%
SAR-10081	IRIDIUM 23 (SPV)	888	31%
SAR-10081	IRIDIUM 24 (SPV)	888	31%
SAR-10081	IRIDIUM 25 (SPV)	888	31%
SAR-10081	IRIDIUM 26 (SPV)	888	31%
SAR-10081	IRIDIUM 27 (SPV)	888	31%
SAR-10081	IRIDIUM 28 (SPV)	888	31%
SAR-10081	IRIDIUM 29 (SPV)	888	31%
SAR-10081	IRIDIUM 30 (SPV)	701	31%
SAR-10081	IRIDIUM 31 (SPV)	701	31%
SAR-10081	IRIDIUM 32 (SPV)	701	31%
SAR-10081	IRIDIUM 33 (SPV)	701	31%
SAR-10081	IRIDIUM 34 (SPV)	701	31%
SAR-10081	IRIDIUM 35 (SPV)	82	31%

ON-ORBIT NiH₂ SPV BATTERY HERITAGE

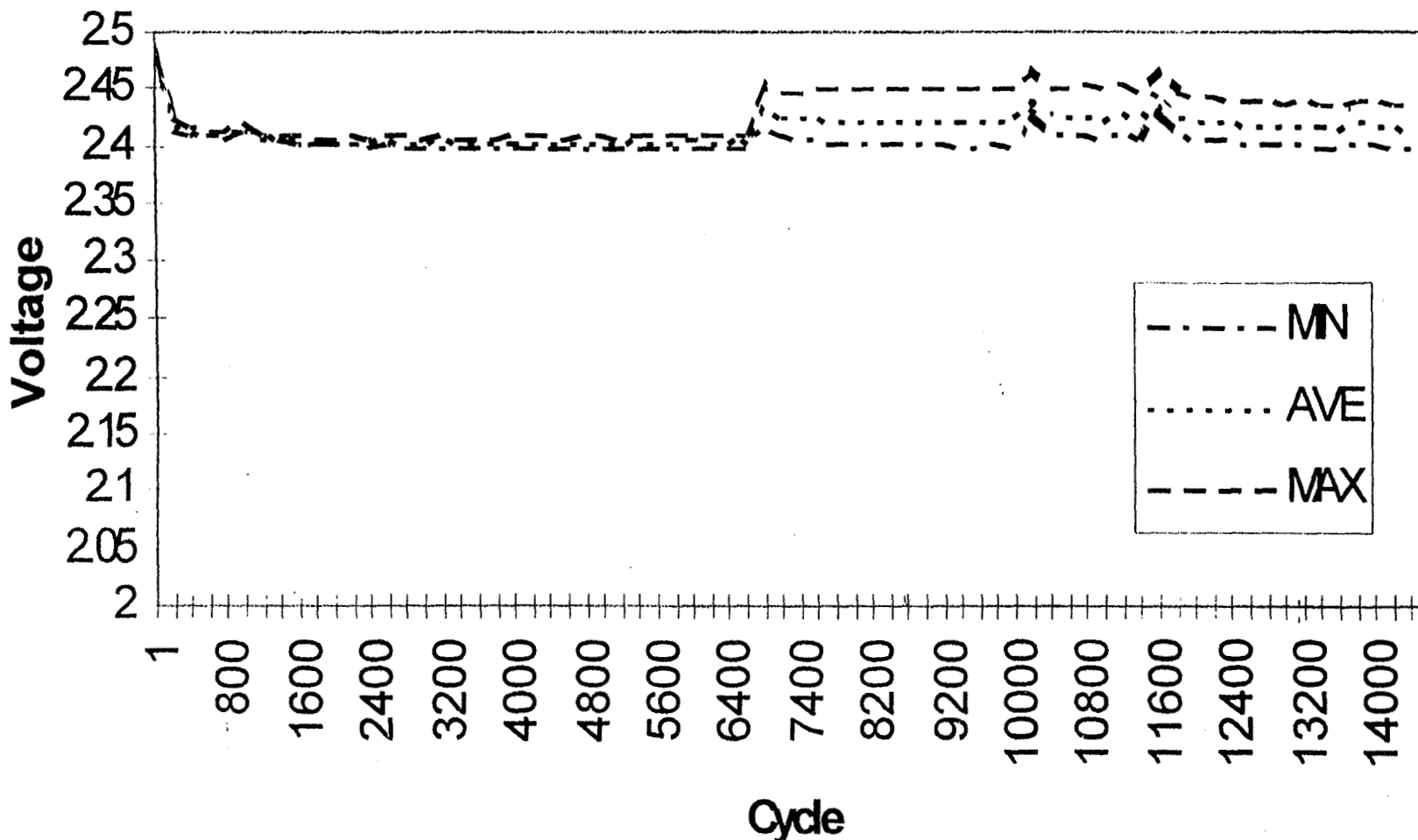
EAGLE P P ICHEP
Technologies Division

<u>CELL/ BATTERY</u>	<u>PROGRAM NAME</u>	<u>TOTAL CYCLES</u>	<u>DOD</u>
SAR-10081	IRIDIUM 36 (SPV)	82	31%
SAR-10081	IRIDIUM 37 (SPV)	82	31%
SAR-10081	IRIDIUM 38 (SPV)	82	31%
SAR-10081	IRIDIUM 39 (SPV)	82	31%

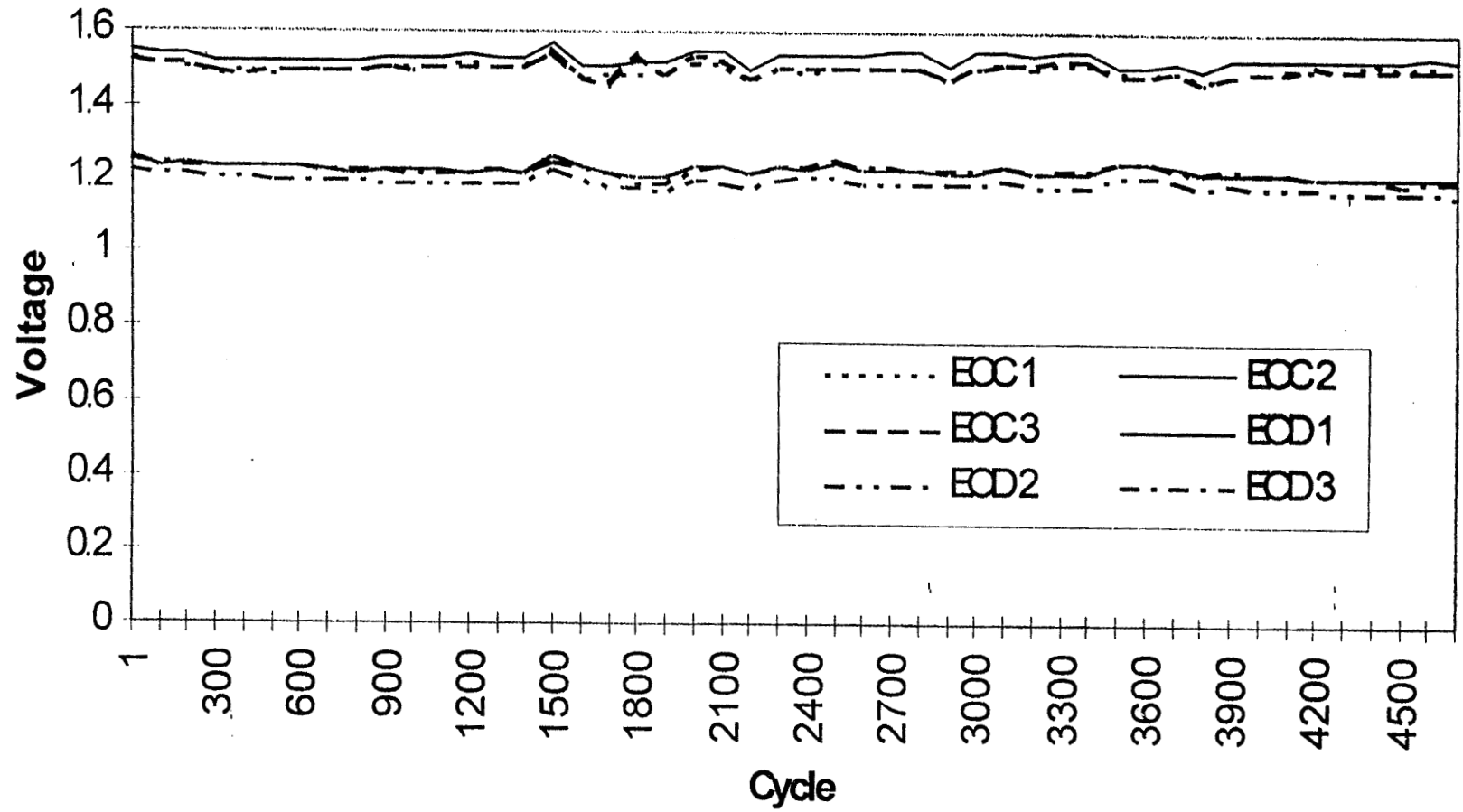
RNHC-10-1 End-of-Charge-Voltage (EOCV)



RNHC-10-1 End-of-Discharge-Voltage (EODV)

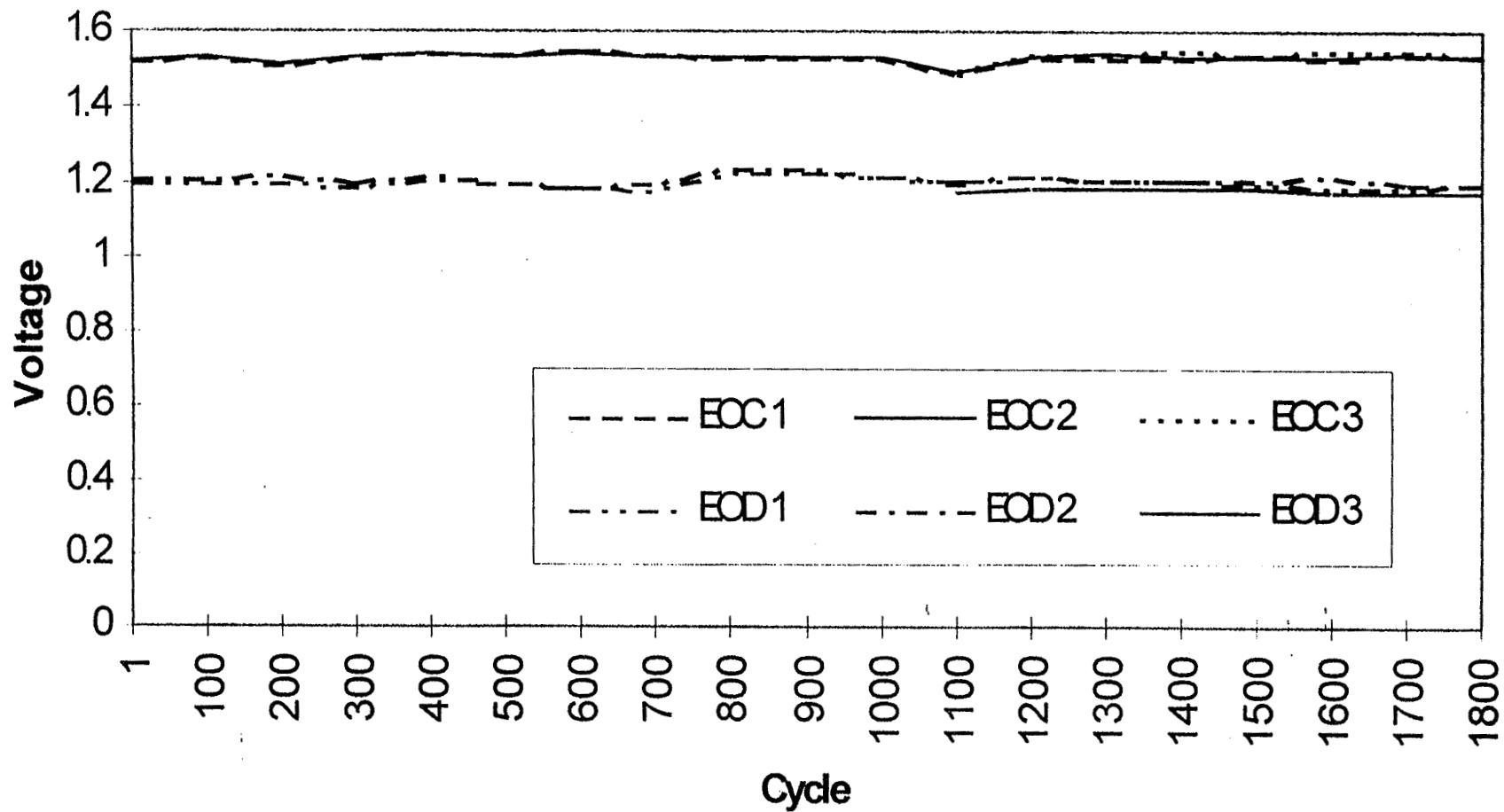


RNHD-40-1 LIFE TEST





RNHD-60-1 LIFE TEST

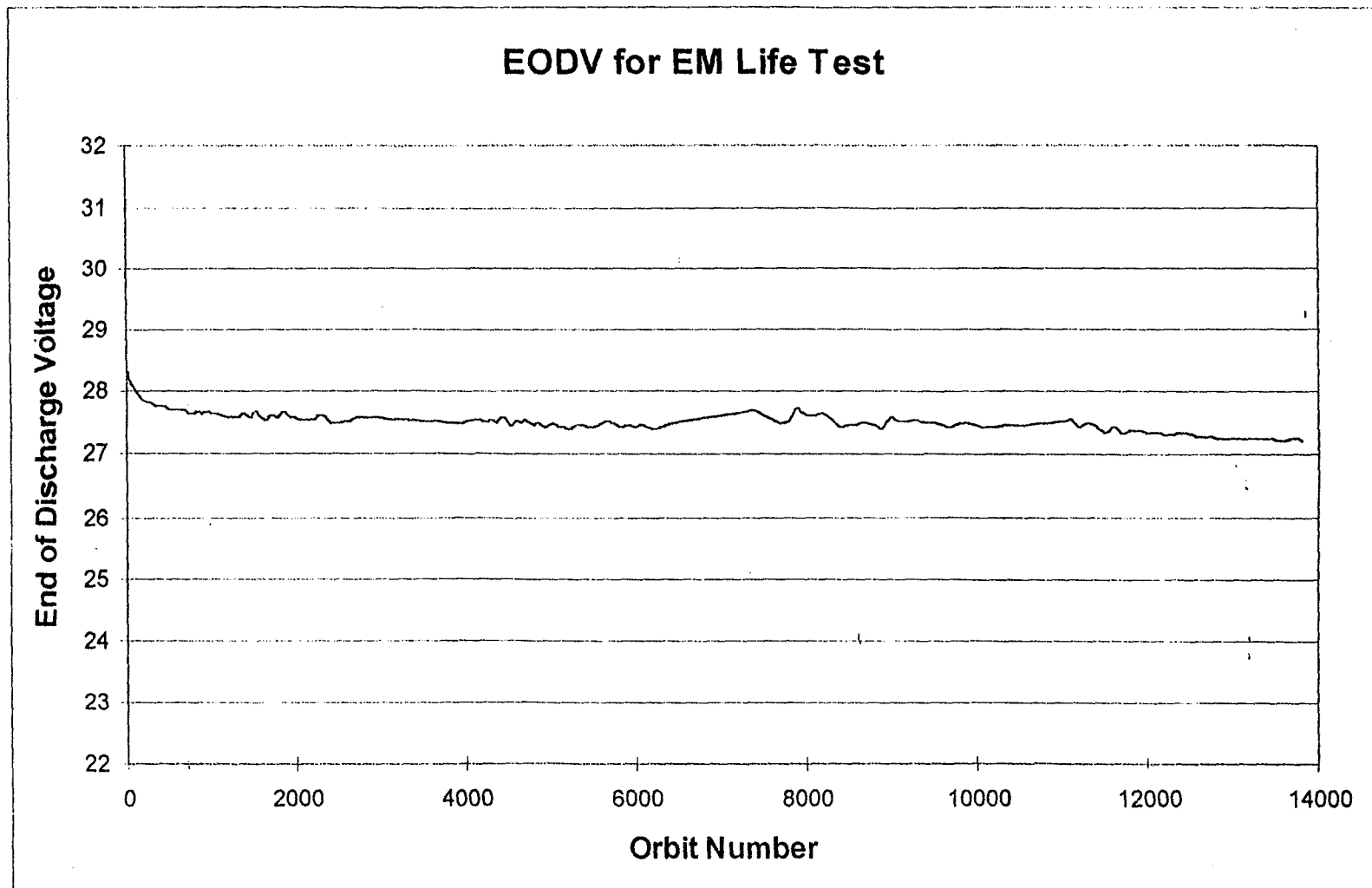


FULL LENGTH SPV LIFE TESTS

EAGLE EPICHER
Technologies Division

- ✦ 100 minute, 31% DOD LEO cycles
- ✦ Charge and discharge waveforms are pulsed
- ✦ Three on-going tests
 - 14,111 orbits at 10°C
 - 5,744 orbits at -5°C
 - 2,320 orbits at 5°C

31% DOD SPV LIFE TEST



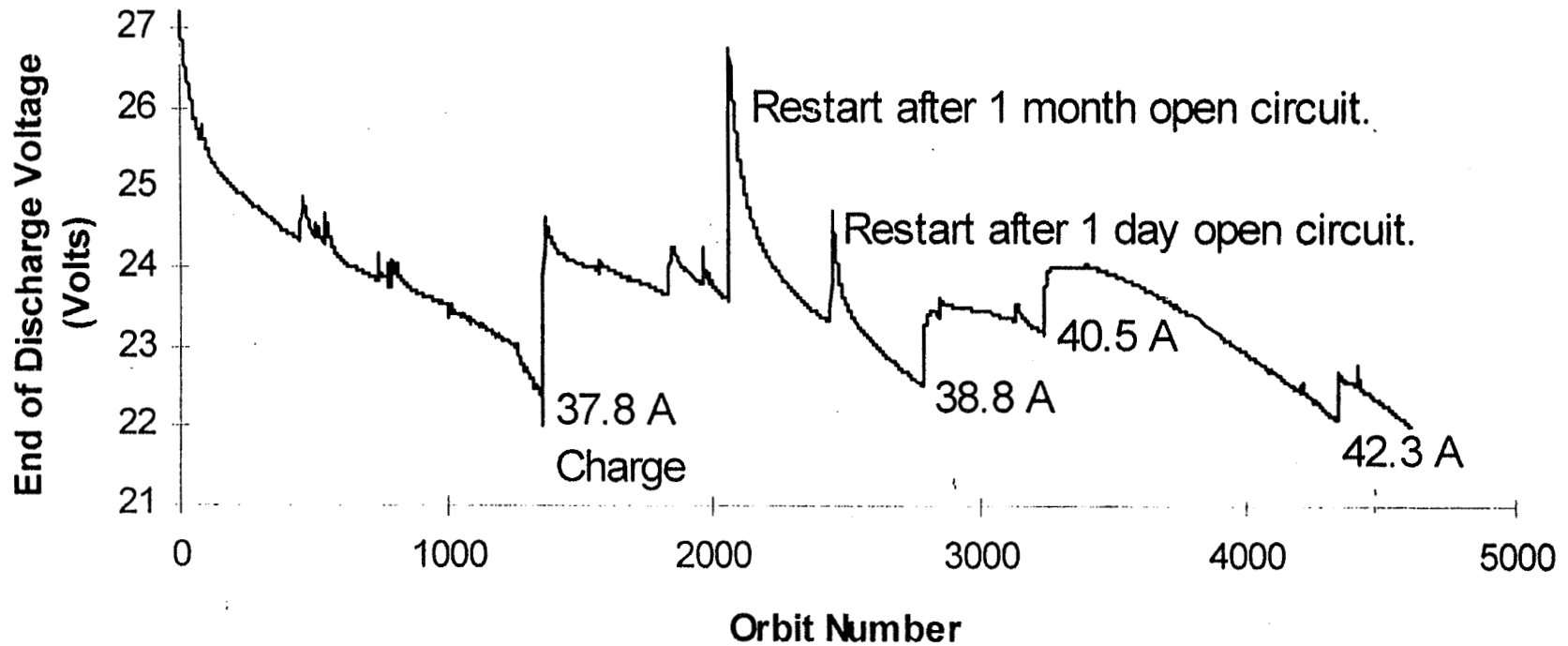
ACCELERATED SPV LIFE TEST

- ✦ **10°C test**
- ✦ **100 minute LEO cycles**
- ✦ **70% DOD**
- ✦ **Increased charge rate as necessary to maintain 22V minimum**
- ✦ **Completed requirement of 4,612 total cycles**
- ✦ **Continued with low rate (31% DOD) 100-minute LEO cycles**
- ✦ **Completed an additional 4,812 cycles**
- ✦ **DPA revealed cells in excellent condition**

HIGH RATE CYCLES - ACCELERATED LIFE TEST



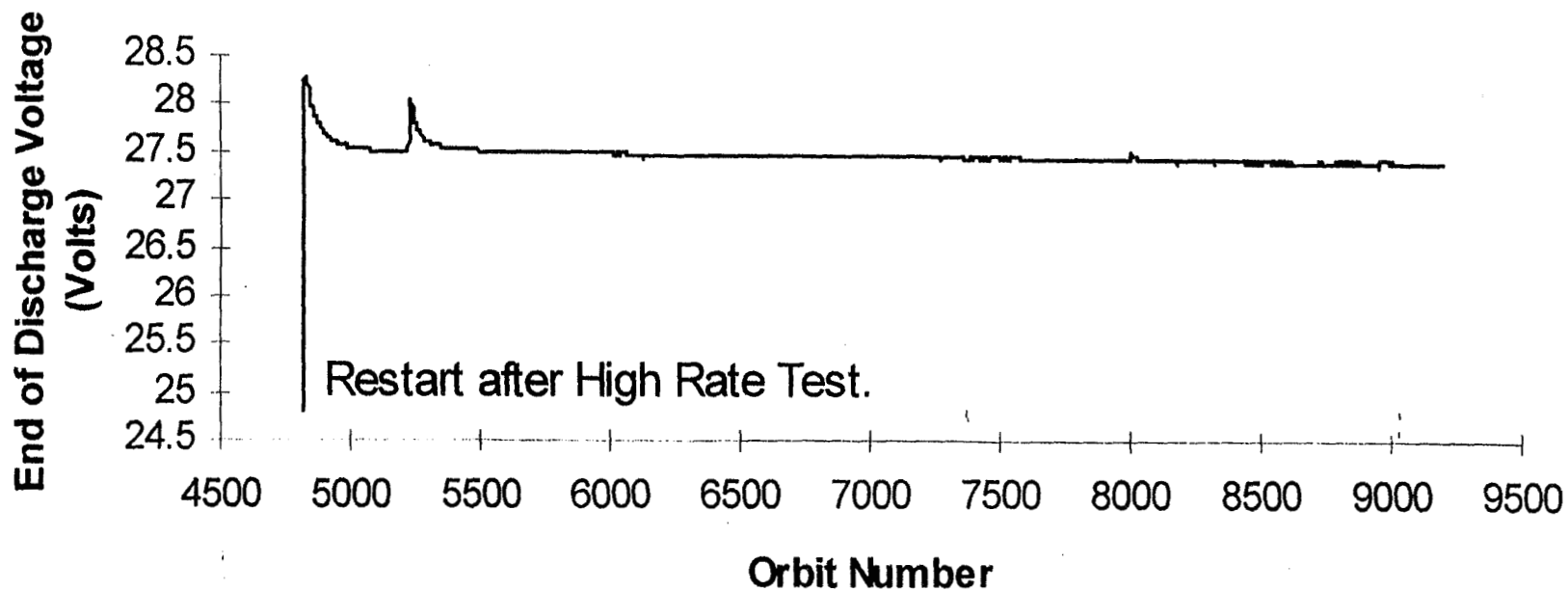
Graph 1. High Rate EODV vs. Orbit Number



LOW RATE CYCLES - ACCELERATED LIFE TEST



Graph 2. Low Rate EODV vs. Orbit Number



Conclusions

◆ Total Spacecraft On-Orbit	128
◆ Total Cells On-Orbit	5,966
◆ Total Operational Cell Hours On-Orbit	209,089,724
◆ Longest Running ACC LEO	127,770 + Cycles
◆ Longest Running RT LEO	69,806 + Cycles
◆ Longest Running ACC GEO	44 + Seasons
◆ Longest Running RT GEO	42 + Seasons
◆ Longest Running On-Orbit LEO	41,410 + Cycles
◆ Longest Running On-Orbit GEO	29 + Cycles

EOS-AM1 Nickel Hydrogen Cell Interim Life Test Report

by

C.W. Bennett

Lockheed Martin Missiles and Space

D.J. Keys, G.M. Rao

NASA/GSFC

H.E. Wannemacher

Jackson and Tull

H. Vaidyanathan

COMSAT Laboratories

(Performed under NASA Contracts NAS5-32500 and NAS5-32600)

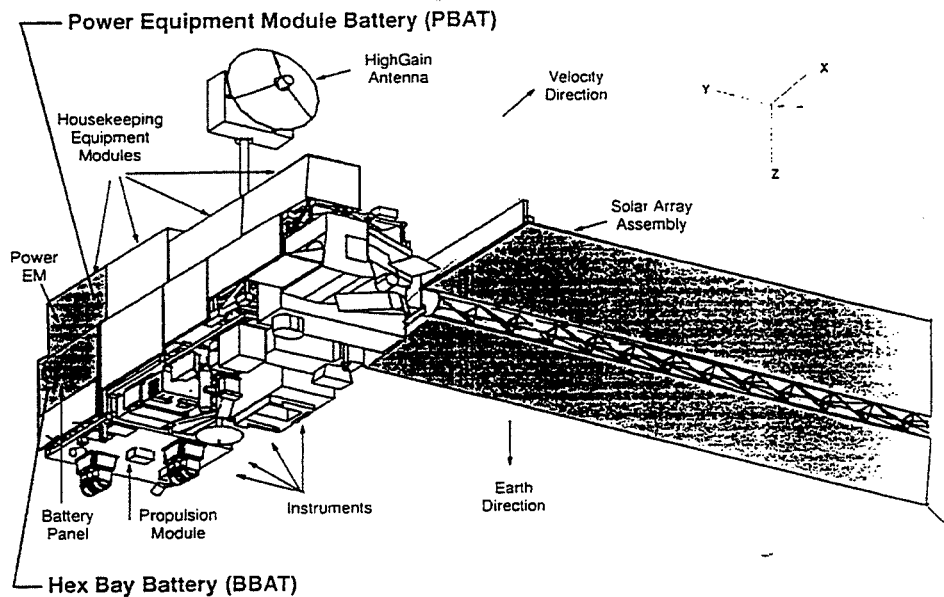
Abstract



This paper reports the interim results of the Earth Observing System AM-1 project (EOS-AM-1) nickel hydrogen cell life test being conducted under contract to National Aeronautics and Space Administration (NASA) Goddard Space Flight Center (GSFC) at the Lockheed Martin Missiles and Space (LMMS) facility in East Windsor, NJ; and at COMSAT Labs., Clarksburg, MD. The purpose of the tests is to verify that the EOS-AM-1 cell design can meet five years of real-time Low Earth Orbit (LEO) cycling. The tests include both real-time LEO and accelerated stress tests. At LMMS, the first real-time LEO simulated 99 minute orbital cycle started on February 7, 1994 and the test has been running continuously since that time, with 18202 LEO cycles completed as of September 1, 1997. Each cycle consists of a 64 minute charge (VT at 1.507 volts per cell, 1.06 C/D ratio, followed by 0.6 ampere trickle charge) and a 35 minute constant power discharge at 177 watts (22.5% DOD). At COMSAT, the accelerated stress test consists of 90 minute orbital cycles at 60% DOD with a 30 minute discharge at 60 amperes and a 60 minute charge at 40 amperes (VT at 1.54 volts per cell to 1.09 C/D ratio, followed by 0.6 ampere trickle charge).

The real-time LEO life test battery consists of seven, 50AH (nameplate rating) Eagle-Picher, Inc. (EPI) Mantech cells manufactured into three, 3-cell pack assemblies (there are two place holder cells that are not part of the life test electrical circuit). The test pack is configured to simulate the conductive thermal design of the spacecraft battery, including: conductive aluminum sleeves, 3-cell pack aluminum baseplate, and honeycomb panel all mounted to a liquid (-5°C) cold plate. The entire assembly is located in a thermal chamber operating at +3°C. The accelerated stress test unit consists of five cells mounted in machined aluminum test sleeves and is operating at +10°C.

The real-time LEO life test battery has met all performance requirements through the first 18,202 cycles, including: end of charge and discharge cell voltages and voltage gradients; end of charge and discharge cell pressures; within cell and between cell temperature gradients; discharge capacity; current and power levels; and all charge parameters. The accelerated stress test battery has completed 11998 cycles when the test was terminated. The stress test unit met all test parameters. This paper reports battery performances as a function of cycle life for both the real-time LEO and the accelerated life test regimes.



Outline

- EOS-AM cell parameters
- Real-time LEO test conditions
- Real-time LEO test results
 - Figures 1-9
- Accelerated LEO stress test conditions
- Accelerated LEO stress test results
 - Figures 10-18
- Summary and conclusions

EOS-AM Cell Parameters



- Single stack, IPV, Mantech design
- Rabbit ear terminals
- 40, 30 mil slurry electrodes
- Back to back with double layer Zircar, catalyzed wall wick
- 31% KOH, nickel precharge
- Average cell weight = 1490 grams
- Average delivered capacity (C/2 discharge)
 - 10°C: 75 AH
 - 0°C: 71 AH
 - +10°C: 63 AH
 - +20°C: 56 AH
 - +30°C: 51 AH
 - +10°C, 72 hour charge retention: 92% lot ave, 89% minimum

Real-time LEO Test Conditions



- Performed at LMMS, East Windsor, NJ
- Number of cells: 7
- Cell configuration:
 - Conductive thermal design with same configuration as spacecraft
 - Machined aluminum sleeves and baseplate
 - Chootherm and RTV 566 isolation
 - Mounted to spacecraft honeycomb panel with Al face sheets
 - Liquid cooled (-5°C) cold plate
- Discharge regime: 177 watts (total) constant power discharge for 35 minutes
- Depth of discharge: 22.5% nominal
- Charge regime:
 - 12.3 ampere to 1.507 V/T (per cell), taper to 1.06 C/D, 0.6 A trickle
 - 64 minute total charge time

Schedule of Test Interruptions and Changes

Event	Date	Cycle	Description
1	2/21/94	200	Charge time reached prior to VT limit. Several test aborts
2	4/26/94	1110	Cells discharged ~ 45 Ah without recharge. Charge time limit reached prior to VT limit
3	10/21/94	3500	VT changed from 10.550 to 10.626
4	10/28/94	3750	Discharge load changed from 177 watts to 88 watts
5	11/5/94	3850	Discharge load changed from 88 watts to 177 watts
6	11/7/94	3900	VT changed from 10.626 to 10.550
7	2/7/95-3/26/95	5200-5900	Data printouts not found
8	5/15/95	6600	Several short duration test aborts
9	6/30/95-7/3/95	7200	Test cells on open circuit due to STE problems
10	9/1/95-9/28/95	8100	Test cells on open circuit due to STE problems
11	11/10/95-11/11/95	8700	Test cells on open circuit due to STE problems
12	9/1/96	12950	Test cells on open circuit due to STE problems
13	2/24/97	15501	Charge parameters changed: Current 12.25A to 15.0A, V/T 10.55 to 10.70, C/D 1.05 to 1.20
14	3/3/97	15601	Charge parameters changed: Current 15.0A to 12.25A, V/T 10.70 to 10.55, C/D 1.20 to 1.05
15	4/7/97	16101	Charge parameters changed: Current 12.25A to 15.0A, V/T 10.55 to 10.70, C/D 1.05 to 1.20
16	4/15/97	16201	Charge parameters changed: Current 15.0A to 12.25A, V/T 10.70 to 10.55, C/D 1.20 to 1.05
17	4/28/97	16401	Charge parameters changed: Current 12.25A to 15.0A, V/T 10.55 to 10.70, C/D 1.05 to 1.20
18	5/5/97	16501	Charge parameters changed: Current 15.0A to 12.25A, V/T 10.70 to 10.55, C/D 1.20 to 1.05
19	8/18/97	18001	Charge parameters changed: Current 12.25A to 11.9A, V/T 10.55 to 10.48, Trickle 0.60A to 2.0A, No C/D, Discharge load 177W to 86.5W
20	8/25/97	18101	Change to standard orbit: 177W discharge, 12.25A charge, V/T=10.55V, C/D=1.05, Trickle=0.60A
21	9/1/97	18202	Final orbital cycle prior to shutdown for move to new facility
22	9/3/97-9/10/97	18205	Special test sequence: 10°C capacity, 10°C 72 hour charge retention, 10°C capacity

Fig 1

End of Charge and Discharge Battery Voltage vs LEO Cycle

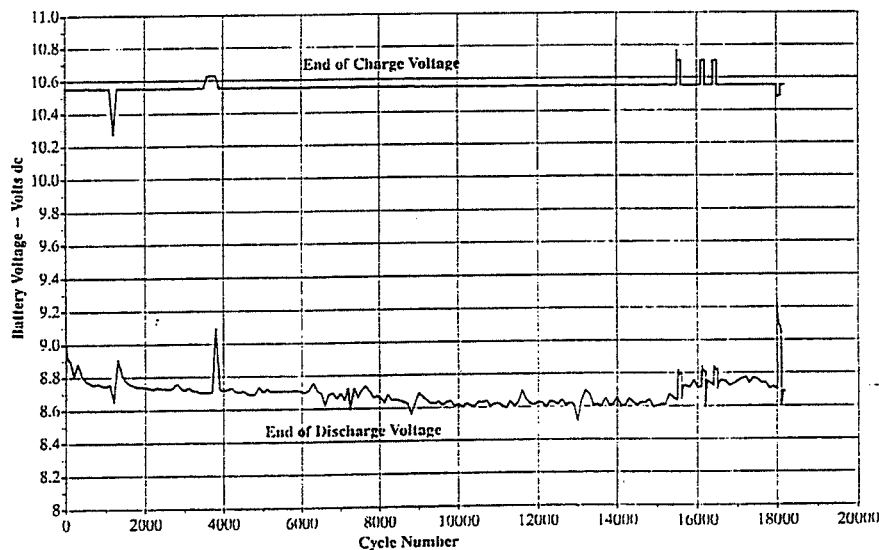


Fig 2



Minimum and Maximum Cell End of Charge Voltage vs LEO Cycle

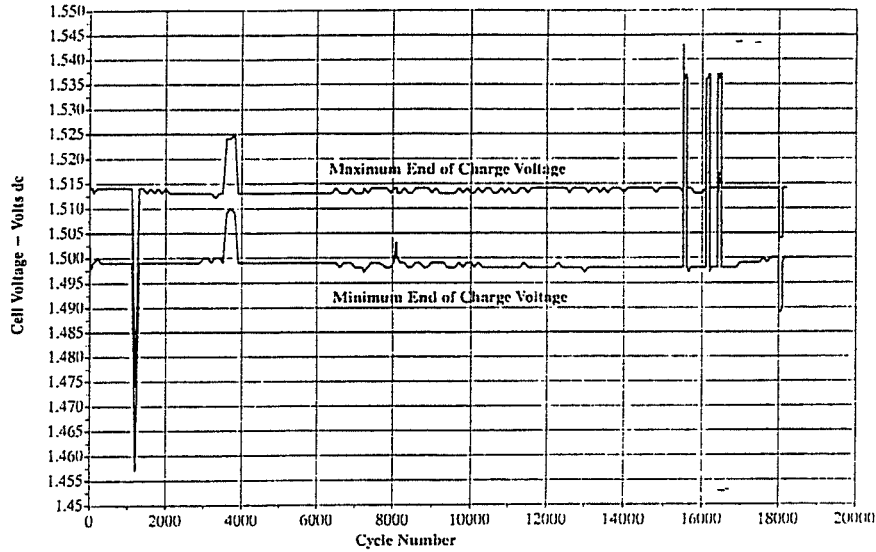


Fig 3



Minimum and Maximum Cell End of Discharge Voltage vs LEO Cycle

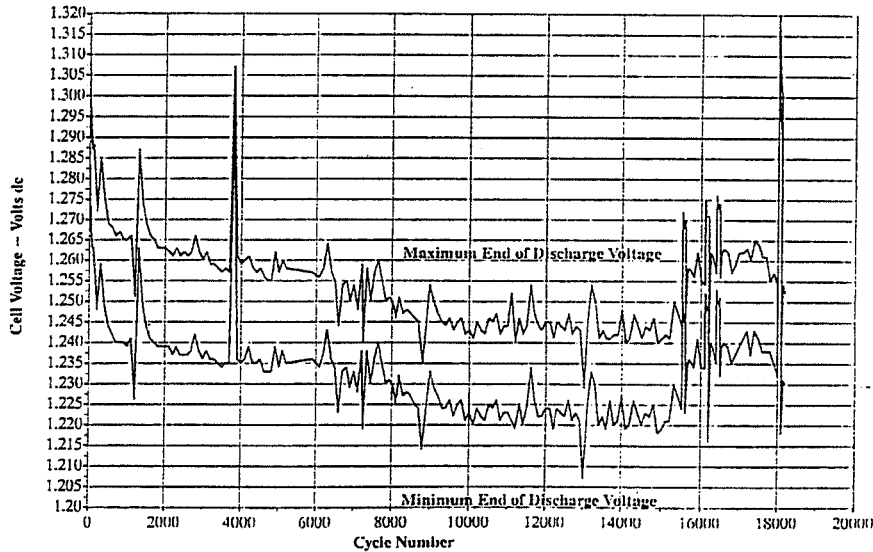


Fig 4



End of Discharge Cell Voltage Gradient vs LEO Cycle

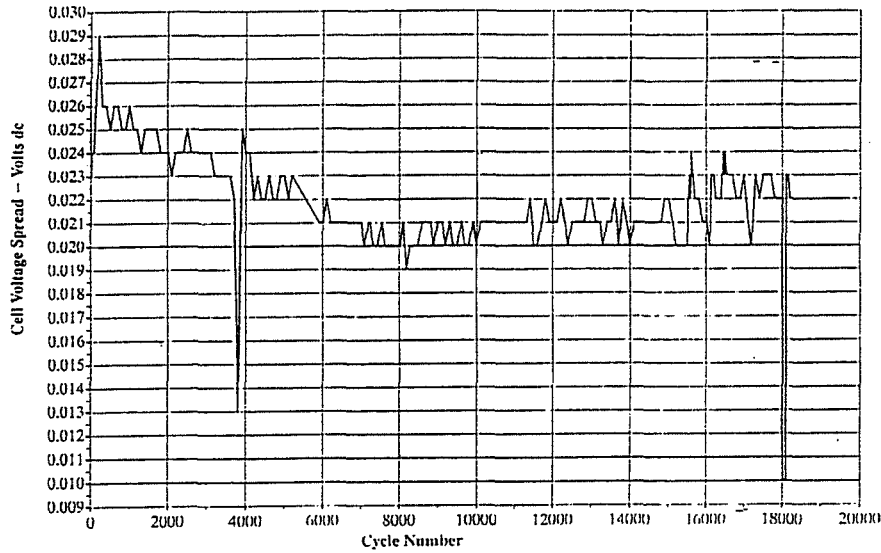


Fig 5



C/D Ratio (Total Charge Capacity/Total Discharge Capacity) vs LEO Cycle

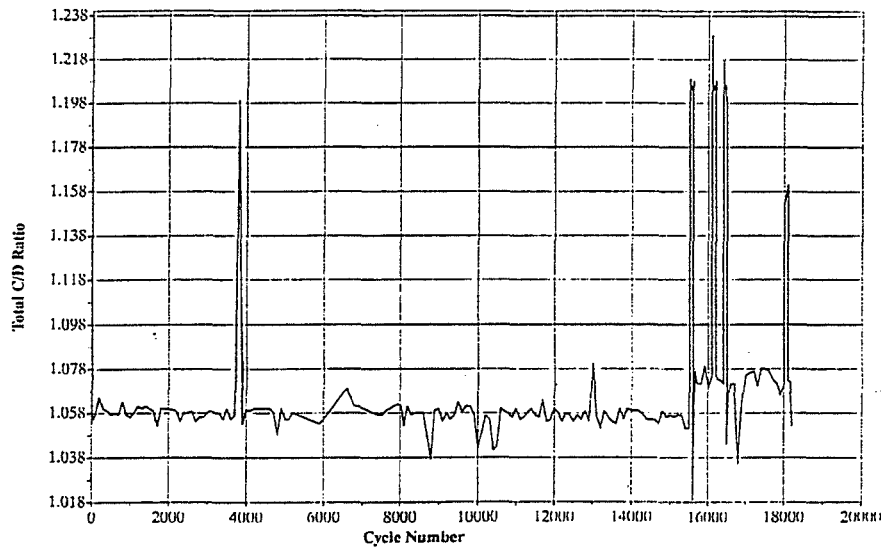


Fig 6



Cell 1 Pressure vs LEO Cycle

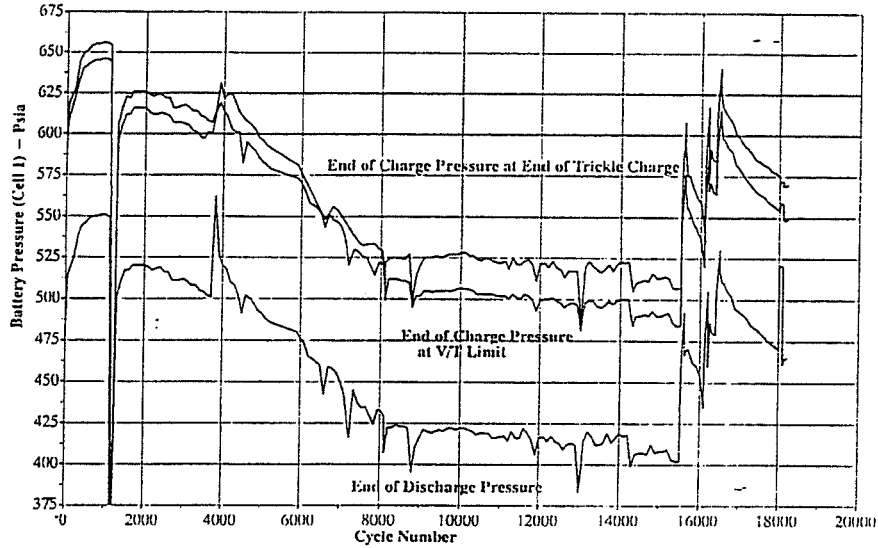


Fig 7



Individual Cell Charge Voltage for Cycle 17830

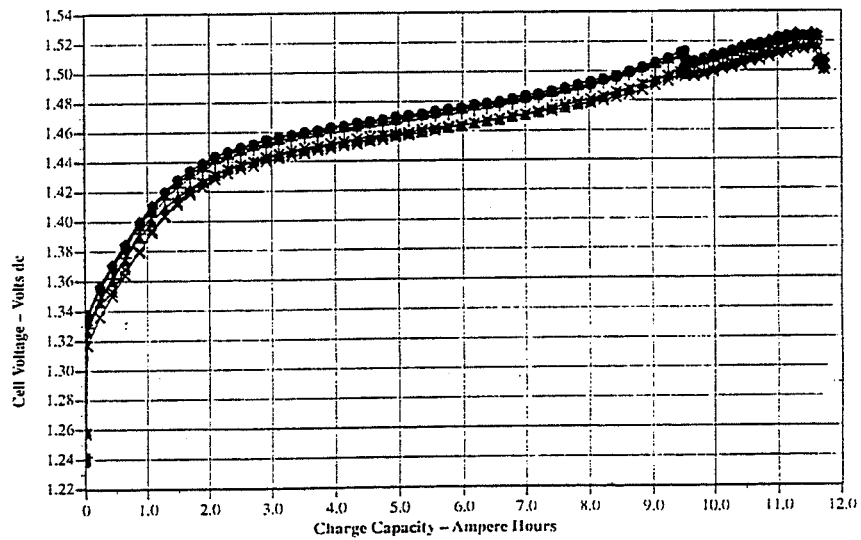


Fig 8

Individual Cell Discharge Voltage for Cycle 17830

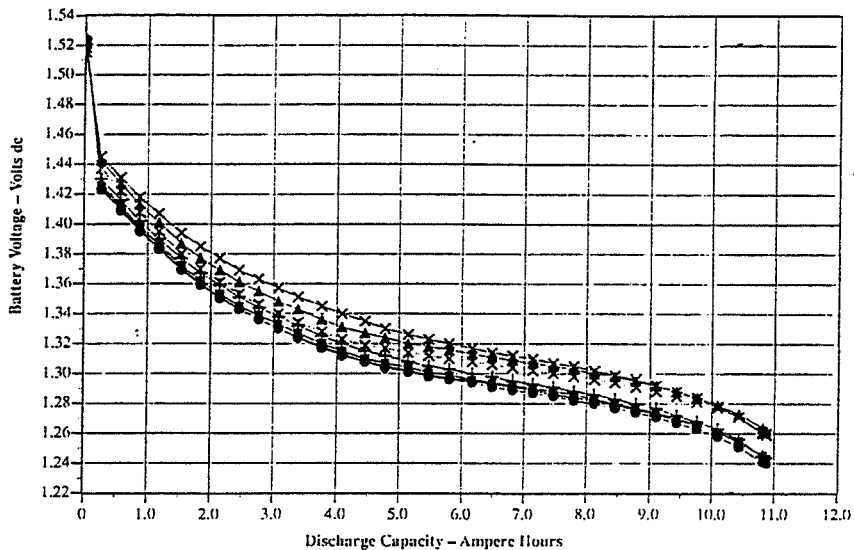
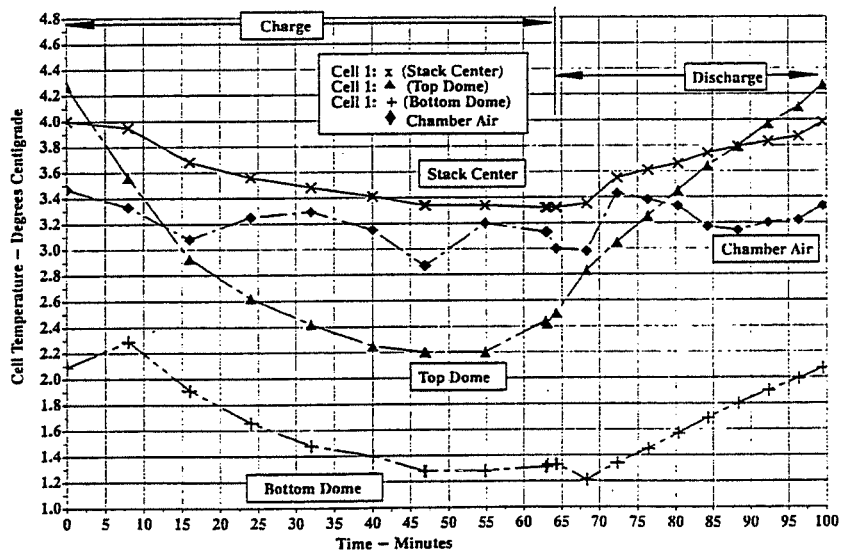


Fig 9

Cell 1 Temperature Profile for Cycle 11800



Accelerated Stress Test Conditions



COMSAT LABORATORIES

- Performed at COMSAT Laboratories
- Number of cells: 5
- Cell configuration:
 - Machined aluminum sleeves
 - Mounted on a cold plate
 - Choitherm and RTV 566 isolation
- Test temperature: 10°C
- Discharge regime:
 - 60 amperes for 30 minutes
- Depth of discharge: 60%
- Charge regime:
 - 40 ampere to 1.54 V/T (per cell), taper to 1.09 C/D, 0.6 A trickle
 - 60 minute total charge time

Fig 10



COMSAT LABORATORIES

Voltage and Current Profiles for Cycle 11998

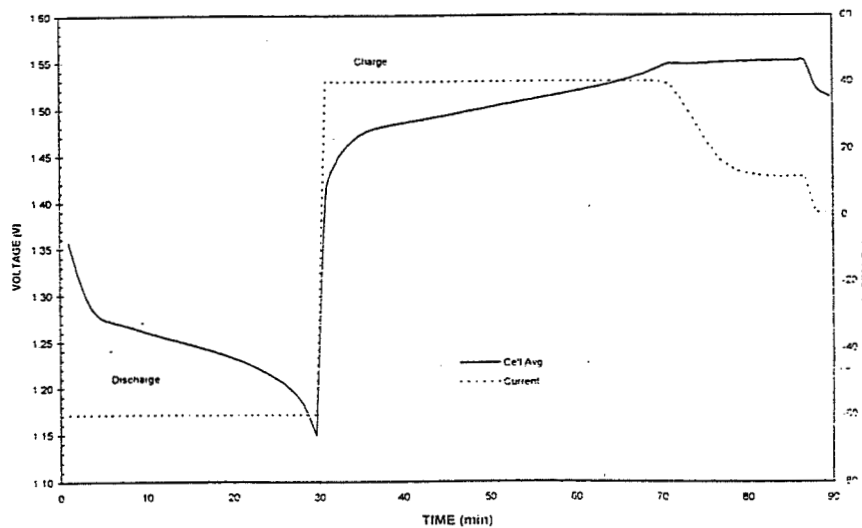


Fig 11



COMSAT LABORATORIES

C/D Ratio

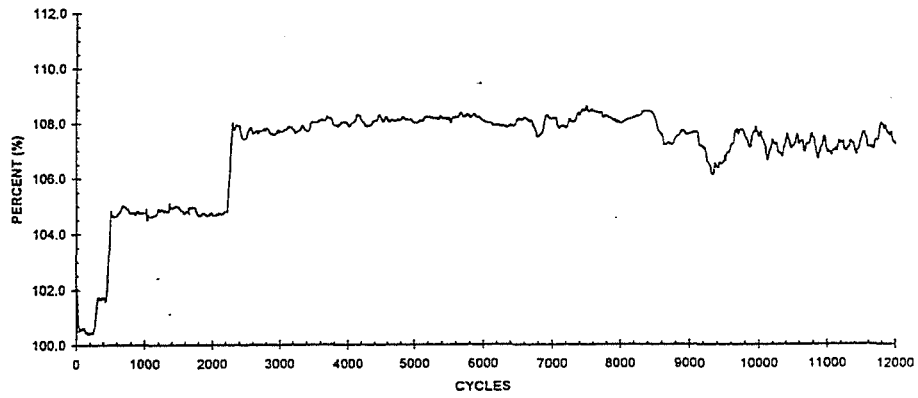


Fig 12



COMSAT LABORATORIES

End of Discharge Sleeve Temperature

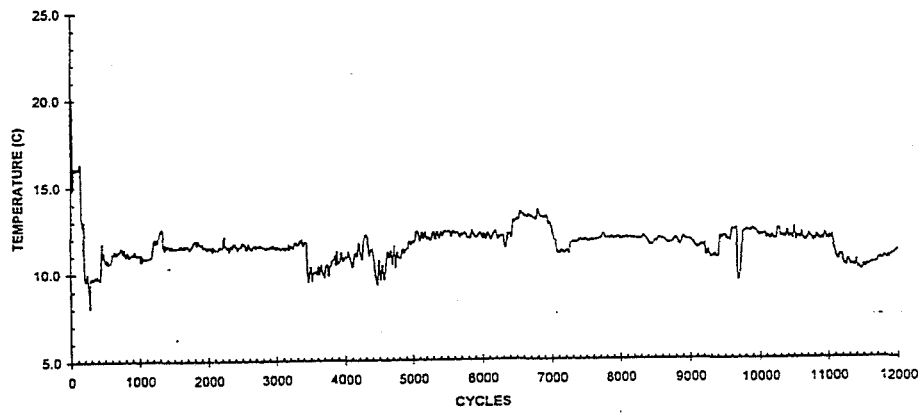


Fig 13



COMSAT LABORATORIES

End of Discharge Average Cell Voltage

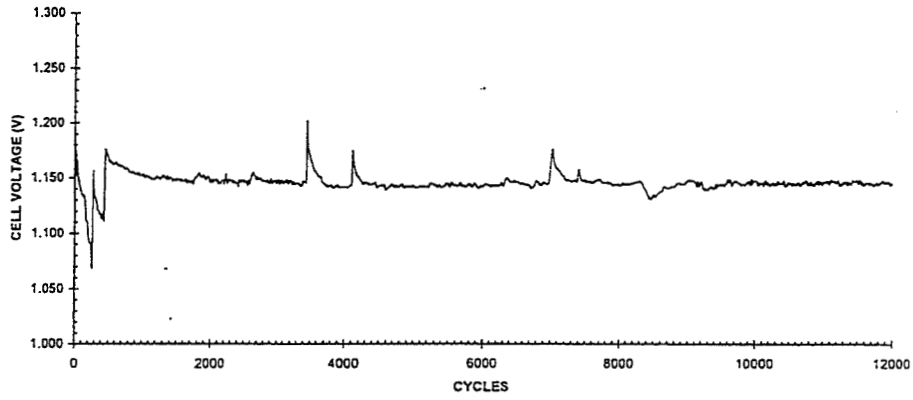


Fig 14



COMSAT LABORATORIES

End of Discharge Individual Cell Voltages

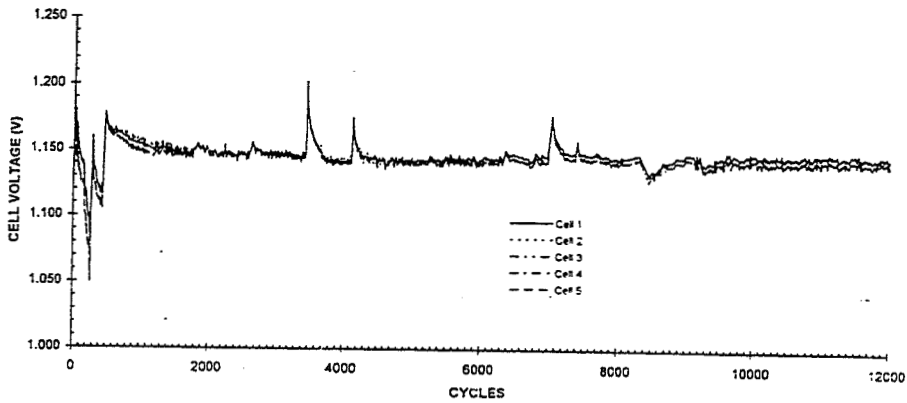


Fig 15



COMSAT LABORATORIES

End of Charge Pressure

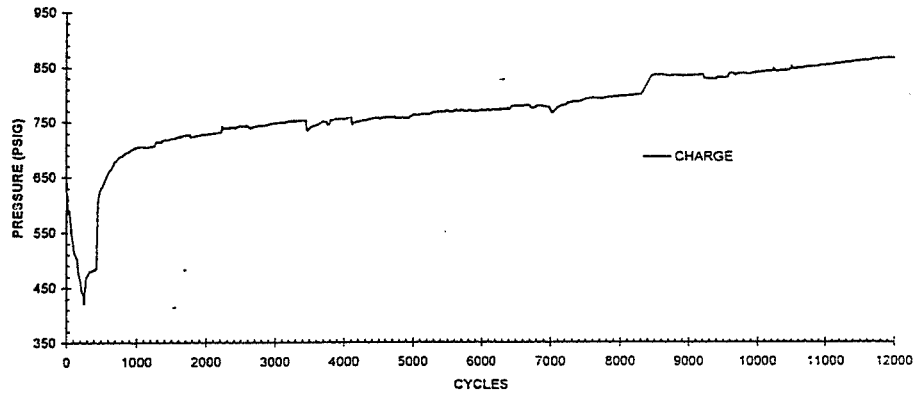


Fig 16



COMSAT LABORATORIES

End of Discharge Pressure

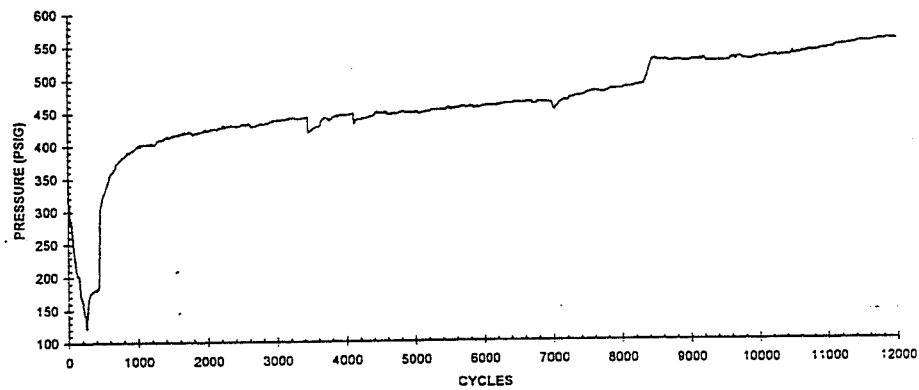


Fig 17



COMSAT LABORATORIES

End of Charge Current

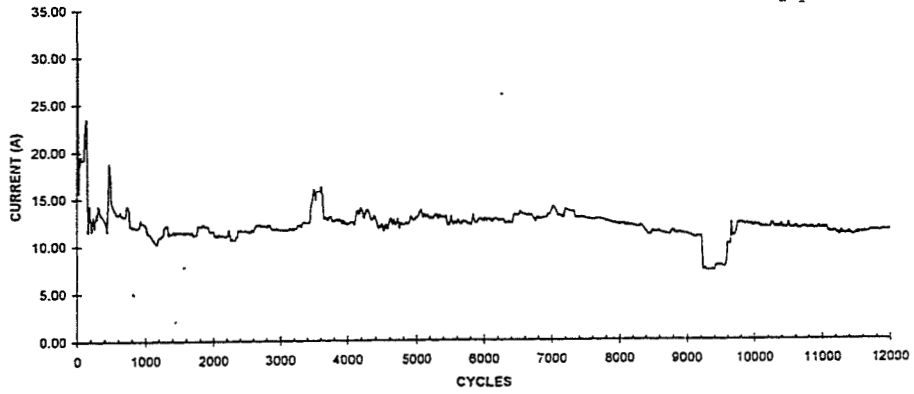
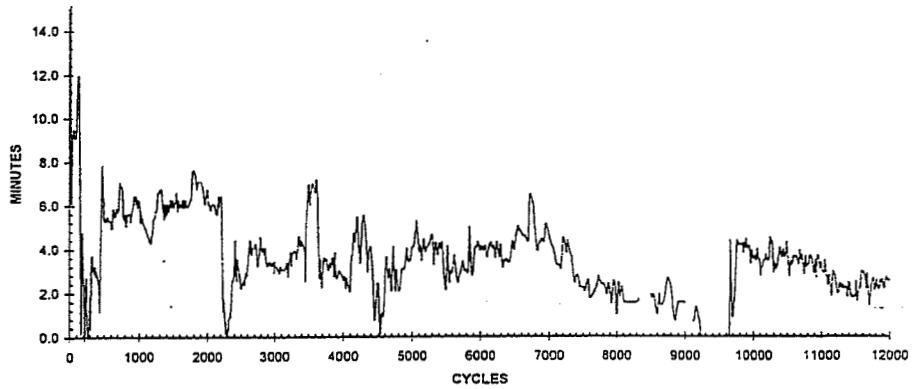


Fig 18



COMSAT LABORATORIES

Trickle Charge Period Duration



Summary and Conclusions



- Real-time LEO life test at Lockheed Martin Missiles and Space
 - Cells have completed 18203 cycles as of 9/1/97
 - End of discharge voltage decreased initially and has stabilized
 - Variation in end of discharge cell voltage has converged with cycling
 - Cell EODP and EOCP stabilized after 8000 cycles
 - – 1.51 V/T limit and 1.06 C/D insufficient to makeup for early test problems (cells on open circuit during all test outages)
 - There was no full reconditioning performed during the first 18203 cycles
- Accelerated LEO stress test at COMSAT Labs.
 - Cells have completed 11998 cycles
 - End of discharge voltage decreased initially and has stabilized
 - Charge termination at 1.55 V and 1.08 C/D is appropriate for 60% DOD cycling
 - EOC and EOD Pressure have increased with cycling
 - Two reconditioning cycles performed
 - – Temporary voltage improvement for approximately 100 cycles

Characterization and Initial Life-Test Data for Computer Designed Nickel Hydrogen Cells

A. Zimmerman, J. Matsumoto, A Prater, D. Smith, and N. Weber
Electronics Technology Center
The Aerospace Corporation
El Segundo, California 90245

Abstract

Five advanced nickel hydrogen battery cells have been acquired based on specifications developed from a first principles battery performance model, with the objective of reducing internal cell impedance by 50%, while improving cycle life and performance. The initial performance of these cells has been characterized and is reported here, and has been found to match the performance predicted by the model quite well. The cells have been placed in a cycle life test at 60% depth-of-discharge and 10 deg C using a standard V/T charge control method. A recharge ratio between 102 and 103% was obtained employing a charge voltage level of 1.488 volts/cell, giving stable performance for the first 830 cycles. At 830 cycles an equipment failure subjected the cells to 9 hr of overcharge at 1.2C, after which capacity was degraded and recharge voltages increased. Cycling is being continued at a higher voltage level.

The standard individual pressure vessel nickel hydrogen cells used in modern satellites have been optimized over the years to have a relatively high energy density, in many respects compromising the voltage, power, or cycle life capability of these cells relative to the ultimate capability of nickel hydrogen battery technology. For applications not involving low altitude orbits, cell weight is often not the overriding battery issue. Efficiency, high pulse power capability, improved voltage regulation, or improved life capability (operation at greater depth-of-discharge) are often highly desirable battery performance traits. To evaluate how nickel hydrogen battery technology may better power these kinds of satellites, an effort has been made to optimize the state-of-the-art nickel hydrogen technology to reduce internal cell impedance by at least 50%, while enhancing the cycle life capability and overall robustness of the cell to handle high rates and high depths-of-discharge. This optimization was performed utilizing a first-principles nickel hydrogen battery model developed at The Aerospace Corporation. This model performed a full optimization of the standard MANTECH design with the constraint that no redesign of existing electrode types was allowed, and considered hydrogen, oxygen, electrolyte, and thermal management issues in addition to electrical performance.

The optimized cell design basically consisted of a "dual anode" stacking arrangement, in which each nickel electrode has both of its faces in contact with separator and a hydrogen electrode. This stacking arrangement requires twice the number of hydrogen electrodes as does the more standard back-to-back stack design, but has the advantages of equally utilizing both faces of the nickel electrodes, doubling the available surface area in contact with the separator, cutting mass transport and conduction distances within the nickel electrodes in half, and doubling the oxygen management capability of the cell. The computer model found that a nearly optimum electrolyte level was obtained using a single layer of Zircar separator, which provides a total electrolyte fill approximately the same as that obtained in the standard back-to-back stack design having two layers of Zircar separator. The optimized cell design also contained a zirconium oxide wall wick, twice the number of leads from the plates, 31% KOH electrolyte, a nickel precharge, and an axial cell terminal configuration. Because of the doubling in the number of hydrogen electrodes and the improved oxygen gas management capabilities of the design, the advantages of a recombination wall wick were found to be less significant than in the standard back-to-

back design, and therefore was not included. The optimized cell design utilizes a 4.5 inch diameter cell assembly, and 30 mil thick nickel electrodes having 80% porosity plaque.

Following these general design specifications, five cells were built by Eagle-Picher Industries, and are referred to as RNH 60-3 cells. Several compromises in the optimized design were made to obtain these cells using components that were readily available. First, a 3.5 inch rabbit-ear cell assembly was employed, giving a longer cell and longer thermal dissipation paths than were optimum. The 3.5 inch diameter cell hardware also did not provide enough core space to contain a lead from each plate, thus resulting in leads from each plate only for the plates in the lower half of the stack. This change was predicted to reduce the improvement in cell impedance by about 25%, but still giving an approximately 50% impedance improvement over the more standard cell designs. Finally, 35 mil thick nickel electrodes were used (slurry type), a change that was not expected to have a significant impact on performance. The maximum pressure expected in these cells is about 600 psi of hydrogen at full charge.

The five cells were placed into an extensive characterization test regime to evaluate their capacity, voltage behavior, charge efficiency, and self-discharge rates as functions of state-of-charge and temperature. Characterization was done at 20, 10, 0, and -10 deg C. Figures 1 and 2 indicate charge and discharge voltages respectively over this temperature range for a standard charge (16 hr at C/10) and discharge (C/2 to 1.0 volts). As predicted and indicated in Fig. 3, these cells have a higher discharge voltage and a lower charge voltage than do standard cells. Voltage behavior at a given temperature can best be summarized in terms of a set of I/V curves which track voltage as a function of current at discrete states-of-charge. Figures 4 and 5 provide a summary of I/V behavior at 0 and 20 deg C for 25, 50, and 75% states-of-charge. The slopes of these I/V lines at high currents provide the best indication of internal cell impedance, including electrochemical reaction impedance, lead resistance, and the resistance of the polarized separators and plates. These cells have impedances of about 1 mohm at the higher states of charge, with a slightly higher impedance being seen at 0 deg C than at 20 deg C. Cells of this size (60 Ah) typically have an internal impedance of 1.5 to 1.8 mohm when all polarizations are included.

The capacity of the cells was found to range from 58 Ah at 20 deg C, to nearly 80 Ah at -10 deg C. The capacity trend is indicated in Fig. 6, and shows that the capacity is best at about -10 deg C, having appeared to level off just below 80 Ah. Thus, these cells are conservatively rated at 60 Ah for usage in the normal temperature range of 0 to 10 deg C. For these cells, there appears to be no reason why the lower operating temperature range could not be extended down to -10 deg C. Figure 7 indicates charge efficiency as a function of state-of-charge for each test temperature. The trends in Fig. 7 mirror the cell capacity function of Fig. 6, with the quite high charge efficiency obtained at low temperatures giving a very high stored capacity.

The self-discharge rate in this cell design based on the variations in observed total capacity from different duration discharges. Figure 8 indicates self-discharge as a function of state-of-charge at 20 deg C. As expected, the self-discharge rate increases with increasing state of charge. This increase is because the hydrogen pressure increases with state-of-charge and because the oxygen evolution rate increases exponentially at high states-of-charge. Fig. 8 indicates that even at 20 deg C, 100% state-of-charge can be maintained with a C/60 trickle charge rate. Trickle charge rates as low as C/240 can maintain a 70% state-of-charge. A standard 72 hr charged stand test was conducted on these cells at 20 deg C, with the result that they retained 83.9% of their capacity. These results indicate that the increases in plate area exposed to the separators and hydrogen electrodes have not resulted in a significant increase in charge losses for this cell design.

After completion of characterization testing, the cells were placed into a cycle life test at 60% depth-of-discharge, utilizing a 90 minute cycle (30 minute discharge, 60 minute charge). The average cell temperature during the life test cycle was held at 10 deg C. The discharge was at 72 amps for the full 30 minute period. Recharge utilized a peak charge rate of 72 amps, with a voltage limit that at present is 1.488 volts per cell. When the voltage hits this level, the current is tapered back at a rate that maintains a constant voltage level within a 5 mv band. The goal at present is to return 102 to 103% of the discharged capacity during recharge for each cycle. The voltage level of 1.488 volts per cell gave 102-102.4% recharge ratio and stabilized performance for about 830 cycles, after which a test equipment failure resulted in the cells being overcharged at 72 amps (1.2C) for 9 hr. After this event, as indicated in Fig. 9, the charge return ratio dropped to just above 100%, and the cells quickly ran down in capacity due to inadequate charge return. Re-characterization of the cells showed an increase of at least 30 mv in the

recharge voltage curves for the cells, as well as about a 25% reduction in cell capacity. However, the cells all still delivered over 52 Ah of capacity at the 72 amp discharge rate. The cells are presently resuming life testing with an increased charge voltage level.

Figures 9-11 indicate the end-of-discharge voltage, end-of-charge voltage, and recharge ratio during the first 1100 cycles of the life test. At about cycle 200 the cells went through about 16 cycles with no discharge, but repeated recharge. Between cycles 200 and 830 the end-of-discharge voltages dropped about 6 mv, and the end-of-charge voltages have spread apart 3-4 mv. These changes are quite small, thus at present it is not clear if they signify drift in cell performance or simply a stabilization at slightly different levels. There was no significant change in end-of-charge or end-of-discharge pressure since cycle 200 up to the test anomaly at cycle 830, suggesting that there was not any significant loss in stored capacity. Performance will continue to be trended after the life test is restarted, again trying to attain the minimum stable recharge ratio that keeps end of discharge voltage above 1.1 volts.

The intent in this life test is maintain the recharge voltage at the minimum level that is just sufficient to maintain capacity of the cells. Failure is defined as voltage falling below 1.0 volts, combined with an inability to correct the low voltage by increasing recharge voltage level. It is anticipated that many years of cycling will be completed prior to cell failures, even after the accelerated aging that the cells experienced as a result of the recent test anomaly. Cells will be disassembled and analyzed when any failures occur, to determine the cause of the failure and whatever cell degradation modes are occurring along with the life cycling or as a result of the test anomaly.

Figure 1

C/10 Charge Voltage vs. Temperature

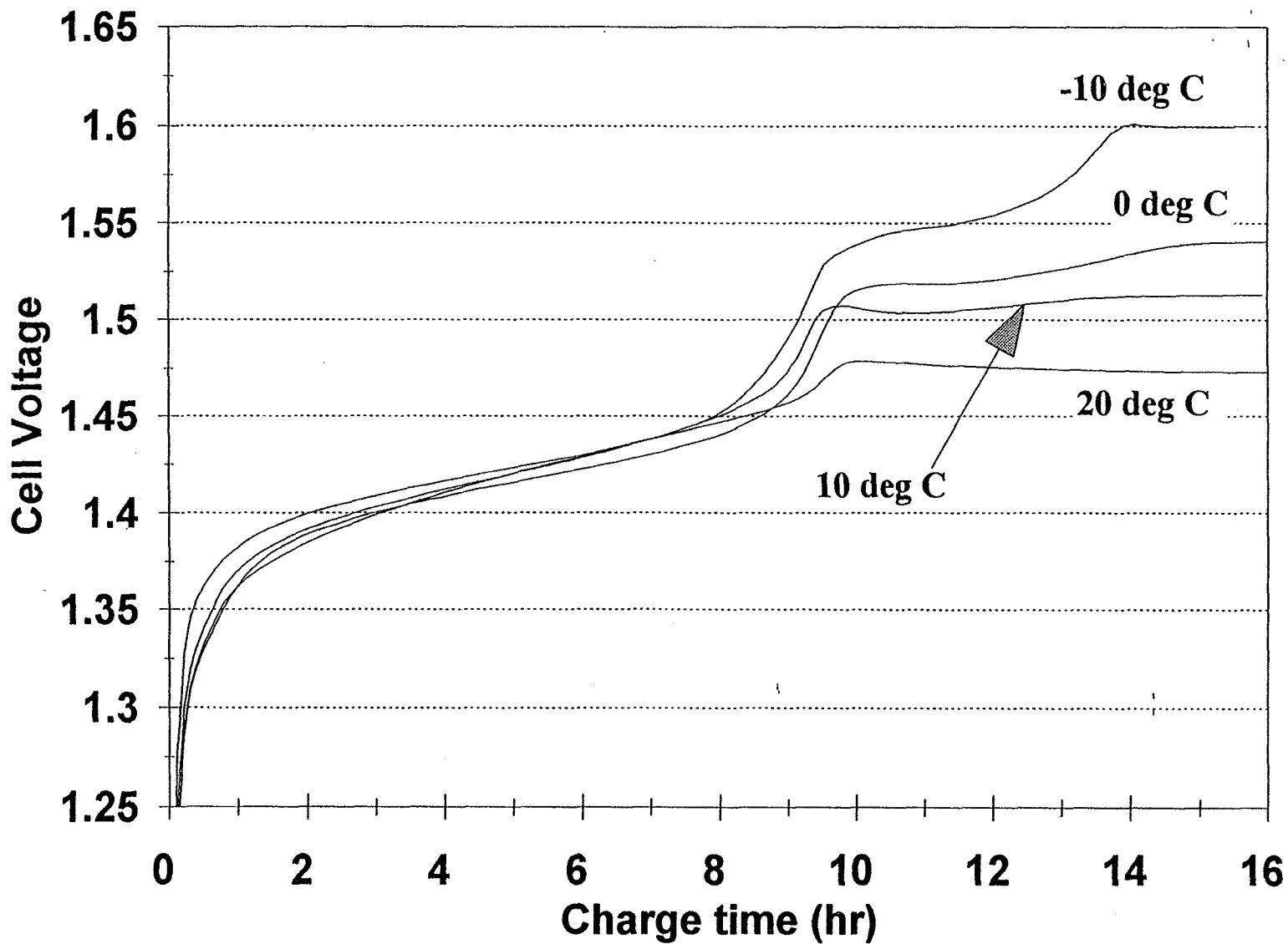


Figure 2

C/10 Discharge Voltage vs. Temperature

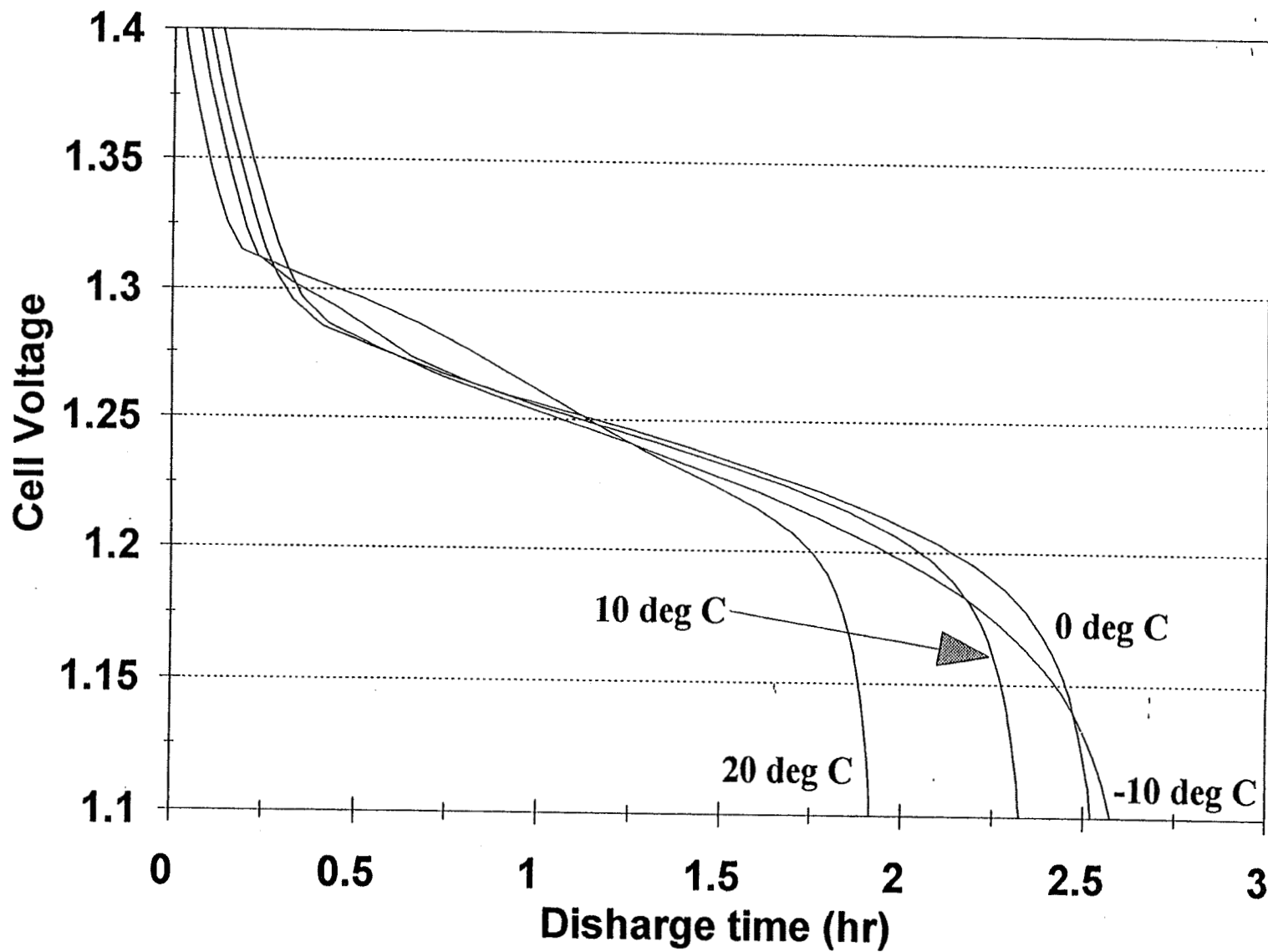


Figure 3

Charge/Discharge Voltages for Different Cell Designs

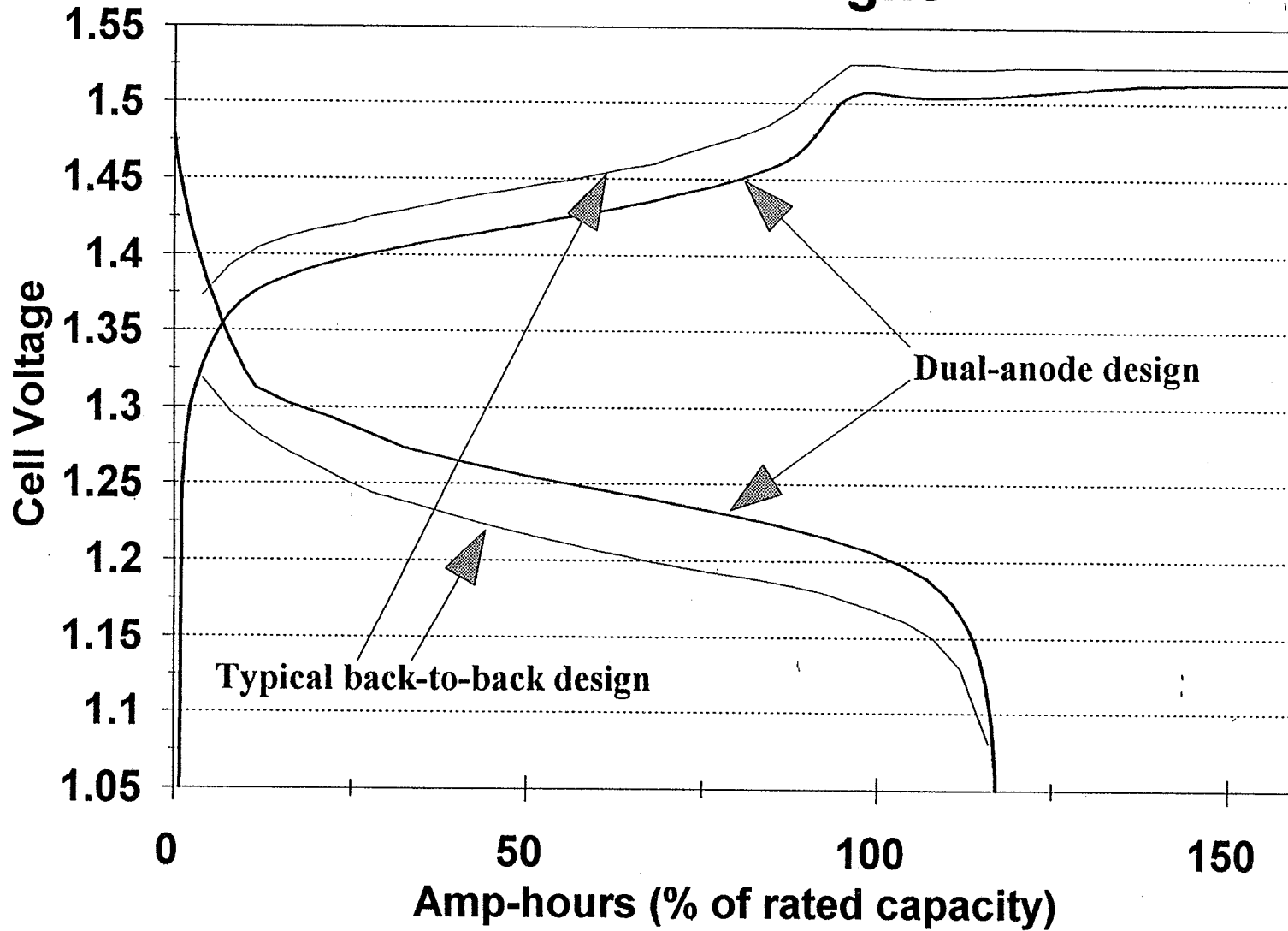


Figure 4

I/V Curves for Dual Anode Cells, 0 C at 25%, 50%, and 75% State-of-Charge

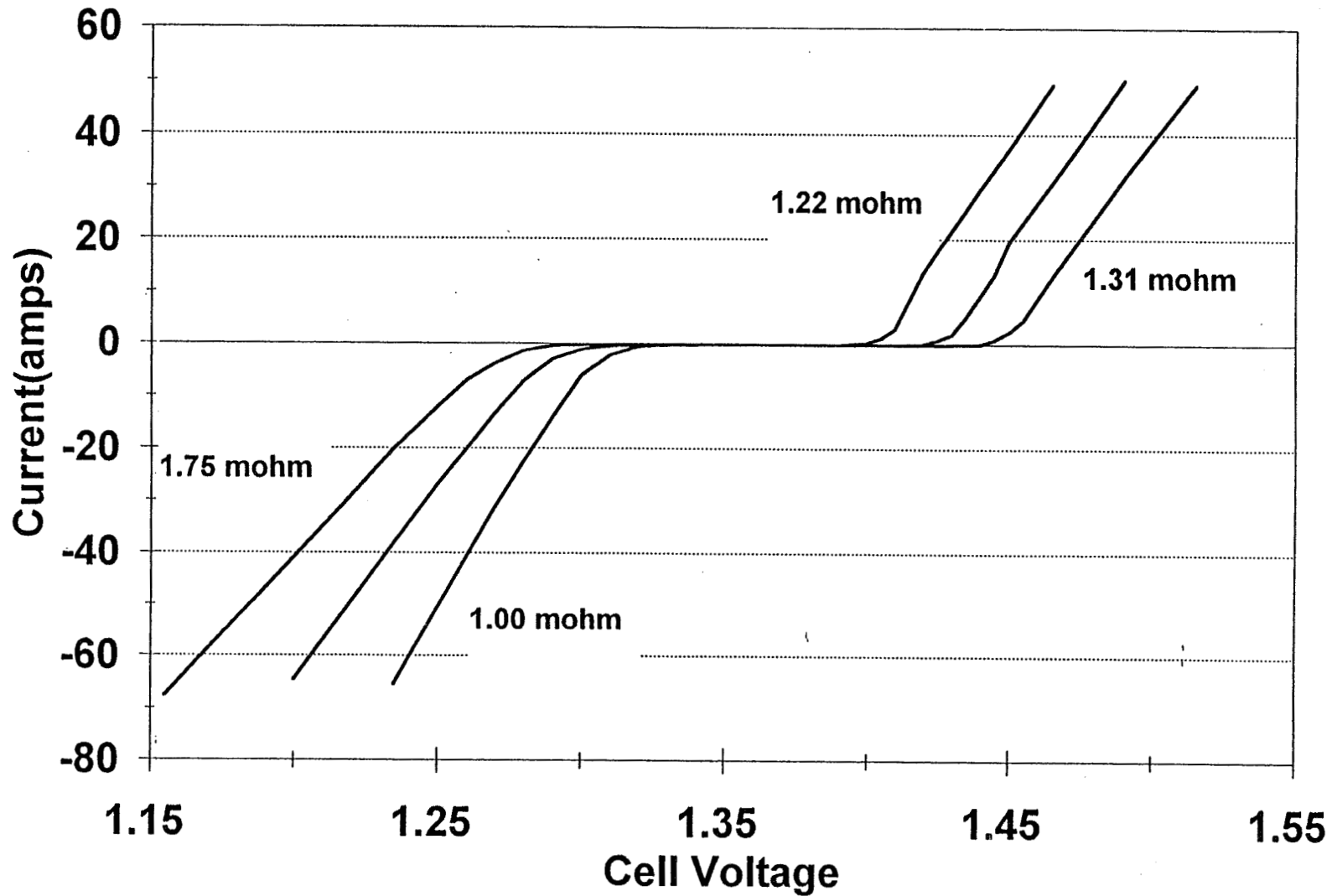


Figure 5

I/V Curves for Dual Anode Cells, 20 C at 25%, 50%, and 75% State-of-Charge

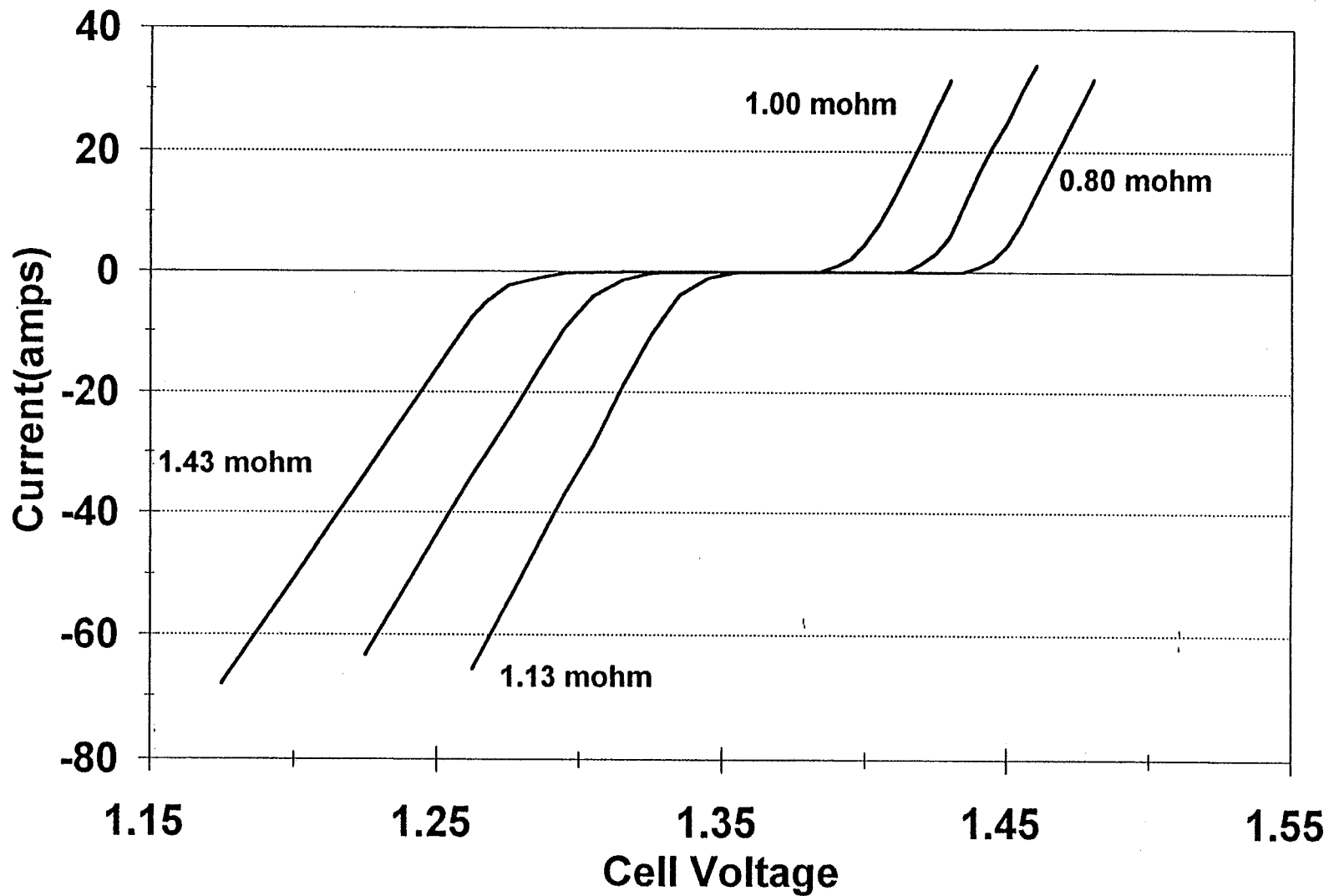


Figure 6

Standard Capacity vs. Temperature for Dual Anode Cells

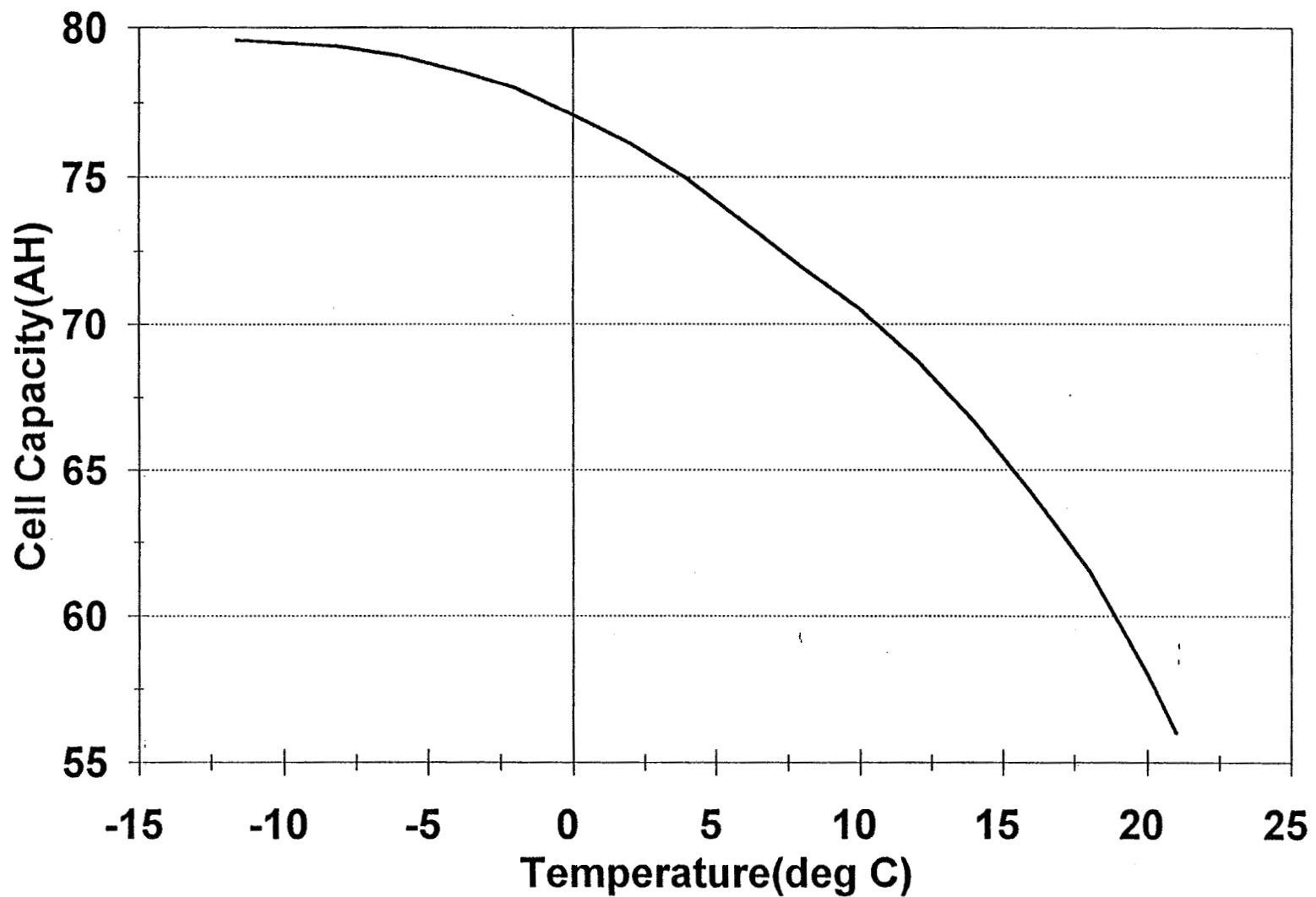


Figure 7

Charge Efficiency for Dual-Anode Cells C/10 Charge Rate

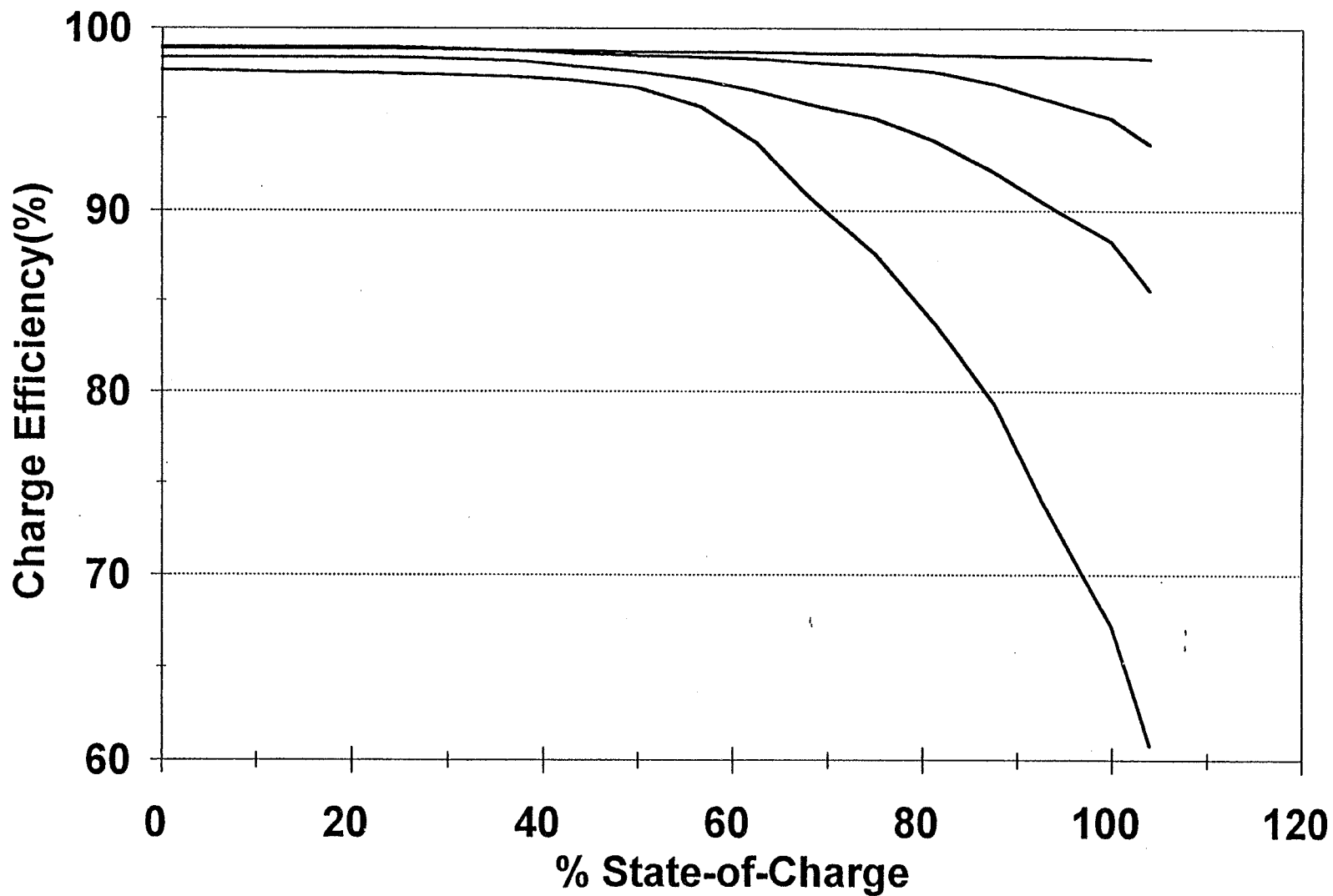


Figure 8

Self-Discharge Rate at 20 deg C for Dual Anode Cells

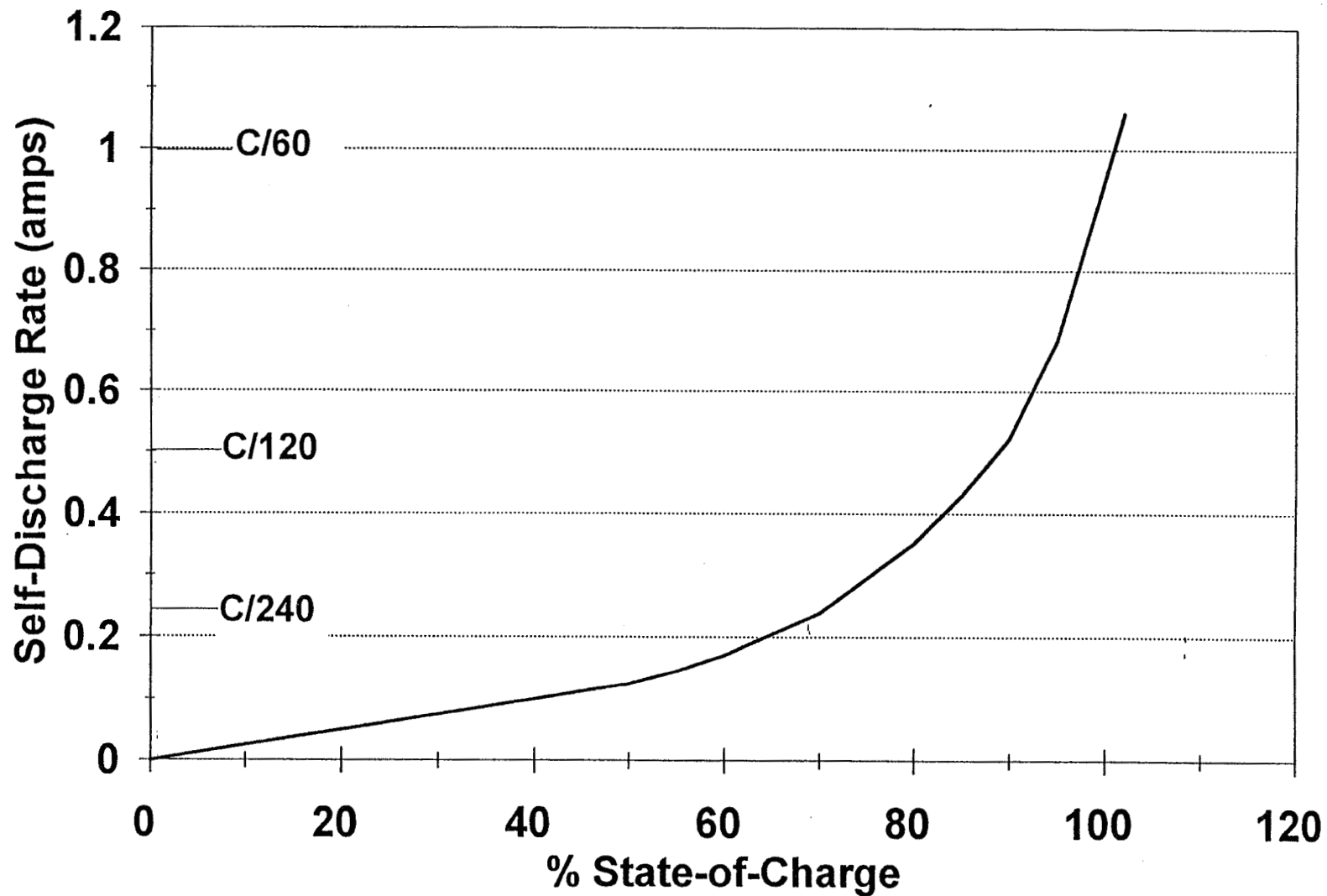


Figure 9

Dual Anode EODV in Life Test

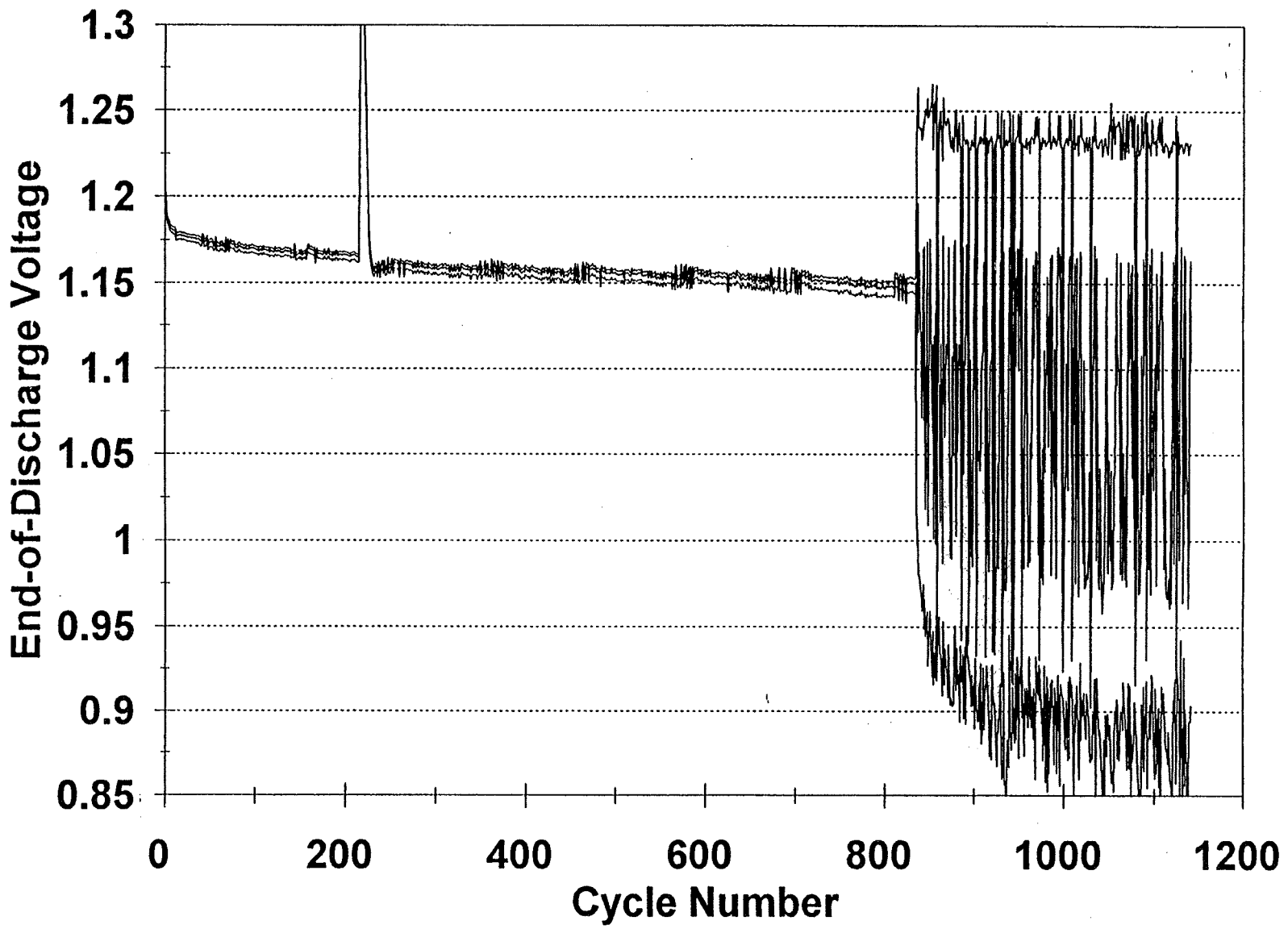


Figure 10

Dual Anode EOCV in Life Test

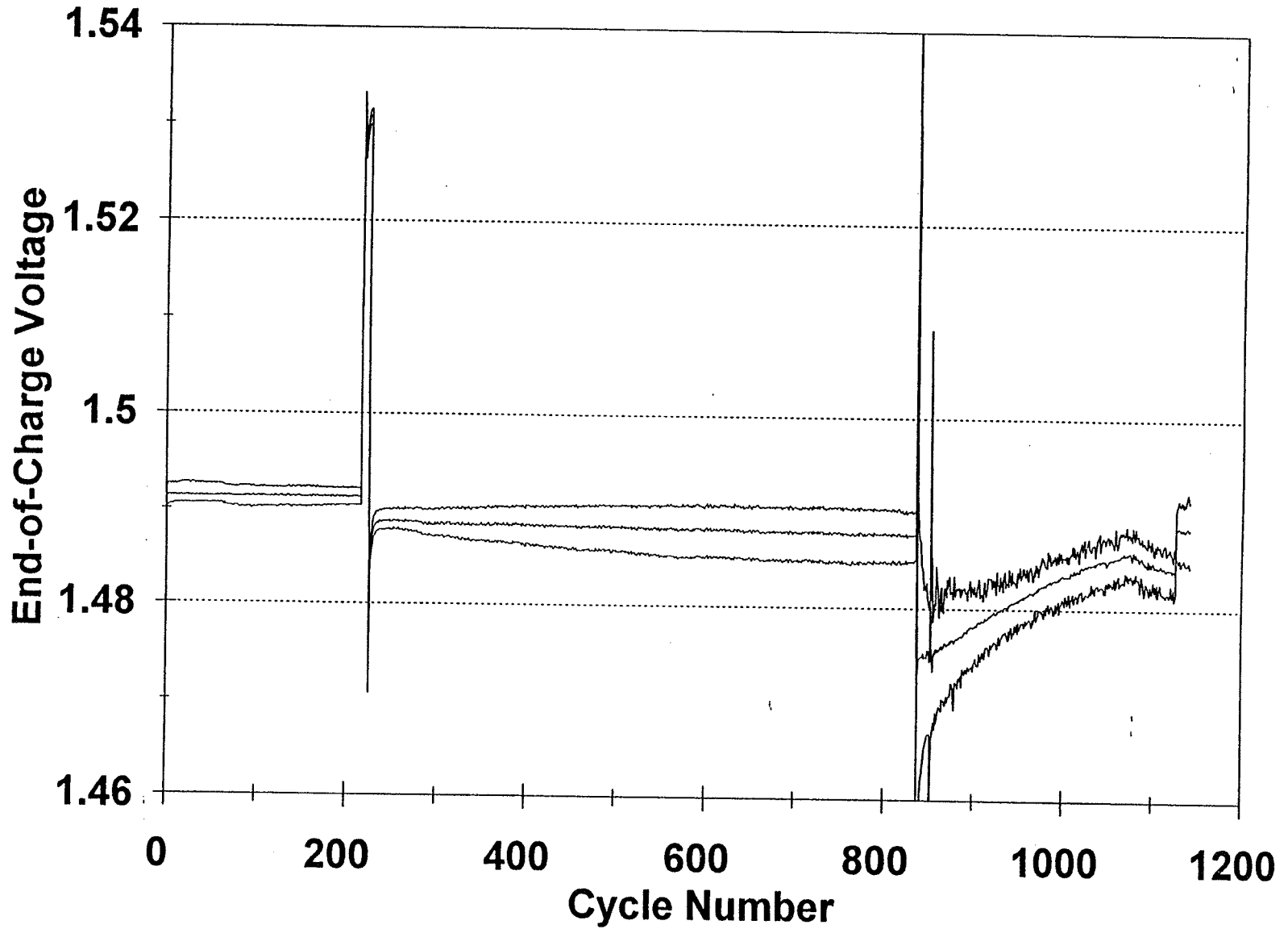
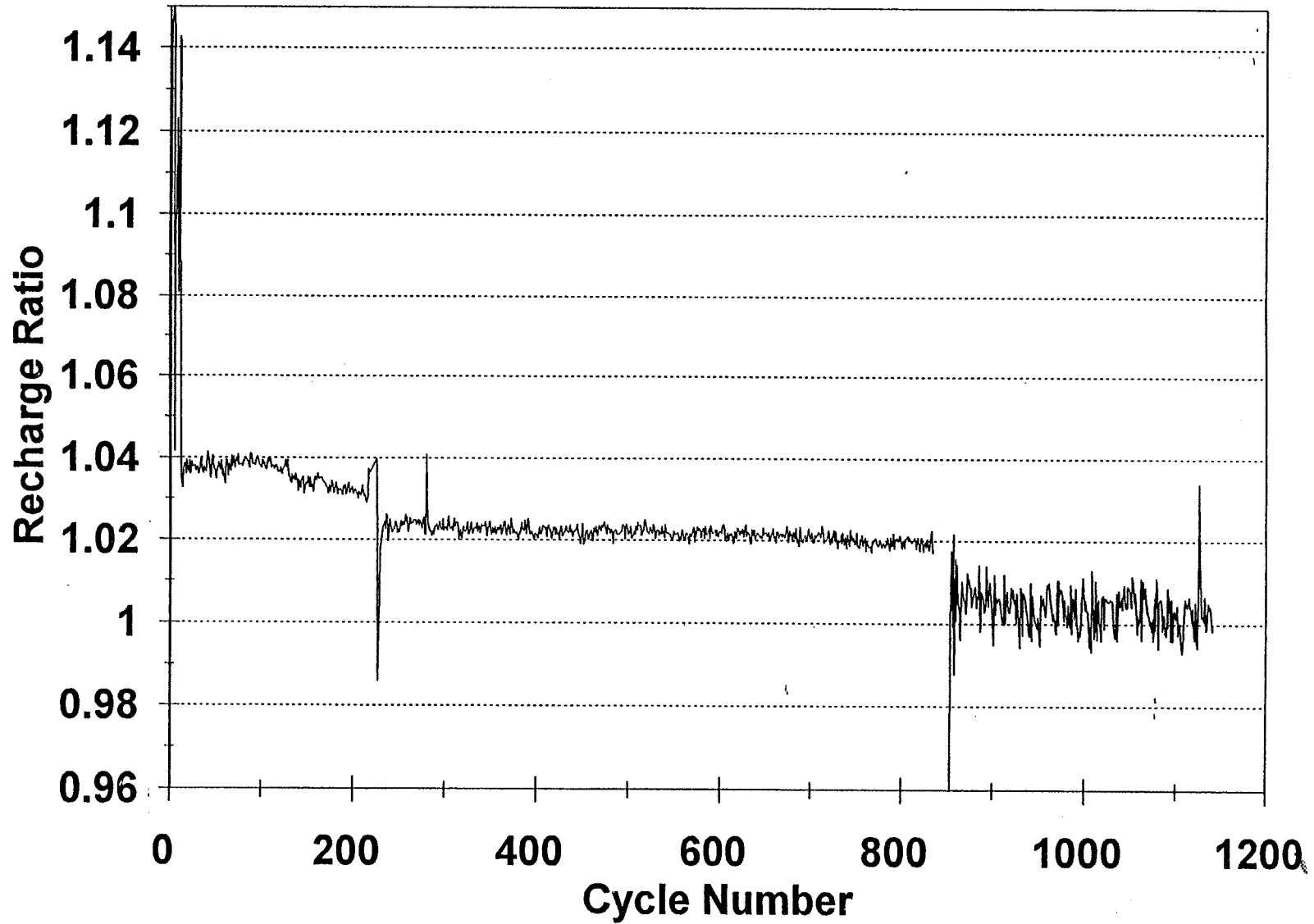


Figure 11

Dual Anode Recharge Ratio in Life Test





Development of a Large Diameter (5.5 Inch) Nickel-Hydrogen (NiH₂) Individual Pressure Vessel (IPV) Battery Cell

**Dwight Caldwell, Jim Morgan, Jack Brill
Technologies Division, Eagle-Picher Industries, Inc.
Joplin, MO 64802
(417) 623-8000**



*Development of a Large Diameter (5.5 Inch)
Nickel-Hydrogen (NiH₂) Individual Pressure
Vessel (IPV) Battery Cell*

OUTLINE

- **HERITAGE**
- **DESIGN RATIONALE**
- **DEVELOPMENT PLAN**
- **CELL DESIGN**
 - **Mechanical**
 - **Electrical**
 - **Thermal**
- **ACCEPTANCE TESTING**
- **LIFE TESTING**
- **FUTURE DEVELOPMENT PLANS**
- **SUMMARY**



Development of a Large Diameter (5.5 Inch) Nickel-Hydrogen (NiH₂) Individual Pressure Vessel (IPV) Battery Cell

NiH₂ ADVANTAGES

- *Reliable, Durable*
- *High Energy Density*
- *High Power Density*
- *Sealed, Maintenance-Free Battery*
- *Excellent Overcharge, Overdischarge and Deep Cycle Capabilities*
- *SOC Easily Determined by Internal Hydrogen Pressure*
- *No Toxic Materials*
- *Competitive Life Cycle Cost*



Development of a Large Diameter (5.5 Inch) Nickel-Hydrogen (NiH₂) Individual Pressure Vessel (IPV) Battery Cell

- | | | |
|--|--|---|
| 1. NTS-2 (US NAVY) [35 AH] ¹ | 23. GPS IIR (GE/ASTRO/
AIR FORCE) [40 AH] ¹⁽²⁾ | 44. INSAT 2E (ISRO) [55 AH] |
| 2. INTELSAT V
(FACC/INTELSAT) [30 AH] ¹⁽⁸⁾ | 24. KOREASAT (GE/ASTRO) [42 AH] ¹⁽²⁾ | 45. APSTAR 2R (SS/LORAL) [120 AH] ¹ |
| 3. G-STAR (RCA/GTE) [30 AH] ¹⁽⁴⁾ | 25. SUPER (MARTIN-MARIETTA/
AIR FORCE) [50 AH] ³ | 46. P-81 (Lockheed-Martin) [77 AH] |
| 4. SPACENET
(RCA/SOUTHERN PACIFIC) [40 AH] ¹⁽⁴⁾ | 26. BS3N (GE/ASTRO) [50 AH] ¹ | 47. TELSTAR 402R (GE/ASTRO) [45 AH] ¹ |
| 5. ASC (AMERICAN SATELLITE
CORPORATION) [35 AH] ¹ | 27. AXAF (TRW/NASA) [40 AH] | 48. SSTI Lewis (TRW) [23 AH] ^{1,4} |
| 6. SATCOM K (RCA SPACE
COMMUNICATION) [50 AH] ¹⁽²⁾ | 28. AXAF (NASA-MSFC) [50 AH] | 49. ISSA (SS/LORAL, NASA) [81 AH] |
| 7. ITALSAT (FACC/SELENIA) [30 AH] ¹ | 29. SPACE STATION FREEDOM
(SS/LORAL/NASA) [81 AH] | 50. GOES (SS/LORAL, NASA) [16 AH] |
| 8. MILSTAR (LMSC/AIR FORCE) [76 AH] ¹⁽²⁾ | 30. GEOSAT Follow-on
(BALL AEROSPACE/NAVY) [20 AH] ⁴ | 51. DBSC (Lockheed-Martin) [100 AH] |
| 9. ASTRA 1A, 1B (GE/ASTRO) [50 AH] ¹⁽²⁾ | 31. TUBSAT-B (TECHNICAL UNIV.
OF BERLIN)[6 AH] ^{1,4} | 52. PanAmSat 7 (SS/LORAL) [120 AH] |
| 10. ANIK-E
(RCA/TELESAT-CANADA) [30 AH] ¹⁽²⁾ | 32. GE1 (MARTIN-MARIETTA ASTRO)
[100 AH] ¹ | 53. PanAmSat 8 (SS/LORAL) [120 AH] |
| 11. PAN AM SAT (GE/ASTRO) [35 AH] ¹ | 33. GE2 (MARTIN-MARIETTA ASTRO)
[100 AH] ¹ | 54. CHINASTAR (Lockheed-Martin) [100 AH] |
| 12. INTELSAT K (GE/ASTRO) [50 AH] ¹ | 34. TEMPO (SS/LORAL) [120 AH] ¹ | 55. PIONEER 1&2 (SS/LORAL) [120 AH] |
| 13. ASC II (GE/ASTRO) [40 AH] ¹ | 35. LANDSAT 7(MARTIN-MARIETTA/
AIRFORCE) [50 AH] | 56. Whitetail 1& 2(Lockheed Martin
Missiles & Space)[100 AH] |
| 14. C3/C4 (GE/ASTRO) [50 AH] ¹⁽²⁾ | 36. GLOBALSTAR (SS/LORAL) [64 AH] | 57. ACeS (LOCKHEED MARTIN
MISSILES & SPACE) [131 AH] |
| 15. AURORA II (GE/ASTRO) [40 AH] ¹ | 37. PanAmSat 6 (SS/LORAL) [120 AH] | 58. SMTS (TRW) [60 AH] |
| 16. TELSTAR 401 (GE/ASTRO) [50 AH] ¹ | 38. AGILA 2 (SS/LORAL) [120 AH] ¹ | 59. IR&D
(NAVAL RESEARCH LAB) [90 AH] ⁶ |
| 17. INMARSAT 3 (GE/ASTRO) [50 AH] ¹⁽⁴⁾ | 39. 2828 (TRW) [98 AH] | 60. EOS Common (TRW) [160 AH] |
| 18. 8482 (TRW) [65AH-76 AH] | 40. TUBSAT-C (TECHNICAL UNIV.
OF BERLIN) [10 AH] ⁴ | 61. QUICKBIRD (BALL AEROSPACE) [40 AH] ⁴ |
| 19. SALT
(INTRASPACE/NAVY) [12 AH] ^{3,4} | 41. MICROLAB
(ORBITAL SCIENCES) [10 AH] ^{1,4} | 62. MTI (BALL AEROSPACE) [40 AH] ⁴ |
| 20. EOS (GE/ASTRO/NASA) [50 AH] | 42. TELSTAR 501 (SS/LORAL) [120 AH] ¹ | 63. 4171 (TRW) [86 AH] |
| 21. TESS(McDonnell Douglas/
NASA) [50 AH] ³ | 43. GE3 (Lockheed-Martin) [100 AH] ¹ | 64. MILITARY (CLASSIFIED) ¹ |
| 22. ORBCOMM
(ORBITAL SCIENCES) [10 AH] ^{1(2),4} | | 1 One (or More) Spacecraft in Orbit
(128 Total) |
| | | 2 Waiting for Launch Availability. |
| | | 3 Flight Qualified Hardware Delivered,
Program on Hold or Terminated |
| | | 4 Common Pressure Vessel (CPV) |
| | | 5 Dependent Pressure Vessel (DPV) |



Development of a Large Diameter (5.5 Inch) Nickel-Hydrogen (NiH₂) Individual Pressure Vessel (IPV) Battery Cell

- | | | |
|---|--|---|
| 1. FLIGHT EXPERIMENT (US AIR FORCE) [50 AH] ¹ | 18. BRILLIANT EYES (ROCKWELL/AIRFORCE) [30 AH] | 38. 3890 [90 AH] |
| 2. OLYMPUS (BAe/ESA) [58 AH] ¹ | 19. TIMED (JACKSON & TULL/ NASA-GFSC) [19 AH] ⁵ | 39. 3893 [90 AH] |
| 3. EUTELSAT II (AEROSPATIALE) [58 AH] ¹⁽⁵⁾ | 20. SPV BATTERY (TRW/IR&D) [35 AH] ⁵ | 40. EUTELSAT W24A (AEROSPATIALE) [58 AH] |
| 4. TV-SAT II (AEG - TELEFUNKEN) [30 AH] ¹ | 21. SMALLSAT/IRIDIUM (LMSC) [50 AH] ⁶ | 41. ARABSAT 2B (AEROSPATIALE) [52 AH] |
| 5. HUBBLE SPACE TELESCOPE (LMSC/NASA) [90 AH] ¹ | 22. TURKSAT 2 (AEROSPATIALE) [65 AH] | 42. NAHUEL 1B (AEROSPATIALE) [58 AH] |
| 6. TELECOM II (MATRA) [78 AH] ¹⁽⁴⁾ | 23. NAHUEL 1A (AEROSPATIALE) [58 AH] ¹ | 43. IRAD-15 (LOCKHEED MARTIN) [15 AH] ⁶ |
| 7. HISPASAT (MATRA) [78 AH] ¹⁽²⁾ | 24. CLEMENTINE [15 AH] ^{1, 5} | 44. IRIDIUM (LOCKHEED MARTIN) [60 AH] ^{1(19), 6} |
| 8. ORION (BAe) [78 AH] ¹ | 25. IRIDIUM (LMSC) [50 AH] ^{1(20), 5} | 45. MSP (SPECTRUM ASTRO) [16 AH] ⁴ |
| 9. TURKSAT 1B (AEROSPATIALE) [65 AH] ¹ | 26. TURKSAT 1C (AEROSPATIALE) [58 AH] ¹ | 46. GPS IIF (ROCKWELL/BOEING) [76 AH] |
| 10. APEX (ORBITAL SCIENCES/ AIR FORCE) [6 AH] ^{1, 4} | 27. SSTI-Clark (CTA) [15 AH] ⁵ | 47. SICRAL (ALENIA SPAZIO) [55 AH] |
| 11. SEA STAR (ORBITAL SCIENCES/NASA) [10 AH] ^{1, 4} | 28. MGS (MARTIN-MARIETTA) [20 AH] ^{1, 4} | 48. STARDUST (LMA) [16 AH] ⁴ |
| 12. INTELSAT 8 (GE/ASTRO) [45 & 50 AH] ¹⁽³⁾ | 29. HST Follow-On (LMSC) [90 AH] | 1. One (or More) Spacecraft in Orbit (128 Total). |
| 13. P91-1/ARGOS (ROCKWELL/AIR FORCE) [45 AH] | 30. DMPS (LOCKHEED MARTIN) [100 AH] | 2. Waiting for Launch Availability. |
| 14. ASIASAT 2 (GE/ASTRO) [45 AH] ¹ | 31. ARABSAT 2A (AEROSPATIALE) [52 AH] | 3. Flight Qualified Hardware Delivered, Program on Hold or Terminated |
| 15. ECHOSTAR (GE/ASTRO) [50 AH] ¹⁽³⁾ | 32. SAFIR (OHB) [4 AH] ⁴ | 4. Common Pressure Vessel (CPV) |
| 16. MSTI-2 (SPECTRUM ASTRO/SDIO) [10 AH] ^{1, 4} | 33. 3810 [90 AH] | 5. Single Pressure Vessel (SPV) |
| 17. MSTI-3 (SPECTRUM ASTRO/SDIO) [12 AH] ^{1, 4} | 34. 3822 [90 AH] | |
| | 35. 3857 [90 AH] | |
| | 36. 3866 [90 AH] | |
| | 37. 3889 [90 AH] | |



*Development of a Large Diameter (5.5 Inch)
Nickel-Hydrogen (NiH₂) Individual Pressure
Vessel (IPV) Battery Cell*

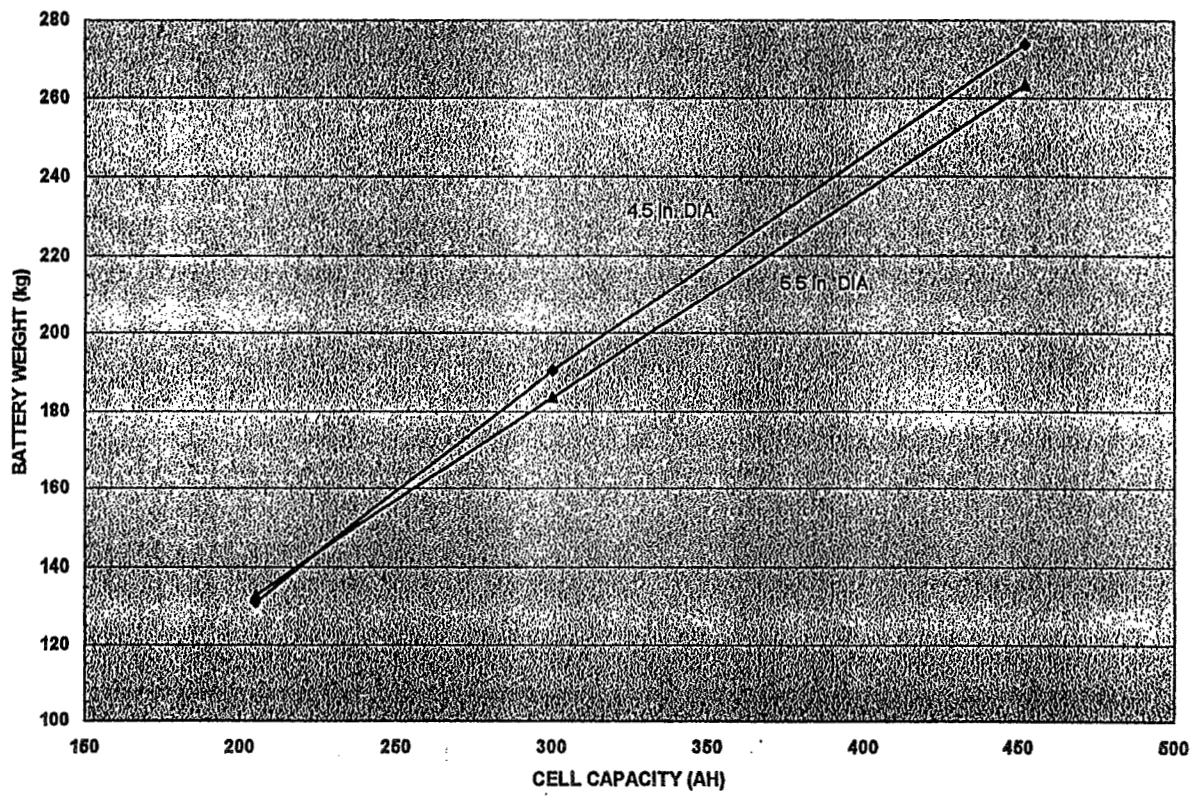
RATIONALE FOR 5.5 INCH CELL DEVELOPMENT

- *Satellite Manufacturers are Demanding Increased Power*
- *Large Diameter, High Capacity Cells Demonstrate the Following Benefits*
 - *Reduced Cell and Battery Weight*
 - *Increased Specific Energy*
 - *Decreased Length*



Development of a Large Diameter (5.5 Inch) Nickel-Hydrogen (NiH₂) Individual Pressure Vessel (IPV) Battery Cell

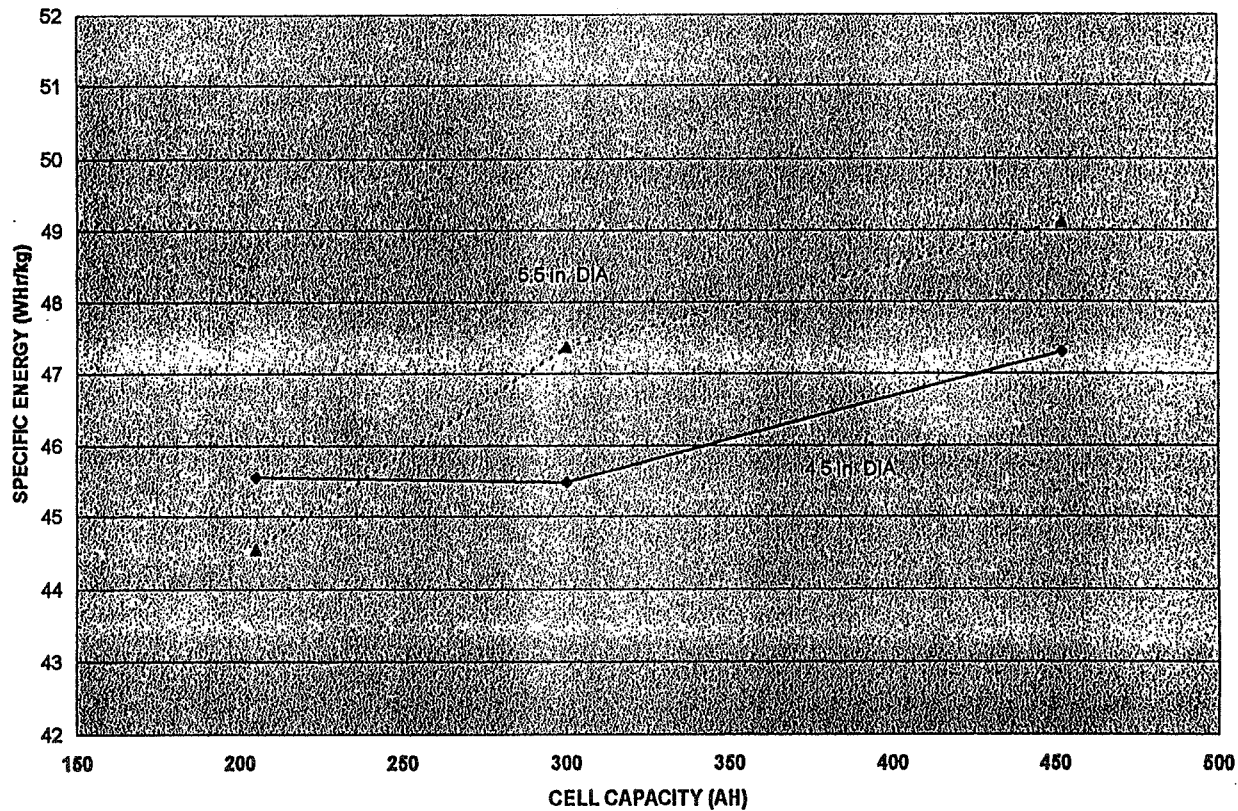
COMPARISON OF 4.5 in. AND 5.5 in. DIAMETER 22 CELL BATTERY CONFIGURATIONS





Development of a Large Diameter (5.5 Inch) Nickel-Hydrogen (NiH₂) Individual Pressure Vessel (IPV) Battery Cell

COMPARISON OF 4.5 in. AND 5.5 in. DIAMETER 22 CELL BATTERY CONFIGURATIONS





*Development of a Large Diameter (5.5 Inch)
Nickel-Hydrogen (NiH₂) Individual Pressure
Vessel (IPV) Battery Cell*

5.5 INCH CELL DEVELOPMENT PLAN

***Guideline: The 5.5 Inch Technology is Scaled-Up
Directly from the 2.5, 3.5, and 4.5 Inch Designs***

- ***Electrochemistry is Unchanged***
- ***Stack Component Materials and Processes
are Identical***
 - ***Positive Electrode***
 - ***Negative Electrode***
 - ***Separator***
 - ***Gas Screen***

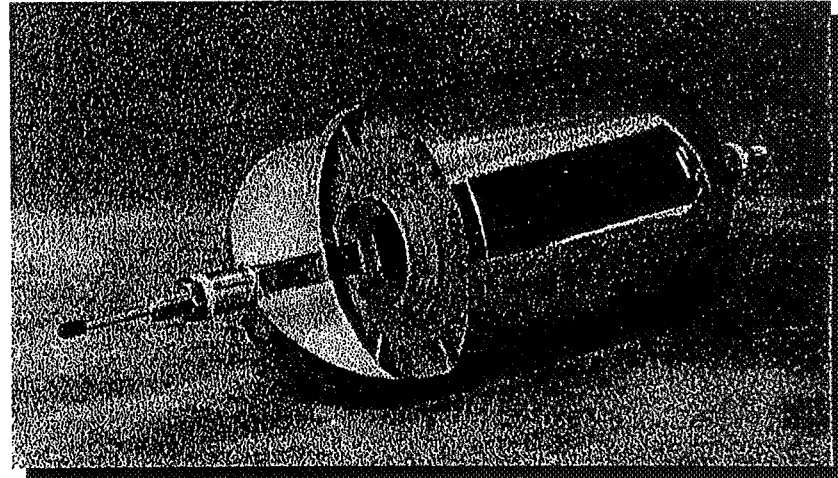


Development of a Large Diameter (5.5 Inch) Nickel-Hydrogen (NiH₂) Individual Pressure Vessel (IPV) Battery Cell

5.5 INCH CELL DESIGN

MECHANICAL:

- *Pressure Vessel - Inconel 718*
- *Max Design Pressure - 800 psi*
- *3.5 : 1 Safety Factor*
- *All Pressure Vessel Welds
Laser or Electron Beam*
- *MIL-STD-1522A Cycle and Burst Test
Complete*
- *Core/End Plates Designed Proportional
to Expected Loads and Growth*
- *Zirconium Oxide Wall Coating*



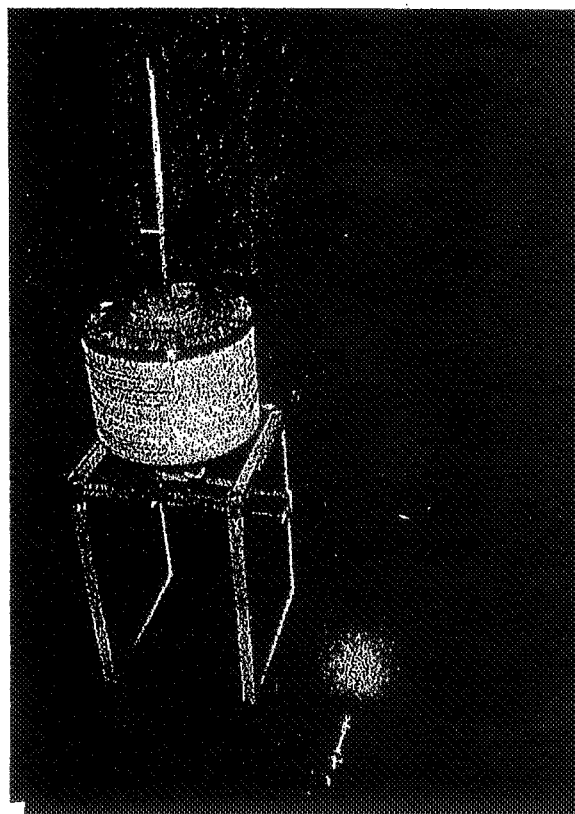


Development of a Large Diameter (5.5 Inch) Nickel-Hydrogen (NiH₂) Individual Pressure Vessel (IPV) Battery Cell

5.5 INCH CELL DESIGN

ELECTRICAL:

- *"Mantech" Design, "Back to Back" Electrode Arrangement*
- *Slurry Sinter Positive Electrode*
- *Lightweight Catalytic Hydrogen Negative Electrode*
- *31% KOH Electrolyte*
- *Zircar Separator*
- *Polypropylene Gas Screen*



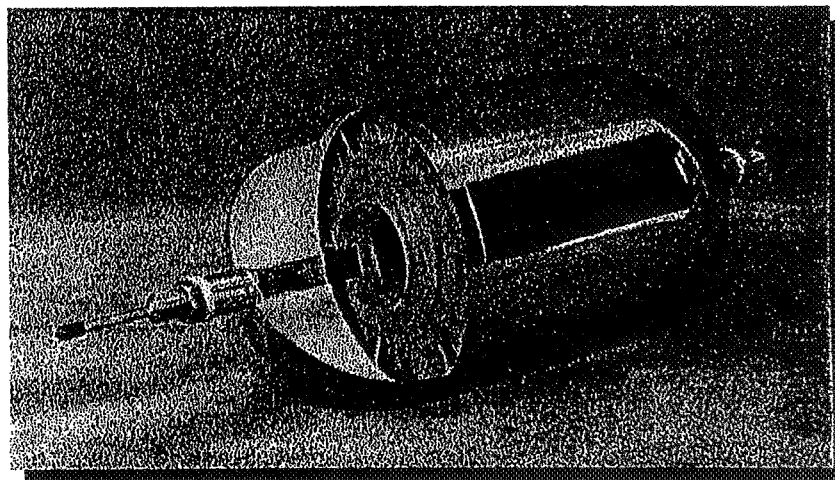


Development of a Large Diameter (5.5 Inch) Nickel-Hydrogen (NiH₂) Individual Pressure Vessel (IPV) Battery Cell

5.5 INCH CELL DESIGN

THERMAL:

- *Thermal Cross-Section Maintained
in Sizing Cell Components*
 - *Thermal Gradient Optimized*
 - *Large Thermal Transfer Area
Along P.V. Wall*
- *Minimal Stack Edge to Vessel Wall Gap*
- *Thermal Model will be Developed
Early Next Year*





Development of a Large Diameter (5.5 Inch) Nickel-Hydrogen (NiH₂) Individual Pressure Vessel (IPV) Battery Cell

5.5 INCH CELL DESIGN SUMMARY

- *Cell Type* RNH 200-1
- *Nominal Voltage* 1.25 Volts
- *Rated Capacity* 200 Ampere-hours
- *Actual Capacity* 205 Ampere-hours
(C/2 to 1.0V @ 10°C)
- *Weight* 12 lbs. (5.45 Kg)
- *Diameter* 5.71" (14.50 cm)
- *Length* 14.41" (36.60 cm)
w/terminals - axial design
- *Specific Energy* 47.02 Wh/Kg
- *Vessel Wall Thickness* 0.040" (1.02 mm)
- *MEOP* 800 psig (55.17 bar)
- *Safety Factor* 3.5 : 1



*Development of a Large Diameter (5.5 Inch)
Nickel-Hydrogen (NiH₂) Individual Pressure
Vessel (IPV) Battery Cell*

5.5 INCH ACCEPTANCE TESTING

- **20°C Capacity Test: 188 Ah (Avg.)**
- **10°C Capacity Test: 205 Ah (Avg.)**
- **10°C Charge Retention: 185 Ah (Avg.) (90% of 10°C Capacity)
(72 Hour Open Circuit)**
- **0°C Capacity Test: 220 Ah (Avg.)**
- **-10°C Capacity Test: 210 Ah (Avg.)**

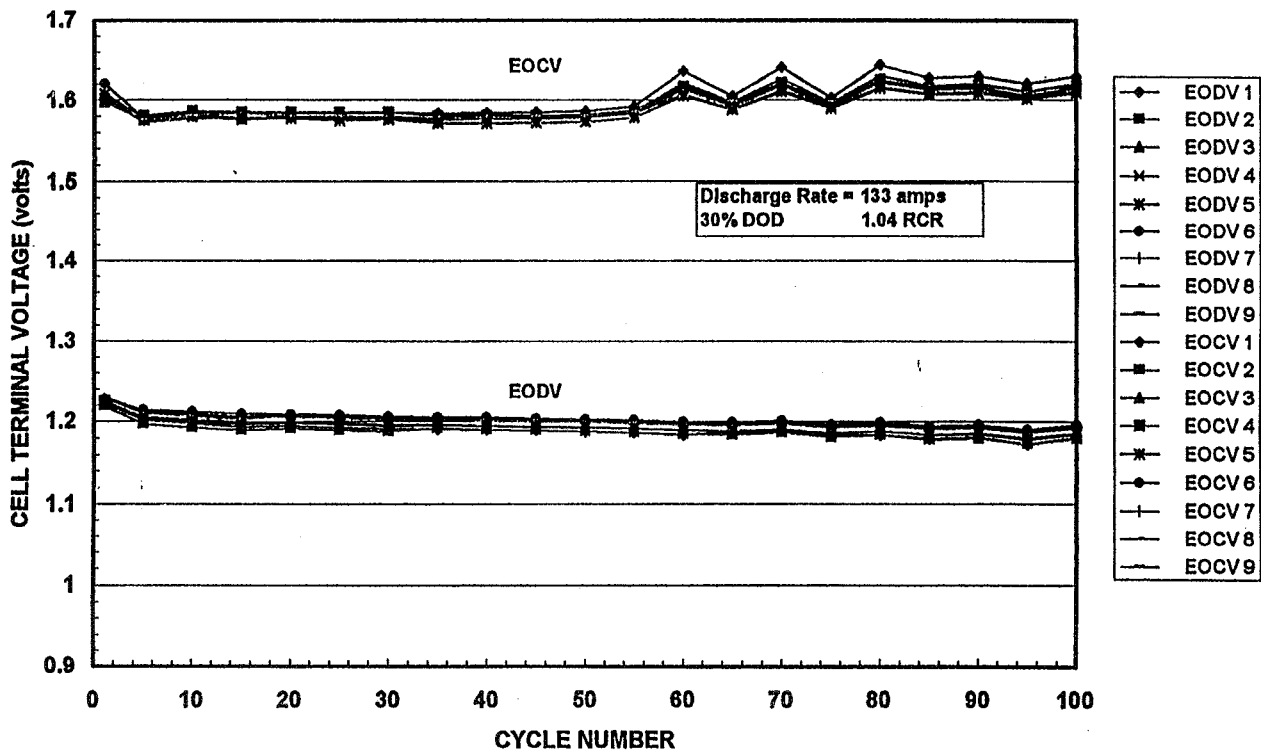
*Note: Charge rate - C/10 or 20 Amps
Discharge Rate - C/2 or 100 Amps
Capacity Measured at 1.0 Volt*



Development of a Large Diameter (5.5 Inch) Nickel-Hydrogen (NiH₂) Individual Pressure Vessel (IPV) Battery Cell

5.5 INCH CELL LIFE TEST

RNH 200 -1 LIFE TEST SUMMARY (LEO)





*Development of a Large Diameter (5.5 Inch)
Nickel-Hydrogen (NiH₂) Individual Pressure
Vessel (IPV) Battery Cell*

FUTURE 5.5 INCH DEVELOPMENT PLANS

- ***RNH 350-1***
 - ***350 Ah IPV Cell***
 - ***Parts in Production***
 - ***Activation and Testing Scheduled Early 1998***

- ***RNHC 100-1***
 - ***100 Ah CPV Cell***
 - ***Parts in Production***
 - ***Activation and Testing Scheduled Early 1998***



*Development of a Large Diameter (5.5 Inch)
Nickel-Hydrogen (NiH₂) Individual Pressure
Vessel (IPV) Battery Cell*

SUMMARY

- **5.5 INCH RNH 200-1 CELLS BUILT AND ON TEST**
- **CELL PERFORMANCE AS PREDICTED**
- **FURTHER DEVELOPMENT IS PROCEEDING RAPIDLY**

Page intentionally left blank

Charge Temperature Characterization of Nickel-Hydrogen Batteries

D. Coates, R. Smith, D. Judd, J. Brill
J. McDermott* and G. Gates*

Eagle-Picher Technologies
Joplin, Missouri

*Lockheed-Martin
Denver, Colorado

Nickel-Hydrogen Battery Charge Characterization Test

The purpose of the test is to determine the V/T level charging characteristics and charging efficiency of the battery as a function of temperature and current under realistic mission-oriented conditions.

Test Article

- Eight-cell pack
- RNH-100-9 cells
- Dual-stack IPV
- Flight configuration hardware
- Sleeve mounted

Test Configuration

- Eight cells sleeve mounted into battery pack
- Pack mounted on coldplate in chamber
- No chamber refrigeration
- 2 fans for air circulation
- 4 baseplate thermocouples
- 1 chamber air thermocouples
- 1 thermocouple per cell

Test Conditions

- V/T level 7 thru 12 (0.5 step increments)
- Testing from 0° to 20°C (5°C increments)
- Charge rates of 35A and 50A
- 155 steps total
- Two charge characterization sequences
- 98 minute cycles (63/35)
- Discharge load profile

Test Sequence

- Charge to the V/T level
- Taper charge to 105% return
 - if 105% is reached - switch to trickle charge
- Perform constant current capacity (C/2)
- Re-charge to V/T level as above
- Cycle to stabilization
- Perform constant current capacity (C/2)

Charging Methodology

- 63 minutes total charge time
- Charge to V/T level (35A or 50A)
- Taper charge until:
 - 105% recharge level reached
- Trickle charge 1.57A

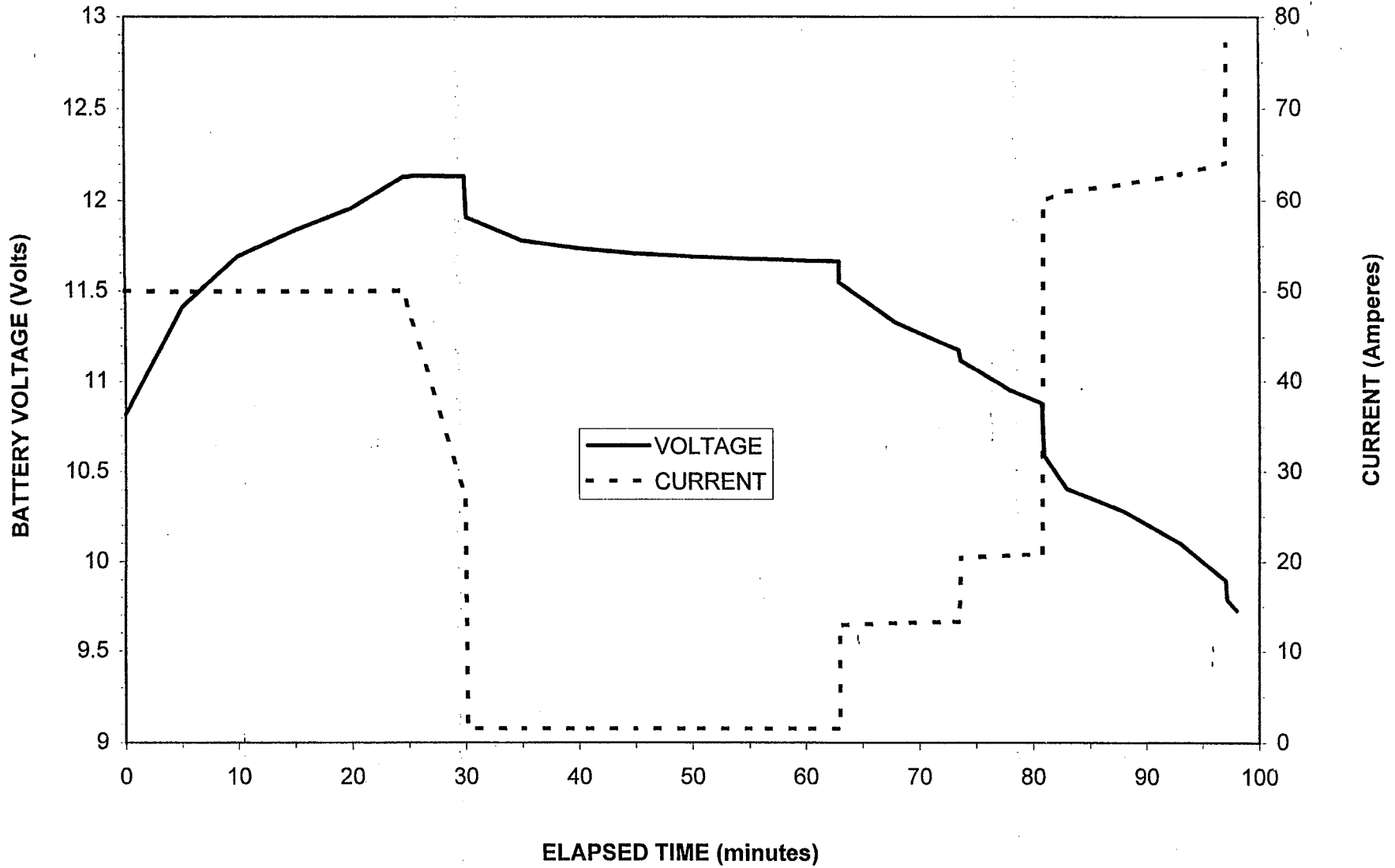
Stabilization Criteria

- The EOD voltage over 5 consecutive cycles changes by less than 0.003V
- The EOD pack voltage drops below 9.164V

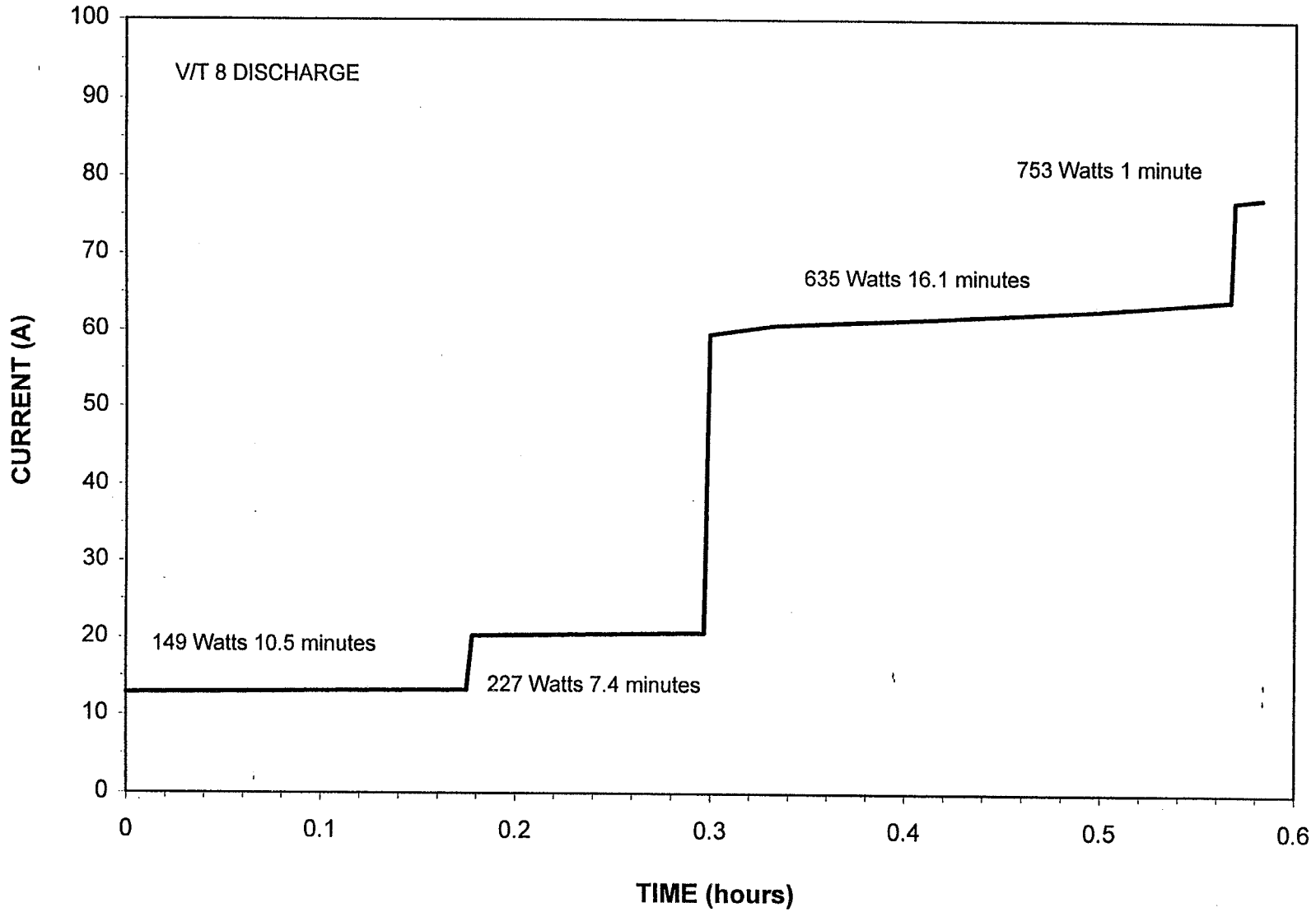
Discharge Load Profile

- 149 Watts for 10.5 minutes
- 227 Watts for 7.4 minutes
- 635 Watts for 16.1 minutes
- 753 Watts for 1 minute

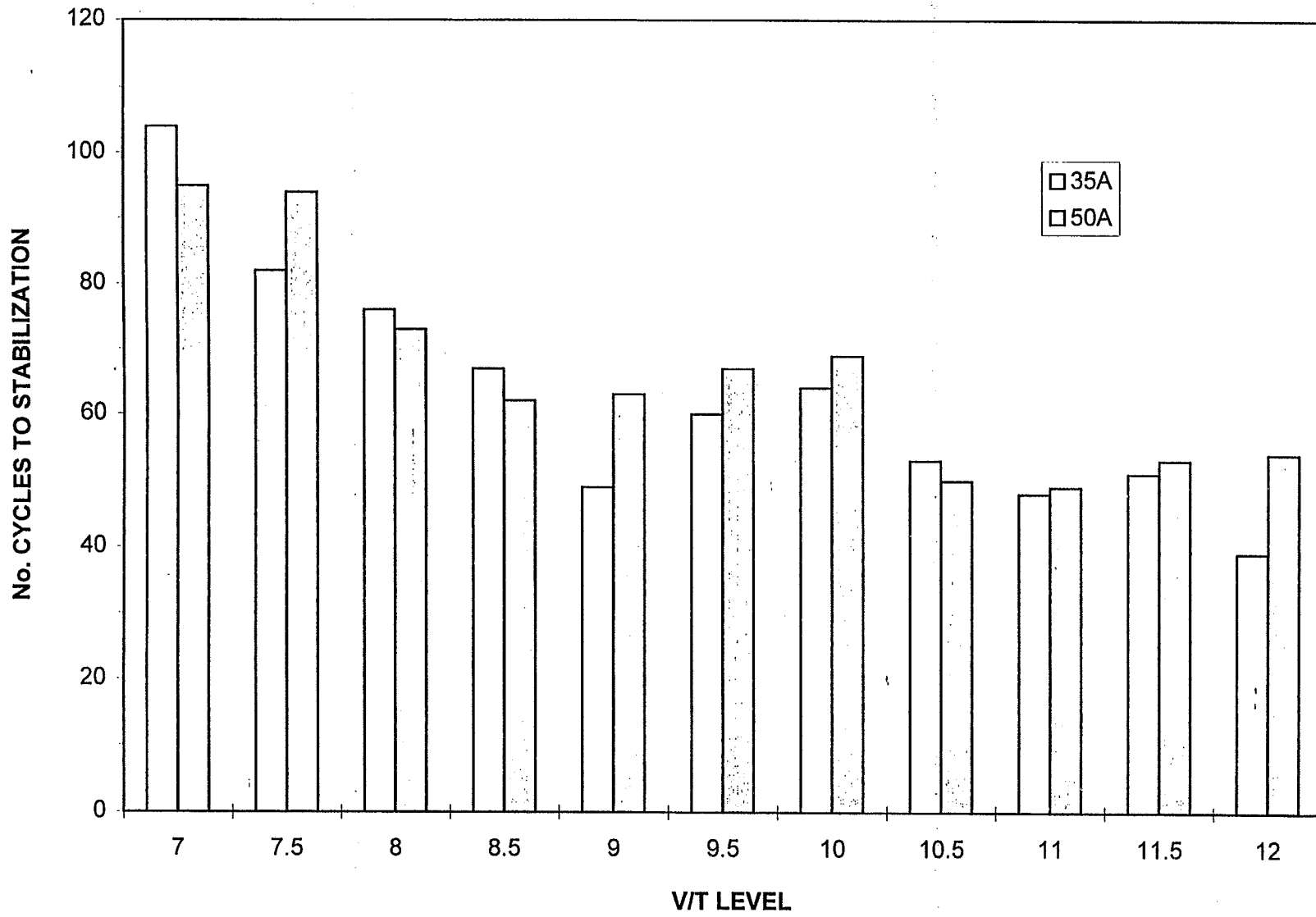
V/T 9 STABILIZATION CYCLE



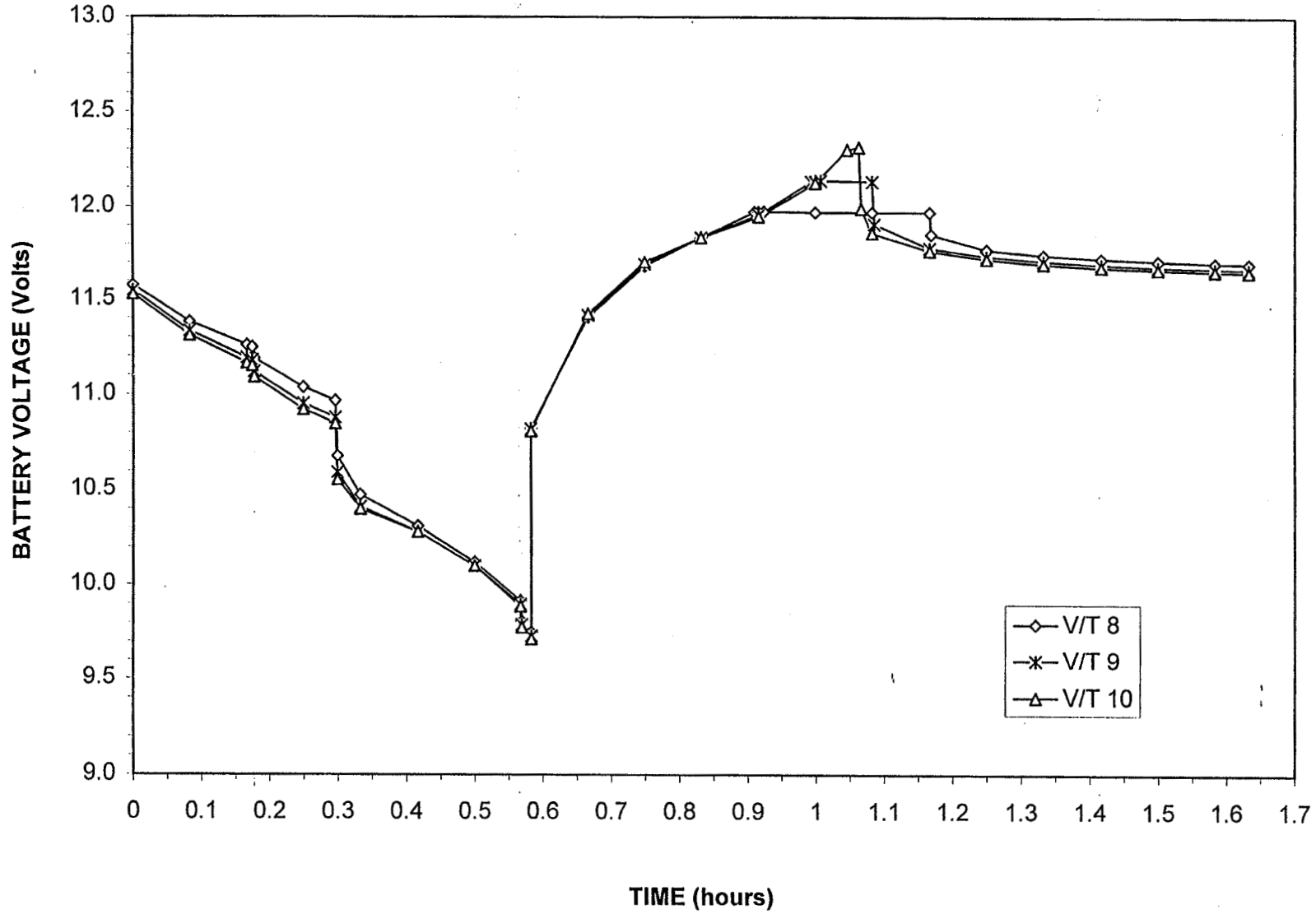
TYPICAL DISCHARGE LOAD PROFILE



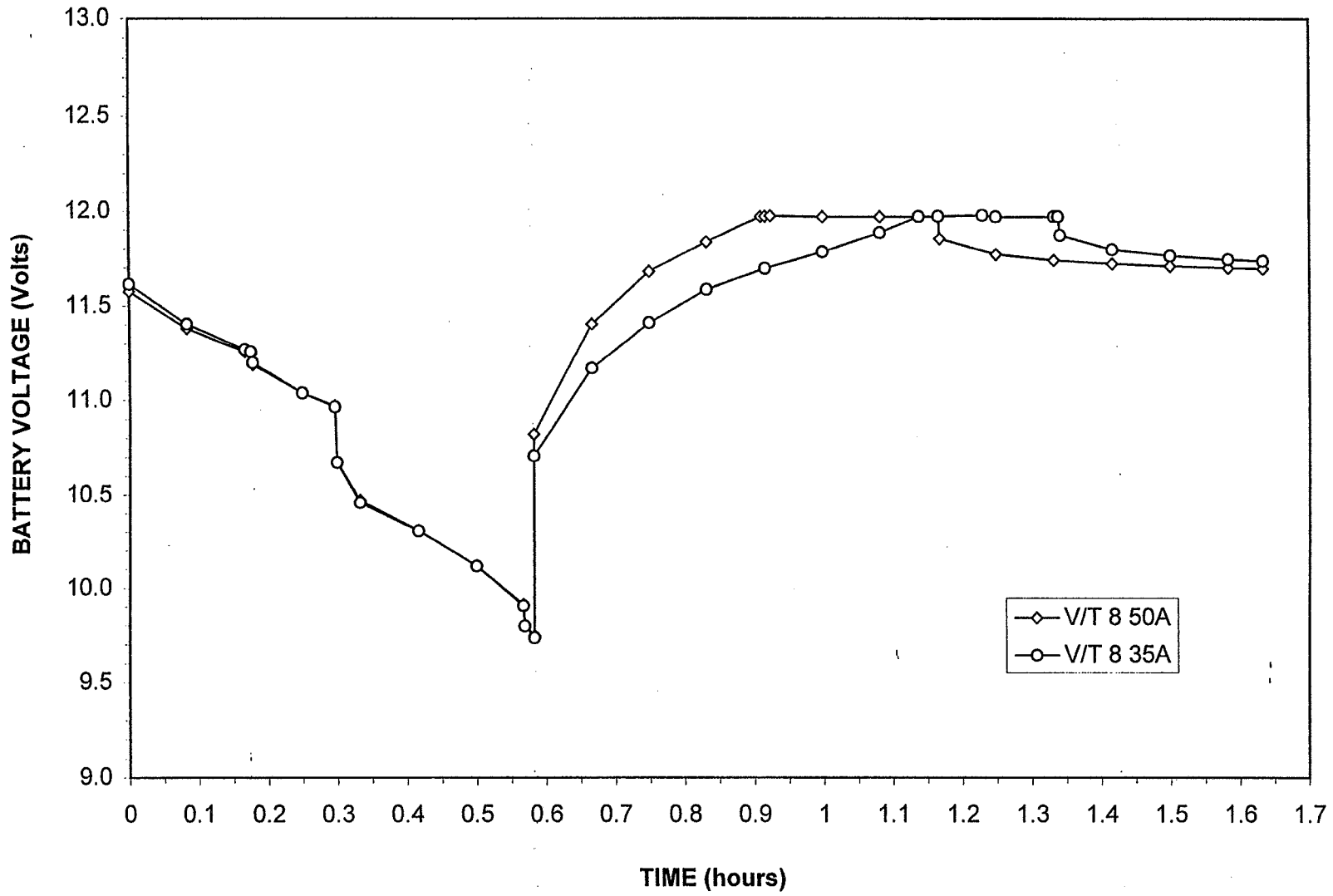
STABILIZATION CYCLES



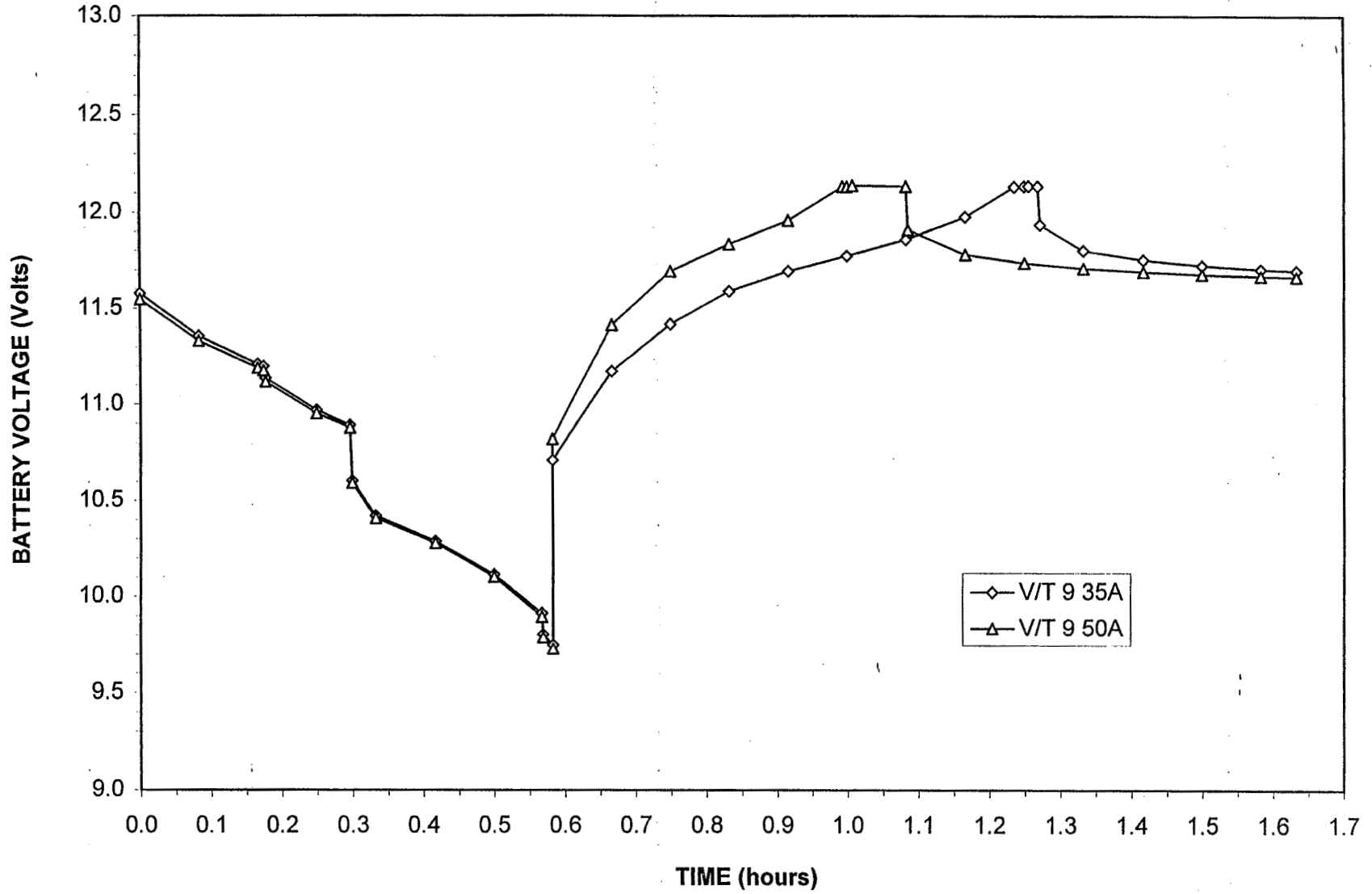
50A CHARGE STABILIZATION CYCLES



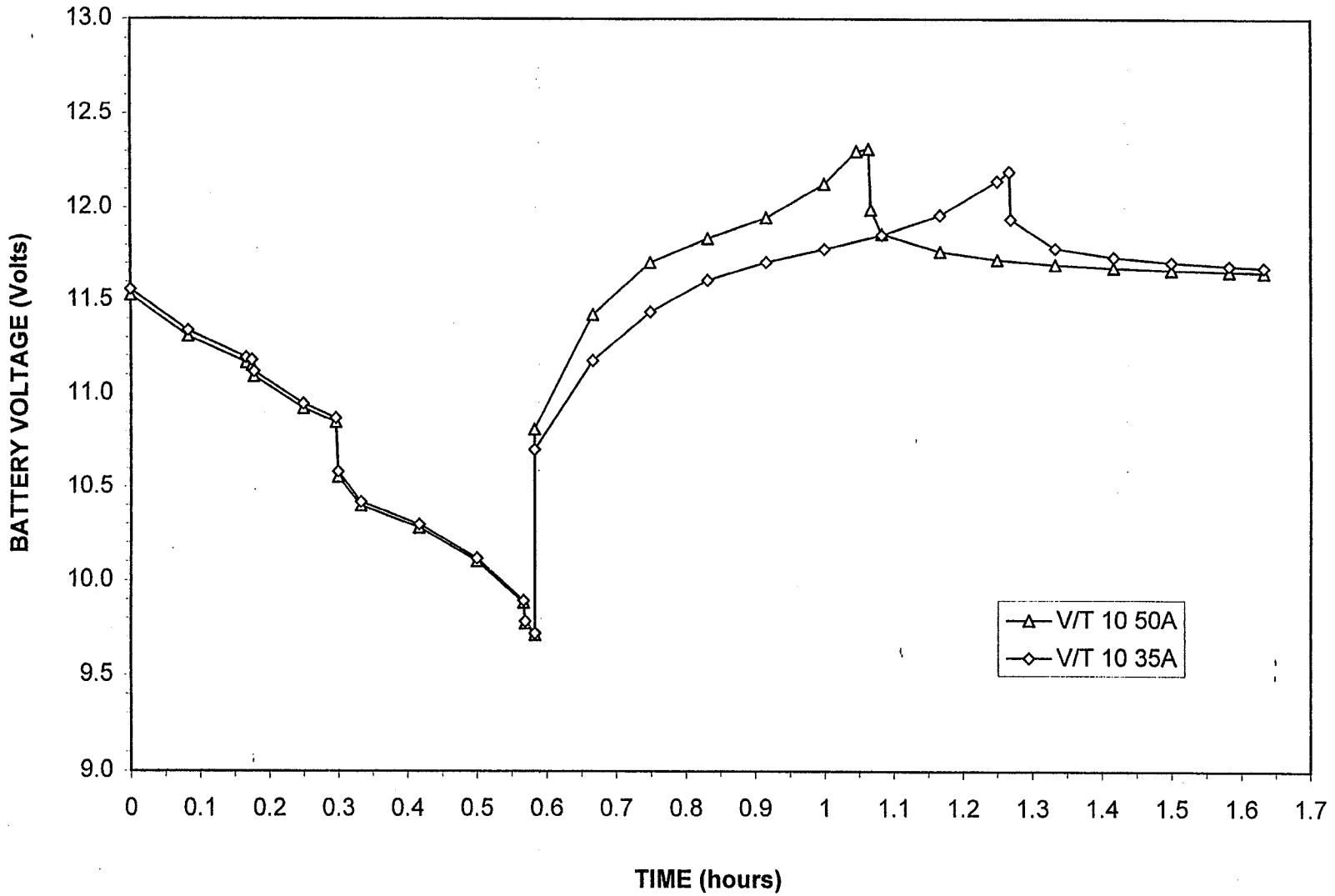
CHARGE STABILIZATION CYCLES



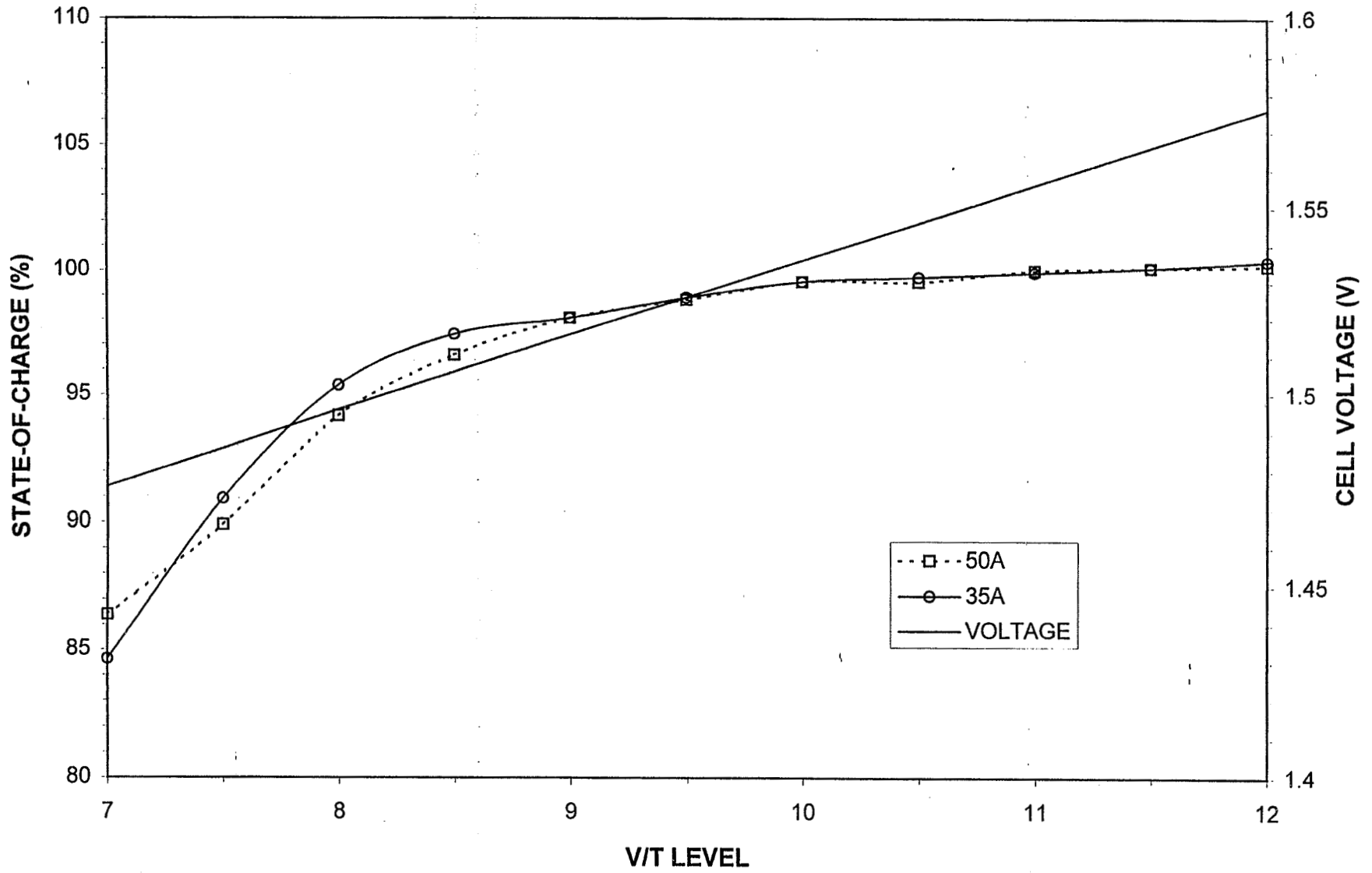
CHARGE STABILIZATION CYCLES



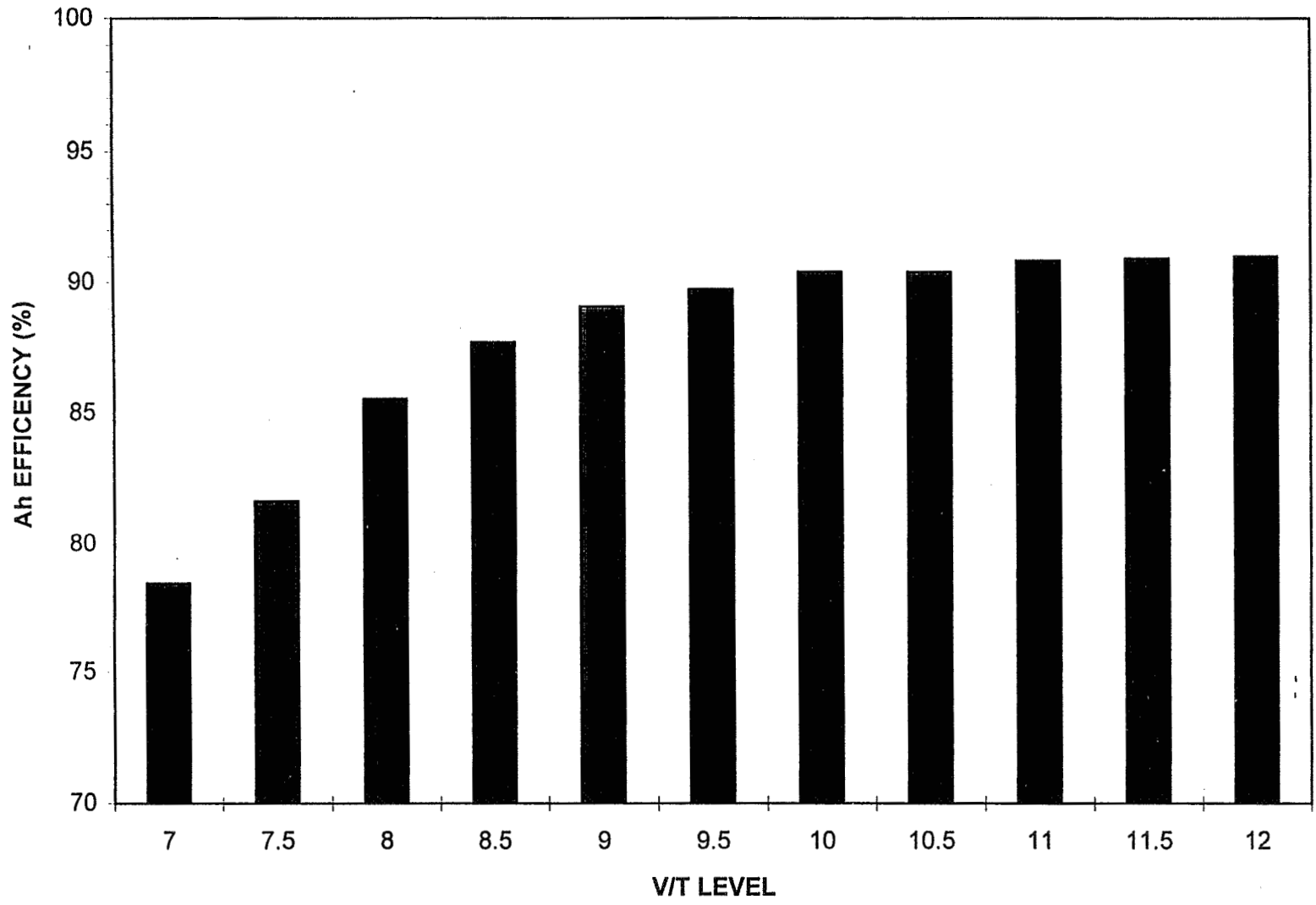
CHARGE STABILIZATION CYCLES



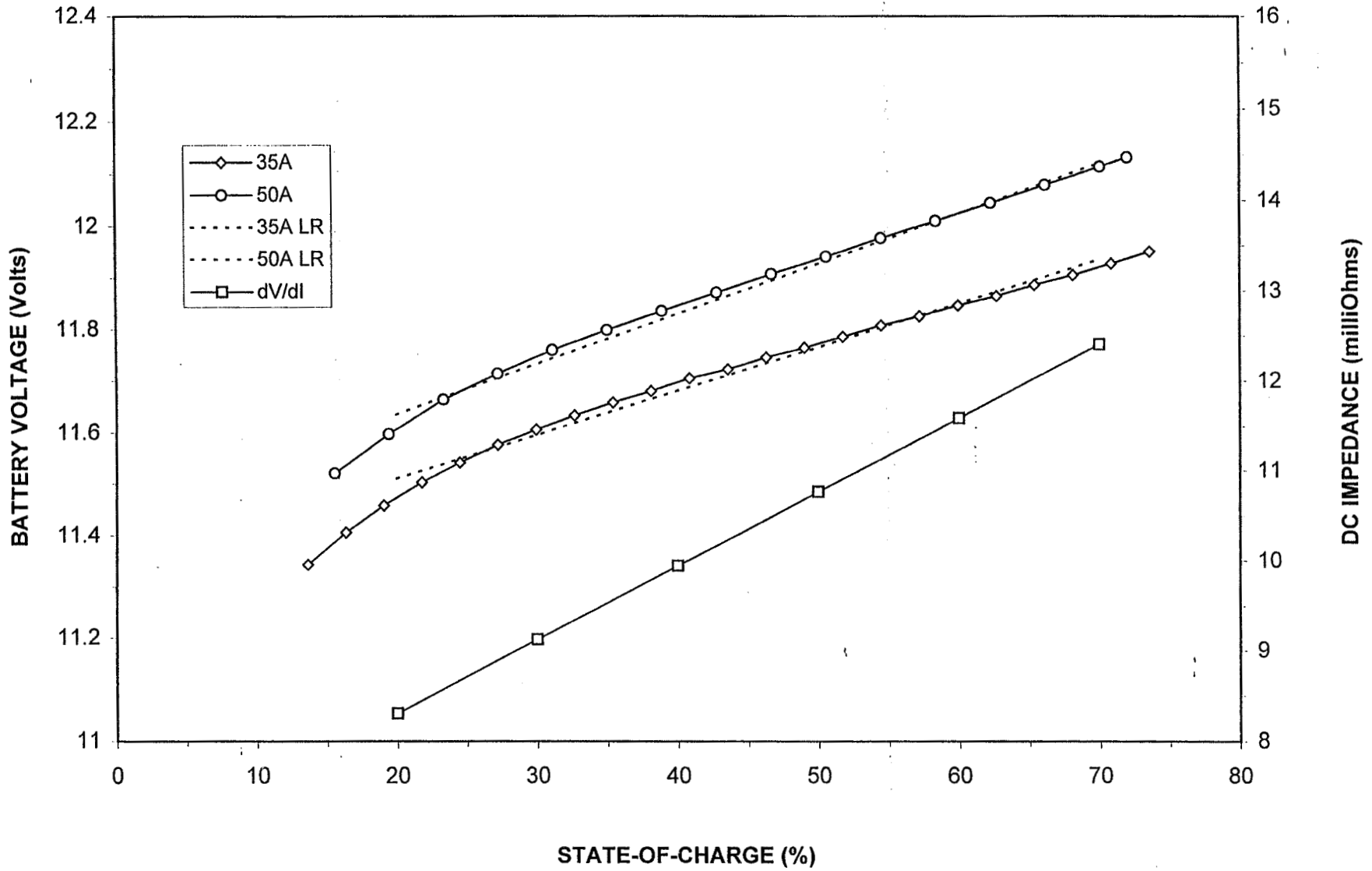
50A / 35A - 10°C CHARGE CHARACTERIZATION



50A - 10°C CHARGE CHARACTERIZATION



V/T 9 IMPEDANCE ANALYSIS



Conclusions

- 10°C testing completed
- Optimal charging occurs at:
 - V/T 9.5 at 35A
 - V/T 10 at 50A
- Charge efficiency is similar at both rates
- Temperature effects have not yet been determined

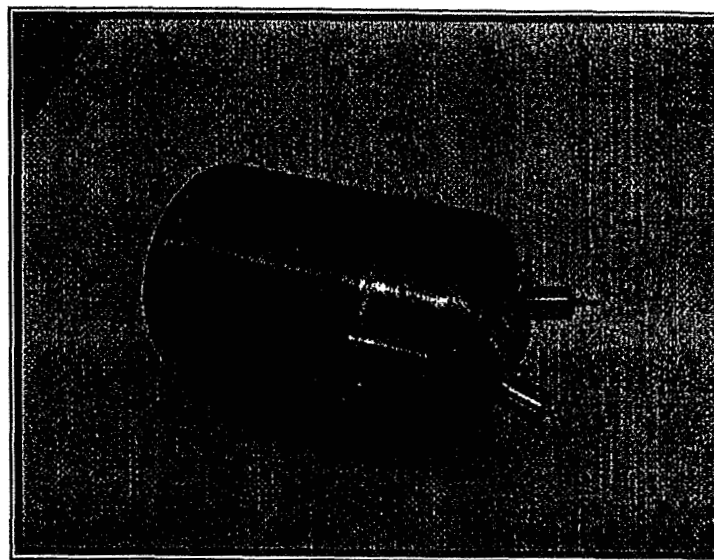
***MEETING THE DEMANDS OF THE
COMMERCIAL AEROSPACE MARKET***

**VERIFICATION TESTING AND PRODUCT
QUALIFICATION AT A NEW BATTERY
MANUFACTURING FACILITY**

***Jeff Dermott and Dwight Caldwell
Eagle-Picher Industries, Inc.
Joplin, MO.***

Outline

- ◆ **Background/History of Facility**
- ◆ **Matrix Life Test Data**
- ◆ **Acceptance Test Data**
- ◆ **Acknowledgements**



Range Line Facility (RLF)

- ◆ **Originally Designed for High Volume Nickel-Iron Production.**
- ◆ **Conversion to Nickel-Hydrogen Production Began in 1994.**
- ◆ **Manufacturing Philosophy**
 - **Implement a Paperless System for Data Management, Quality Control, Process Control.**
 - **Reduce Inspection Points by Incorporating Operator Inspections.**
 - **Build Quality Into the Product by Using Process Control.**

Qualified Processes

◆ Since 1994 the Following Processes at RLF Have Been Qualified for Flight Use:

- Positive Electrode Manufacturing and Testing
- Negative Electrode Manufacturing and Testing
- Pressure Vessel LASER Welding
- Pressure Vessel Cycle and Burst Testing
- Pressure Vessel Flame Spraying
- IPV Assembly
- SPV Assembly
- SPV and IPV Acceptance Testing

Qualified Designs

- ◆ **10 Inch Diameter, 50 and 60 AH Single Pressure Vessel (SPV) Batteries.**
- ◆ **4.5 Inch Diameter, 120 AH Independent Pressure Vessel (IPV) Cells**
- ◆ **3.5 Inch Diameter, 64 AH IPV Cells**
- ◆ **All Three Designs Are Produced on Programs Requiring Monthly and/or Weekly Deliveries.**

RNH 64-1 Matrix Life Test

- ◆ **First RLF, IPV Life Test**
- ◆ **Test Uses High Rate 70% DOD Cycles to Accumulate Wear on the Cells.**
- ◆ **Every 1000 Cycles the Cells Are Run for 100 Cycles at 40% DOD As a Health Check.**

Matrix Life Test Cycle Regime

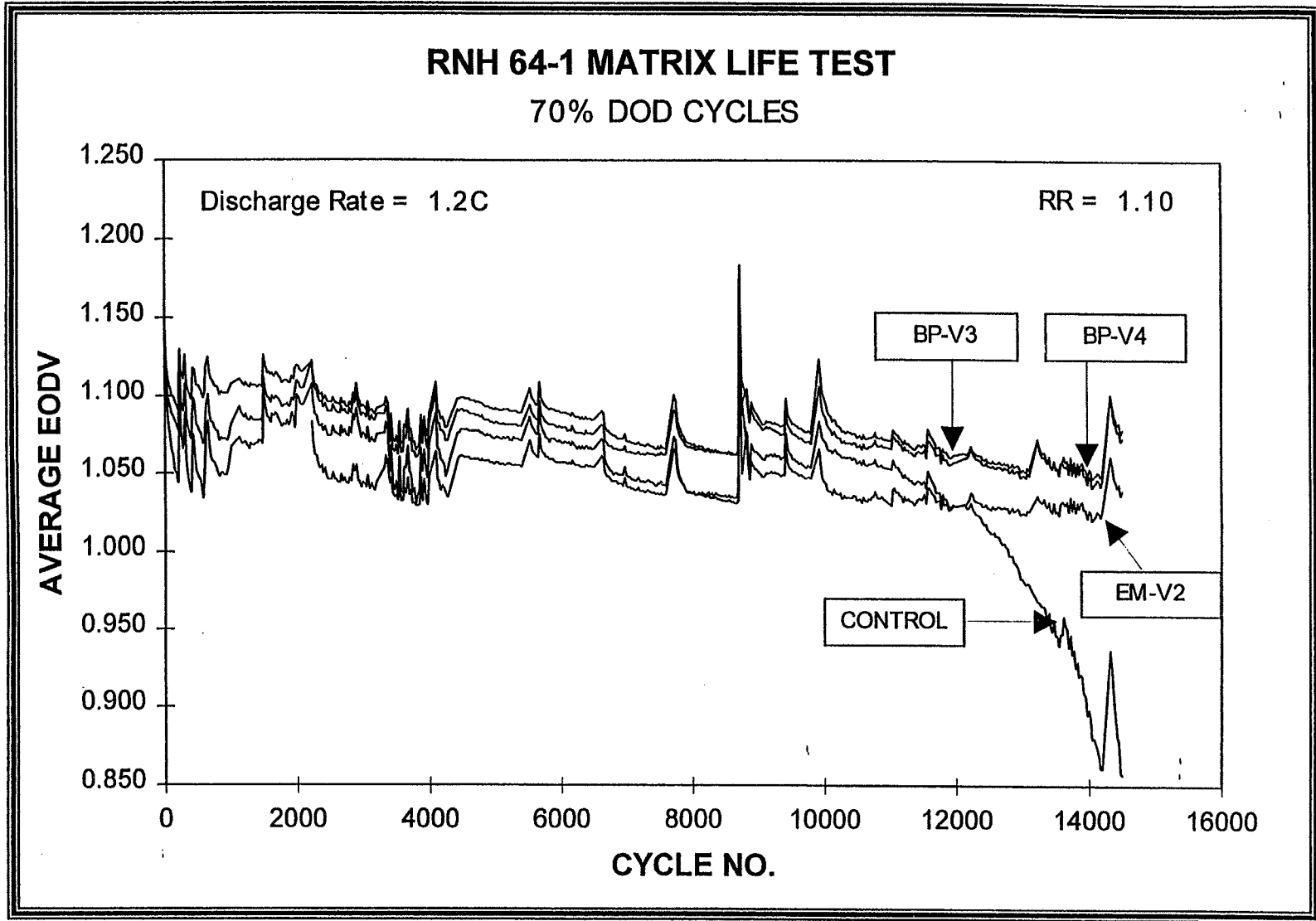
- ◆ **Test Temperature = 0 C**
- ◆ **70% DOD Cycles:**
 - **Charge at a C Rate With a Taper at the End of Charge.**
 - **Discharge at a 1.2C Rate for 35 Minutes.**
 - **RR = 110%, Total Cycle Time = 90 Minutes**
- ◆ **40% DOD Cycles:**
 - **Charge at a C/2 Rate With a Taper at the End of Charge.**
 - **Discharge at a C/1.45 Rate for 35 Minutes.**
 - **RR = 110%, Total Cycle Time = 90 Minutes**

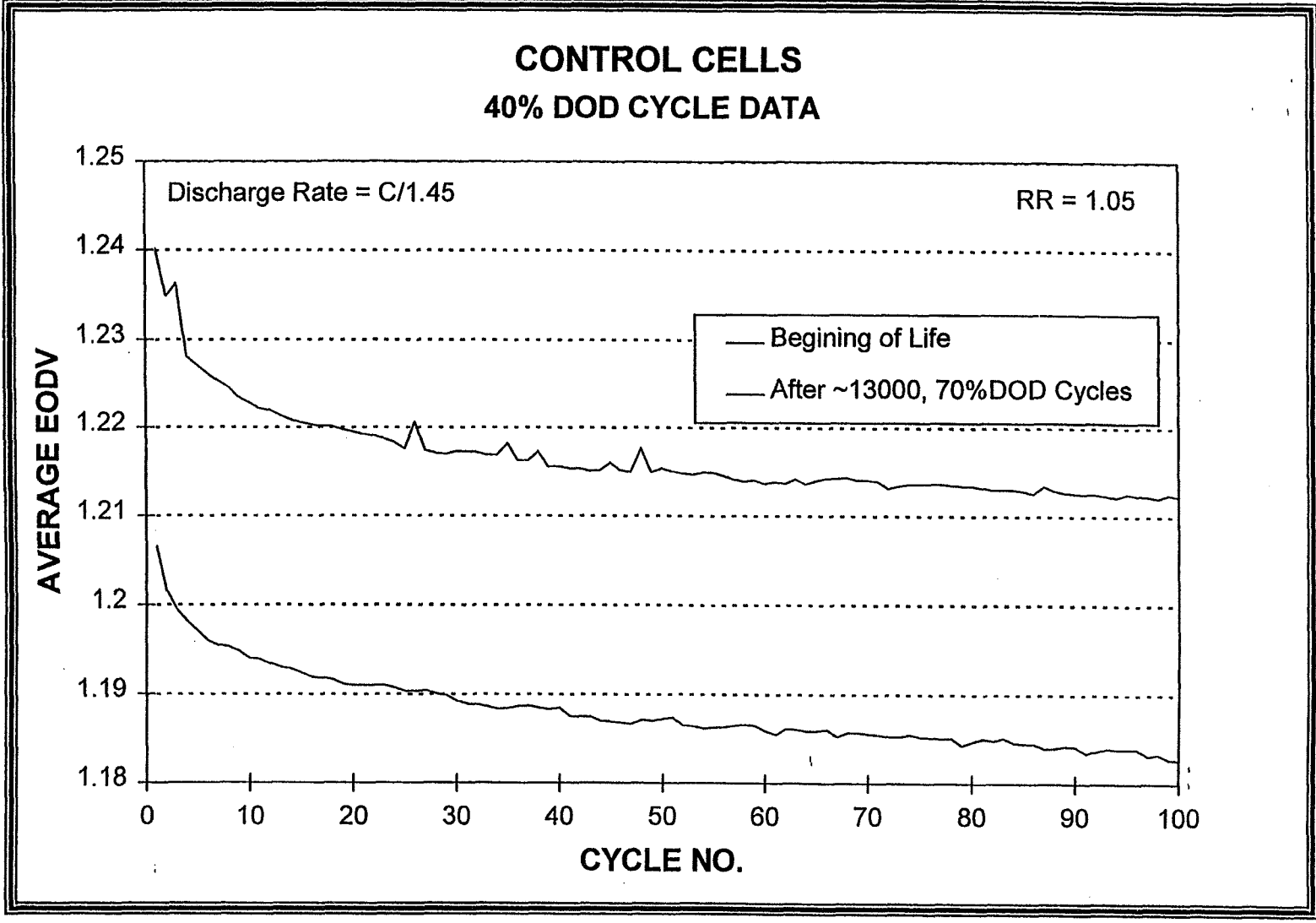
Description of Cells in Test

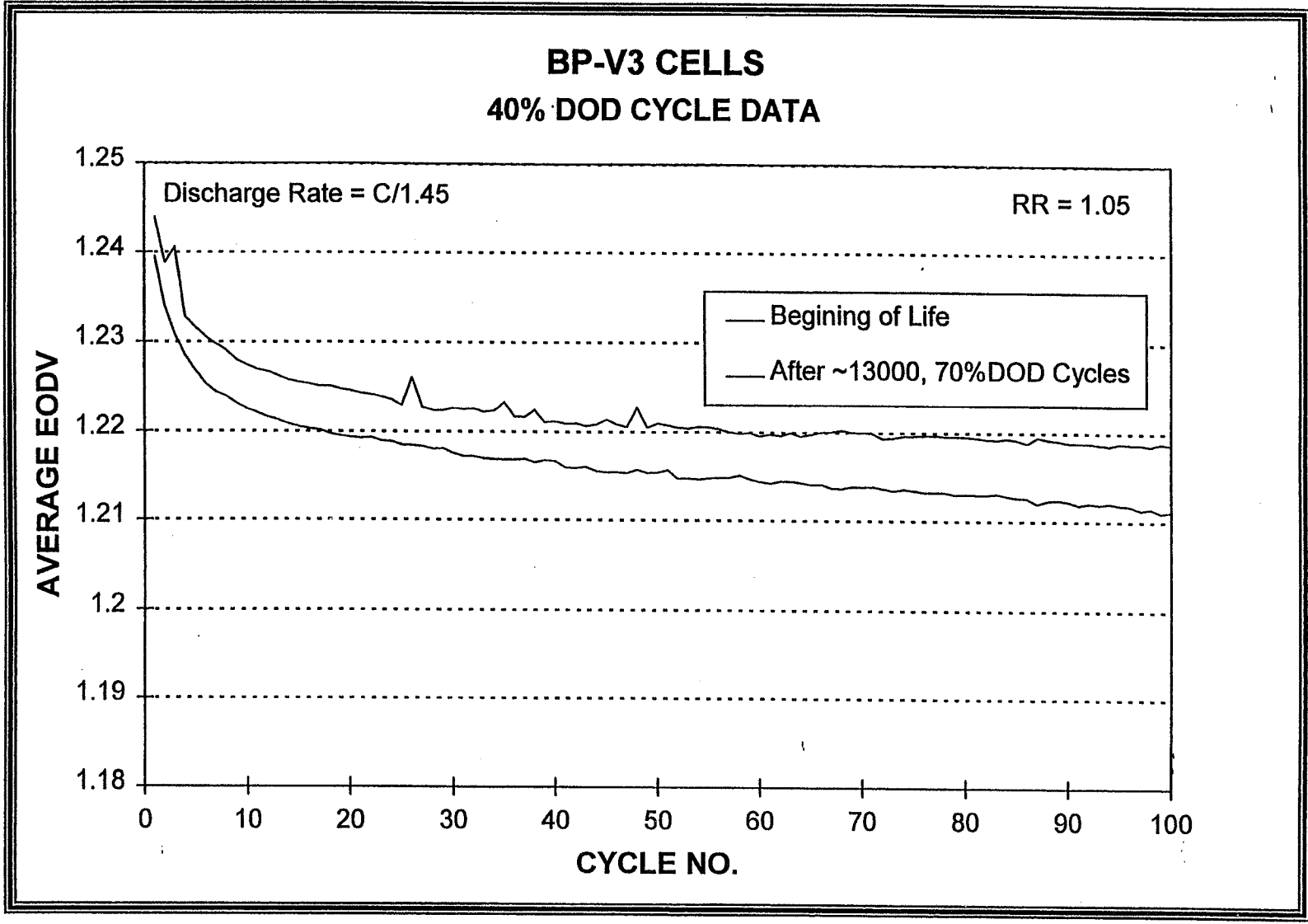
Cell Lot	Identifier	Positive Porosity	Positive Thick.	Electrolyte (%KOH)	# of Cells
Boiler Plate	Control	80%	0.030"	31%	3
Boiler Plate	BP-V3	80%	0.035"	26%	4
Boiler Plate	BP-V4	84%	0.035"	26%	4
Engineer. Models	EM-V2	80%	0.035"	31%	3

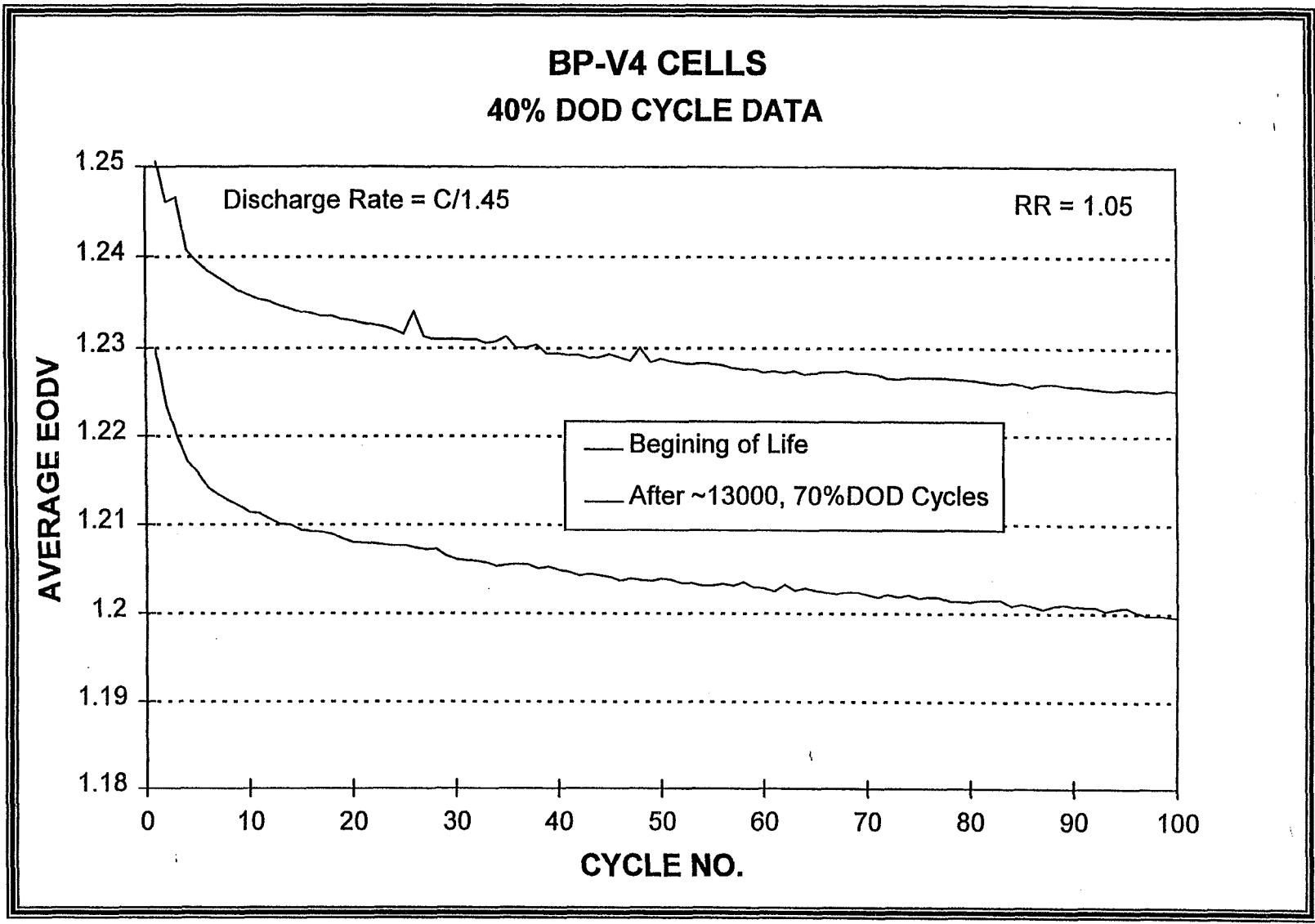
Cycle Status

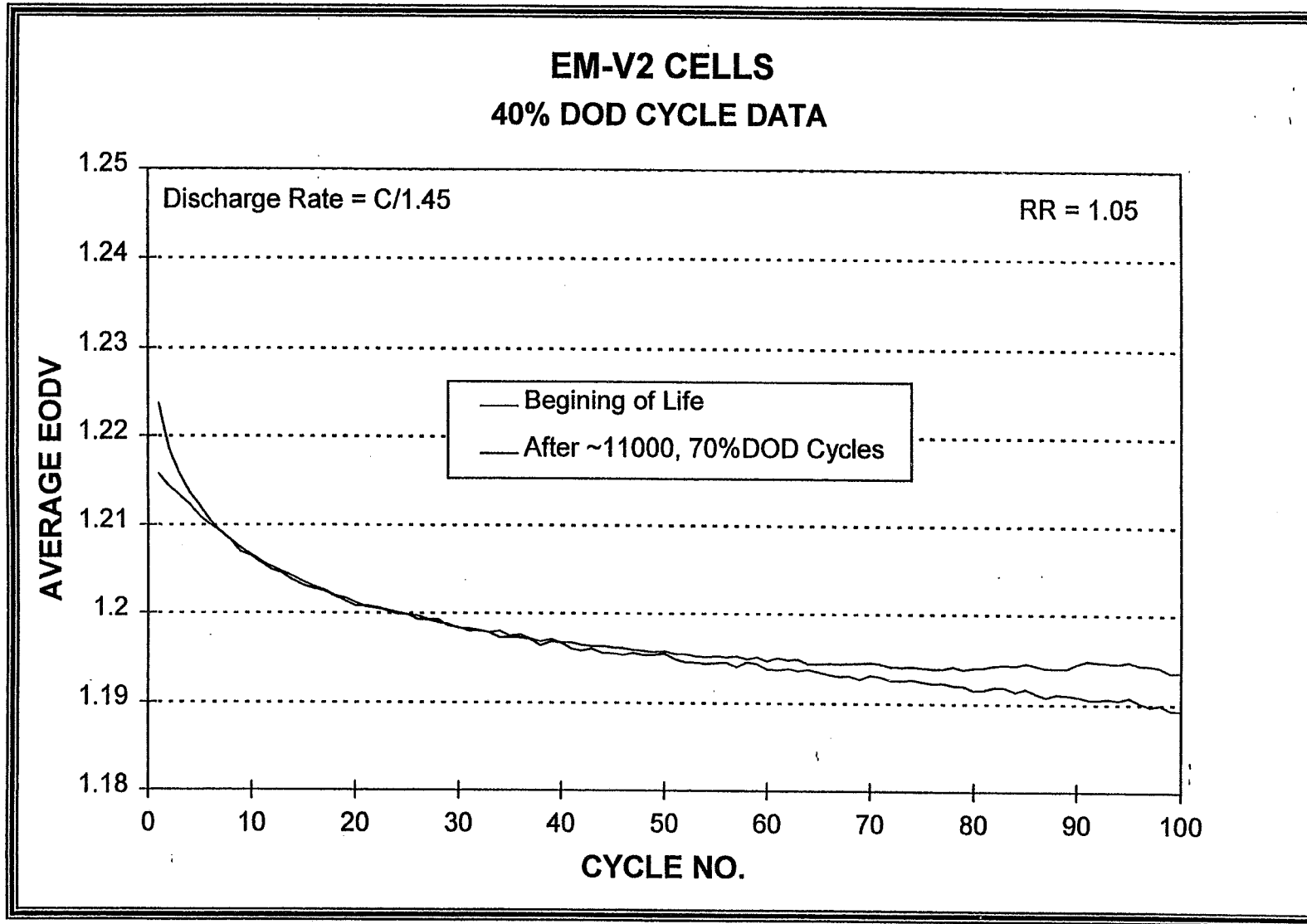
- ◆ **Currently the Cells From Boiler Plate Lot Have Accumulated 13,400 70%DOD Cycles and 1,300 40%DOD Cycles.**
- ◆ **The Engineering Model Cells Have Accumulated 11,400 70%DOD Cells and 1,100 40%DOD Cells.**









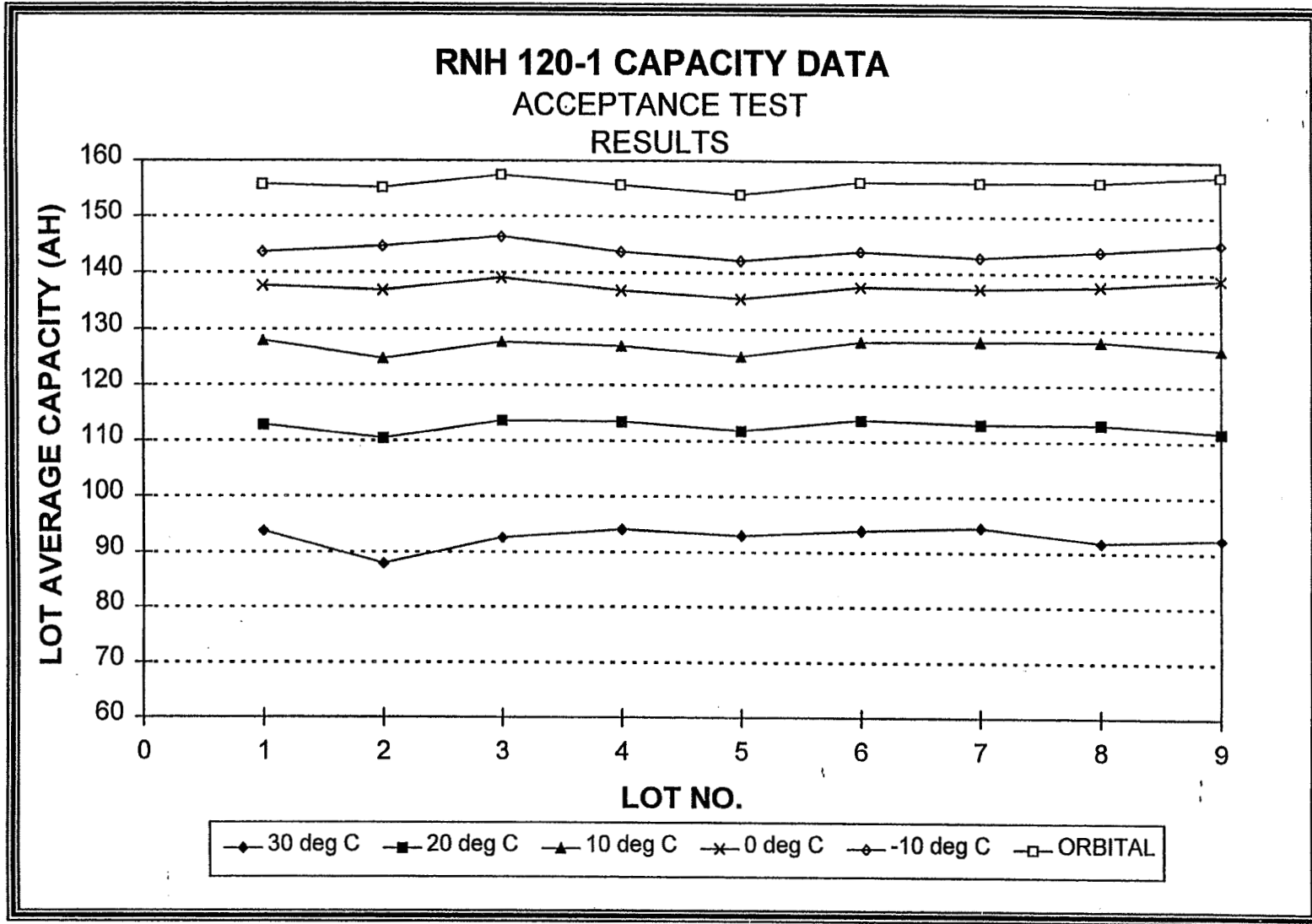


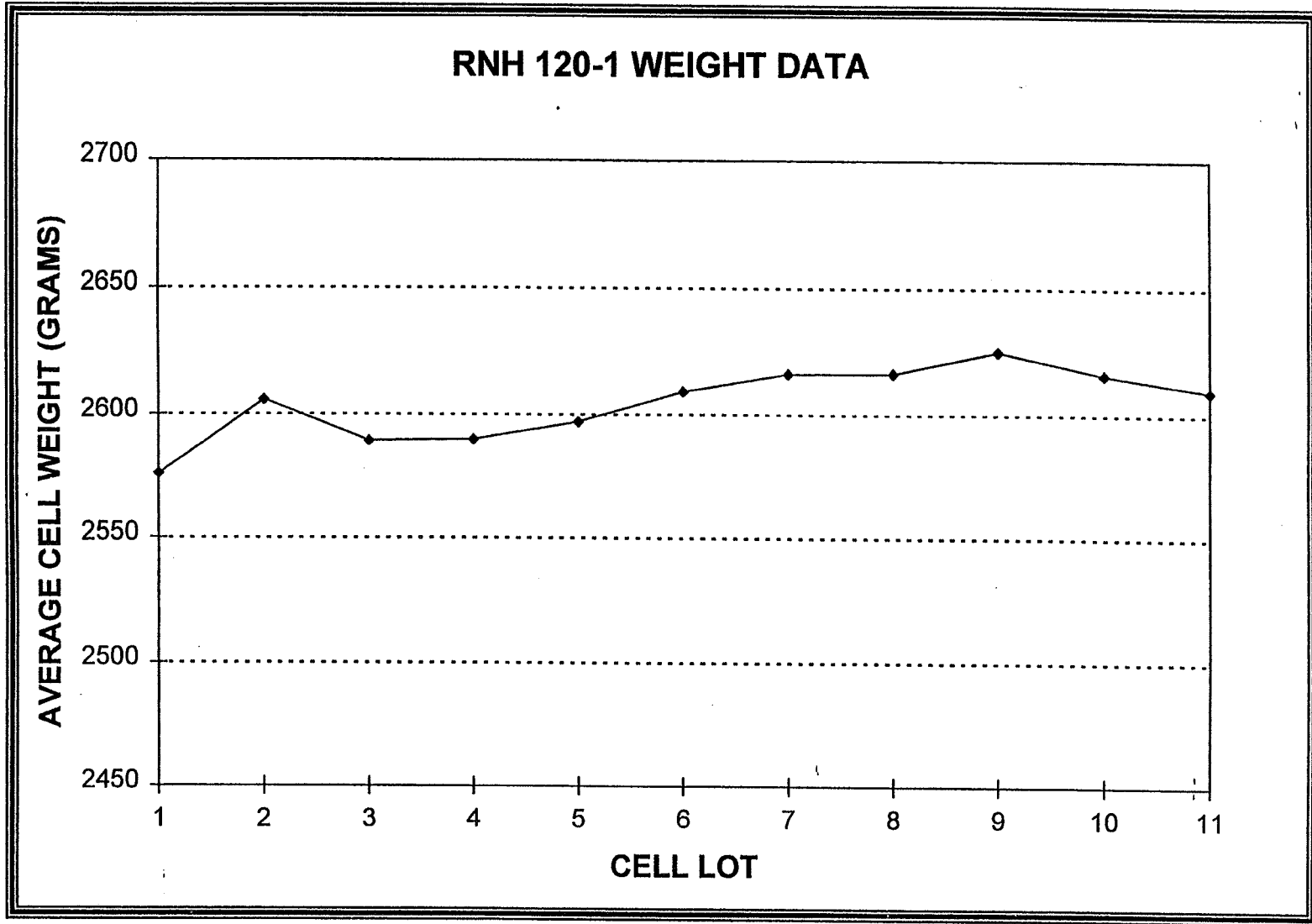
Summary

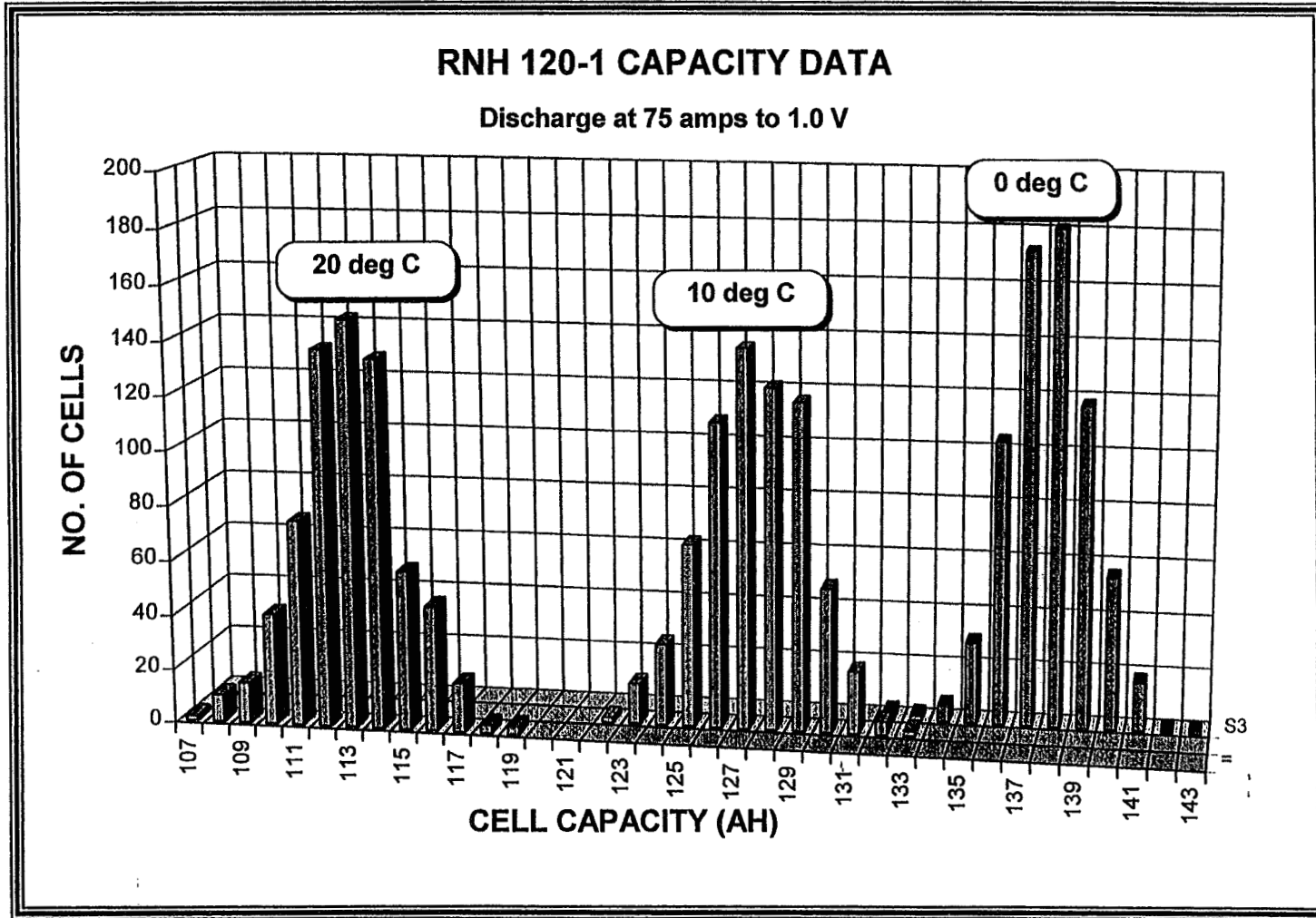
- ◆ **All 0.035” Slurry Designs Are Still Performing Well.**
- ◆ **The RLF Impregnated Electrodes (EM-V2) Show the Least Amount of Voltage Decay.**
- ◆ **Three Additional Cell Designs Have Been Added to the Test Recently.**
- ◆ **A Control Cell DPA Is Planned to Determine Cause of EODV Decline.**

RNH 120-1 Acceptance Test Data

- ◆ **First 4.5" IPV Flight Programs (800 Cells Delivered).**
- ◆ **Represents a Mixture of Data From C Street Impregnated Positives and RLF Impregnated Positives.**
- ◆ **Cell Lots Are Being Shipped on 4 to 6 Week Centers With 6 Month Build Times.**







Summary

- ◆ **RNH 120-1 Data Has Established the Ability to Repeat Cell Performance Over Multiple Lots.**
- ◆ **Tracking This Data Has Aided in the Consistency Achieved.**

Page intentionally left blank

Nickel Electrode Design Focused Session

Page intentionally left blank

Cause for Second Plateau Discharge in Nickel Electrodes

**A. Zimmerman and N. Weber
Electronics Technology Center
The Aerospace Corporation
El Segundo, California 90245**

**for presentation at
The 1997 NASA Battery Workshop
18-20 November 1997
Huntsville, Alabama**

Cause for Second Plateau Discharge in Nickel Electrodes

A. Zimmerman and N. Weber
Electronics Technology Center
The Aerospace Corporation
El Segundo, California 90245

Abstract

Nickel electrodes typically exhibit a lower discharge plateau at about 0.9 volts vs. hydrogen. This lower plateau can become quite significant in degraded nickel hydrogen cells. The possible mechanisms for this lower plateau are presented, and the data either supporting or refuting each mechanism described. It will be demonstrated that only one mechanism for the second plateau is fully consistent with the existing data base. This mechanism predicts the second plateau to result from coupling between parasitic oxygen reduction and the I/V behavior of a barrier layer at the junction between the semiconducting active material and the current collector. Methods will also be described that are capable of either accentuating or reducing the second plateau discharge in nickel hydrogen battery cells.

Capacity loss from nickel electrode degradation in nickel hydrogen battery cells is often manifested by the loss of discharge capacity from the normal discharge voltage plateau at about 1.25 volts, accompanied by an increase in discharge capacity at a lower (or "second") plateau at about 0.9 volts, as illustrated in Figure 1. While this lower discharge level is always present to some degree in the discharge of nickel electrodes, it is only in the nickel hydrogen cell environment that is seen to become accessible for lengthy discharge at quite high discharge rates. A number of mechanisms for this lower plateau have been proposed over the years. Here the consistency of each of these mechanisms with the available data base will be evaluated, for the purpose of determining the underlying mechanism for the second plateau.

The following list of mechanisms have been either proposed, or have the possibility of causing a lower discharge plateau in nickel electrodes:

1. An alternative electrochemical reaction. Possibilities include reduction of oxygen gas, reduction of gamma-phase active material, or the reduction of some unidentified material. These possibilities all require significant quantities of an alternative active phase.
2. The drop from the upper discharge plateau is caused either by depletion of charge in the active material or by the development of a high resistance in the active material due to charge depletion, and probably in most instances is caused by a combination of these two effects. If conductivity can increase with decreasing electrode voltage, and there exists a parasitic electrochemical process that can pin the voltage at the interface between the active material and the current collector, a lower discharge plateau can occur at the pinned voltage level. This mechanism can give multiple lower plateaus if there are different types of interfaces present, since each interface can pin the voltage at a different level.

3. Physical variations in contact area of active material to current collector can shift the overpotential for the normal discharge reactions to greater values, thus moving the discharge plateau downwards. If there are two populations of active material, distinguished by either very good or very poor contact area with the current collector, it is possible for these populations to discharge at different voltage levels.

To differentiate between these or other mechanisms, it is necessary to have a collection of observed data. The following list is a collection of observations made for nickel electrodes that are pertinent to the mechanisms for the second plateau.

1. In some cases, the amount of capacity discharged in the second plateau can exceed the amount discharged in the upper plateau.
2. The second plateau disappears when oxygen gas is not present at the nickel electrode, i.e. evacuating all gas from a nickel hydrogen cell then backfilling with hydrogen. However, the capacity encompassed by the second plateau remains in an undischARGEABLE state. This behavior is indicated in Figure 2. The regeneration of oxygen allows the lower plateau material to be again discharged.
3. The gamma-NiOOH phase, in a homogeneously discharging electrode, discharges at a voltage about 40 mv below that of the beta-NiOOH phase. This reaction occurs with kinetics that are not significantly poorer than discharge of the normal beta-phase, as indicated in Figure 3. For this reason it is thermodynamically impossible for significant gamma-phase active material to exist in close proximity to the current collector when the voltage has dropped down to the second plateau.
4. The depleted nickel oxyhydroxide active material is a semiconductor, having a doping density equal to the density of charged sites remaining. Thus, if a voltage exceeding a bandgap of about 0.3 volts develops across a layer of this active material, its electronic conductivity will increase exponentially as the voltage across the layer increases.
5. The heat produced by a nickel electrode while discharging on the second plateau gives an enthalpy change for the second plateau reaction that is identical to that for the reaction on the normal discharge plateau, i.e. the added voltage drop between the upper and lower discharge plateau all shows up as heat according to the product of the voltage drop and the current. Data measured utilizing dynamic calorimetry, which has a time constant of less than 30 seconds, indicate this in Figure 4.
6. In the hydrogen gas environment of the nickel hydrogen cell, extensive second plateaus are often seen, with the amount of second plateau capacity generally being proportional to the amount of gamma-phase active material generated. However, typically there is much more overcharge when larger amounts of gamma-phase are formed. When the same kind of sintered electrode is evaluated in a flooded test cell, there is no good correlation between the amount of second plateau seen and the amount of gamma-phase or the amount of overcharge.
7. The reversible potential seems to be the same on both the upper and lower discharge plateaus.
8. Increasing the amount of cobalt additive in the active material shifts capacity from the lower plateau to the upper plateau, and also increases the rate of recovery from the lower plateau to the upper plateau if the discharge current is decreased.
9. The voltage level associated with the second plateau depends on the pressure of hydrogen gas in the nickel electrode, increasing with increasing hydrogen pressure.
10. The kinetics for the discharge reaction undergo a significant change, as indicated by the $\log I/V$ curves in Figure 5 for a nickel hydrogen cell undergoing discharge on the upper and lower plateaus.

The first mechanism to be considered is simply that reduction of oxygen, either adsorbed or gaseous, causes the second plateau. There are several reasons why this is not likely to be a valid mechanism. First, the amount of oxygen needed to give 50% of the electrode capacity in a second plateau is prohibitive, particularly in a nickel hydrogen cell where the oxygen will burn in the hydrogen atmosphere. Second, the reversible potential and enthalpy change due to oxygen reduction should be slightly different from the normal discharge process, a difference that has not been detected. Third, the second plateau position should vary with oxygen activity in the nickel electrode. The second plateau voltage level actually seen does not vary significantly, but seems pinned somehow to a relatively narrow range of potentials. We have constructed a nickel-oxygen cell employing a sintered nickel electrode, which when filled with 114 psia of oxygen gas could continuously support oxygen reduction at 0.1 ma/cm^2 at an overpotential of 800 mv. Clearly this kind of process cannot support the 10 ma/cm^2 discharge rates seen on second plateaus in nickel hydrogen cells.

The second mechanism to be considered is that electrochemical reduction of gamma-phase to some other reduced phase causes the second plateau. Since gamma-phase is reduced at voltages about 40 mv below beta-phase reduction (Fig. 3), it is thermodynamically impossible to retain significant gamma-phase in the face of a 300-400 mv overpotential, unless it is stabilized by a high resistance layer between the gamma-phase material and the current collector. If this is the case, then it is the high resistance layer and its conduction properties that are responsible for the lower discharge plateau. In addition, it is difficult to envision any electrochemically active material that always discharges at an overpotential of 300-400 mv independent of rate, structure, or other parameters that normally alter electrochemical overpotentials.

The third mechanism to be considered is the possibility that two distinct populations of active material exist, one having a very high surface area contact with the current collector and the other having a very low surface area contact. This is consistent with the observation that the amount of second plateau seen in nickel hydrogen cells typically increases as the electrodes degrade. Here again, one would expect to see second plateau levels covering the entire voltage range from the upper level and downwards, as the physical structure of the active material shifts and degrades. Since this behavior is not seen, this cannot be regarded as a viable mechanism.

The final mechanism to be considered attributes the lower voltage plateau to the intrinsic semiconducting characteristics of the active materials in nickel electrodes. As the discharge process begins to deplete the active material at its junction with the current collector, a layer of depleted material begins to grow out from the current collector. Because, this layer has poor conductivity, a significant voltage drop develops across the layer, i.e. between the current collector and the remaining charged active material. When this voltage drop exceeds the bandgap of the nickel oxyhydroxide, about 0.3-0.4 volts, the depleted layer will increase in conductivity much like a diode responds when forward biased. While this enables electronic conduction through the depleted layer and discharge of otherwise isolated charged material, it cannot give a second plateau unless some electrochemical process can act to pin the potential at the junction between the active material and the current collector. The oxygen reduction process provides just such a process, requiring only microamps or less current to support the potential at the current collector surface, while the bulk of the current is carried electronically through the depleted layer to discharge remaining charged active material. If there is only a very limited supply of oxygen gas at the surface of the current collector, the second plateau will terminate. The diagram in Fig. 6 illustrates this mechanism.

This last mechanism seems to be fully consistent with all the observed behavior of nickel electrodes. By definition, it involves identically the same reactions on the lower plateau

as on the upper plateau. Since it requires electronic conductivity through a depleted layer, it should be sensitive to any materials that can alter the conductivity of the depleted layer. Cobalt additives provide sites that can significantly improve proton diffusion rates, thus increasing the ability of the active material to maintain conductivity. Similarly, hydrogen gas can undergo catalytic reaction at the metal surfaces at low rates, resulting in the direct injection of protons into the depleted active material and its enhanced ability to conduct charge through the depleted layers. It is this exchange between hydrogen gas and protons in the active material that enhances the ability to obtain lower plateau discharge at high rates in the gaseous environment of the nickel hydrogen cell.

The mechanism described above and illustrated in Fig. 6, which is consistent with the body of performance data, indicates precisely how one should go about minimizing the second plateau. First, assure that all active material is in intimate and close contact with the current collector. The sintered electrode, until it undergoes significant expansion, blistering, or corrosion after extensive cycling, is an excellent example of this kind of structure. Second, improve the proton diffusion rate in the active material. This will delay the formation of depleted layers, as well as improving electronic conductivity. The use of cobalt additives provides this function, when the cobalt occupies a site in the active material lattice that otherwise would contain a nickel ion. Additives that do not occupy nickel sites within the lattice can also improve conductivity by enhancing conduction across the grain boundaries between the active material crystallites.

Figure 1

C/2 Discharge Voltage for NiH2 Cell Showing second plateau

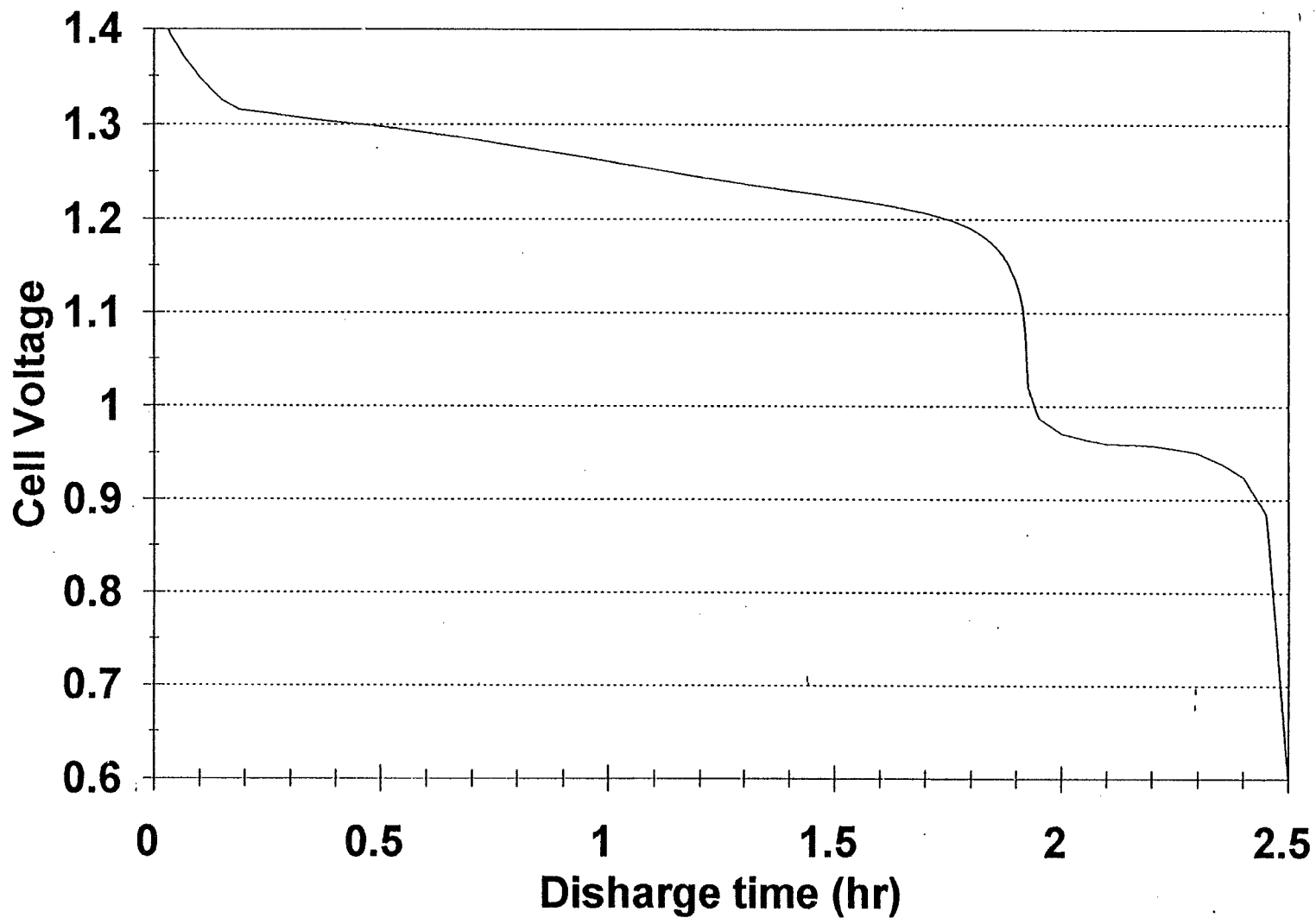


Figure 2

C/2 Discharge Voltage for NiH₂ Cell Showing second plateau

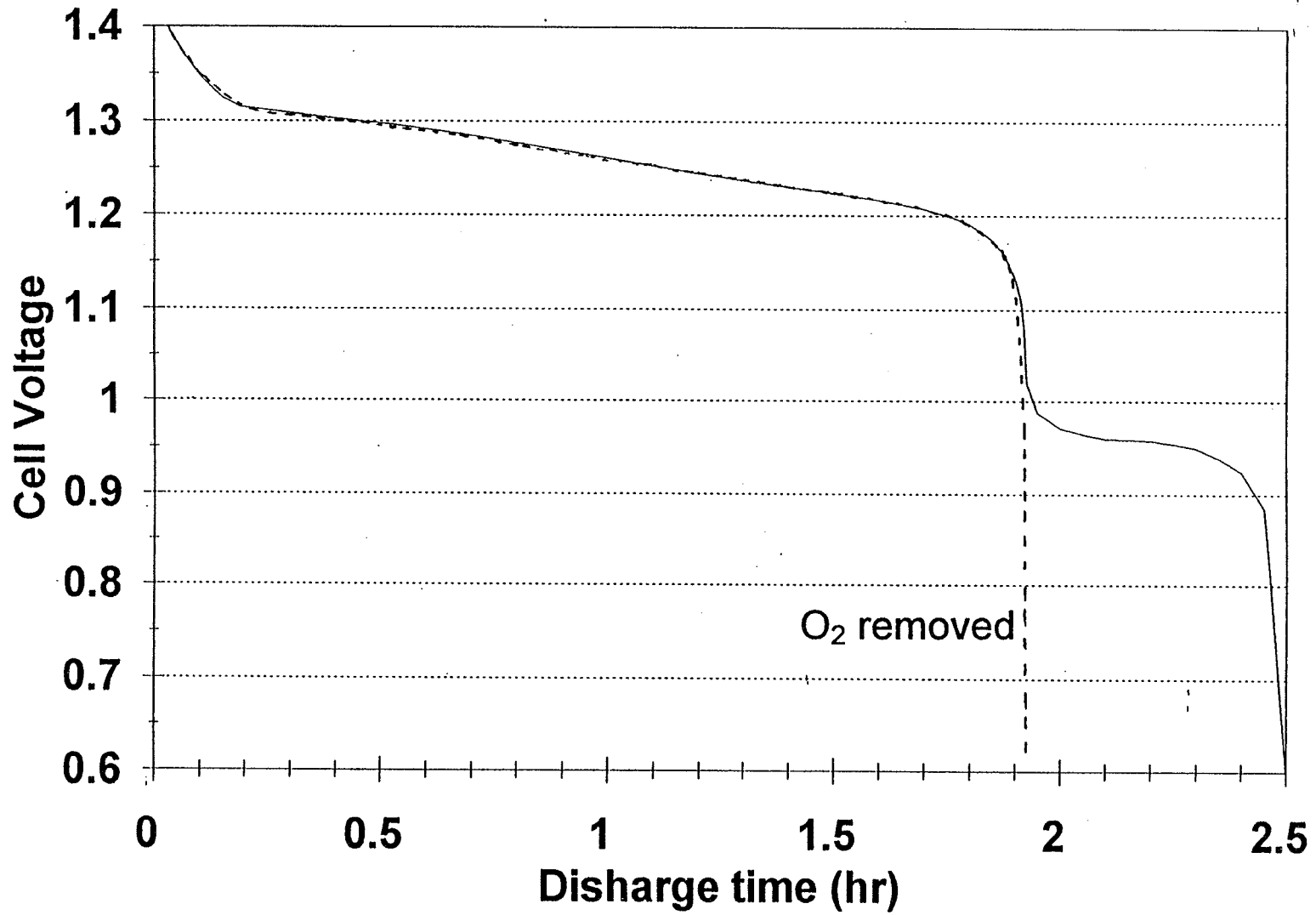


Figure 3

Relative Redox Potentials of β -NiOOH and γ -NiOOH

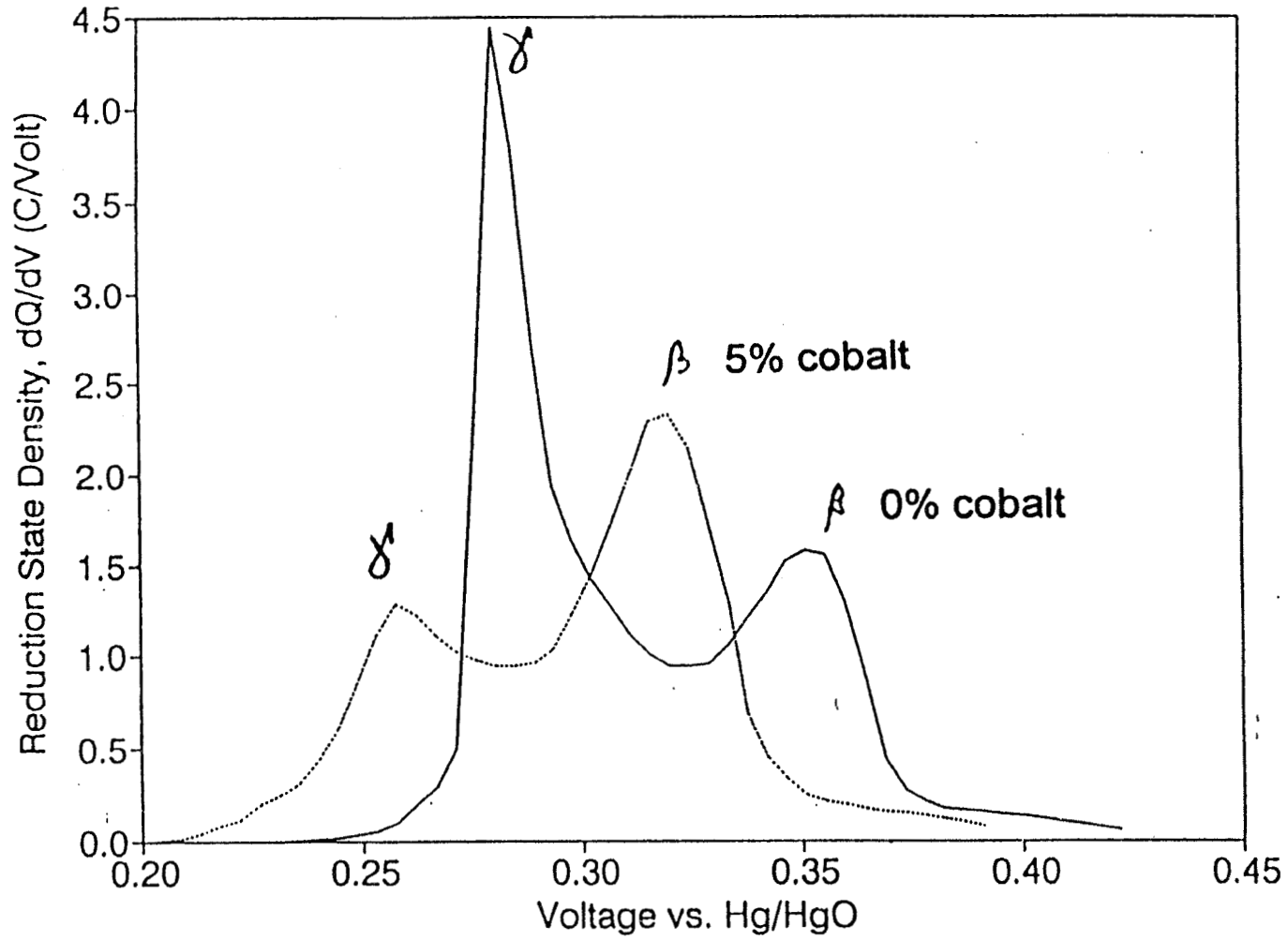


Figure 4
Enthalpy Change for Discharge Reaction During Discharge on Upper and Lower Plateaus

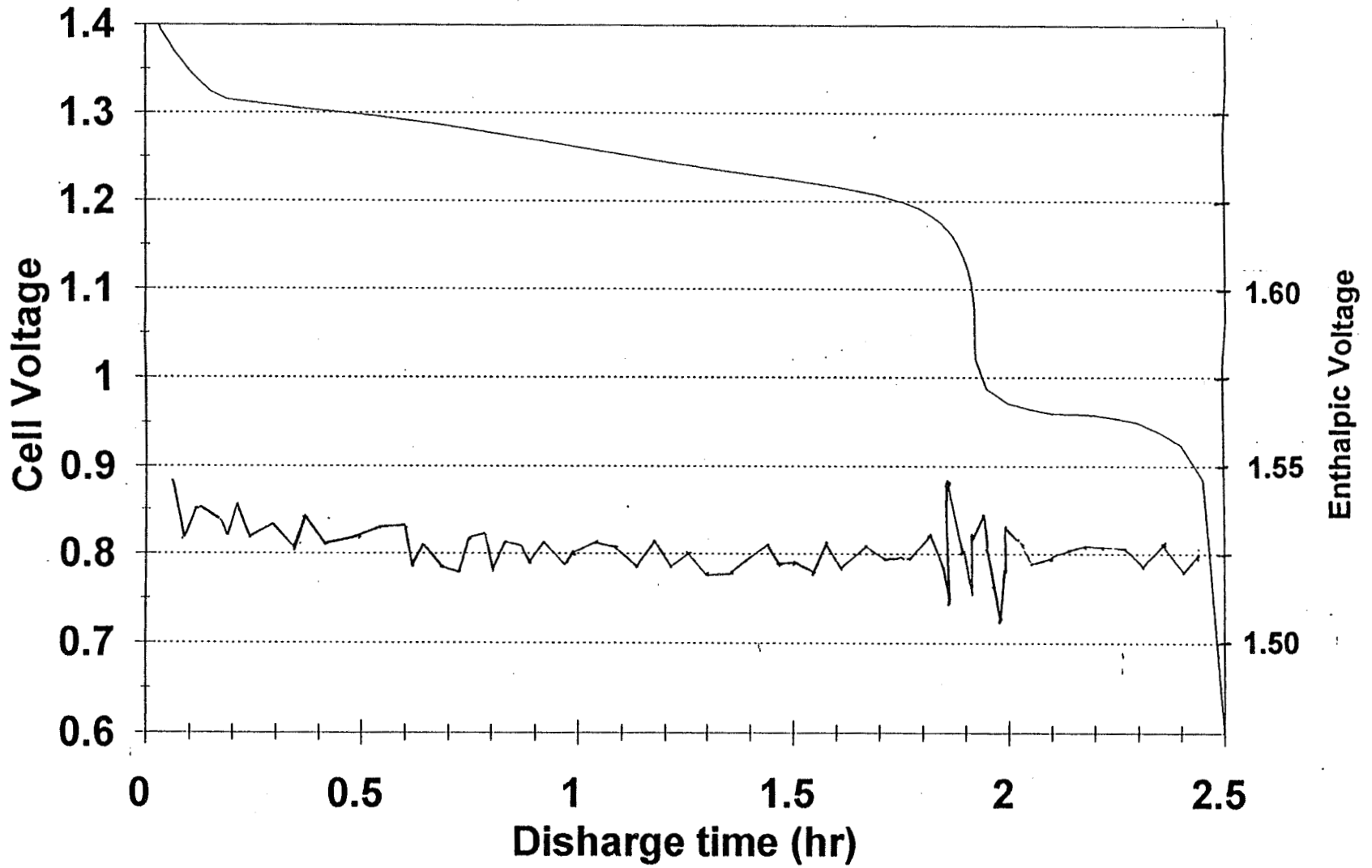


Figure 5

I/V Plot for Nickel Electrode on Upper and Lower Voltage Plateaus

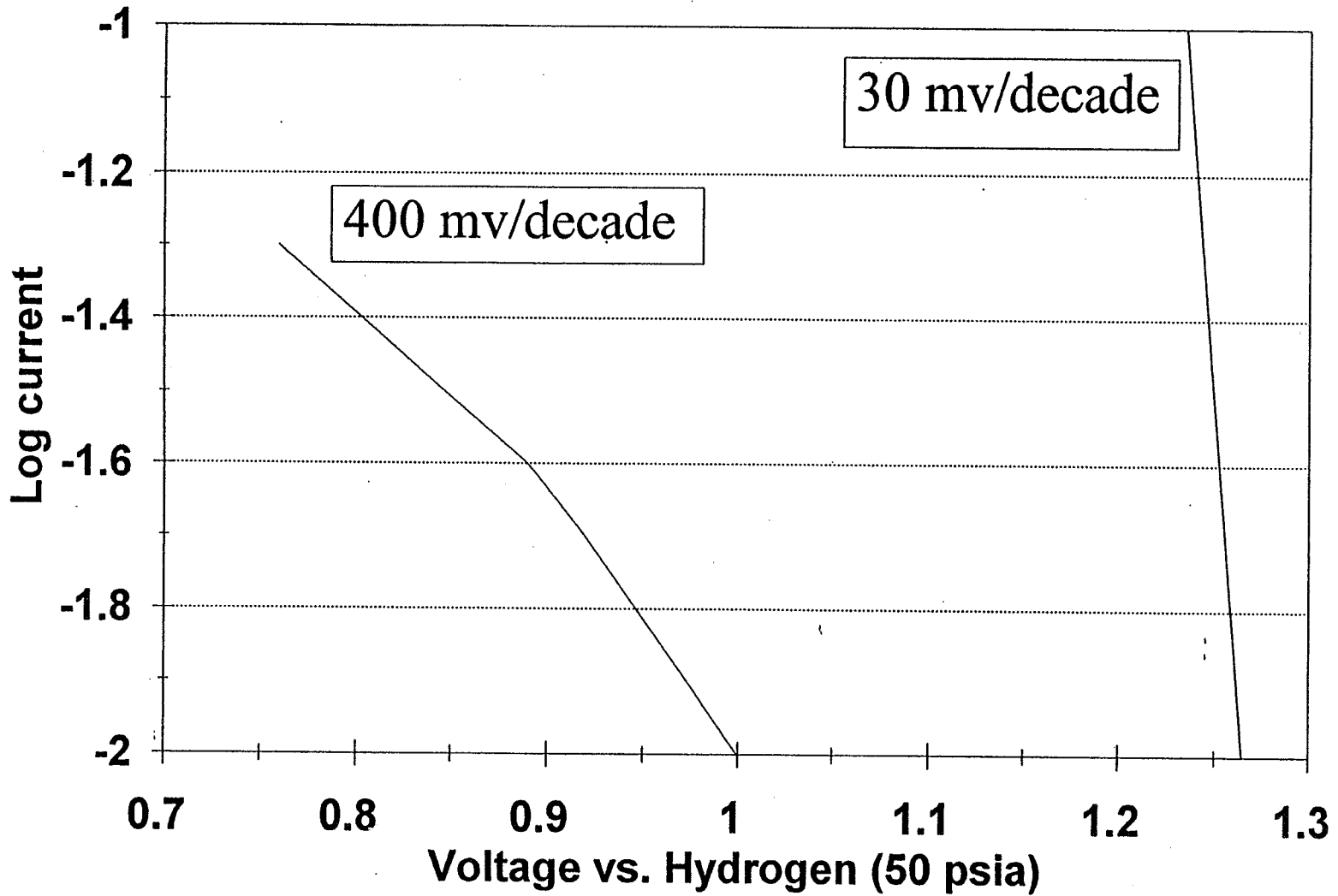
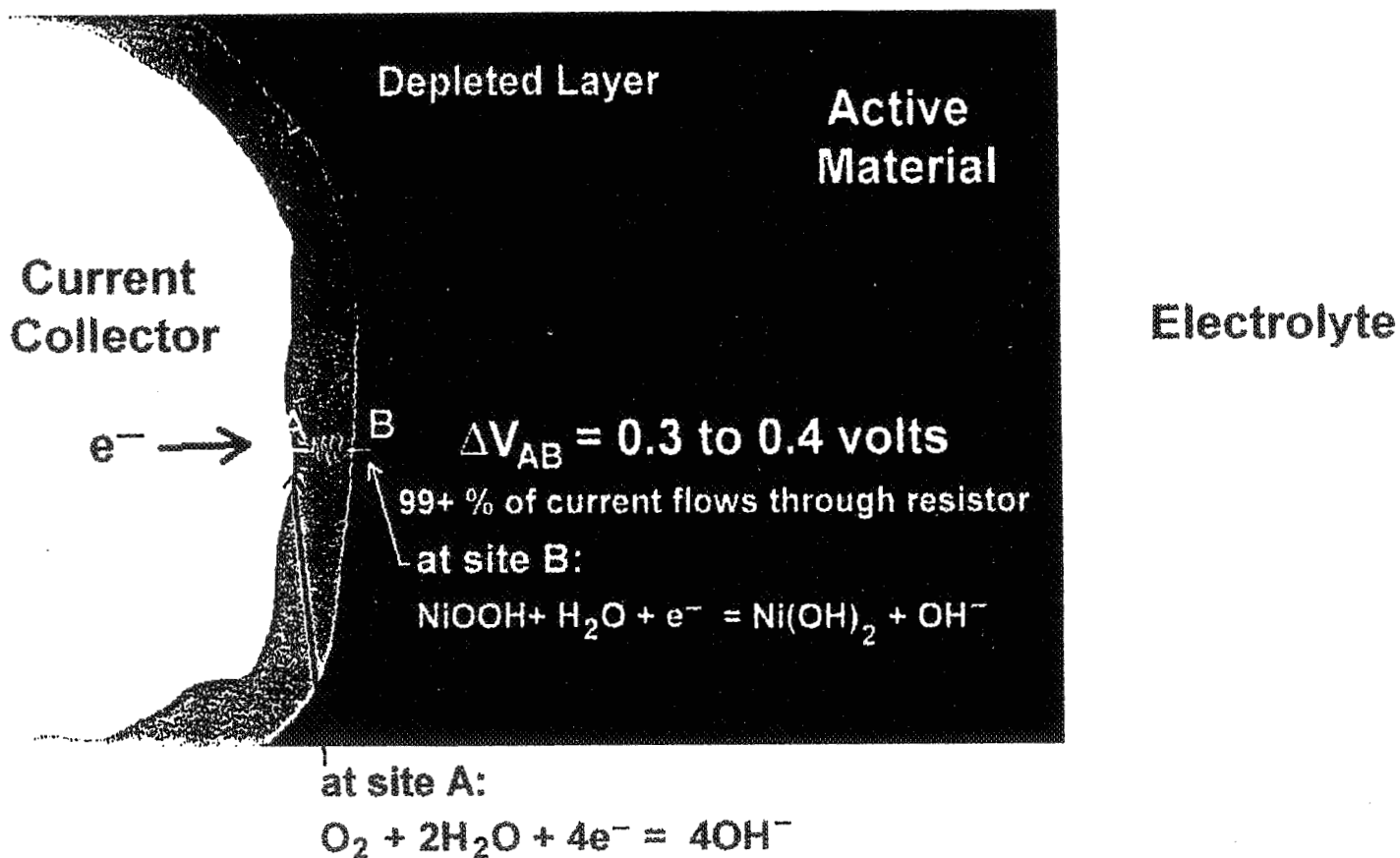


Figure 6
**Role of Barrier Layer
 in Producing Lower Voltage Plateau
 in Nickel Electrode**

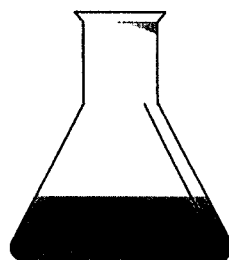


Page intentionally left blank

**EAGLE-PICHER INDUSTRIES INC.
TECHNOLOGIES DIVISION
POWER SYSTEMS DEPARTMENT
COLORADO SPRINGS, CO 80911**

**FABRICATION OF NICKEL
ELECTRODES USING ETHANOL
SOLUTIONS**

DAVID F. PICKETT, JR.



AGENDA

- **BACKGROUND**
 - STUDIES OF AQUEOUS EI PROCESSES AT BELL LABS.
 - EARLY EFFORTS AT WRIGHT LABORATORIES
 - CONTRACTUAL STUDIES
- **DEVELOPMENT HISTORY**
 - WRIGHT LABORATORIES BENCH DEVELOPMENT
 - EAGLE-PICHER MANUFACTURING TECHNOLOGY
 - NASA LEWIS STUDIES
- **SCALE-UP TO MANUFACTURING AT EAGLE-PICHER**
- **FLIGHT QUALIFICATION**
 - GOVT PROGRAMS
 - HUGHES AIRCRAFT
- **FLIGHT DATA BASE**
 - NICKEL HYDROGEN
 - SUPER NiCd
- **CURRENT USES**
- **CONTINUING DEVELOPMENT EFFORTS**

BACKGROUND

- **DEVELOPMENT**
 - **GERMAN EFFORTS IN EI PLATE PROCESSING (AQUEOUS)**
 - **KANDLER, HAUSLER, *ET AL***
 - **BELL TELEPHONE LABORATORIES (AQUEOUS)**
 - **MAURER, MACARTHUR, McHENRY, BEAUCHAMP, O'SULLIVAN, WILLIS**
 - **ACTED AS ADVISOR TO USAF AND INDUSTRY**
 - **IN-HOUSE EFFORTS AT WL/AFAPL (AQUEOUS, ETHANOL)**
 - **LANDER, PICKETT**
 - **INDUSTRY(CONTRACTS THROUGH USAF/ WL)**
 - **SPECTROLAB, EAGLE-PICHER**
 - **NASA LeRC**
 - **CONTRACT WITH HUGHES**
- **MANUFACTURING TECHNOLOGY (USAF)**
 - **EAGLE-PICHER**

FLIGHT QUALIFICATION

- **NICKEL HYDROGEN PROGRAMS AT HUGHES AIRCRAFT (1975-1984)**
- **INTELSAT VI (1985 - 1990)**
- **HUGHES NICKEL HYDROGEN CELLS {HSC IN HOUSE EFFORT - (1990 - PRESENT)}**
- **HUGHES SUPER NiCd (1987 - PRESENT)**
 - **NOW MANUFACTURED EXCLUSIVELY BY EAGLE-PICHER**
 - **USED BY HUGHES, NASA, TRW, APL, *ET AL.***
- **EAGLE-PICHER MAGNUM (1990 - PRESENT)**

WHY ETHANOL?

- **CAN BE CARRIED OUT AT LOWER TEMPERATURES THAN AQUEOUS SOLUTIONS**
 - FORMS AZEOTROPE WITH WATER
 - REDUCES SURFACE TENSION
- **RETARDS NICKEL ATTACK ON SUBSTRATE WITHOUT FURTHER PASSIVATION OF SINTER**
 - USED TO IMPREGNATE NICKEL PLATED CARBON FIBERS
- **REDUCING AGENT DOES NOT BUILD UP IN SOLUTION**
- **ENHANCES PRECIPITATION IN PORES OF SINTER**
- **PROVEN TO GIVE LONG LIFE ELECTRODE**
 - LIM AND SMITHRICK REPORT >20,000 LEO CYCLES AT 80% DOD
 - IN-HOUSE STUDIES AT HSC

WHAT MAKES THE BEST ELECTRODE - AQUEOUS OR ALCOHOL PROCESS?

- **"IT'S NOT WHAT YOU LINE UP WITH, IT'S WHO YOU LINE UP WITH"-
DARRAL ROYAL**
 - THE USAF, NASA, HUGHES AND EAGLE-PICHER (COLO SPGS) ARE THE "FOUR HORSEMEN" WHO MADE THE ALCOHOL PROCESS SUCCESSFUL
 - THE BELL LABS HIGH TEMPERATURE PROCESS ALSO MAKES EXCELLENT ELECTRODES
 - BELL LABS., TYCO, GENERAL ELECTRIC, AND EAGLE-PICHER (JOPLIN) PARTICIPATED IN ITS DEVELOPMENT
- **APPLICATION AND ECONOMICS, NOT ONLY CYCLE LIFE PERFORMANCE, ARE ALSO KEY IN DECIDING WHICH IS THE BEST ELECTRODE FOR AN APPLICATION.**
 - GEO ONLY REQUIRES ~2500 CYCLES FOR MISSION
 - PLANETARY MISSIONS USUALLY REQUIRE LONG STAND LIFE AND MINIMAL CYCLE LIFE
 - LONGEST LEO CYCLE LIFE HAS BEEN DEMONSTRATED USING 26% KOH AND ALCOHOL ELECTRODES.
- **QUALITY IS NO ACCIDENT - THE BEST ELECTRODE WILL BE MADE BY THE ORGANIZATION WHO HAS THE COMMITMENT AND DEDICATION TO MAKE IT - BE IT AQUEOUS OR ALCOHOL BASED.**

CURRENT USES OF ELECTRODES IMPREGNATED WITH ETHANOL SOLUTIONS

- **HSC NICKEL HYDROGEN CELLS**
 - **GEO COMMUNICATIONS SATELLITES**
- **EAGLE-PICHER SUPER NiCd CELLS**
 - **GEO**
 - **LEO**
 - **SPACE PROBES**
 - **SPACE STATION EMERGENCY LIGHTING**
- **MAINTENANCE FREE AIRCRAFT BATTERIES**
 - **BOMBERS**
 - **FIGHTERS**
 - **MILITARY TRANSPORT**
 - **HELICOPTERS**
 - **OTHER**

CONTINUING DEVELOPMENT EFFORTS

- **LIGHTWEIGHT NICKEL ELECTRODES**
 - HSC
 - NASA LEWIS RESEARCH CENTER
- **SPECIALTY APPLICATIONS**
 - EAGLE-PICHER POWER SYSTEMS DEPT.
- **MODELING OF IMPREGNATION PROCESS**
 - ORD/UNIV. OF S. CAROLINA

Effects of Cycling Conditions of Active Material from Discharged Ni Positive Plates Studied by Inelastic Neutron Scattering Spectroscopy

Juergen Eckert

Los Alamos National Laboratory

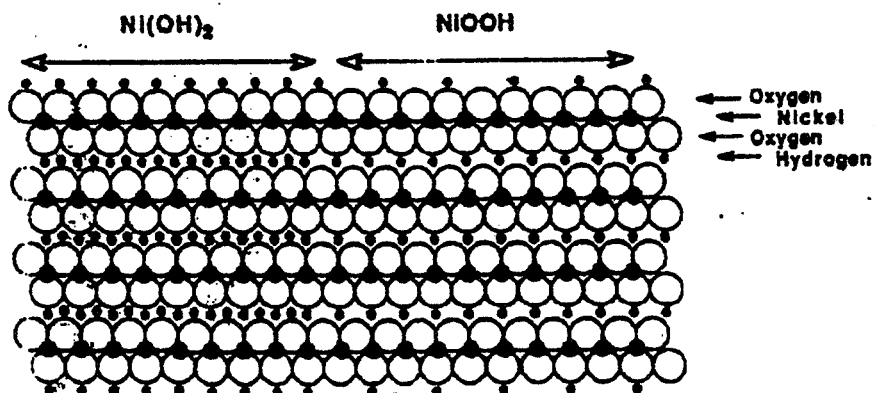
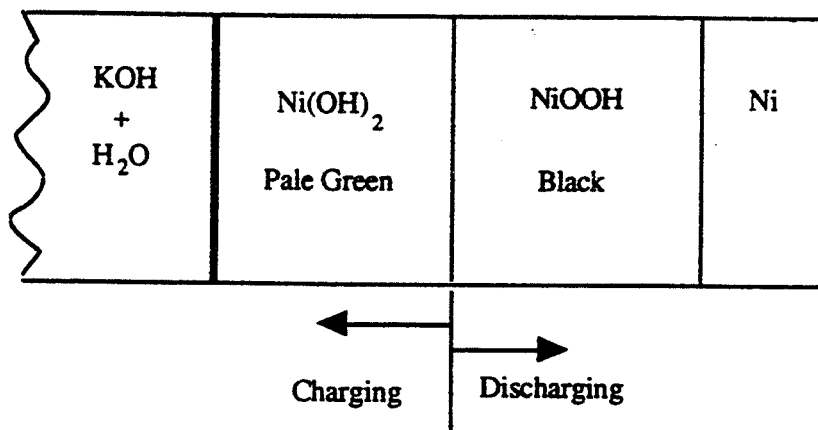
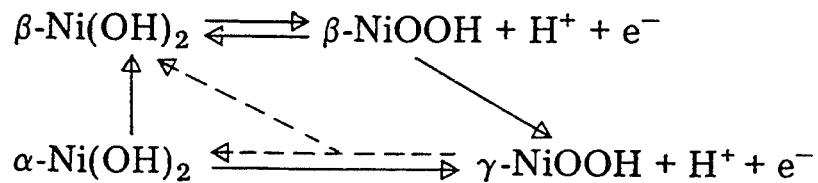
and

Ravi Varma, Lisa Diebolt and Margaret Reid

Objectives

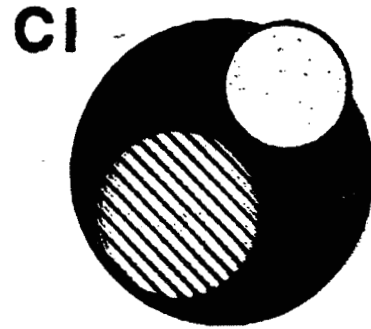
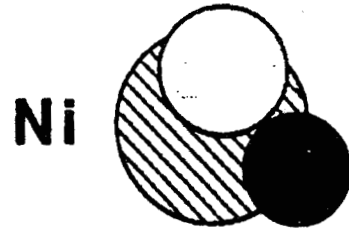
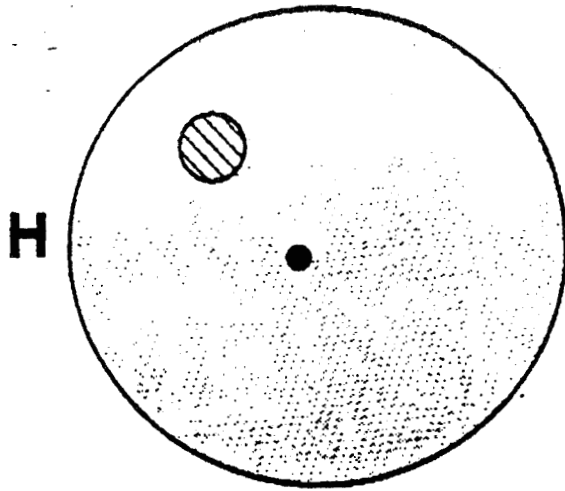
- Identify atomic-level signatures of electrochemical activity of the active material on the Ni positive plate of Ni-H₂ batteries.
- Relate findings to cycling conditions and histories
- Develop INS spectroscopy as a non-destructive testing technique for the evaluation of Ni-positive plates of Ni-H₂ batteries.

Charge/Discharge of $(\alpha, \beta)\text{-Ni(OH)}_2 / (\gamma, \beta)\text{-NiOOH}$ Couples



Fundamentals of Vibrational Spectroscopy by Inelastic Neutron Scattering

- neutrons are scattered by the atomic nuclei and not the electrons (as are photons)
 - scattering cross-sections a nuclear property
 - H scatters neutrons >10 times more strongly than other atoms
- absorption cross-sections for neutrons are very low:
 - probe the bulk of the sample
 - in-situ methods are easy(no windows required)
- all vibrational modes are observable
 - intensities are weighed by nuclear cross-sections:INS spectra are dominated by modes involving large displacements of H atoms.
 - intensities are readily quantifiable and are proportional to the number of scatterers.



Incoherent scattering cross section



Coherent scattering cross section

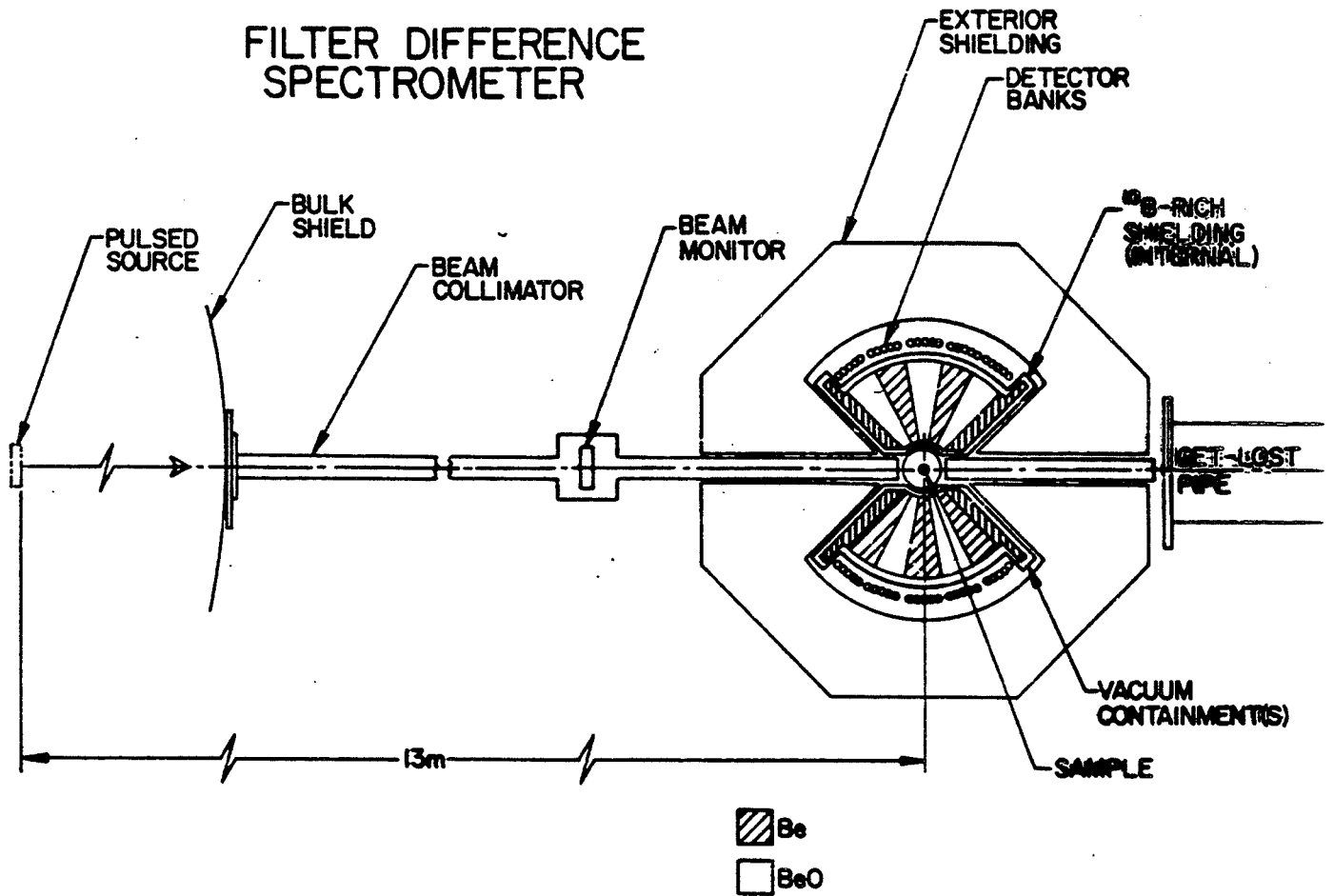


Absorption cross section

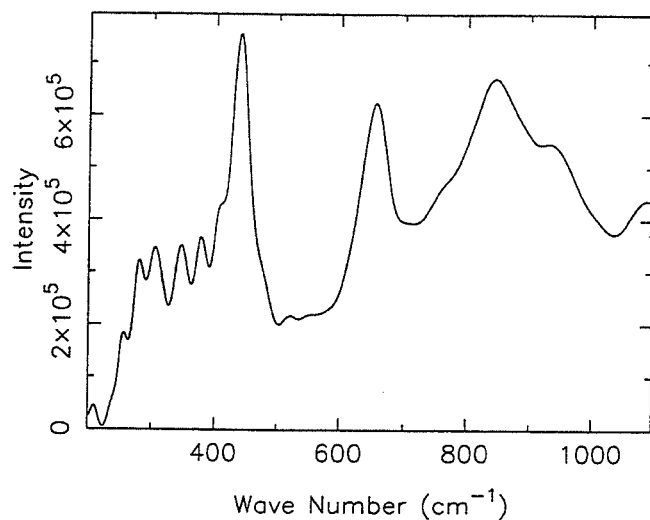
INS Vibrational Spectroscopy

- technique is well suited for application to battery material
 - bulk probe
 - sensitivity to protons (H)
- experiments are carried out at the Lujan Center of LANL
 - 5 - 10g samples from battery plates
 - FDS instrument; $\Delta E = 50 - 4000 \text{ cm}^{-1}$
 - 12-24 hrs. data collection time
 - $T=15\text{K}$

FILTER DIFFERENCE SPECTROMETER

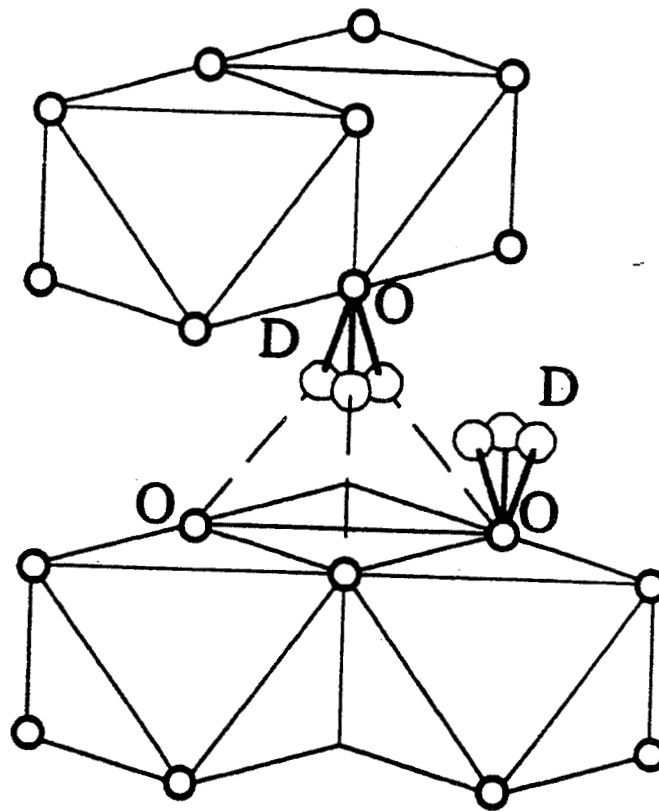


Assignment of β -Ni(OH)₂ vibrational bands



	INS (cm ⁻¹)	IR, Raman (cm ⁻¹)	Assignment
	315,290	318	$\nu(\text{NiO}); A_{1g}$
	358	350	$\delta(\text{ONiO}); E_u$
	390		$\nu(\text{NiO}); A_{2u}$
	451,412	449	$\delta(\text{ONiO}); E_g$
		452	accoust. + E_u
		530	
	673		$\gamma(\text{OH}) E_u$
	867		$\gamma(\text{OH}) E_g$
	929		

Hydrogen disorder in brucite structures



Raman Scattering Spectra of Ni electrode materials

B. C. Cornilsen and collaborators

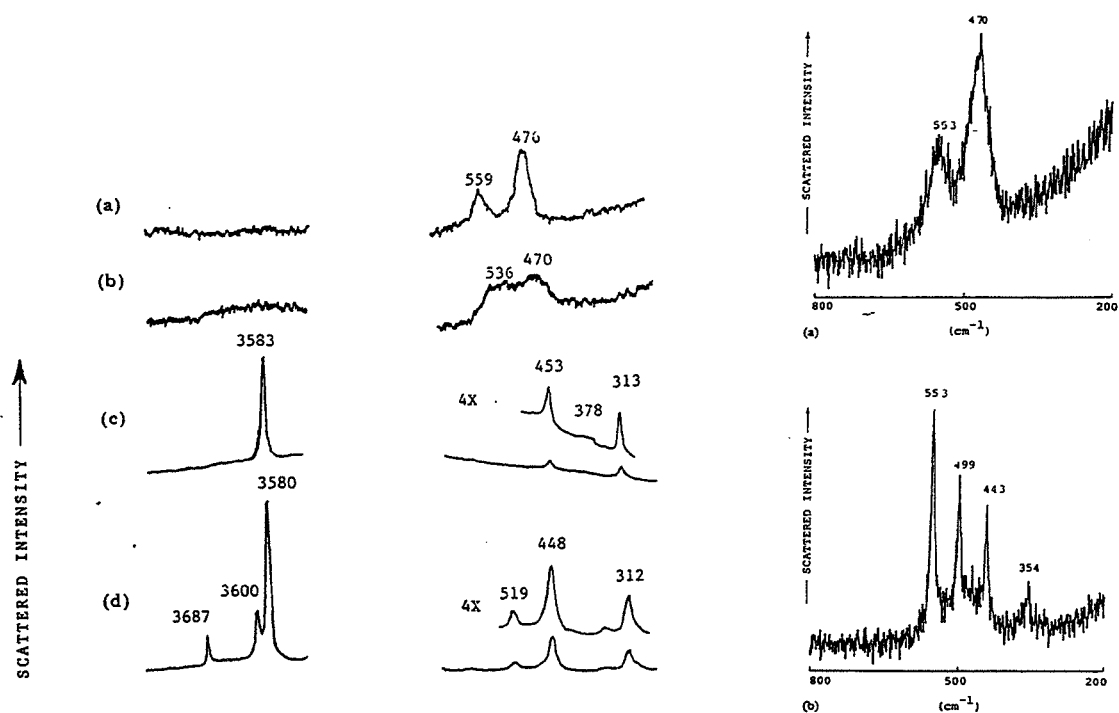
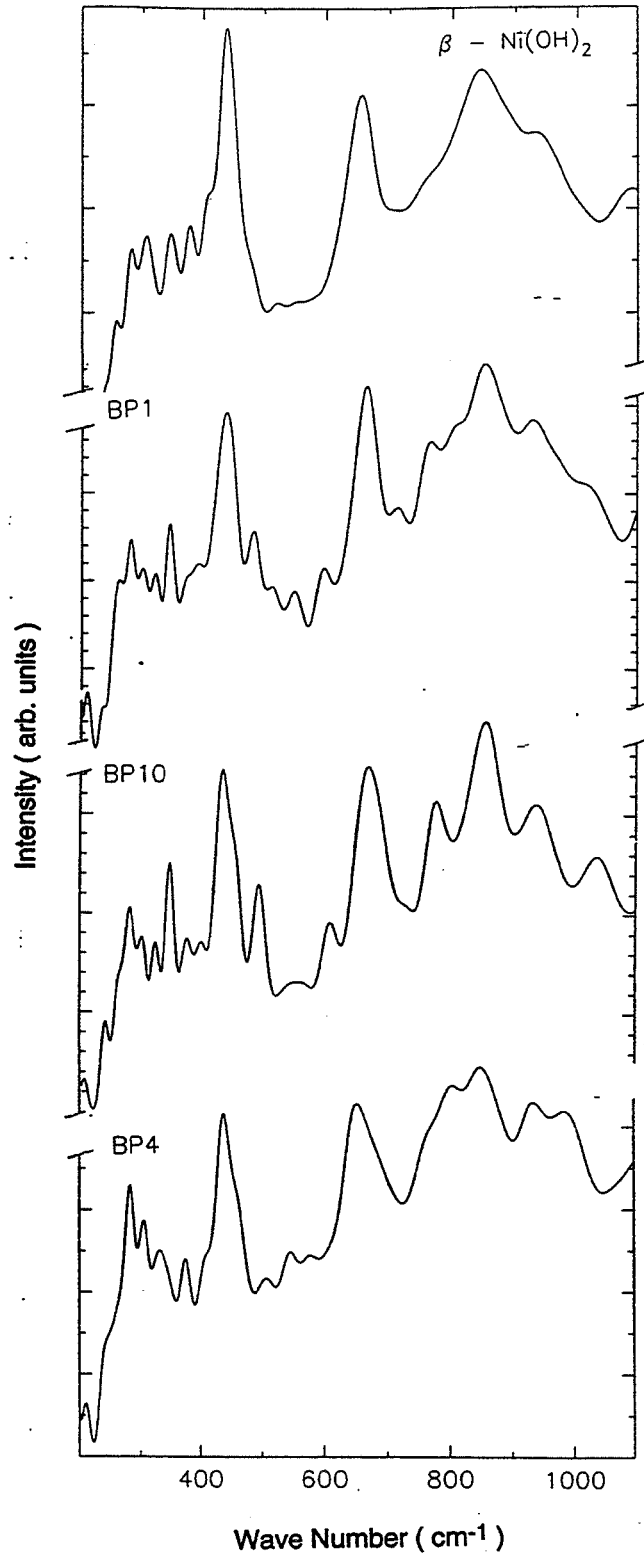


Fig. 1. Raman spectra of nickel electrode active mass and model compounds. (a) Charged γ active mass; (b) discharged α active mass; (c) recrystallized β -Ni(OH)₂; (d) first precipitate β -phase

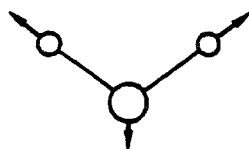
Raman spectra of: (a) discharged active mass (ID no. 16-09); (b) 'phase-X'

<u>KOH Concentration</u>	<u>Number of Cycles</u>
BP1 21 %	38,191
BP4 31 %	3,286
BP10 23.5%	28,495

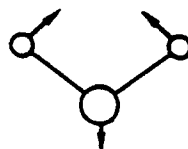


Vibrational Modes of Hydration Water

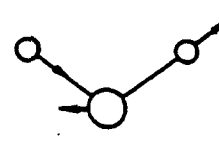
Internal modes



$V_1 (V_{sym})$

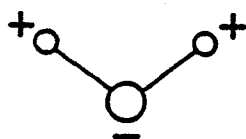


$V_2 (\delta)$

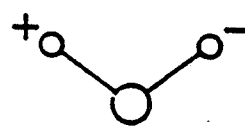


$V_3 (V_{asym})$

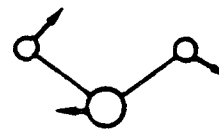
Librations



$R_1 (wag)$



$R_t (twist)$



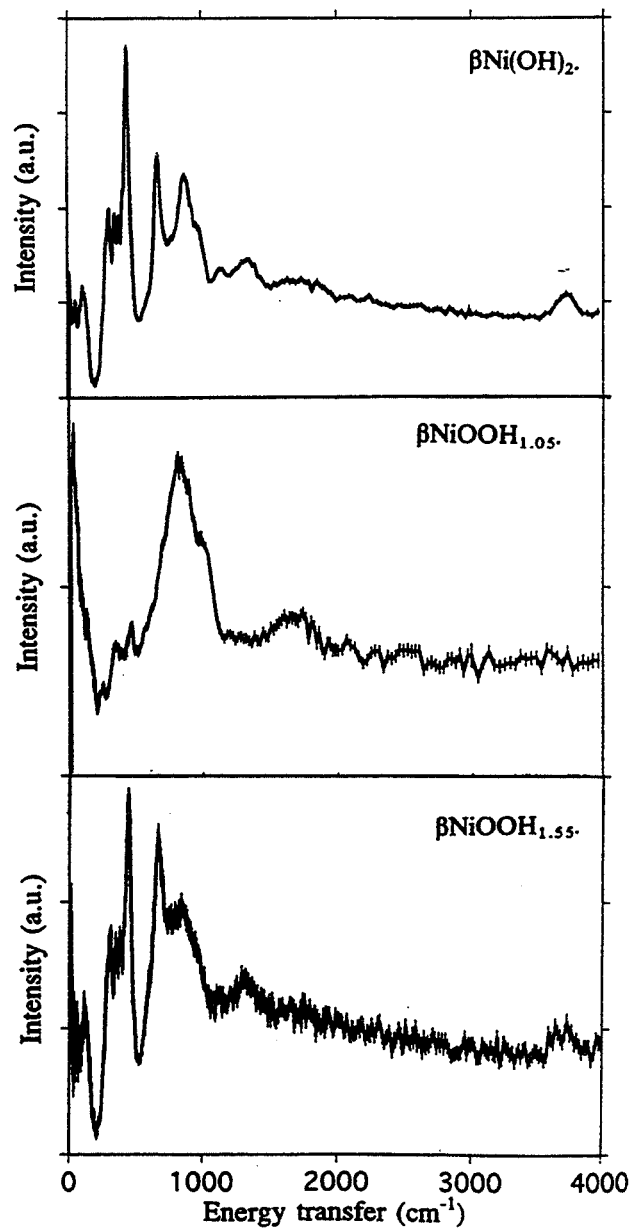
$R_r (rock)$

frequency ranges (cm^{-1})

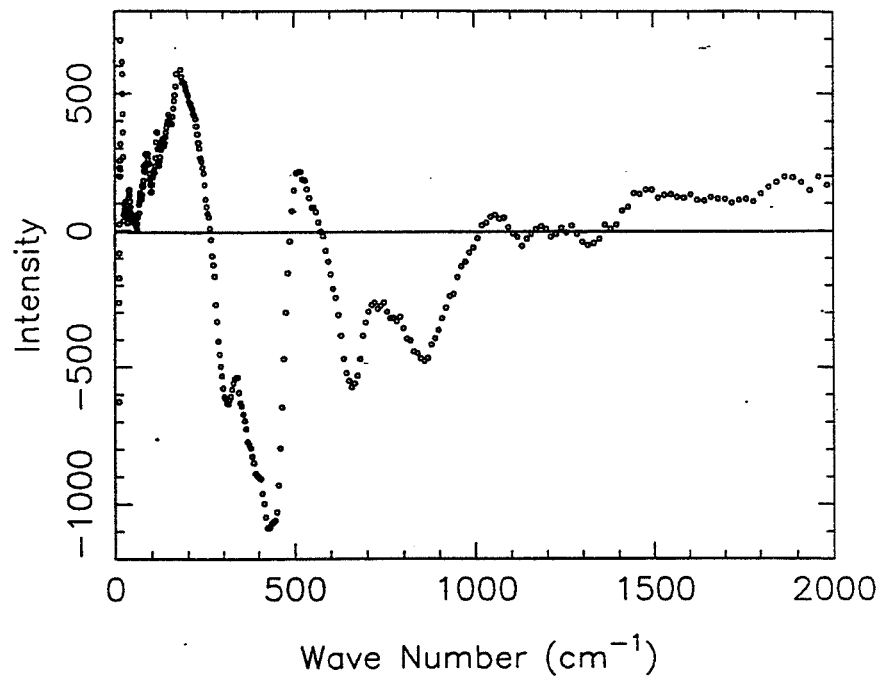
stretching modes (ν)	3600 - 3000
bending modes (δ)	1660 - 1590
librations (R)	1050 - 350
translatory modes (T)	350 - 100

INS Spectra of Reference Compounds

F. Fillaux et al., Physica B 213&214, 637 (1995)



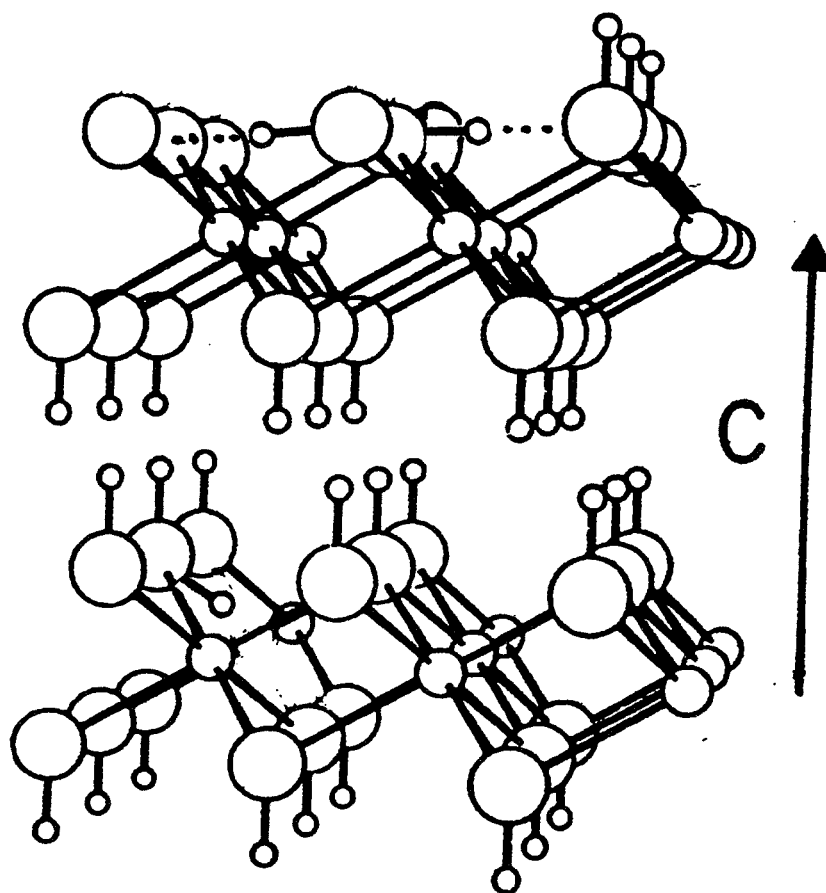
Ni(OH)₂ {BP1 - β}



INS results

- discharged materials are mainly β -Ni(OH)₂
- changes in the Ni-O stretching and bending regions:
 - a decreases from 3.13 Å (β -Ni(OH)₂) to 2.89Å (β -NiOOH)
 - distortion of NiO₆ octahedron
 - frequency shifts and band splittings result
- water librations above ~ 500 cm⁻¹
 - vacancies may allow formation of Ni(H₂O)
- protons in O-H...O hydrogen bonds: β -NiOOH

Structural Models for Hydrogen in NiOOH and bound H₂O



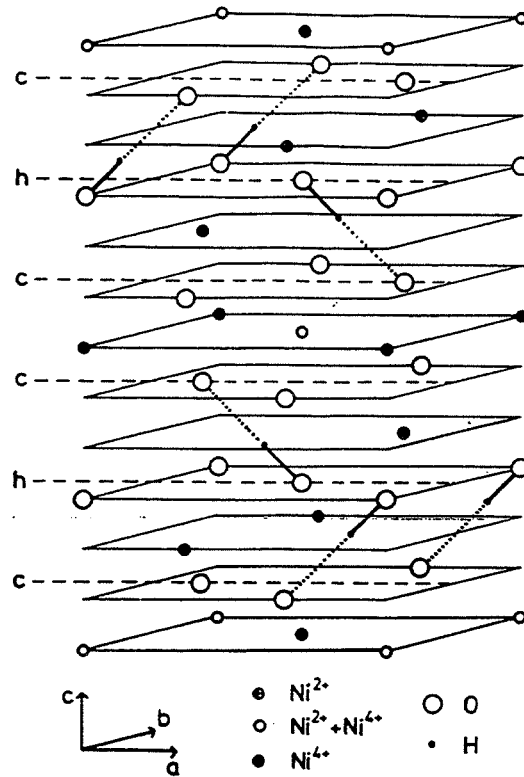


FIGURE 2
Schematic representation of the structure of Ni_2O_3H

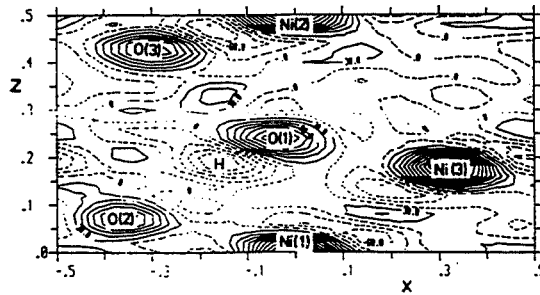


FIGURE 3
Fourier section, $y = 0$, based on observed intensities and calculated phases

Conclusions

- (1) Irreversible formation of NiOOH; scales with number of cycles
- (2) additional protons are bound in the lattice to form Ni-(H₂O) complexes; increases with KOH concentration in the cell.
- (3) These processes occur only in the outermost layers of the plate material but lead to the failure of the battery cells.

Acknowledgments

**Support from the NASA Lewis Research
Center (NASA grant NAS-3-119)**

**DOE/OBES for use of facilities at the
Manuel Lujan Jr. Neutron Scattering
Center of Los Alamos National
Laboratory**

Page intentionally left blank



Advanced and Industrial Battery Group
Defense and Space Division

STUDY OF PARAMETERS CAUSING SECOND PLATEAU EFFECT ON NiH₂ CELLS

STUDY OF PARAMETERS CAUSING SECOND PLATEAU EFFECT ON NICKEL HYDROGEN CELLS

Y. BORTHOMIEU
SAFT Defense and Space Division
POITIERS FRANCE

N. SAC-EPEE
Laboratoire de Réactivité et de Chimie des Solides du CNRS
AMIENS FRANCE

T. JAMIN
CNES
TOULOUSE FRANCE

1997 NASA Aerospace Battery Workshop
Huntsville Hilton, AL
November 18-20, 1997



Advanced and Industrial Battery Group
Defense and Space Division

STUDY OF PARAMETERS CAUSING SECOND PLATEAU EFFECT ON NiH₂ CELLS

OUTLINE

- 1- NiCd CELL SECOND PLATEAU
- 2- EFFECTS OF HYDROGEN PRESSURE AND NiH₂ CELL SECOND PLATEAU



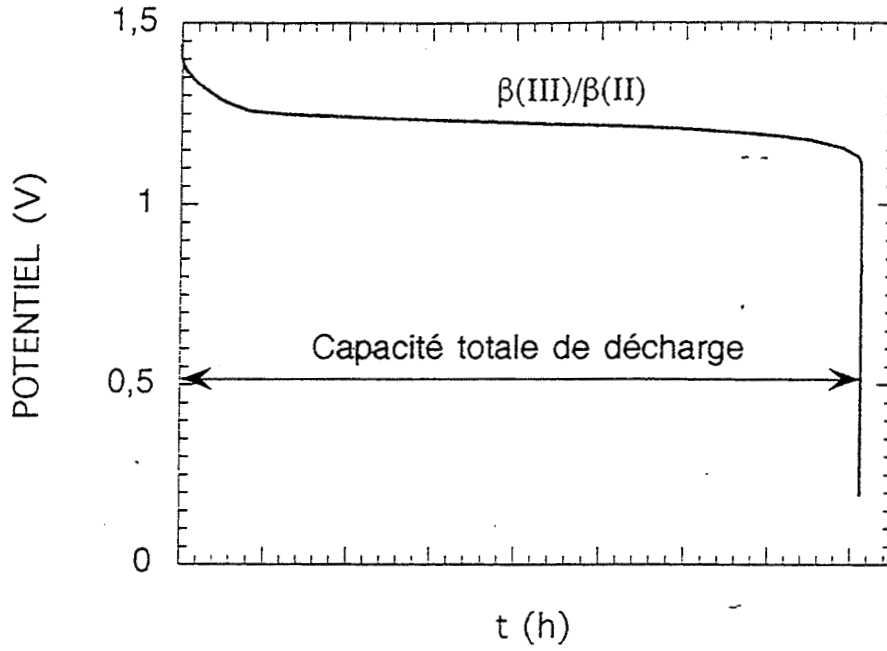
Advanced and Industrial Battery Group
Defense and Space Division

STUDY OF PARAMETERS CAUSING SECOND PLATEAU EFFECT ON NiH₂ CELLS

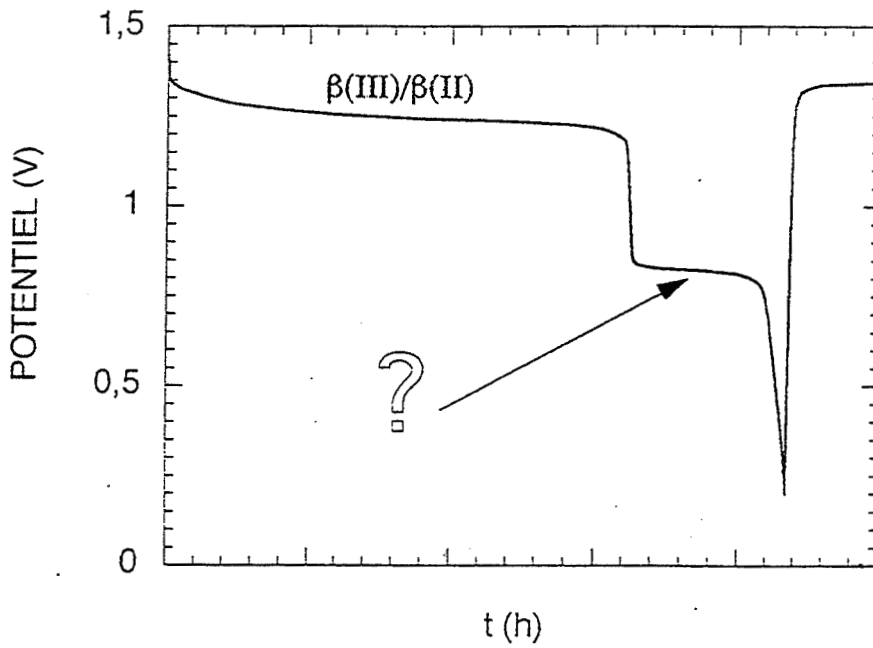
THE SECOND PLATEAU

WHAT IS IT ?

FONCTIONNEMENT NORMAL



SECOND PLATEAU





STUDY OF PARAMETERS CAUSING SECOND PLATEAU EFFECT ON NiH₂ CELLS

INTRODUCTION

SECOND PLATEAU IS GENERALLY OBSERVED IN ALL NICKEL COUPLES :
NiCd, NiMH and NiH₂

BUT IS EXACERBATED IN NiH₂ CELLS

OUR APPROACH :

- MANY OF ELECTROCHEMISTRY STUDIES HAVE BEEN PERFORMED
(ZIMMERMAN AND BARNARD)
- NO CHEMICAL STUDY DONE



SEPARATE AND IDENTIFY THE VARIOUS
PARAMETERS ACTING AT THE POSITIVE ELECTRODE



Advanced and Industrial Battery Group
Defense and Space Division

STUDY OF PARAMETERS CAUSING SECOND PLATEAU EFFECT ON NiH₂ CELLS

INTRODUCTION

DIAGRAM OF THE STUDY

ACTIVE MATERIAL BEHAVIOR

EFFECT OF THE γ PHASE

ROLE OF THE INTERFACE

γ/β (II) TRANSITION

NICKEL HYDROGEN CELL

STORAGE IN KOH

STORAGE AT CHARGED
STATE WITH H₂

DISCHARGE ON
RESISTOR WITH H₂

BEST KNOWLEDGE OF THE SECOND PLATEAU PHENOMENON



Advanced and Industrial Battery Group
Defense and Space Division

STUDY OF PARAMETERS CAUSING SECOND PLATEAU EFFECT ON NiH₂ CELLS

1- STUDY OF SECOND PLATEAU APPEARANCE IN NiCd

- 1.1 EFFECT OF THE γ PHASE
- 1.2 ROLE OF THE INTERFACE
- 1.3 STUDY OF γ/β (II) TRANSITION



Advanced and Industrial Battery Group
Defense and Space Division

STUDY OF PARAMETERS CAUSING SECOND PLATEAU EFFECT ON NiH₂ CELLS

1- STUDY OF SECOND PLATEAU APPEARANCE IN NiCd

1.1 EFFECT OF THE γ PHASE

- PREPARATION OF VARIOUS OXIDIZED PHASES FROM β (II)

LEVEL OF OXIDATION CONTROLLED BY :

- THE QUANTITY OF KOH
- THE TEMPERATURE (55 TO 80 °C)
- NaClO CONCENTRATION

- OXIDATION LEVEL BETWEEN 2.8 AND 3.6



Advanced and Industrial Battery Group
Defense and Space Division

STUDY OF PARAMETERS CAUSING SECOND PLATEAU EFFECT ON NiH₂ CELLS

1- STUDY OF SECOND PLATEAU APPEARANCE IN NiCd

1.1 EFFECT OF THE γ PHASE

- X-RAY DIFFRACTION PATTERN STUDY

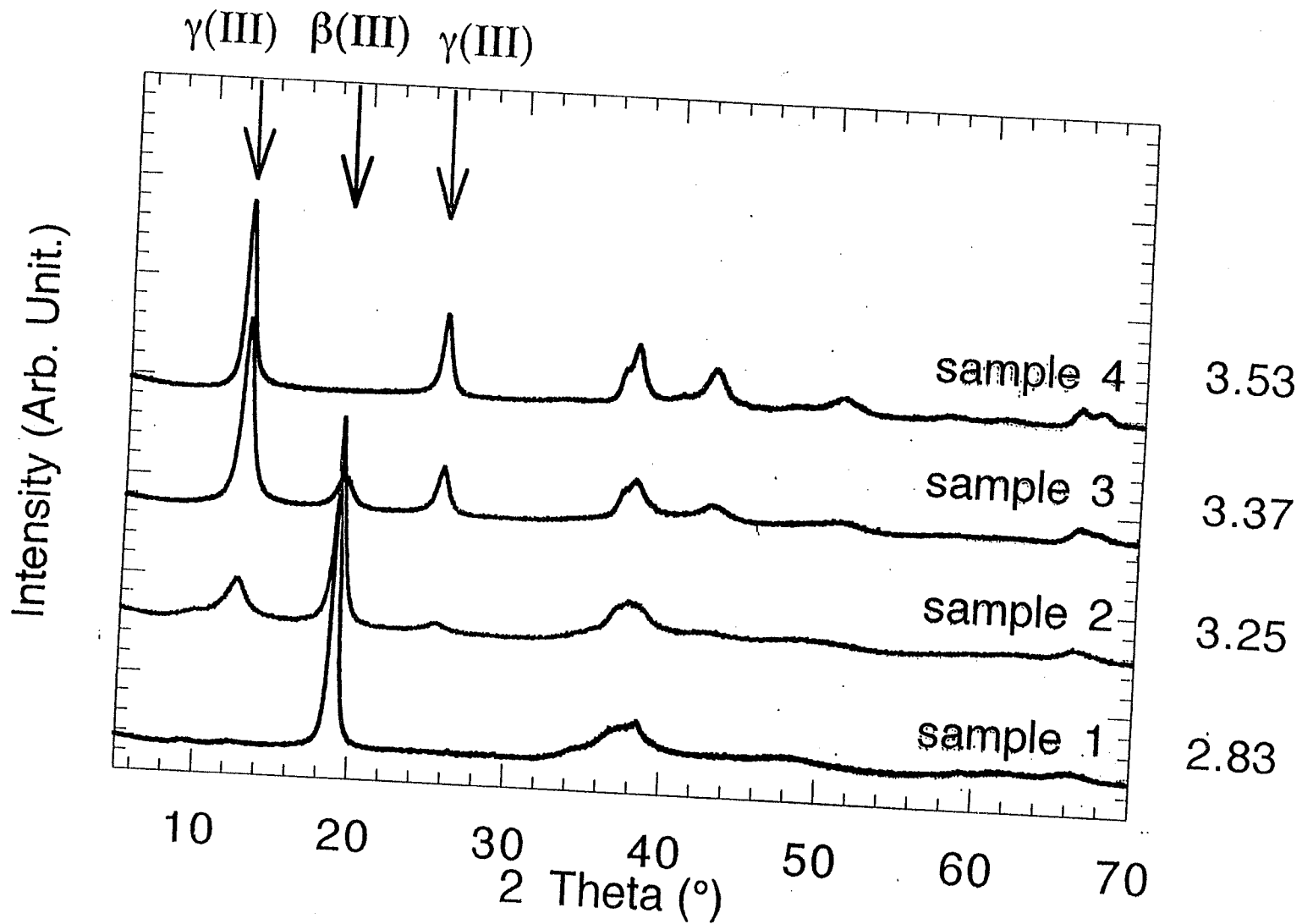


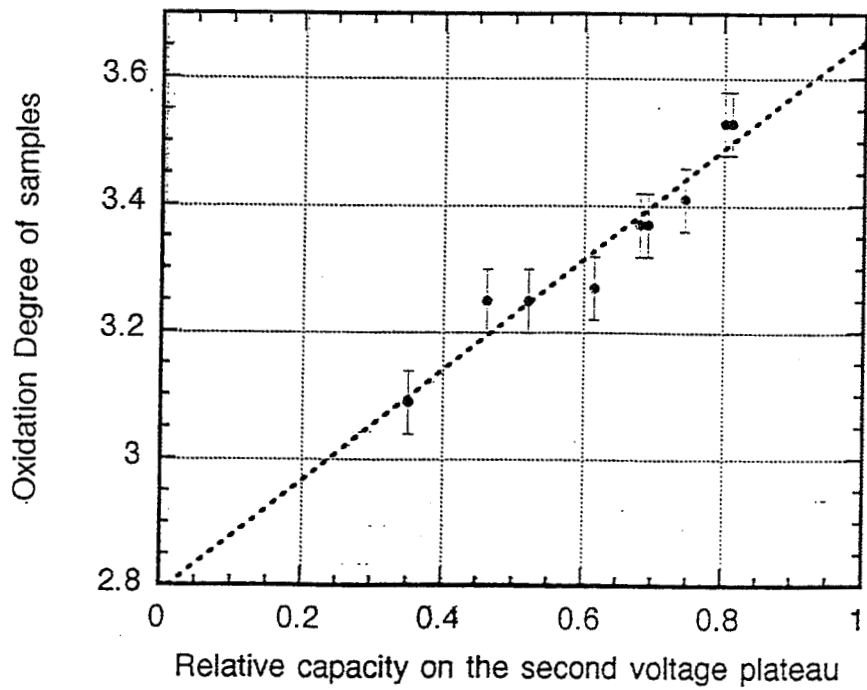
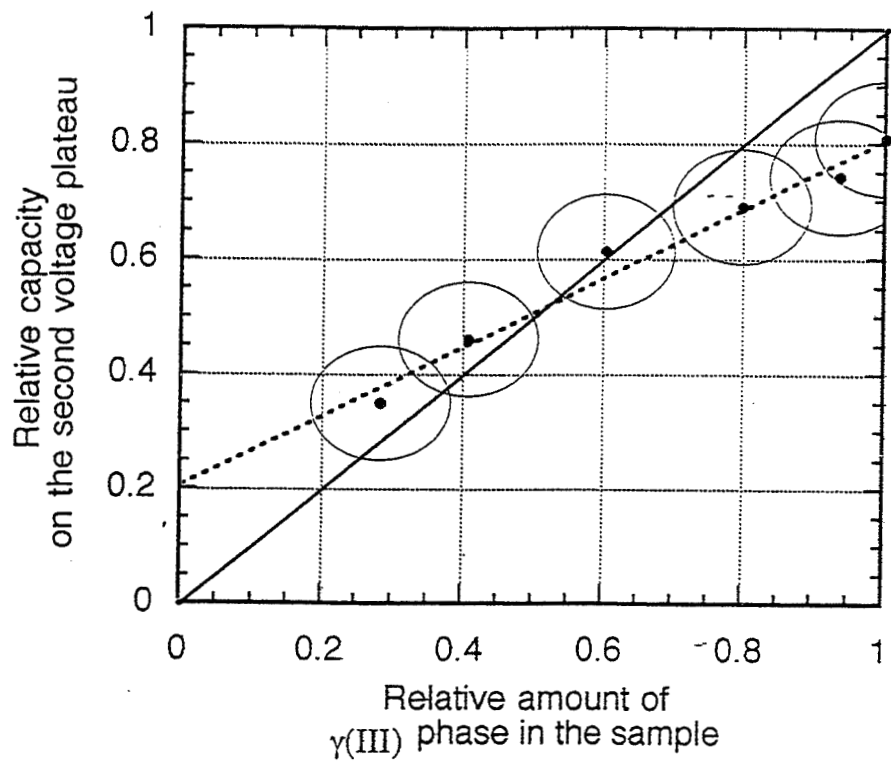
RELATIVE AMOUNT OF γ PHASE IN ACTIVE MATERIAL
IS PROPORTIONAL TO OXIDATION LEVEL

- ELECTROCHEMICAL STUDY (BOILER-PLATES)



PERCENTAGE OF SECOND PLATEAU DIRECTLY LINKED TO THE
RELATIVE AMOUNT OF γ PHASE IN ACTIVE MATERIAL







Advanced and Industrial Battery Group
Defense and Space Division

STUDY OF PARAMETERS CAUSING SECOND PLATEAU EFFECT ON NiH₂ CELLS

1- STUDY OF SECOND PLATEAU APPEARANCE IN NiCd

HOW TO EXPLAIN THE γ PHASE DURING THE CHARGE ?

OR

WHICH PARAMETERS DO DETERMINE THE γ PHASE FORMATION
FROM AN ELECTROCHEMICAL POINT OF VIEW ?

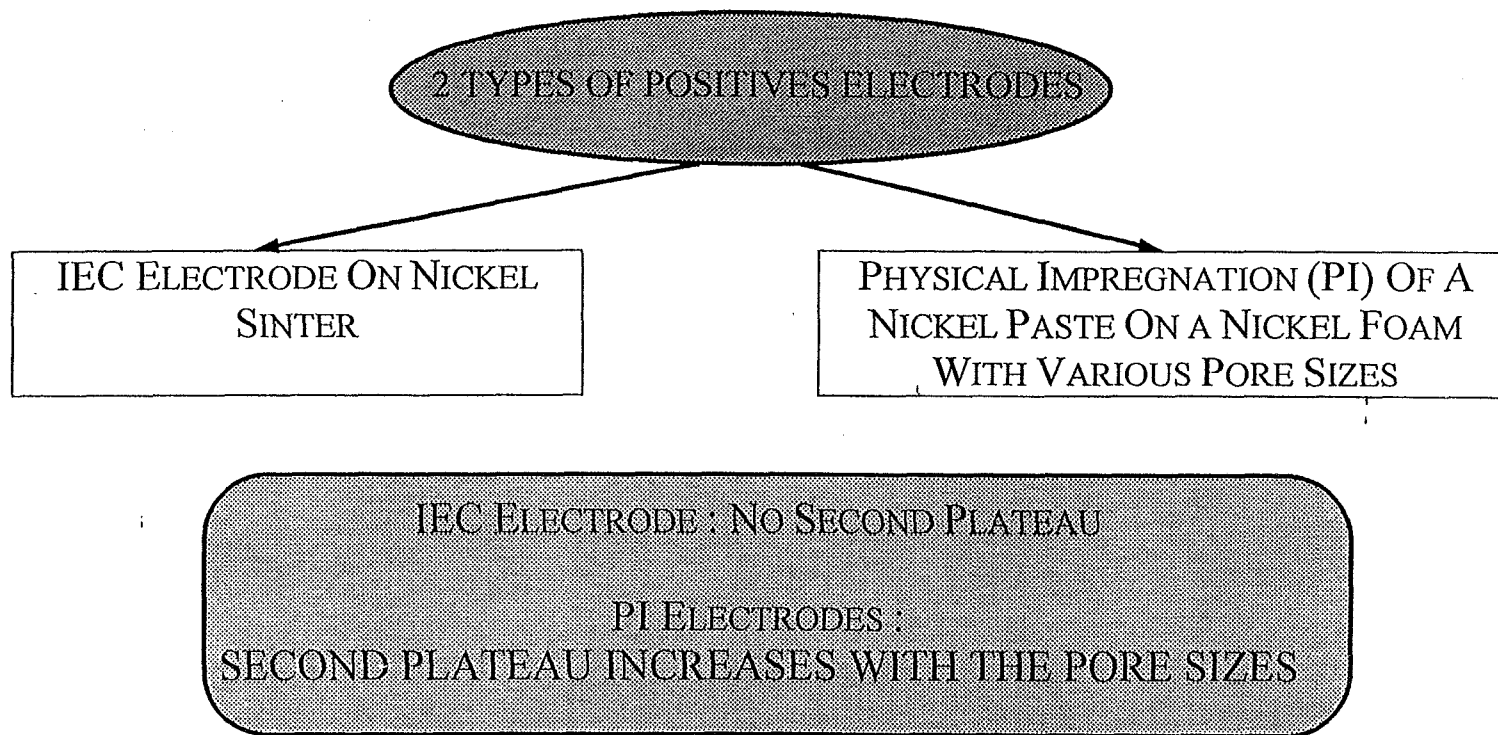


Advanced and Industrial Battery Group
Defense and Space Division

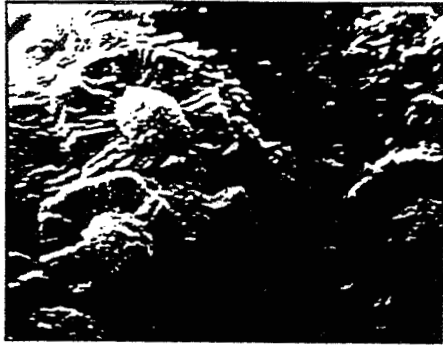
STUDY OF PARAMETERS CAUSING SECOND PLATEAU EFFECT ON NiH₂ CELLS

1- STUDY OF SECOND PLATEAU APPEARANCE IN NiCd

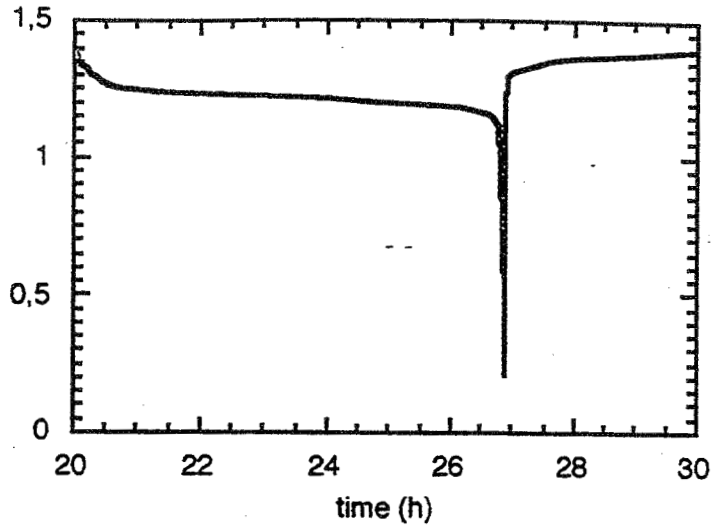
1.2 EFFECT OF THE COLLECTOR



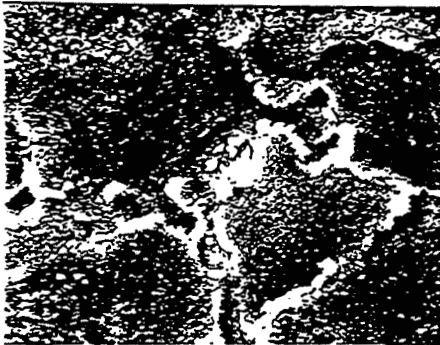
ECI electrode



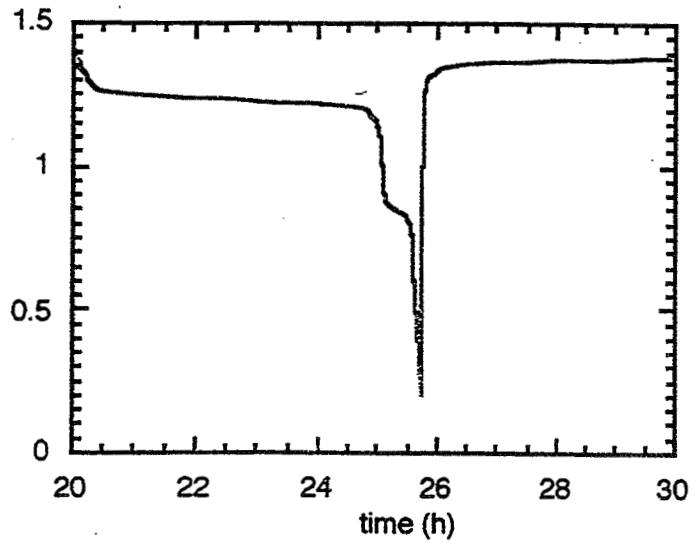
Voltage vs Cd (V)



PI electrode with small pores



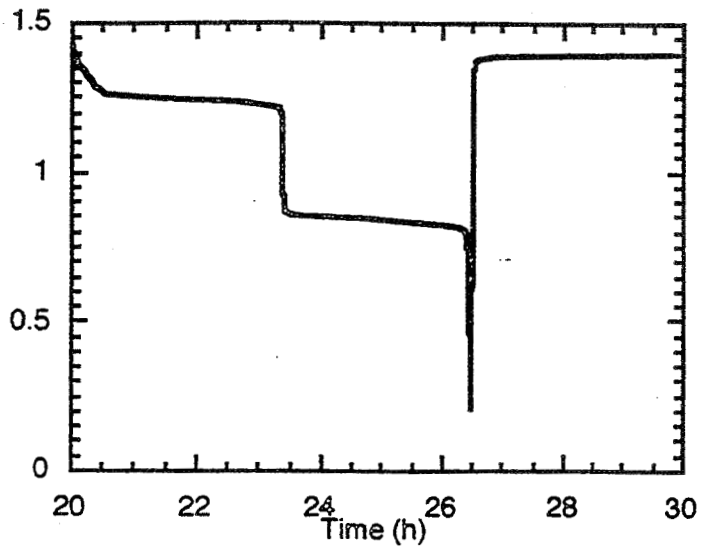
Voltage vs Cd (V)



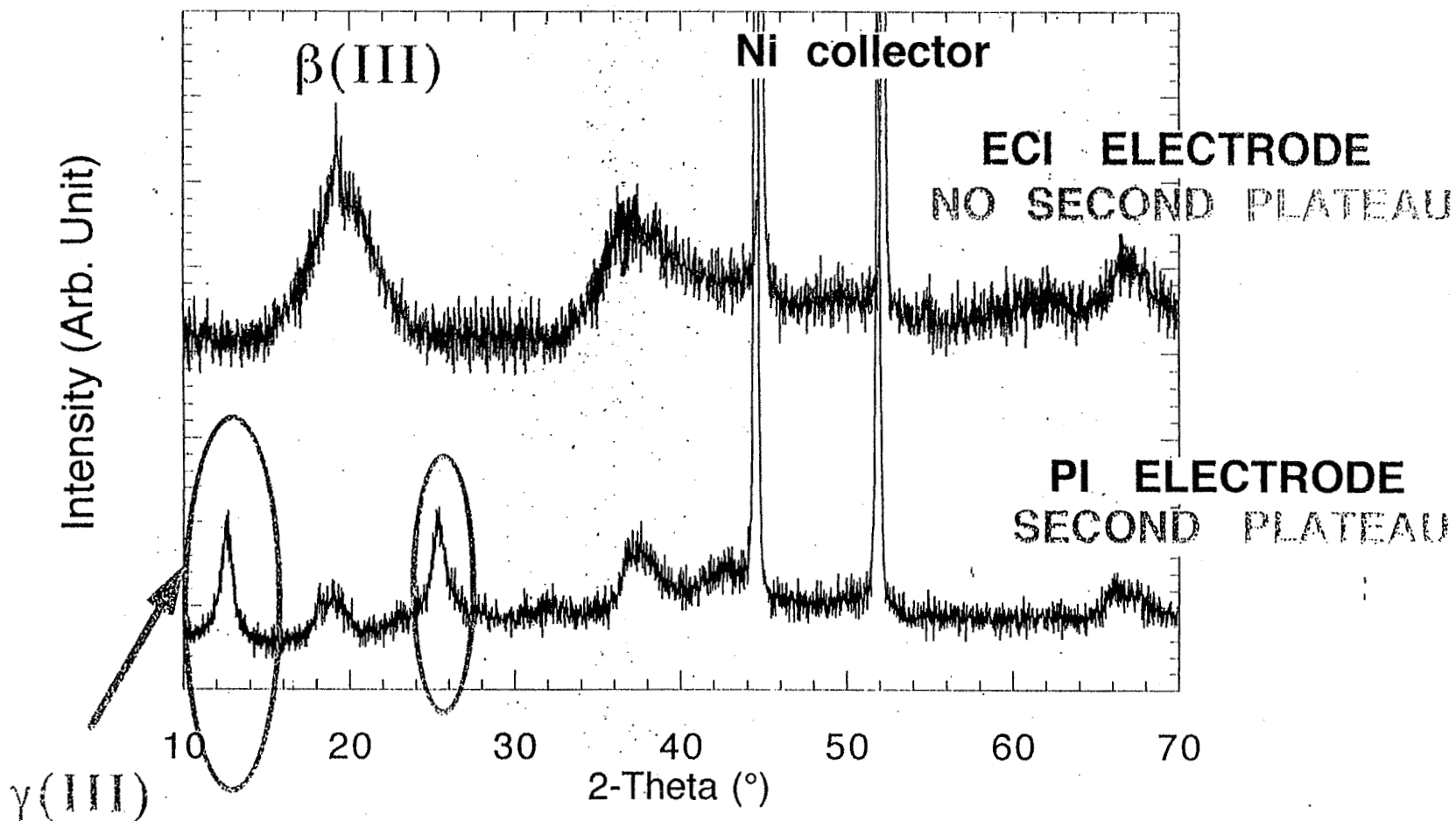
PI electrode with large pores



Voltage vs Cd (V)



X-RAY DIFFRACTION PATTERNS AT THE END OF CHARGE



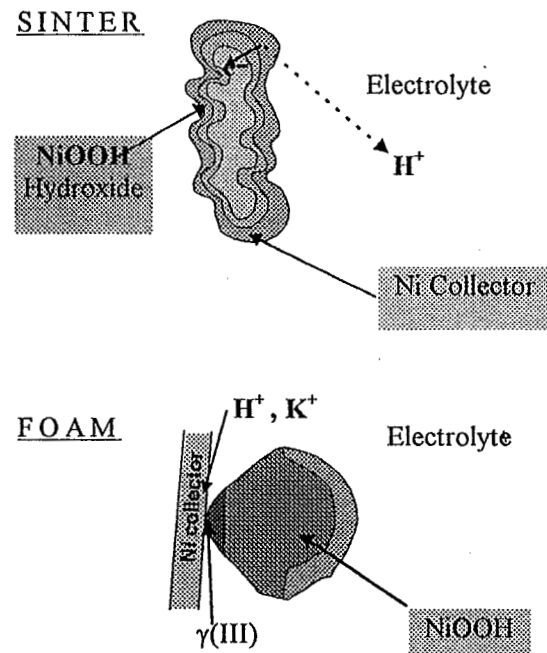


Advanced and Industrial Battery Group
Defense and Space Division

STUDY OF PARAMETERS CAUSING SECOND PLATEAU EFFECT ON NiH₂ CELLS

1- STUDY OF SECOND PLATEAU APPEARANCE IN NiCd

ROLE OF THE COLLECTOR

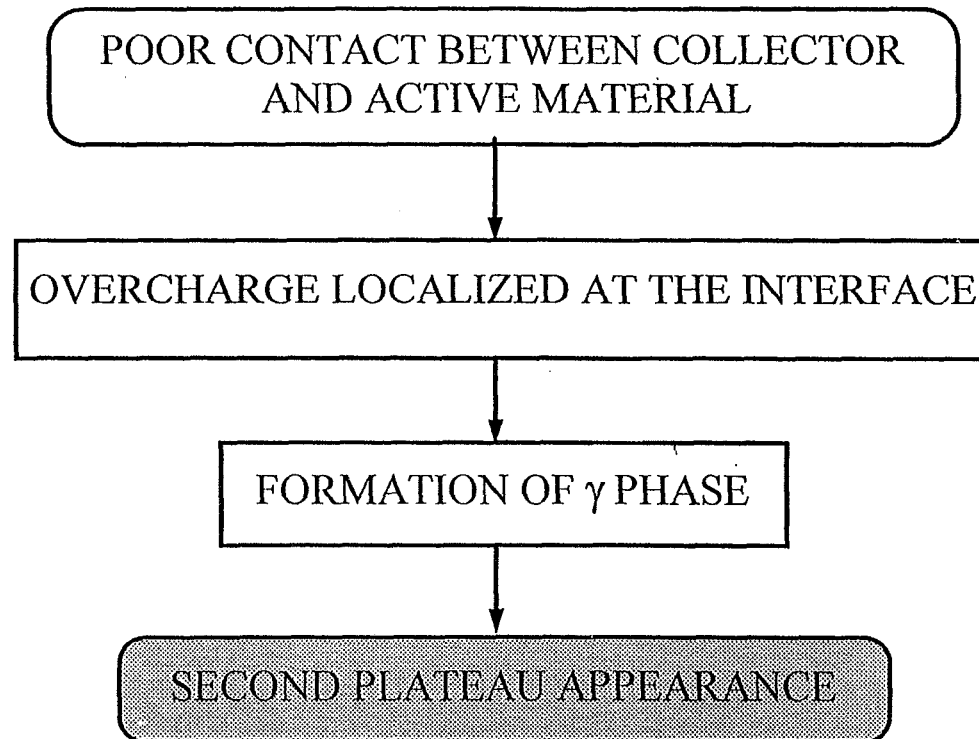




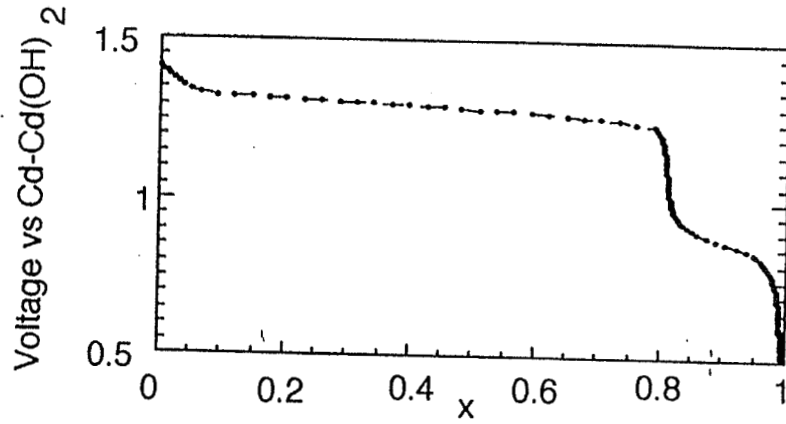
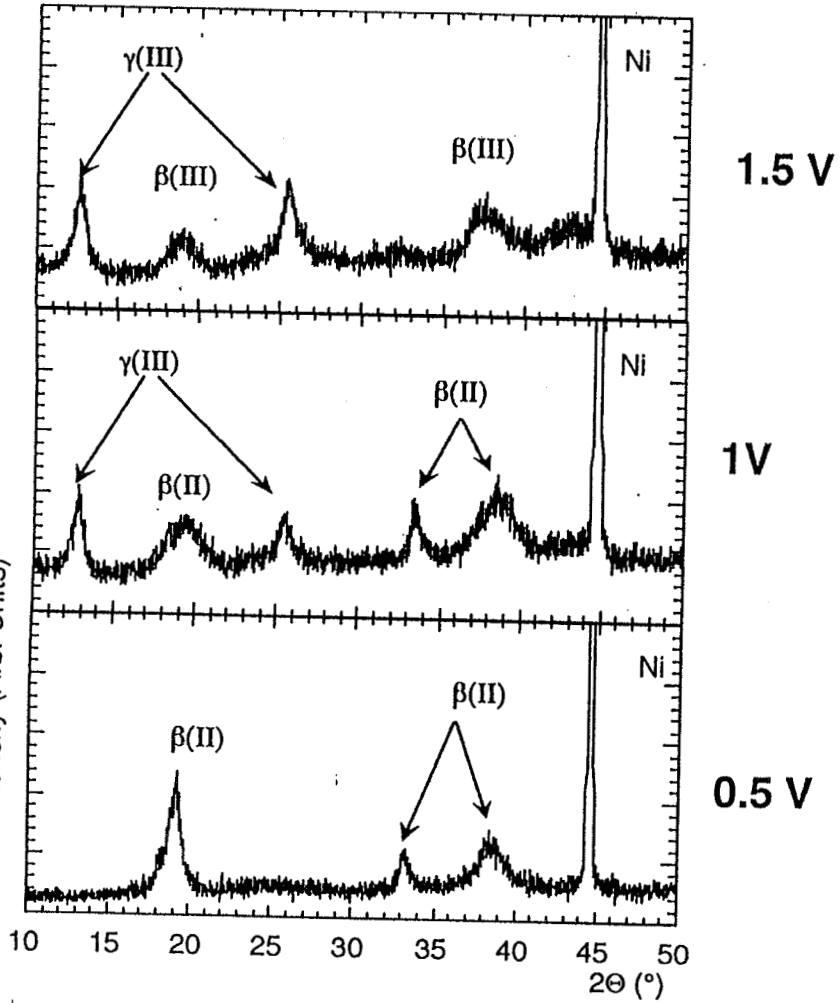
Advanced and Industrial Battery Group
Defense and Space Division

STUDY OF PARAMETERS CAUSING SECOND PLATEAU EFFECT ON NiH₂ CELLS

1- STUDY OF SECOND PLATEAU APPEARANCE IN NiCd



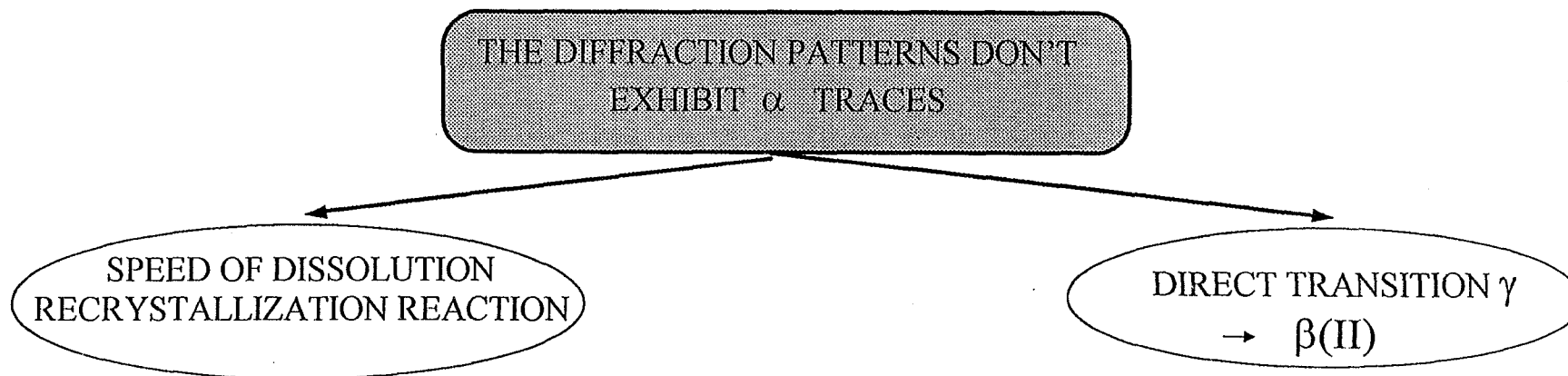
XRD on discharge



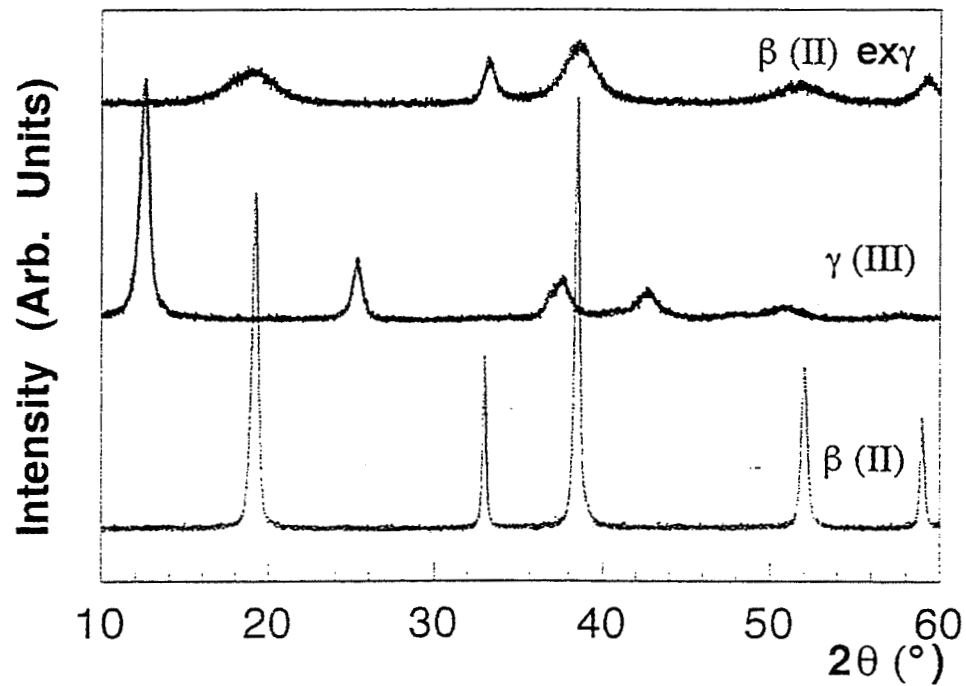
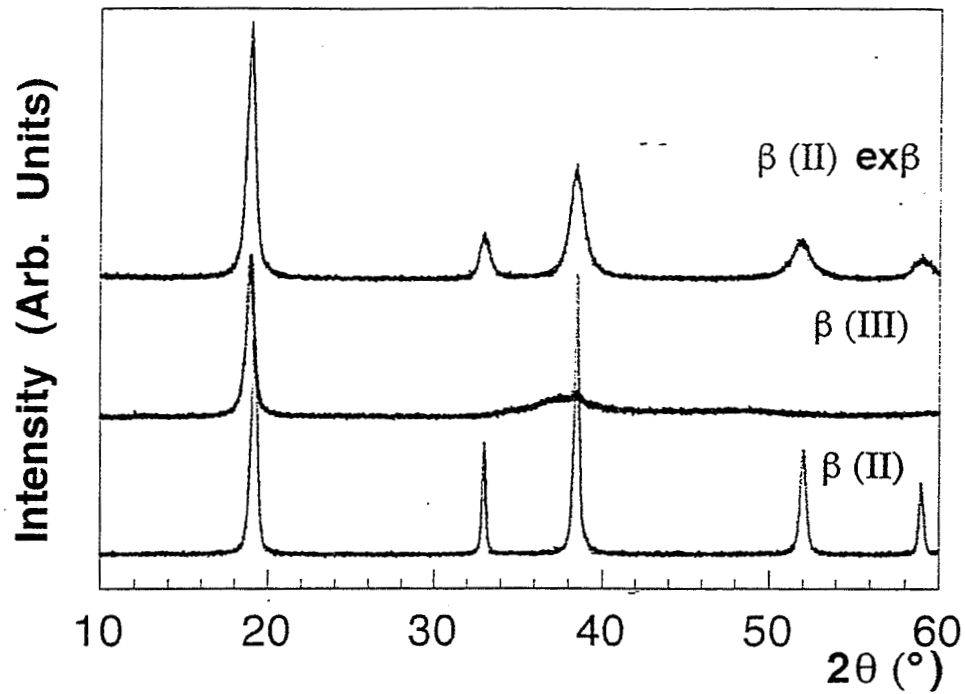


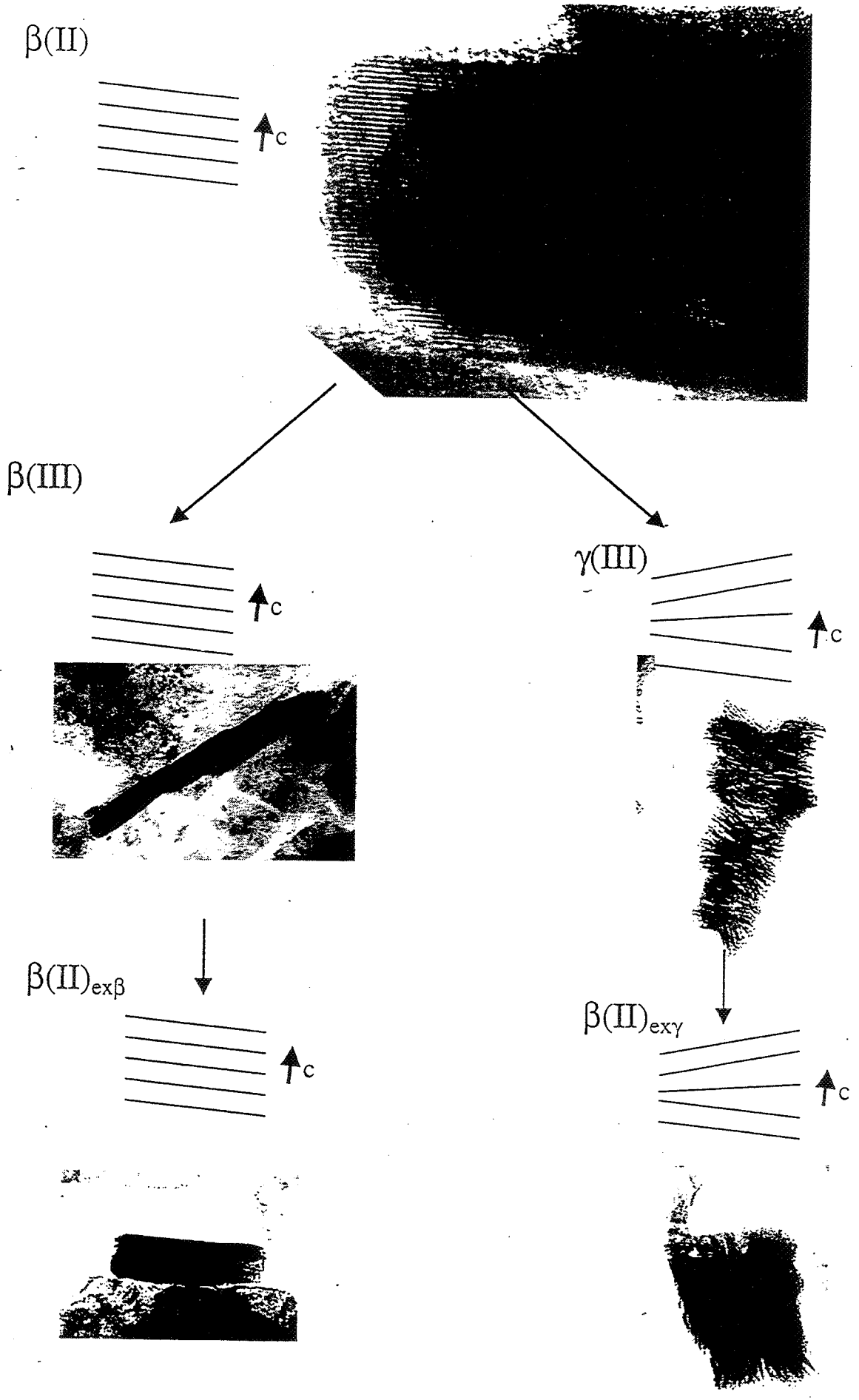
STUDY OF PARAMETERS CAUSING SECOND PLATEAU EFFECT ON NiH₂ CELLS

1- STUDY OF SECOND PLATEAU APPEARANCE IN NiCd

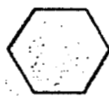


- HIGH RESOLUTION TEM ANALYSES SHOW :
- $\beta(II)_{EX\gamma}$ EXHIBITS SAME MOSAIC STRUCTURE AS γ
 - PLATELETS ARE MAINTAINED FROM γ TO $\beta(II)$
 - THE REACTION IS PSEUDOMORPHOUS





1st
C
H
A
R
G
E



$\alpha(\text{II})$

$< 1.40\text{V}$

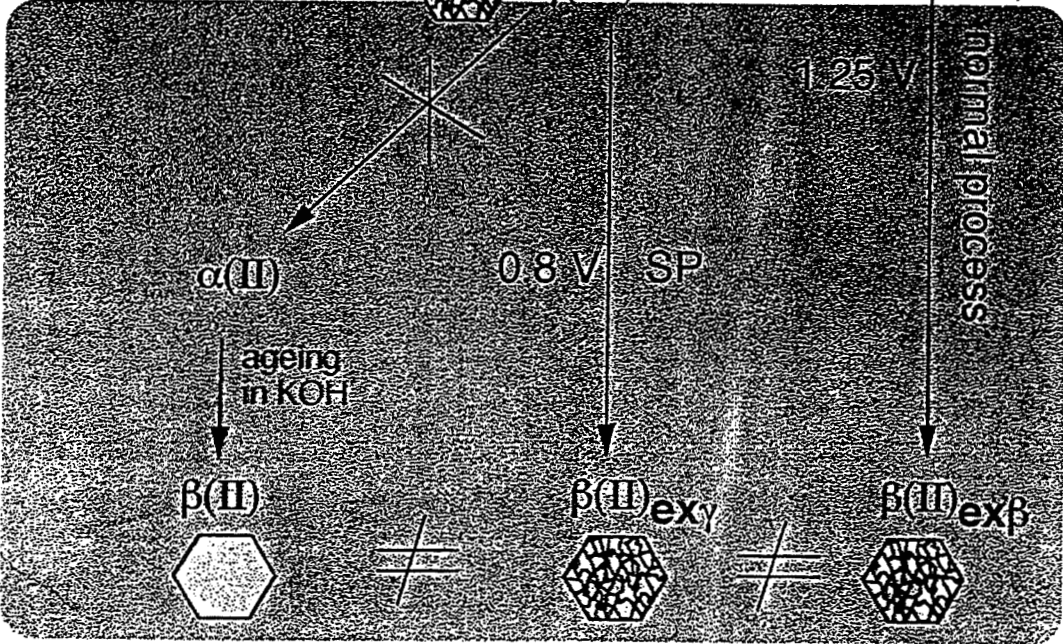


$\beta(\text{III})$

overcharge $> 1.40\text{V}$



$\gamma(\text{III})$



Next
C
H
A
R
G
E

textural memory

$\gamma(\text{III})$

$\beta(\text{III})$



Advanced and Industrial Battery Group
Defense and Space Division

STUDY OF PARAMETERS CAUSING SECOND PLATEAU EFFECT ON NiH₂ CELLS

1- STUDY OF SECOND PLATEAU APPEARANCE IN NiCd

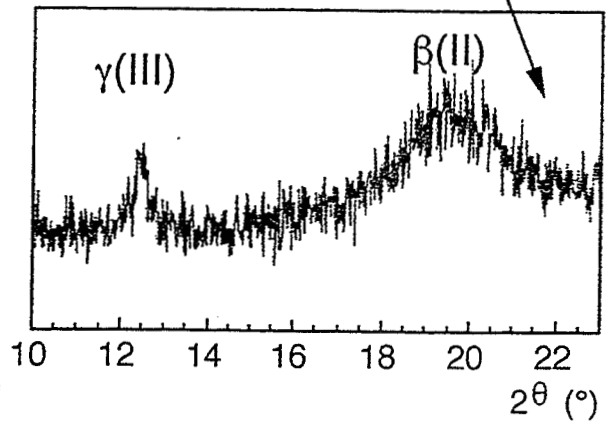
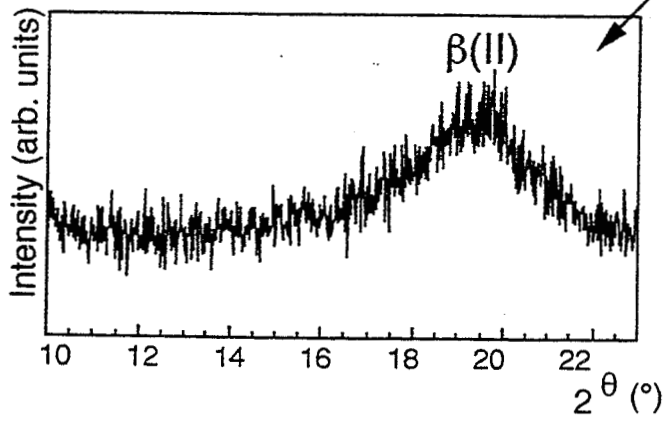
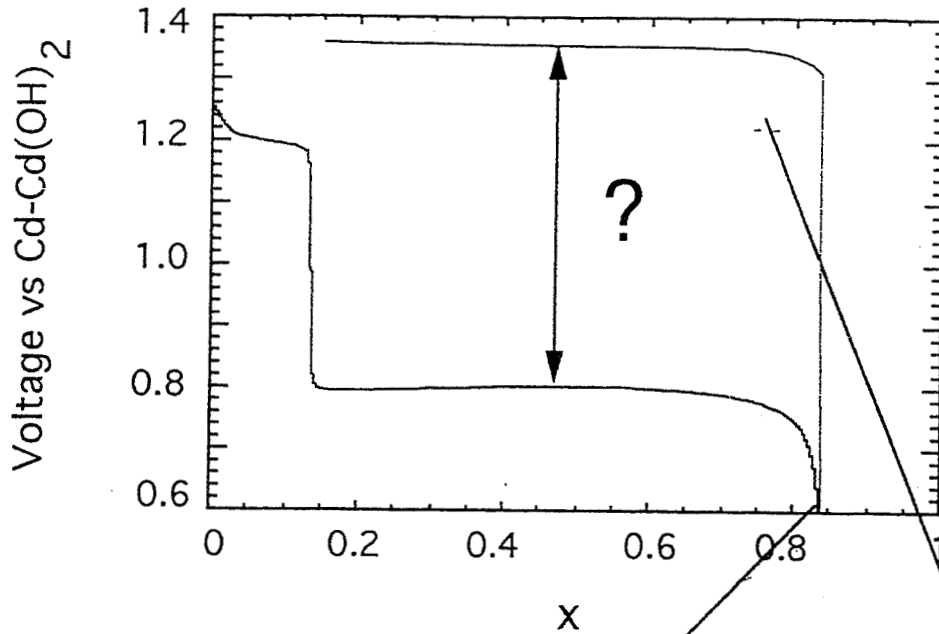
EVEN WITH ALL THE STUDIES PERFORMED ON
NICKEL ELECTRODE, IT IS THE FIRST TIME
THE DIRECT TRANSITION γ TO β (II) HAS BEEN DESCRIBED

MEB, SAED, XRD TECHNICS CONFIRM THIS TRANSITION

A RECHARGE ON β (II)_{EX γ} YIELDS IMMEDIATELY γ PHASE

CHARGE

begins at 1.36V
(no 0.8 V plateau)



γ(III) at the beginning of
charge: β_{exγ} → γ



Advanced and Industrial Battery Group
Defense and Space Division

STUDY OF PARAMETERS CAUSING SECOND PLATEAU EFFECT ON NiH_2 CELLS

1- STUDY OF SECOND PLATEAU APPEARANCE IN NiCd

SUMMARY ON ACTIVE MATERIAL BEHAVIOR :

- THE γ PHASE IS INVOLVED IN SECOND PLATEAU
- THE SECOND PLATEAU CAN BE INFLUENCED BY THE COLLECTOR INTERFACE
- THE TRANSITION $\gamma/\beta(\text{II})$ IS RESPONSIBLE FOR THE SECOND PLATEAU



Advanced and Industrial Battery Group
Defense and Space Division

STUDY OF PARAMETERS CAUSING SECOND PLATEAU EFFECT ON NiH_2 CELLS

2- EFFECTS OF HYDROGEN PRESSURE

- 2.1 STORAGE IN KOH

- 2.2 STORAGE AT CHARGED STATE UNDER H_2

- 2.3 DISCHARGE ON RESISTOR UNDER H_2



Advanced and Industrial Battery Group
Defense and Space Division

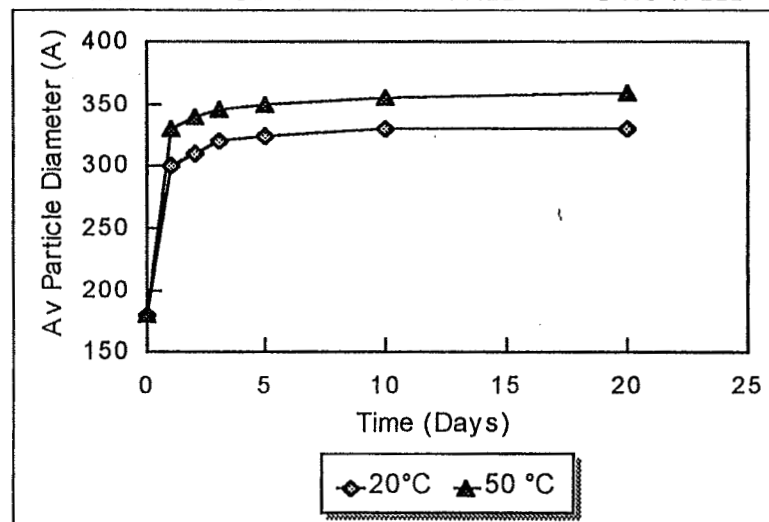
STUDY OF PARAMETERS CAUSING SECOND PLATEAU EFFECT ON NiH₂ CELLS

2- EFFECTS OF HYDROGEN PRESSURE

2.1 STORAGE IN KOH

- β (II) WITH SMALL PLATELETS (30 Å * 200 Å)
- TREATMENT AT 20 °C (AND 50°C) UNDER KOH 8N

EVALUATION OF THE PARTICLE GROWTH

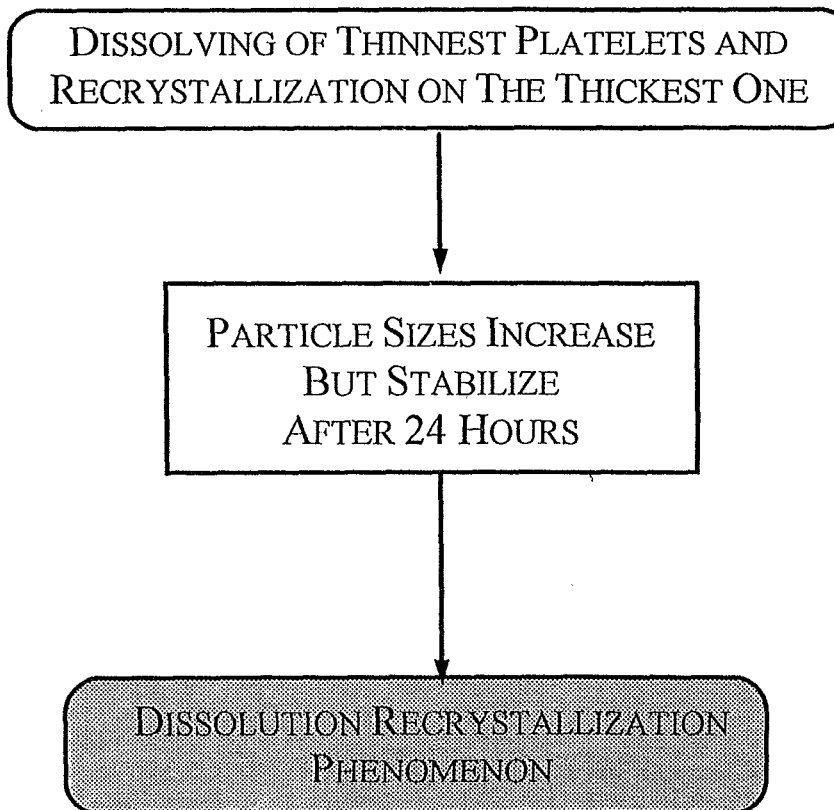


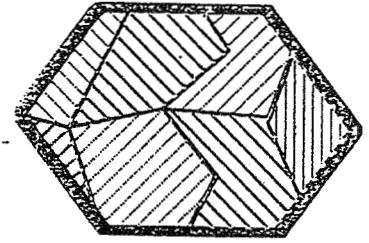
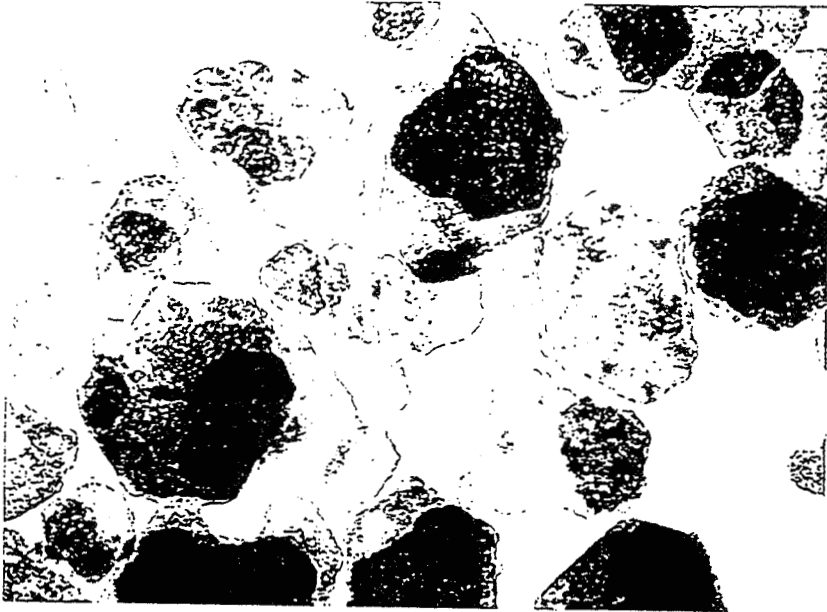


Advanced and Industrial Battery Group
Defense and Space Division

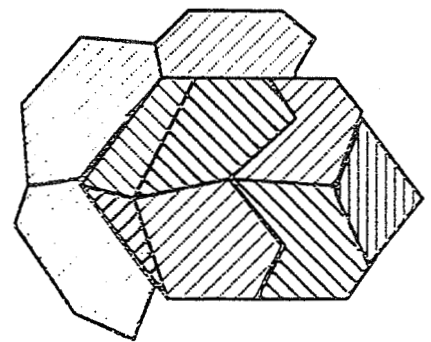
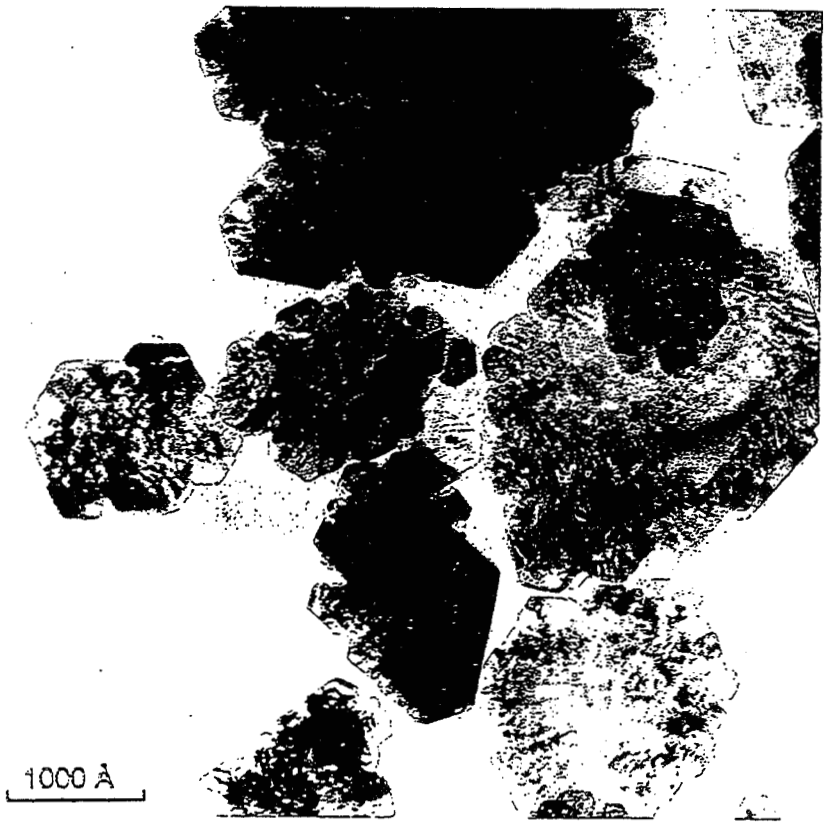
STUDY OF PARAMETERS CAUSING SECOND PLATEAU EFFECT ON NiH_2 CELLS

2- EFFECTS OF HYDROGEN PRESSURE





DISSOLUTION-RECRISTALLIZATION PROCESS





Advanced and Industrial Battery Group
Defense and Space Division

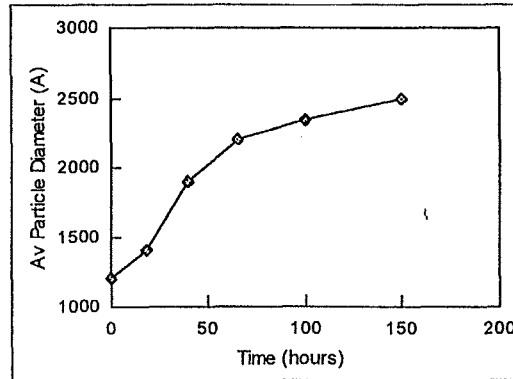
STUDY OF PARAMETERS CAUSING SECOND PLATEAU EFFECT ON NiH₂ CELLS

2- EFFECTS OF HYDROGEN PRESSURE

2.2 STORAGE AT CHARGED STATE UNDER H₂

- β (III) IS OBTAINED WITH CHEMICAL OXIDATION OF β (II) : ($\approx 1300 \text{ \AA}$)
- TREATMENT 80 BARS (1100 PSI) OF H₂ IN KOH AT 60°C

EVOLUTION OF PARTICLE SIZE VERSUS TIME





Advanced and Industrial Battery Group
Defense and Space Division

STUDY OF PARAMETERS CAUSING SECOND PLATEAU EFFECT ON NiH₂ CELLS

2- EFFECTS OF HYDROGEN PRESSURE

AFTER 150 HOURS IN H₂ :
AVERAGE DIAMETER > 2* INITIAL ONE AFTER 150 HOURS



HYDROGEN ACTS AS A CATALYST OF THE DISSOLUTION
RECRYSTALLIZATION DUE TO ITS REDUCTION POWER



STUDY OF PARAMETERS CAUSING SECOND PLATEAU EFFECT ON NiH₂ CELLS

2- EFFECTS OF HYDROGEN PRESSURE

2.3 DISCHARGE ON RESISTOR STATE UNDER H₂

- $\beta(\text{II})$ WITH SMALL PLATELETS (30 Å * 200 Å)
- VARIOUS NEGATIVE PRECHARGE LEVELS (10 TO 25 BARS)

DISCHARGE TO 1V

DISCHARGE TO 0V ON RESISTOR

ANALYSES :

- SECOND PLATEAU EVALUATION
 - TEM AND XRD

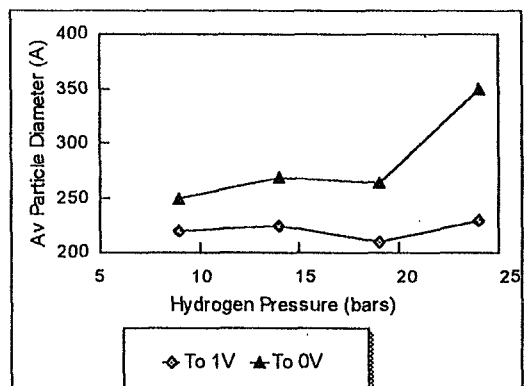


Advanced and Industrial Battery Group
Defense and Space Division

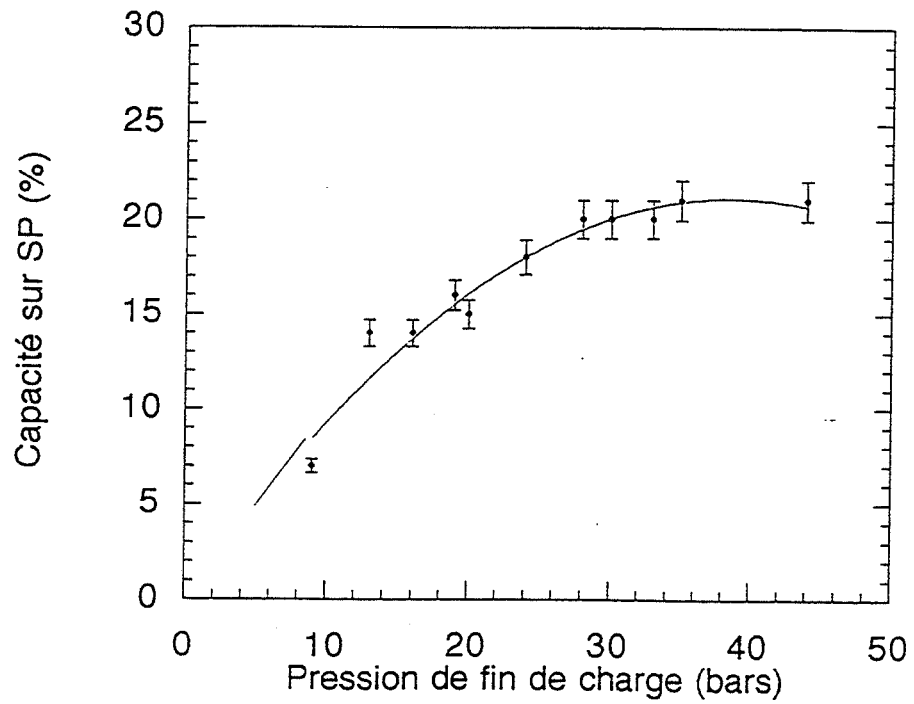
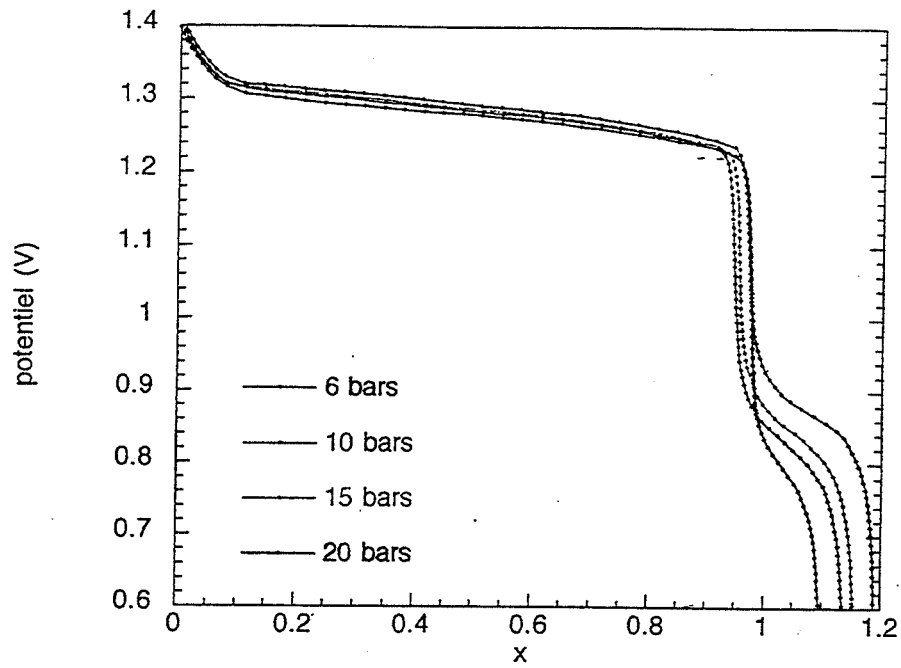
STUDY OF PARAMETERS CAUSING SECOND PLATEAU EFFECT ON NiH_2 CELLS

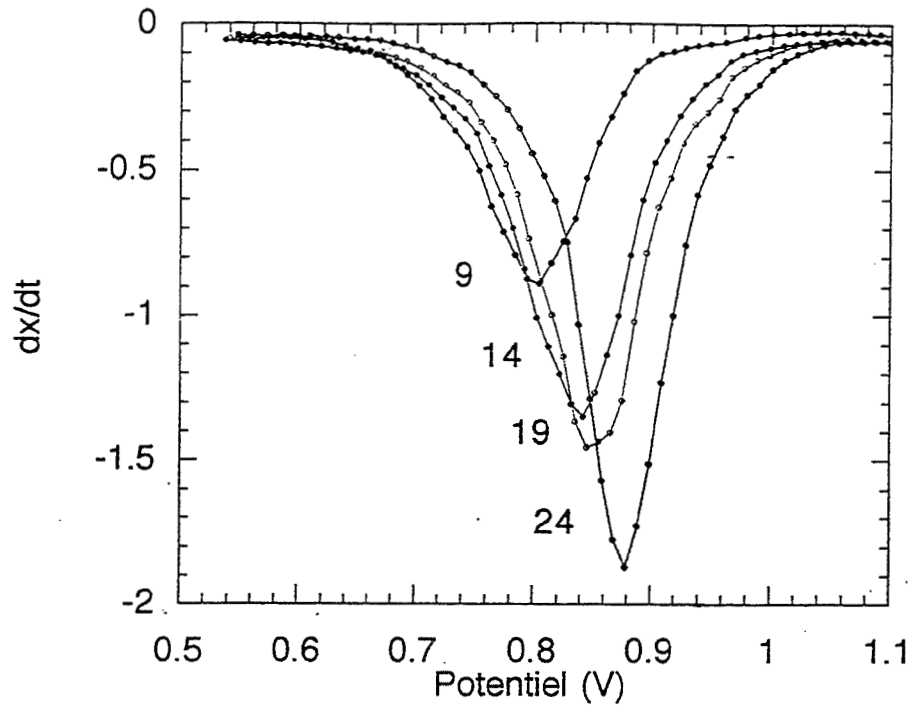
2- EFFECTS OF HYDROGEN PRESSURE

- INCREASE OF THE PARTICLE SIZE DIAMETER WITH PRECHARGE LEVEL:

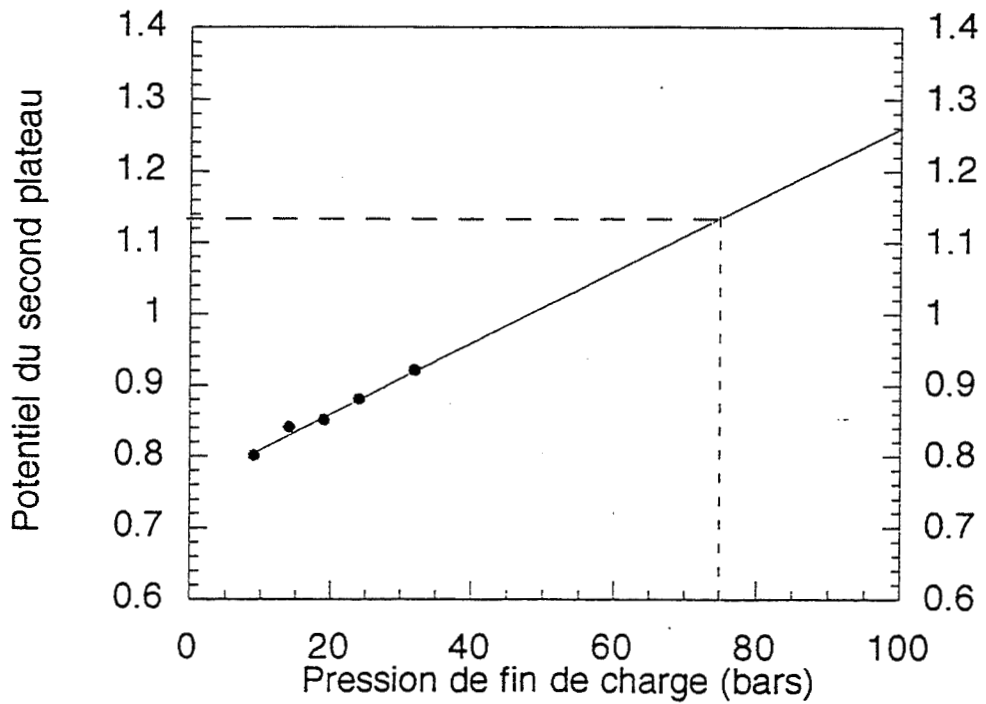


- INCREASE OF SECOND PLATEAU WITH THE PRECHARGE LEVEL WHEN DISCHARGED TO 0 V
- INCREASE OF PARTICLE DIAMETER AND SECOND PLATEAU





Evolution du potentiel du second plateau en fonction de la pression atteinte en fin de charge

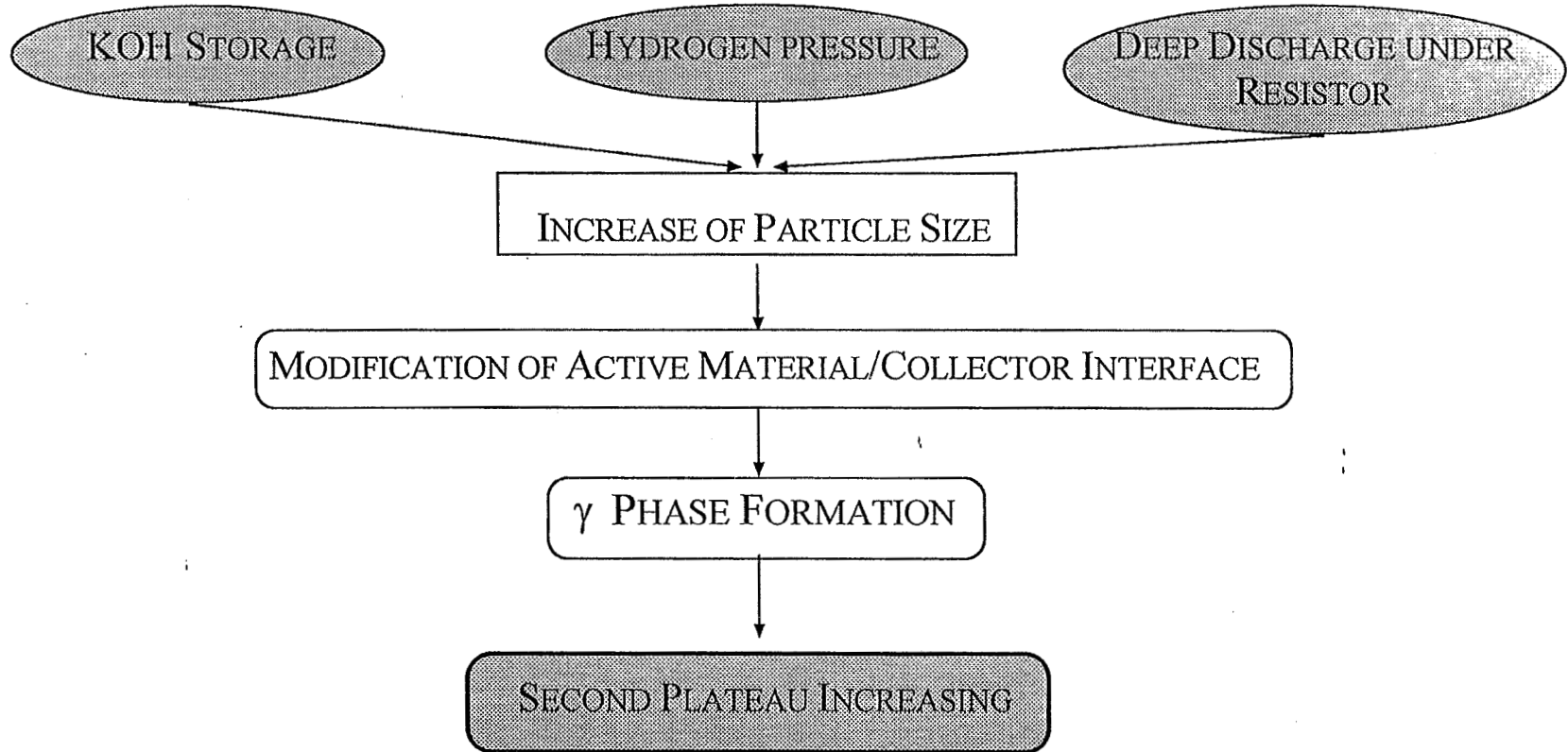




STUDY OF PARAMETERS CAUSING SECOND PLATEAU EFFECT ON NiH₂ CELLS

2- EFFECTS OF HYDROGEN PRESSURE

SUMMARY ON HYDROGEN EFFECTS





Advanced and Industrial Battery Group
Defense and Space Division

STUDY OF PARAMETERS CAUSING SECOND PLATEAU EFFECT ON NiH₂ CELLS

CONCLUSION

THE SECOND PLATEAU IS :

- LINKED TO THE γ PHASE
- INFLUENCED BY THE COLLECTOR/ACTIVE MATERIAL INTERFACE
 - DUE TO THE TRANSITION $\gamma/\beta(\text{II})$
 - INCREASED BY THE PARTICLE SIZE
- EXACERBATED BY THE PRECHARGE LEVEL
- AMPLIFIED BY THE DEEP DISCHARGES



Advanced and Industrial Battery Group
Defense and Space Division

STUDY OF PARAMETERS CAUSING SECOND PLATEAU EFFECT ON NiH₂ CELLS

CONCLUSION

RECOMMENDATIONS FOR NiH₂ CELL MANAGEMENT

IN ORDER TO DIMINISH SECOND PLATEAU APPEARANCE :

- AVOID OVERCHARGE AND γ FORMATION : LIMIT THE RECHARGE RATIO
- USE POSITIVE PRECHARGE INSTEAD NEGATIVE
- AVOID DEEP DISCHARGE (BETWEEN 0.5 AND 0 V) UNDER RESISTOR DURING RECONDITIONNING



STUDY OF PARAMETERS CAUSING SECOND PLATEAU EFFECT ON NiH₂ CELLS

ACKNOWLEDGEMENTS

A.DELAHAYE AND J.M TARASCON FOR FRUITLESS DISCUSSIONS

T.JAMIN FROM CNES FOR FINANCIAL SUPPORT

**PERFORMANCE COMPARISON BETWEEN
NiH₂ DRY SINTER AND SLURRY ELECTRODE CELLS**

J. D. Armantrout

Presented at
1997 NASA Battery Workshop
Focused Session - Design of the Nickel Electrode

November 19, 1997

Background

- LAUNCHED IN 1990 WITH A 7-YEAR BATTERY DESIGN LIFE (5-YEAR MISSION).
 - 88 Ah NiH₂ CELLS, DRY SINTER PROCESS PLATES, HYDROGEN PRECHARGE.
 - NOMINAL 12 PERCENT BATTERY DEPTH OF DISCHARGE (DOD).
- BATTERY DATA THRU 1995 SHOWED CAPACITY LOSSES OF 4.5 Ah/YEAR.
- BASELINE BATTERY REFURBISHMENT IN 2002 ON SERVICING MISSION 4.
 - UPGRADE TO SLURRY PROCESS PLATE; INCORPORATE POSITIVE PRECHARGE.
 - COULD REPLACE BATTERIES IN 1999 BASED ON CAPACITY TREND ANALYSIS.
- NEED TO KNOW OPERATING V/T CHARGE LEVEL (SLOPE AND INTERCEPT) AND HEAT DISSIPATION OF NEW CELL DESIGN.

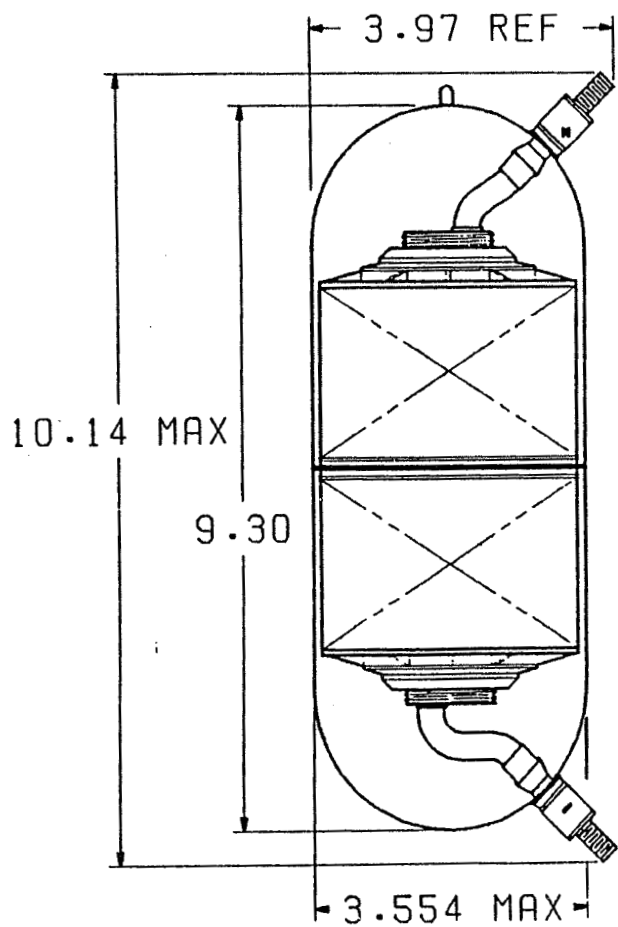
HST Refurbishment Cell Design Summary

“Pineapple Slice” Cell Design with the Following Components:

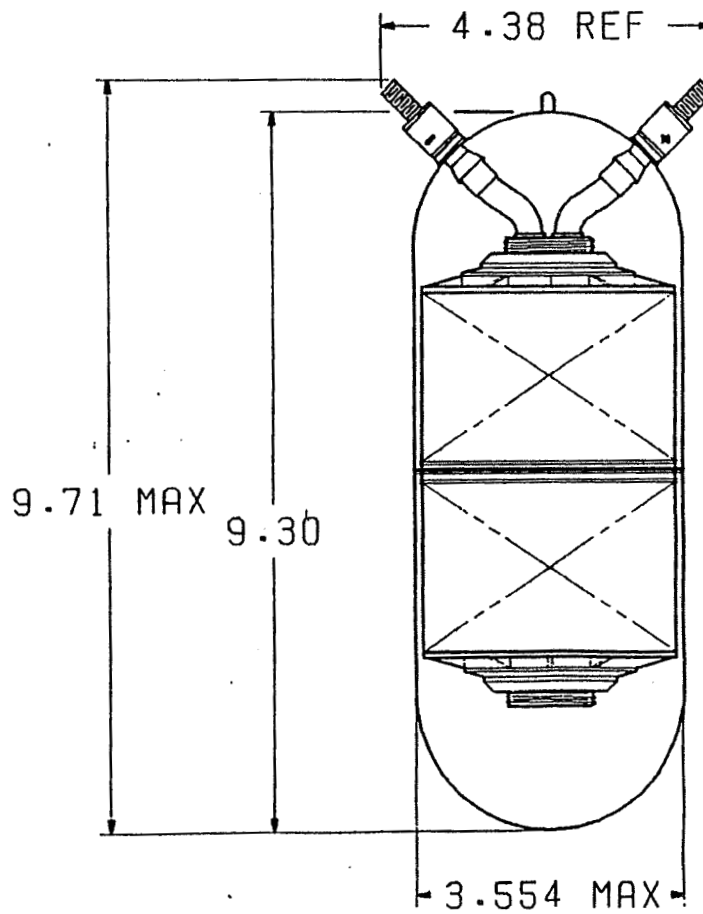
- 48 Slurry Process Nickel Positive Electrodes 0.035 in. thick
- 48 Platinum Negative Electrodes (0.006 in. thick)
- Back-to-back Electrode Stack Configuration
- Zirconium Oxide Cloth Separators and Gas Screens
- Polysulfone End Plates, Core and Retaining Nut
- Belleville and Whiteley Washers
- Inconel 718 Pressure Vessel 0.040 in. thick
- Zirconium Oxide Pressure Vessel Wall Wick
- Inconel 718 Terminal Bosses and Weld Ring
- Injection Molded Nylon Terminal Seals
- “Rabbit Ear” Terminal Configuration
- Positive Precharge

Offset Non-Opposing vs. Rabbit Ear Cell

OFFSET NON-OPPOSING



RABBIT EAR



HST NICKEL-HYDROGEN BATTERY OVERVIEW

- CONTRACT MOD 593 DATED 2 JUNE 1987 DIRECTED LMSC TO DESIGN, DEVELOP AND DELIVER NICKEL-HYDROGEN (NiH_2) BATTERY MODULES TO REPLACE NiCd BATTERIES FOR THE HUBBLE SPACE TELESCOPE (HST) LOW EARTH ORBIT (LEO) MISSION PER NAS 8-32697.
- A NiH_2 MODULE WITH THREE ELECTRICALLY DISTINCT BATTERIES IN A COMMON MECHANICAL STRUCTURE WAS DESIGNED AS AN ORBITAL REPLACEMENT UNIT (ORU). TWO MODULES WERE INSTALLED ON BAY DOORS 2 AND 3 OF THE HST SUPPORT SYSTEM MODULE (SSM).
- TWO MODULES MAKE UP THE FULL NiH_2 BATTERY COMPLEMENT OF SIX BATTERIES, EACH RATED AT 88Ah TO 26.4 VDC PER CELL AT A 15 AMP DISCHARGE RATE AT 0°C AND HAVING A MINIMUM ORBITAL LIFE OF 5 YEARS.
- ONE STRUCTURAL ENGINEERING MODULE (SEM) AND FIVE MODULES WERE MANUFACTURED AND DELIVERED BY EAGLE PICHER INDUSTRIES (EPI).

HST NiH₂ BATTERY RECONDITIONING CAPACITY

- THE HST NICKEL HYDROGEN BATTERIES BUILT FROM 88 Ah CELLS MANUFACTURED WITH DRY SINTER PROCESS ELECTRODES HAVE EXCEEDED THEIR 7-YEAR DESIGN LIFE (5-YEAR MISSION).
 - PERIODIC BATTERY CAPACITY MEASUREMENTS SHOW IMPROVED PERFORMANCE SINCE SWITCHING FROM PRIMARY TO SECONDARY HEATERS IN NOVEMBER 1995.

BATTERY POSITION	BATTERY CAPACITY (Ah)					
	<u>1990</u>	<u>1992</u>	<u>1994</u>	<u>1995</u>	<u>1996</u>	<u>1997</u>
1	94.2		80.4	74.5		83.7
2		88.5	79.3	72.4		78.5
3		85.6		73.5	74.7	74.4
4	93.4					83.7
5		94.0		78.3	73.7	76.4
6		88.3	74.6	70.5		75.3

Figure 1. HST Battery Capacity Trend Data

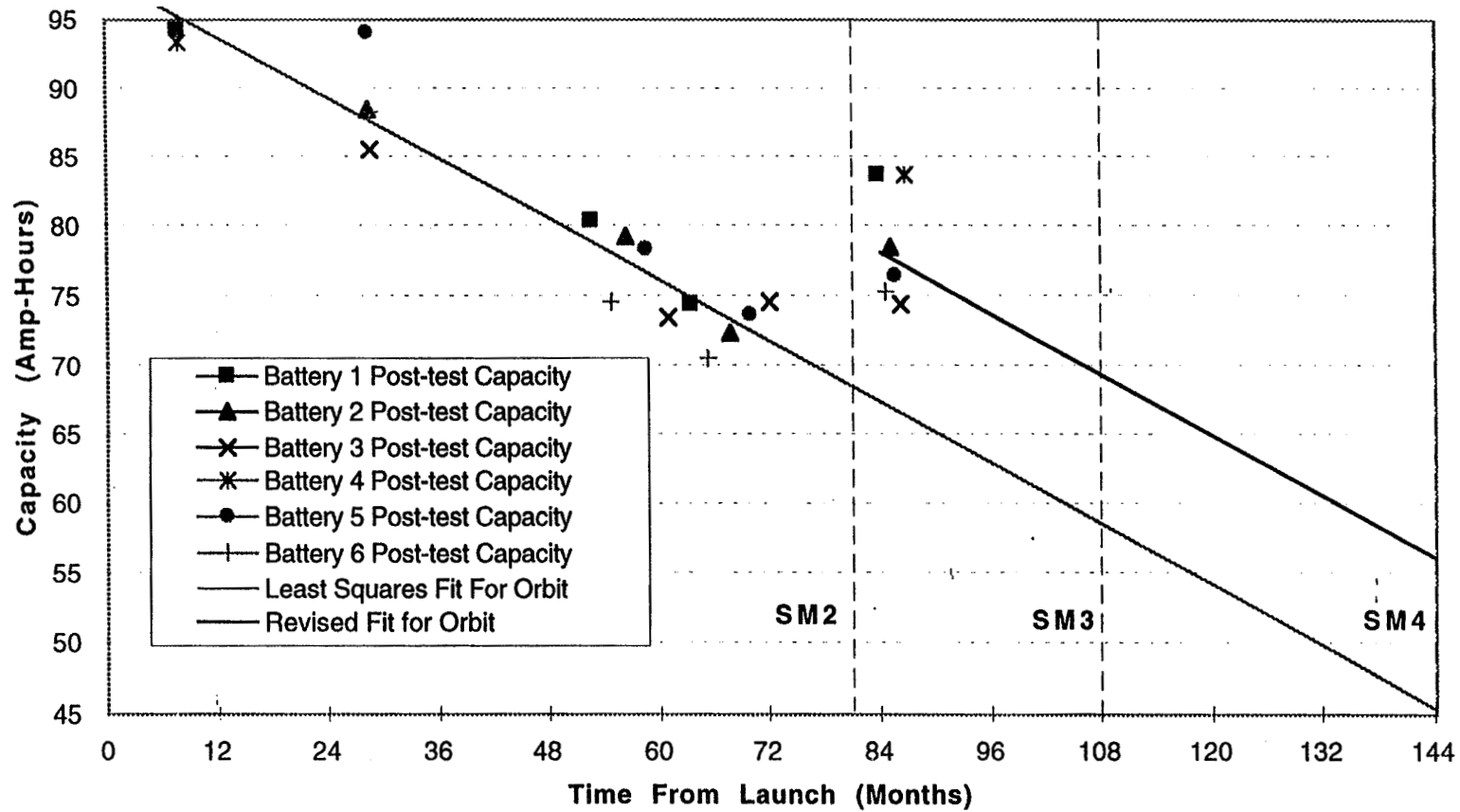


Figure 2. Effect of Temperature and Cutoff Voltage on Capacity

Charge current is 15 amperes.

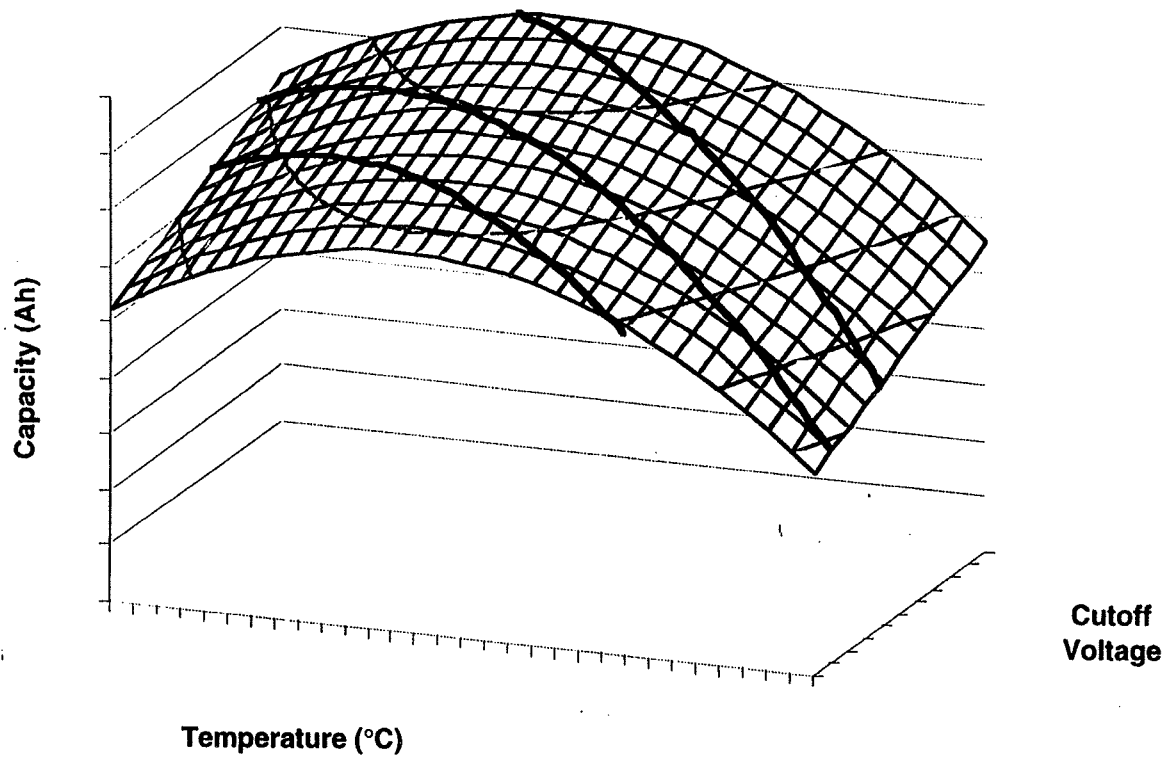
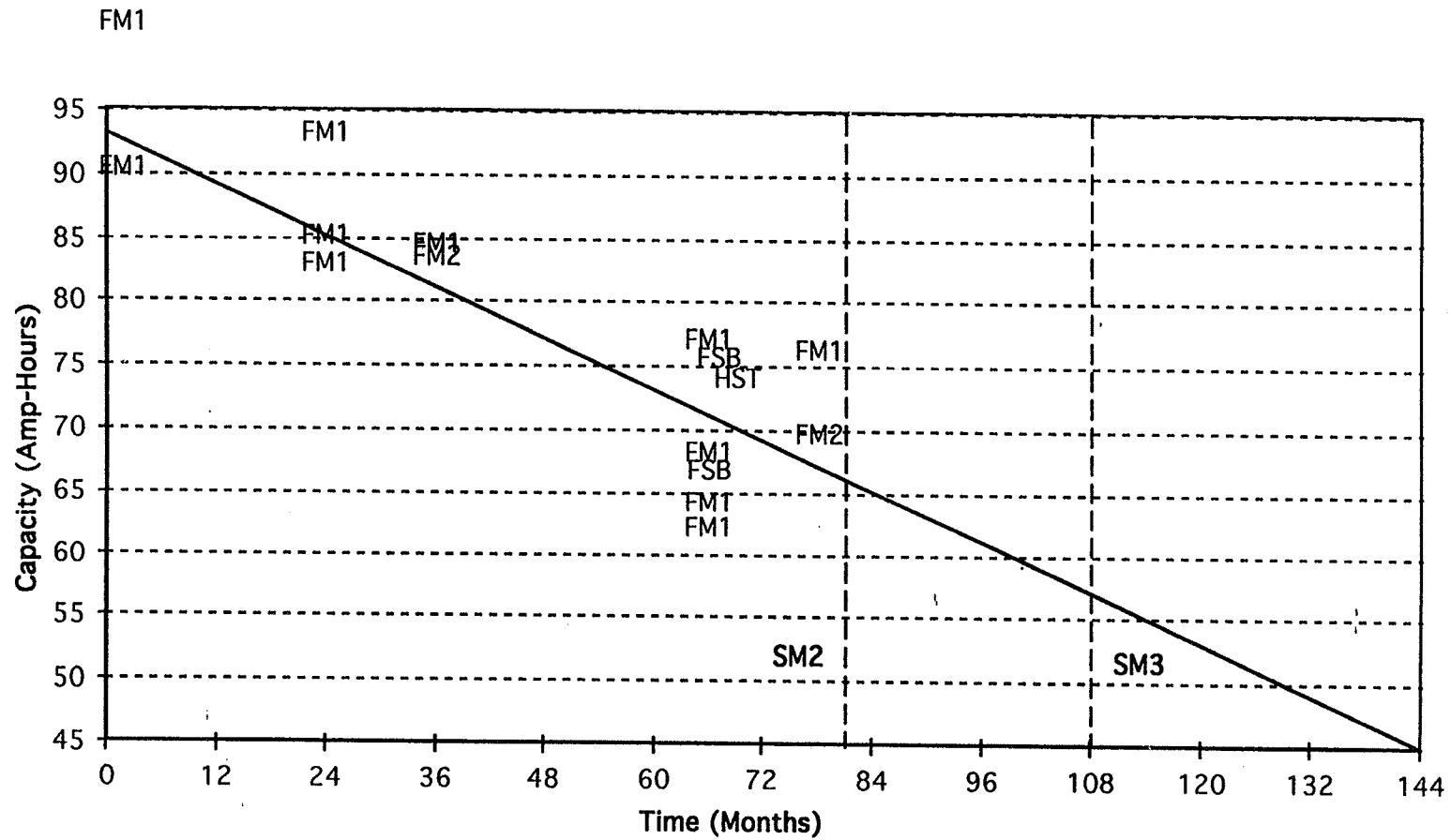


Figure 3. Ground Test Capacity Data



HST CHARACTERIZATION TEST PROCEDURE

- BATTERY CELLS BUILT WITH SLURRY PROCESS ELECTRODES TESTED TO CHARACTERIZE PERFORMANCE FOR EXPECTED OPERATING CONDITIONS.
 - TESTED VARIOUS CHARGE VOLTAGE LIMITS OVER 23°F TO 50°F RANGE.
- TESTING PERFORMED UNDER ISOTHERMAL CONDITIONS THAT ALLOW FIRST LAW CALCULATION OF HEAT DISSIPATION AND RECHARGE RATIO.
 - CHARGING PERFORMED AT 14 AMPS TO VOLTAGE LIMIT FOLLOWED BY 2 AMP TRICKLE CHARGE FOR DURATION OF SUN PERIOD.
 - 9.6 Ah DOD ACHIEVED USING 12 AMP AND 24 AMP DISCHARGES DURING ECLIPSE.
- PERIODIC CAPACITY MEASUREMENTS MADE TO DETERMINE EFFECTS OF VARIOUS TEST CONDITIONS ON PERFORMANCE.
- CELLS MANUFACTURED WITH DRY SINTER PROCESS ELECTRODES INCLUDED IN THE TEST FOR COMPARISON WITH ORIGINAL DESIGN.
- OPERATING CAPACITY MEASUREMENTS TO 1.2 AND 1.1 VOLTS PER CELL MADE AT 18 AMP AND/OR 40 AMP RATES.

HST CHARACTERIZATION TEST RESULTS

- CELLS WITH SLURRY ELECTRODES HAVE SLIGHTLY HIGHER ORBITAL AVERAGE THERMAL DISSIPATION THAN DRY SINTER CELLS.
 - DATA SUMMARIZED IN TABLE 1 SHOW PERFORMANCE FOR EACH CELL TYPE.
 - DATA SUMMARIZED IN TABLE 2 AND PRESENTED IN TABLE 3 SHOW CORRELATION OF HEAT DISSIPATIONS AND RECHARGE RATIOS.
 - DATA ILLUSTRATED IN FIGURES 4 THROUGH 10 SUMMARIZE TEST RESULTS.
- SLURRY PROCESS ELECTRODE CELLS HAVE LOWER RELATIVE CAPACITY AT LOWER TEMPERATURES (FIGURE 11 AND TABLE 1).
 - VOLTAGE DATA IN FIGURES 12 THROUGH 15 SHOW LOWER RELATIVE DISCHARGE VOLTAGE PLATEAU FOR SLURRY CELLS VERSUS DRY SINTER CELLS.
 - RECONDITIONING CELL VOLTAGE DRAINS ARE SHOWN IN FIGURES 16 AND 17.
 - CYCLING PERFORMANCE DATA IN FIGURES 18 THROUGH 21 ILLUSTRATE AN INDEPENDENT TEST RUN UNDER ISOTHERMAL CONDITIONS.
- THERE WAS A DRAMATIC EFFECT OF CHARGE CUTOFF VOLTAGE ON HEAT DISSIPATION (FIGURES 5 AND 6).
- CAPACITY INCREASED ONLY SLIGHTLY WITH HIGHER CHARGE CUTOFF VOLTAGES (FIGURES 7 THROUGH 10).

Table 1. HST CHARACTERIZATION TEST RESULTS

Slurry Recharge Ratio				
	23°F	32°F	41°F	50°F
VT5	100.88%	100.55%		
VT4.5	101.79%	101.76%	101.81%	
VT4	103.02%	104.77%	105.51%	104.63%
VT3.5	105.30%	108.59%	109.50%	109.74%
VT3	107.65%	113.14%	115.83%	116.56%
VT2.5	111.93%	120.20%	124.96%	128.48%

Note: Recharge Ratios for Dry Sinter Cells not measured.

Dissipation (watts)								
	Slurry Cells				Dry Sinter Cells			
	23°F	32°F	41°F	50°F	23°F	32°F	41°F	50°F
VT5	11.8	10.8			10.2	9.1		
VT4.5	14.0	13.3	13.1		12.1	11.5	11.3	
VT4	16.4	19.3	20.4	18.4	14.5	17.4	18.5	16.5
VT3.5	20.9	26.9	28.5	28.5	19.2	24.8	26.5	26.6
VT3	25.9	36.1	41.4	42.2	24.1	34.0	39.1	40.3
VT2.5	34.7	50.7	60.0	66.2	33.2	48.8	57.6	64.2

Table 1 (Cont). HST CHARACTERIZATION TEST RESULTS

	Operating Capacity (Ah) to 1.2 Volts				Operating Capacity (Ah) to 1.2 Volts			
	Slurry Cells				Dry Sinter Cells			
	23°F	32°F	41°F	50°F	23°F	32°F	41°F	50°F
VT5	46.19	47.60			70.56	69.35		
VT4.5	46.79	50.43	50.25		70.87	70.51	62.05	
VT4	47.23	51.71	54.11	51.77	71.29	72.55	69.80	58.87
VT3.5	47.64	52.16	55.85	55.77	72.42	74.64	70.47	62.59
VT3	48.05	52.68	57.03	59.12	73.45	75.23	71.31	66.30
VT2.5	47.02	53.19	58.26	61.45	70.72	72.50	70.46	68.13

	Operating Capacity (Ah) to 1.1 Volts				Operating Capacity (Ah) to 1.1 Volts			
	Slurry Cells				Dry Sinter Cells			
	23°F	32°F	41°F	50°F	23°F	32°F	41°F	50°F
VT5	81.53	81.35			94.12	85.73		
VT4.5	82.29	84.14	79.68		95.31	86.19	71.38	
VT4	82.64	84.97	82.88	73.91	93.90	88.26	83.40	74.07
VT3.5	82.84	85.55	84.08	77.44	93.61	90.41	83.86	77.41
VT3	83.15	85.90	85.12	80.52	94.63	90.72	84.86	80.60
VT2.5	82.6	85.19	84.98	82.86	90.02	86.93	84.32	82.44

Table 2. CHARACTERIZATION TEST RESULTS SUMMARY

Cond	V/T Level	Temp	Cutoff	Recharge Ratio	Dissipation (watts)	Operating Capacity (Ah)
1	VT 4	23°F	33.02V	102.96	16.2	82.56
2	VT 3.5	23°F	33.33V	105.3	20.9	82.84
3	VT 3	23°F	33.64V	107.65	25.9	83.15
16	VT 2.5	23°F	33.95V	111.93	34.7	82.6
4	VT 4	32°F	32.71V	104.91	19.5	84.97
5	VT 3.5	32°F	33.02V	108.59	26.9	85.55
6	VT 3	32°F	33.33V	113.14	36.1	85.9
15	VT 2.5	32°F	33.64V	120.2	50.7	85.19
7	VT 4	41°F	32.40V	105.51	20.4	82.88
8	VT 3.5	41°F	32.71V	109.5	28.5	84.08
9	VT 3	41°F	33.02V	115.83	41.4	85.12
14	VT 2.5	41°F	33.33V	124.96	60	84.98
10	VT 4	50°F	32.09V	104.63	18.4	73.91
11	VT 3.5	50°F	32.40V	109.74	28.5	77.44
12	VT 3	50°F	32.71V	116.56	42.2	80.52
13	VT 2.5	50°F	33.02V	128.48	66.2	82.86
17	VT 5	23°F	32.40V	100.88	11.8	81.53
18	VT 4.5	23°F	32.71V	101.79	14	82.29
19	VT 4	23°F	33.02V	103.22	16.9	82.72
20*	VT 4	23°F	33.02V	102.88	16.2	99.52
21	VT 5	32°F	32.09V	100.55	10.8	81.35
22	VT 4.5	32°F	32.40V	101.76	13.3	84.14
23	VT 4	32°F	32.71V	104.63	19.1	85.67
24*	VT 4	32°F	32.71V	104.76	19.4	96.89
25	VT 4.5	41°F	32.09V	101.81	13.1	79.68

Table 2 (Cont). CHARACTERIZATION TEST RESULTS SUMMARY

Points from LMMS heat dissipation test

x40	VT3	41°F	33.02V	114	38.5
x40a	VT3	50°F	32.71V	117	42.8
x40b	VT3.5	50°F	32.40V	110	29.1
x46	VT3	50°F	32.71V	112	34.2

(*) Note: Operating capacity for condns 20 and 24 measured at 18A to 1.2V and 9A to 1.1V. (40A to 1.1V for all other conditions)

x46 should be vt3.5, 41°F

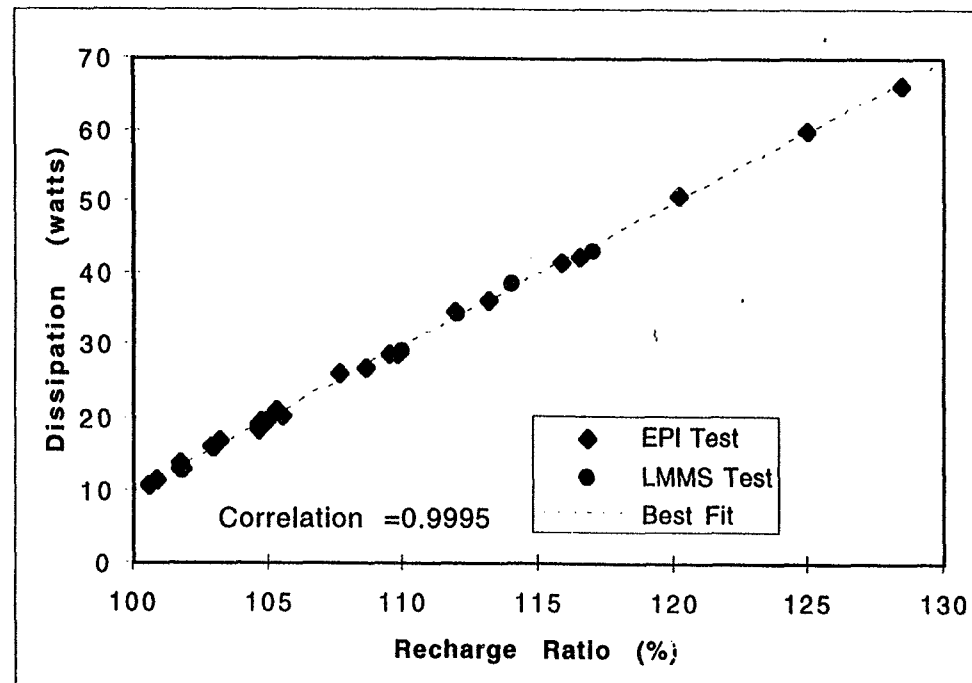


Table 3. LMMS HEAT DISSIPATION TEST CONDITION x46

Date	RNH-90-3 Rechg Ratio(%)	RNH-90-3 Dissipation (W)	RNH-90-9 Rechg Ratio(%)	RNH-90-9 Dissipation (W)
29-Mar-97	104.5	18.8	104.3	18.3
30-Mar-97	105.1	19.9	104.9	19.5
31-Mar-97	106.4	22.5	106.3	22.3
1-Apr-97	107.2	24.2	106.7	23.2
2-Apr-97	108.2	26.2	107.6	25.1
3-Apr-97	109.0	27.8	108.3	26.4
4-Apr-97	109.2	28.3	108.4	26.7
5-Apr-97	109.9	29.7	108.8	27.7
6-Apr-97	110.2	30.4	109.3	28.6
7-Apr-97	110.4	30.8	109.5	29.1
8-Apr-97	110.4	30.9	109.5	29.2
9-Apr-97	110.6	31.4	109.9	30.1
10-Apr-97	110.7	31.7	109.9	30.1
11-Apr-97	111.0	32.3	110.0	30.3
12-Apr-97	111.2	32.6	110.1	30.6
13-Apr-97	111.3	32.9	110.2	30.9
14-Apr-97	111.5	33.4	110.3	31.1
15-Apr-97	111.5	33.4	110.3	31.1
16-Apr-97	111.3	33.2	110.5	31.7
17-Apr-97	111.5	33.7	110.3	31.3
18-Apr-97	111.6	33.9	110.4	31.5
19-Apr-97	111.5	33.6	110.6	31.8
20-Apr-97	111.8	34.2	110.5	31.8
21-Apr-97	111.7	34.2	110.6	32.0

Table 3 (Cont). LMMS HEAT DISSIPATION TEST CONDITION x46

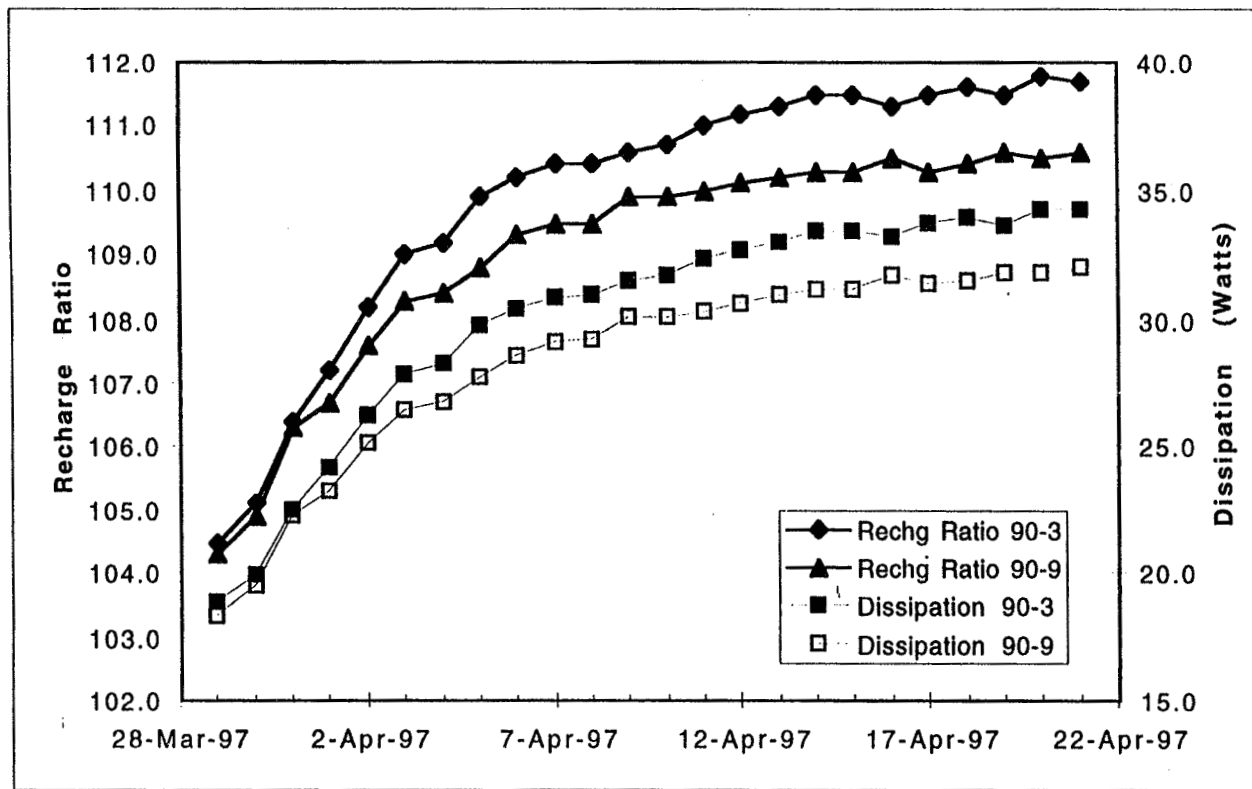


Figure 4. HST Characterization Test Slurry Recharge Ratios

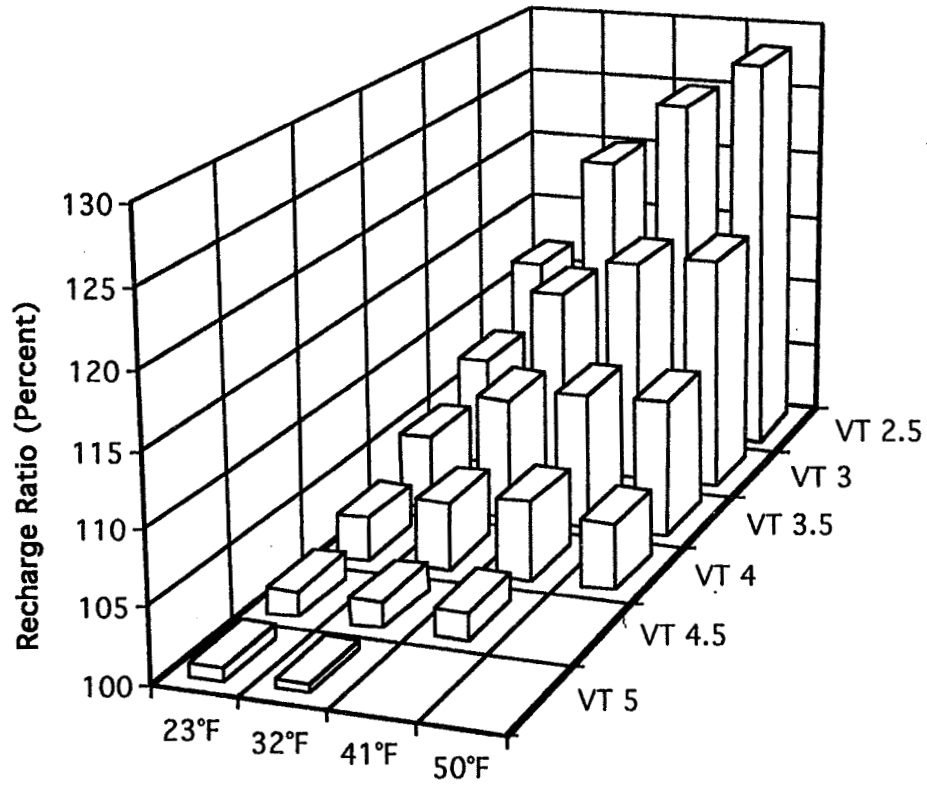


Figure. 5. HST Characterization Test Dissipations-Slurry Cells

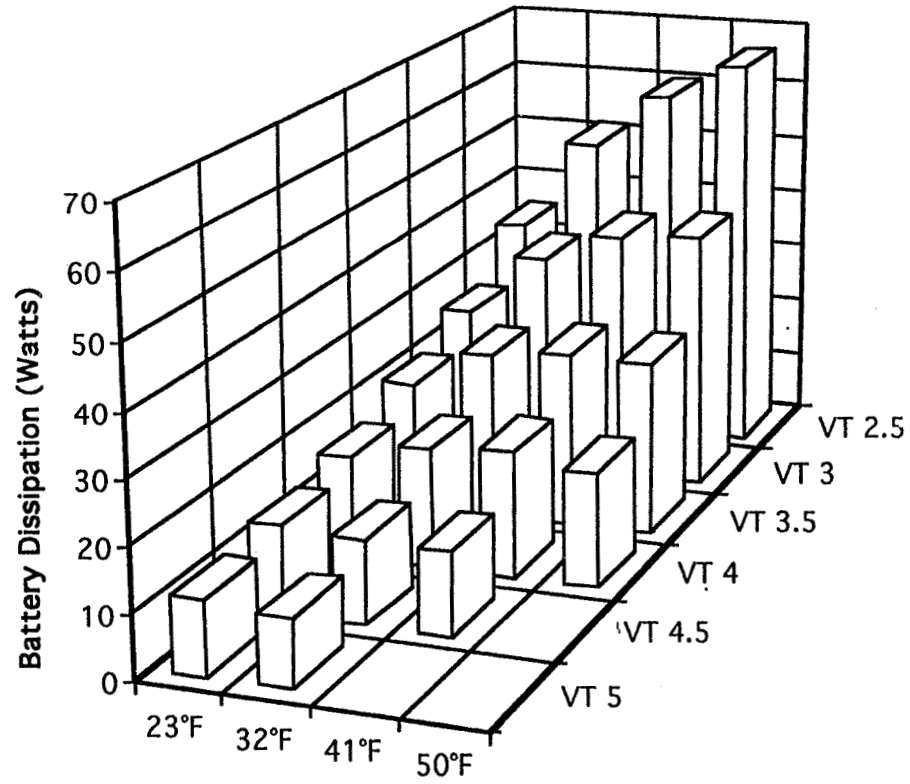


Figure 6. Characterization Test Dissipations for Dry Sinter Cells

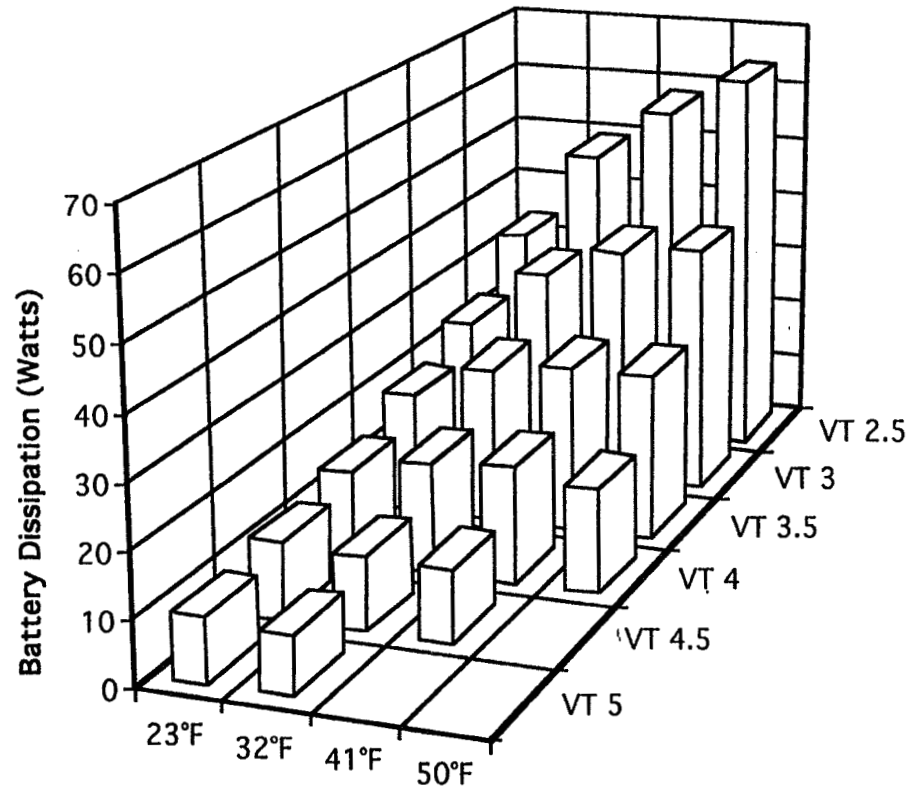


Figure 7. Operating Capacity to 1.2V for Slurry Cells

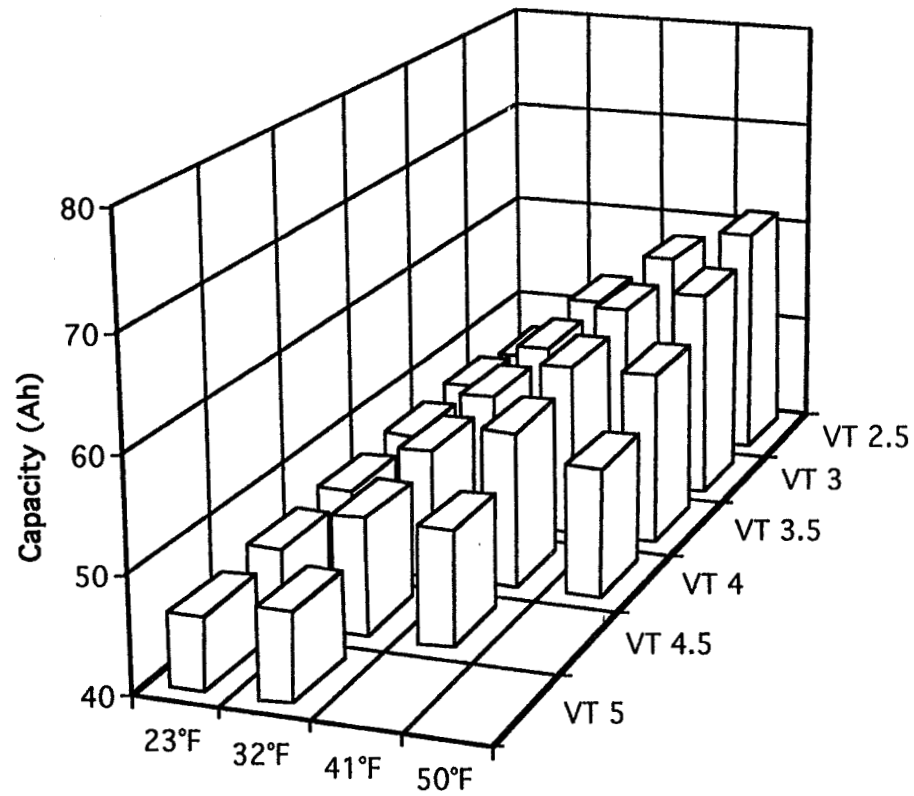


Figure 8. Operating Capacity to 1.1V for Slurry Cells

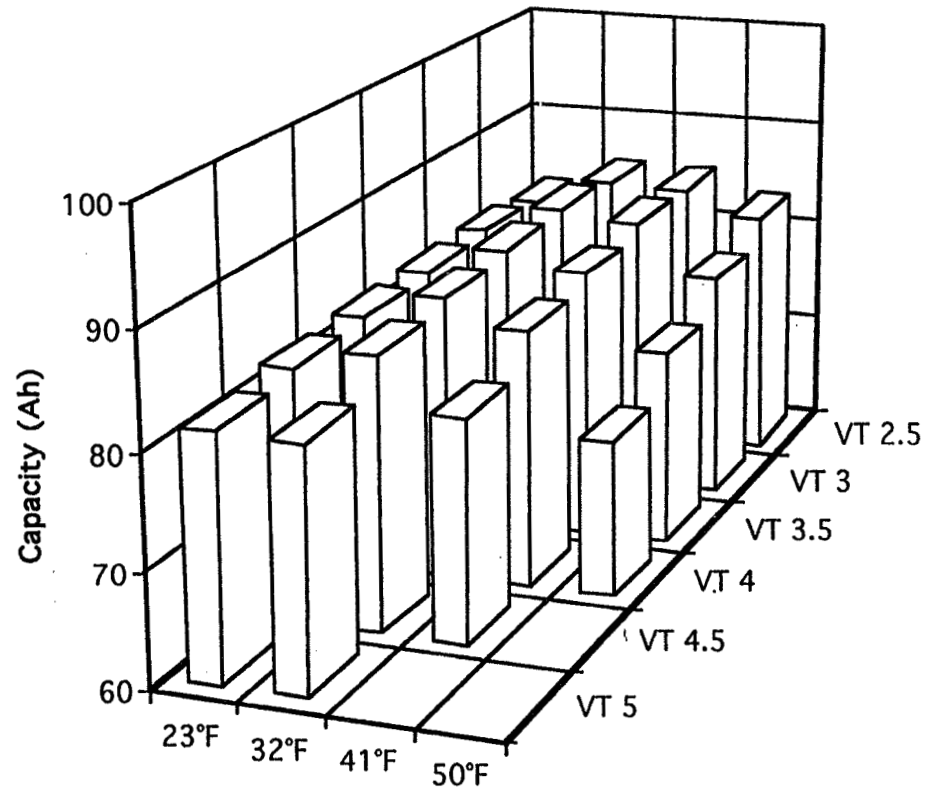


Figure 9. Operating Capacity to 1.2V for Dry Sinter Cells

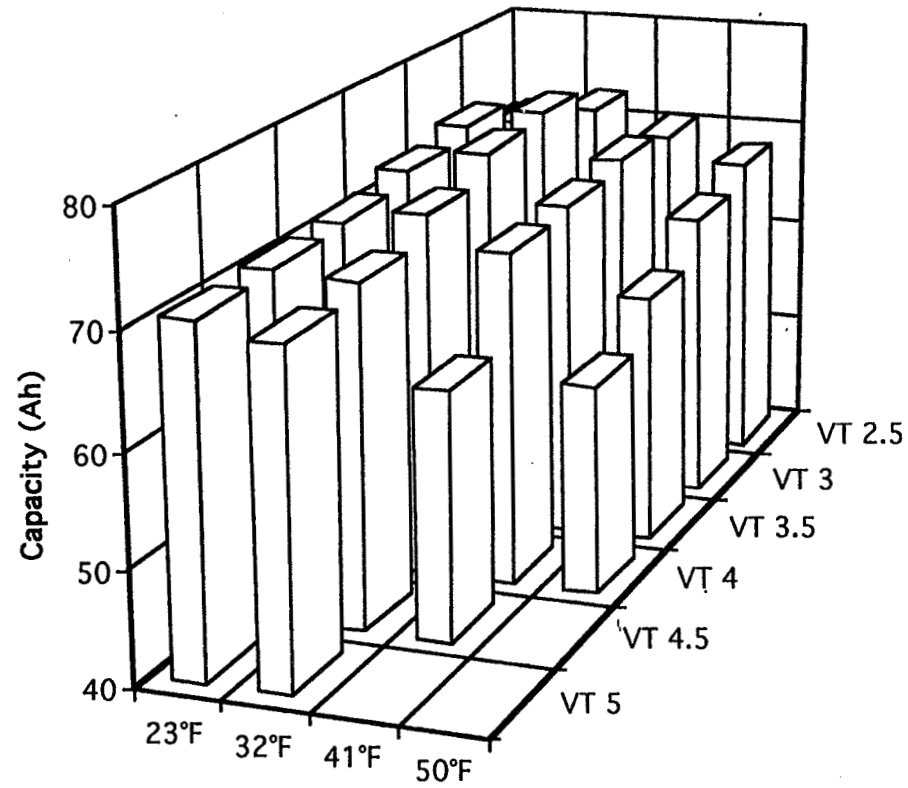


Figure 10. Operating Capacity to 1.1V for Dry Sinter Cells

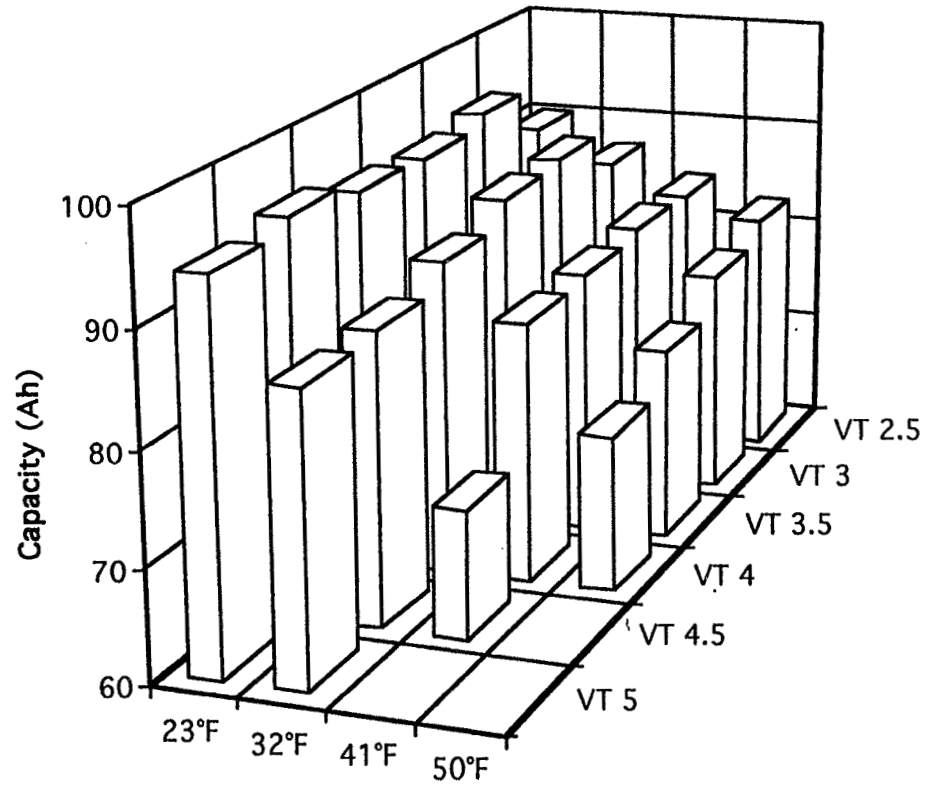


Figure 11. HST Cell Impedance and Capacity Performance

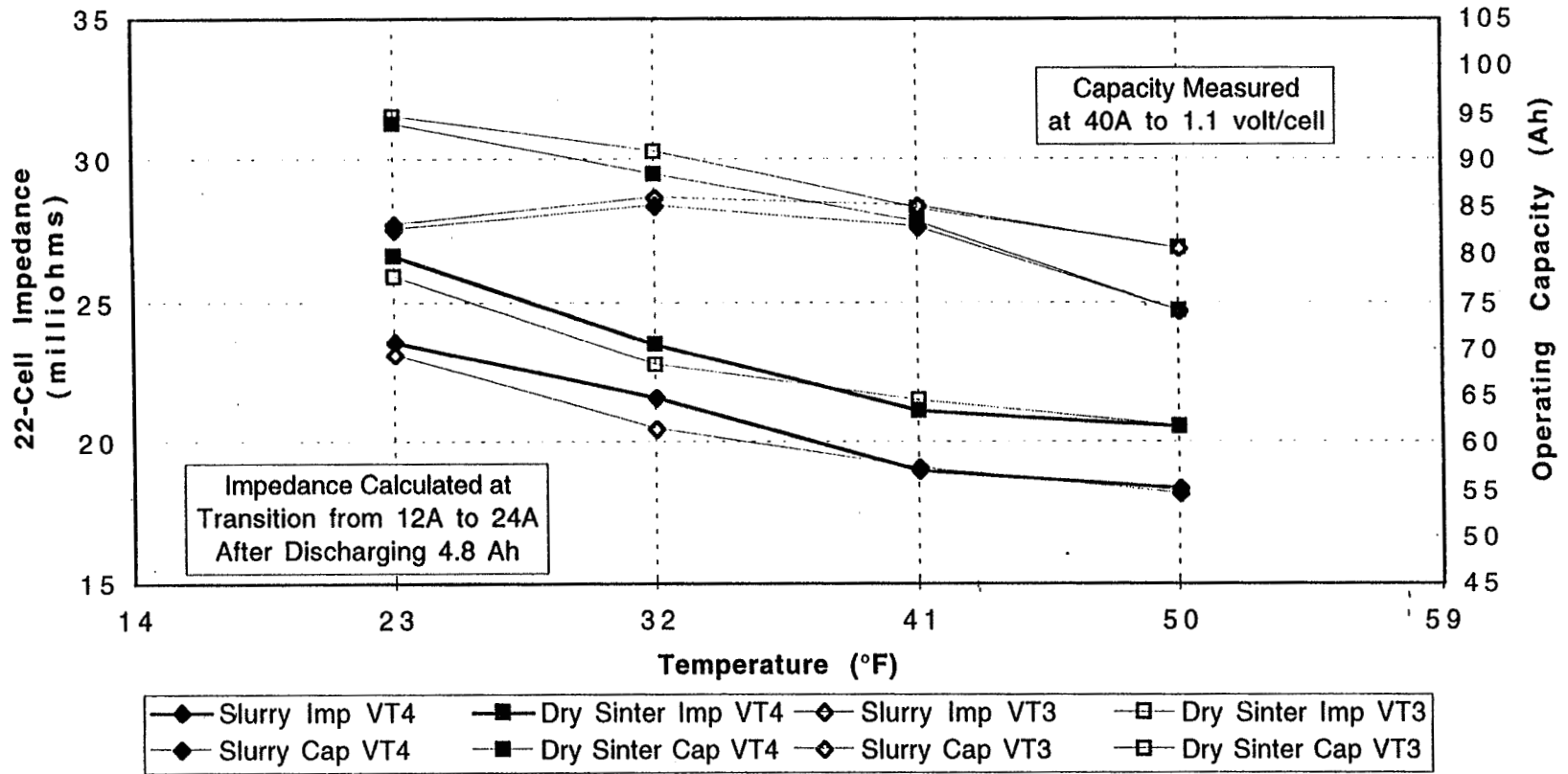


Figure 12. Slurry Cell Voltage vs. Discharge Rate
V/T 4 23°F

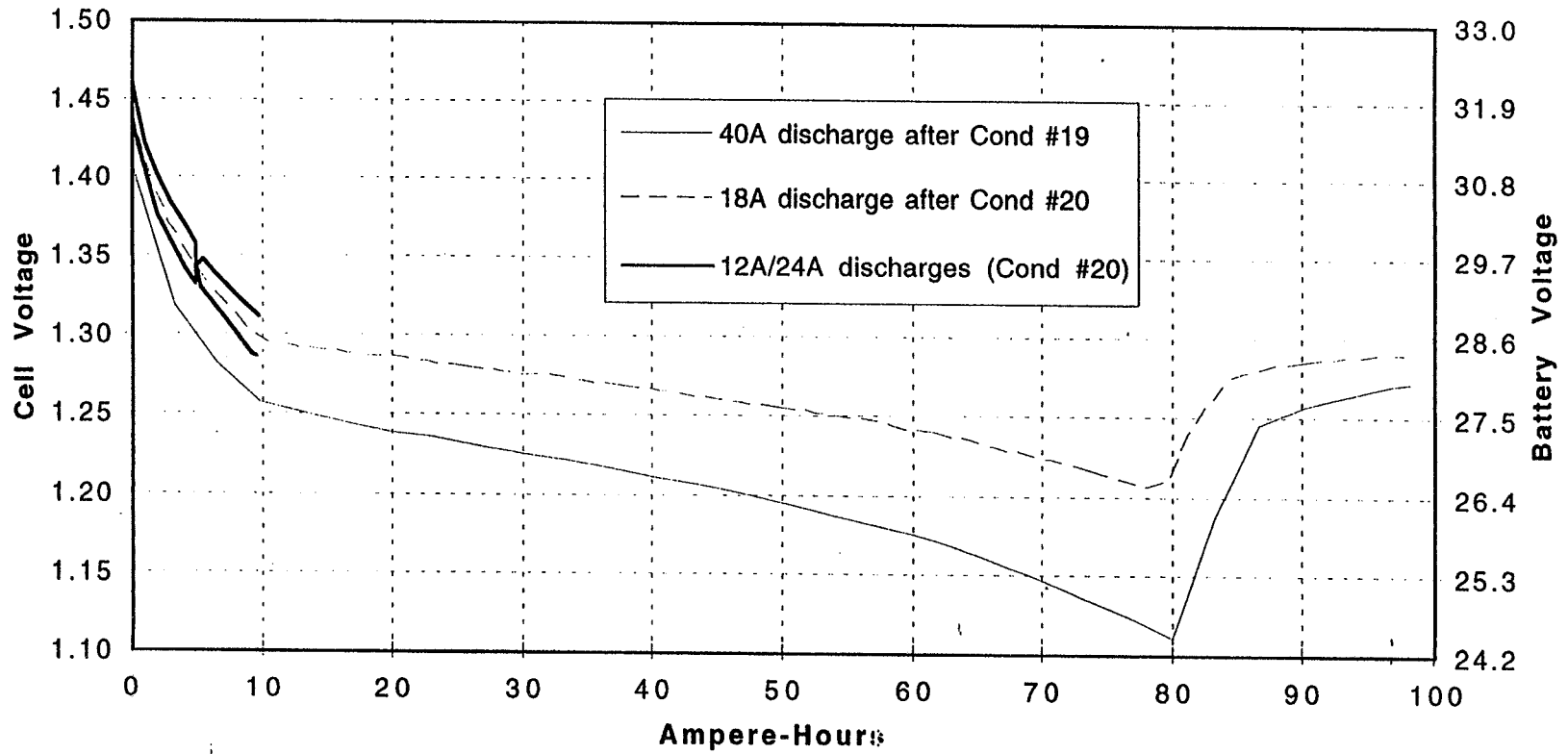


Figure 13. Dry Sinter Cell Voltage vs. Discharge Rate
V/T 4 23°F

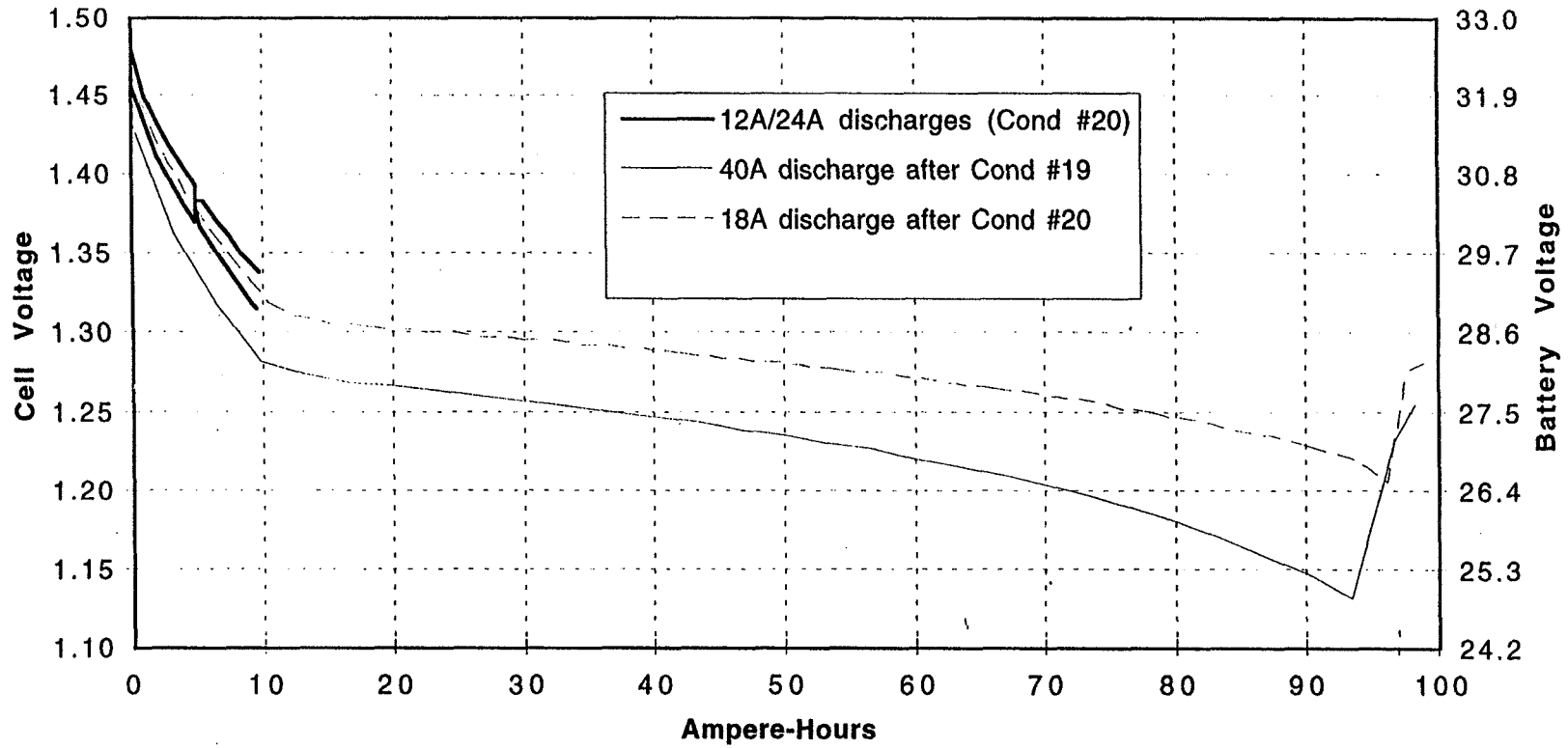


Figure 14. Slurry Cell Voltage vs. Discharge Rate
V/T 4 32°F

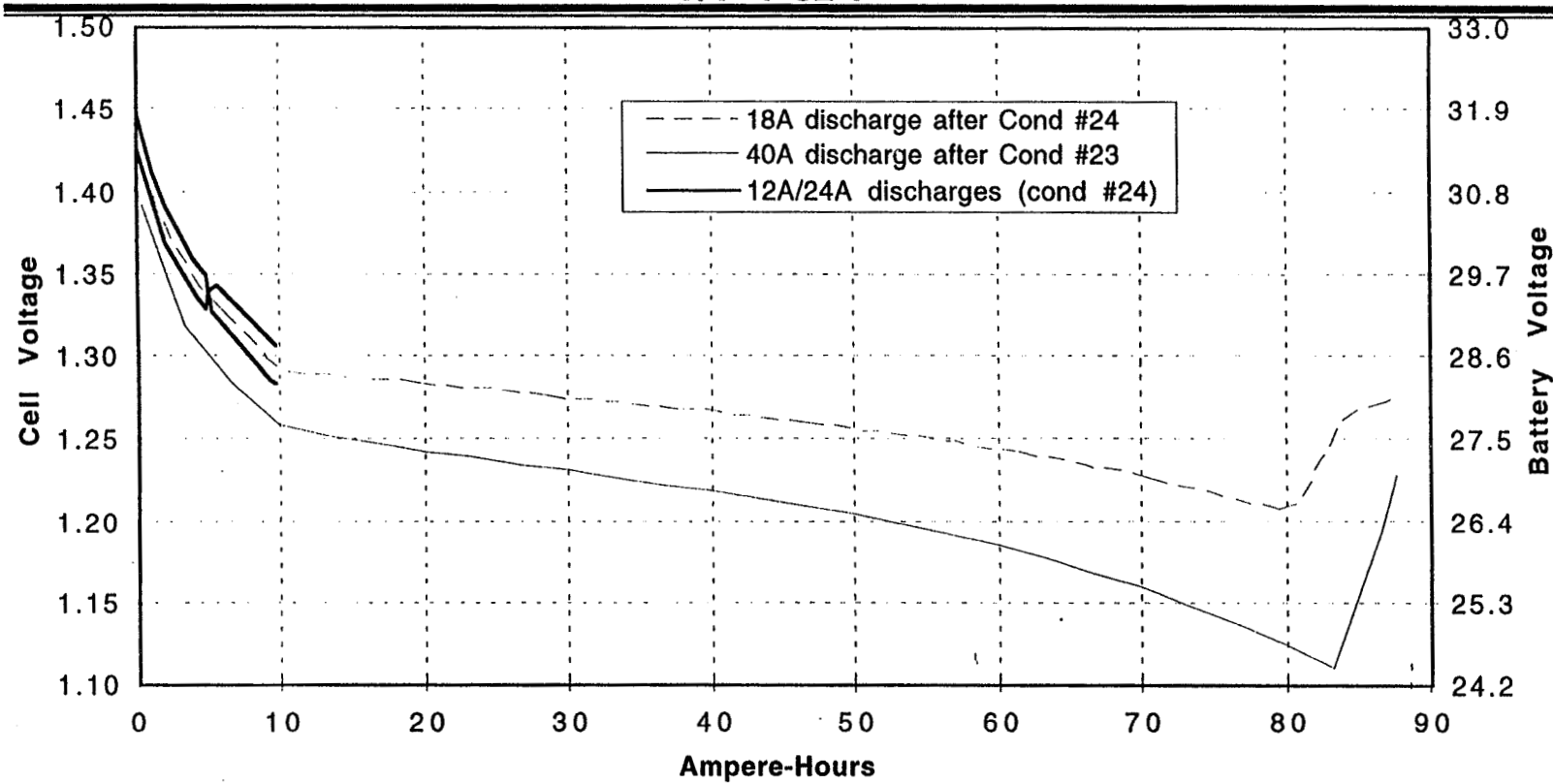


Figure 15. Dry Sinter Cell Voltage vs. Discharge Rate
V/T 4 32°F

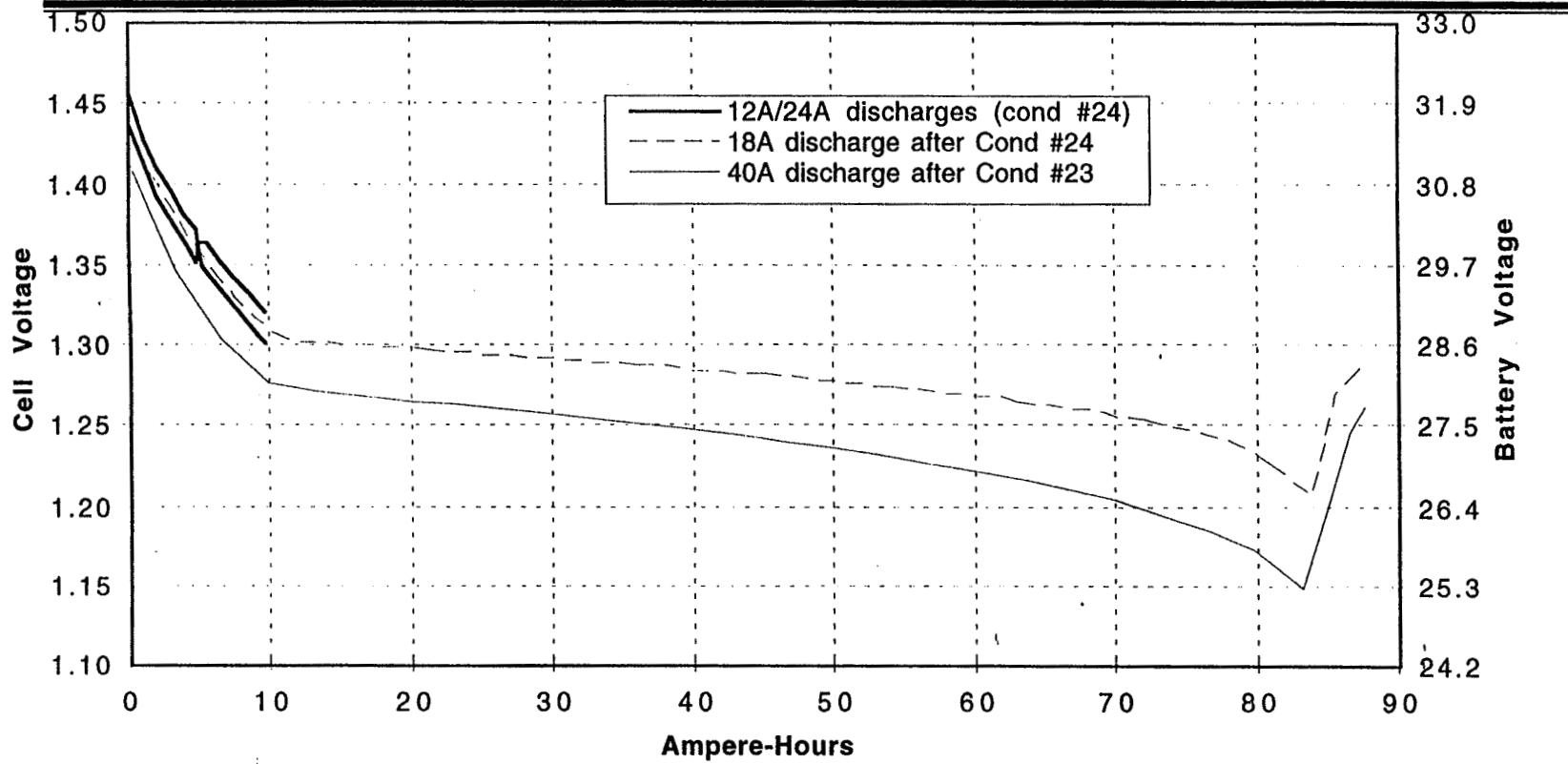


Figure 16. Slurry Cell Drains

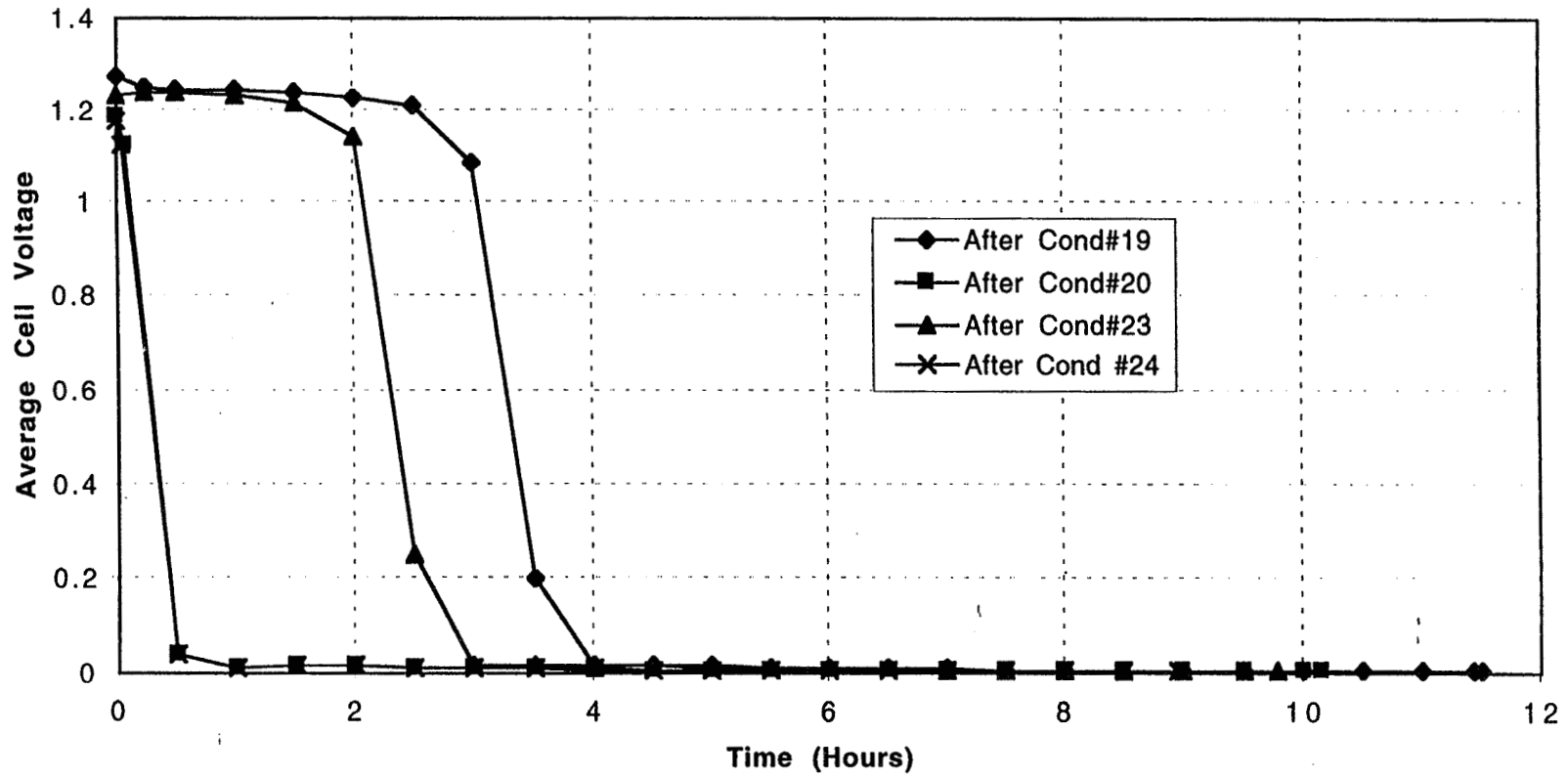


Figure 17. Dry Sinter Cell Drains

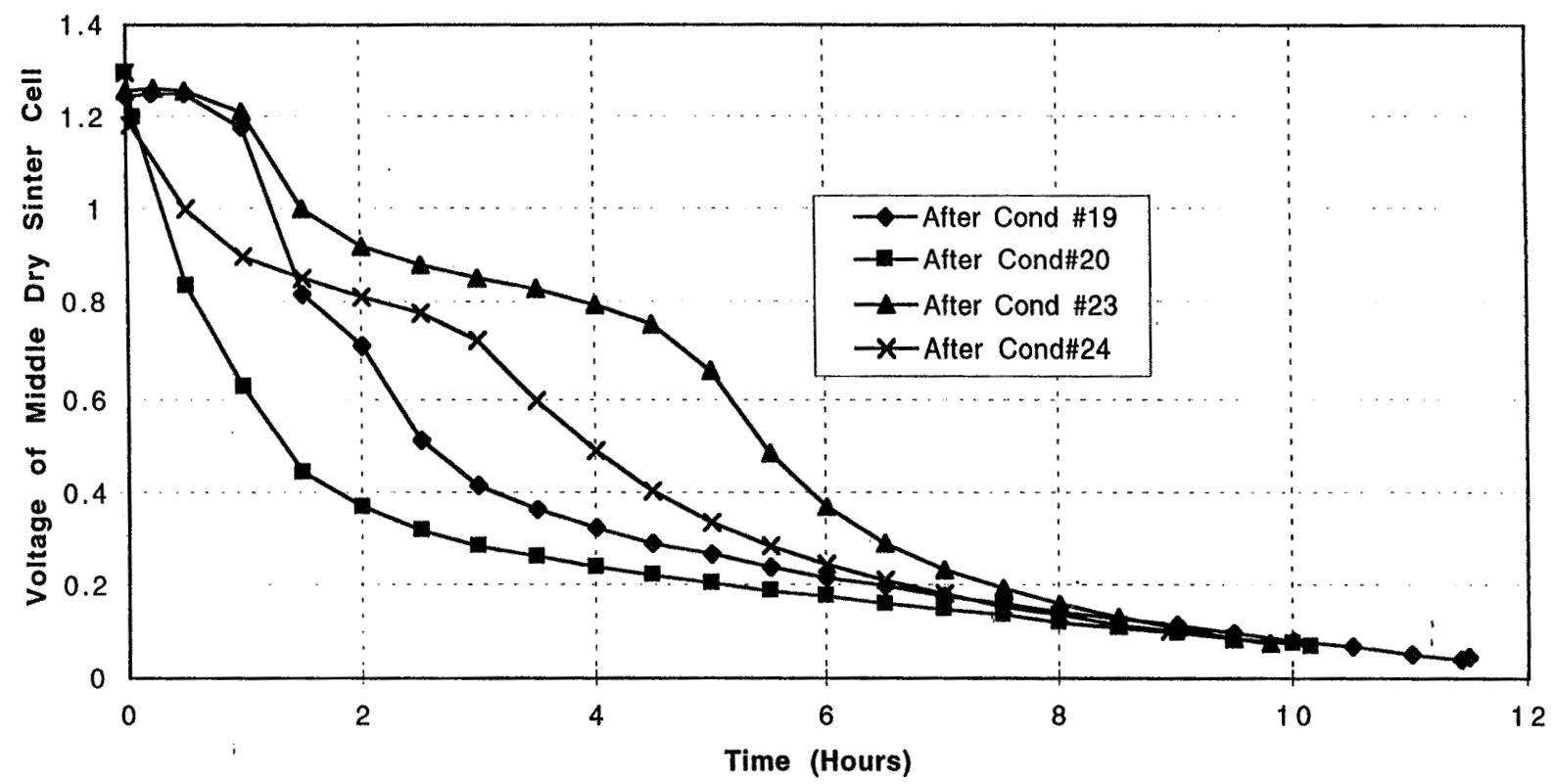


Figure 18. RNH-90-3 Condition X46

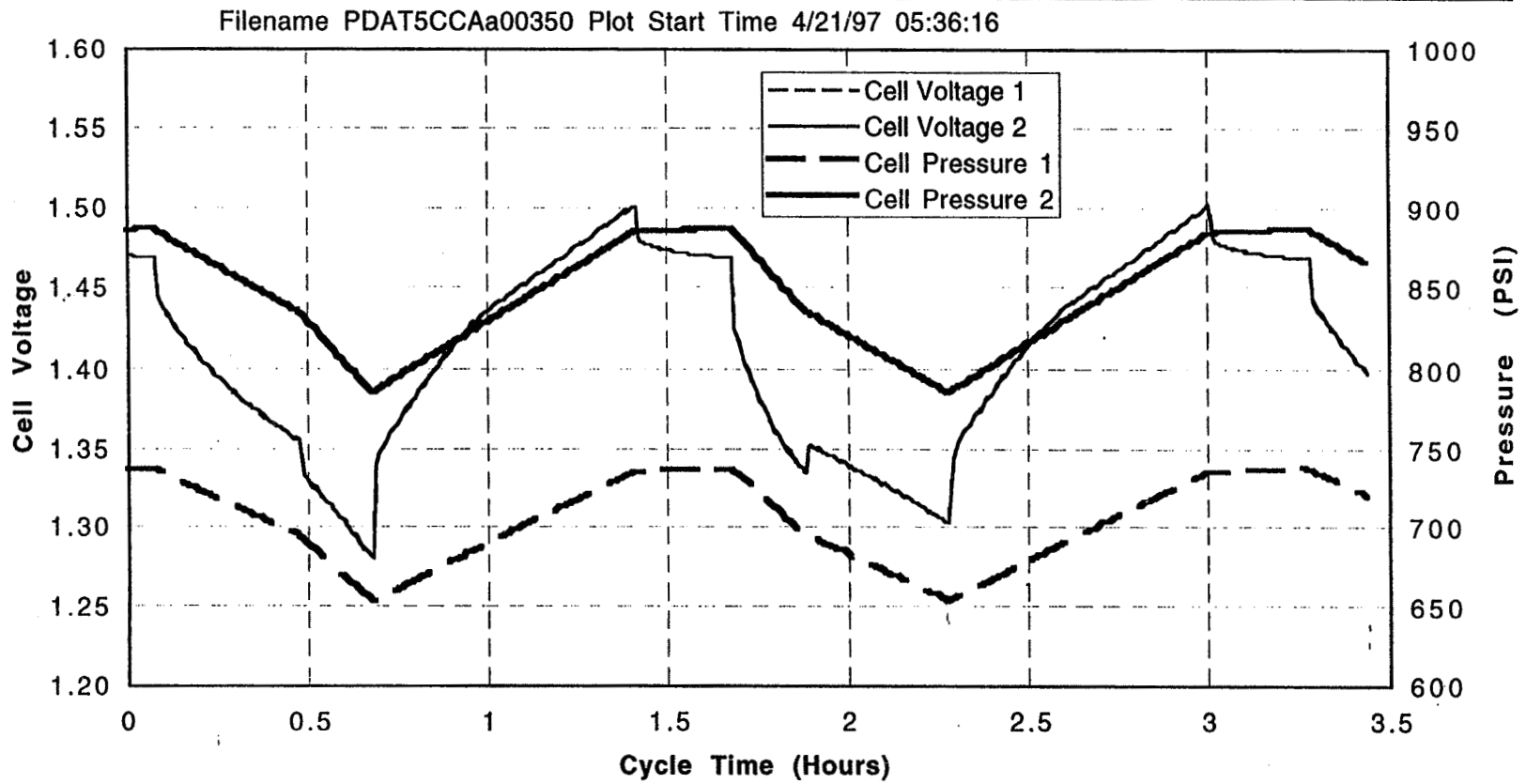


Figure 19. RNH-90-3 Condition X46

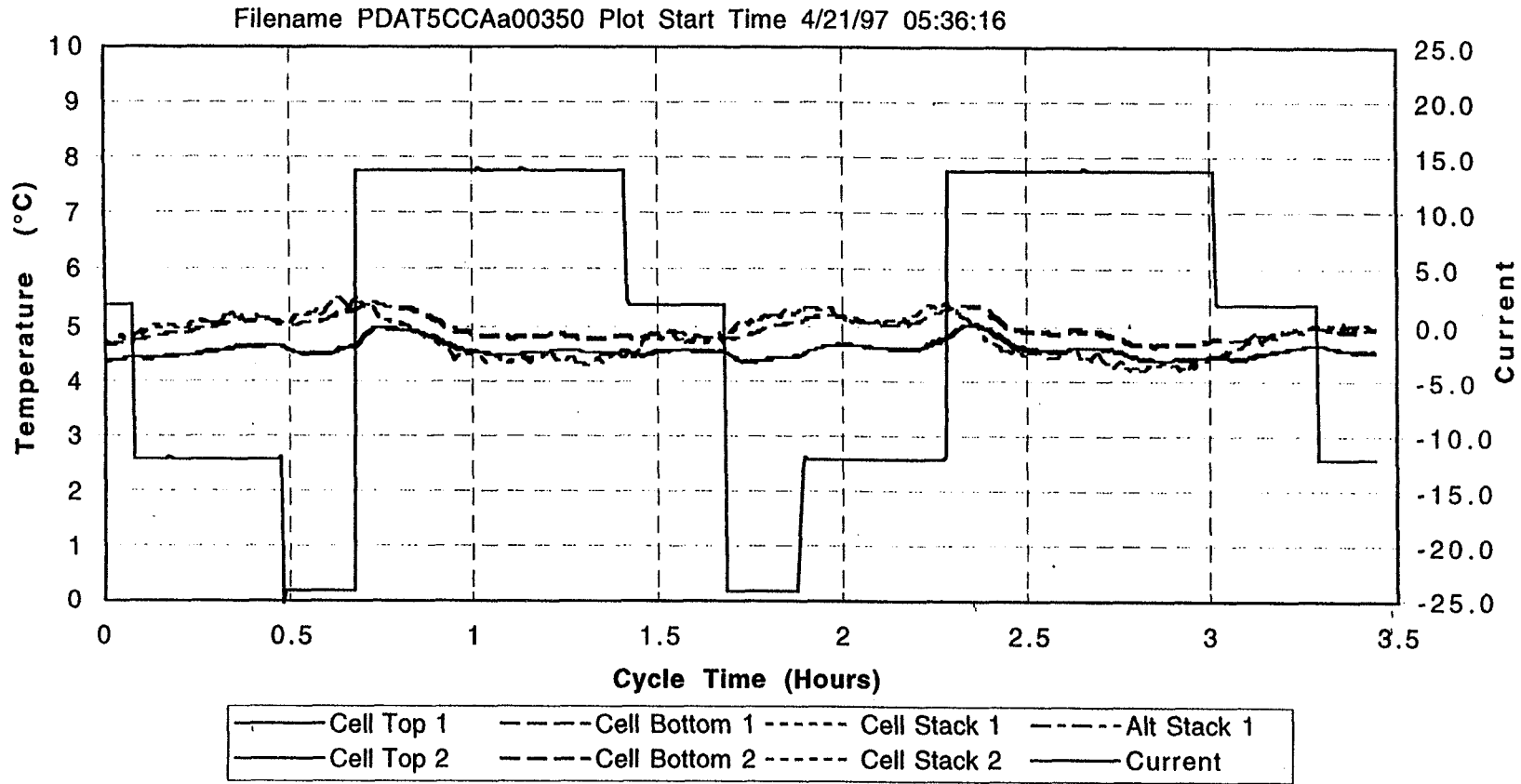


Figure 20. RNH-90-9 Condition X46

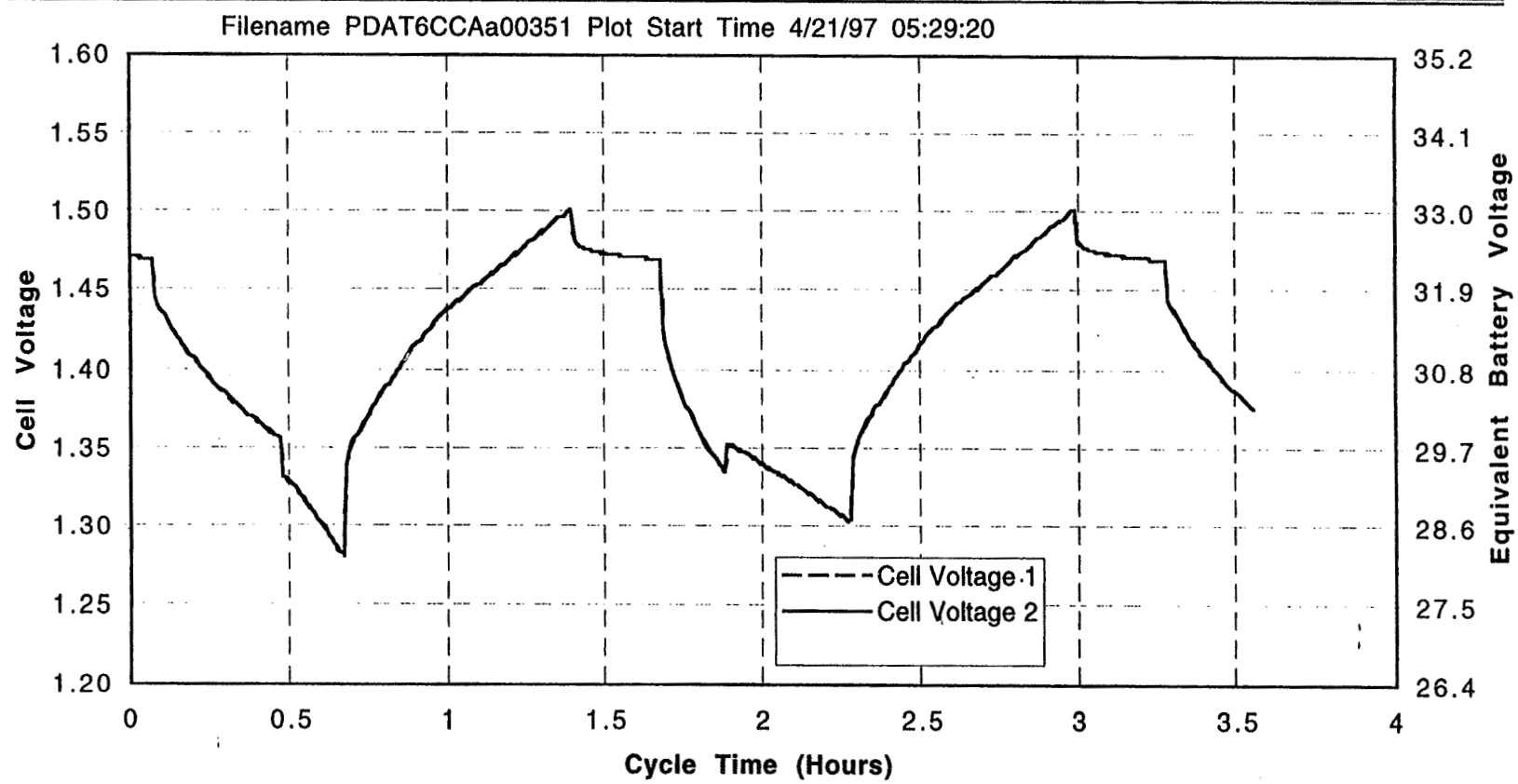
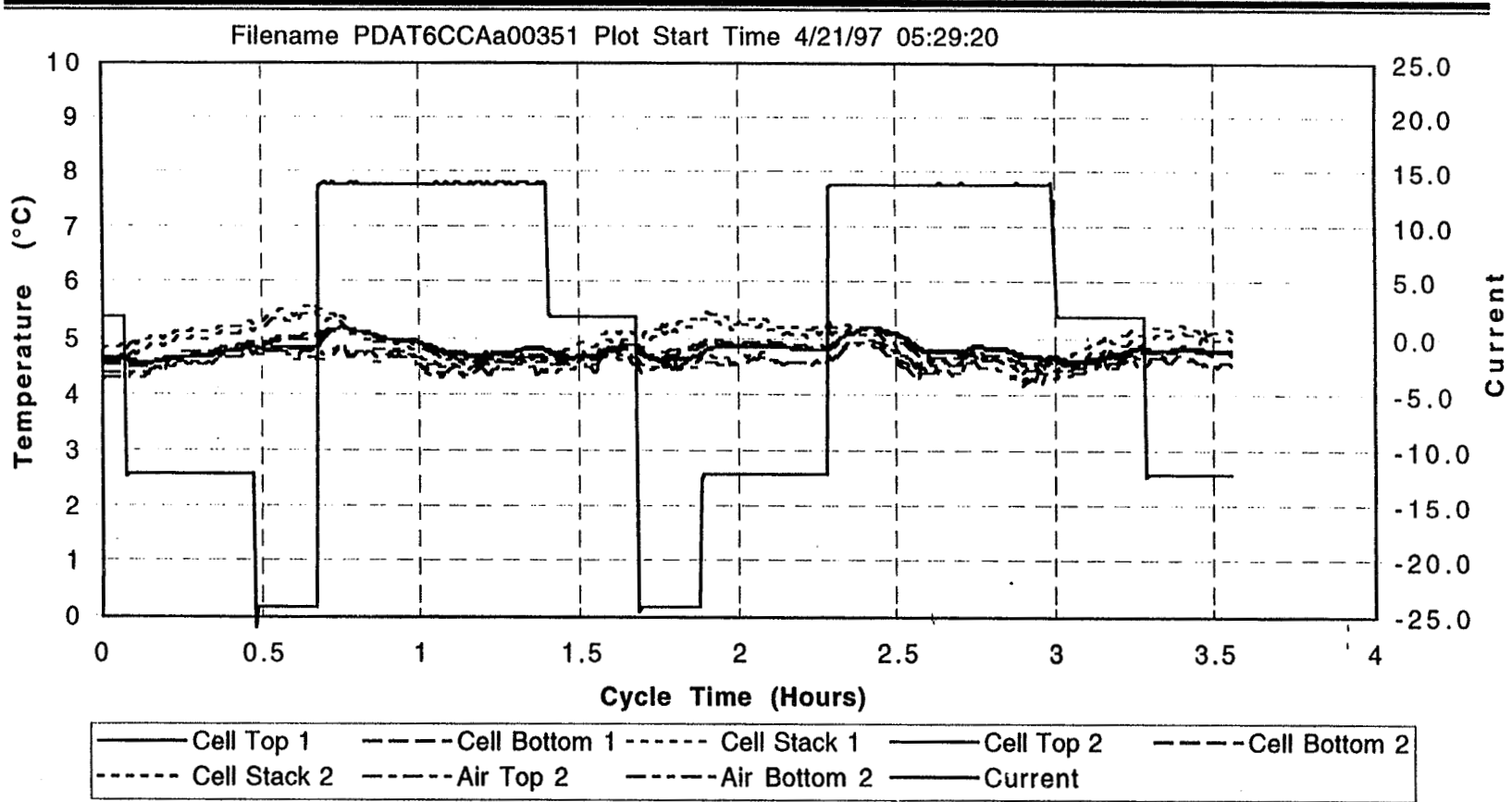


Figure 21. RNH-90-9 Condition X46



CONCLUSIONS

- CELLS WITH SLURRY ELECTRODES HAVE SLIGHTLY HIGHER THERMAL DISSIPATION THAN DRY SINTER CELLS FOR CONDITIONS TESTED.
- SLURRY ELECTRODE CELLS HAVE LOWER RELATIVE OPERATING CAPACITY TO 1.2 V AND 1.1 V AT LOWER TEMPERATURES FOR V/T LEVELS 3 AND 4.
- THERE WAS A DRAMATIC EFFECT OF CHARGE CUTOFF VOLTAGE ON HEAT DISSIPATION AT HIGHER OPERATING TEMPERATURES.
- HST ONBOARD BATTERY MANAGEMENT SINCE NOVEMBER 1995 SHOWS IMPROVEMENT IN CAPACITY REQUIRING FURTHER TREND ANALYSIS.
 - LONG TERM CAPACITY LOSSES ATTRIBUTED TO PREMATURE CHARGE CUTOFF AT LOWER VT LEVEL (KIL4) TO LIMIT BATTERY HEAT DISSIPATION.
 - OPERATION AT LOWER TEMPERATURES AFTER SWITCHING FROM PRIMARY TO SECONDARY HEATERS HAVE INDICATED IMPROVEMENTS IN BATTERY CHARGE EFFICIENCIES AND PERFORMANCE.

Advanced Ni-H₂ / Nickel Electrode Session

Page intentionally left blank

EAGLE P ICHER

**SAR10085/10083
BATTERY PRESENTATION**

LANDER AND ORBITER BATTERY

**PRESENTED BY
WILLIAM COOK
EAGLE P ICHER INC.**



SAR10085/10083 BATTERY PRESENTATION

PRESENTATION OUTLINE

- PROGRAM OVERVIEW
- TWO CELL CPV DESIGN SUMMARY
- CPV PERFORMANCE SUMMARY
- BATTERY DESIGN SUMMARY "LANDER"
- BATTERY DESIGN SUMMARY "ORBITER"
- BATTERY PERFORMANCE SUMMARY
- QUESTIONS AND ANSWERS

MSP PROGRAM OVERVIEW

- **EXTREMELY TIGHT COST CONSTRAINT**
- **USE PROVEN DESIGN WHEREVER POSSIBLE**
- **TWO SATELLITE DEVELOPMENT**
- **LANDER (11) CPV/ (1) IPV DESIGN**
- **ORBITER (11) CPV DESIGN**

ref. AVIATION WEEK & SPACE TECHNOLOGY 12/9/96:

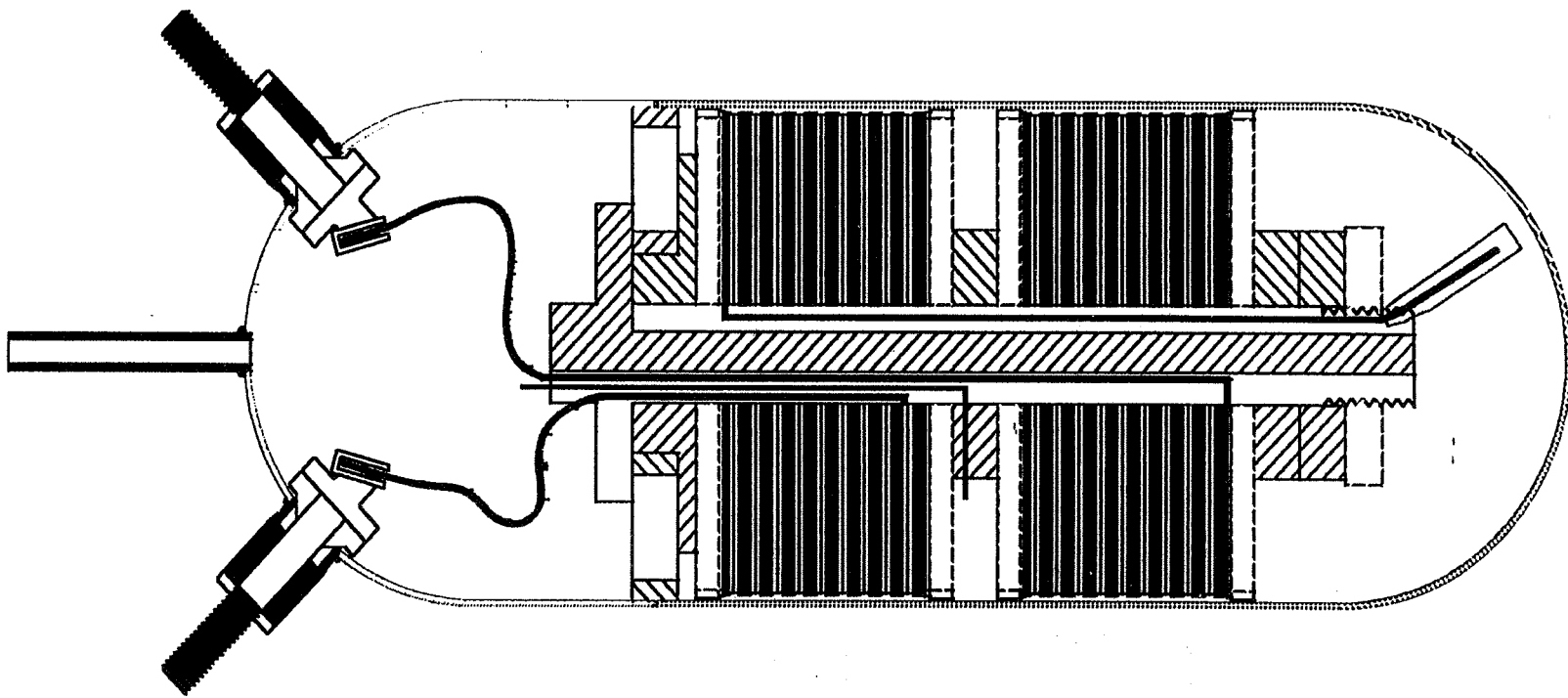
Common Pressure Vessel Flight History

- Salt (Interspace Navy)
- Apex (Orbital Sciences)
- SeaStar (Orbital Sciences)
- Orbcomm (Orbital Sciences)
- MSTI-2 (Spectrum Astro)
- MSTI-3 (Spectrum Astro)
- Tubsat-B (Technical Univ. of Berlin)
- Tubsat-C (Technical Univ. of Berlin)

EAGLE EPICHER

SAR10085/10083 BATTERY PRESENTATION

RNHC-16-1





SAR10085/10083 BATTERY PRESENTATION

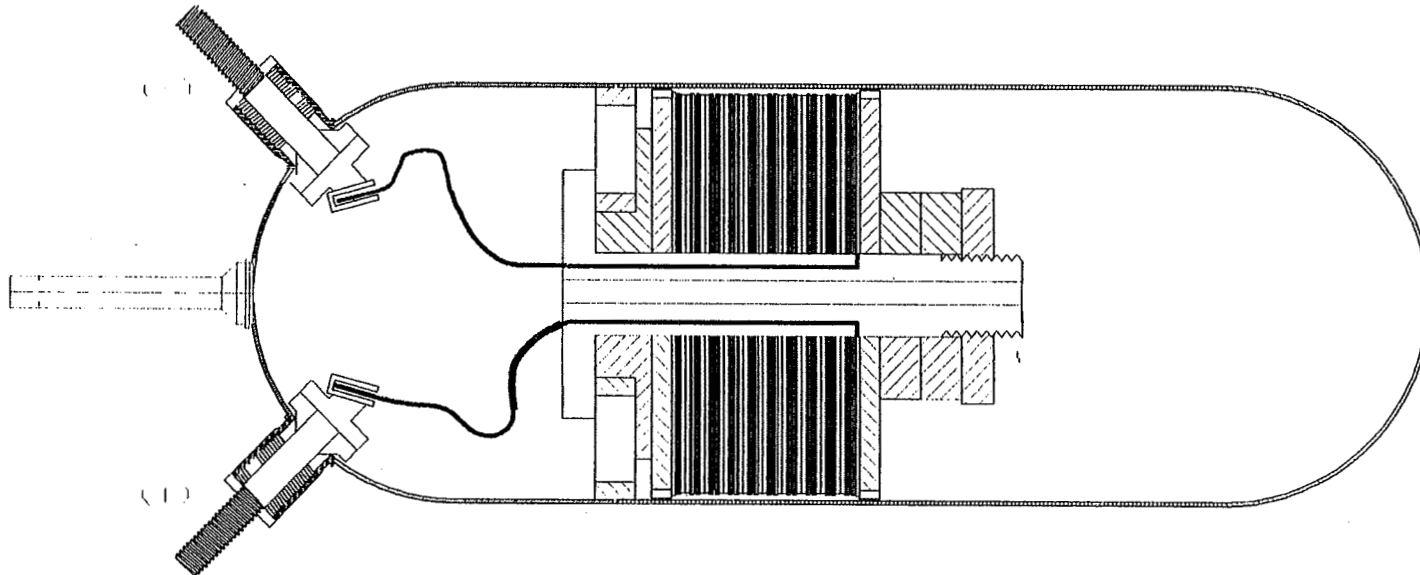
RNHC 16-1 SPECIFICATION

•Terminal Type(10/32 thread)	Rabbit Ear
•Nominal Capacity 10°C	17.5 AH
•Pressure Vessel Length	9.00in (22.86)
•Pressure Vessel Diameter	2.53in (6.43)
•Pressure Vessel Material	Inconel)
•Separator Material	Zircar
•Cell Weight (Nominal)	950 g
•Electrolyte Concentration	31%
•MEOP	800 PSIG
•Specific Energy Wh/lb	21.03 (46.39)
•Safety Factor	3.0:1

EAGLE EPICHER

SAR10085/10083 BATTERY PRESENTATION

RNH 16-3 CELL DESIGN





SAR10085/10083 BATTERY PRESENTATION

Cell Performance Specification RNH-16-3

•Terminal Type(10/32 thread)	Rabbit Ear
•Nominal Capacity 10°C	17.5 AH
•Pressure Vessel Length	9.00 in (22.86)
•Pressure Vessel Diameter	2.53 in (6.43)
•Pressure Vessel Material	Inconel
•Separator Material	Zircar
•Cell Weight (Nominal)	606 g
•Electrolyte Concentration	31%
•MEOP	400 PSIG
•Specific Energy Wh/lb	16.38 (36.09)
•Safety Factor	3.0:1



SAR10085/10083 BATTERY PRESENTATION

RNHC 16-1 TEST RESULTS

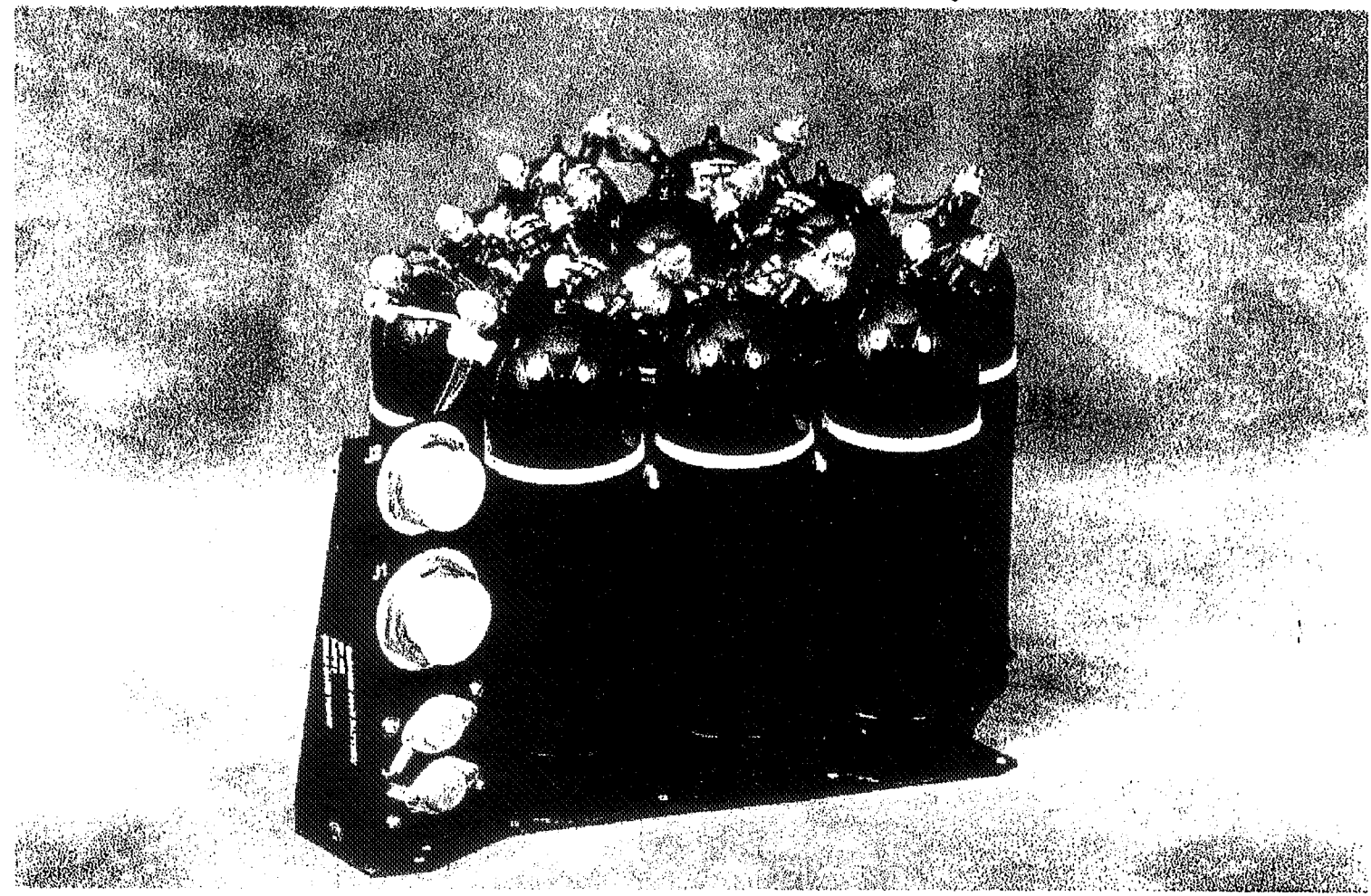
<u>TEST</u>	<u>MINIMUM</u>	<u>MAXIMUM</u>	<u>AVERAGE</u>
-10°C Ah to 2.0v	18.99	19.50	19.24
-5°C AH to 2.0V	19.20	19.87	19.57
0°C AH to 2.0V	19.22	19.86	19.53
CHARGE RET	82%	86%	85%
10°C AH to 2.0v	17.17	17.86	17.58
20°C AH to 2.0V	15.03	15.60	15.31
25°C AH to 2.0V	14.53	14.95	14.74
35°C AH to 2.0V	10.92	11.37	11.19
IMPEDANCE mOHMS	7	8	7

SINE VIBRATION, RANDOM VIBRATION, PYRO-SHOCK (all passed)

EAGLE P P ICHER

SAR10085/10083 BATTERY PRESENTATION

SAR 10085 Lander Battery



**SAR10085/10083
BATTERY PRESENTATION**

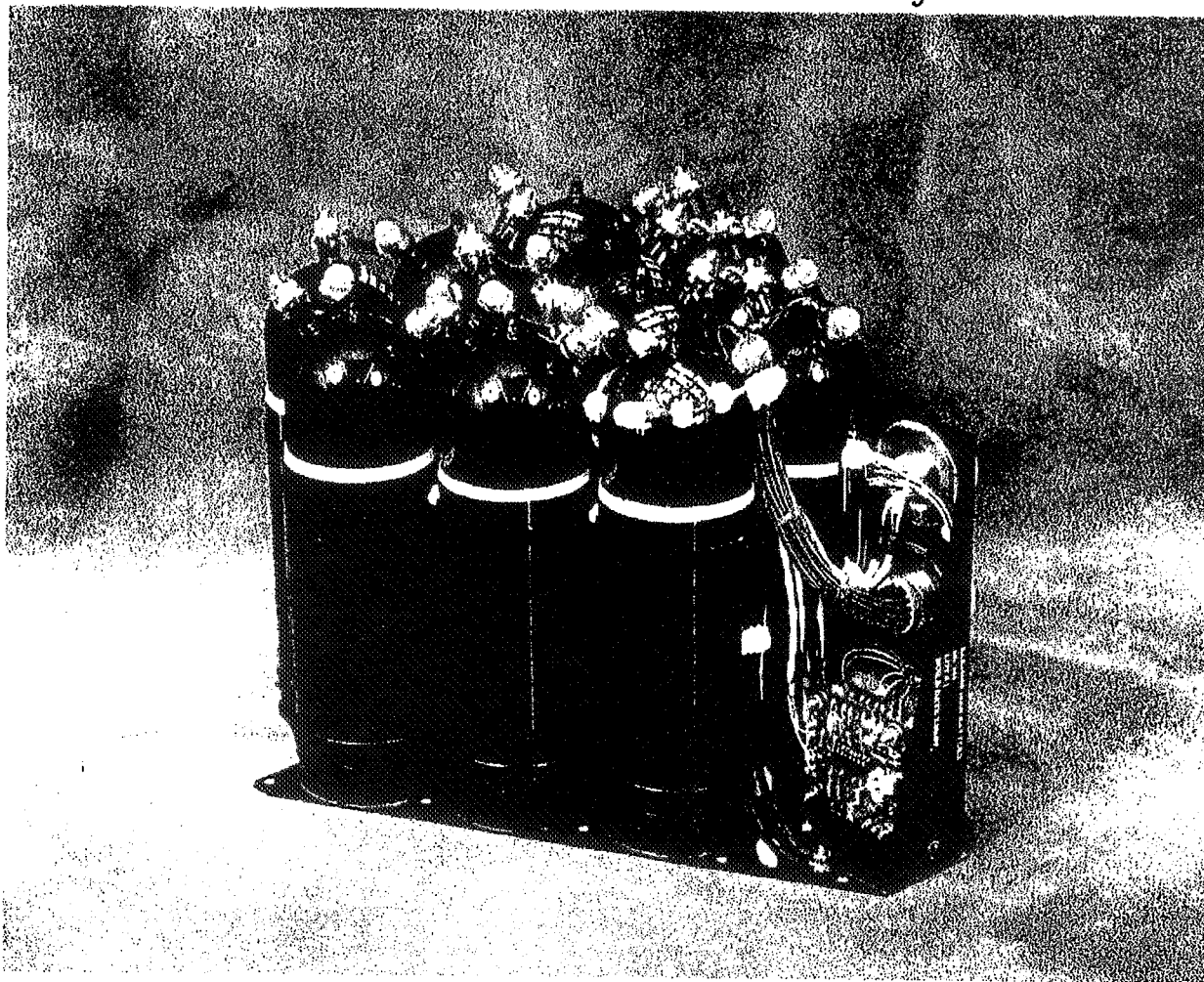
LANDER UNIQUE FEATURES

- **UTILIZES IPV AND CPV COMBINATION**
- **SIMPLE CONSTRUCTION**
- **FOUR TRANSDUCER TEMPERATURE CONTROL**
- **0.080 THICK 7075-T6 ALUM BASE PLATE**
- **COFFEE CAN SLEEVE DESIGN**
- **VOLTAGE REGULATOR FOR ELECTRONIC**
- **STRAIN GAGE AMPLIFICATION 1-5VDC**

EAGLE EPICHER

SAR10085/10083 BATTERY PRESENTATION

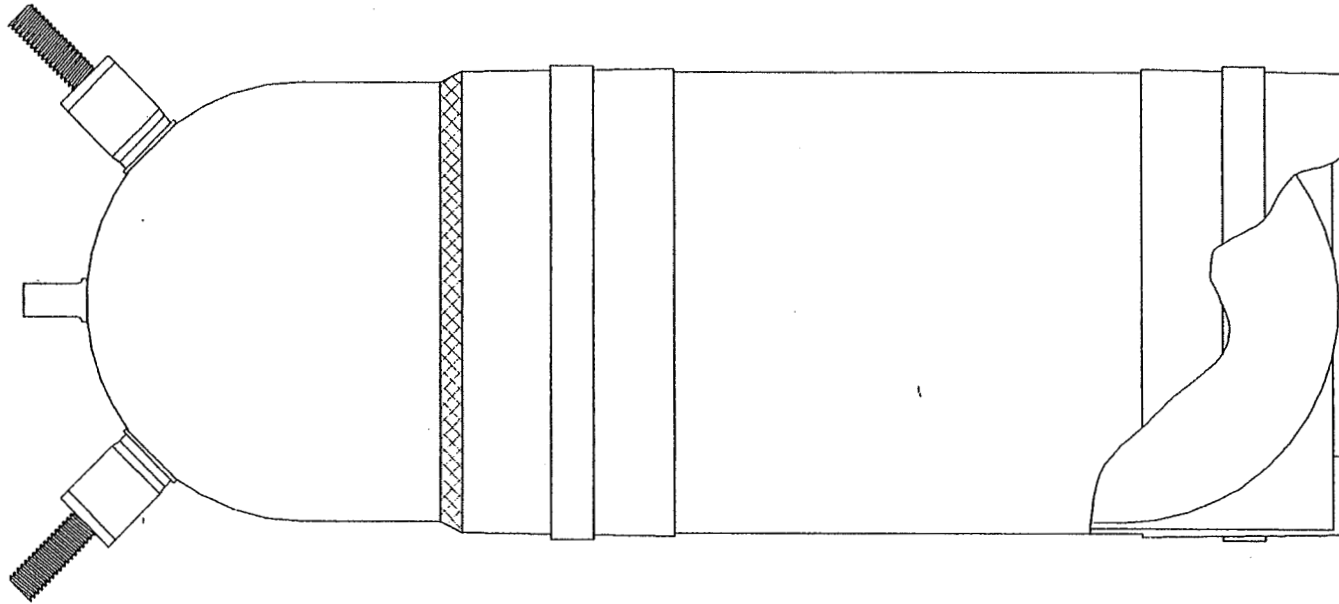
SAR 10085 Lander Battery



EAGLE EPICHER

SAR10085/10083 BATTERY PRESENTATION

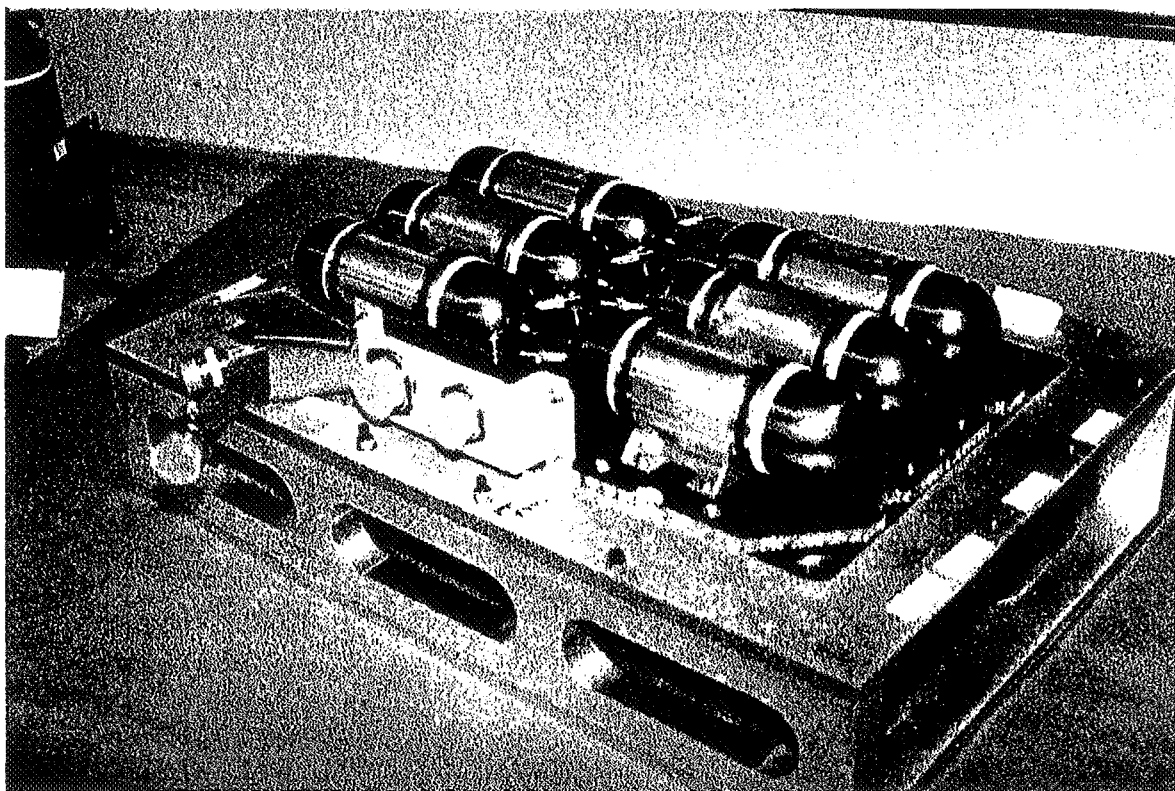
LANDER / SLEEVE ASSEMBLY





SAR10085/10083 BATTERY PRESENTATION

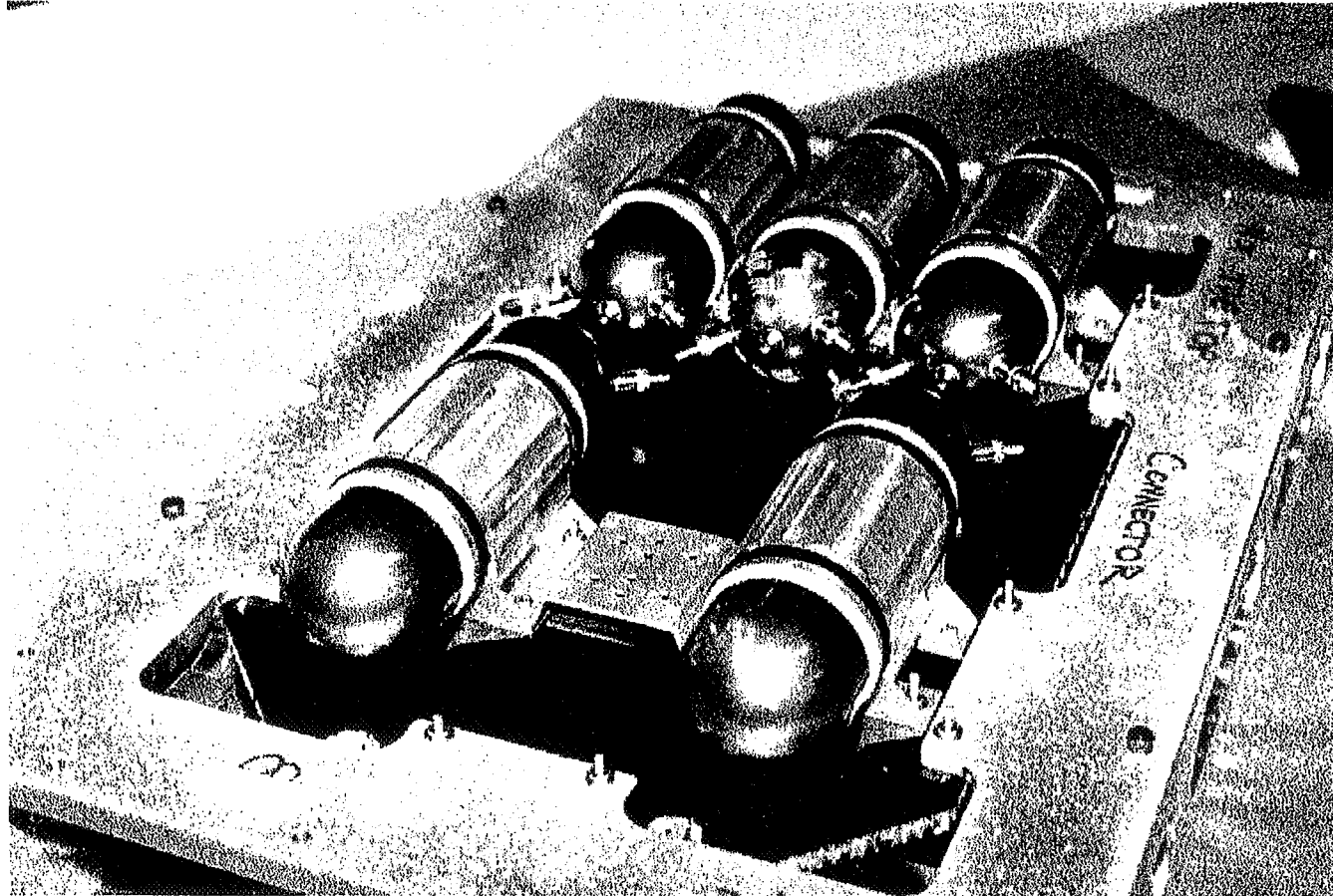
SAR10083 ORBITER BATTERY



EAGLE EPICHER

SAR10085/10083 BATTERY PRESENTATION

SAR10083 BATTERY ASSEMBLY



NASA BATTERY WORKSHOP 1997



SAR10085/10083 BATTERY PRESENTATION

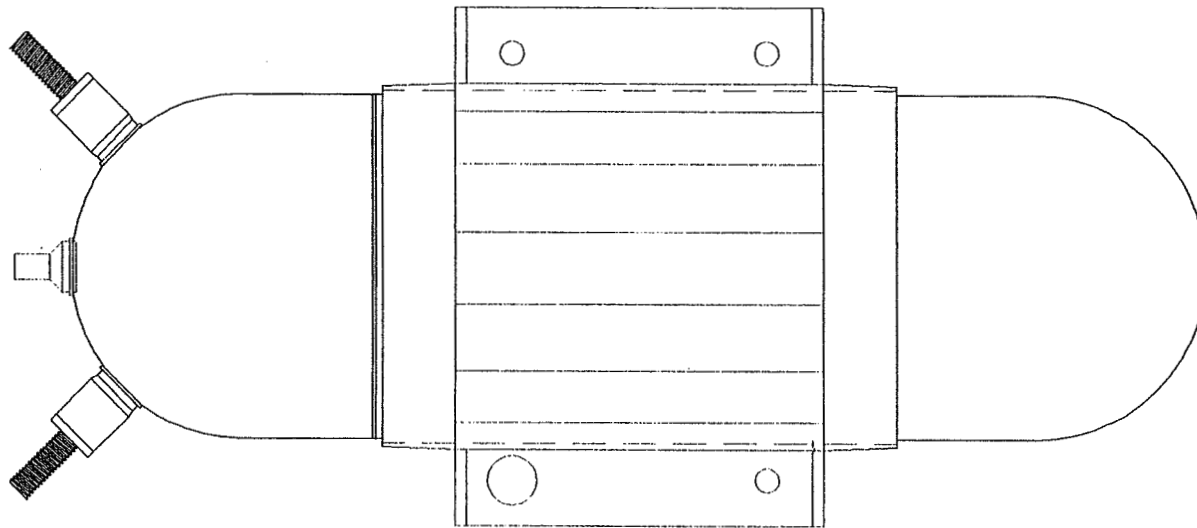
ORBITER UNIQUE FEATURES

- HONEYCOMB BASEPLATE DESIGN
- SIMPLE CONSTRUCTION
- FOUR TRANSDUCER TEMPERATURE CONTROL
- HORIZONTAL MOUNT SLEEVE DESIGN
- VOLTAGE REGULATOR FOR ELECTRONIC
- STRAIN GAGE AMPLIFICATION 1-5VDC

EAGLE EPICHER

SAR10085/10083 BATTERY PRESENTATION

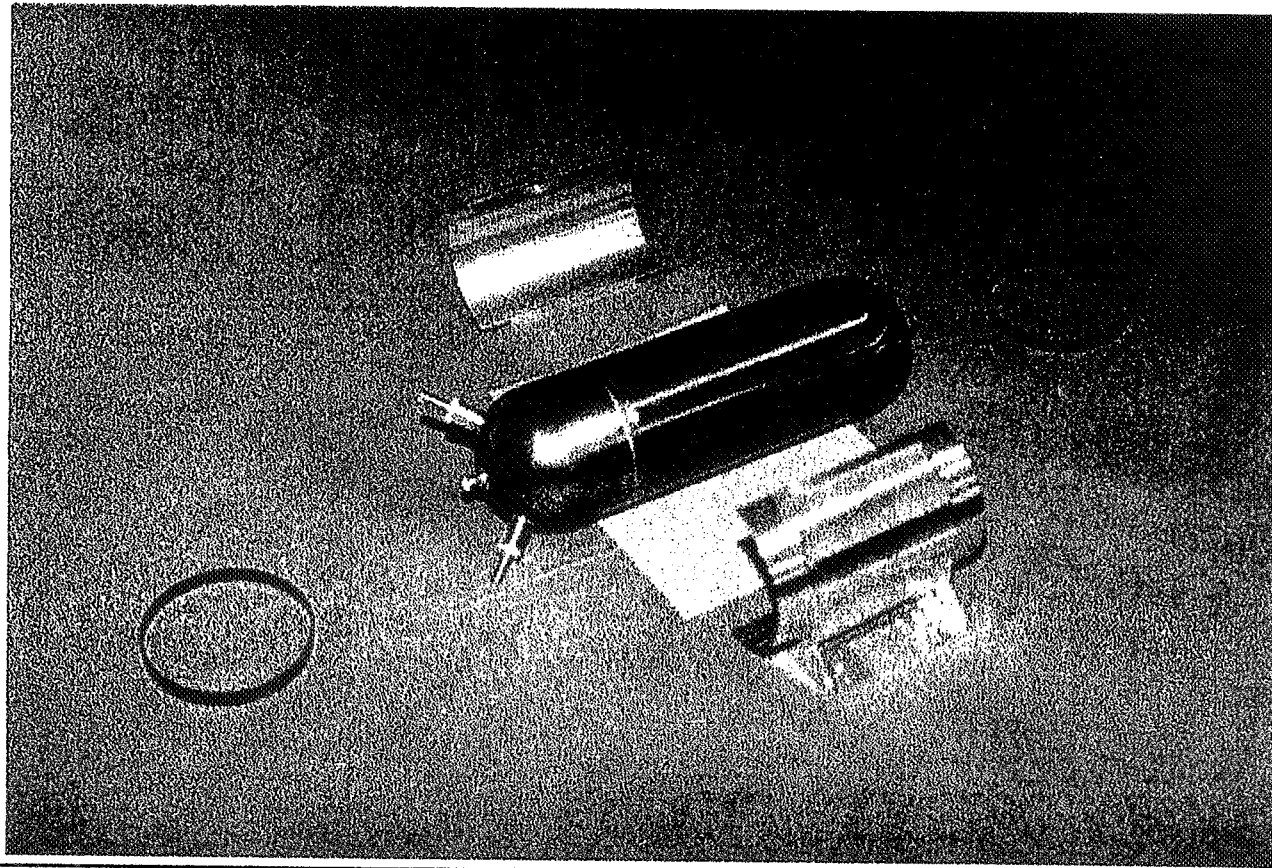
ORBITER CELL/SLEEVE ASSEMBLY



EAGLE EPICHER

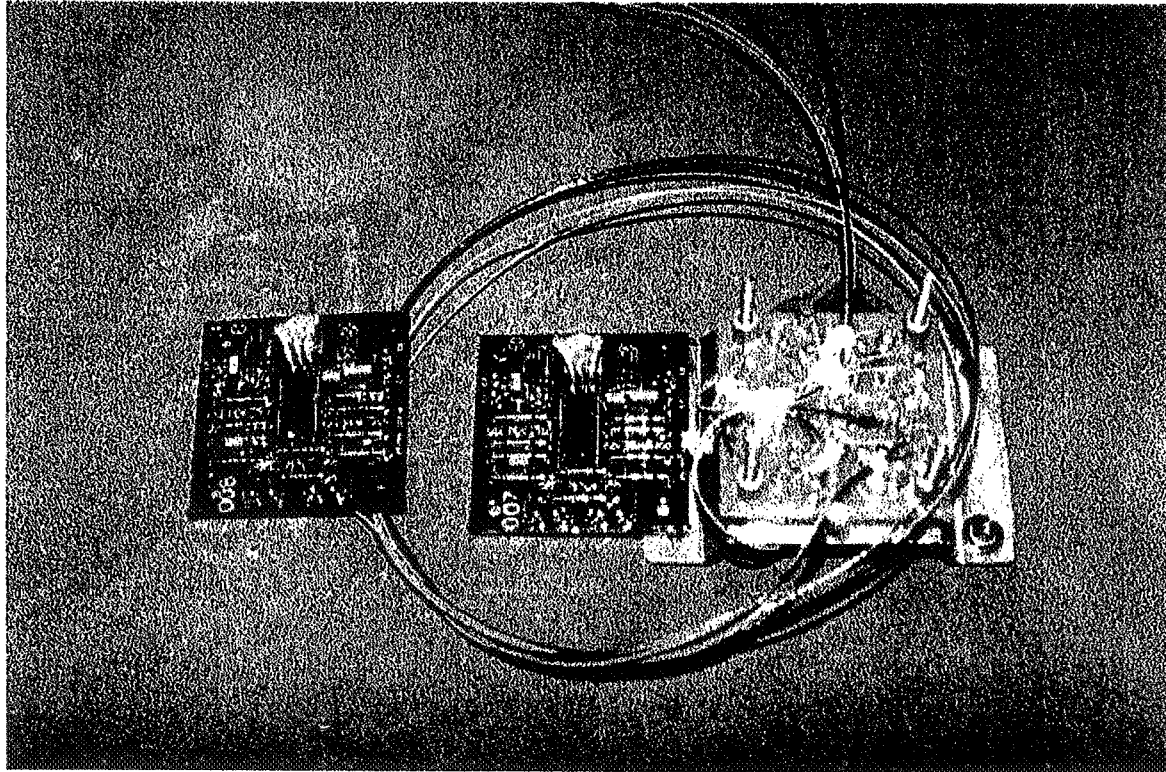
SAR10085/10083 BATTERY PRESENTATION

SAR10083 SLEEVE ASSEMBLY



SAR10085/10083 BATTERY PRESENTATION

ELECTRONICS ASSEMBLY



EAGLE EPICHER

**SAR10085/10083
BATTERY PRESENTATION**

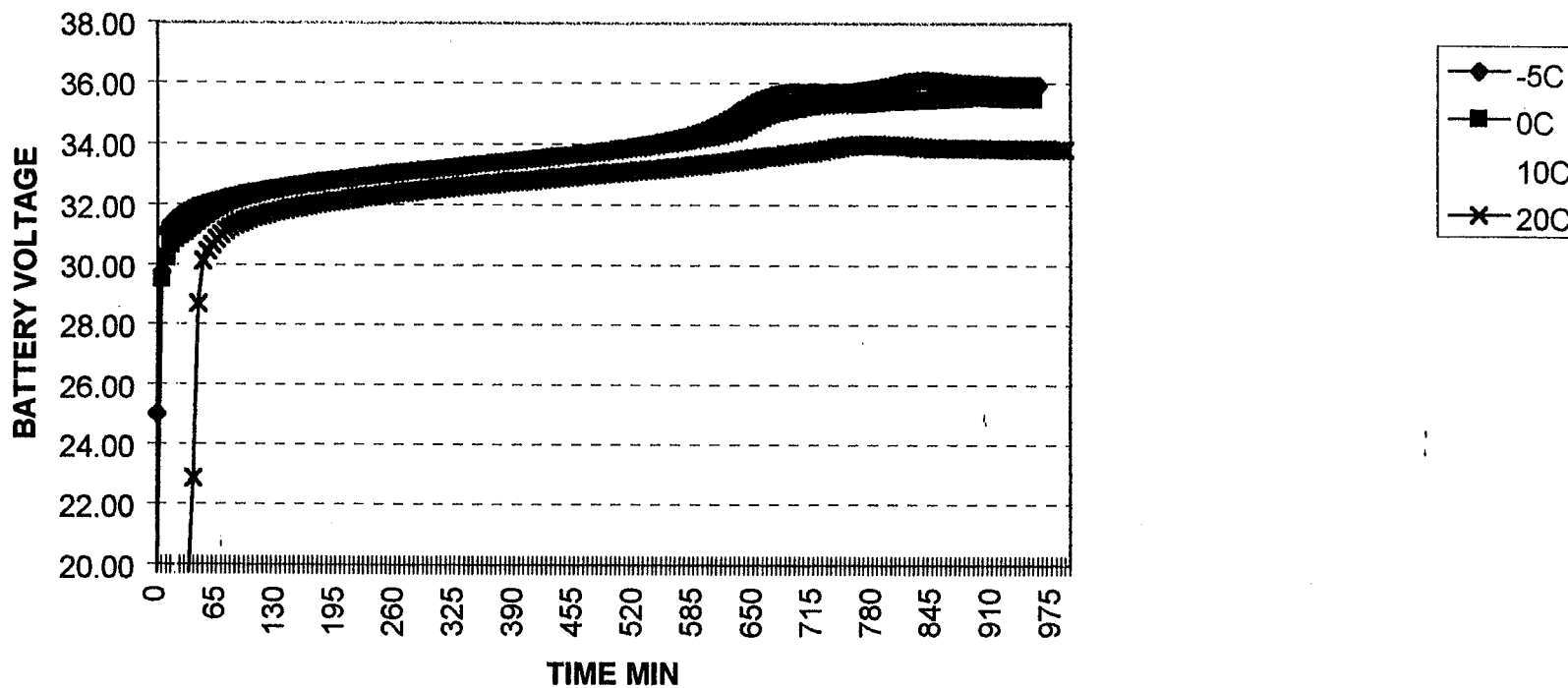
BATTERY PERFORMANCE SUMMARY

**LANDER
BATTERY**



SAR10085/10083 BATTERY PRESENTATION

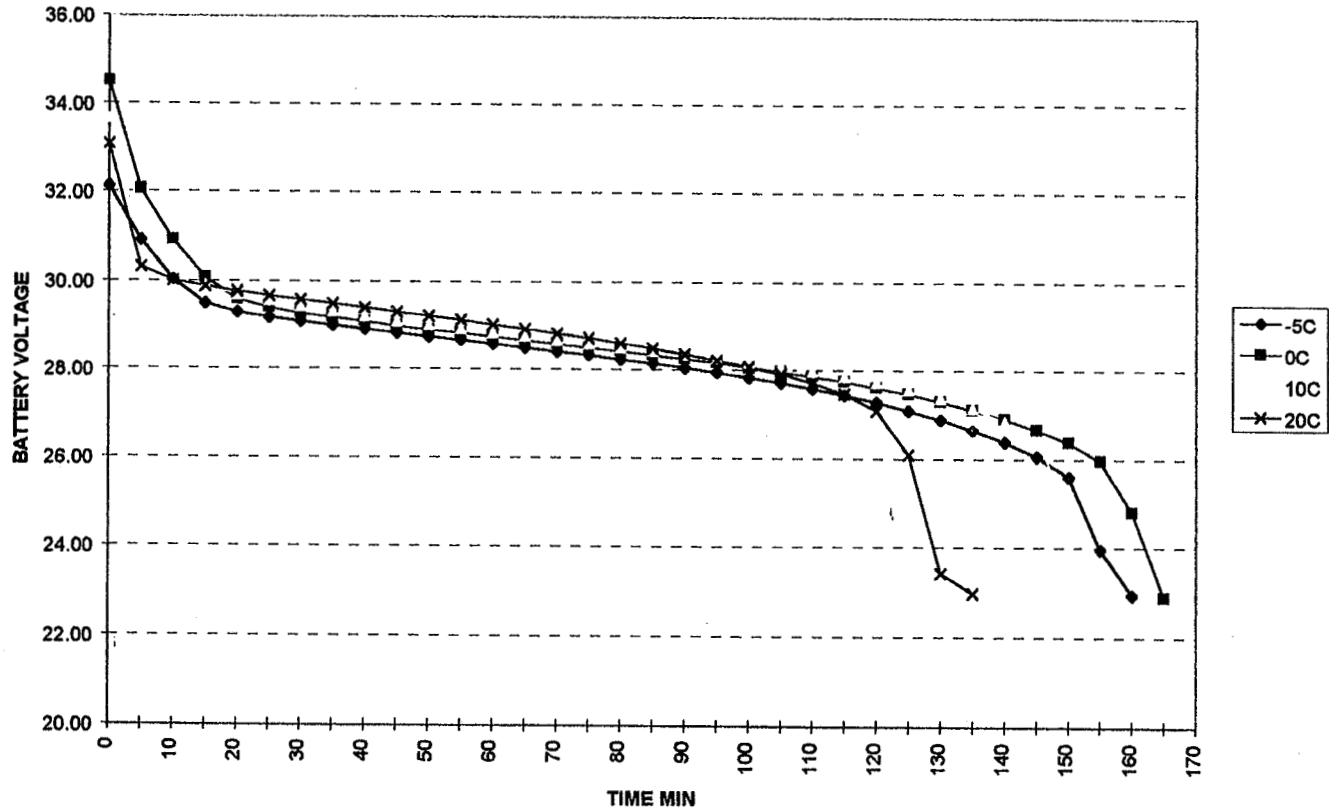
SAR10085 CHARGE VOLTAGE VS TEMP





SAR10085/10083 BATTERY PRESENTATION

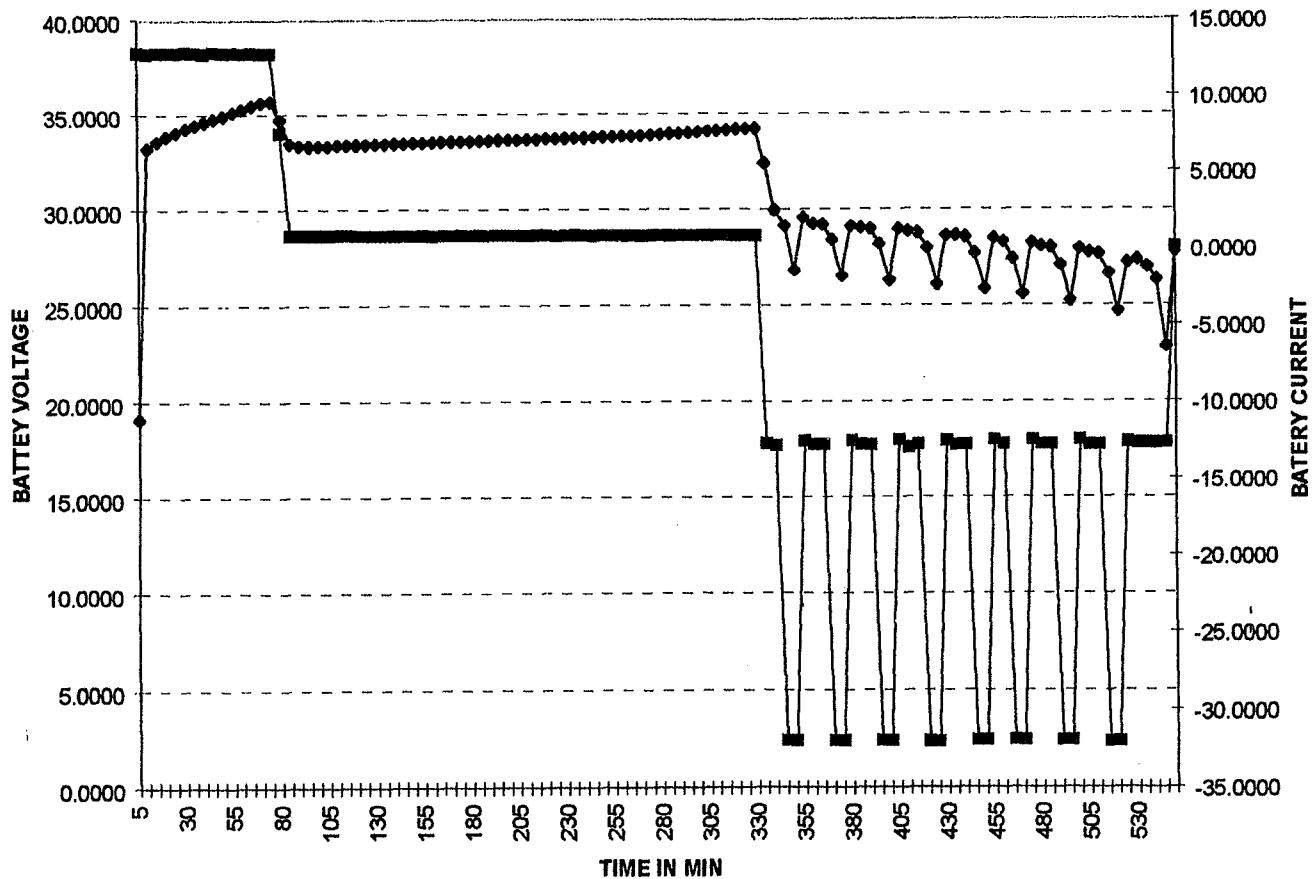
SAR10085 DISCHARGE VS TEMP
C/2 DISCHARGE TO 23 VOLTS





SAR10085/10083 BATTERY PRESENTATION

SAR10085 BATTERY HIGH RATE TEST





**SAR10085/10083
BATTERY PRESENTATION**

QUESTIONS AND ANSWERS

IRIDIUM® Satellite Batteries: Flight Observations “By the Dozen”

**PRESENTED TO:
1997 NASA BATTERY WORKSHOP
NOVEMBER 18 - 20, 1997**

**BY:
MARK R. TOFT
MOTOROLA SPACE SYSTEMS TECHNOLOGY
GROUP**

IRIDIUM is a registered trademark and service mark of IRIDIUM LLC © 1997

MOTOROLA SPACE SYSTEMS TECHNOLOGY GROUP

IRIDIUM SATELLITE BATTERY OVERVIEW

- **AS OF NOVEMBER 15, 1997 - 39 IRIDIUM SPACE VEHICLES HAVE BEEN LAUNCHED:**
 - **LOCKHEED BUS DESIGN**
 - **EACH SPACE VEHICLE CONTAINS A SINGLE PRESSURE VESSEL NICKEL-HYDROGEN BATTERY**
 - **BATTERIES MANUFACTURED BY EAGLE-PICHER, IND. JOPLIN, MO**
 - **SOLAR ARRAY PROVIDES ENERGY BY SWITCHING INDIVIDUAL STRINGS ON AND OFF**
- **SPACE VEHICLES IN 86.4 DEGREE ORBIT INCLINATION WITH THE BATTERIES MAINTAINED AT 0 °C WITH AN AVERAGE DEPTH-OF-DISCHARGE OF ~10% (WITHOUT TELEPHONY)**

BATTERY CHARGE CONTROL OVERVIEW

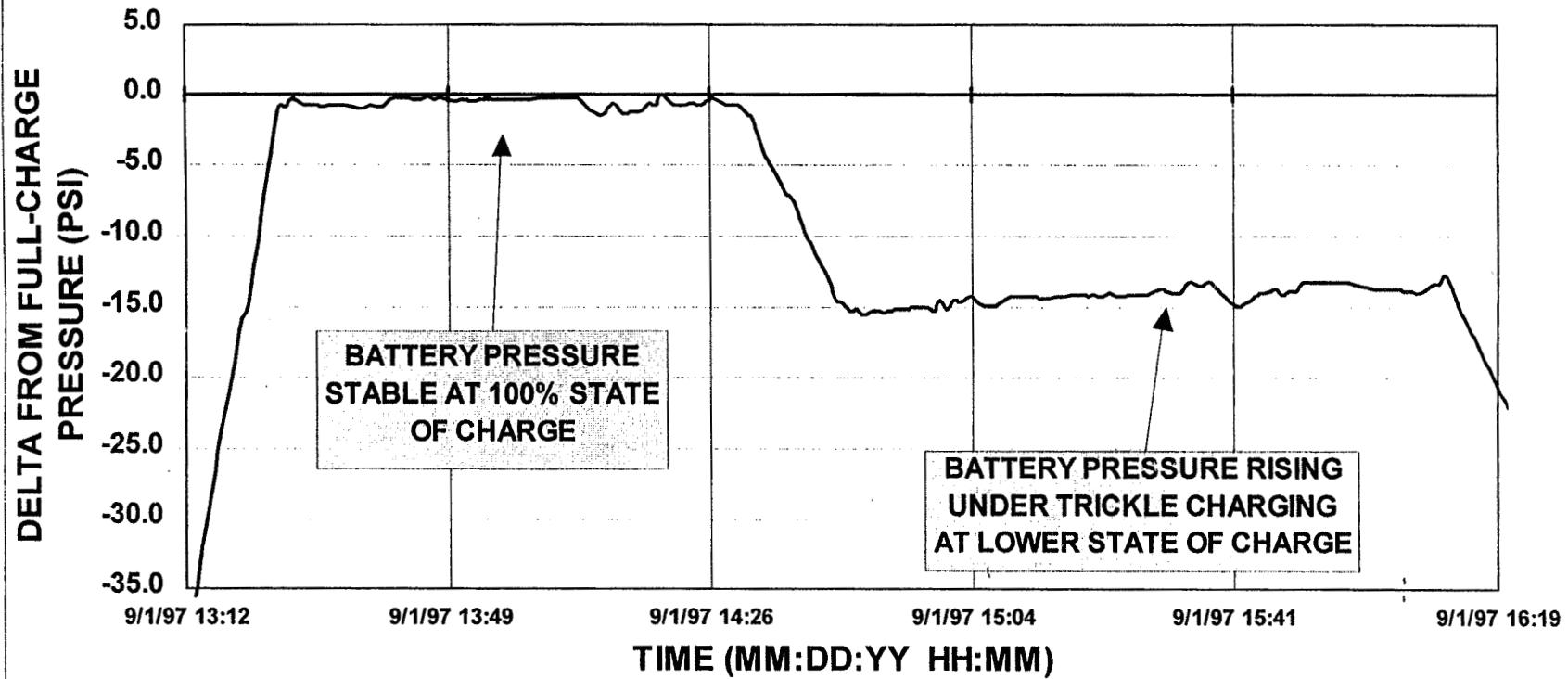
- **ON-ORBIT BATTERIES MAINTAINED AT PRESSURE LEVEL CORRESPONDING TO 85% OF FULL-CHARGE PRESSURE FROM VENDOR'S 10 DEG. C CAPACITY TEST**
- **BATTERY CHARGE MODE (FULL & TRICKLE) CAN BE CONTROLLED BY COMBINATIONS OF PRESSURE, PRESSURE SLOPE, VOLTAGE, C/D RATIO AND TEMPERATURE LIMITS**
 - **CHARGE BACK TO BATTERY-SPECIFIC PRESSURE LIMIT, AND RECHARGE RATIO (1.02) OR VOLTAGE LEVEL (~33.8V)**
 - **BATTERY REMAINS IN TRICKLE UNTIL DISCHARGE REACHES A CERTAIN THRESHOLD**
 - **PARTIALLY REDUCE STRESS BY PREVENTING FREQUENT RECHARGES AT SHALLOW DOD'S (ENTERING AND EXITING FULL-SUN)**

MOTOROLA SPACE SYSTEMS TECHNOLOGY GROUP

EXPERIENCE WITH FIRST-LAUNCH VEHICLES

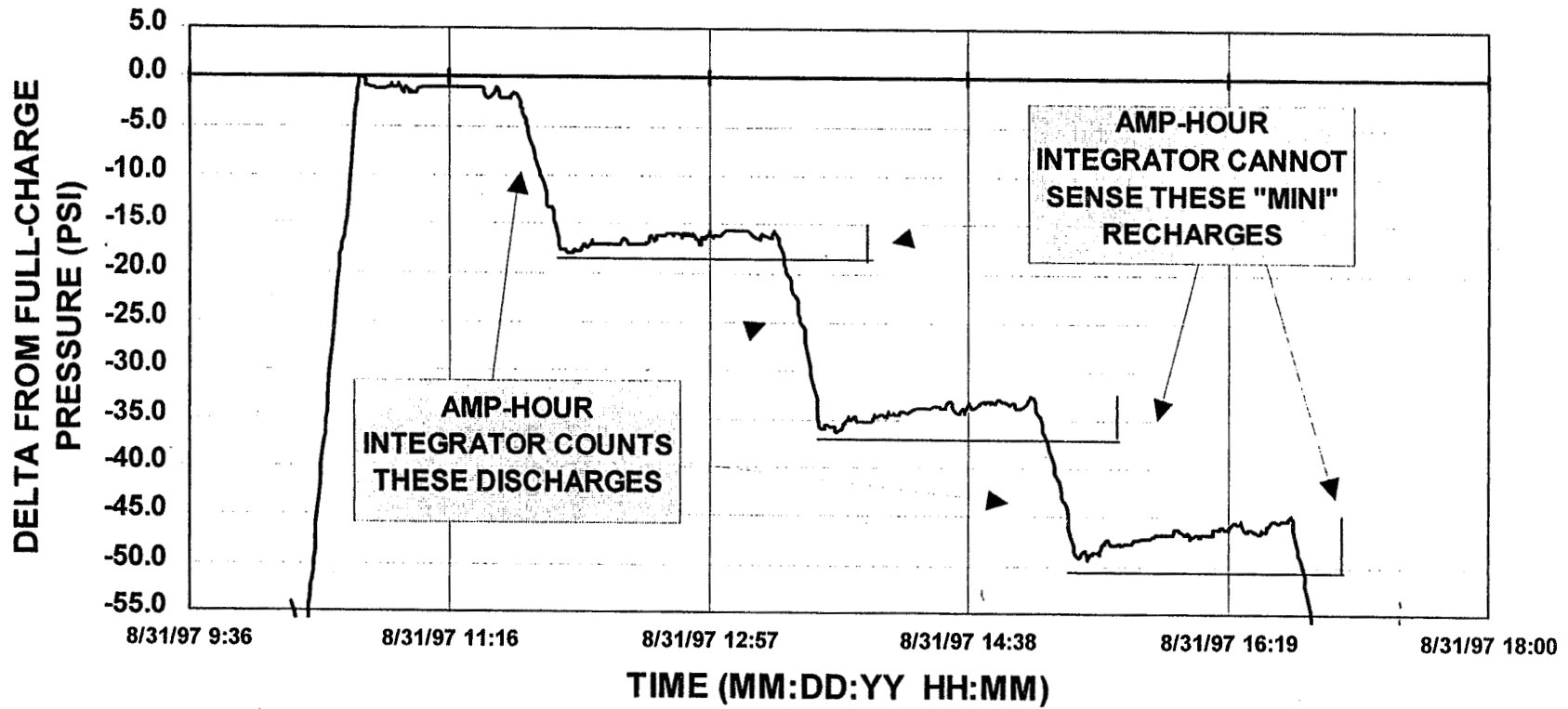
- **FIRST FIVE SV's LAUNCHED INTO FULL-SUN**
- **INITIAL TRICKLE RATE (C/100) CAUSED PRESSURE AND STATE OF CHARGE TO SLOWLY INCREASE (ABOVE DESIRED LEVELS)**
 - **TEMPERATURE PERFORMANCE STABLE UNDER THIS INITIAL TRICKLE RATE**
- **WHEN ECLIPSING BEGAN AFTER ~4 WEEKS, THIS "EFFICIENT" TRICKLE CHARGING CORRUPTED C/D RATIO CALCULATIONS AS WELL AS THE LOGIC THRESHOLDS FOR RETURNING TO FULL CHARGE**
- **TRICKLE CHARGE RATE WAS LOWERED**
 - **PRESSURE DECAYS UNDER TRICKLE AT 100% STATE-OF-CHARGE**
 - **PRESSURE MAINTAINED AT LOWER STATES-OF-CHARGE**

IRIDIUM SV005 BATTERY PRESSURE PERFORMANCE WITH C/100 TRICKLE CHARGE

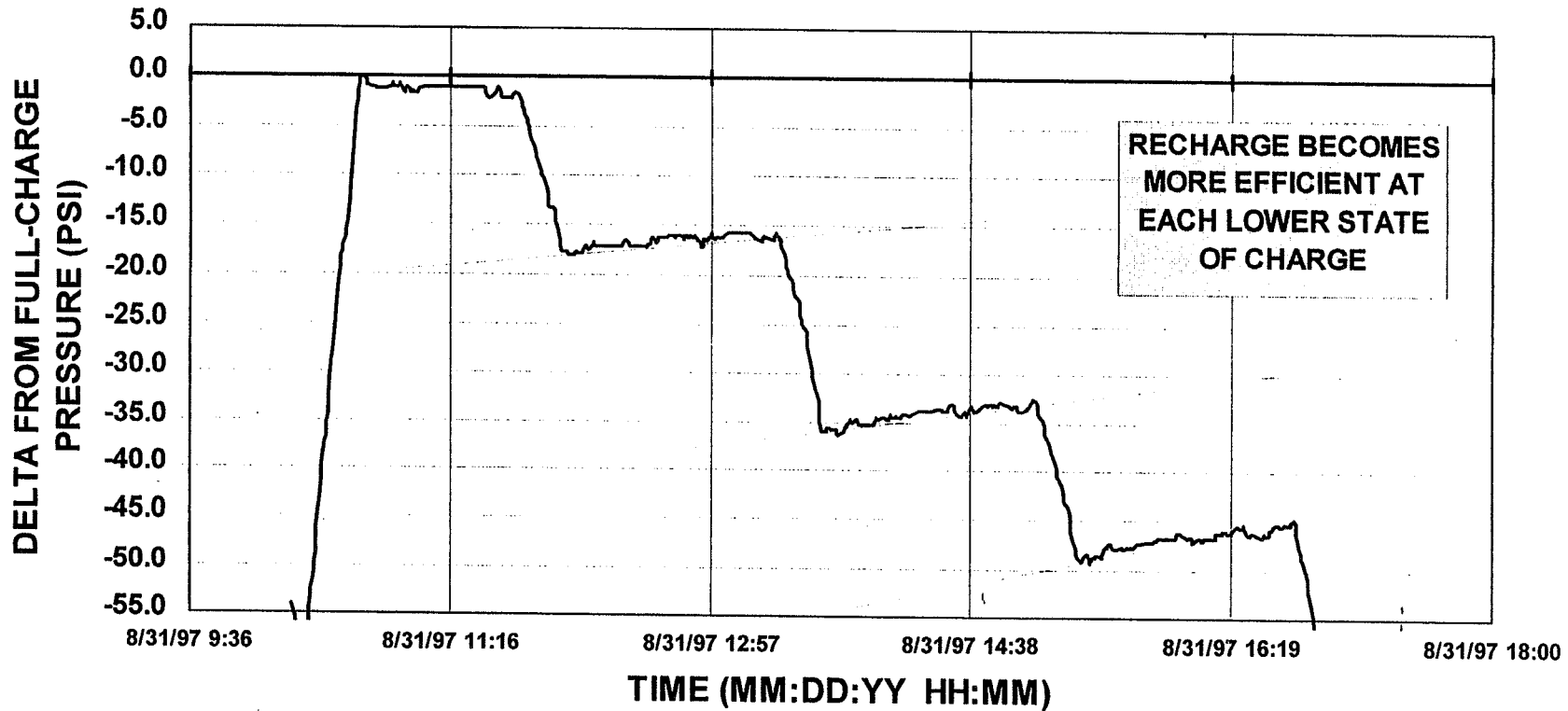


MOTOROLA SPACE SYSTEMS TECHNOLOGY GROUP

IRIDIUM SV005 BATTERY PRESSURE PERFORMANCE WITH C/100 TRICKLE CHARGE

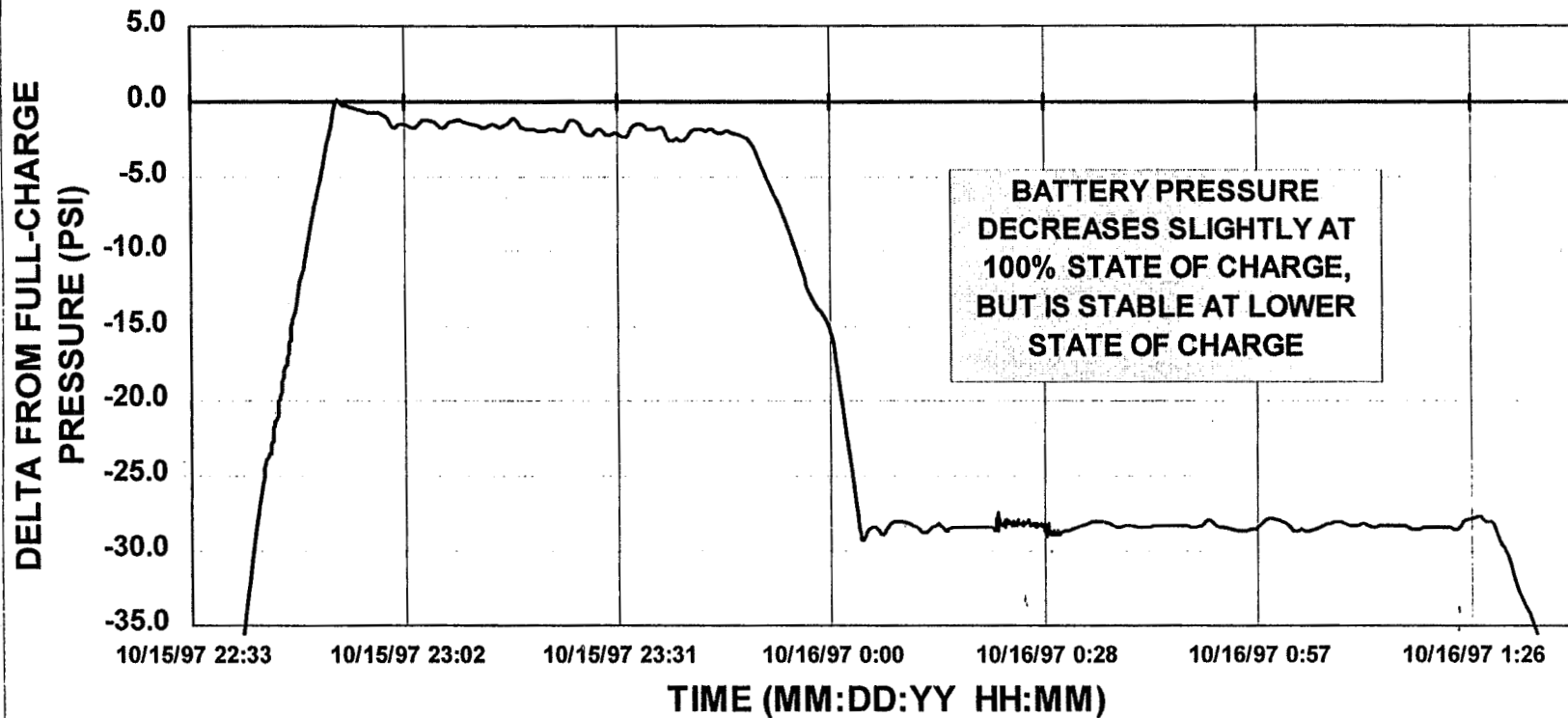


IRIDIUM SV005 BATTERY PRESSURE PERFORMANCE WITH C/100 TRICKLE CHARGE



MOTOROLA SPACE SYSTEMS TECHNOLOGY GROUP

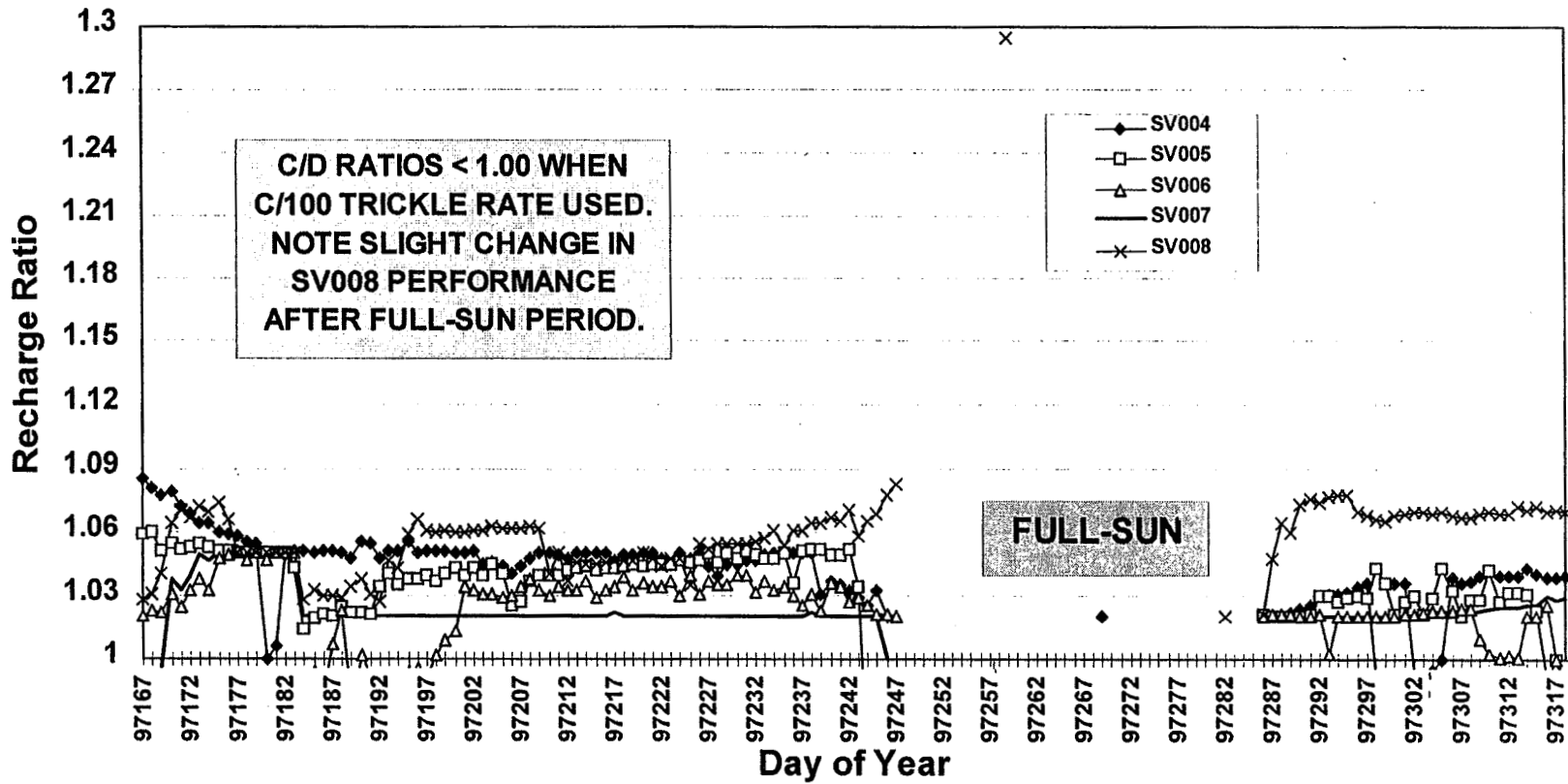
IRIDIUM SV005 BATTERY PRESSURE PERFORMANCE WITH C/250 TRICKLE CHARGE



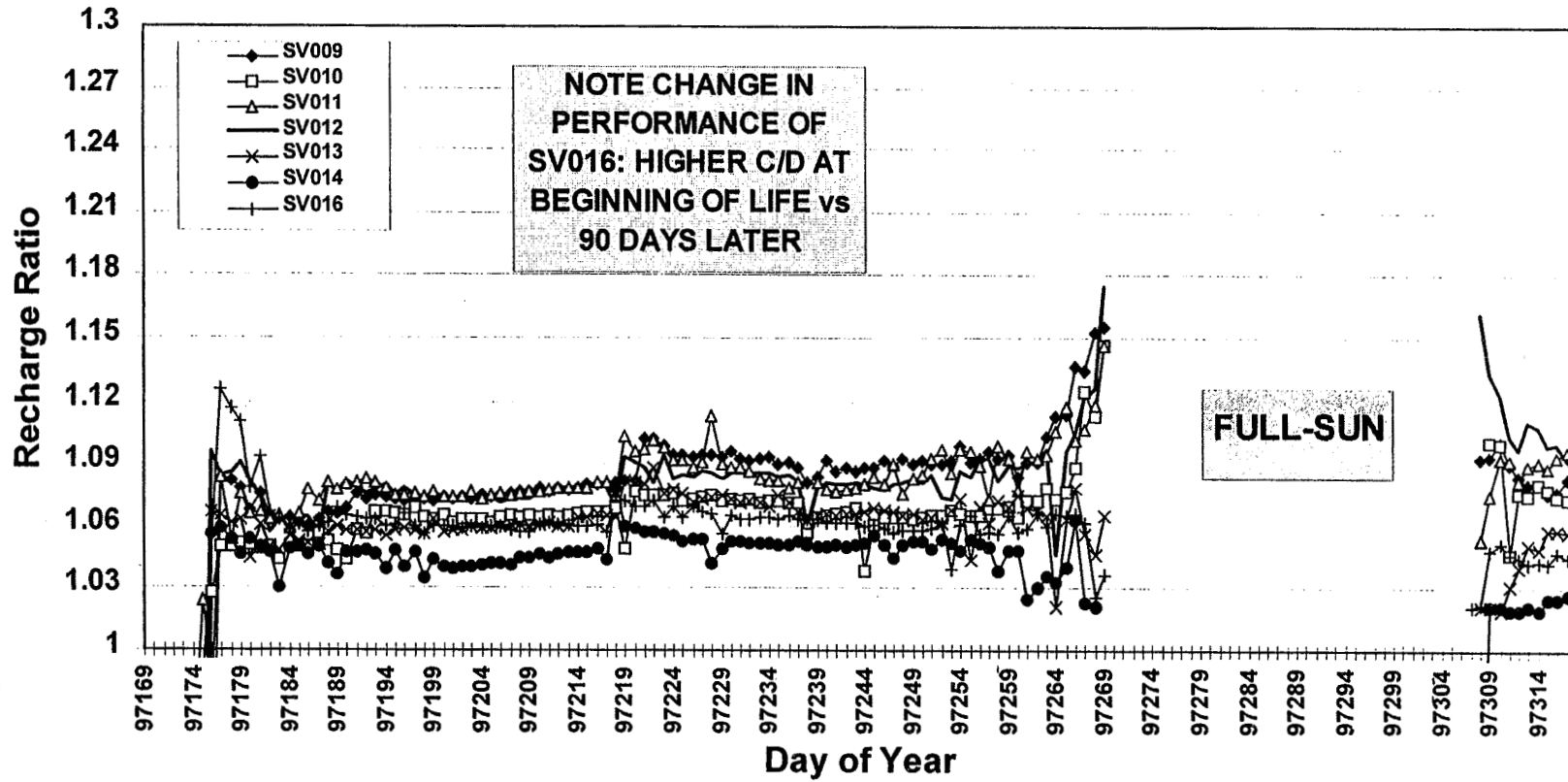
LOWER TRICKLE RATE DOES NOT ALWAYS OVERCOME BATTERY SELF-DISCHARGE

- **SUBSEQUENT SV's LAUNCHED INTO, OR THAT HAVE SINCE TRANSITIONED TO FULL-SUN OPERATIONS, HAVE BEEN AFFECTED IN DIFFERENT WAYS BY THE LOWER TRICKLE RATE**
- **VOLTAGE AND PRESSURE PERFORMANCE AFFECTED WHETHER IN FULL-SUN OR IN ECLIPSING**
 - **BATTERIES GAIN OR LOSE CHARGE AT VARIOUS RATES WHILE TRICKLING IN FULL-SUN**
 - **WILDLY VARYING C/D RATIOS FOR THOSE BATTERIES IN ECLIPSING OPERATIONS (TRICKLING BETWEEN THE END OF FULL-CHARGE AND THE BEGINNING OF ECLIPSE)**

Comparison of Battery Recharge Ratios for First Launch SV's

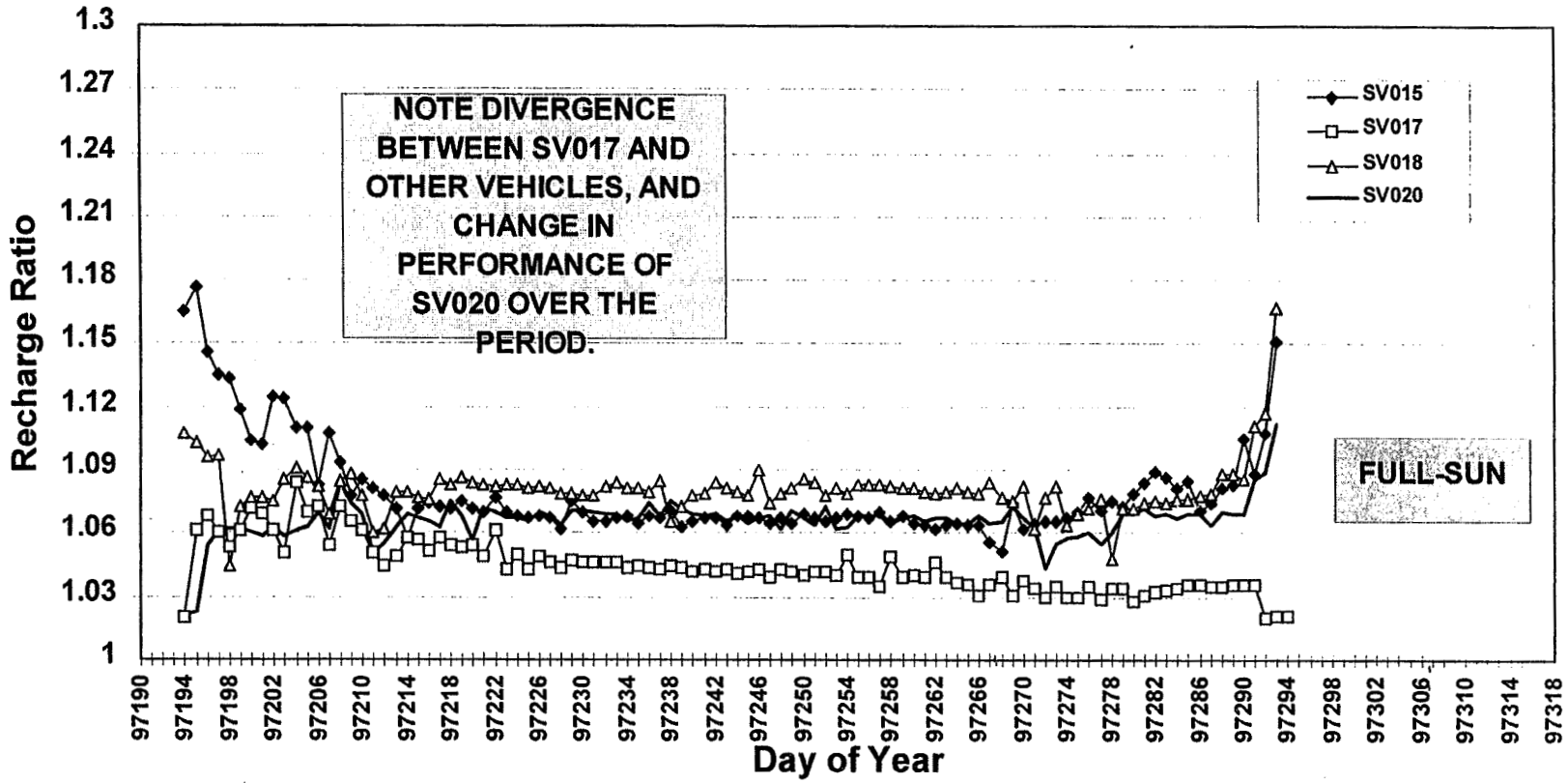


Comparison of Battery Recharge Ratios for Second Launch SV's

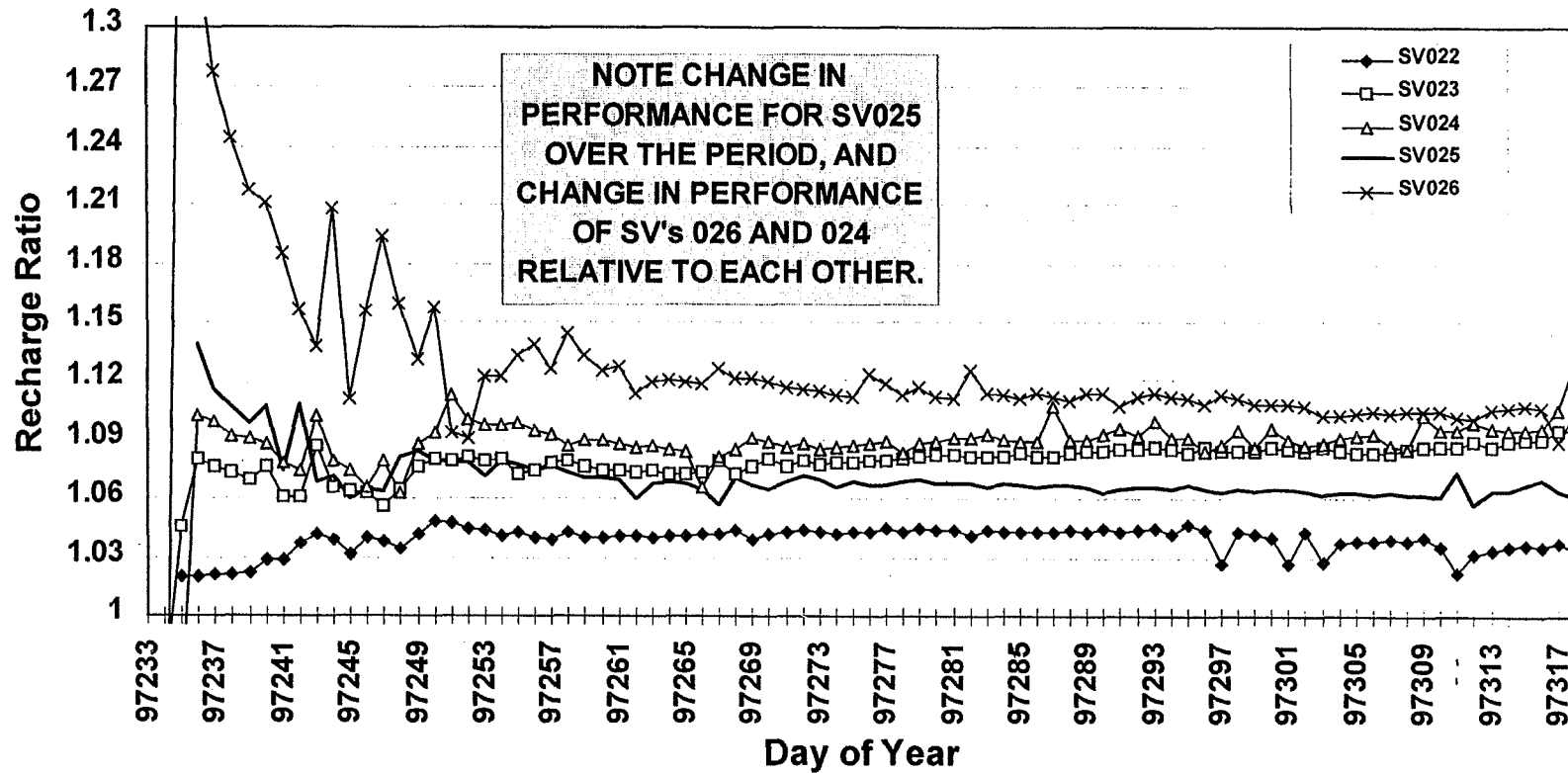


MOTOROLA SPACE SYSTEMS TECHNOLOGY GROUP

Comparison of Battery Recharge Ratios for Third Launch SV's

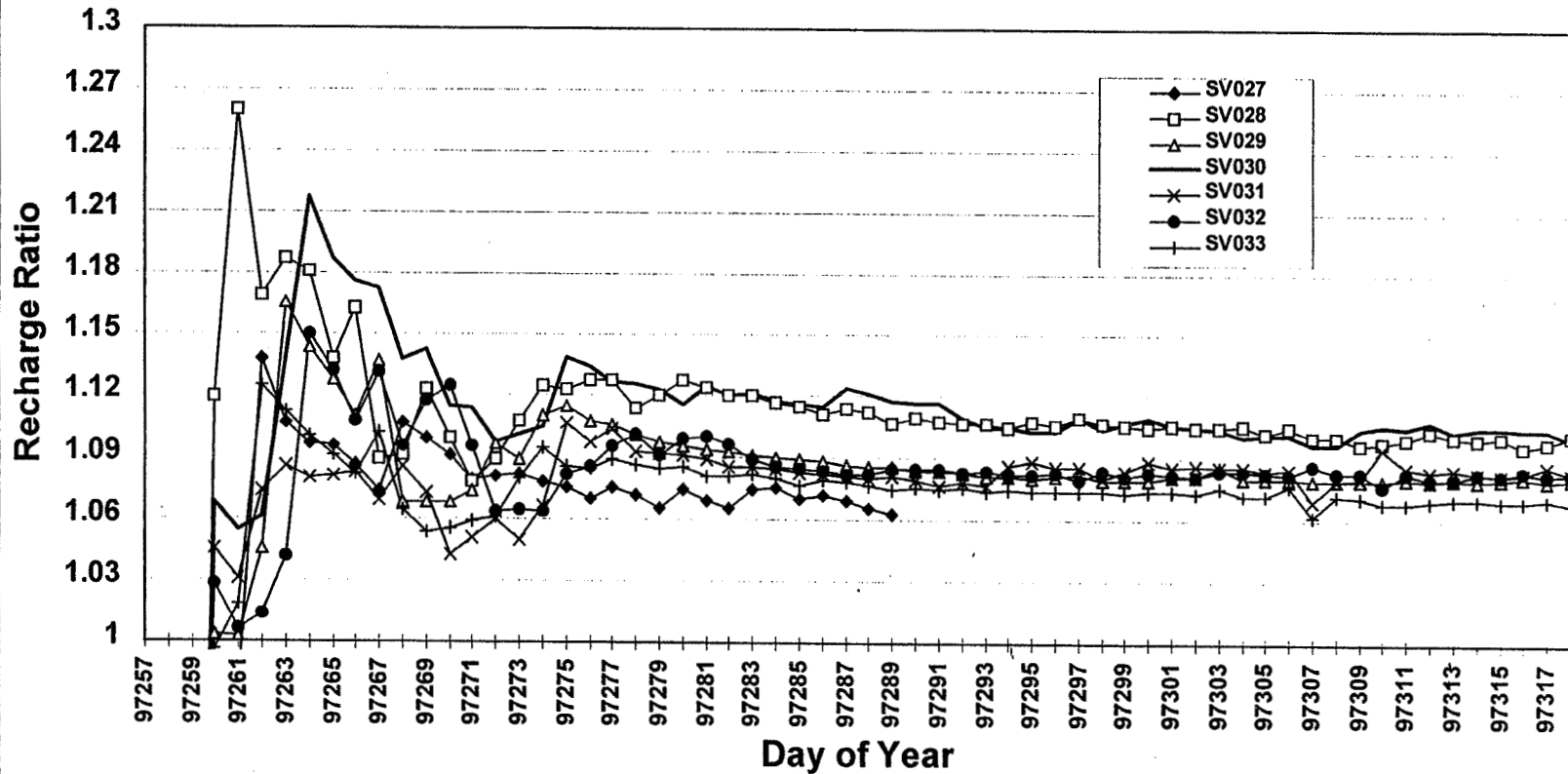


Comparison of Battery Recharge Ratios for Fourth Launch SV's

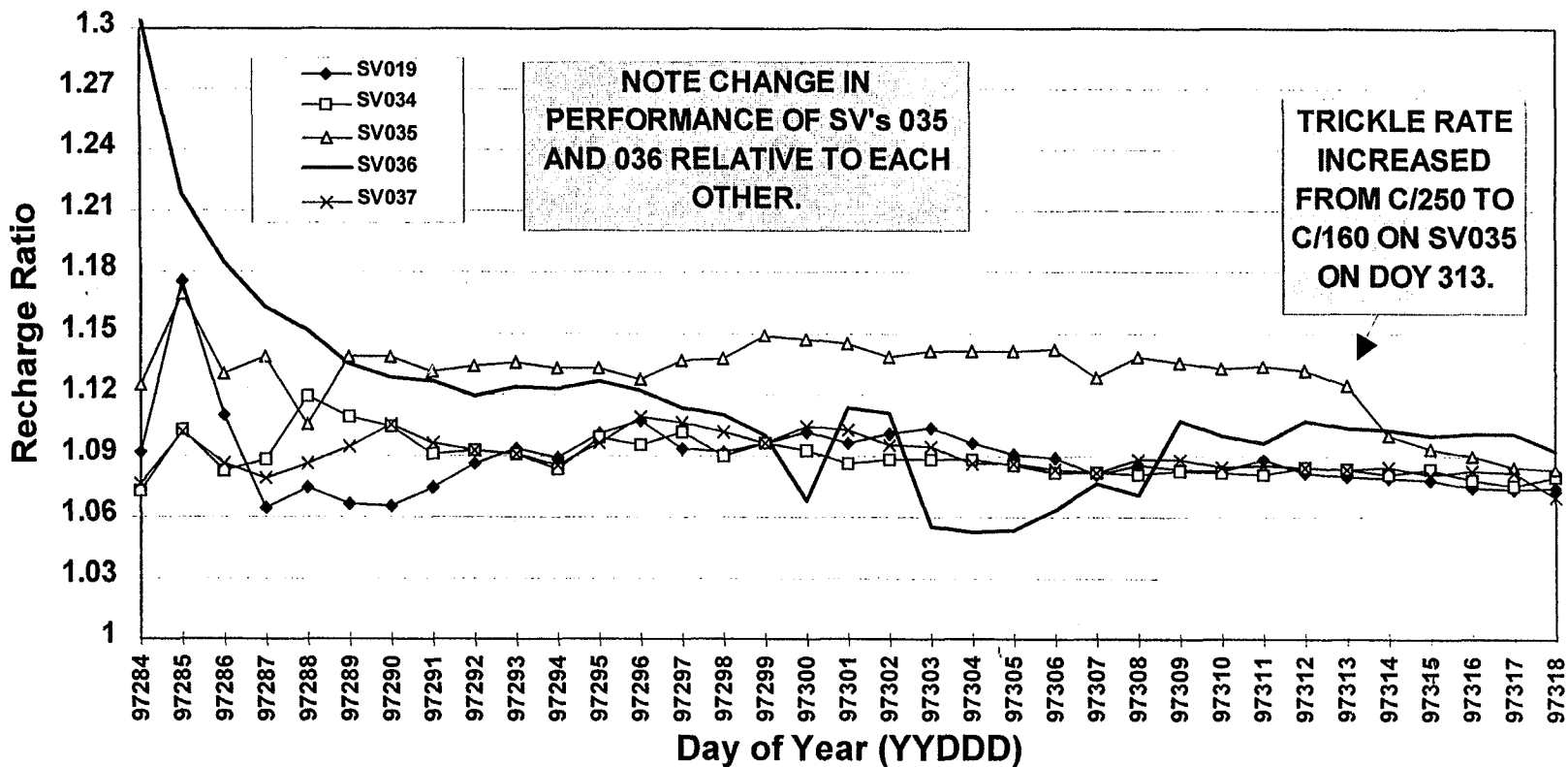


MOTOROLA SPACE SYSTEMS TECHNOLOGY GROUP

Comparison of Battery Recharge Ratios for Fifth Launch SV's

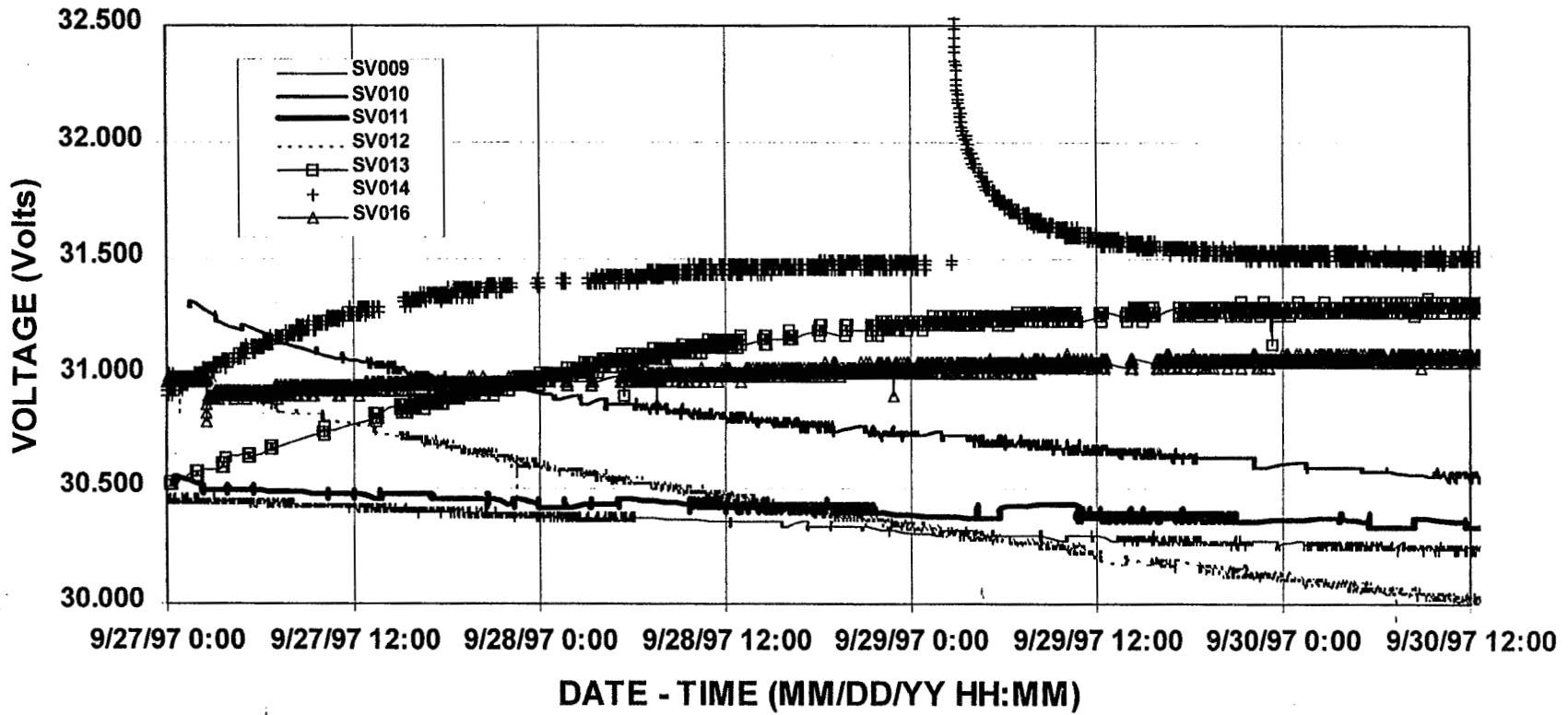


Comparison of Battery Recharge Ratios for Sixth Launch SV's

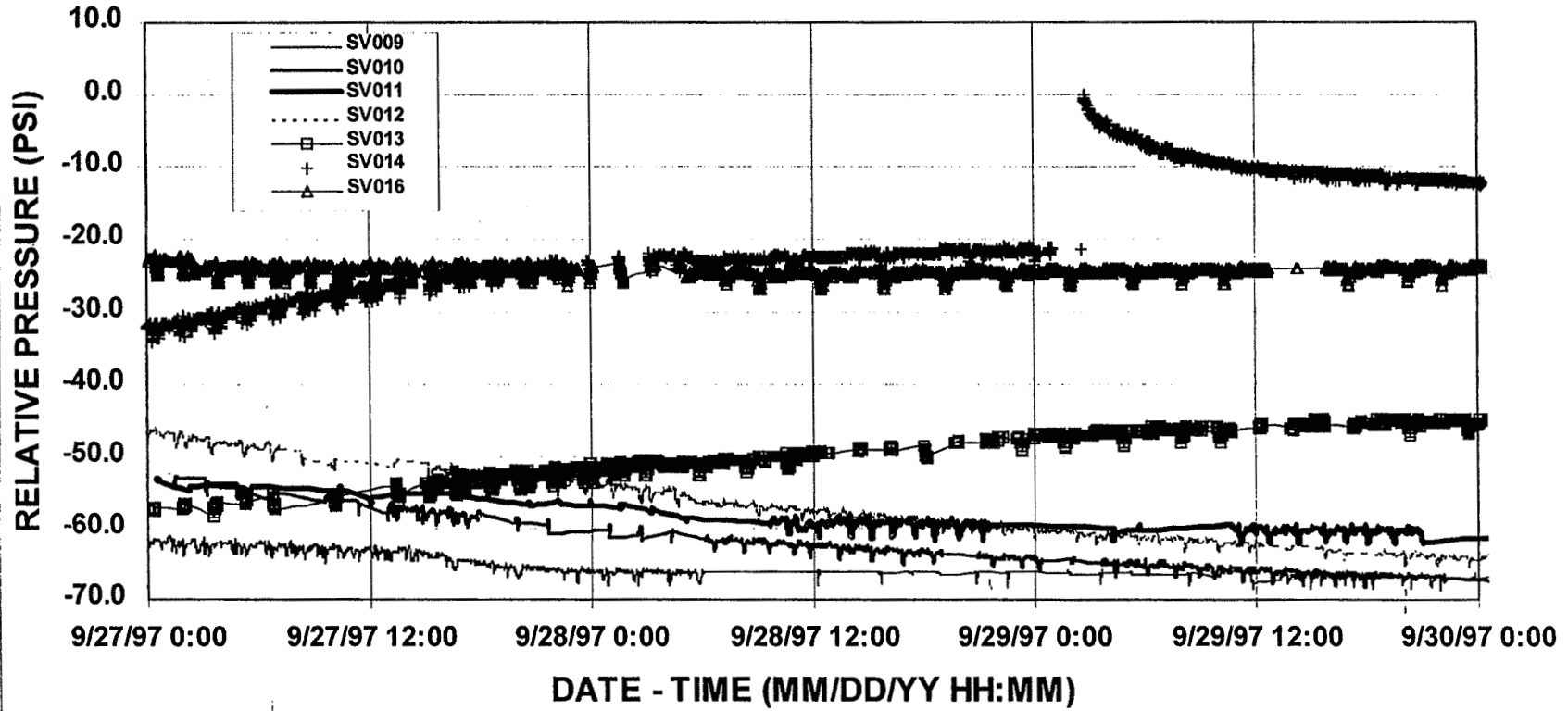


MOTOROLA SPACE SYSTEMS TECHNOLOGY GROUP

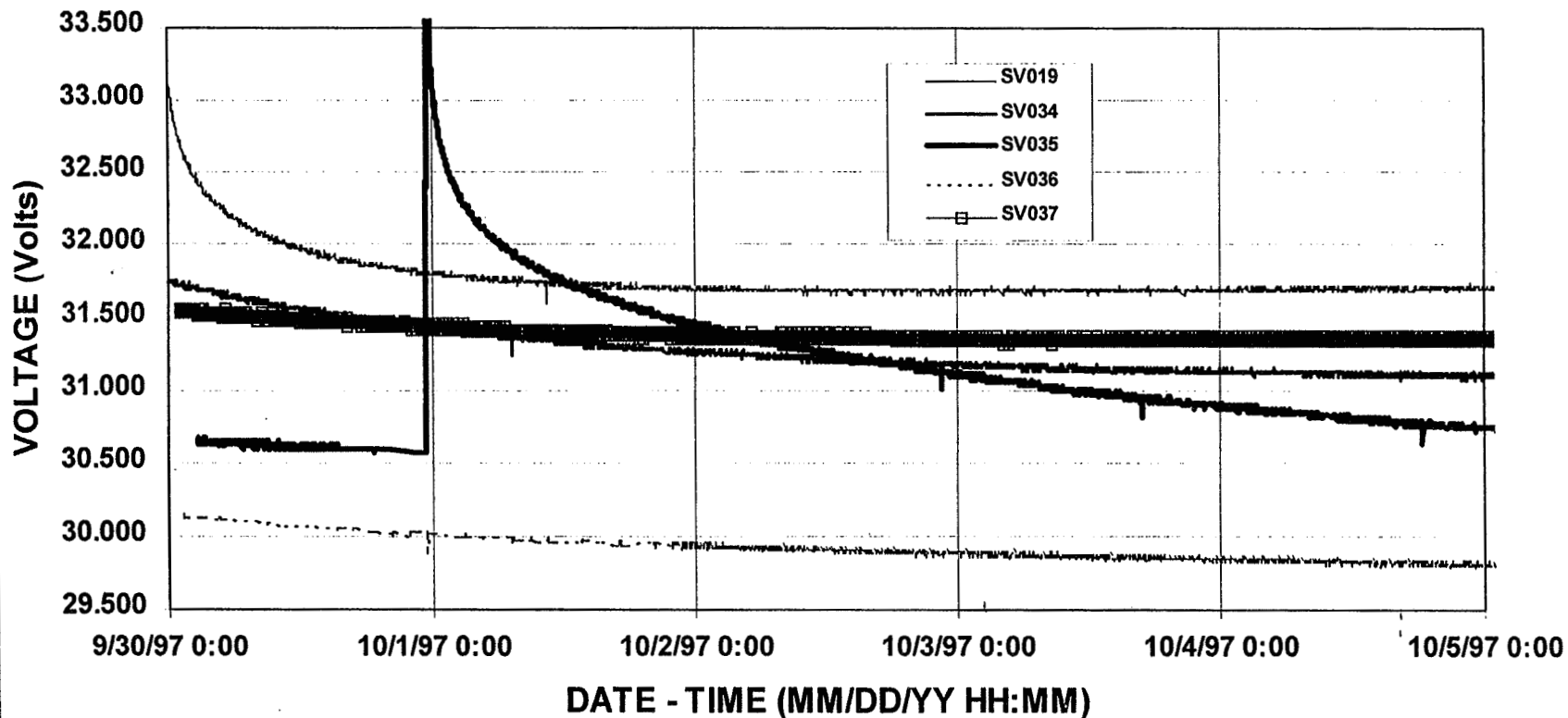
IRIDIUM 2ND LAUNCH VEHICLES: VOLTAGE PERFORMANCE IN FIRST FULL-SUN PERIOD UNDER C/250 TRICKLE-CHARGE RATE



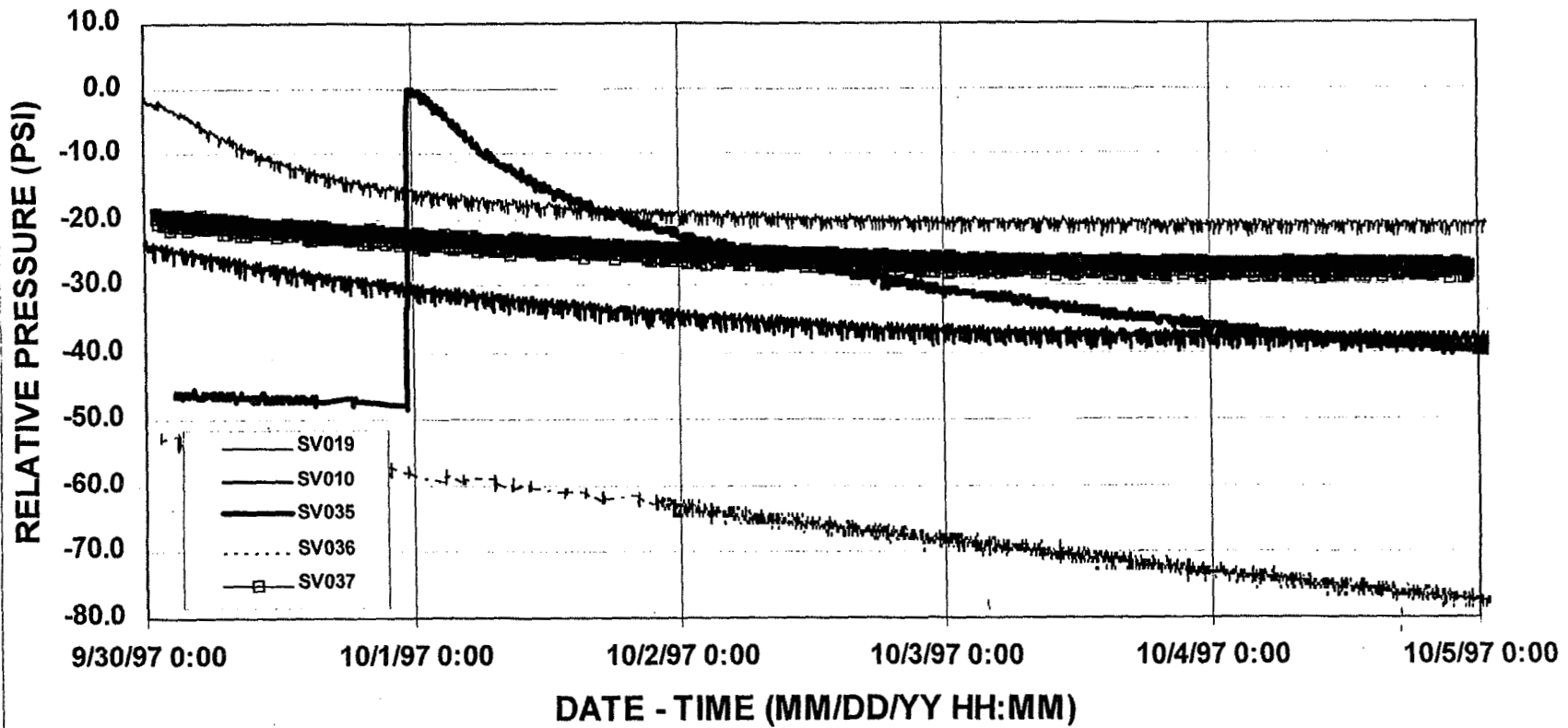
IRIDIUM 2ND LAUNCH VEHICLES: PRESSURE PERFORMANCE IN FIRST FULL-SUN PERIOD UNDER C/250 TRICKLE-CHARGE RATE



IRIDIUM 6TH LAUNCH VEHICLES: VOLTAGE PERFORMANCE IN FIRST FULL-SUN PERIOD UNDER C/250 TRICKLE-CHARGE RATE



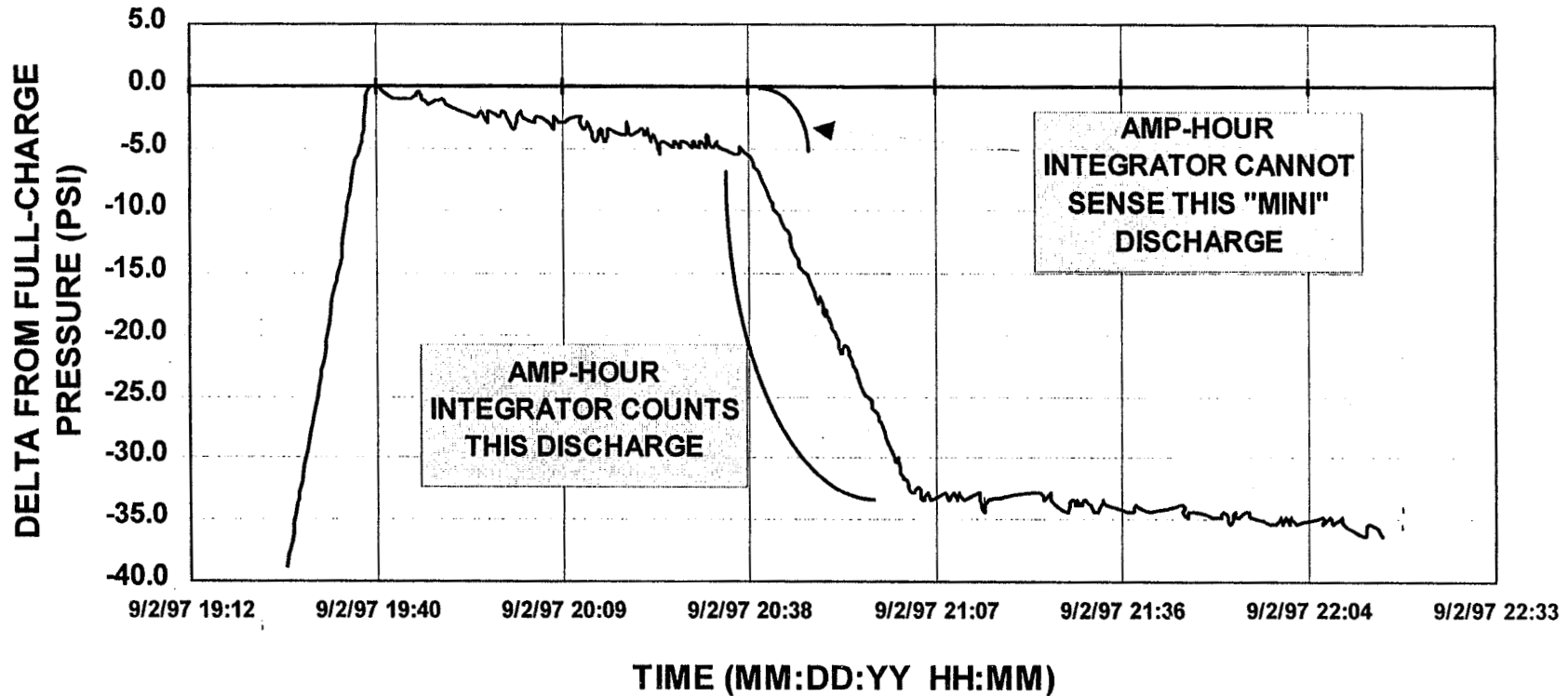
IRIDIUM 6TH LAUNCH VEHICLES: PRESSURE PERFORMANCE IN FIRST FULL-SUN PERIOD UNDER C/250 TRICKLE-CHARGE RATE



MOTOROLA SPACE SYSTEMS TECHNOLOGY GROUP

LOWER TRICKLE RATE CAN RESULT IN SIGNIFICANT SELF-DISCHARGE WITH ASSOCIATED HIGHER C/D RATIOS

IRIDIUM SV026 BATTERY PRESSURE PERFORMANCE WITH C/250 TRICKLE CHARGE



MOTOROLA SPACE SYSTEMS TECHNOLOGY GROUP

ANALYSIS

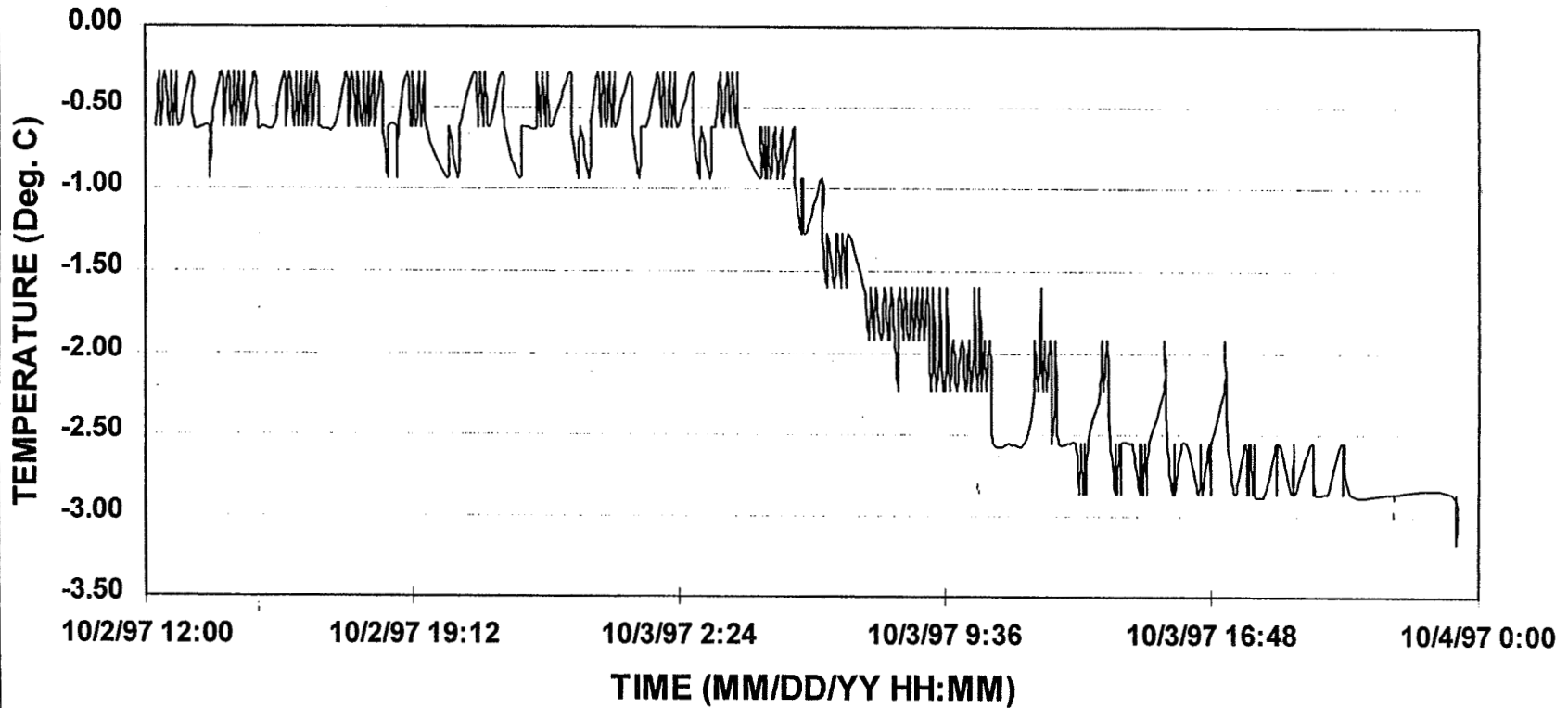
- **PROBABLE CAUSE(S):**
 - SELF-DISCHARGE RATE VARIES FROM ONE BATTERY TO ANOTHER
 - CURRENT SENSOR ERROR (ACCURACY ± 0.1 AMPS)
 - SENSOR READS PROPER CURRENT BUT IS IN FACT TOO LOW
- **INVESTIGATION:**
 - CURRENT SENSOR ERROR SHOULD PROVIDE STATIC DIFFERENCES IN PERFORMANCE (e.g. C/D RATIO ALWAYS 5% HIGHER)
 - THE FACT THAT PERFORMANCE CHANGES WITH TIME AND/OR RELATIVE TO ANOTHER BATTERY UNDER SIMILAR CONDITIONS SUGGESTS THAT BATTERY IS SOURCE OF PHENOMENON
- **SOME BATTERIES WILL NEED TO HAVE TRICKLE RATE INCREASED REGARDLESS OF THE SOURCE OF THE PHENOMENON**

ADDITIONAL INVESTIGATION

- **AS A TRIAL, THE TRICKLE RATE WAS INCREASED FROM C/250 TO C/160 ON SVO18 (FULL-SUN OPERATIONS) AND SV035 (ECLIPSING)**
 - **SELF-DISCHARGE WAS REVERSED ON SV018; C/D RATIO WAS REDUCED BY 4.5% ON SV035**
- **ANY INCREASES IN TRICKLE CHARGE MUST BE CAREFULLY CONSIDERED AND CLOSELY MONITORED**
 - **SINCE BATTERY PERFORMANCE SEEMS TO BE CHANGING, TRICKLE RATES MAY HAVE TO KEEP CHANGING TO KEEP UP**
 - **E.g. FIRST-LAUNCH SV TOLERANCE OF HIGHER TRICKLE RATE HAS CHANGED**
 - **RECENT CHANGE BACK TO HIGHER TRICKLE RATE INCREASED BATTERY TEMPERATURE ~2 DEG. C**
 - **REMOVAL OF HIGHER RATE REDUCED BATTERY TEMPERATURE**

FIRST-LAUNCH SV TEMPERATURE RESPONSE TO REDUCTION IN TRICKLE CHARGE

SV006: BATTERY TEMPERATURE RESPONSE TO DECREASE IN TRICKLE CHARGE RATE FROM C/100 TO C/250



MOTOROLA SPACE SYSTEMS TECHNOLOGY GROUP

CONCLUSIONS AND FUTURE STRATEGY

- **BATTERIES NEED DIFFERENT TRICKLE CHARGE RATES EITHER BECAUSE OF CURRENT SENSOR ERROR OR VARIABLE SELF-DISCHARGE RATES**
- **HIGHER TRICKLE RATES WILL OFFSET THIS EFFECT BUT MAY CREATE UNDESIRABLE WASTE HEAT**
- **AVOIDING EXCESSIVE WASTE HEAT SHOULD CONTRIBUTE TO BATTERY LONGEVITY, WHICH IN TURN CONTRIBUTES TO IRIDIUM SUCCESS**
- **BATTERY OVERCHARGE AND THERMAL STRESS WILL CONTINUE TO BE MINIMIZED**

BEHAVIOR OF 2-CELL CPV NI-H₂ BATTERY DURING PULSE DISCHARGE

Hari Vaidyanathan
COMSAT Laboratories
Clarksburg, MD

AND

Gopalakrishna Rao
NASA-GODDARD SPACE FLIGHT CENTER
Greenbelt, MD

ABSTRACT

A study was carried out to determine the transient voltage behavior of the 2-cell CPV nickel-hydrogen battery with the objective of using the results as a basis for mathematical modeling. The 2-cell CPV battery which is manufactured by Eagle Picher, Inc. for the GOES program yields 18.5 Ah at C/2 rate of discharge at 10°C with a mid-discharge voltage of 2.514 V. The capacity increased with decrease of temperature and a maximum capacity of 22 Ah was obtained at -5°C. The pulse tests consisted of obtaining the voltage profile in the first 20 milliseconds of the one minute pulse discharge at 37 A and pulse discharge was repeated as a function of state-of-charge. The pulse test at 10°C and 20°C provided voltage profiles with the expected decrease in voltage as the pulse was applied. The end of pulse voltage decreased with the state-of-charge. The battery voltage was above 2V at the end of the one-minute pulse at 8% state-of-charge at 10°C. The voltage profile during the 37 A pulse discharge consists of an initial drop in voltage which was independent of the state of charge. The invariability in the value for the initial drop in voltage with state of charge is a very important observation. The results show that towards the end of discharge the dominant resistance is not ohmic in nature. It could be hypothesized from the nature of the voltage transients that the dominant mechanism towards the end of discharge is proton diffusion. The study also shows that the dominant resistance in the voltage plateau during discharge is activation polarization.

INTRODUCTION

The 2-Cell CPV nickel-hydrogen battery manufactured by Eagle Picher is a variation of the aerospace individual pressure vessel cell (IPV) with the same electrochemical performance features but with an operating voltage of 2.5 V and a specific energy of 58 Wh/Kg. The purpose of this work is to examine the characteristics of the 2-cell CPV battery including the behavior during pulse discharge. The purpose of the pulse test was to determine lowest state of charge at which the battery can sustain a 37 A pulse discharge

with minimum voltage degradation and assess the effect of high burst currents on the usable capacity. Another objective is to analyze the transient voltage response to determine the dominant mechanism for the abrupt decrease in voltage at low states-of-charge.

CAPACITY AND SELF DISCHARGE

The capacity of the four 2-cell CPV batteries at 10°C was determined to be 18.5 Ah (to 2V) and the mid-discharge voltage to be 2.514 V. The capacity remaining after 72-hours of open-circuiting at 10°C was 86.7%. Thus, the self-discharge rate is similar to that of single cells. Figures 1 and 2 show the voltage profiles during charge and discharge, respectively and the features are such as voltage roll-over during charge and plateau region during discharge are identical to that of IPV cells. The mid-discharge voltage during discharge at C/2 after the 72-hour stand test was 2.485 as shown in Figure 3. Thus, the initial capacity tests indicate performance features of two properly connected cells in series.

RATE AND TEMPERATURE DEPENDENCY

The variation of capacity with the rate of charge and discharge and temperature was determined. The capacity was the highest with a value of 22 Ah at -5°C at a charge rate of C/10 and discharge rate of C/10. The capacity increased from 19.58 Ah to 20.35 Ah when the charge rate was increased from C/20 to C/2 at 10°C. The capacity at a charge rate of 0.8 C and discharge rate of 0.8 C was 20.05 Ah. The capacity increased with decrease of temperature and at -5°C, a charge rate of C/2 yielded a capacity of 20.97 Ah. Figure 4 shows the voltage profiles at different rates of discharge at 10°C for one of the CPVs. As expected the mid-discharge voltage decreased with increase in the rate. The capacity decreased when the discharge rate was increased from 0.5 C to 0.8 C. Figure 5 shows the voltage profiles at C/2 rate of discharge at different temperatures. At -5°C the discharge voltage is high in the beginning and low towards the end. In the plateau region the mid-discharge voltage is almost the same at all temperatures studied. Figure 6 shows the voltage profiles at C/10 rate of discharge at different temperatures. The profiles at C/10 differ from that obtained at C/2 rate with respect to the appearance of a shift in the mid-discharge region and the observation of higher discharge voltages at -5°C towards the end of discharge. It is to be noted that the negative electrode polarization is higher at -5°C and this characteristic results in a slightly lower discharge voltage at -5°C. The reason for the higher voltage beyond the mid-discharge region at C/10 rate compared to C/2 is due to the overwhelming influence of the polarization at the nickel electrode. The variation of capacity with temperature when charged and discharged at 0.8 C was also determined as shown in Table 1. The mid-discharge voltage and capacity showed marginal changes with the temperature.

PULSE TEST

The pulse test was performed using a Hewlett-Packard 6050 A programmable electronic load which has a slew rate of 400,000 A/s to reach the pulse current of 37 A in <150 μ s. The CPV battery voltage was measured using a Nicolet 460 storage oscilloscope. The procedure consisted of obtaining the transient voltage profile in the first 20 milliseconds of a one-minute pulse at 37 A. The application of the 37 A pulse was done by increasing the discharge rate from 9.3 A to 37 A during discharge at regular intervals such as 90% state-of-charge, 80%, 70 %, etc. The application of pulses were concluded when the voltage reached 2 V during the 9.3 A discharge. The pulse discharge was first done with the CPV battery stabilized at 10°C and then the test was repeated at 20°C.

Figure 7 shows the voltage transient obtained during the first 2 milliseconds of pulse discharge. The voltage of the battery decreases by 0.71 V in first few microseconds and then the voltage recovers to a value 200 mV less than that obtained during the 9.3 A discharge. This is an expected behavior and the initial drop of 710 mV translates to an ohmic resistance of 25.6 milliohms.

Figure 8 shows the variation of end of pulse battery voltage as a function of state-of-charge at 20°C. The features of the curve are similar to a discharge voltage profile with an initial decline, a plateau region and final decrease in voltage. Thus, the battery is able to sustain pulse discharges at states-of-charge as low as 12%. A very similar behavior was observed at 10°C and the lowest state-of-charge at which the battery would support a pulse current was 8 %.

Figure 9 shows the variation of initial drop in voltage with the state-of-charge. The trend in the data showed that the initial drop was ~ 670 mV and it did not change with state-of-charge. The initial drop in voltage is related to the ohmic resistance at the nickel electrode surface. It is known that, the discharged active material, Ni(OH)₂ grows on the surface of the charged active material. The electronic conductivity is expected to decrease with the growth of the discharged active material on the nickel electrode with the consequent increase in polarization. The pulse behavior data indicates that the ohmic resistance calculated from the initial drop in voltage amounts to ~ 25.6 mohms and it does not increase with the accumulation of discharged active material.

DOMINANT RESISTANCE

During constant current discharge the reaction rates at the nickel and hydrogen electrode proceed at a constant rate, the reaction at the nickel electrode being the limiting factor. The hydrogen electrode functions with an average polarization loss of 25 mV at 15 mA/cm² at a discharge rate of C/2.

Thus the shape of the voltage - time curve depends primarily on the reactions of Ni(OH)₂ which consists of processes like the diffusion of OH⁻ ions in the bulk electrolyte, diffusion of protons into the bulk of the solid phase, increase of OH⁻ concentration on the nickel electrode surface, and build-up of Ni(OH)₂ on the surface of NiOOH active material. The voltage of the nickel electrode and the cell is therefore governed by:¹

- Concentration polarization due to a rise in the KOH concentration
- Activation polarization or charge transfer resistance of the nickel electrode reaction
- Diffusion polarization related to proton
- Ohmic effects: resistance polarization at the solid phase

The dominant resistance at different segments of the discharge curve is not known with certainty. The dominant resistance in the plateau region of the discharge curve is said to be activation polarization. The dominant resistance towards the end of discharge (knee of the curve) during constant current discharges is said to be ohmic in nature. The invariability in the initial voltage drop obtained in the pulse test indicates that the dominant resistance is not ohmic. The other possibilities such as concentration polarization and activation polarization can be excluded based on published information in the literature. The other alternative is polarization loss attributable slow proton diffusion. A previous study by Salkind et al² attributed the suppressed discharge voltages at 1C rate of discharge at 25% state of charge by sintered impregnated electrodes to a diffusion problem since an ohmic effect would have magnified the effect in a fiber mat electrode. The results of this study also suggests that the voltage drop is attributable diffusion and specifically proton diffusion. Weidner et al³. pointed out that the ohmic effect is not significant during a major portion of discharge and contributes very little to the overall polarization loss, but conductivity at the end of discharge causes significant polarization losses. The results obtained in our study are contrary to this and the reason for the large polarization loss towards the end of discharge is not ohmic in nature.

CONCLUSIONS

The results of this study suggest the following conclusions:

- The CPV battery yields a capacity of 22 Ah and retained 86.7% of the capacity in the 3-day open-circuit stand test.
- The battery can sustain a 3C rate pulse for one minute at low states-of-charge (8%). The initial decline in the voltage during the 3C rate pulse is about 670 mV and the voltage recovers in less than one millisecond.

- Analysis of the initial decline in voltage during the pulse test indicates that the resistance polarization is not significant and the polarization loss at very low states-of-charge is attributable to slow proton diffusion.

REFERENCES

1. Z. Mao and R.E.White and John Newman, J.Electrochem. Soc., Vol 141, 1994,p.54
2. Salkind, A.J., Kelly, J.J., and Ockerman, J.B. Proc. Symp.on the Nickel Electrode, 176th Meeting of the Electrochemical Society, Hollywood, Fl, Pennington, N.J. Vol.90-4, pp247-260
- 3.J.W.Weidner, and P. Timmerman, J. Electrochem. Soc ,Vol 141,1994,p 346

FIGURE 1: VOLTAGE PROFILES DURING CHARGE AT C/10 AT 10°C

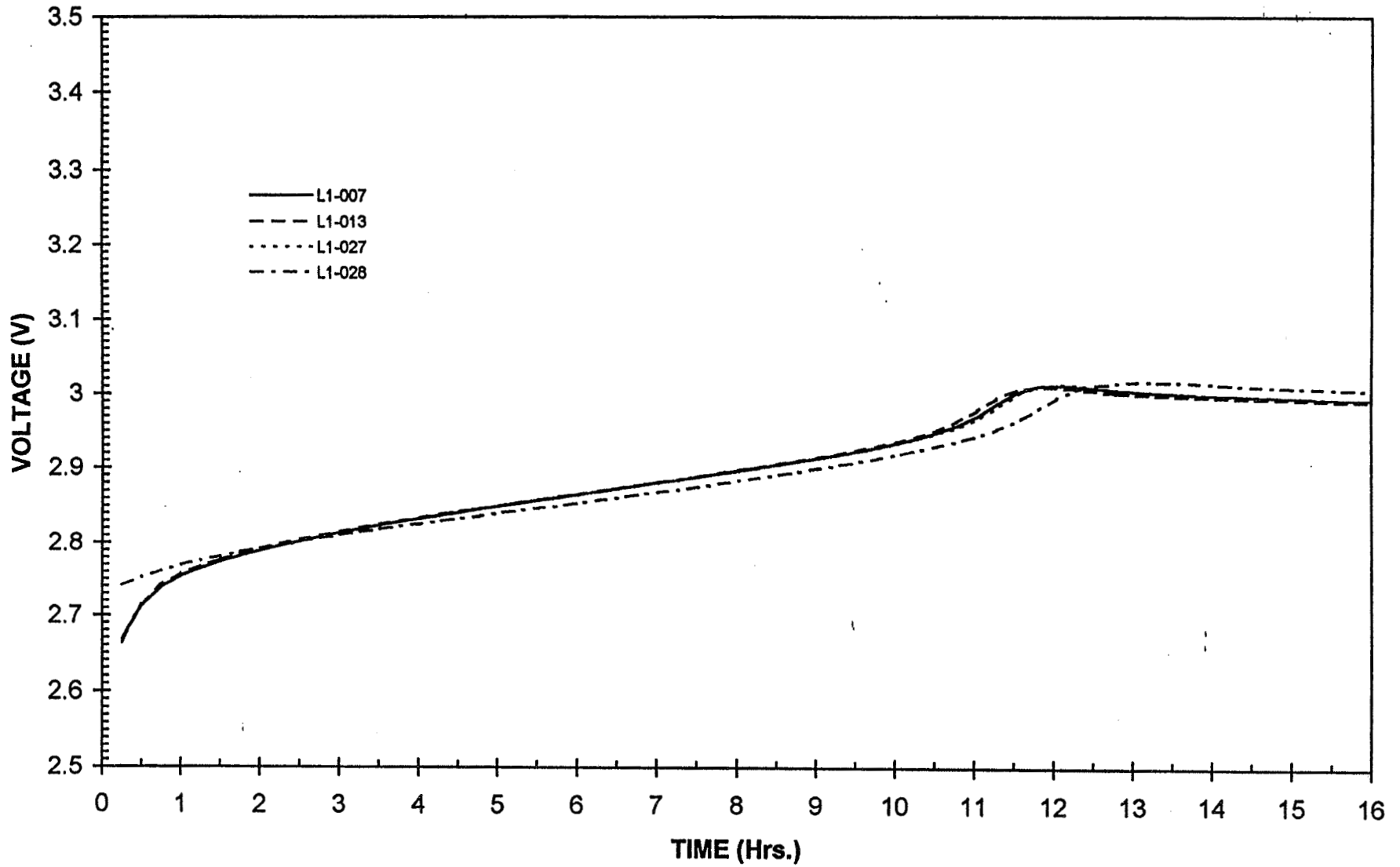


FIGURE 2: VOLTAGE PROFILES DURING DISCHARGE AT C/2 AT 10°C

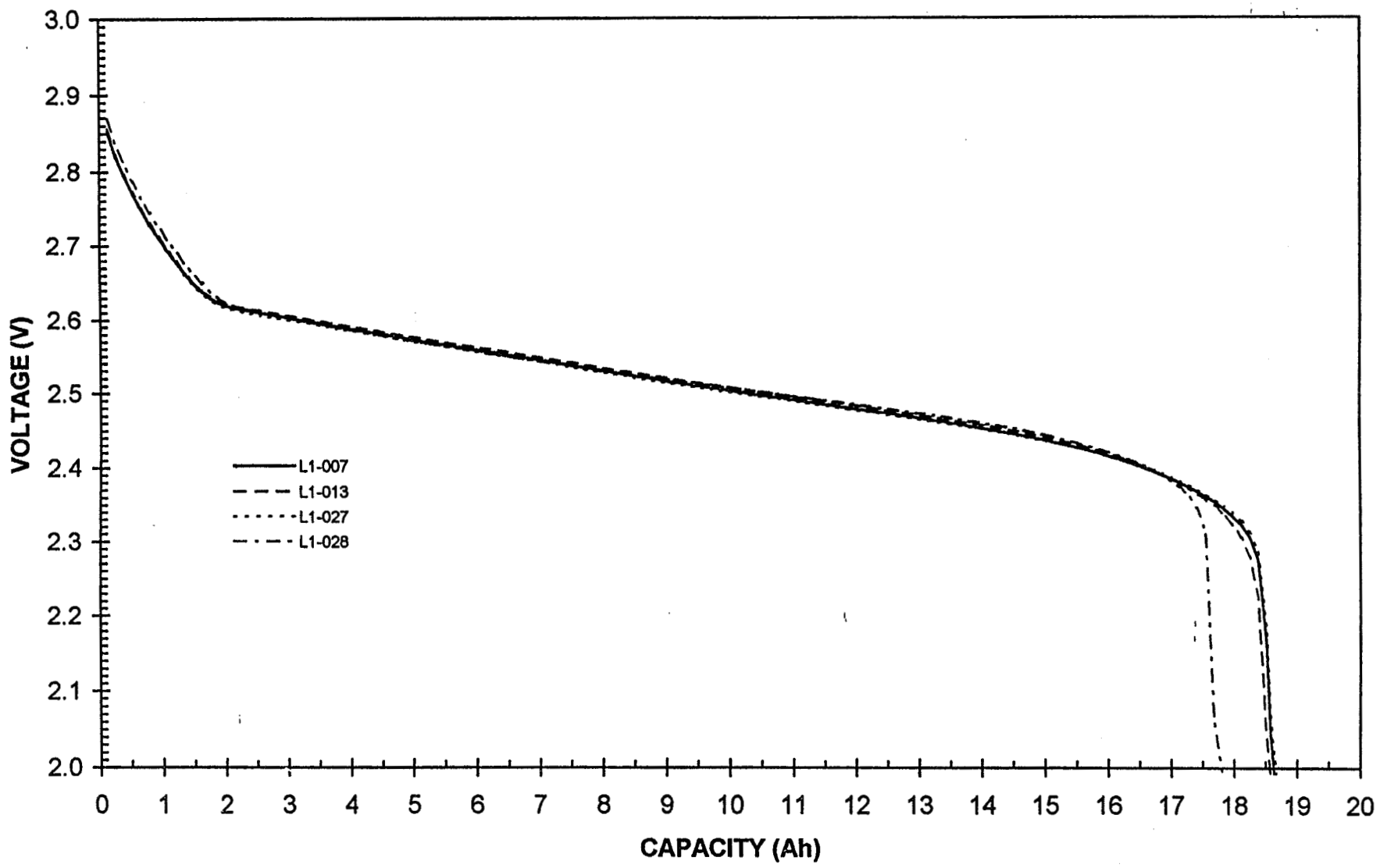


FIGURE 3: VOLTAGE PROFILES AFTER OPEN-CIRCUIT STAND AT 10°C

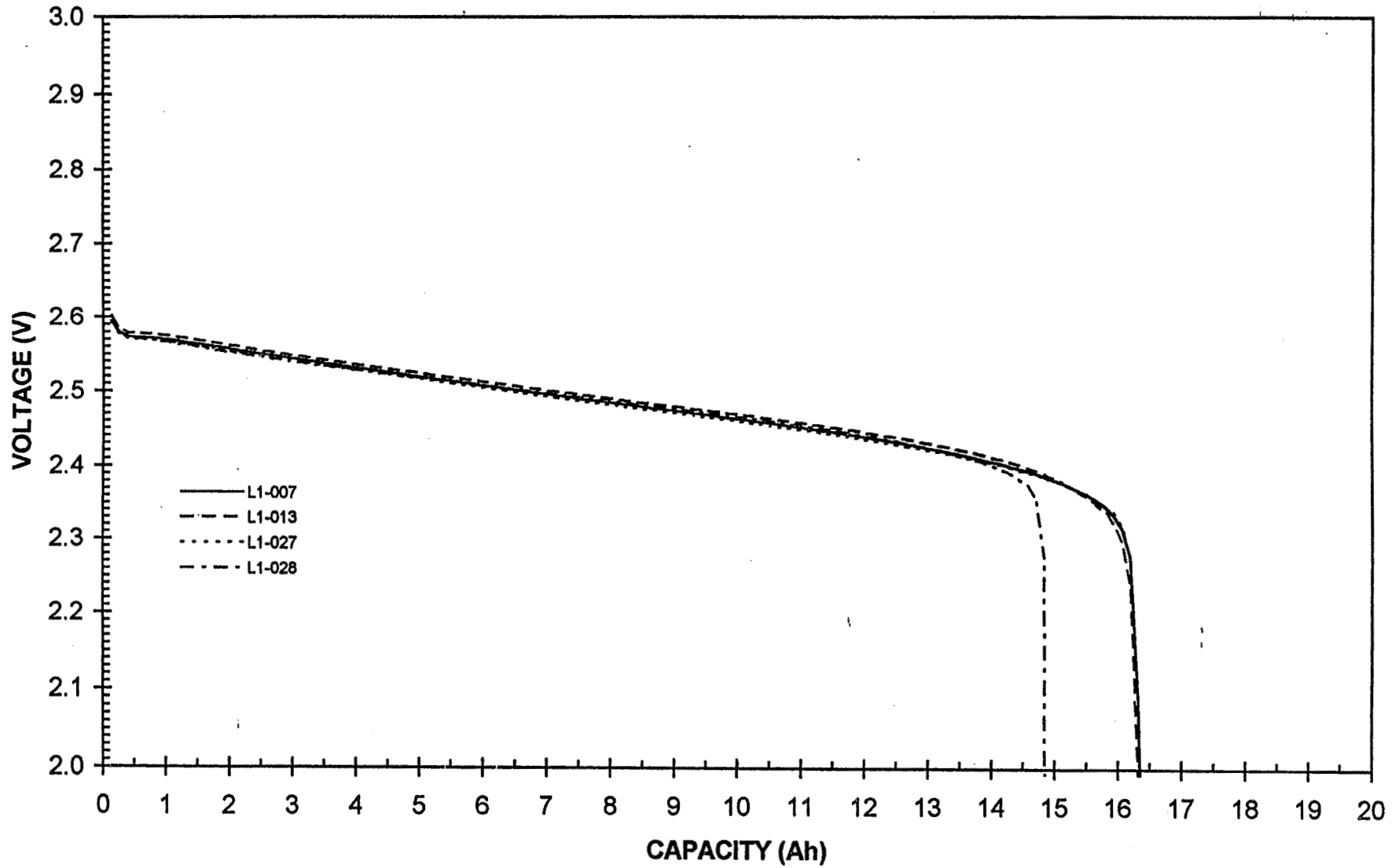


FIGURE 4: VOLTAGE PROFILES AT DIFFERENT RATES OF DISCHARGE AT 10°C

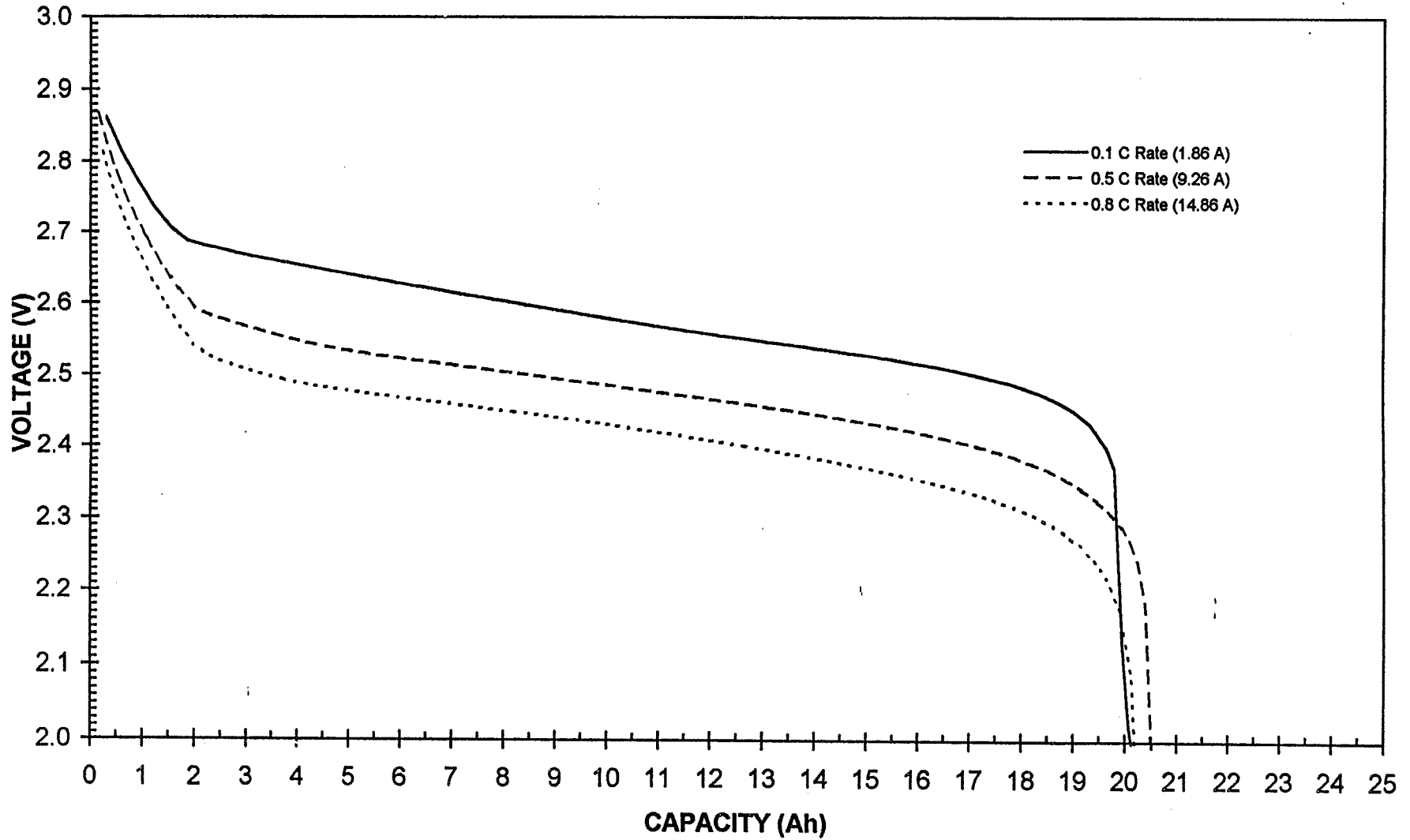


FIGURE 5: VOLTAGE PROFILES AT DIFFERENT TEMPERATURES DURING DISCHARGE AT C/2

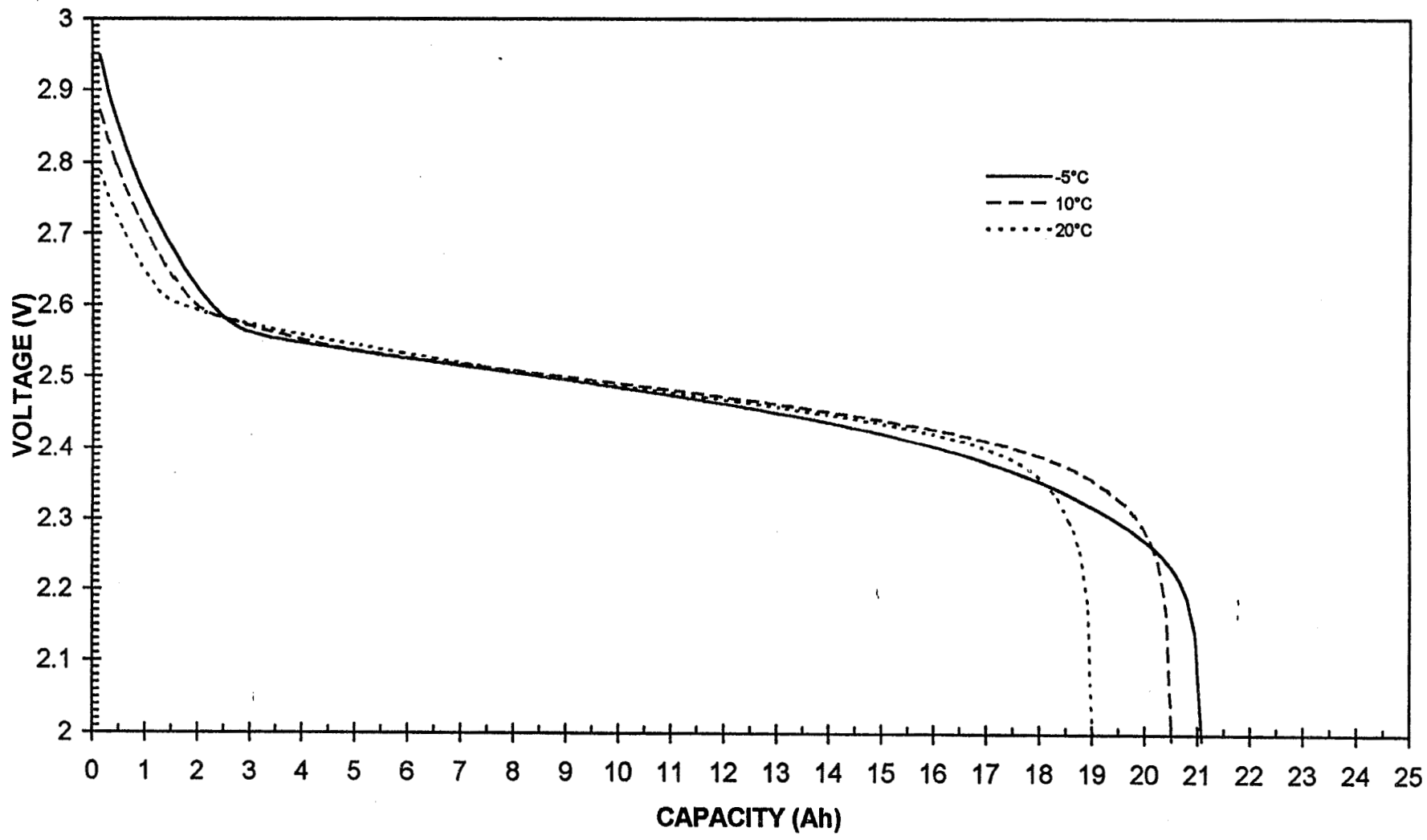


FIGURE 6: VOLTAGE PROFILES DURING C/10 DISCHARGE AT DIFFERENT TEMPERATURES

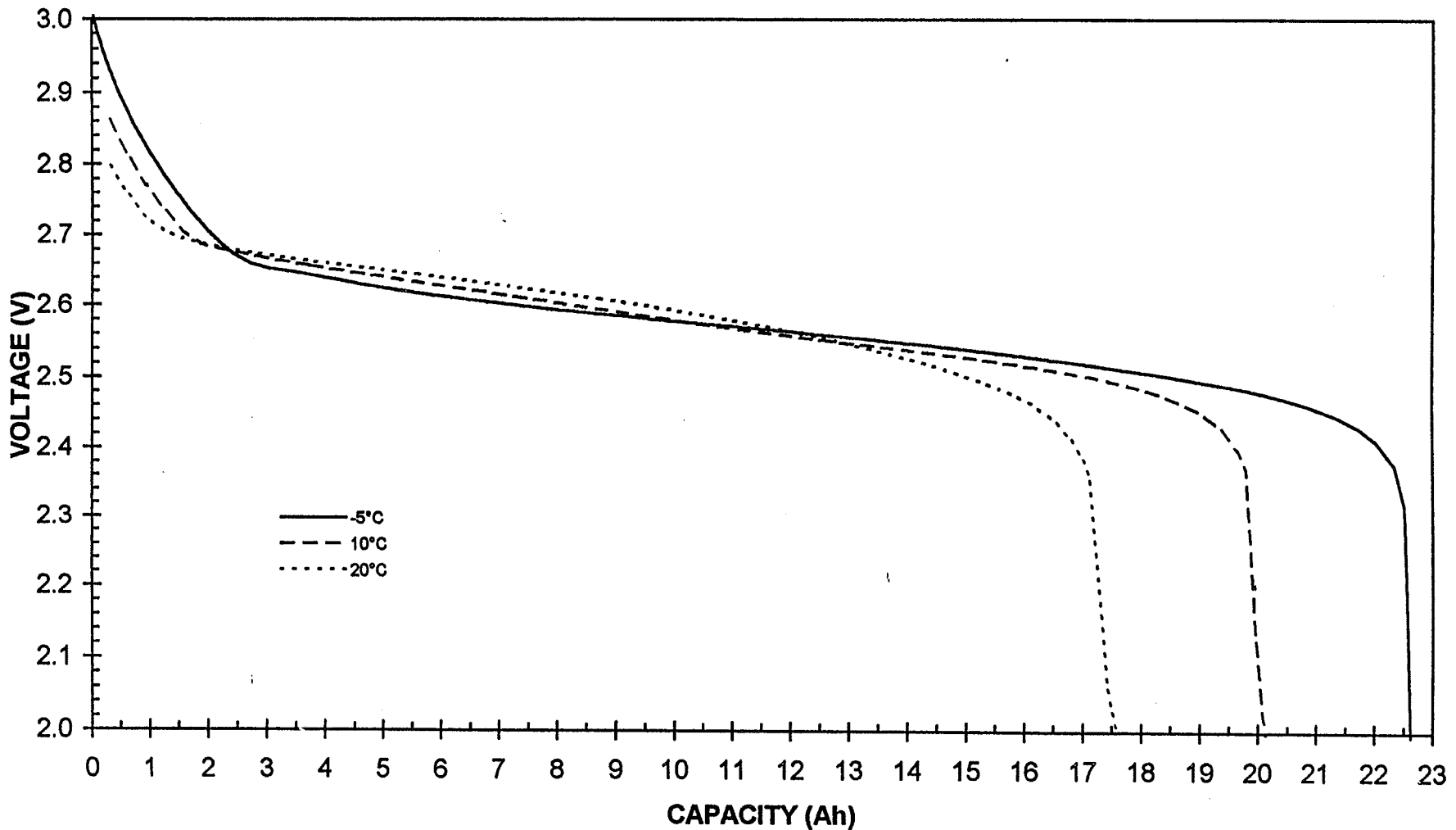


FIGURE 7: VOLTAGE TRANSIENT OBTAINED AT 21% STATE OF CHARGE

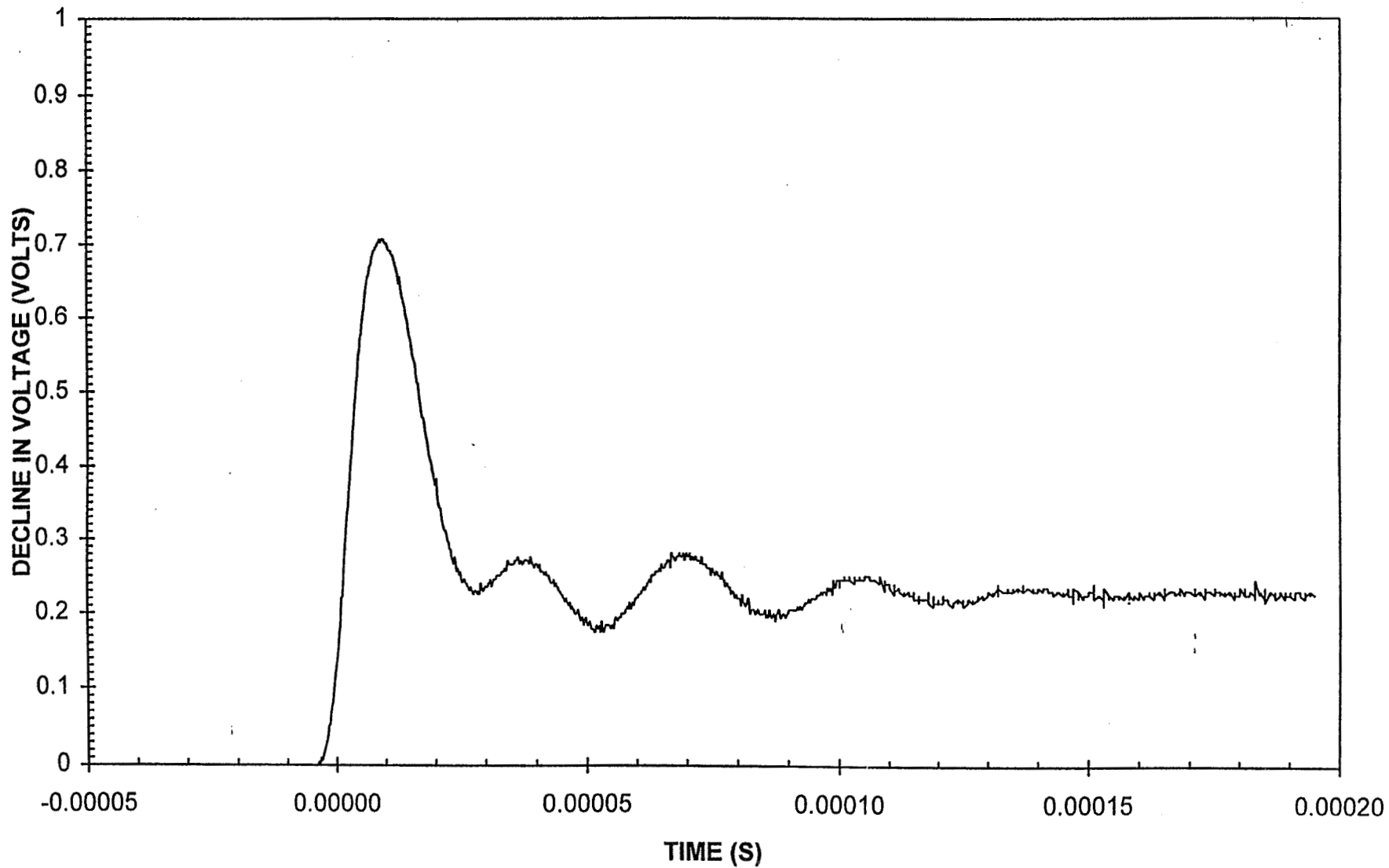


FIGURE 8. VARIATION OF END-OF-PULSE VOLTAGE WITH THE STATE-OF-CHARGE

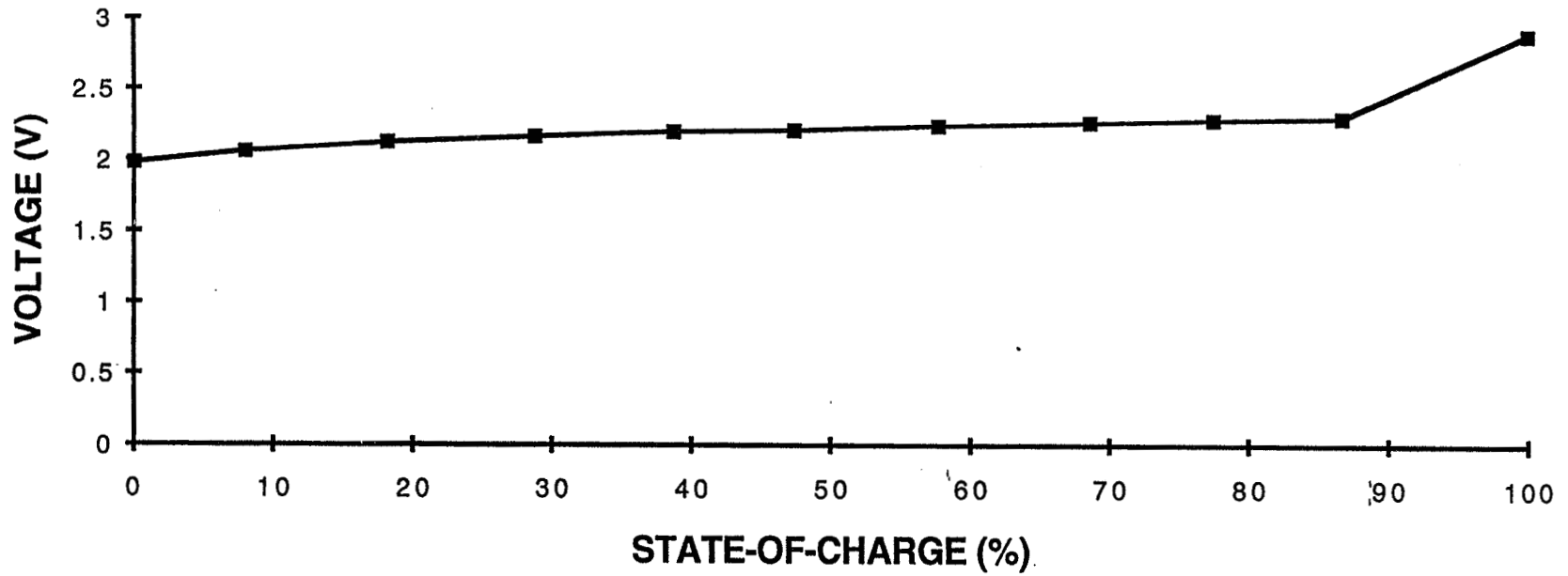


FIGURE 9. VARIATION OF INITIAL DROP IN VOLTAGE WITH STATE-OF-CHARGE

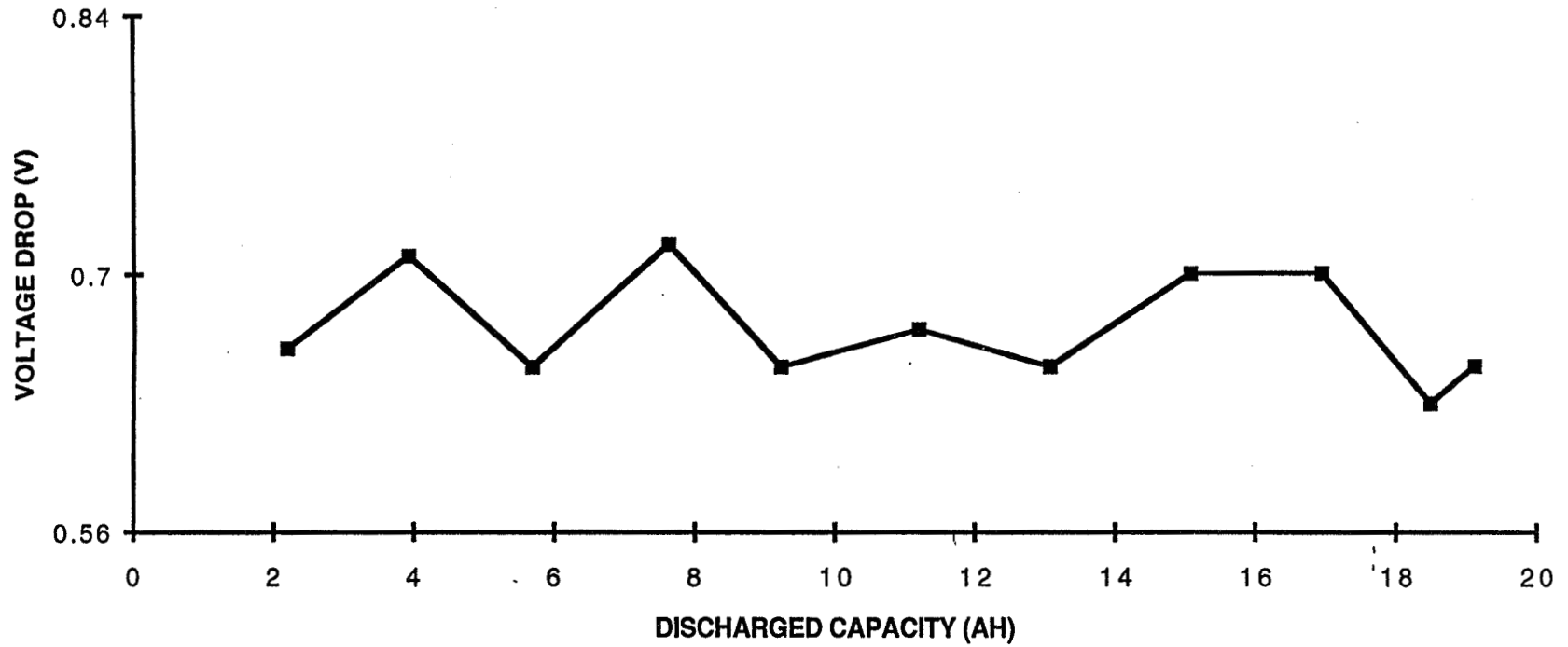


TABLE 1.

Cycle	Temp (°C)	Current		L1-007			L1-013			L1-027			L1-028		
		Charge (A)	Discharge (A)	EOCV (V)	Mid-Dch V (V)	Capacity (Ah)									
1	10	0.8	8	2.976	2.495	19.57	2.970	2.498	19.42	2.976	2.498	19.57	2.998	2.495	19.77
2	0	1.6	8	3.082	2.491	20.27	3.076	2.498	20.17	3.080	2.498	20.23	3.093	2.499	19.45
3	10	1.6	8	2.992	2.513	18.64	2.990	2.516	18.57	2.993	2.510	18.68	3.005	2.519	17.80
4*	10	1.6	8	3.010	2.482	16.36	3.008	2.488	16.32	3.010	2.480	16.36	3.022	2.492	14.90
5	20	1.6	8	2.941	2.548	16.45	2.941	2.552	16.34	2.943	2.545	16.58	2.944	2.558	15.67
6	-5	1.86	1.86	3.044	2.567	22.61	3.043	2.570	22.51	3.042	2.566	22.69	3.048	2.573	21.71
7	10	1.86	1.86	2.992	2.576	20.13	2.991	2.576	20.08	2.992	2.576	20.27	2.999	2.577	19.79
8	20	1.86	1.86	2.944	2.607	17.59	2.945	2.610	17.48	2.945	2.609	17.75	2.949	2.611	16.96
9	-5	9.26	9.26	3.258	2.470	21.16	3.252	2.478	21.10	3.265	2.471	21.21	3.233	2.482	20.43
10	10	9.26	9.26	3.135	2.483	20.53	3.129	2.487	20.53	3.144	2.482	20.61	3.115	2.492	19.74
11	20	9.26	9.26	3.019	2.489	18.96	3.020	2.491	19.03	3.032	2.487	19.17	3.004	2.494	18.54
12	10	14.81	14.86	3.220	2.429	20.21	3.213	2.434	20.21	3.235	2.426	20.28	3.193	2.437	19.52
13	15	14.81	14.86	3.190	2.428	19.98	3.184	2.433	19.89	3.204	2.425	20.05	3.160	2.436	19.20
14	20	14.81	14.86	3.143	2.429	19.55	3.135	2.431	19.48	3.158	2.425	19.66	3.114	2.433	18.91

* 72-hour open circuit stand

Page intentionally left blank

NICKEL-HYDROGEN (NiH₂) SINGLE PRESSURE VESSEL (SPV) BATTERY DEVELOPMENT UPDATE

Steve Sterz, Beth Parmley, Dwight Caldwell and John Bennett
Technologies Division, Eagle-Picher Industries, Inc.
Joplin, MO 64802
(417) 623-8333

ABSTRACT

The NiH₂ battery system is the dominant rechargeable technology for communications, scientific and military satellites and is recognized for its long life, reliability and durability. Eagle-Picher Industries, Inc. (EPI) has developed the Single Pressure Vessel (SPV) NiH₂ battery, which houses all cells within a single vessel, as an evolutionary step in NiH₂ technology. The SPV configuration was developed to improve the performance, producibility and reliability of the NiH₂ system at the battery level and ultimately to reduce overall battery cost and weight.

Recognition of the benefits and advantages of the SPV resulted in its choice as the battery design for a large-scale communications satellite program. After instituting high-volume production procedures and undergoing a significant life test effort at EPI, this program is proceeding very smoothly, on time and on cost. This particular application requires a 22 cell, 60 Ah Low Earth Orbit (LEO) battery, however, 50 Ah, 30 Ah and 15 Ah battery configurations have been produced and capacities up to 120 Ah are possible with a short development time. An accelerated (70% depth-of-discharge for 4612 cycles) life test of an early prototype and an independent design review have both shown the design to be robust. The advanced SPV battery has the flexibility to fulfill the requirements of any mission needing a reliable, durable, space-qualified battery with a high duty cycle capability. This presentation discusses SPV design features and presents life test data. Also addressed are the production features of the SPV battery which have resulted in cost and performance benefits for the IRIDIUM® global communications system.

INTRODUCTION

The nickel-hydrogen (NiH₂) battery system has been extensively developed over the past twenty years, primarily for space applications such as communications satellites. The battery combines a traditional nickel/nickel-hydroxide electrode, as is used in nickel-cadmium and nickel-iron batteries, with a fuel-cell type catalytic hydrogen electrode. Since hydrogen is a very lightweight, efficient energy storage material, this allows the prospect of higher energy density than typical chemical-type electrodes such as cadmium or iron.

Several distinct NiH₂ cell and battery designs are currently in production and under development for a wide variety of applications. These include traditional aerospace applications such as earth-orbital communications satellites as well as terrestrial uses such as telecommunications equipment, utility load leveling and remote location power systems. Existing Individual Pressure Vessel (IPV) NiH₂ technology has been supplemented by newer Common Pressure Vessel (CPV) cell designs and other cell and battery designs such as the Dependent Pressure Vessel (DPV) and Low Pressure Vessel (LPV) battery. The SPV battery design is the next step in the continued development and evolution of the NiH₂ battery system, and with the launch of the first five IRIDIUM® satellites in May, 1997, EPI has the distinction of being the first battery manufacturer to orbit SPV NiH₂ battery technology used in a telecommunications application.

NiH₂ BATTERY DESIGN CONCEPTS

Traditional NiH₂ battery design (Figure 1) consists of multiple IPV cells connected in series to develop the required battery voltage. The cylindrical cells are packaged together in a rectangular battery footprint. The cells are sleeve mounted perpendicular to the

1997 NASA Aerospace Battery Workshop, Huntsville, AL, Nov.18-20, DC041097.PM6

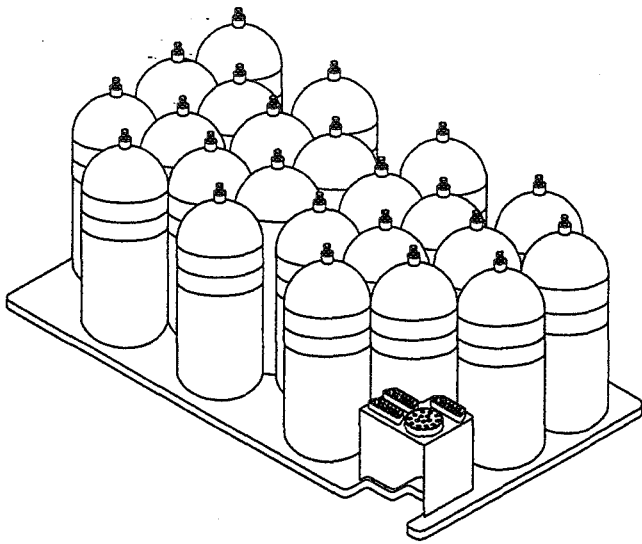


FIGURE 1

baseplate. Volumetric packaging efficiency is low. Each individual cylindrical pressure vessel contains a single cell. The individual cells are sized to deliver the rated ampere-hour (Ah) capacity of the battery and delivers 1.25 VDC, which is characteristic of the nickel-hydrogen electrochemical couple. In larger sizes, typically above 60 Ah, each cell contains two discrete electrode stacks, connected electrically in parallel, within the pressure vessel. This type of internal dual-stack cell construction is shown in Figure 2. The next step for the dual-stack IPV is the common pressure vessel (CPV) cell design. This design incorporates two discrete electrode stacks, connected electrically in series, within a common pressure vessel. The design is mechanically identical to a dual-stack IPV cell with the only difference being the electrical connection of the two electrode stacks. The CPV cell has a terminal voltage of 2.5 VDC, which is the additive voltage of the two series-connected electrode stacks. The electrical capacity of the cell is the rated capacity of either electrode stack (the two stacks are of equal capacity).

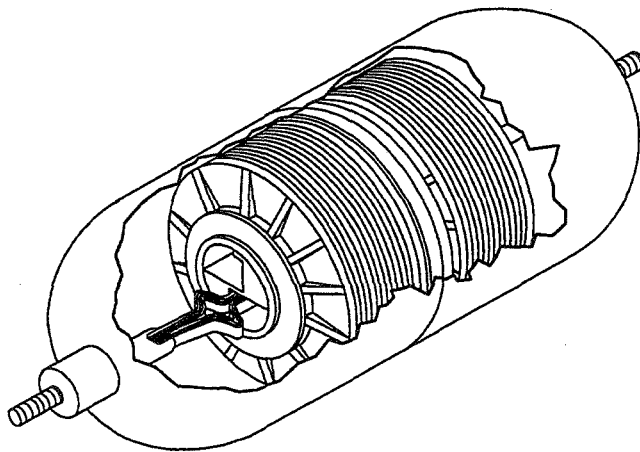


FIGURE 2

SINGLE PRESSURE VESSEL DESIGN FEATURES

The next logical step after the CPV design, which contains only two cell stacks, is to incorporate an entire multicell battery within a single pressure vessel. The single pressure vessel NiH_2 battery design concept is a full battery of series-connected cells within a single hermetically sealed container (Figure 3). The number of cells within the battery is a function of the desired voltage. Each SPV cell delivers the 1.25 VDC typical of the NiH_2 couple. In this design, each cell shares a common hydrogen atmosphere within the battery pressure vessel. Therefore each cell is operating at the same hydrogen pressure throughout charge and discharge. This provides a pressure balance between cells. The individual cell doesn't contain a net pressure differential with the internal battery atmosphere. The advantages of this design concept are increased volumetric energy density and specific energy, improved performance, reduced complexity of construction and decreased overall battery cost. For a typical 28 VDC spacecraft battery, a single container of twenty-two series-connected cells is more efficient than twenty-two individual, smaller pressure vessels. (1)

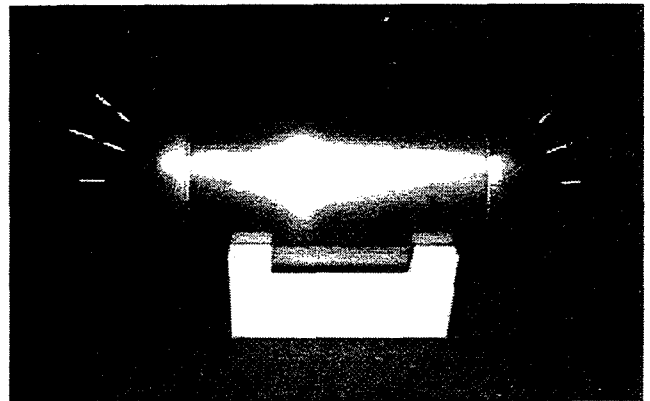


FIGURE 3

SINGLE PRESSURE VESSEL CELL DESIGN

Cell design is a critical aspect of the SPV battery system. The cell design must conform to a variety of mechanical, electrical and thermal interface requirements at the battery level. The semi-circular lightweight plastic cells use a dual-layer plastic bag and conform to a ten inch diameter battery pressure vessel. Cell geometry is designed to fit a cylindrical pressure vessel, which is discussed in the next section as part of the overall battery design. The overall cell design concept is to maintain electrolyte integrity and isolation for each cell while allowing the free exchange of common hydrogen gas throughout the battery. This is accomplished by venting the plastic cell case with a microporous plug which selectively allows the diffusion of hydrogen gas while preventing the passage of water or electrolyte. The holes in the material are small enough so that the surface tension of the electrolyte blocks its passage but large enough to allow sufficient hydrogen flow into and out of the

1997 NASA Aerospace Battery Workshop, Huntsville, AL, Nov.18-20, DC041097.PM6

cell. The hydrogen gas pressure inside the SPV cell remains equalized with the ambient pressure within the battery pressure vessel. This eliminates the requirement of the individual cell case to contain any pressure. The SPV cell operates in a starved electrolyte mode, as with other NiH₂ cell designs, so there is virtually no free electrolyte. Nearly all of the electrolyte contained by the cell is absorbed within the electrodes and separators.

Cell mechanical design is oriented primarily towards electrolyte containment. The physical structure of the cell is simply the interleaved electrode stack containing the electrodes and separators. Electrical design of the cell consists of connecting electrodes of the same type electrically in parallel. The capacity of the cell is determined by the number of nickel electrodes connected in parallel. (The hydrogen electrodes are likewise connected electrically in parallel.) The electrical connections are made by welding electrical tabs to a comb-type bus bar. The hydrogen electrode contains an integral tab and the nickel electrode has a welded tab. Because of the cell geometry, the tabs in an SPV cell are much shorter than those in an IPV cell. This results in an overall low impedance cell design (typically less than half the impedance of an IPV cell). The bus bar design also provides some additional mechanical support to the electrodes and helps preclude electrical short-circuit between opposing electrodes.

SINGLE PRESSURE VESSEL BATTERY DESIGN

The SPV battery design is similar to standard 3.5 inch NiH₂ space-flight cell technology. The Inconel alloy pressure vessel is a cylinder with hemispherical domes on either end. This configuration allows the maximum strength-to-weight ratio for containing gas pressure with the minimum material weight. The pressure vessel maintains a 2.5:1 safety margin, based on the maximum operating pressure of the battery, and is classified as a leak before burst container under MIL-STD-1522. Normal battery operating pressure may range up to 800 psi, depending on the specific battery design and the free volume available to contain the hydrogen gas required for operation.

The electrical feedthroughs for the battery use a mechanical compression seal. The battery electrical terminal passes through, and is insulated from, an Inconel terminal boss. A machined polymeric material is mechanically crimped into place and forms the actual seal around the battery electrical terminal. The Inconel pressure vessel is closed by laser welding the two dome ends to the cylindrical body of the battery. This provides a hermetic seal. A weld ring is incorporated into each of the two weld joints.

The internal design and construction of the battery is shown in Figure 4. The semi-circular cells are arranged in pairs to form a circle and those circular pairs are arranged along, and perpendicular to, the central longitudinal axis of the battery. The number of cells included determines the battery output voltage. Each pair of cells is contained in a flat thermal cooling plate with radial fins which contact the battery pressure vessel wall. The fins on each cooling plate are sprung outward slightly in order to make positive

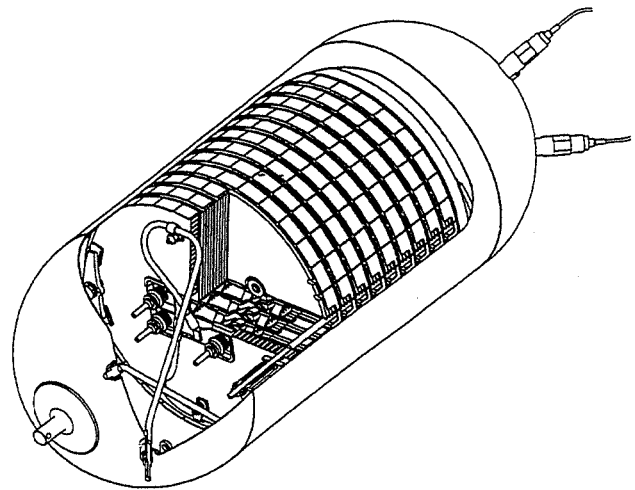


FIGURE 4. SPV BATTERY.

mechanical contact with the pressure vessel wall when inserted during battery assembly. This provides a maximum, direct thermally conductive path to remove heat from the cell to the pressure vessel where it can be dissipated into an exterior heat sink, such as a battery baseplate or thermal radiator in the spacecraft. The thermal plate is constructed of lightweight aluminum and has a nickel coating. The plate is electrically isolated from the adjacent cells by the plastic cell case.

The cell electrical terminals are arranged along the central axis of the battery to minimize resistance within the plates. A mechanical connection is used between the terminals of the adjacent cells; all of the connections within the cell are welded. Large conductor cross-sections are used to further minimize IR voltage drop.

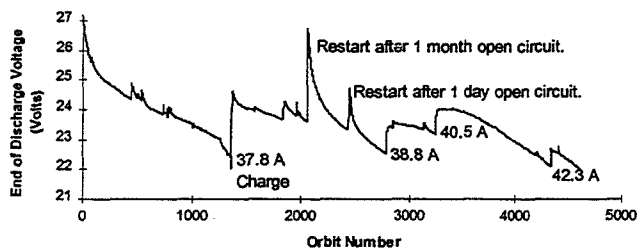
TESTING

The EPI SPV design has been optimized for electrical performance. The impedance of the 50 Ah SPV battery, SAR 10065, is less than half that of a representative 50 Ah IPV battery. Beyond the immediately apparent benefits of lower charge voltage and higher discharge voltage, this also increases the current carrying capability of the battery. As part of its acceptance test procedure, the SAR-10065 undergoes current rates in excess of C/2 for charge and 2C for discharge. In addition, heat generation increases directly with impedance, thus the SPV allows the use of a smaller, lighter weight cooling system.

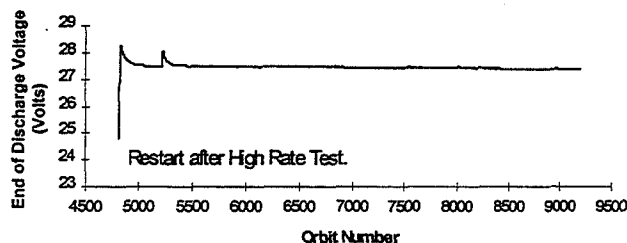
In order to prove the durability of the design, an accelerated life test and three full length life tests were initiated. The recently completed accelerated life test, run at 10°C, subjected a 43 Ah actual capacity battery to successive 100 minute LEO cycles. The cycles consisted of a 36.7 A charge for 51 minutes followed by 36.7 A discharge for 49 minutes, for a depth-of-discharge (DOD) of approximately 70%. Over the course of the test, the charge rate was increased as necessary to keep the end of discharge voltage (EODV)

above 1 V/cell. An EODV plot for the 4612 cycle test is shown in Graph 1. Where not otherwise noted, discontinuities represent short (four hours or less) periods of open circuit.

After the high rate test, a low rate test was performed. In this test, also a 100 minute LEO cycle, the battery was charged at 16.1 A for 51 minutes and discharged at 15.6 A for 49 minutes, for a DOD of approximately 31%. The 4812 cycle EODV plot of this test is shown in Graph 2.



GRAPH 1. HIGH RATE EODV VS ORBIT NUMBER



GRAPH 2. LOW RATE EODV VS ORBIT NUMBER

The ongoing full length life tests are 100 minute, 31% DOD LEO cycles. Both the charge and discharge waveforms are pulsed (the details of the profile are proprietary). After more than 15,900 cycles, a 50 Ah nameplate test battery, operating at 10°C, has exhibited excellent electrical characteristics and is expected to exceed the 25,000 cycle specification requirement. Two other full-length life test batteries, operating at -5°C and 5°C, have completed over 7500 and 4100 cycles respectively, and have shown the same positive results.

MANUFACTURING CAPABILITY

By virtue of its design, the SPV battery is better suited to high volume production than the IPV battery. The use of one pressure vessel requiring only 2 girth welds is much easier produced than a 22 cell IPV battery requiring 22 welds. Proof pressure testing of a single pressure vessel is also much faster and easier than repeating the same process on 22 IPV cells. In addition, gas management is simplified by reducing the number of hydrogen seals from 66 to 4

and all cells are at the same pressure, leaving only one pressure to be monitored and set. Efficiency is also gained by activating and testing the cells in the final battery configuration. With an IPV battery, there is a cell acceptance test procedure (ATP) and a battery ATP, so the cells are subjected to essentially the same test procedure twice.

The internal design of the SPV is also well suited to production speed and efficiency. The plastic cell cases require less fabrication time and fewer high tolerance parts than the metal IPV enclosures. There are less than one third as many plates in each cell (the SPV plates are larger). This reduces the amount of plate preparation, speeds cell assembly and helps to decrease the total part count to less than half that of an equivalent IPV battery.

These factors, along with intensive process development, continuous refinement, capital investment and an ISO 9001 style quality system (certification anticipated June, 1998), have helped EPI achieve a single shift manufacturing capability of one 22 cell, 60 Ah SPV battery per week, as well as a testing capacity of 12 finished batteries. EPI has produced 15 Ah, 30 Ah, 50 Ah and 60 Ah, 27 volt (22 cell) SPV batteries, and the modular nature of the design allows rapid development of capacities up to 120 Ah as well as higher or lower voltages. As of this writing, over 60 SPV's have been delivered.

ACKNOWLEDGMENTS

The authors would like to acknowledge the contributions of Lockheed Martin-Sunnyvale, and the assistance of Sharon Wecker in the editing, manuscript preparation and publication of this paper.

CONCLUSIONS

The Eagle-Picher NiH₂ SPV battery provides lighter weight, smaller volume and better electrical performance than a comparable IPV system. This, combined with high rate production capability, short development time for different configurations and low cost make the Eagle-Picher SPV well-suited for satellite energy storage.

REFERENCES

- Coates, D.K., Ansley R.E., Cooper, S.C., Morgan, J.L. and Fox, C.L., 1995, "The Design and Manufacture of Nickel-Hydrogen Batteries for Spacecraft Power Systems," 16th ICSSC, Washington D.C.
- Coates, D.K., Grindstaff, B.S. and Fox, C.L., 1995, "Single Pressure Vessel (SPV) Nickel-Hydrogen Battery Design," in Proc. 10th Annual Battery Conference on Applications and Advances, California State University, Long Beach, CA.

MECHANICAL BEHAVIOR OF NICKEL OXIDE ELECTRODE UNDER SHALLOW CYCLES AND OVERCHARGE

G. Davolio, E. Soragni, P. Zannini and P. Baraldi

Department of Chemistry, University of Modena
183, Via G. Campi, I 41100 Modena, Italy.

1. Introduction

Mechanical effects of cycling on Nickel Oxide Electrode (NOE) have been observed for a long time: swelling and bulging, with shedding of active mass are the main physical defects, often associated with capacity fading. Studies of the mechanical aspects related to the electrochemical reactions on NOE are rather new. Such studies were not possible on pocket electrodes, since the external perforated metal strip constrains the active mass, so hindering any measurement of that phenomena. They can be done, on the other hand, on NOEs with an interior current collector, such as sintered, metal felt or metal foam supported and plastic bonded electrodes. Some physical properties of these electrodes (expansion, elongation, Young's elastic modulus), are related to volume changes, associated to phase transitions caused by the electrochemical reactions. These studies open a possible way for a better understanding of the failure mechanisms, by evaluating the effects of fabrication variables and cycling conditions on the electrode internal stresses, therefore giving experimental bases for a reliable prediction of the electrode life.

Several works have been done on this line by various authors; the following physical properties have been studied: bending of asymmetric electrodes (1, 2), elongation (3), thickness changes (4,5), electrical resistivity (6), Young's flexural elastic modulus (7, 8). In Figures 1-4 are reported drawings of some experimental set-up of measurements. The main results of these studies are that on cycling of NOE the active mass expands during the discharge half-cycle and contracts during recharging half-cycle; the stress exerted on the supporting structure (sinter) brings about the expansion of the electrode. The expansion-contraction process is only partially reversible; the irreversible part being due to the plastic deformations of the supporting structure and to some degree of irreversibility of the phase transitions of the active material. Some effects of manufacture and cycling variables on NOE expansion have

also been established, confirming the experimental findings that both the increase of the level of impregnation or the depth of discharge enhance electrode expansion with a negative effect on cycle life (9,10).

Sintered NOEs show often a more or less evident asymmetry with respect to net or perforated sheet acting as the current collector (Fig. 5). In this cases a volume expansion of active mass originates a bending moment, which acts against the stiffness of the structure and is related to the asymmetry of the electrode. In Fig. 5a is sketched the longitudinal section of an asymmetric uncycled electrode, and in Fig. 5b, the same section of a discharged Nickel electrode, bent as a result of the active mass expansion. The opposite behavior is shown, for example, by an asymmetric metal-hydride electrode, since its active mass expands during charge and contracts during discharge (11, 12). In the case of an asymmetric iron electrode we observe a bending during the first plateau, corresponding to the reaction: $Fe \rightarrow Fe(OH)_2$. The bending decreases during the second plateau, owing to the contraction of the active mass by the reaction $Fe(OH)_2 \rightarrow FeOOH$ (13).

By applying the *Mechanics of deformable bodies* and the theory of *cantilevered beam* (14) to a bent asymmetric electrode, clamped at one end, we have that the bending moment M , is balanced by a Force F , applied at a distance L . This force cancels the displacement, z , of the free end, brought about by the changes of the active mass: the following relation holds (Fig. 6):

$$z = FL^3/3YI \quad (1)$$

where I is the *momentum of inertia of the cross section* ($I=bh^3/12$), relating to a beam cross section of length b and eighth h .

and Y is the *Young flexural elastic modulus*.

If we consider the model of sintered NOE as a *composite material*, constituted by sinter, active mass and voids, (Fig. 7), and apply the principles of *Micromechanics*, holding for composite materials (14), we obtain:

$$Y_{\text{electrode}} = (Y_s Y_{am} / (Y_s V_{am} + Y_{am} V_s)) (V_{am} + V_s) \quad (2)$$

where :

Y is Young's flexural elastic modulus

V is the Volume fraction of a component

and the subscripts s and am refer to sinter and active mass respectively.

If the displacement z is kept constant, the force F , balancing the bending moment, depends only on the properties of the active mass (Volume fraction and Modulus), which in turn depend on the state of charge, then by combining the relations (1) and (2) we have:

$$F = z/L^3/3YI = \text{const.} (Y_s Y_{am} / (Y_s V_{am} + Y_{am} V_s)) (V_{am} + V_s) \quad (3)$$

It follows from the equation (3) that phase transitions and/or volume changes of the active mass influence the balancing force F , whose changes can be measured by a balance in the experimental set-up as reported in the draw of Fig. 8. The electrode E is

clamped at one end to the cell and the free end is mechanically connected to a balance through a rigid rod and a weight, w . This weight allows the maintaining a constant deflection, z of the electrode and the possibility of recording the values of the force F during a charge-discharge cycle, and measuring the changes in the bending moment of the electrode.

The aim of this work is to find a correlation between mechanical behavior and structural changes of the active mass. Another task is to collect data in order to establish efficient conditions of accelerated tests for reliable life predictions. The latter problem is related to the stability of the sinter structure under the stress produced by the active mass changes; in effect the force we measure is a direct measure of the stress suffered by the supporting structure during cycling.

Experimental.

Owing to the irreversible expansion, the shape of an asymmetric electrode, working as a *cantilevered beam*, bound at one end, shows after cycling a permanent bending, as sketched in Fig. 9a; the permanent expansion leads also the electrode to take the shape represented in Fig. 9b. In order to maintain the original shape of the electrode, such as normally occurs in practical cells, we have applied the principle of Fig. 9c, accomplished as sketched in Fig. 9d. The electrode is clamped both at the extremities: the end with the current collector is clamped at C, fixed to the electrolytic cell, the other end is clamped to the frame A, free of pivoting around the axis X: the bending moment is equal to $F \cdot b$.

By using the electrode assemblage of Fig. 9d, placed in the cell of Fig. 8 we have studied the electrochemical and mechanical behavior of Nickel oxide electrodes, with these characteristics:

Type A: chemical impregnation, Co content: 2,9%.

Type B: electrochemical impregnation, Co content 4,3%

Type C: electrochemical impregnation, Co content 8,2%.

All the tested electrodes had been manufactured on a sintered nickel support.

The testing procedure was as follows: a strip, 5 cm long and 0.5 cm wide, is cut from the asymmetric plate. After the conducting tab is welded, the two extremities are masked with teflon tape, leaving it uncovered for a length of 2cm. The asymmetric electrode is then placed in the cell, the masked areas are clamped within the frames, as in Fig. 9d. The cell is filled with the solution and the level of the balance is lowered in order to have a force of some grams with a displacement, z , in the order of tenth of mm. These values depend upon the characteristics of the electrode, the only important condition is to maintain the electrode in the elastic range of the supporting structure. On the other end one must remember that ΔF , and not the absolute value of F , is of interest.

Once the experiment was started no further change in the dimensional parameters of the apparatus was done. The change of the solution, for example, is performed by rotating taps without touching the cell. Each cycle of one test, consisting of various

runs, was numbered and the cycle number (#) is reported in the *legenda* of the following figures.

Three runs of experiments have been performed: i) regular cycles, ii) shallow cycles, iii) overcharge. KOH solutions of different concentrations (6 N and 10 N in deionized water) and different temperatures (0°C, 20°C and 40°C) have been used in the tests. The electrodes were cycled at constant current, with an AMEL galvanostat (model. 545) controlled by a timer (in charge and in shallow cycles) or a voltage sensor. A Hg/HgO reference electrode and a cadmium counter electrode were used.

The regular cycle was performed by charging 75 minutes at 1C current; shallow cycles were performed by discharging to 30%-50% DoD, recharging with a 20% overcharge of the discharged capacity. The overcharge lasted normally two hours at 1C.

All the data refer to discharges following said cycling schedule (regular, shallow or overcharge) and a regular recharge.

Results and discussion.

Electrode voltage ($V_{vs. Hg/HgO}$) and $F(N-2)$ values were recorded vs. Time during the discharge-charge cycles. The records vs. Time were changed in vs. Capacity records, a representation giving a more immediate view of the related physical phenomena. For example in Fig. 10a is shown a typical record of Force, Voltage and Current vs. Time, and in Fig 10b the plots of Force and Voltage vs. Capacity. In the latter plot the capacity has positive values during charge and negative in discharge. The arrows indicate the temporal sequence of experimental points. The origin of the plots, zero value Capacity, is represented by the charged electrode, so in Fig 10b the discharge of the electrode begins at point O and proceeds to be completed at point P, where the current is reversed and starts the recharge. A first comment on the mechanical behavior concerns a "negative hysteresis" in the Force/Capacity plot: the stress slowly increases during the discharge and it is quickly relieved during the first 10-15% of recharging. On the far left of the same plot we observe some negative value of Capacity, corresponding to overcharge. In this case overcharge does not bring about increase of Force. We will see later that an increase of Force occurs during overcharge in some particular conditions (γ -phase formation).

We have studied the NOE behavior during shallow cycling and overcharging, owing to the related practical interest, since these cycling conditions often occurs in the normal use of nickel-based storage batteries and produce in discharge the well known 40-60 mV Voltage depressions, the so called '*memory effect*' (15), related to phase changes in the active mass (16).

Several are the variables tested, such as type of impregnation, Co content, KOH concentration and temperature. The electrochemical and mechanical parameters one can take into account for a comparison are the amount and shape of Voltage depression and the dependence of the Force upon the Capacity delivered or accepted by the electrode.

Some of the most significant results are presented in Figures 11-13, relating to the three electrodes in 6N KOH at 20°C. In all the conditions the full discharge following shallow cycles shows a voltage depression at the same capacity as that of the repeated shallow discharges. The voltage depression is accompanied by an increase in Force, with respect to the behavior after regular cycle. This means that higher internal stress is suffered by the electrode during the shallow cycling. Two hours overcharge at 1C do not produce notable changes on the electrochemical and mechanical behavior of A and C type electrodes. A remarkable effect is observed on B type electrode (Fig. 12): it appear greatly stressed after overcharge. In discharge the stress remains high for about the 30% of the capacity, then it decreases at the end of the discharge. The voltage depression appears in discharge and the voltage/capacity slope is lower than after normal charge.

All these results are in agreement with the hypothesis that γ -NiOOH is formed during overcharge, as suggested by the well known Bode cycle (Fig.14), and by the physical parameters of the Nickel compounds, reported in Table 1.

Table 1
Crystallographic parameters of exagonal unit cell and densities of Nickel oxhydroxides, related to NOE.

(reference)	a/cm-8 (18, 19)	c/cm-8 (18, 19)	Density/g.cm-3 (20)
α -Ni(OH) ₂ ,	3.13	8-9	2.82
β -Ni(OH) ₂	3.13	4.6	3.97
β -NiOOH	2.82	4.7	4.68
γ -NiOOH	2.82	7,2	3,79

The discharge of γ -phase gives rise to α -phase of high molar volume, so the stress remains unchanged for some time, then the stress goes down due to the transition α -Ni(OH)₂ ----> β -Ni(OH)₂, with molar volume decrease.

The comparison with the various types of electrodes shows that the factors (temperature and KOH concentration) enhancing γ -NiOOH formation bring about stressed electrodes during overcharge. The electrode type C, for example, did not show voltage depression nor mechanical stress in the discharge after overcharge in 6N KOH at 20°C (Fig. 13). This electrode becomes susceptible to γ -NiOOH formation when cycled in 10 N KOH at 20°C, under both shallow cycling and overcharge (Fig. 15).

The electrode type A, when it is overcharged in 10N KOH at 40°C.during 3.5 hours shows to be susceptible to γ -NiOOH formation, whereas it did not do it when

had been overcharged 5 hours at 0°C nor 3.5 hours at 20°C in the same solution: 10 N KOH (Fig. 16)

Regarding to the effect of the method of impregnation-one observes a different behavior of chemically impregnated electrode (type A), with respect to the electrochemically impregnated one (types B and C): in the regular cycling the former shows a force increase as soon as the discharge begins (Fig. 11, 16), the latter shows the force increase after the 20-30% DoD has been reached (Figures 12, 13, 15). One must note that shallow cycling reduces that DoD (Fig. 12) and the same effect has the overcharge in the case of low susceptibility to γ -phase formation (Fig. 13, type C, 6N KOH, 20°C) The model of sintered NOE of fig 7 can help in explaining the different mechanical behaviors: the electrochemical impregnation deposits the active material on the walls of the sinter network, so the voids are regularly distributed in the porous structure. At the beginning of the discharge these voids can accommodate part of the expanded mass; only after that, the further expansion brings about stress on the structure and the bending moment arises. In chemically impregnated electrodes the active mass is distributed at random into the structure, no well distributed voids are present, so that the stress arises as soon as starts the discharge. The different aspects of the surfaces of the electrodes type A and C are shown on the SEM micrographs reported in Figures 17 and 18.

Conclusions

- Mechanical stress on the supporting structure, related to phase changes, can be detected, *in situ* during cycling, with the aid of the technique described.
- Overcharge originates γ -phase, with active mass expansion; further expansion may occur in discharge, due to reduction $\gamma\text{-NiOOH} \rightarrow \alpha\text{-Ni(OH)}_2$: the following transition $\alpha\text{-Ni(OH)}_2 \rightarrow \beta\text{-Ni(OH)}_2$ occurs spontaneously with volume contraction.
- Repeated shallow discharges also originates γ -phase, the stress on the structure, developed when the discharge occurs is higher than after regular cycles. This stress arises at the same time of the voltage depression and occurs at the same DoD of the shallow cycles.
- An increase of temperature or concentration enhances the susceptibility to γ -phase formation in overcharge.

Aknowledgments.

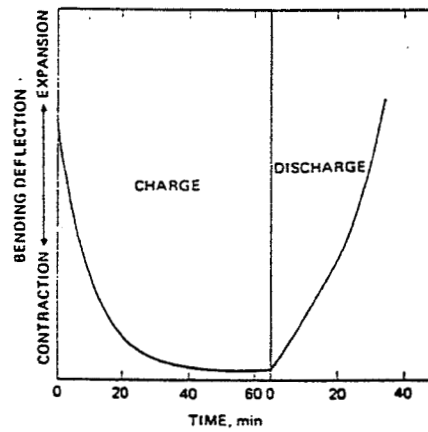
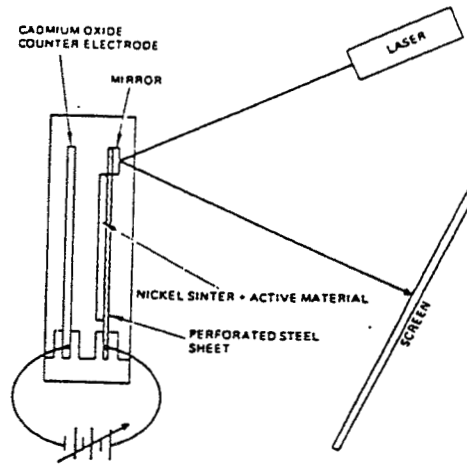
This work has been funded by MURST (Ministero dell'Università e della Ricerca Scientifica), Rome.

Test electrodes have been supplied by :

- Eagle-Picher Industries, Joplin (MO) and Colorado springs (CO).
- Office of Research and Development, Washington (DC)

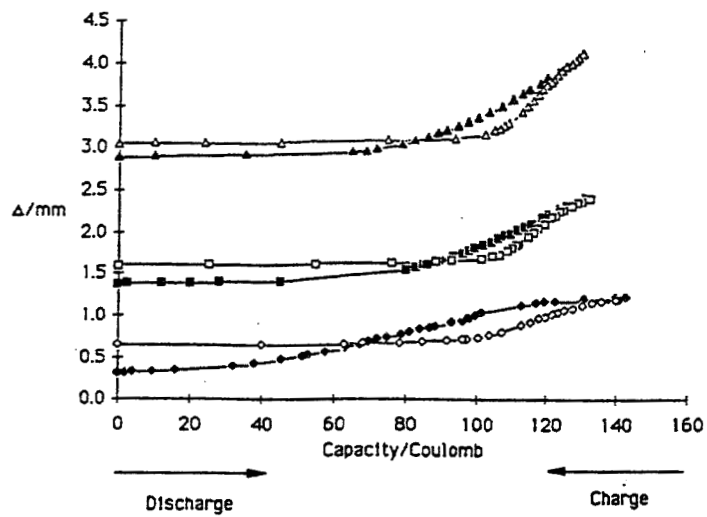
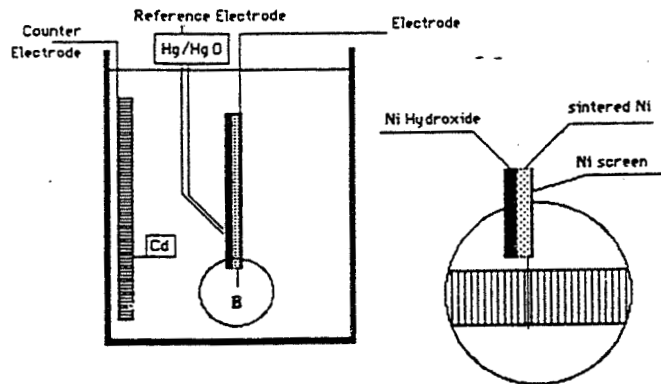
References;

- 1) H. S. Lim and S. A. Werzwyvelt, *NASA Conference Publication* no. 2177, 175 (1980)
- 2) G. Davolio, E. Soragni, "Power Sources 11", L.J. Pearce editor, International Power Sources Symposium Committee, Leatherhead (U.K.), 1987, p.227
- 3) D.H. Fritts, *J. Electrochem. Soc.*, **129**, 118 (1982).
- 4) M. Oshitani, T. Takayama, K. Takashima and S. Tsuji, *J.Appl.Electrochem.*, **16**, 403 (1986).
- 5) K. Micka, J. Mrha and B. Klapste, *J. Power Sources*, **5**, 207 (1980)
- 6) D. H. Fritts, "Power Sources 7", J. Thompson, editor., Academic Press, London, 1981, p.105.
- 7) G. Davolio, A. Da Pieve and E. Soragni, *Power Sources 12*, T. Keily and B.W. Baxter, editors, International Power Sources Symposium Committee, Leatherhead (U.K.), 1989, p. 253.
- 8) L. H. Thaller and T. P. Barrera, *Proceedings E.S.A. Conference*, Florence, 2-6 Sept., 1991.
- 9) H. S. Lim and S. A. Werzwyvelt, *Proceedings of 20th IECEC Conference*, Miami Beach, FL, August 1985, p.164.
- 10) G. Davolio, A. Da Pieve and E. Soragni, *Nickel Hydroxide Electrodes*, D.A. Corrigan and A. H. Zimmerman editors, The Electrochemical Society Inc., Proceedings Volume 90-4, p. 281.
- 11) G. Davolio, E. Soragni and C. Fontanesi, in Ext. Abst. of the Spring 1986 Meeting of the Electrochem. Soc., The Electrochemical Society Inc., Pennington, New Jersey, Vol. 96-1, p. 91
- 12) A. Pecheron-Guegan, M. Latroche, A.J. Achard, Y.Chabre, J. Bouet, *Hydrogen and Metal-Hydride Batteries*, P. D. Bennet and T. Sakai eds, The Electrochem. Soc. Inc., Pennington, New Jersey, Proc. Vol; 94-27, 1994, p. 196
- 13) G. Davolio, A. Da Pieve, P. Baraldi and E. Soragni, *Journées DElectrochimie 89*, Montpellier (France), Résumé des Communications, A 7-12
- 14) M. P. Feynman, R. B. Leighton and M. Sands, *Lectures in Physics*, Addison Wesley, Reding, Mass. 1966, Vol. 2, sect. 18-9
- 15) G.Weidmann, P. Lewis and N. Reid, editors. "Structural Materials", Butterworths, London, 1990, p. 332.
- 16) R.N. Thomas, *Modern Battery Technology*, C.D.S. Tuck, editor, Ellis Horwood Ltd, New York 1991, p. 276.
- 17) Y. Sato, K. Ito, T. Arakawa, and K. Kobayakawa, *J. Electrochem. Soc.*, **143**, L225 (1996).
- 18) C. Faure, C. Delmas, M. Fouassier, *J. Power Sources*, **35** (1991) 279.
- 19) H. Bode, K. Dehemelt and J. Witte, *Zeit. An. All. Chemie*, **366** (1969) 1.
- 20) H. Bode, K. Dehemelt and J. Witte, *Electrochim. Acta* **11** (1966) 1079.



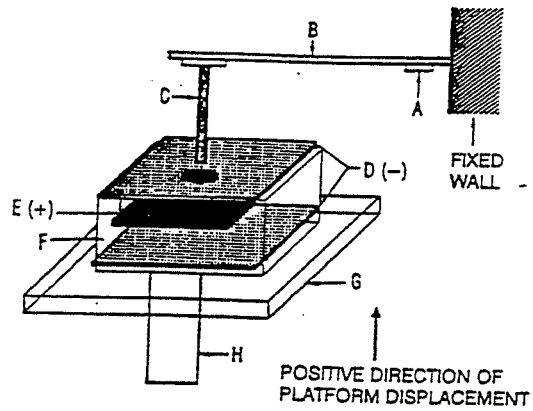
H. S. Lim and S. A. Werzwyveit, NASA Conference publ. n° 2177
 (1980) p. 175. (Bending of asymmetric electrode)

Fig. 1



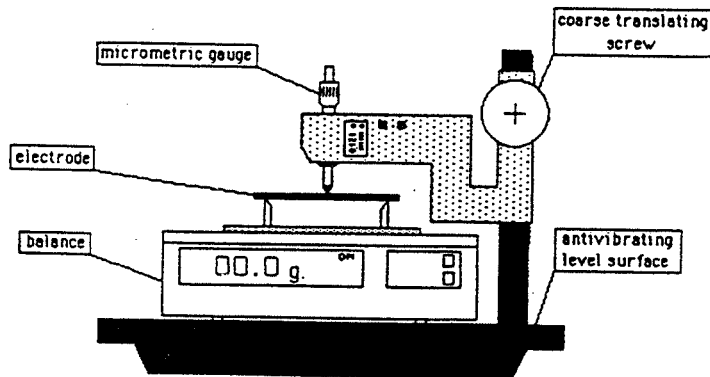
G. Davolio, E. Soragni, "Power Sources 11", L. J. Pearce editor, International Power Sources Symposium Committee, Leatherhead (U.K.), 1987, p.227 (Bending of asymmetric electrode)

Fig. 2



L. H. Thaller and T. P. Barrera, *Proceedings E.S.A. Conference*, Florence, 2-6 Sept., 1991. (Elastic modulus of electrodes)

Fig 3



G. Davolio, A. Da Pieve and E. Soragni, *Power Sources 12*, T. Keily and B.W. Baxter, editors, International Power Sources Symposium Committee, Leatherhead (U.K.), 1989, p. 253. (Elastic modulus of electrodes)

Fig. 4

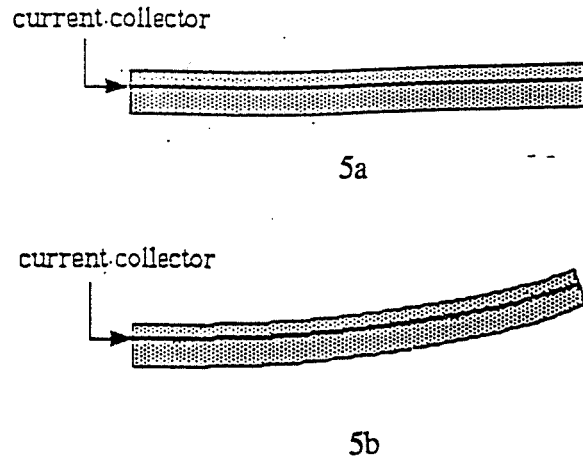


Fig. 5. Sketch of the cross-section of asymmetric NOE.
 5a) charged (or uncycled)
 5b) discharged.

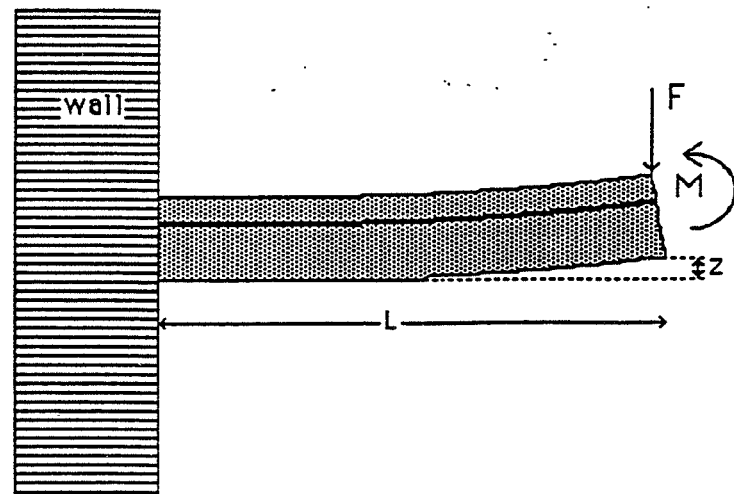


Fig. 6 Asymmetric electrode as a *Cantilevered beam* fixed at one end

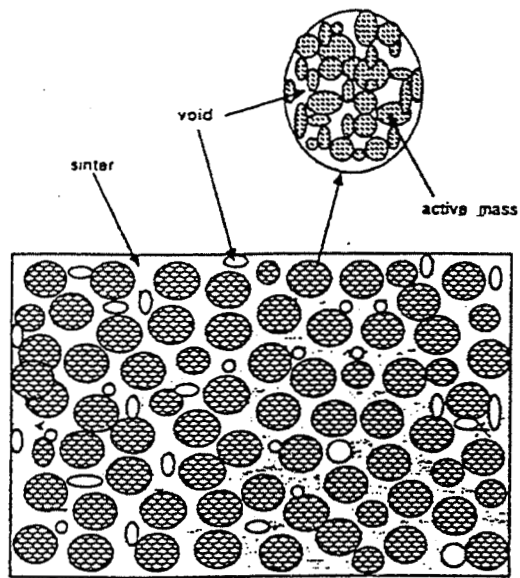


Fig. 7 Sketch of a model of sintered NOE, as a *composite material*, made by sinter, active mass and voids

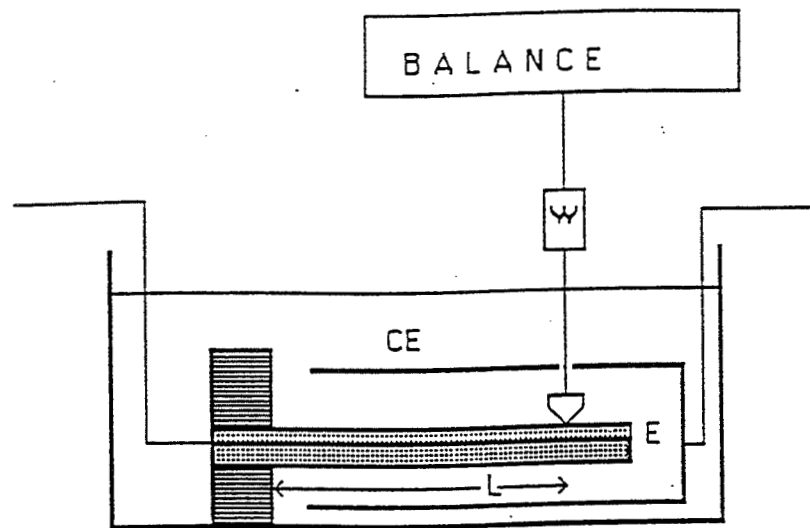


Fig.8. Draft of the cell for electrochemical and mechanical tests.

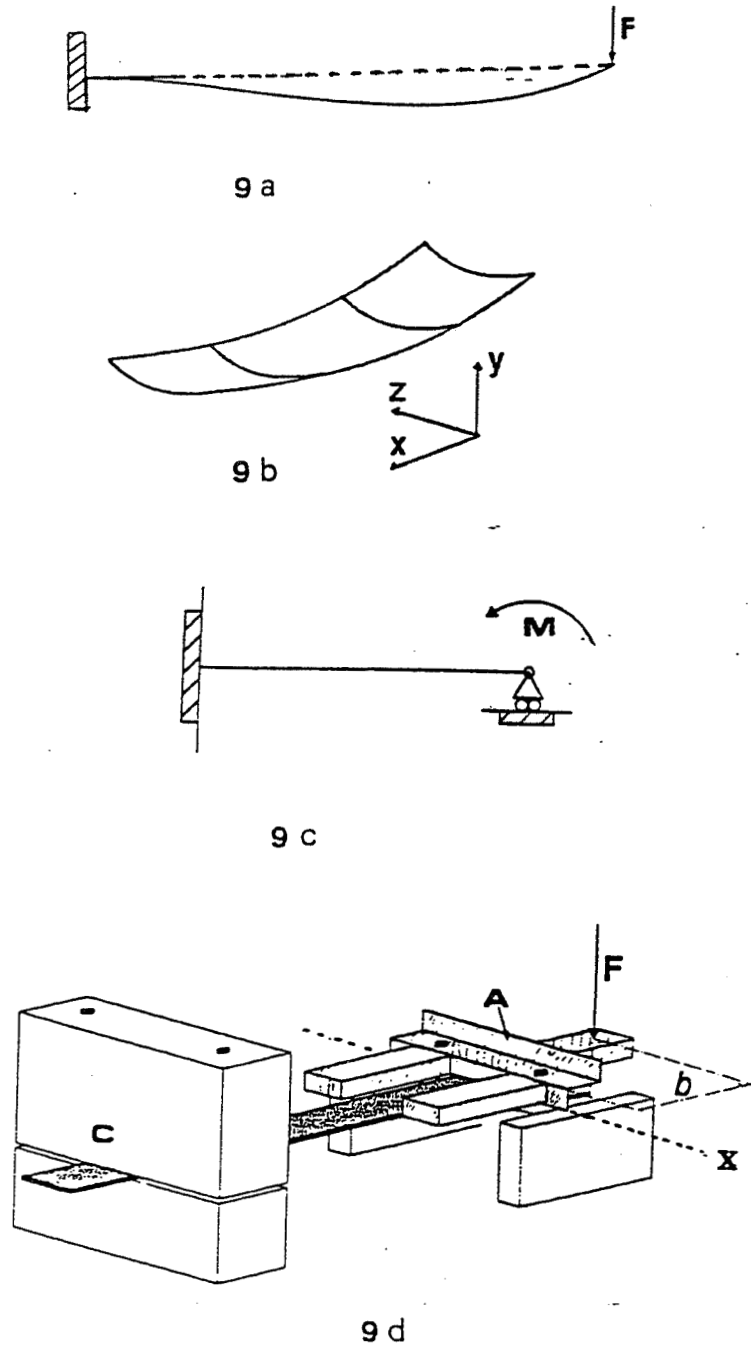


Fig. 9 System for maintaining the electrode planarity during cycling.

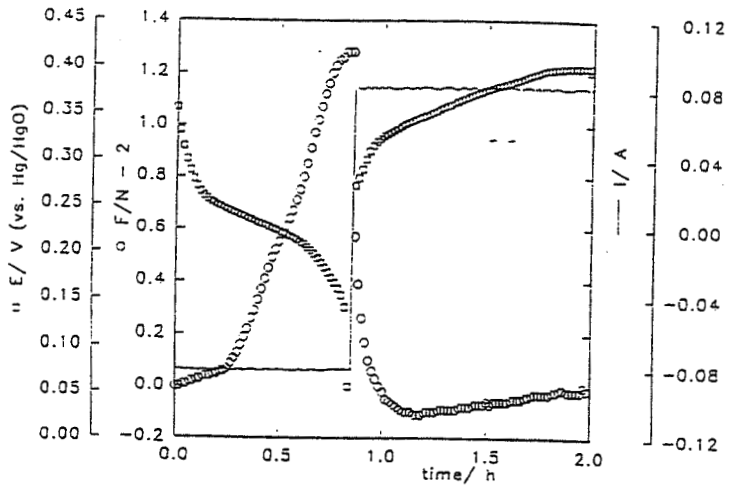


Fig. 10 a) Typical record of Force (F) , Voltage (V) and Current (I) vs. Time , during a discharge- charge cycle

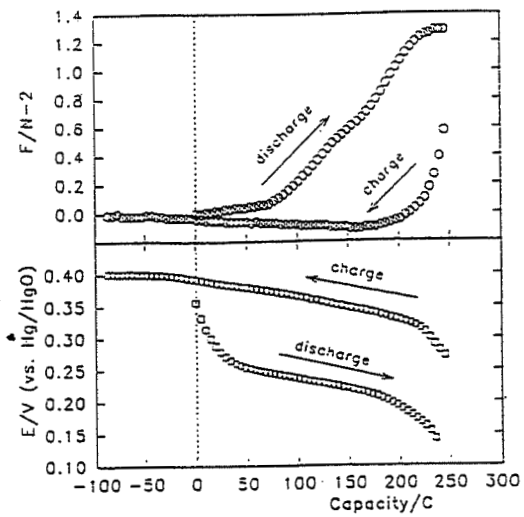


Fig. 10b) Plot of the data of Fig. 10a vs. Capacity

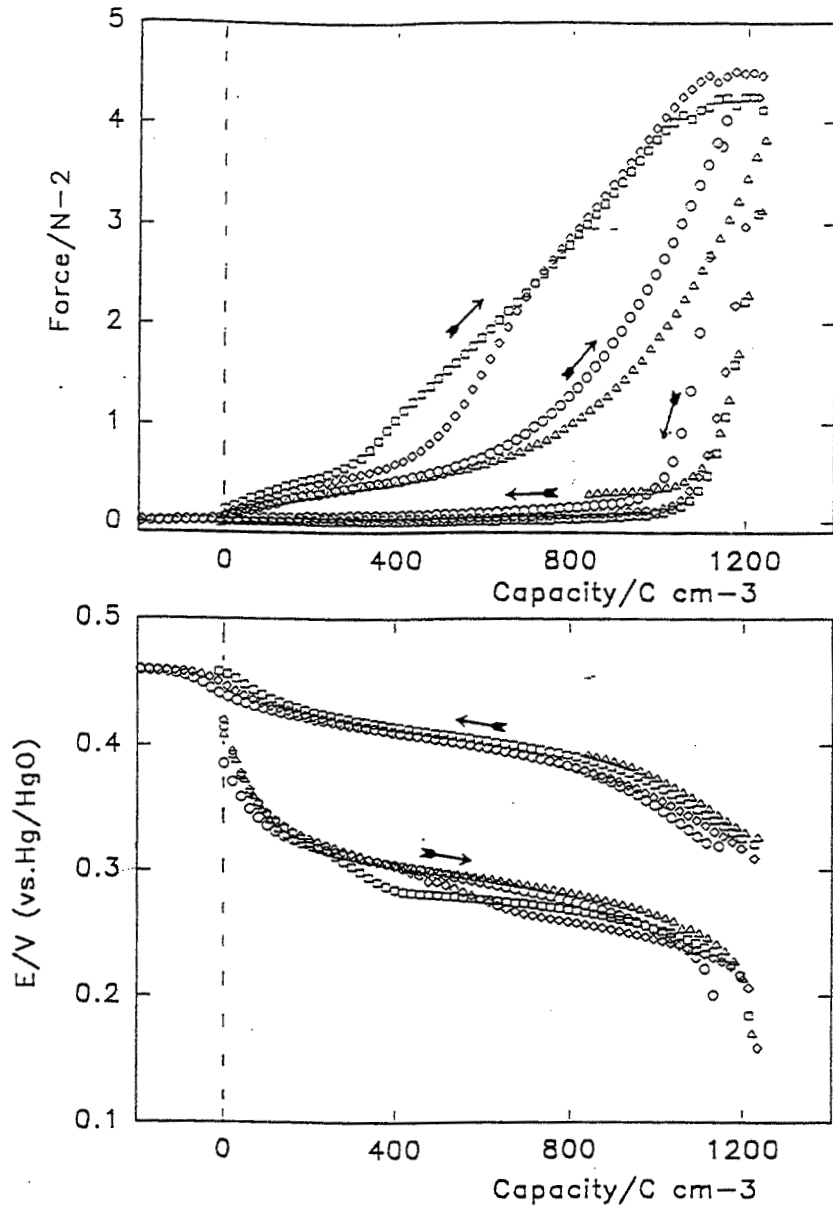


Fig. 11. Force and Potential vs. Capacity. type A, 6N KOH, 20°C.
 ○ cycle # 135, regular charge, □ : cycle # 114, 19 shallow cycles, disch. 30% DOD, ◇ : cycle # 132, 11 shallow cycles, disch. 36% DOD, △ : cycle #116, overcharge 1C 2 hours.

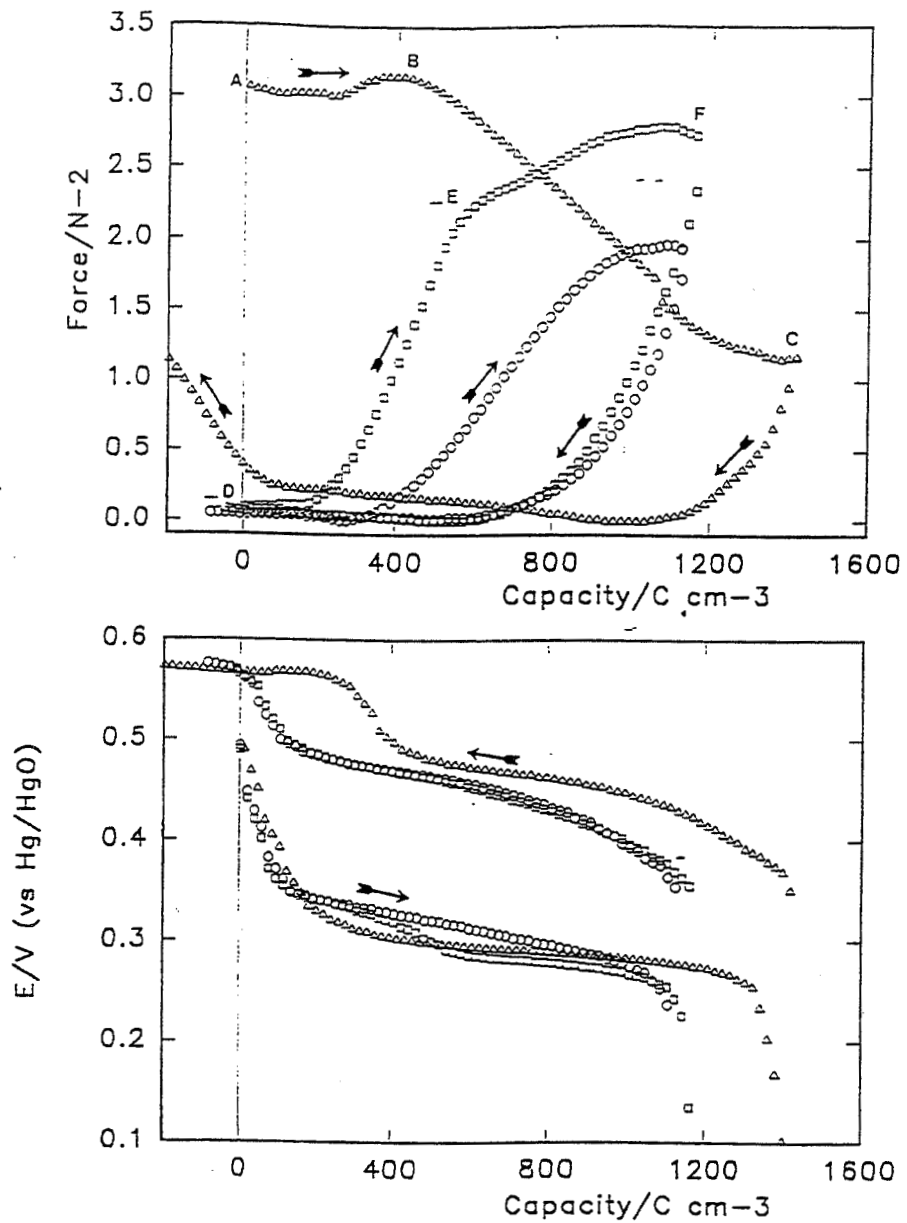


Fig.12. Force and Potential vs. Capacity. type B, 6N KOH, 20°C.
 ○ : cycle # 118, regular charge, □ : cycle # 114, 48 shallow cycles,
 disch. 50% DOD, △ : cycle #122, overcharge 1C 2 hours.

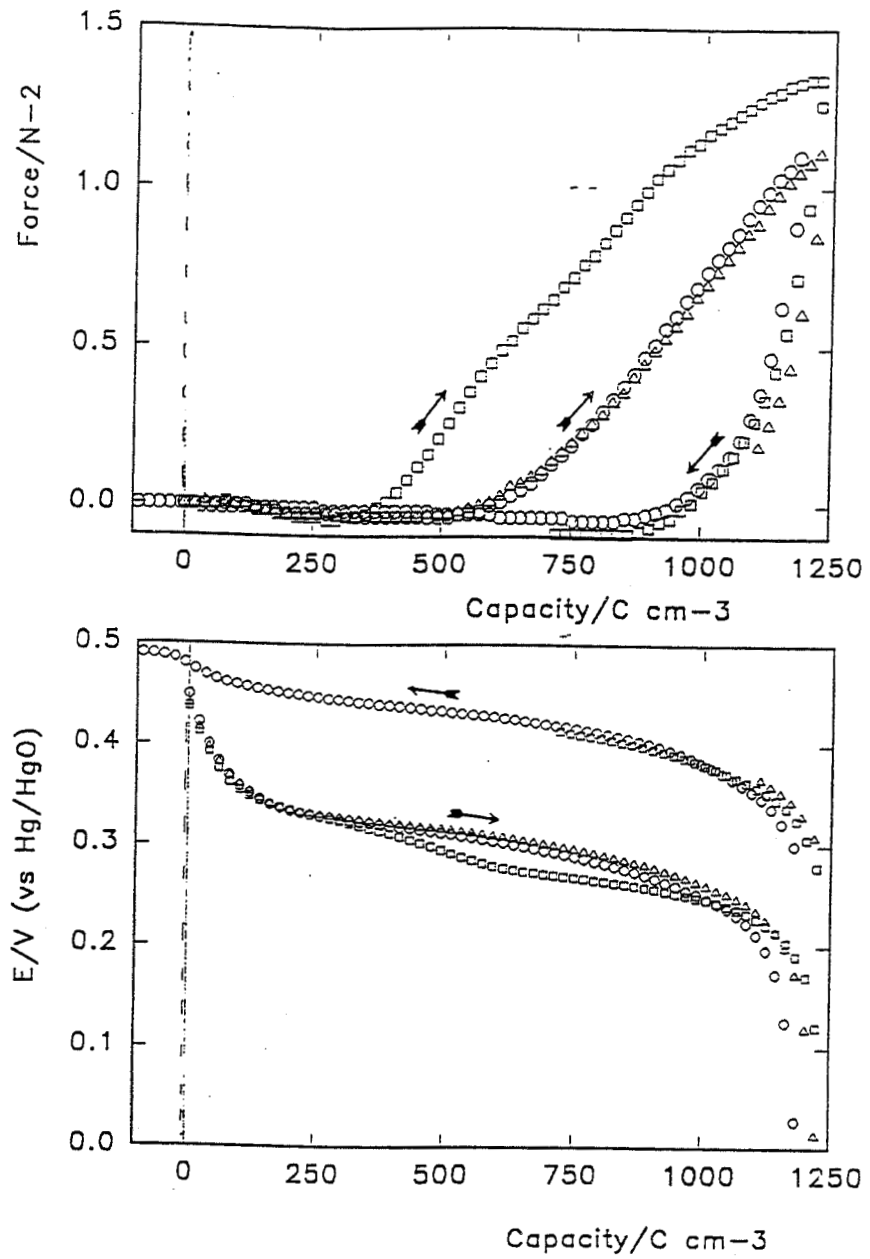


Fig. 13. Force and Potential vs. Capacity. type C, 6N KOH, 20°C.
 \circ : cycle # 190, regular charge, \square : cycle # 183, 22 shallow cycles,
 disch. 50% DOD, \triangle : cycle #191, overcharge 1C 2 hours.

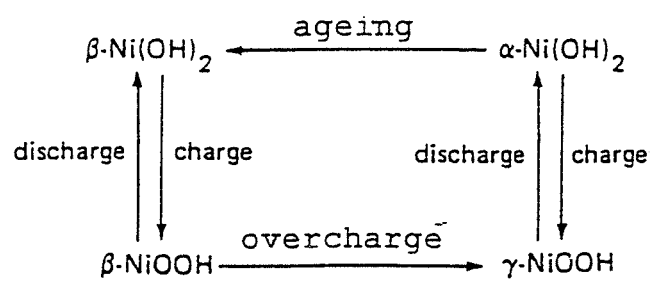


Fig. 14 The Bode's Cycle

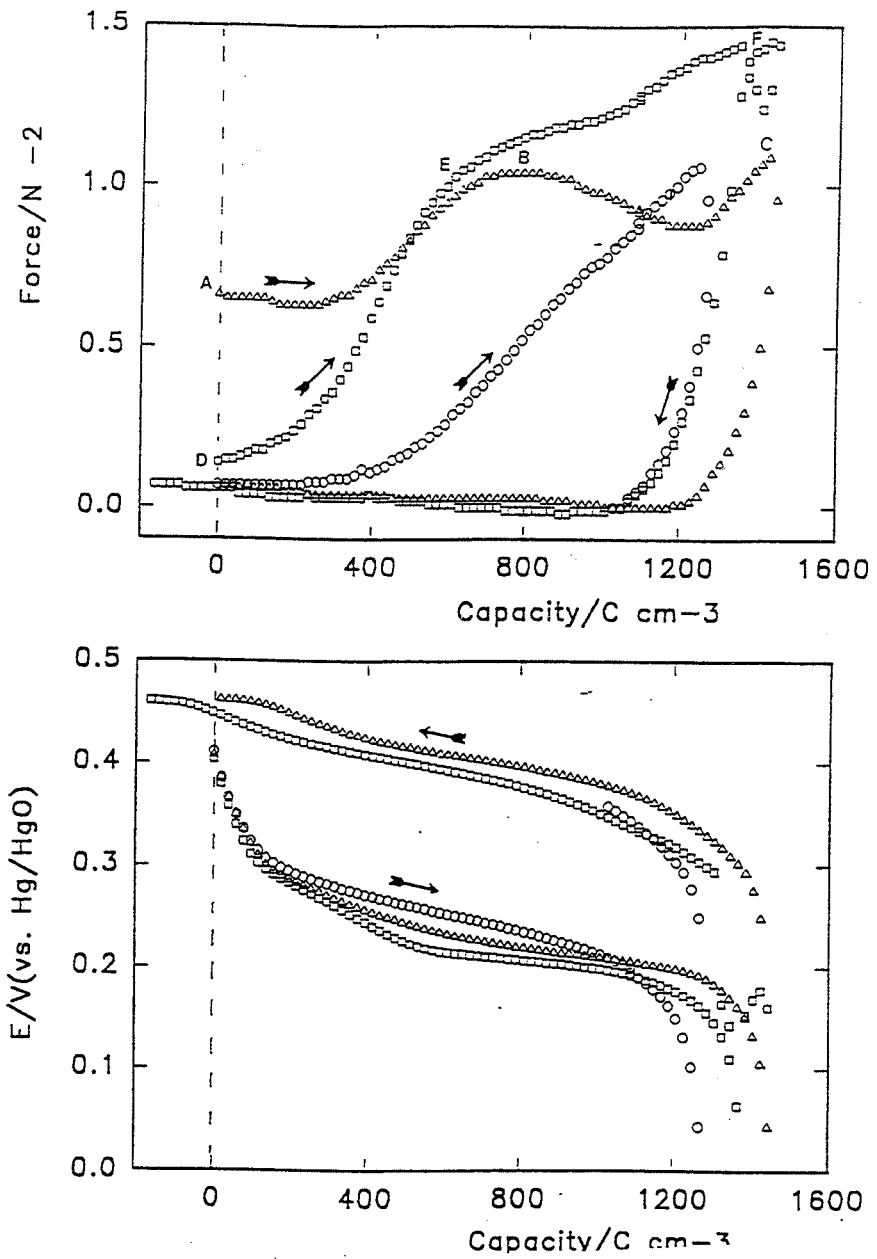


Fig. 15. Force and Potential vs. Capacity. type C, 10 N KOH, 20°C
 ○ : cycle # 213, regular charge, □ : cycle # 210, 16 shallow cycles,
 disch. 40% DOD, △ : cycle #212, overcharge 1C 2-hours.

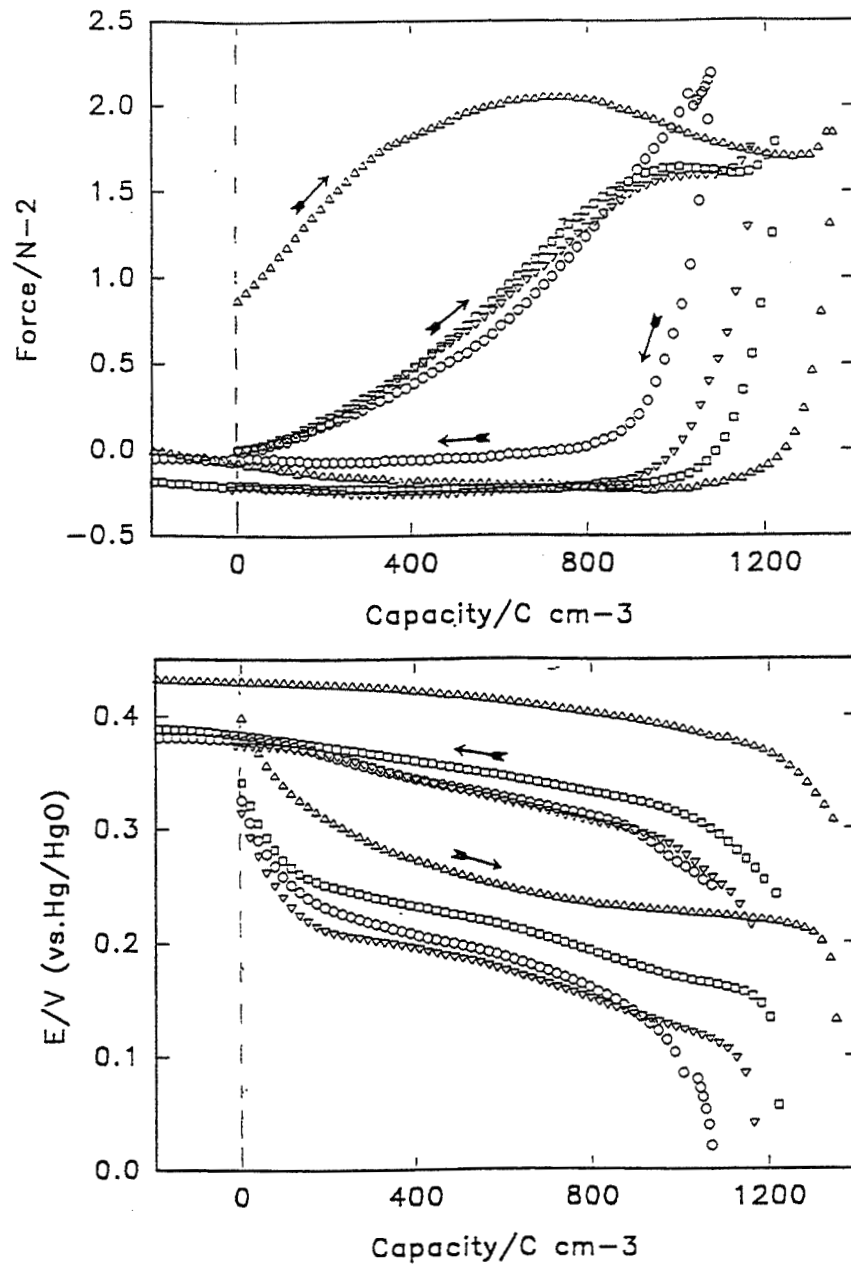
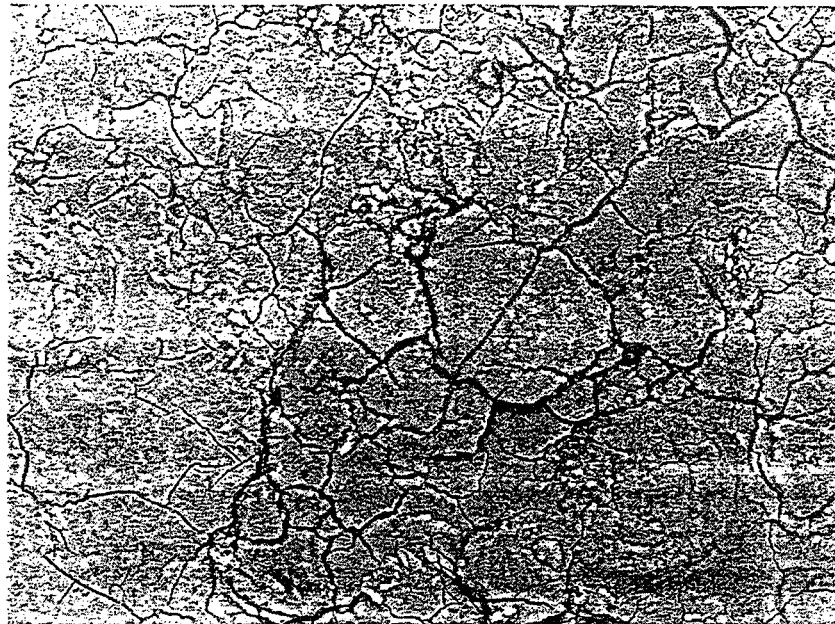
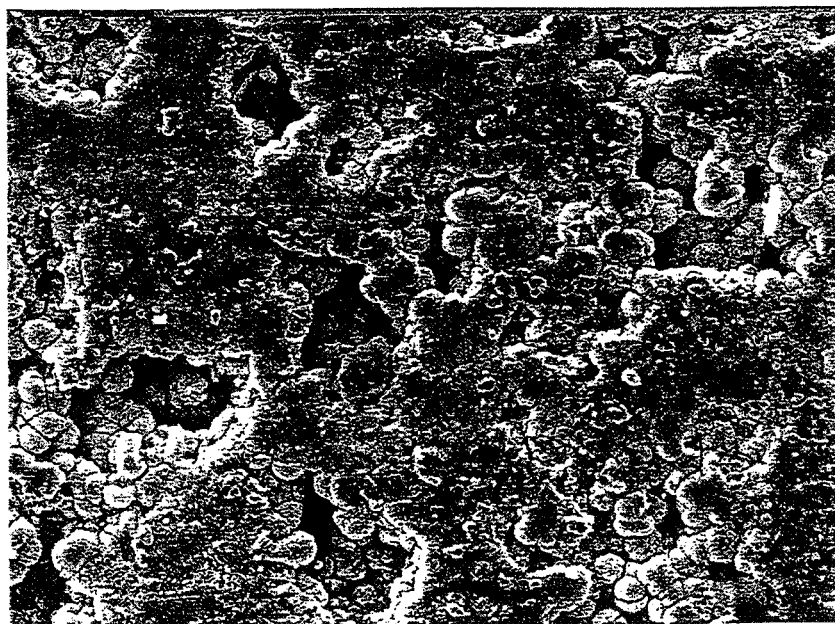


Fig. 16 Force and Potential vs. Capacity. type A, 10 N KOH;
 ○ cycle # 567, 0°C., 2hrs. overcharge, ▽ : cycle # 568, 0°C., 5
 hrs. overcharge, □ : cycle # 520, 20°C. 3.5 hrs. overcharge,
 △ : cycle # 558, 40°C. 3.5 hrs. overcharge.



— 20 μm .

FIG. 17. Aspect of the surface of Type A electrode.



— 20 μm .

FIG. 18. Aspect of the surface of Type C electrode.

Page intentionally left blank

Characterization of Electrochemically Impregnated Fiber Nickel Electrodes

D. Coates, J. Francisco, D. Chiappetti and J. Brill
Eagle-Picher Technologies - Power Subsystems
Joplin, Missouri

Possible Approaches to Improve the Specific Energy of the Nickel Electrode

- High porosity sintered nickel powder
- Heavy loading
- Nickel metal fiber
- Carbon fiber
- Nickel coated graphite fiber
- Carbon composite fiber/powder
- Pasted electrodes
- Nanostructured materials
- Additives
- Increased electron transfer

Metal / Carbon Fiber Composite Nickel Electrode Structures

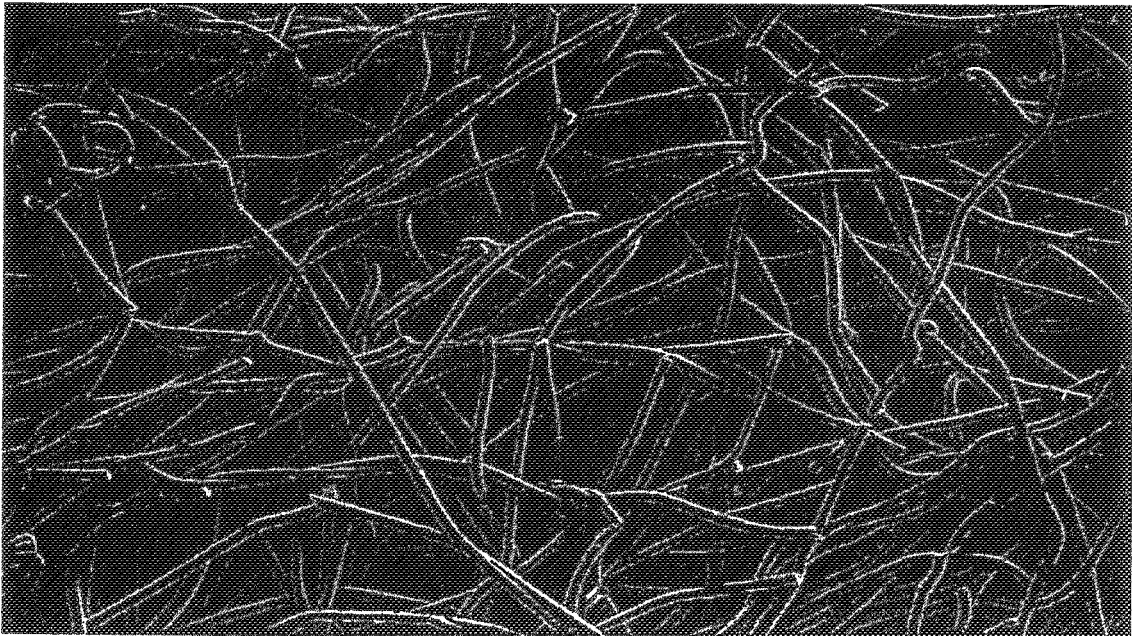
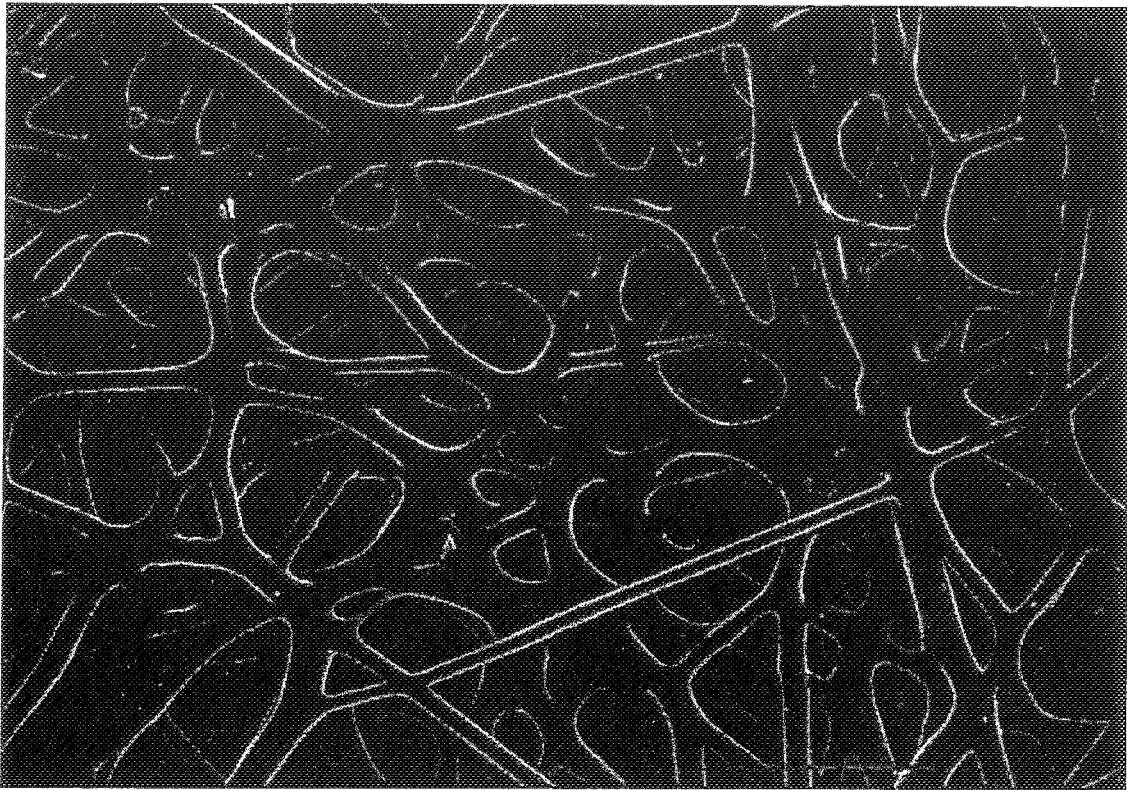
- W. Ferrando, W. Lee, A. Salkind, D. Hall, B. Tatarchuk, DAUG / Acme, et. al.

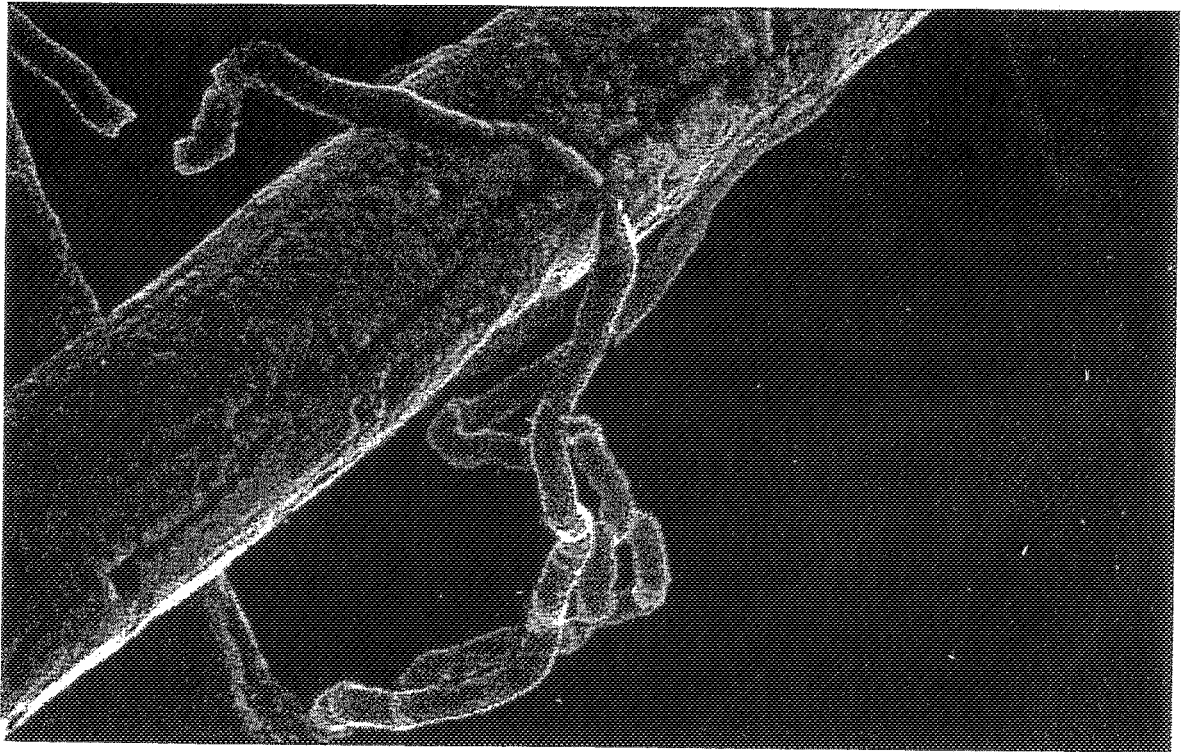
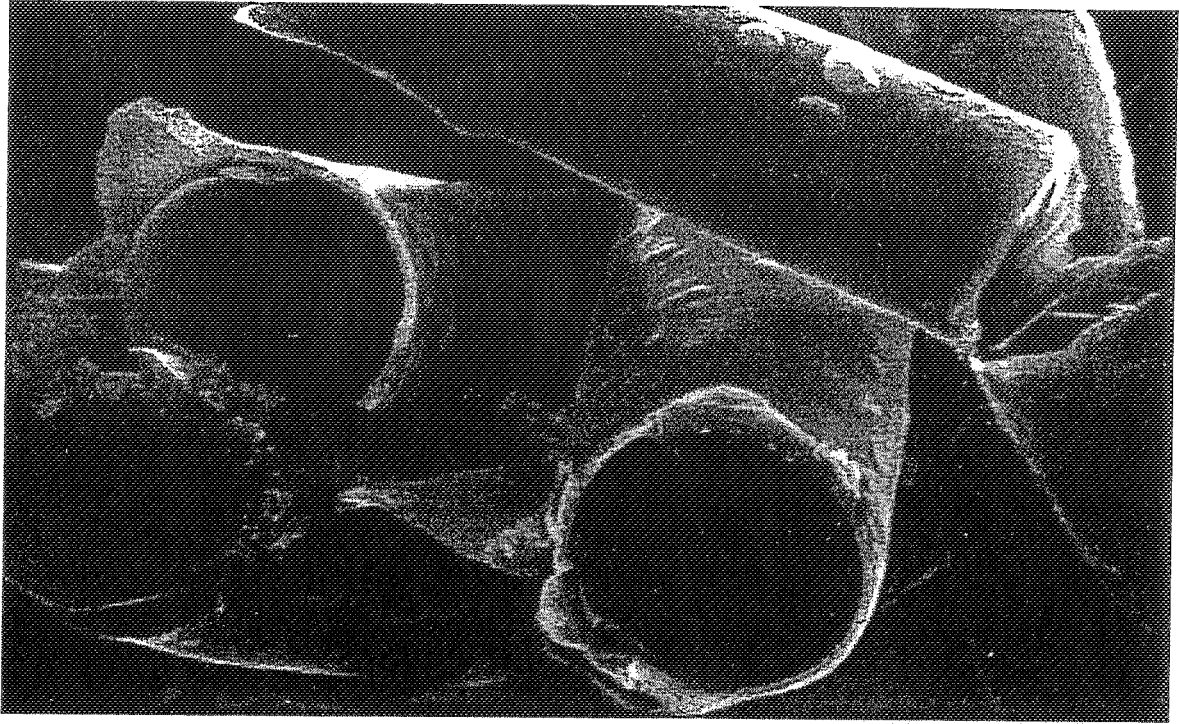
1984 - present

- Nickel-coated carbon fibers
- Carbon / stainless steel
- Cellulose mat-type preforms
- Sintered structures
- Pasted / electrochemical impregnation

Electroplated Nickel on Carbon

- **Florida Atlantic University**
 - Electroplating process using a proprietary plating cell technology
 - Process for the continuous through-plating of carbon fiber tows
 - Batch process for electroplating carbon fiber mats
 - Very thin, pure contiguous coating of the fiber

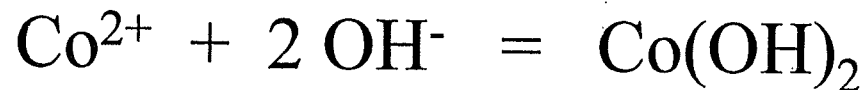
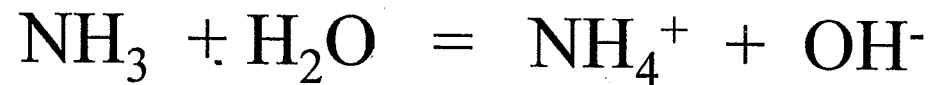




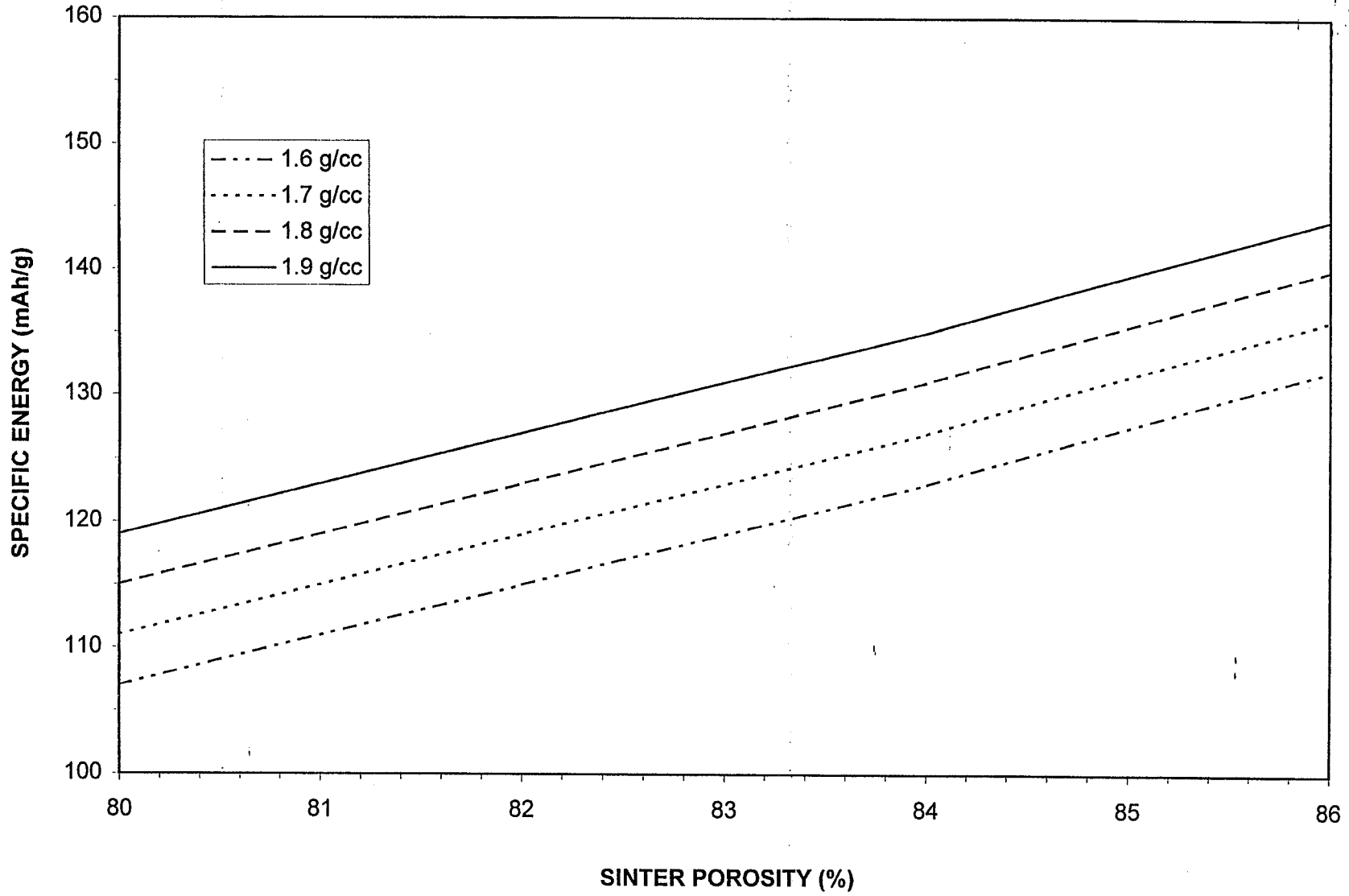
Fiber Electrode Substrates

- **Ribbon Technology**
 - Melt overflow fiber process
 - Dry air-layered mat process
- **Memtec America**
 - Fibers produced by drawing process
 - Wet-layering process for making mats
- **National Standard**
 - Fiber / powder substrates

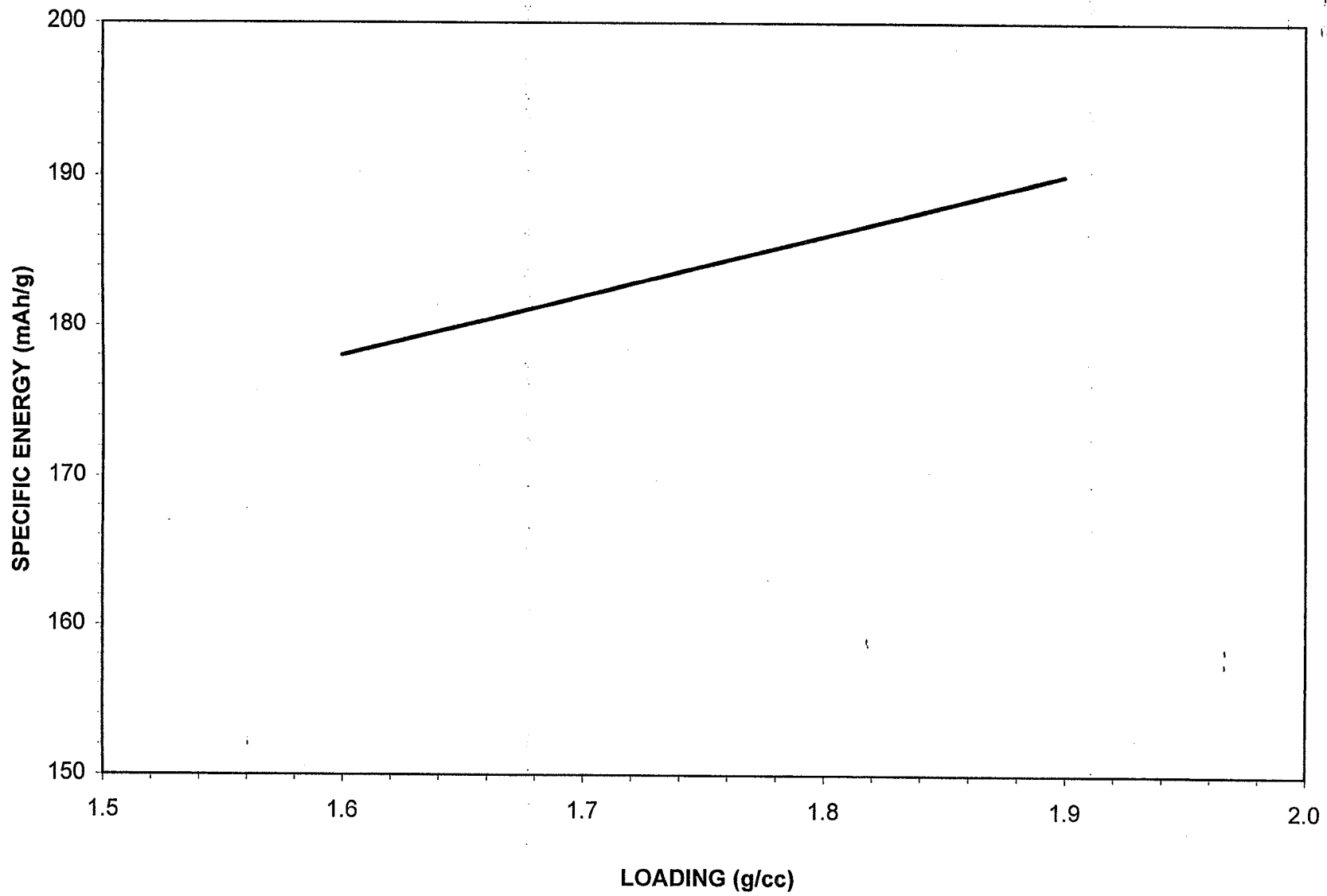
Electrochemical Impregnation Process

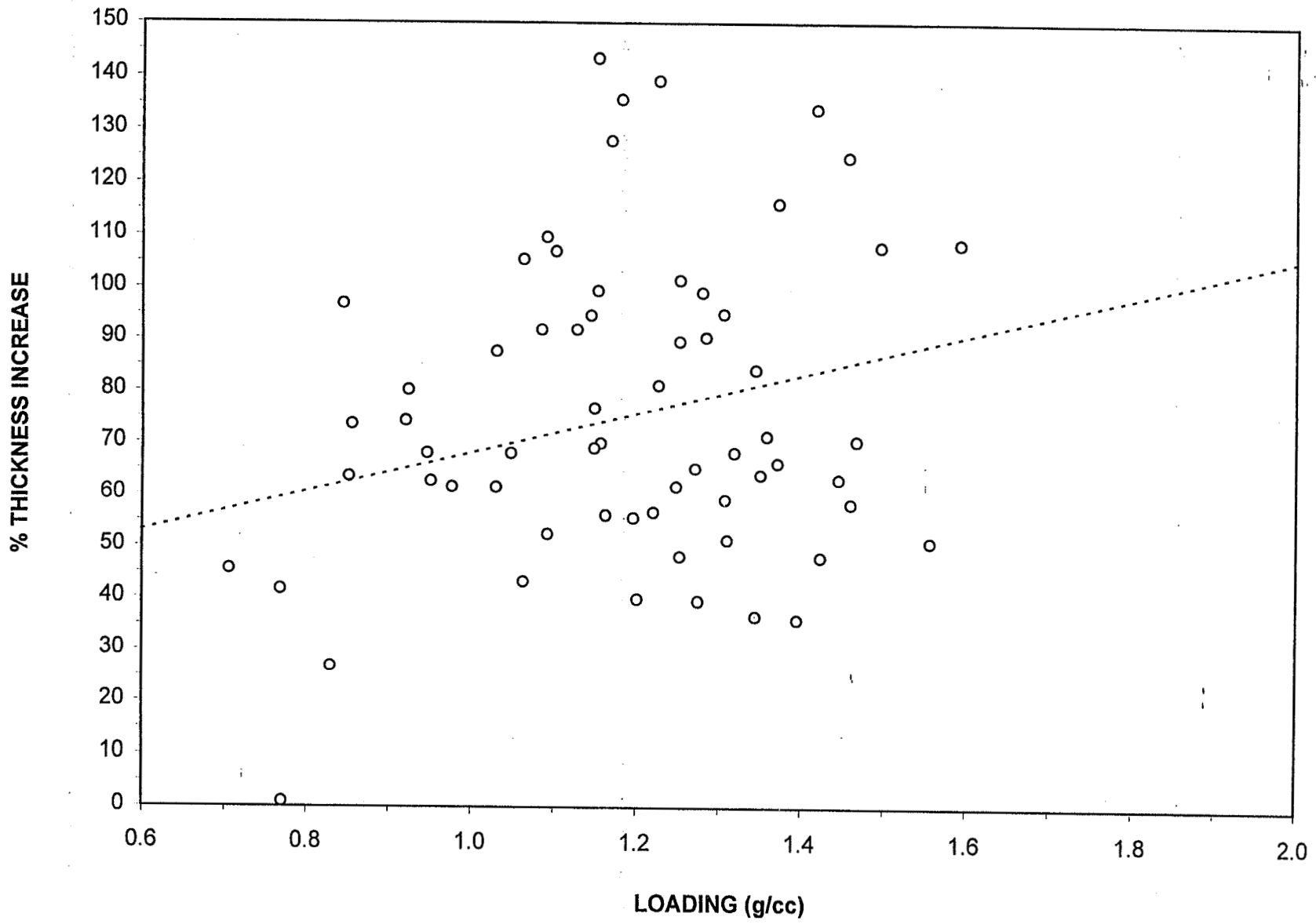


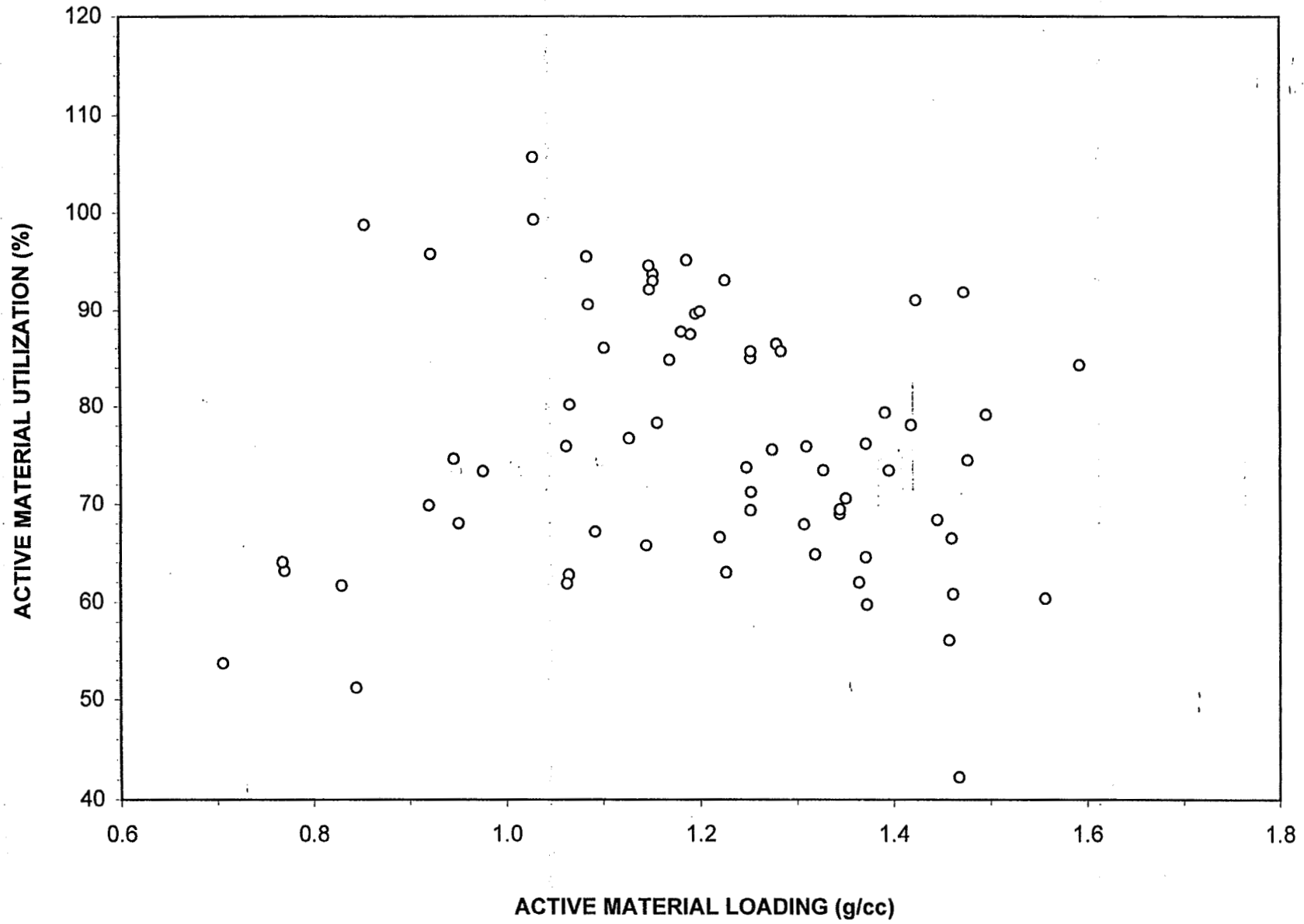
SPECIFIC ENERGY vs POROSITY

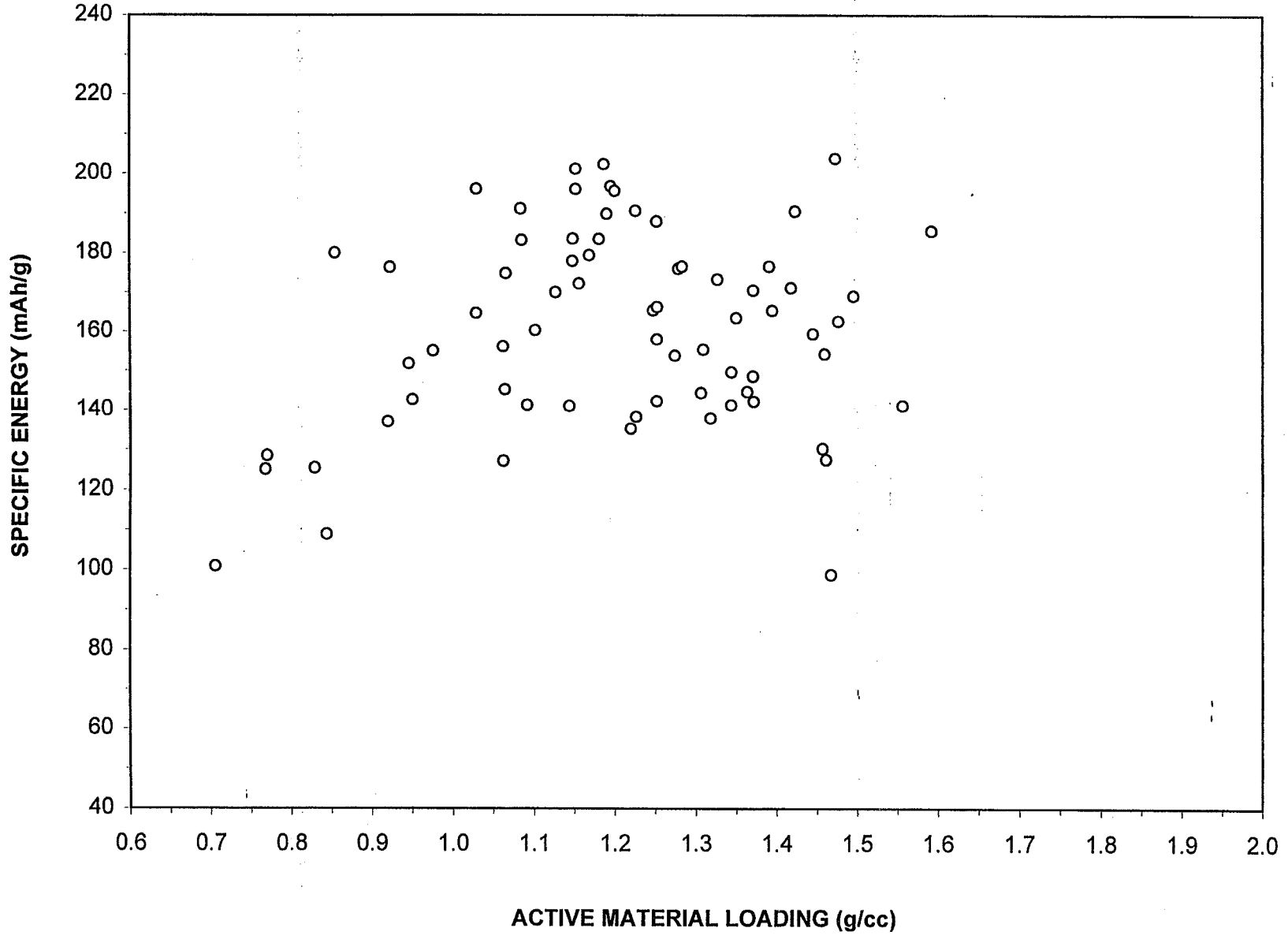


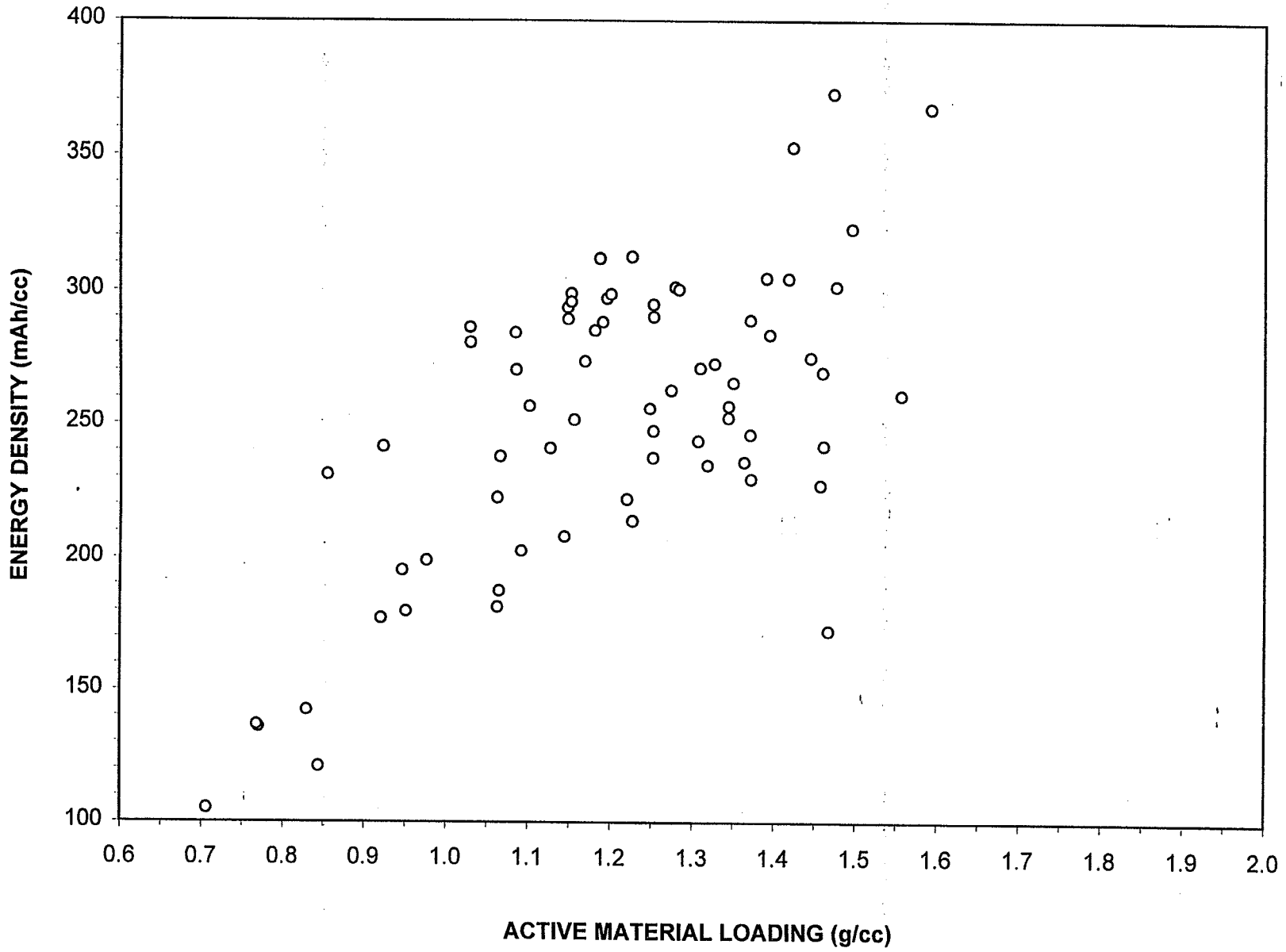
SPECIFIC ENERGY vs. LOADING - ncg ELECTRODE

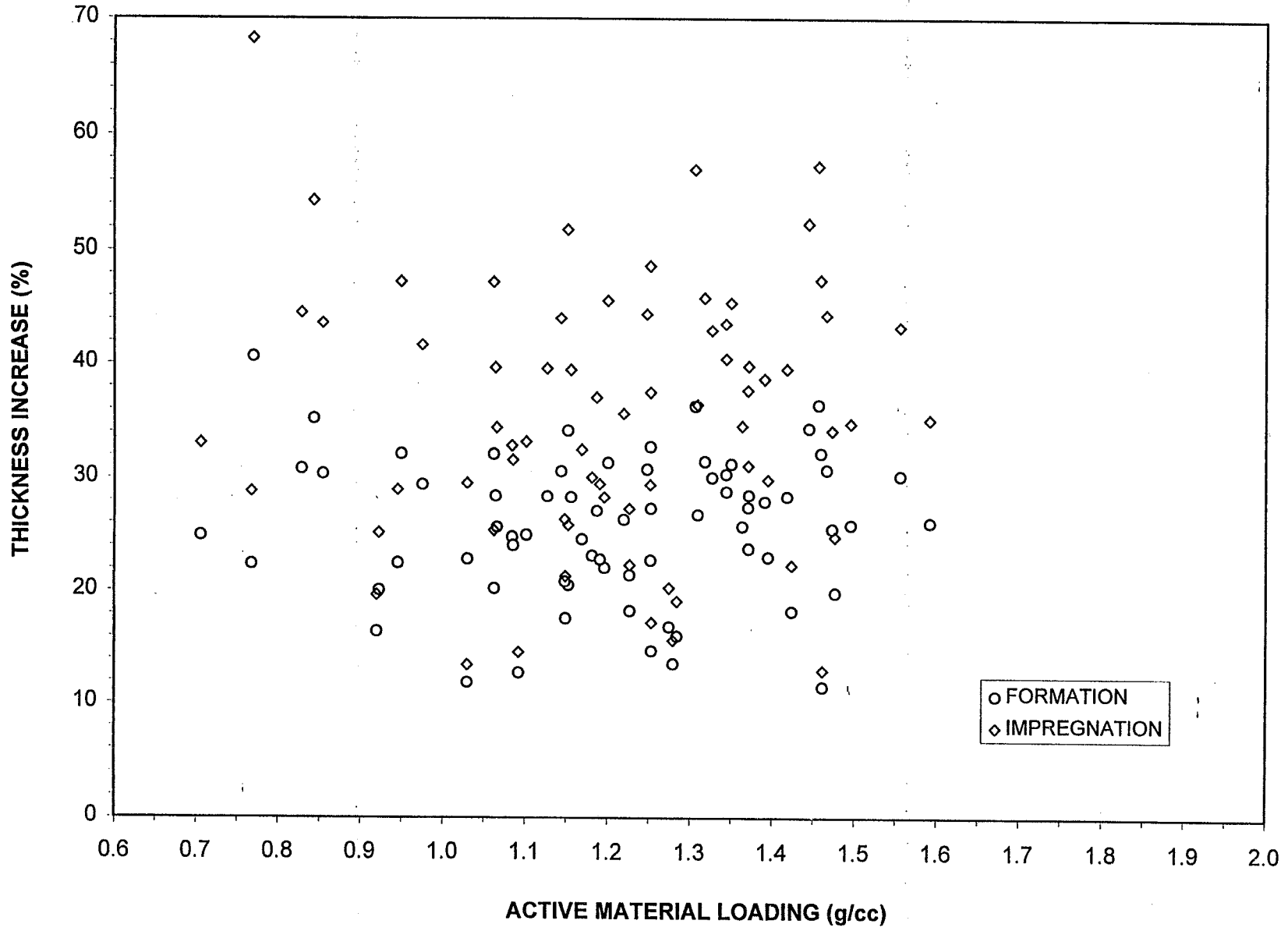


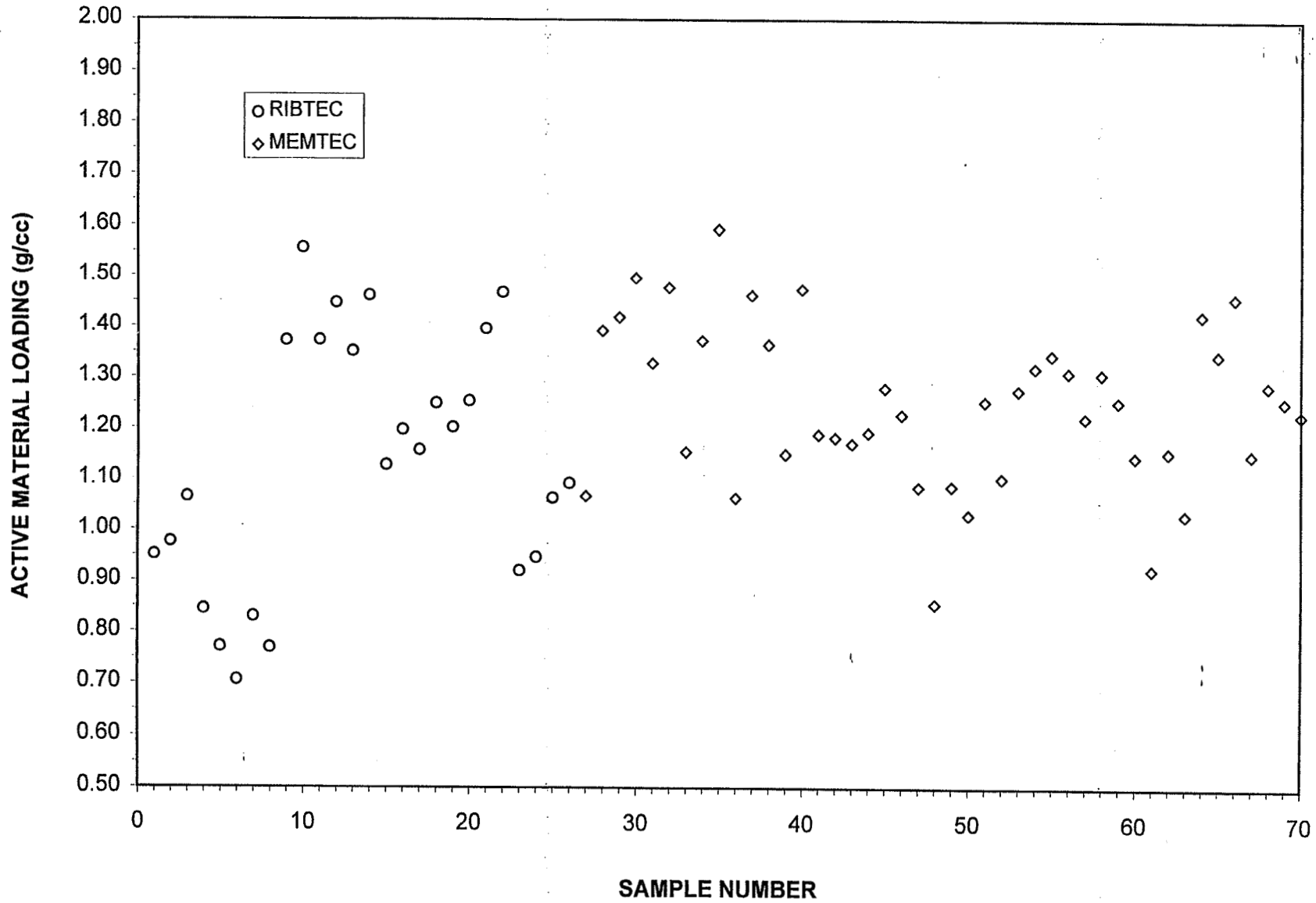


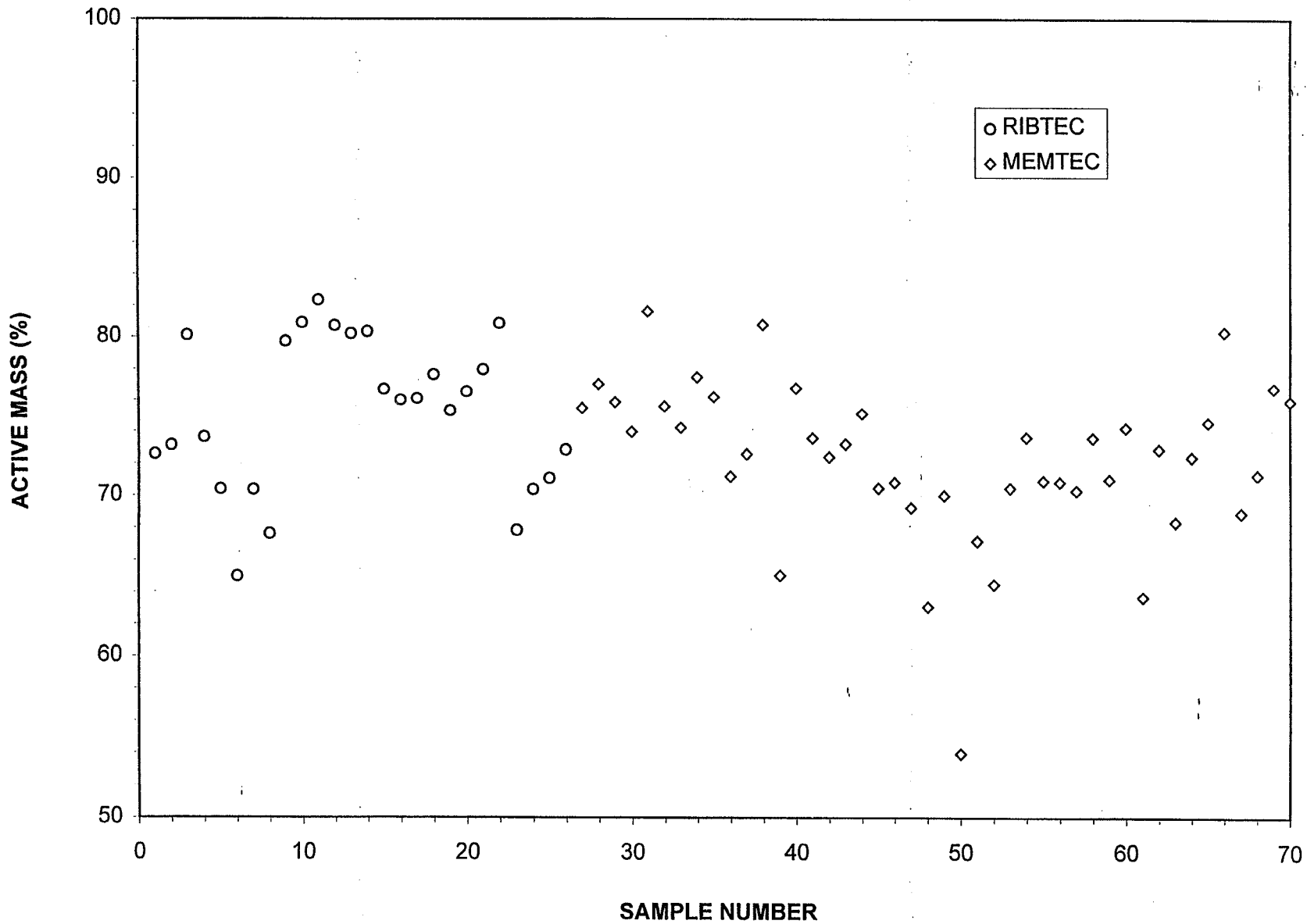


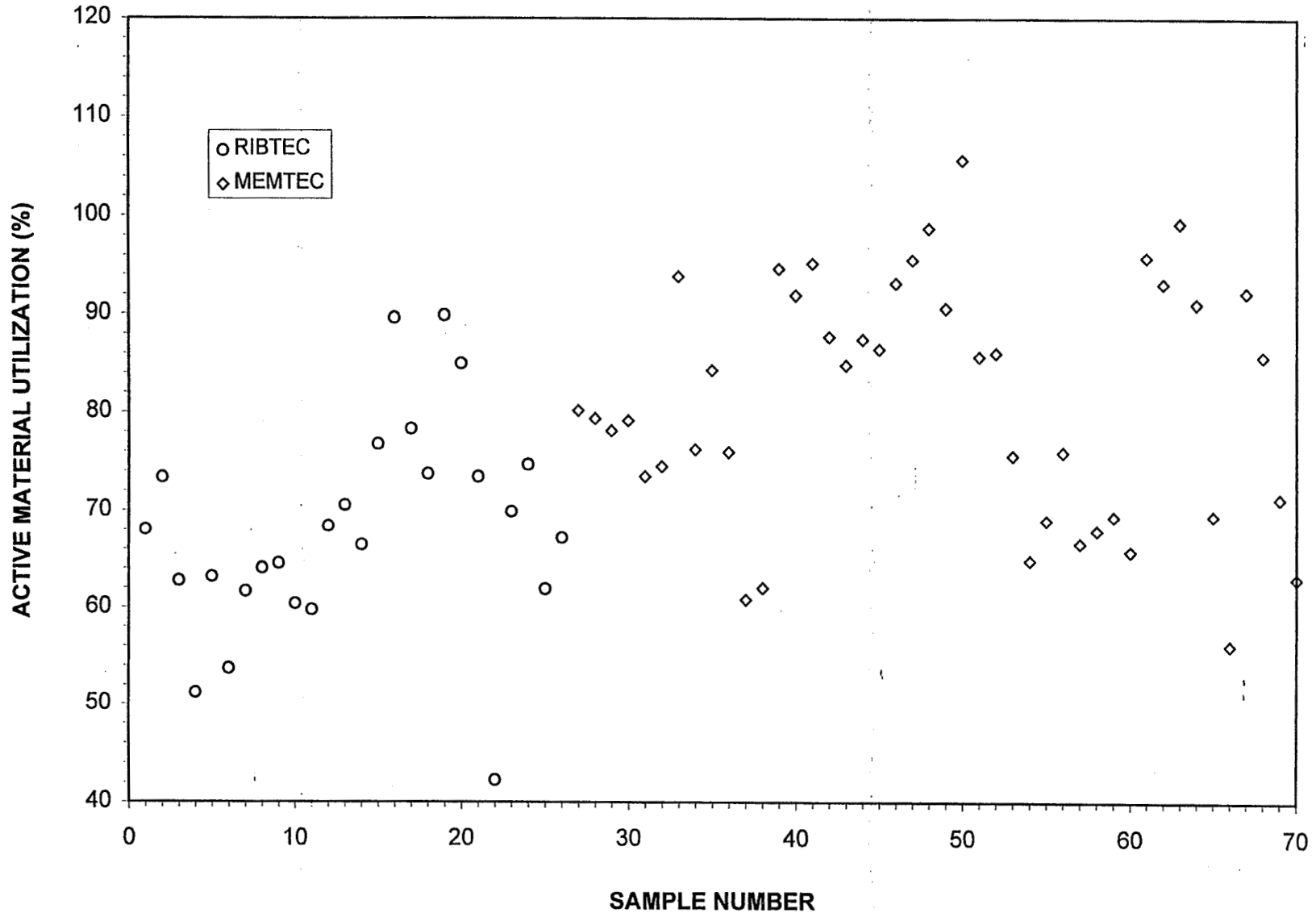


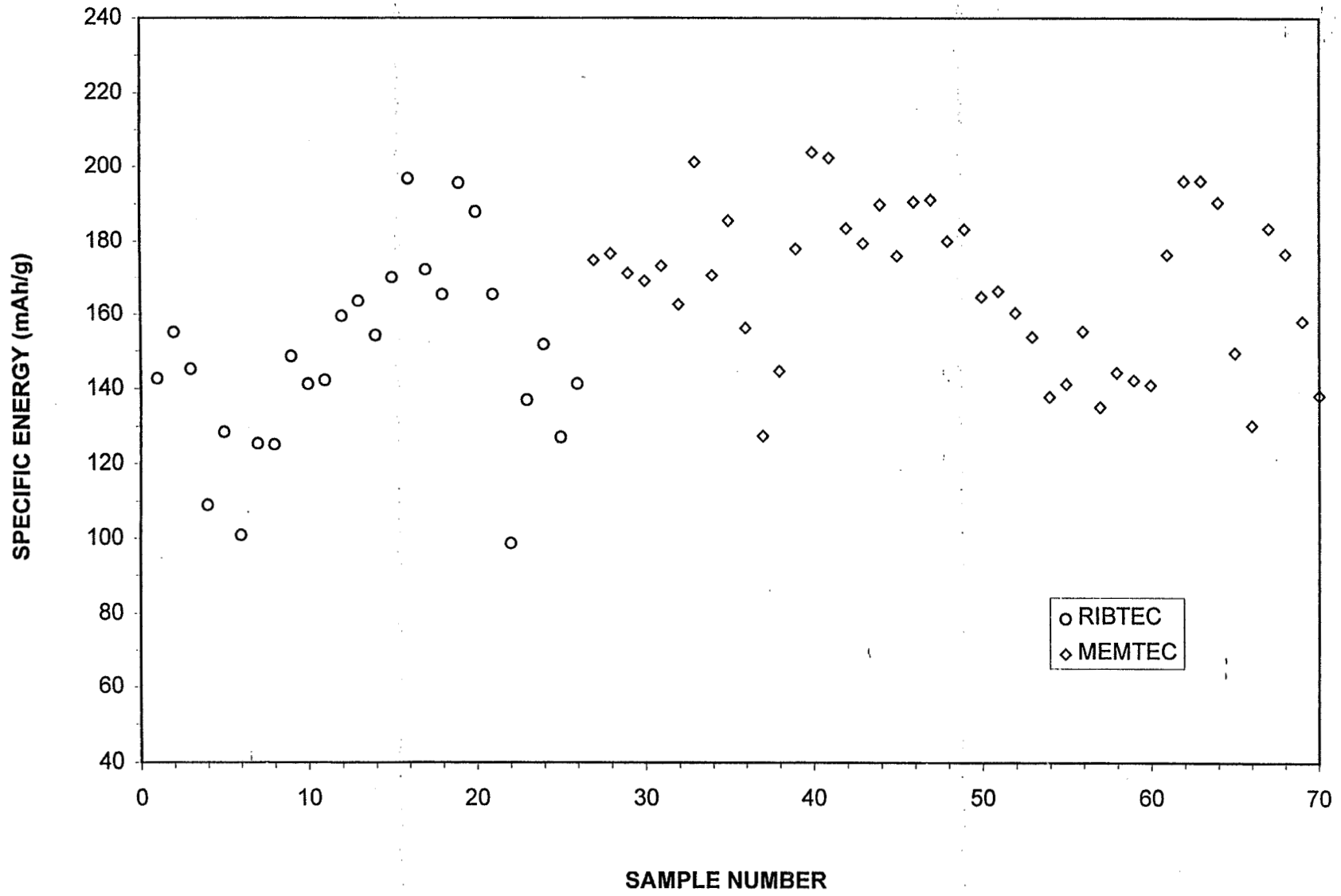


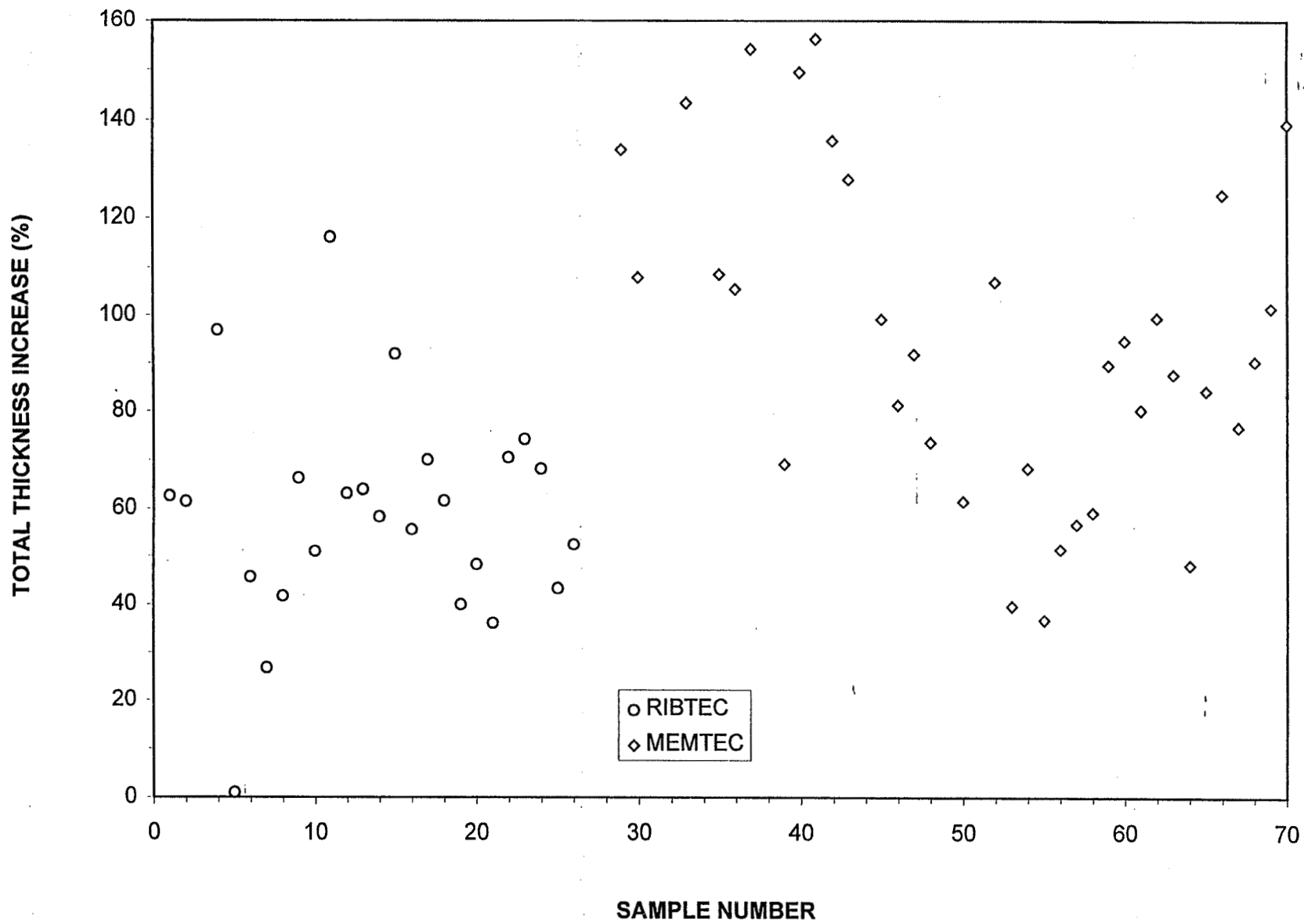


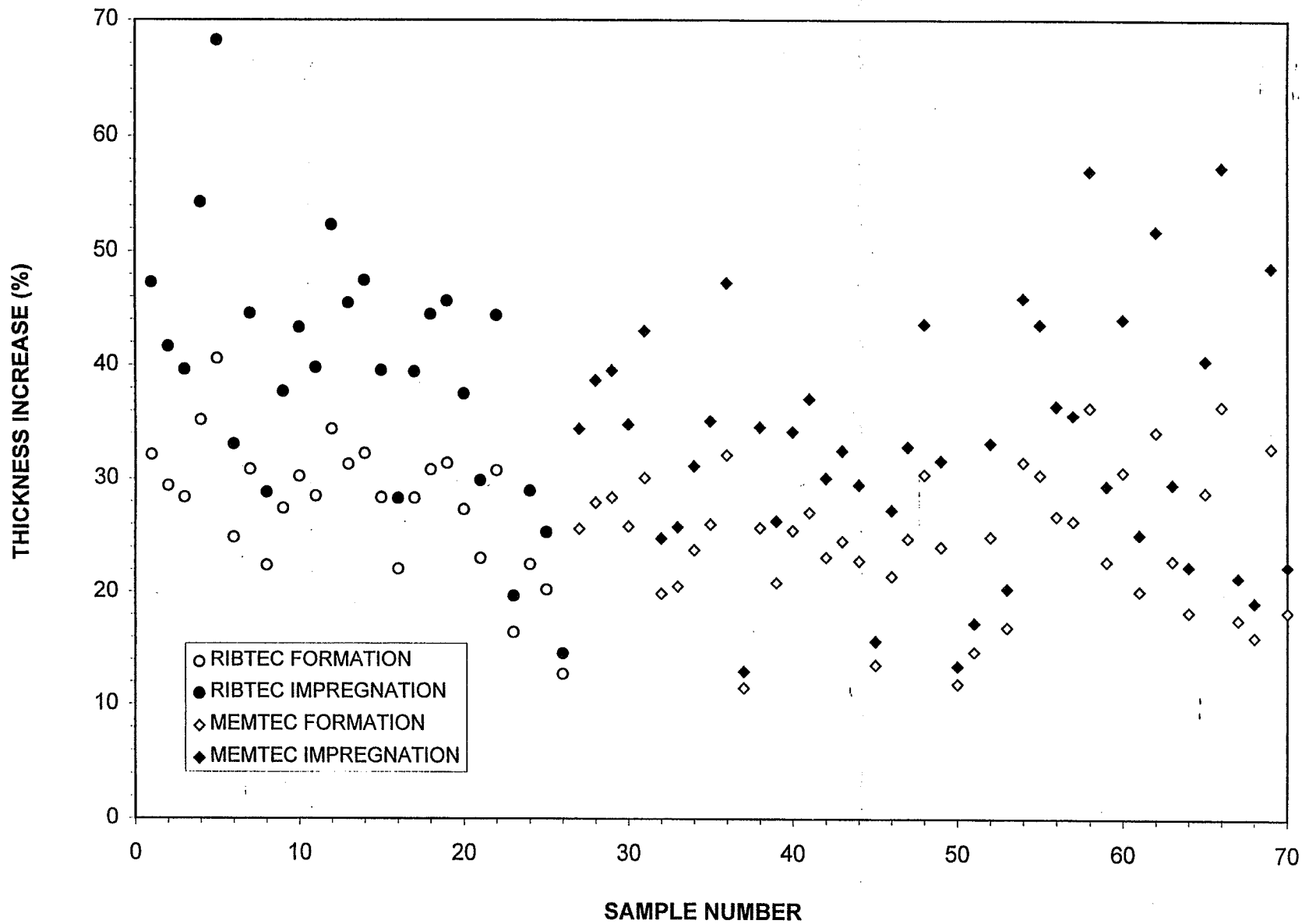












Conclusions

- Sintered powder electrode designs are limited to approximately 140 mAh/g maximum
- Fiber / graphite composite electrodes are limited to approximately 185 mAh/g maximum
- A variety of trends have been identified relating electrode design parameters such as fiber construction type, porosity and loading to electrode performance parameters such as active material utilization, specific energy, energy density and thickness growth

Nickel Electrode Corrosion During Nominal On-Orbit Operation

**Chuck Lurie and Bob Tobias
TRW Space and Electronics Group
Redondo Beach, California 90278**

**The 1997 NASA Aerospace Battery Workshop
The Huntsville Hilton
Huntsville, Alabama
November, 17 - 20, 1997**

Background

- **The increase in capacity often observed during early nickel-cadmium battery mission life is attributed to corrosion of nickel electrode sinter forming active nickel hydroxide.**
- **An example of this phenomenon is examined using the 20-year, on-orbit history of the FLTSATCOM F1 spacecraft.**
- **At 20 years into the mission:**
 - **Battery eclipse discharge performance continues to be nominal.**
 - **Reconditioning discharge capacity increased during the first 6 - 7 years of operation, plateaued, and then started a continuing decrease.**

The FLTSATCOM F1 spacecraft provides an excellent opportunity to examine the phenomenon of nickel electrode sinter corrosion using on-orbit data. Extensive eclipse season and reconditioning operating data has been collected throughout its 20-year mission life.

The Spacecraft and Mission

- **Geosynchronous orbit communications satellite**
- **Eclipse power provided by three 24-cell, 24-Ah, NiCd batteries**
- **Cell characteristics:**
 - **Rated capacity** **24 Ah**
 - **Measured capacity** **28.5 Ah**
 - **Number of plates** **11 positive, 12 negative**
 - **Plate loading** **Positive 13.4 ± 0.6 gms/dm²**
Cd treatment
Negative 16.1 ± 0.6 gms/dm²
Ag treatment
 - **Neg /Pos ratio** **1.7:1**
 - **Electrolyte quantity** **68 ml, 34% KOH**

The mission of FLTSATCOM is to provide a satellite communication capability that is shared by the United States Navy and Air Force.

During eclipse, spacecraft power is provided by three 24-cell nickel-cadmium batteries. The batteries are connected to the main spacecraft bus, during charge, through a diode path. When the spacecraft enters into eclipse, relays are switched to connect the batteries directly to the bus, which is powered by the spacecraft solar array.

Each battery weighs approximately 65 pounds and has envelope dimensions of 15.5 by 11.7 by 8.5 inches. The cells were manufactured by General Electric Battery Division in Gainesville, Florida.

Battery Operation

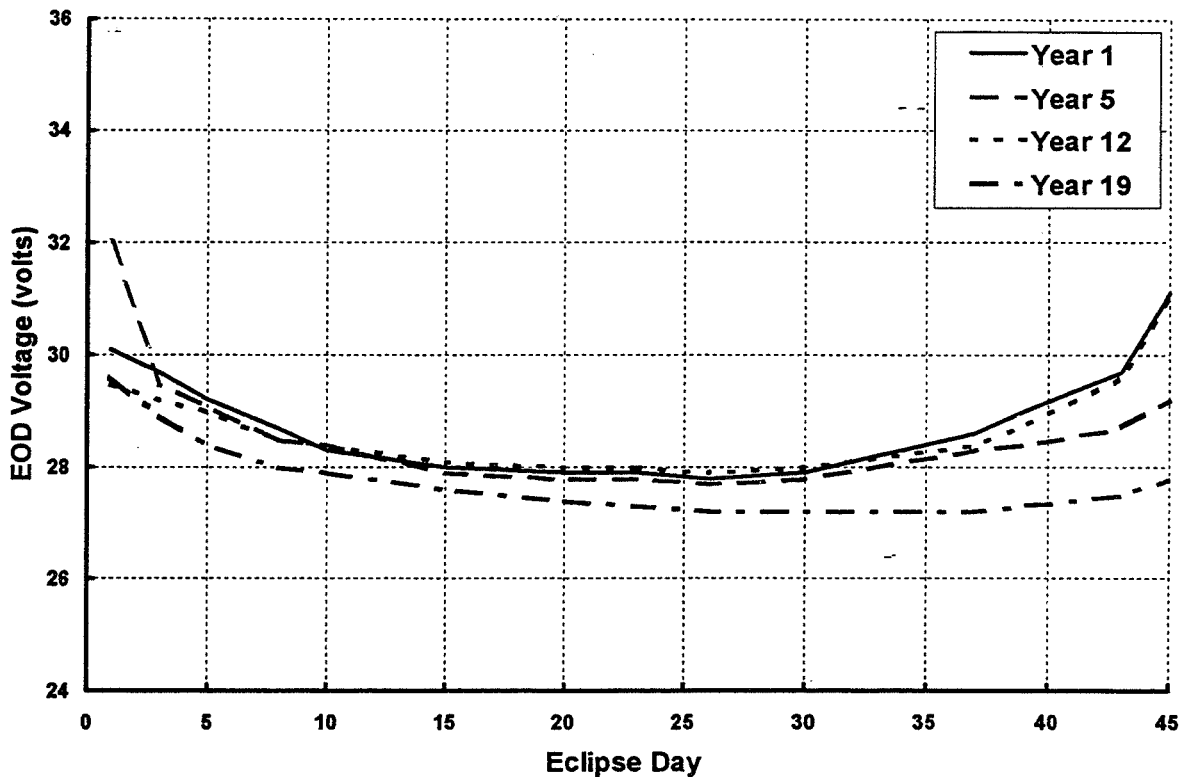
- **DOD**
 - 75% of rated capacity
 - 63% of measured capacity
- **Charge**
 - Charge at C/15 - C/10 rate to a recharge ratio of ~ 1.0
 - Trickle charge at ~C/100 rate until following discharge
- **Reconditioning**
 - Immediately prior to each eclipse season
 - Discharge into 85.7 ohm load to 18 volts (~100 hours)
 - Provision for manual termination
- **Temperature**
 - 0°C to 10°C

Battery depth-of-discharge (DOD) has remained close to 63% of measured capacity (75% of rated capacity) during on-orbit eclipse season operations.

Battery charging consists of a full rate charge period followed by trickle charge. During full charge, current is provided by the battery charge section of the solar array. Full charge current is limited to approximately 2.1 amperes by the current limiting characteristics of the charge section of the solar array. Full charge is terminated when the battery voltage reaches a preselected temperature compensated voltage limit. The charge current is then reduced to a trickle charge rate of 0.24 amperes and maintained on trickle charge for the remainder of the sunlight period.

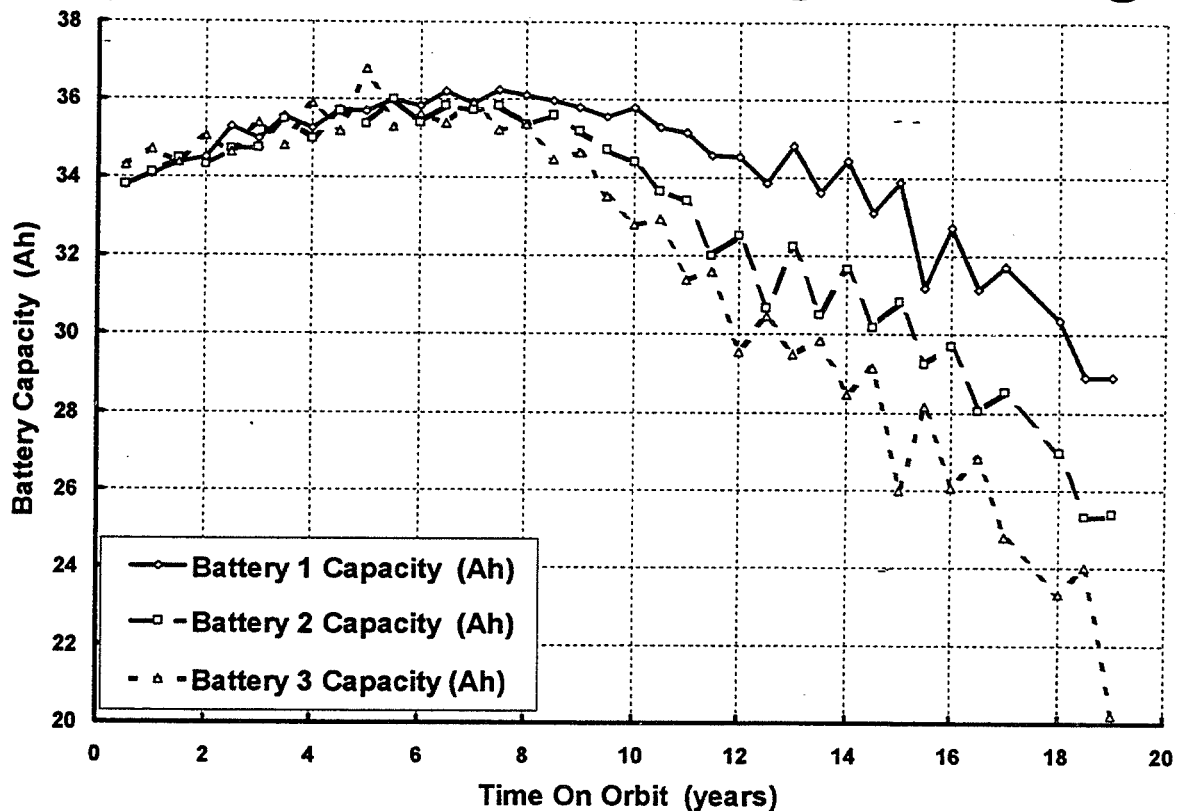
Reconditioning is performed prior to each eclipse season. The batteries are discharged through 85.7 ohm resistors. Discharge is terminated automatically when the battery reaches 18 volts. The reconditioning discharge can also be terminated manually at lower voltages.

History: Eclipse Performance



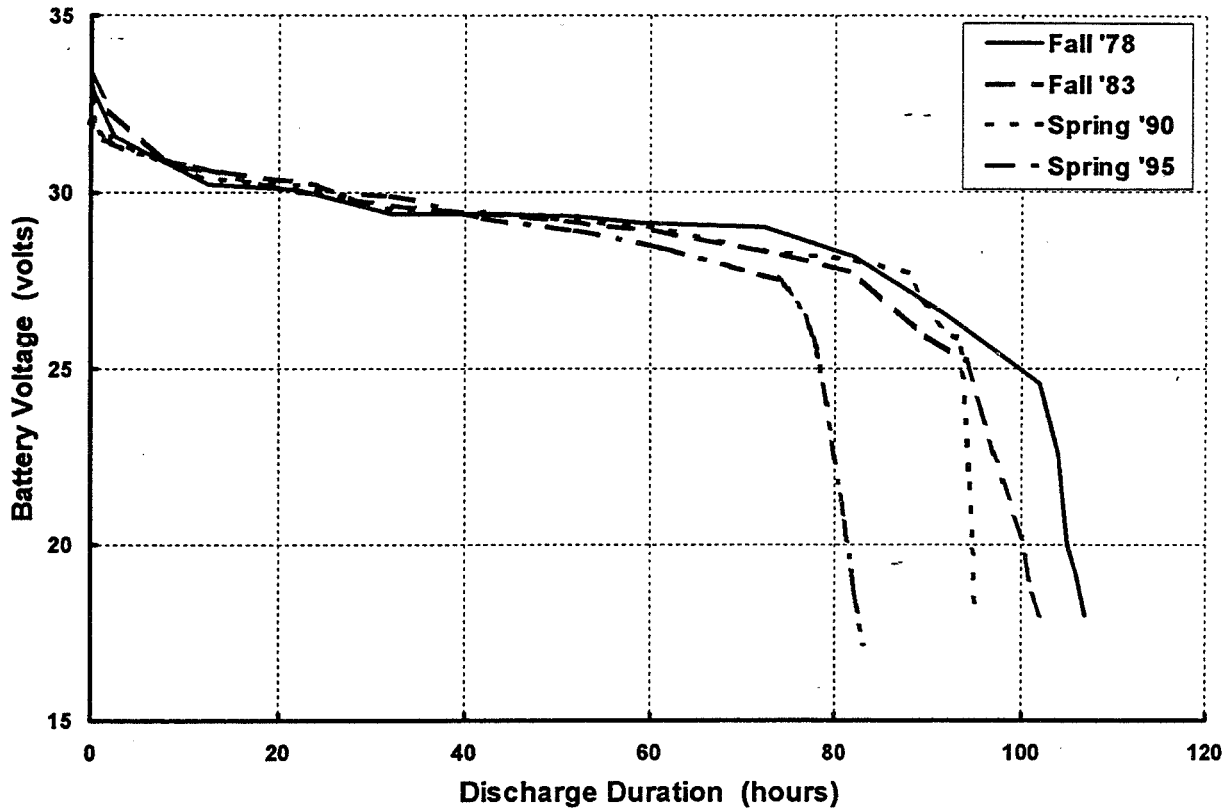
The data presented here summarizes the eclipse season performance of the spacecraft. Performance is tracked by observing the trends in end of discharge voltage from season to season. The data shows a gradual decrease in end of discharge voltage during the mission. However, the end of discharge voltages remain at satisfactory levels.

History: Reconditioning Discharge



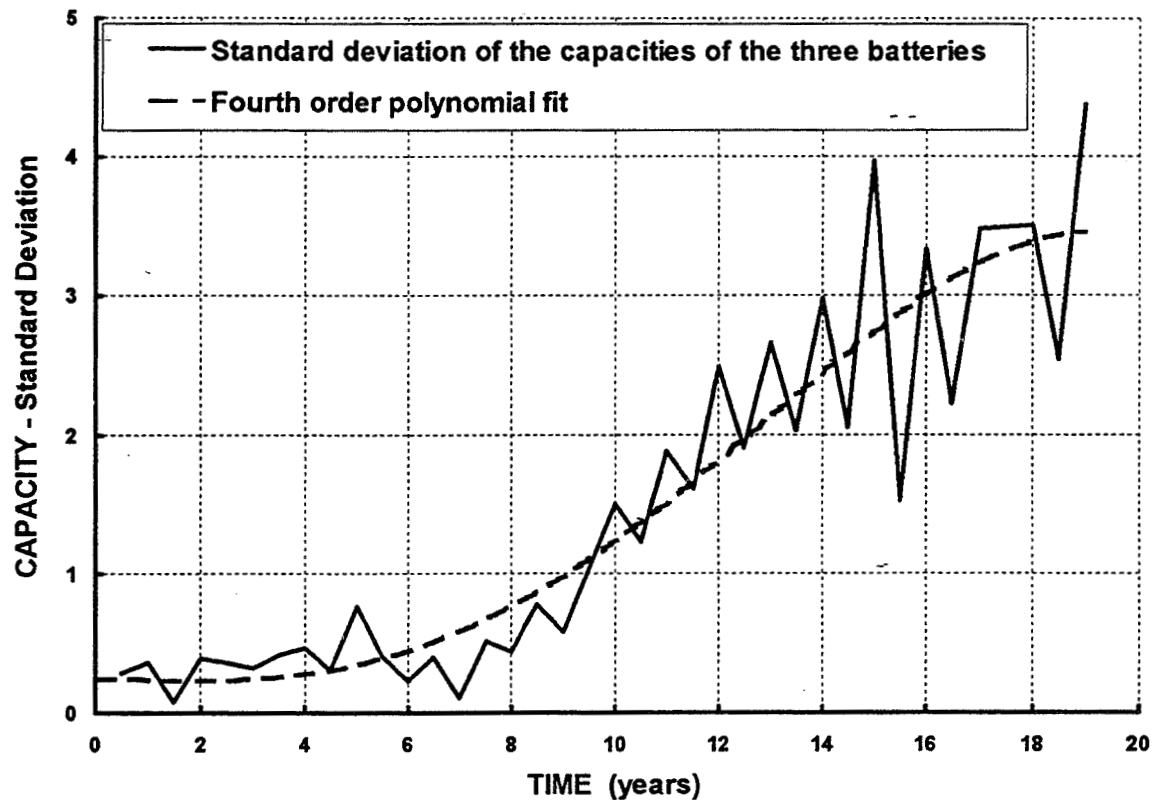
This chart shows the reconditioning discharge capacity history for FLTSATCOM F1 mission from inception. During the first eight years capacity is increasing and individual battery capacities are very close. After a short plateau the capacities begin to decrease and dispersion begins to increase. It is interesting to note that, while the batteries continue to support the eclipse season requirements with margin, the reconditioning discharge data suggests that the batteries are near end of life.

Reconditioning Discharge Profiles



As the mission progresses the reconditioning discharge profiles continue to have smooth knees indicating that cell capacities, within a battery, are not diverging significantly. This is an interesting observation because cell capacity dispersion, due to the presence of soft shorts, is frequently observed as cells age.

Reconditioning Capacity Dispersion



Capacity dispersion is defined as the standard deviation of the capacities of the three batteries. As can be seen from the chart, dispersion is small during the first six to seven years, when the capacity is increasing, and becomes increasingly larger, during the remaining years as the capacity decreases. The small dispersion, initially, reflects careful cell matching. The trajectory of the dispersion growth suggests a mechanism that is common to all cells in all batteries and is well behaved.

Capacity Growth

Ni Corrosion at the Current Collector

- The rate of capacity increase is stable at approximately 0.34 Ah/year, during the first 6 -7 years of operation.
- Capacity growth is assumed to be due to the formation of NiOOH by corrosion of Ni electrode sinter during overcharge.
- 0.34 Ah of additional NiOOH per year suggests that 0.75 gms of the Ni sinter is consumed per cell per year.
- This rate of Ni loss is equivalent to 8% of the Ni electrode sinter mass, at year 10.

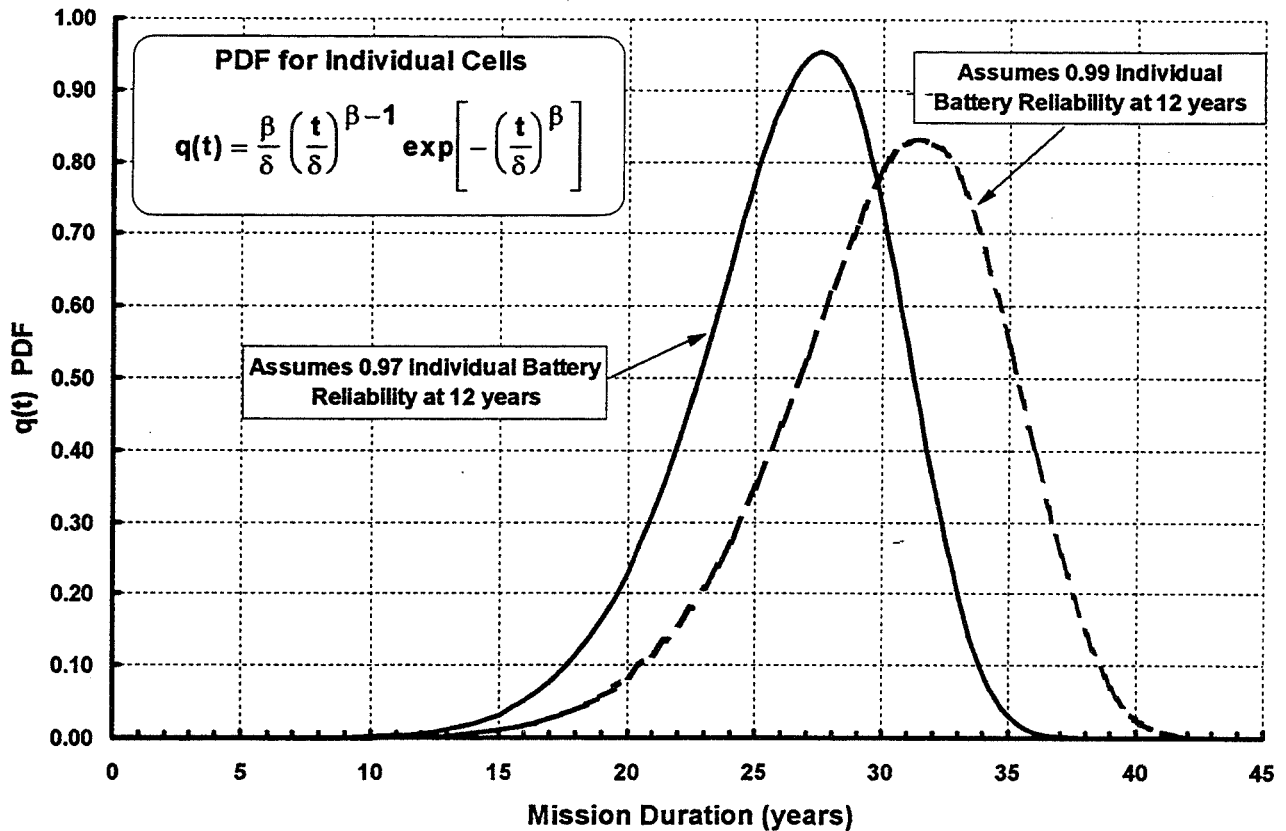
Corrosion of the nickel electrode sinter, during overcharge, can occur uniformly during early life because of the inherent uniformity of the cell plate stacks. As more and more sinter is corroded the plates become less uniform and increased capacity dispersion can occur. The amount of sinter corroded, approximately 8% at year 10, appears to be sufficient to significantly alter the interface between the active material and the current collector .

Prediction of Remaining Life

- **The reconditioning capacity trend curves provide a signature describing processes which limit battery life.**
- **This signature may be useful in determining remaining life, at some point in the mission.**
- **This hypothesis has been tested.**
 - **Assuming a Weibull reliability model**
 - **Shape parameter, β , assumed to be 8**
 - **Scale parameter, δ , estimated from the orbital data**

Spacecraft and electrical power system designers are usually concerned with battery system performance and life. Most of the related effort reported has focused on determining battery life as a function of battery and mission characteristics. The FLTSATCOM F1 battery reconditioning performance data base provides an opportunity to explore a different aspect of life prediction. The hypothesis that the reconditioning discharge history may be useful in determining remaining life was tested using a two-parameter Weibull reliability model. The Weibull distribution has been used by many investigators and is generally considered to be appropriate for battery reliability modeling.

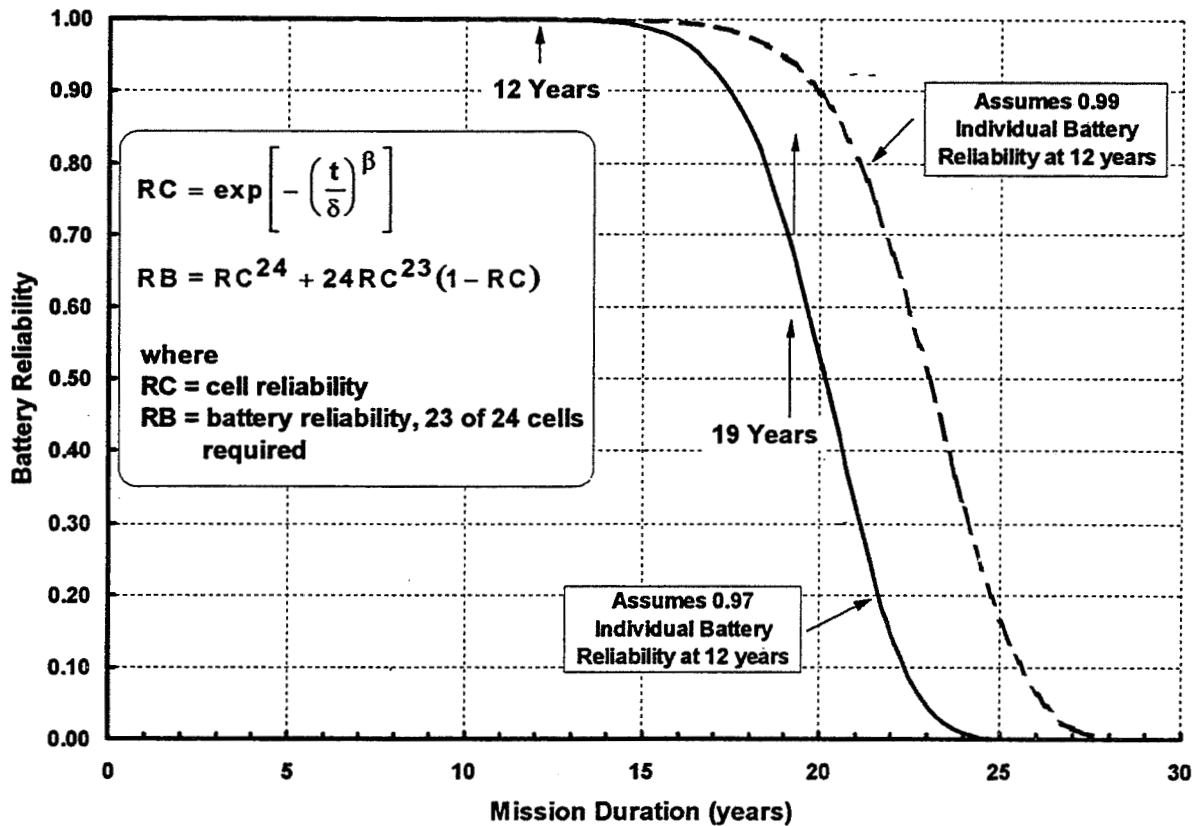
Weibull Reliability Model



The two-parameter Weibull distribution was chosen as being the distribution most representative of the aerospace battery data and experience base.

The most familiar distribution is the normal (Gaussian) distribution. Unfortunately battery lifetime data is markedly skewed and not bell shaped. Also the normal distribution, applied to aerospace battery lifetime data, is mathematically difficult complicating determination of failure/hazard rates. The log-normal distribution is more convenient and has been used by others. However its hazard rate increases to a maximum and then decreases in the long-life range, whereas the normal distribution has a continuously increasing hazard rate. The Weibull distribution is convenient mathematically and has an increasing hazard rate that, with the appropriate choice of Weibull parameters, faithfully models the historical aerospace battery data base.

Battery Life, Predicted at Year 12



The hypothesis that remaining life can be predicted with the Weibull model was tested at the twelve-year point, in the FLTSATCOM F1 mission. The β variable was assumed to be 8. This value assumes that failures are the result of wearout and that random failures contribute insignificantly to the hazard rate. Values of δ equivalent to individual battery reliabilities of 0.97 and 0.99, at year 12, were calculated. These are considered conservative in that the three batteries were functioning nominally at year 12. The resulting PDF's are shown on the previous chart. Battery reliability is calculated, from cell reliabilities, using a binomial model, assuming one cell is redundant. As can be seen from the curves above the model predicts that reliability is high for a twenty year mission, and falls rapidly thereafter. This prediction is in good agreement with conclusions drawn, using engineering judgment, from observation of on-orbit battery performance and reconditioning data.

Summary

- **Data has been presented which tracks NiCd battery reconditioning discharge capacity during the continuing 20-year FLTSATCOM F1 mission.**
- **The data trend describes a reconditioning discharge capacity growth/decay signature. The capacity signature is postulated to be the result of corrosion of the sinter, in the Ni electrode, forming NiOOH.**
- **The hypothesis that this reconditioning discharge signature can be used to predict remaining life was tested using a Weibull reliability model.**
 - **Predictions are consistent with observations.**
 - **A larger data base is needed before this approach can be validated.**

Page intentionally left blank

1997 NASA Aerospace Battery Workshop Attendance List

Walter Alsbach
KRIS Engineering Inc. / J & T
GSFC Code 734
Greenbelt, MD 20771
Ph: (301) 286-4822 Fax:

Jon D. Armantrout
Lockheed Martin
O/E201-B/154
1111 Lockheed Way
Sunnyvale, CA 94089
Ph: (408) 742-1800 Fax: (408) 742-2731

Chris Baker
Acme Electric Corporation
528 W. 21st
Tempe, AZ 85282
Ph: (602) 894-6864 Fax: (602) 921-0470
E-mail: cbaker@acmepower.com

Doug Bearden
Marshall Space Flight Center
EB12
Marshall Space Flight Center, AL 35812

Bob Bechtel
Marshall Space Flight Center
EB11
Marshall Space Flight Center, AL 35812
Ph: (205) 544-3294 Fax: (205) 544-5841

Charles W. Bennett
Lockheed Martin Astro Space
230 E. Mall Blvd.
King of Prussia, PA 19406-2995
Ph: (610) 354-6155 Fax: (610) 354-3434
E-mail: ebennett@voicenet.com

Samuel Birken
The Aerospace Corporation
MS M4/986
POB 92957
Los Angeles, CA 90009-2957
Ph: (310) 336-6080 Fax: (310) 336-5581
E-mail: samiam@lafn.org

Yannick Borthomieu
SAFT Advanced Batteries
Rue G. Leclanche
BP 1029
86060 Poitiers Cedex
France
Ph: 33-549-55-4014 Fax: 33-549-55-5620
E-mail: yannick.borthomieu@saft.alcatel-althom.fr

Rita Brazier
Marshall Space Flight Center
EB11
Marshall Space Flight Center, AL 35812
Ph: (205) 544-3295 Fax: (205) 544-5841

Jeffrey C. Brewer
Marshall Space Flight Center
EB12
Marshall Space Flight Center, AL 35812
Ph: (205) 544-3345 Fax: (205) 544-5841
E-mail: jeff.brewer@msfc.nasa.gov

Harry Brown
Naval Surface Warfare Center - Crane Div.
Code 6095 B2949
300 Highway 361
Crane, IN 47522
Ph: (812) 854-6149 Fax: (812) 854-3589
E-mail: brown_harry@crane.navy.mil

Ratnakumar Bugga
Jet Propulsion Laboratory
MS 277-207
4800 Oak Grove Dr.
Pasadena, CA 91109
Ph: (818) 354-0110 Fax: (818) 383-6951
E-mail: kumar@hyperfine.caltech.edu

Shirley Butler
Marshall Space Flight Center
EB12
Marshall Space Flight Center, AL 35812
Ph: (205) 544-3298 Fax:

Dwight Caldwell
Eagle-Picher Industries, Inc.
1216 W. C St.
Joplin, MO 64801
Ph: (417) 623-8000 Fax: (417) 623-5319
E-mail: pwrsubsys@epi-tech.com

1997 NASA Aerospace Battery Workshop Attendance List

John E. Casey
Lockheed Martin Space Mission Sys & Services
2400 NASA Rd. 1, EP5
Houston, TX 77058-3799
Ph: (281) 483-0446 Fax: (281) 483-3096
E-mail: john.e.casey1@jsc.nasa.gov

Marie-Pierre Cassagne
ALCATEL
av champollion
Toulouse Cedex
France-31037
Ph: (33) 5-61-19-62-58 Fax: (33) 5-61-19-61-69

Dwaine Coates
Eagle-Picher Industries
"C" and Porter Streets
Joplin, MO 64801
Ph: (417) 623-8000 Fax:

William D. Cook
Eagle-Picher Industries, Inc.
C and Porter Streets
Joplin, MO 64801
Ph: (417) 623-8000 Fax:

Dr. Marsha Daman
Lockheed Martin Missiles and Space
Org. E6-01; Bldg 149
1111 Lockheed Martin Way
Sunnyvale, CA 94089
Ph: (408) 756-0749 Fax: (408) 756-0645
E-mail: marsha.daman@lmco.com

Giovanni Davolio
University of Modena
Department of Chemistry
183, Via G. Campi
Modena, Italy I-41100
Ph: 39-59-378461 Fax: 39-59-373543
E-mail: davolio@c220.unimo.it

Jeff Dermott
Eagle-Picher Industries, Inc.
Joplin, MO 64802
Ph: (417) 623-8333 Fax: (417) 623-0233

Sal Di Stefano
Jet Propulsion Laboratory
MS 277-212
4800 Oak Grove Drive
Pasadena, CA 91109
Ph: (818) 354-6320 Fax: (818) 393-6951

Juergen Eckert
Los Alamos National Laboratory
Lujan Center, MS H805
Los Alamos, NM 87545
Ph: (505) 665-2374 Fax: (505) 665-2676
E-mail: juergen@lanl.gov

Ted Edge
Marshall Space Flight Center
EB12
Marshall Space Flight Center, AL 35812
Ph: (205) 544-3381 Fax:

Beth Fleming
The Boeing Company
689 Discovery Drive
Huntsville, AL 35806
Ph: (205) 922-7359 Fax: (205) 922-7525
E-mail: beth.fleming@boeing.com

Pete George
Marshall Space Flight Center
EB12
Marshall Space Flight Center, AL 35812
Ph: (205) 544-3331 Fax:

Donald Georgi, P.E.
Batteries Digest Newsletter
1261 Town Line Road
Maple Plain, MN 55359
Ph: (612) 479-6190 Fax: (612) 479-3657
E-mail: teksym@aol.com

Shirley Georgi
Batteries Digest Newsletter
1261 Town Line Road
Maple Plain, MN 55359
Ph: (612) 479-6190 Fax: (612) 479-3657
E-mail: teksym@aol.com

1997 NASA Aerospace Battery Workshop Attendance List

Charles Hall
Marshall Space Flight Center
EB12
Marshall Space Flight Center, AL 35812
Ph: (205) 544-3330 Fax:

David Hall
Marshall Space Flight Center
EB12
Marshall Space Flight Center, AL 35812
Ph: (205) 544-4215 Fax:

Steve Hall
Naval Surface Warfare Center - Crane Div.
Code 6095
300 Highway 361
Crane, IN 47522
Ph: (812) 854-4172 Fax: (812) 854-3589

Gerald Halpert
Jet Propulsion Laboratory
MS 277-207
4800 Oak Grove Dr.
Pasadena, CA 91109
Ph: (818) 354-5474 Fax: (818) 393-6951
E-mail: gerald.halpert@jpl.nasa.gov

Jeff Hayden
Eagle-Picher Industries, Inc.
3820 South Hancock Expressway
Colorado Springs, CO 80911
Ph: (719) 392-4266 Fax: (719) 392-5103

Susan M. Herczeg
National-Standard Co.
2401 N. Home St.
Mishawaka, IN 46545
Ph: (219) 259-8505 x257 Fax: (219) 259-8507

Albert Himy
Navy / JJMA
2341 Jefferson Davis Highway
Suite 715
Arlington, VA 22202
Ph: (703) 418-4257 Fax: (703) 418-4269

Scott Hoover
Orion Satellite Corporation
2440 Research Blvd.
Suite 160
Rockville, MD 20850
Ph: (301) 258-3325 Fax: (301) 258-3319
E-mail: shoover@onsi.com

Charles Huang
Lockheed Martin
3700 Bay Area Blvd.
Houston, TX 77058
Ph: (281) 335-6036 Fax: (281) 335-6284
E-mail: huang@ips.jsc.nasa.gov

Scott Hutchison
Lockheed Martin SMS&S
16100 Space Center Blvd. #112
Houston, TX 77062
Ph: (281) 335-6464 Fax: (281) 335-6400
E-mail: hutchison@mscips.jsc.nasa.gov

Nathan Isaacs
Mine Safety Appliances Company
38 Loveton Circle
Sparks, MD 21152
Ph: (410) 628-5432 Fax: (410) 628-0613
E-mail: nedizakmsa@aol.com

Lorna Jackson
Marshall Space Flight Center
EB12
Marshall Space Flight Center, AL 35812
Ph: (205) 544-3318 Fax:

Jason E. Jenkins
Johns Hopkins University / APL
MS 23-214
Johns Hopkins Rd.
Laurel, MD 20723-6099
Ph: 410 792-5106 Fax:

Grady S. Jobe
Marshall Space Flight Center
EA01
Marshall Space Flight Center, AL 35812
Ph: (205) 544-0027 Fax:

1997 NASA Aerospace Battery Workshop Attendance List

Walter Kaden
Lockheed Martin Missiles and Space
Mail Stop 419-3A
POB 800
Princeton, NJ 08543-0800
Ph: (609) 490-2310 Fax: (609) 490-2856
E-mail: walter.kaden@lmco.com

Chad O. Kelly
Eagle-Picher Industries
C & Porter
Joplin, MO 64801
Ph: (417)-623-8000 x436 Fax: (417) 623-0850
E-mail: eplion@aol.com

Marcie Kennedy
Marshall Space Flight Center
EB12
Marshall Space Flight Center, AL 35812
Ph: (205) 544-3724 Fax:

Donald R. Kleis
ENSER
227 Silverwood Ln.
Hazel Green, AL 35750
Ph: (205) 828-0569 Fax: (205) 890-6707 x247
E-mail: slvrstreek@aol.com

Randolph Leising
Wilson Greatbatch Ltd.
10000 Wehrle Dr.
Clarence, NY 14031

Danny Liu
Intelsat
Intelsat VIII Program Office
c/o Lockheed Martin Astropace
POB 800 / MS 93
Princeton, NJ 08543-0800
Ph: (609) 426-9225 Fax: (609) 426-8968
E-mail: danny.liu@intelsat.int

Eric Lowery
Marshall Space Flight Center
EB12
Marshall Space Flight Center, AL 35812
Ph: (205) 544-0080 Fax:

Dave Lucero
Eagle-Picher Industries, Inc.
3820 South Hancock Expressway
Colorado Springs, CO 80911
Ph: (719) 392-4266 Fax: (719) 392-5103

Chuck Lurie
TRW
MS R4/1082
One Space Park
Redondo Beach, CA 90278
Ph: (310) 813-4888 Fax: (310) 812-4978
E-mail: chuck.lurie@trw.com

Michael Mackowski
The Boeing Co.
1022 W. Juanita Ave.
Gilbert, AZ 85233
Ph: (602) 732-3064 Fax: (602) 732-3885
E-mail: 71571.330@compuserve.com

Dr. Tyler X. Mahy
U.S. Government
c/o OTS, NHB
Washington, DC 20505
Ph: (703) 874-0739 Fax: (703) 641-9830

Michelle Manzo
Lewis Research Center
MS 309-1
21000 Brookpark Rd.
Cleveland, OH 44135
Ph: (216) 433-5261 Fax: (216) 433-6160

Lynn Marcoux
BlueStar Advanced Technology Corporation
1155 West 15th Street
North Vancouver, B.C.
Canada V7P 1M7
Ph: (604) 986-4020 Fax: (604) 986-1048

Dr. Nehemiah Margalit
Tracor Applied Sciences Inc.
1601 Research Blvd.
Rockville, MD 20850-3176
Ph: (301) 838-6223 Fax: (301) 838-6222
E-mail: nmargalit@tracor.com

1997 NASA Aerospace Battery Workshop Attendance List

Richard Marsh
AFRL / PRPB
1950 Fifth St.
Wright-Patterson AFB, OH 45433
Ph: (937) 255-7770 Fax: (513) 255-1759
E-mail: marshra@wl.wpafb.af.mil

Jeff Martin
Marshall Space Flight Center
EB12
Marshall Space Flight Center, AL 35812

Dean W. Maurer
Loral Skynet
292 Johnston Dr.
Watchung, NJ 07060
Ph: (908) 753-4457 Fax: (732) 949-8082
E-mail: dwmaurer@attmail.com

Louis C. Maus
Marshall Space Flight Center
PD11
Marshall Space Flight Center, AL 35812
Ph: (205) 544-0484 Fax: (205) 544-4225

Kurt McCall
Marshall Space Flight Center
EB12
Marshall Space Flight Center, AL 35812
Ph: (205) 961-4501 Fax:

George Methlie
2120 Natahoa Ct.
Falls Church, VA 22043
Ph: (202) 965-3420 Fax: (703) 641-9830

Martin Mildner
2212 So. Beverwil Dr.
Los Angeles, CA 90034-1034
Ph: (310) 836-7794 Fax: (310) 836-4494
E-mail: mmildner@worldnet.att.net

Thomas L. Miller
Barrios Technology, Inc.
MS DF75
NASA Johnson Space Center
Houston, TX 77058
Ph: (281) 244-0048 Fax: (281) 244-0031
E-mail: thomas.l.miller1@jsc.nasa.gov

Thomas R. Newbauer
SMC / AXEN
SMC / AXE
160 Skynet St.
Los Angeles, CA 90245-4683
Ph: (310) 363-5176 Fax: (310) 363-2532
E-mail: newbauertr@post6.laafb.af.mil

Pat O'Donnell
Lewis Research Center
MS 309-1
21000 Brookpark Rd.
Cleveland, OH 44135
Ph: (216) 433-5248 Fax: (216) 433-6160
E-mail: seodo@lms02.lerc.nasa.gov

Burton Otzinger
Jet Propulsion Laboratory
4800 Oak Grove Drive
Pasadena, CA 91109
Ph: (626) 354-2351 Fax:

John Pajak
ZAE Research, Inc.
555 Sparkman Dr.
Suite 450
Huntsville, AL 35816
Ph: (205) 890-0507 Fax: (205) 890-0857

Rick Parmley
LaBarge Electronics
1505 Maiden Lane
POB 1210
Joplin, MO 64802-1210
Ph: (417) 781-3200 x258 Fax: (417) 781-2175

Dave Perrone
Jet Propulsion Laboratory
MS 277-212
4800 Oak Grove Dr.
Pasadena, CA 91109
Ph: 818 354-9044 Fax: 818 393-6951

1997 NASA Aerospace Battery Workshop Attendance List

David F. Pickett
Eagle-Picher Industries
Power Systems Department
3820 S. Hancock Expressway
Colorado Springs, CO 80911
Ph: (719) 392-4266 Fax: (719) 392-5103
E-mail: aaaa_energy_enterprises@msn.com

Darren Pivarnik
Orion Satellite Corporation
2440 Research Blvd
Suite 160
Rockville, MD 20850
Ph: (301) 258-3219 Fax: (301) 258-3319
E-mail: 695-4848@mcimail.com

Allen R. Powers
Hughes Space & Communications
POB 2999
3100 Lomita Blvd.
Bldg 231 / MS 1918
Torrance, CA 90509-2999
Ph: (310) 517-5435 Fax: (310) 517-7676
E-mail: arpowers@ccgate.hac.com

Dan T. Radzykewycz
AFRL / VSDVP
3550 Aberdeen Ave. SE
Kirtland AFB, NM 87117
Ph: 505 846-5703 Fax:

David L. Randall
Johnson Space Center
Mail Code DF6
Houston, TX 77058
Ph: (281) 483-0746 Fax: (281) 483-3997
E-mail: david.l.randall1@jsc.nasa.gov

Paul L. Reinstein
The Aerospace Corporation
2350 E. El Segundo Blvd.
MS M4/179
El Segundo, CA 90245-4691
Ph: (310) 336-1909 Fax: (310) 336-5581
E-mail: paul.l.reinstein@aero.org

Paul Repligle
USBI
POB 21212
Mail Stop USB-EE
Kennedy Space Center, FL 32815-0212
Ph: (407) 867-7871 Fax: (407) 867-9829
E-mail: repliglep@usbi.com

Ron Replinger
Eagle-Picher Industries, Inc.
POB 47
Joplin, MO 64802
Ph: (417) 623-8000 Fax: (417) 623-5319

Ricky J. Roberson
Huntsville Integrated Voltaic Equipment
2115 Britain Ave.
Huntsville, AL 35803
Ph: (205) 512-3001 Beeper Fax:
E-mail: ricky.roberson@msfc.nasa.gov

Paul S. Rodriguez
ENSER
512 Bain Dr.
Huntsville, AL 35803
Ph: (205) 882-3465 Fax:

Frank Scalici
INTELSAT
3400 International Dr. NW
Box 34
Washington, DC 20008
Ph: (202) 944-7353 Fax: (202) 944-7333
E-mail: frank.scalici@intelsat.int

Charles Scogins
ACM Inc.
3054 D Leeman Ferry Rd.
Huntsville, AL 35807
Ph: (205) 881-5493 Fax: (205) 883-5885
E-mail: ACM@traveller.com

Darren L. Scoles
Lockheed Martin Missiles & Space
GPS IIR Flight Operations
440 Discoverer St.
Suite 79
Falcon AFB, CO 80912-4479

Annie Sennet
SAFT
156 Avenue DeMetz
Romainville, France 93230
France
Ph: 33 1 49 15 36 44 Fax: 33 1 48 91 95 53

1997 NASA Aerospace Battery Workshop Attendance List

Sat P. Singhal
Computer Sciences Corporation
7404 Executive Place
Seabrook, MD 20706
Ph: 301 464-7489 x7579 Fax: 301 464-3352
E-mail: ssinghal@csc.com

Gerald S. Smith
INTELSAT
3400 International Dr., NW
Box 34
Washington, DC 20008-3098
Ph: (202) 944-8194 Fax: (202) 944-7333
E-mail: gerald.smith@intelsat.int

Yoshitsugu Sone
National Space Development Agency of Japan
Tsukuba Space Center
2-1-1 Sengen, Tsukuba-city
Ibaraki-pref. 305 Japan
Ph: 81-(0)298-52-2285 Fax: 81-(0)298-52-2299
E-mail: sone.yoshitsugu@nasda.go.jp

David M. Spillman
Wilson Greatbatch Ltd.
10000 Wehrle Drive
Clarence, NY 14031
Ph: (716) 759-5378 Fax: (716) 759-8579
E-mail: dspillman@greatbatch.com

James A. Stepro
National-Standard Co.
2401 N. Home St.
Mishawaka, IN 46545
Ph: (219) 259-8505 Fax: (219) 259-8507

Tina D. Stewart
United Space Alliance
MS DF75
NASA JSC
Houston, TX 77058
Ph: (281) 483-8900 Fax: (281) 244-0031
E-mail: tina.d.stewart1@jsc.nasa.gov

Joe Stockel
Office of Research & Development
LF-7 Rm 6118
Washington, DC 20505
Ph: (703) 613-8833 Fax: (703) 613-8954

Bradley Strangways
Symmetry Resources, Inc.
POB 785
Arab, AL 35016
Ph: (205) 586-8911 Fax: (205) 586-9443
E-mail: symm@bmtc.mindspring.com

Rao Surampudi
Jet Propulsion Laboratory
4800 Oak Grove Dr.
Pasadena, CA 91109
Ph: (818) 354-0352 Fax: (818) 393-6951
E-mail: rao.surampudi@jpl.nasa.gov

Vijay V. Thakur
Defence Evaluation and Research Agency
Space Power Laboratory
X107 Bldg.
DERA Farnborough
Hampshire. GU140LX.U.K.
Ph: 011-44-1252 393669 Fax: 011-44-1252 392664

Lawrence Thaller
The Aerospace Corporation
MS M2/275
POB 92957
Los Angeles, CA 90009
Ph: (310) 336-5180 Fax: (310) 336-1636
E-mail: lawrence.h.thaller@aero.org

Robert F. Tobias
TRW
MS R4/1074
One Space Park
Redondo Beach, CA 90278
Ph: (310) 813-5784 Fax:

Mark R. Toft
Motorola
44330 Woodridge Parkway
Leesburg, VA 20176
Ph: (703) 724-8188 Fax: (703) 724-8156
E-mail: mark_toft-P27760@email.mot.com

Greta Tracinski
Applied Power International
1236 N. Columbus Ave., #41
Glendale, CA 91202-1672
Ph: (818) 243-3127 Fax: (818) 243-3127
E-mail: 104024.1452@compuserve.com

1997 NASA Aerospace Battery Workshop Attendance List

Walter A. Tracinski
Applied Power International
1236 N. Columbus Ave., #41
Glendale, CA 91202-1672
Ph: (818) 243-3127 Fax: (818) 243-3127
E-mail: 104024.1452@compuserve.com

Dr. Hari Vaidyanathan
COMSAT Laboratories
22300 Comsat Dr.
Clarksburg, MD 20871
Ph: (304) 428-4507 Fax: (301) 428-3686
E-mail: hari.vaidyanathan@comsat.com

Daniel J. Vonderwell
The Boeing Company
MS AHSV-33B1
689 Discovery Drive
Huntsville, AL 35806-2804
Ph: (205) 922-6739 Fax: (205) 922-7525
E-mail: daniel.j.vonderwell@boeing.com

Sammy Waldrop
Symmetry Resources, Inc.
POB 785
Arab, AL 35016
Ph: (205) 586-8911 Fax: (205) 586-9443
E-mail: symm@bmtc.mindspring.com

Steven C. Walker, P.E.
The ENSER Corporation
UAH Johnson Research Center
Huntsville, AL 35899
Ph: (205) 890-6707 x227 Fax: (205) 890-6668
E-mail: royjaxon@aol.com

Bryan Walls
Marshall Space Flight Center
EB12 ~
Marshall Space Flight Center, AL 35812

Harry Wannemacher
Jackson & Tull
7375 Executive Place
Suite 200
Seabrook, MD 20706
Ph: (301) 805-6090 Fax: (301) 805-6099
E-mail: harry.wan@jnt.com

Marvin Warshay
Lewis Research Center
MS 301-5
21000 Brookpark Rd.
Cleveland, OH 44135
Ph: (216) 433-5261 Fax:

Steve Westfall
LaBarge Electronics
1505 Maiden Lane
Joplin, MO 64802
Ph: (417) 781-3200 Fax: (417) 781-2175

Tom Whitt
Marshall Space Flight Center
EB12
Marshall Space Flight Center, AL 35812
Ph: (205) 544-3313 Fax:

Brett Williams
EUTELSAT
70 rue Balard
75502 PARIS CEDEX 15
Ph: 33.1.53.98.46.43 Fax: 33.1.53.98.49.99

Floyd L. Williamson
ZAE Research, Inc.
555 Sparkman Dr.
Suite 450
Huntsville, AL 35816
Ph: (205) 890-0507 Fax: (205) 890-0857
E-mail: fiw@hiwaay.net

Doug Willowby
Marshall Space Flight Center
EB12
Marshall Space Flight Center, AL 35812
Ph: (205) 544-3334 Fax:

Doug Wright
Eagle-Picher Industries
POB 47
Joplin, MO 64802
Ph: (417) 623-8000 Fax: (417) 623-0850
E-mail: dwright@epi-tech.com

1997 NASA Aerospace Battery Workshop Attendance List

Thomas Yi
Goddard Space Flight Center
Code 734
Greenbelt, MD 20771
Ph: (301) 286-3051 Fax: (301) 286-9214

Albert H. Zimmerman
The Aerospace Corporation
MS M2/275
POB 92957
Los Angeles, CA 90009-2957
Ph: (310) 336-7415 Fax: (310) 336-1636

REPORT DOCUMENTATION PAGE			Form Approved OMB No. 0704-0188	
Public reporting burden for this collection of information is estimated to average 1 hour per response, including the time for reviewing instructions, searching existing data sources, gathering and maintaining the data needed, and completing and reviewing the collection of information. Send comments regarding this burden estimate or any other aspect of this collection of information, including suggestions for reducing this burden, to Washington Headquarters Services, Directorate for Information Operation and Reports, 1215 Jefferson Davis Highway, Suite 1204, Arlington, VA 22202-4302, and to the Office of Management and Budget, Paperwork Reduction Project (0704-0188), Washington, DC 20503				
1. AGENCY USE ONLY (Leave Blank)	2. REPORT DATE July 1998	3. REPORT TYPE AND DATES COVERED Conference Publication		
4. TITLE AND SUBTITLE The 1997 NASA Aerospace Battery Workshop			5. FUNDING NUMBERS	
6. AUTHORS J.C. Brewer, Compiler				
7. PERFORMING ORGANIZATION NAME(S) AND ADDRESS(ES) George C. Marshall Space Flight Center Marshall Space Flight Center, AL 35812			8. PERFORMING ORGANIZATION REPORT NUMBER M-885	
9. SPONSORING/MONITORING AGENCY NAME(S) AND ADDRESS(ES) National Aeronautics and Space Administration Washington, DC 20546-0001			10. SPONSORING/MONITORING AGENCY REPORT NUMBER NASA/CP-1998-208536	
11. SUPPLEMENTARY NOTES Proceedings of a workshop sponsored by the NASA Aerospace Flight Battery Systems Program, hosted by the Marshall Space Flight Center, and held at the Huntsville Hilton on November 18-20, 1997.				
12a. DISTRIBUTION/AVAILABILITY STATEMENT Unclassified-Unlimited Subject Category 44 Standard Distribution			12b. DISTRIBUTION CODE	
13. ABSTRACT (Maximum 200 words) This document contains the proceedings of the 30th annual NASA Aerospace Battery Workshop, hosted by the Marshall Space Flight Center on November 18-20, 1997. The workshop was attended by scientists and engineers from various agencies of the U.S. Government, aerospace contractors, and battery manufacturers, as well as international participation in like kind from a number of countries around the world. The subjects covered included nickel-cadmium, nickel-hydrogen, nickel-metal hydride, lithium, lithium-ion, and silver-zinc technologies, as well as various aspects of nickel electrode design.				
14. SUBJECT TERMS battery, nickel-cadmium, nickel-hydrogen, nickel-metal hydride, lithium, lithium-ion, silver-zinc, nickel electrode, electrode, battery tests			15. NUMBER OF PAGES 810	
			16. PRICE CODE A99	
17. SECURITY CLASSIFICATION OF REPORT Unclassified	18. SECURITY CLASSIFICATION OF THIS PAGE Unclassified	19. SECURITY CLASSIFICATION OF ABSTRACT Unclassified	20. LIMITATION OF ABSTRACT Unlimited	

National Aeronautics and
Space Administration
AT01S
George C. Marshall Space Flight Center
Marshall Space Flight Center, Alabama
35812